Casa abierta al tiempo

UNIVERSIDAD AUTÓNOMA METROPOLITANA, UNIDAD IZTAPALAPA

División de Ciencias Biológicas y de la Salud

Posgrado en Biología Experimental

The consumption of a high cholesterol diet conditions the development of a subtype of HCC with high aggressiveness and poor prognosis

TESIS:

Que para obtener el grado de

Doctor en Biología Experimental

PRESENTA:

Mtro. Biol. Exp. Arturo Simoni Nieves

Matrícula: 2163802393 **ORCID:** 0000-0002-1353-260X

Correo electrónico: bioexpp22@gmail.com

COMITÉ TUTORAL:

Co-Director: Dr. Luis Enrique Gómez Quiroz

Co-Director: Dr. Jens Uwe Marquardt

Asesora: Dra. Roxana Uri Miranda Labra

JURADO:

Presidente: Dr. Ju Seog Lee.

Secretario: Dr. Cédric Coulouarn Michel.

Vocal 1: Dra. María Concepción Gutiérrez-Ruiz.

Vocal 2: Dr. Héctor Fernando Serrano.

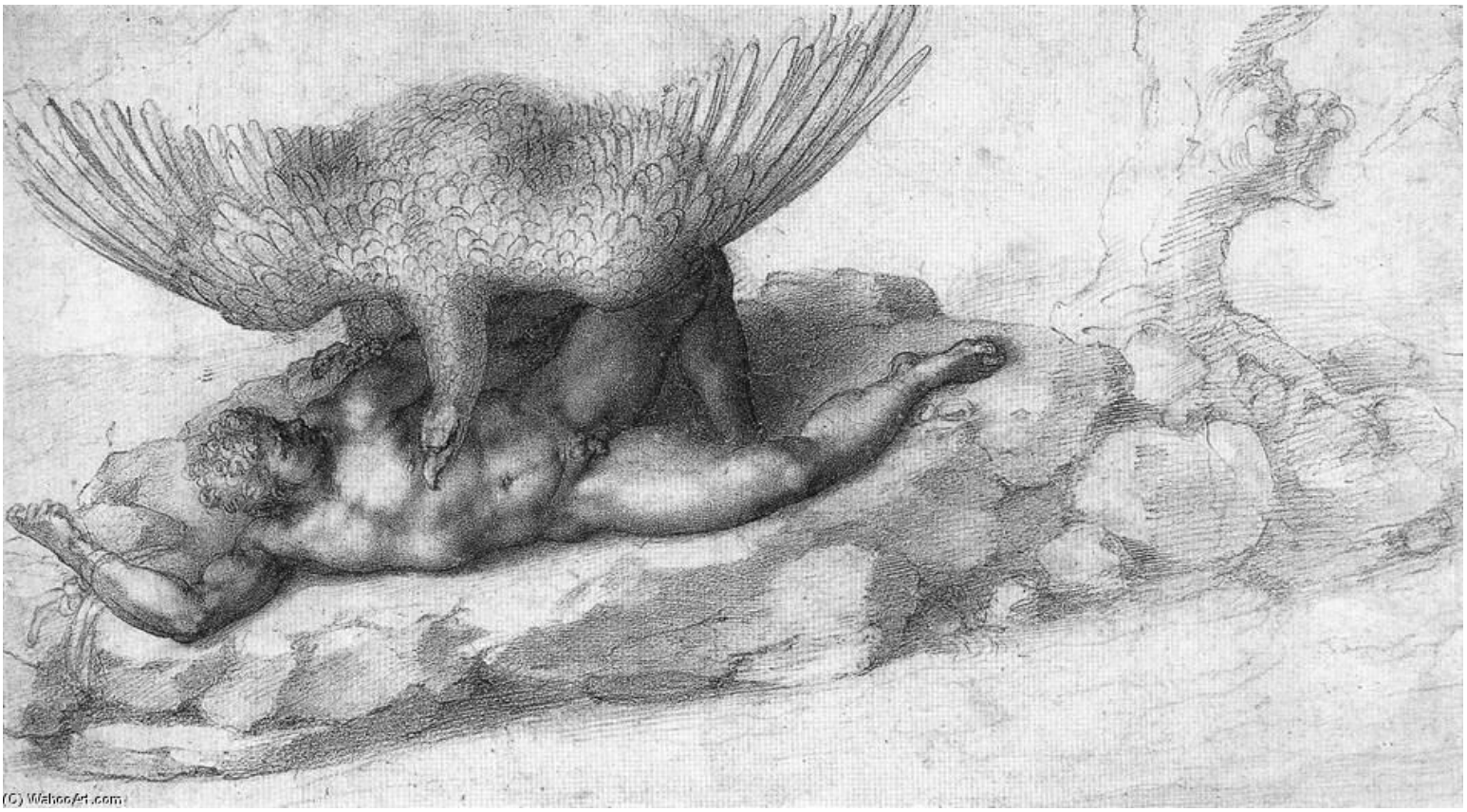
Iztapalapa, Ciudad de México a 10 de marzo del 2021

The consumption of a high-cholesterol diet conditions the development of a subtype of HCC with high aggressiveness and poor prognosis.

El consumo de una dieta alta en colesterol condiciona el desarrollo de un subtipo de HCC con una alta agresividad y mal pronóstico

Thesis to obtain the degree of Doctor of Philosophy in Experimental Biology

Arturo Simoni Nieves, 2021



Michelangelo Buonarroti, The Punishment of Tityus (1532).
Black chalk. Royal Collection, © 2010, Her Majesty Queen Elizabeth II.

The consumption of a high cholesterol diet conditions the development of a subtype of HCC with high aggressiveness and poor prognosis

Arturo Simoni Nieves
Ciudad de México
MARZO 2021

Declaración de originalidad

El (La) que suscribe _____Arturo Simoni Nieves_____, alumno (a) del posgrado _____Biología Experimental_____, de la División de Ciencias Biológicas y de la Salud, de la Universidad Autónoma Metropolitana Iztapalapa y autor(a) de la tesis o idónea comunicación de resultados titulada: "_El consumo de una dieta alta en colesterol condiciona a el desarrollo de un subtipo de HCC con una alta agresividad y mal pronóstico_",

Declaro que:

1. La tesis o idónea comunicación de resultados que presento ante ___el honorable jurado_____ para lo obtención del grado de __Doctor_____ es de mi autoría y original creación, producto del resultado de mi trabajo de investigación personal e individual; el cual cuenta con las correspondientes citas textuales del material bibliográfico utilizado y con el debido otorgamiento de los créditos autorales.
2. En la tesis o idónea comunicación de resultados no he reproducido párrafos completos; ilustraciones, fotografías, diagramas, cuadros y tablas, sin otorgamiento del crédito autoral y fuente correspondiente.
3. En consecuencia, relevo de toda responsabilidad a la Universidad Autónoma Metropolitana de cualquier demanda o reclamación que llegara a formular alguna persona física o moral que se considere con derecho sobre la tesis o idónea comunicación de resultados, respondiendo por la autoría y originalidad de la misma, asumiendo todas las consecuencias económicas y jurídicas si ésta no fuese de mi creación.

La presente declaración de originalidad se firma en la Ciudad de México el 10 de marzo del 2021.

Atentamente



__Arturo Simoni Nieves__

Nombre y firma del alumno

CARTA DE CONFIDENCIALIDAD

Ciudad de México, a 10 de marzo del 2021

Comisión Académica del Posgrado
__en Biología Experimental__
Presente

El(La) que suscribe (____Arturo Simoni Nieves____) alumno(a) con número de matrícula __2163802393__, del posgrado _Biología Experimental_ de la Universidad Autónoma Metropolitana, Unidad Iztapalapa (UAM-I), manifiesto mi compromiso de mantener de forma confidencial y de no utilizar, divulgar o difundir por ningún medio, en beneficio propio o de terceros, la información, la documentación y datos de toda índole a los que tenga acceso y reciba con motivo del proyecto de investigación _ El consumo de una dieta alta en colesterol condiciona a el desarrollo de un subtipo de HCC con una alta agresividad y mal pronóstico_ a desarrollar en la _Universidad Autónoma Metropolitana, Unidad Iztapalapa_, lo anterior en términos del artículo 6, fracción V, de los Lineamientos para el Acceso a la Información de la Universidad Autónoma Metropolitana. Esta obligación subsistirá incluso después de haber obtenido el grado.

En caso de que contravenga este compromiso, la Universidad se reserva el derecho de ejercer las acciones civiles y penales que procedan y en consecuencia, asumo cualquier responsabilidad por el manejo indebido o sin la previa autorización expresa de la UAM-I de la referida información o resultados, así como por los eventuales perjuicios que pudiese ocasionarse a esta Casa de Estudios.



___ Arturo Simoni Nieves ___
Nombre completo y firma autógrafa*

El programa de Doctorado en Biología Experimental de la Universidad Autónoma Metropolitana pertenece al Programa Nacional de Posgrados de Calidad (PNPC) del CONACYT, registro 001482, en el Nivel Consolidado, y cuenta con el apoyo del mismo Consejo, Clave DAFCYT-2003IMPTNNN0020. Número de registro de la beca otorgada por el CONACYT: 570373.

Este trabajo fue financiado por el Consejo Nacional de Ciencia y Tecnología (CONACYT), Fronteras de la Ciencia #1320, CB-252942 y a la Universidad Autónoma Metropolitana Iztapalapa siendo responsable el Dr. Luis Enrique Gómez Quiroz.

Casa abierta al tiempo
UNIVERSIDAD AUTÓNOMA METROPOLITANA
Unidad Iztapalapa

Fecha : 09/03/2021
Página : 1/1

CONSTANCIA DE PRESENTACION DE EXAMEN DE GRADO

La Universidad Autónoma Metropolitana extiende la presente CONSTANCIA DE PRESENTACION DE DISERTACIÓN PÚBLICA de DOCTOR EN BIOLOGIA EXPERIMENTAL del alumno ARTURO SIMONI NIEVES, matrícula 2163802393, quien cumplió con los 315 créditos correspondientes a las unidades de enseñanza aprendizaje del plan de estudio, 45 créditos de PUBLICACION y 45 créditos de EXAMEN PREDOCTORAL. Con fecha diez de marzo del 2021 presentó la DEFENSA de su DISERTACIÓN PÚBLICA cuya denominación es:

The consumption of a high cholesterol diet conditions the development of a subtype of HCC with high aggressiveness and poor prognosis.

Cabe mencionar que la aprobación tiene un valor de 45 créditos y el programa consta de 450 créditos.

El jurado del examen ha tenido a bien otorgarle la calificación de:

Aprobar

JURADO

Presidente	Secretario
DR. JU SEOG LEE	DR. CEDRIC COULOUARN MICHEL
Vocal	**Vocal**
DRA. MARIA CONCEPCION GUTIERREZ RUIZ	DR. HECTOR FERNANDO SERRANO

Av. San Rafael Atlixco No. 186, Col. Vicentina, Del. Iztapalapa, C.P. 09340, México, CDMX, Tels: 5804 4680 y 5804 4883 csera@xanum.uam.mx y csesi@xanum.uam.mx http://cse.izt.uam.mx/cse/

Academic recognition

This thesis was carried out under the mentorship of Dr. Luis Enrique Gomez Quiroz in the Experimental Medicine and Carcinogenesis Laboratory, of the Department of Health Sciences belonging to the Universidad Autonoma Metropolitana, Mexico City, Mexico and Dr. Jens U. Marquardt in the Department of Medicine I, from the Schleswig-Holstein University Hospital, Lübeck, Germany as part of the requirements to obtain the degree of Doctor of Experimental Biology through the PhD Program in Experimental Biology.

Tutoral committee that evaluated the development of this project was composed of:

Codirector. Dr. Luis Enrique Gomez Quiroz
Department of Health Science, Metropolitan Autonomous University, Mexico City, Mexico.
Telephone. 55-58044730 Email. legq@xanum.uam.mx

Codirector. Dr. Jens U. Marquardt
Department of Medicine I, University Hospital Schleswig-Holstein, Lübeck, Germany.
Telephone. +49 0451 / 500-44101 Email. Jens.Marquardt@uksh.de

Advisor. Dra. Roxana U. Miranda Labra
Deparment of Health Science, Metropolitan Autonomus University, Mexico City, Mexico.
Telephone. 55 13780345 Email. roxml@xanum.uam.mx

Monitoring and support my academic situation of the Dra. Laura Josefina Perez Flores, Coordinator of the Doctoral Program in Experimental Biology and the Lic. Angelica Ostos and Lic. Violeta Luna are recognized.

This work was funded by the National Science and Technology Council (CONACYT), Frontiers of Science # 1320, CB-252942 and Universidad Autónoma Metropolitana Iztapalapa being responsible Dr. Luis Enrique Gómez Quiroz.

Finally, I would like to thank to my thesis defense jury for giving me the honor of being part of it:

Chairman: Dr. Ju-Seog Lee

Secretary: Dr. Cédric Coulouarn

Vowel: Dra. María Concepción Gutiérrez-Ruiz

Vowel: Dr. Héctor Fernando Serrano

Acknowledgments

I thank my thesis supervisors who are among the people I most admire for their great intelligence and dedication. Dr. Luis Enrique Gómez Quiroz, who has always been one of my role models to whom I owe the fact that this thesis is finished, thanks for your time and support. To Dr. Jens Marquardt, who welcomed me with open arms in your country and in your laboratory, who has always been willing to support me and enrich this work. Danke.

To Dr. Concepción Gutiérrez Ruiz for allowing me to enter this great laboratory and giving me the opportunity to grow both as a person and as a researcher.

To Dr. Leticia Bucio, Dr. Verónica Souza and Dr. Roxana Miranda for their help and advice within the laboratory.

To Doctors Ju-Seog Lee and Cédric Coulouarn for their invaluable advice and opinions, which enriched the present work.

To my lab colleagues to Lissete, Monse, Natanael, and especially to Joselyn for always messing around with me, thanks for everything.

To the members of the Mainz laboratory (now Lubeck), to Darko, Monika and Sharon, who always made working days in the laboratory enjoyable.

To my first student, Alejandro, for his help and thanks to his questions, he have forced me to read and learn more.

To Denise who was my teacher and you have taught me a lot and you will continue to do so.

To Soraya that more than a friend is already part of my family, thank you for everything you have lived with me, thank you for all the support.

Dedications

I dedicate this thesis to my family who thanks to their support I was able to conclude this great step. To my mom and sister for their support and trust. Thank you for helping me meet my goals as person and student. To my mother for making me a better person through her advice, teachings and love from her. To my sister for always being present. Thank you for all the support and love.

Index

Foreword ----------xv

Resumen ----------xvii

Abstract ----------xxiv

Dramatis Personae ----------xxvi

Chapter 1. A historical overview ----------1

Chapter 2. Non-alcoholic fatty liver disease ----------4

Chapter 3. Hepatocellular Carcinoma ----------8

- Epidemiology ----------8
- The Biology of HCC and cholesterol ----------11
- Translational oncology and personalized medicine ----------14

Chapter 4. Research Proposal ----------16

- Justification ----------16
- Research question ----------16
- Hypothesis ----------16
- Objective ----------17
    - Main objective ----------17
    - Specific objectives ----------17

Chapter 5. Experimental Design and Methods ----------18

- Animal model Page ----------18
- Methods ----------20

Chapter 6. Results ----------28

High lipids diets induce weight gain, liver damage and tumor promotion ---------28

Transcriptional profile of tumors from lipid overloaded livers ----------34

Inflammation present in liver tumors associated to cholesterol consumption ----39

Integrative genomics and four-gene signature ----------42

Chapter 7. Discussion and Conclusions ----------51

- Discussion ----------51
- Conclusions ----------57

Chapter 8. Perspectives ----------58

Reference ----------60

Annexed I. ----------68

Annexed II. ----------84

Epilogue ----------266

Figure Index

Chapter 1

Figure 1. Natural history of liver disease. ----------1

Chapter 2

Figure 2. Prevalence of Nonalcoholic Fatty Liver Disease ----------5

Figure 3. Primary mouse hepatocytes isolated from animals fed with a balanced Chow diet and with a cholesterol-enriched diet ----------6

Chapter 3

Figure 4. Estimated incidence and mortality world rates 2020 ----------9

Figure 5. The estimated proportion of HCC attributed to NAFLD ----------11

Chapter 5

Figure 6. Experimental design overview. ----------19

Chapter 6

Figure 7. High lipid diets induce weight gain and liver damage in mice. ----------29

Figure 8. The consumption of a lipid-enriched diets induce lipid liver overload and hepatic tumors. -------31

Figure 9. Lost of normal liver architecture. ----------33

Figure 10. Tumors from high lipids diets exhibit a profound change in gene expression------35-36

Figure 11. Tumors from high lipids diets exhibit a more aggressive phenotype. ----------37-38

Figure 12. Inflammation as distinctive feature in liver tumors associated to high lipid and cholesterol consumption. ----------40-42

Figure 13. High cholesterol diet consumption promotes specific gene signature. ----------44-45

Figure 14. Lipid-associated four gene signature of HCC correlates with cholesterol overload in human cancer cell lines. ----------46-48
Figure 15. Lipid-associated four gene signature defines a subtype of human liver cancer with poor prognosis. ----------49-50

Table Index

Chapter 5

Table 1. Mice groups under different diets and treatments. ----------19
Table 2. Primers used in the study. ----------23-25
Table 3. Antibodies used in the study. ----------26

Foreword

Although cancer is a disease fundamentally of the genome, where only some mutations trigger a selective advantage of cell growth, most of the mutations being benign passengers that accumulate by chance. We still cannot fully understand the origin and consequences of these evolutionary advantages. One of the biggest paradoxes that researchers face is the so-called Peto´s paradox.

This paradox speaks that cancer is a consequence of multicellularity and a striking example of multilevel selection. The theory of cancer initiation and progression is deeply rooted in evolutionary and environmental concepts. Cancer develops through somatic evolution, with genetic and epigenetic instability that generates variation in fitness between cells in a body. Selection at the organism level has led to the evolution of tumor suppressor mechanisms, such as cell cycle checkpoints and apoptosis, which act as safeguards to prevent somatic mutations from spreading in the cell population. Nonetheless, cancer occurs at staggeringly high rates and can be responsible for 20-46% of all deaths in multicellular animals ranging from mollusks to mammals. In all, as mentioned before, cancer is closely rooted in evolutionary and environmental concepts. Within all this great global health problem that is cancer, this work tries to describe an environmental condition that is already considered a "pandemic", fatty liver disease, focused mainly on cholesterol, which is giving liver cancer an advantage.

This research that has been initiated in the old Cellular Physiology laboratory for several years and now in the new Experimental Medicine and Carcinogenesis

Laboratory where I was trained as a researcher and mainly as a person has developed a lot of knowledge regarding liver cancer, although there is still endless of unknowns to be solved, in the same way there are a large number of future scientists who are yet to enter this great multidisciplinary laboratory, where they will find great support in the researchers who carry the laboratory on their shoulders. I just hope this thesis will be usefull to guide and inspire future scientists, of whom I am sure they will play a great role to finally understand this paradox called cancer.

Resumen

Las dietas desbalanceadas, como las que se encuentran en los países occidentales, basadas en altas proporciones de carbohidratos y lípidos, en particular el colesterol, contribuyen en gran medida a la enfermedad del hígado graso no alcohólico (NAFLD), incluida su forma progresiva de esteatohepatitis no alcohólica (NASH). Es por eso por lo que, la sobrecarga de lípidos es uno de los principales factores de riesgo en el inicio y la progresión del carcinoma hepatocelular (HCC), el principal cáncer de hígado primario que se asocia con una alta incidencia y mortalidad a nivel mundial.

Previamente, demostramos las propiedades de promoción de tumores hepáticos provocadas por el consumo de una dieta alta en colesterol en ratones. Los tumores generados presentaron un fenotipo agresivo, incluida la metástasis pulmonar, en comparación con los animales alimentados con una dieta balanceada. Estos resultados se asociarón fuertemente con daño al DNA mediado por estrés oxidativo, la falla en la activación de la principal maquinaria de la proteína reparadora del DNA y resistencia a la apoptosis. Los principales objetivos del presente trabajo fueron caracterizar la progresión del HCC con una etiología de NAFLD inducida por el consumo de dietas altas en lípidos, particularmente el aporte de colesterol e identificar el perfil de expresión génica asociado a esta característica particular. Por lo tanto, alimentamos a los animales hasta los 8 meses con una dieta tipo Western (altos en lípidos, colesterol y carbohidratos). Posteriormente, los ratones recibieron una dosis única de DEN para inducir la carcinogénesis hepática. Bajo la dieta tipo Western, los ratones presentaban signos de obesidad con aumento de peso y acumulación de grasa

visceral, junto con la presencia de daño hepático. Estos hallazgos concuerdan con los observados en humanos con una dieta occidental y en otros modelos de ratón bien caracterizados de NAFLD. El tratamiento conjunto con DEN indujo eficazmente una mayor generación de tumores hepáticos en comparación con los grupos CW/DEN, lo que sugiere claramente que la sobrecarga de lípidos actúa como un promotor tumoral. Uno de los componentes clave de la dieta occidental es el colesterol alto. Nosotros y otros hemos publicado que este lípido, además de las propiedades fundamentales bien reconocidas para la vida, muestra efectos nocivos cuando se acumula excesivamente en las células, particularmente como resultado de la disfunción mitocondrial y el deterioro de la transducción de señales al alterar la fluidez de la membrana celular. Cuando se acumula en el hígado, demostramos previamente que el colesterol aumenta definitivamente la carga tumoral y la agresividad. Sin embargo, los mecanismos moleculares exactos por los cuales el colesterol favorece el desarrollo de tumores aún no se conocen por completo. El análisis transcriptómico realizado por RNA-seq muestra una buena separación entre los grupos CW/DEN y HC/DEN, W/DEN. Un análisis de GSEA reveló un fenotipo inflamatorio notable, particularmente impulsado por la señalización de IL-6/STAT3, además de otras vías relacionadas con factores de crecimiento como HGF, incluidas las vías PI3K/AKT y ERK. Es muy interesante la abrogación de señales supresoras de tumores clave como p53, PTEN y la señalización de apoptosis en este modelo. Nuestro trabajo anterior identificó un notable efecto mecanicista inducido por la sobrecarga de colesterol en el hígado, incluida la regulación a la baja de las principales proteínas reparadoras del DNA, como ATM, ATR, CHK1 y 2 y p53. Mediante un análisis utilizando el software IPA, confirmó

este efecto en términos de vías de señalización controladas por p53. Desde principios de los años 2000, algunos informes señalaron la represión transcripcional de p53 por STAT3. La pérdida de función de p53 también se ha relacionado con la activación de STAT3 en el cáncer de páncreas. Nuestro trabajo publicado anteriormente informó que la sobrecarga de colesterol en el hígado de ratones alimentados con una dieta alta en colesterol durante 30 días presentó una activación notable de Stat3 y el incremento en la expresión de genes diana clave como Mcl-1. Está claro que el colesterol toma el control de estas vías de señalización relevantes en preparación para la promoción de tumores. Por el contrario, se ha observado que la desfosforilación de STAT3 podría estabilizar p53 y conducir a la apoptosis. De acuerdo con el análisis de RNA-seq, encontramos escasa supervivencia.

Las principales citocinas y factores de crecimiento asociados a la proliferación e inflamación (por ejemplo, IL-6, IL-17, HGF, VEGF-A, entre otros) estaban significativamente elevados en ratones en tratamiento con W/DEN. Inmunofluorescencias de F4/80 y CD206 corroboraron una significativa infiltración inflamatoria en los animales alimentadós con dietas altas en colesterol en comparación con CW/DEN tumoral, lo cúal identificamós una vez más a STAT3 como un factor clave en la inflamación de NASH y HCC.

La modulación de la respuesta inmune que promueve el reclutamiento y la activación de macrófagos ha sido reportada previamente en tumores criados bajo el consumo de dietas altas en lípidos/colesterol. El estrecho contacto de los macrófagos y las células tumorales se asocia a la polarización de los macrófagos tipo M2 aumentando la agresividad de los tumores. De acuerdo con estos hallazgos anteriores, observamos

una señal prominente de F4/80 y CD206 en dietas altas en lípidos, particularmente en la dieta occidental. Curiosamente, se ha observado que los macrófagos M2 podrían proporcionar colesterol a las células tumorales, creando una codependencia del colesterol entre estas células en el microambiente tumoral. La infiltración alta de macrófagos M2 se asocia con una supervivencia más pobre y un aumento en la recurrencia del cáncer. Además de una infiltración de macrófagos bien definida, también observamos un aumento en la respuesta proangiogénica, juzgado por el incremento en la expresión de VEGF-A y HGF, y confirmado por la detección deCD34, lo que apoya el fenotipo agresivo. En consecuencia, informamos que la firma de expresión regulada por HGF/c-Met se asoció con un incremento en la angiogénesis y fue capaz de definir un subtipo de HCC humano con mal pronóstico y fenotipo agresivo. Otra característica observada en esta firma fue la destacada descompensación de la lipogénesis y el estrés oxidativo. Por lo cual decidimos develar algunos de los mecanismos por lo cual HGF/c-Met regula el estado redox celular. Como se muestra en el Anexo II, Es bien sabido que la señalización mediada por el factor de crecimiento de hepatocitos (HGF) y su receptor c-Met en el hígado está involucrada en el control del estado redox celular y el estrés oxidativo, particularmente a través de su capacidad para inducir la expresión de genes hepatoprotectores activando vías de supervivencia. Se ha informado de que el HGF puede regular la expresión de algunos miembros de la familia de la NADPH oxidasa en las células hepáticas, en particular las subunidades catalíticas y $p22^{phox}$. Por lo que nos centramos en caracterizar el mecanismo de regulación de $p22^{phox}$ por HGF/c-Met en hepatocitos primarios de ratón como un determinante clave para la regulación redox celular. Los hepatocitos primarios de ratón

se trataron con HGF (50 ng/ml) durante diferentes tiempos. La expresión de *cyba* (gen que codifica p22phox) o el contenido de proteínas se abordaron mediante RT-PCR en tiempo real, Western blot o inmunofluorescencia. Las interacciones proteicas se exploraron mediante inmunoprecipitación y análisis FRET. Nuestros resultados proporcionaron información mecanicista que apoya la represión transcripcional de *cyba* inducida por HGF en un mecanismo dependiente de la actividad de NF-κB. Identificamos un mecanismo de regulación postraduccional dirigido por la degradación de p22phox por el proteasoma 26S, y un segundo mecanismo mediado por el secuestro de $p22^{phox}$ por c-Met en la membrana plasmática. Nuestros datos muestran claramente que HGF/c-Met ejerce la regulación de la NADPH oxidasa por una amplia gama de mecanismos moleculares. Las especies reactivas de oxígeno derivadas de la NADPH oxidasa reguladas por HGF/c-Met representan uno de los principales mecanismos de transducción de señales provocadas por este factor de crecimiento.

Para obtener una evidencia más mecanicista de la relevancia del desarrollo de tumores en hígados sobrecargados de lípidos, estudiamos otro grupo de ratones alimentados con una dieta alta en colesterol (carbohidratos y otros lípidos en contenido estándar). El análisis de expresión génica en este proceso tumorigénico identificó 194 genes expresados diferencialmente relacionados con CW/DEN. La comparación entre HC/DEN y W/DEN identificó 62 genes comúnmente regulados. Respaldando estos hallazgos, establecimos una genómica comparativa entre los tumores de ratones con alto colesterol y los HCC humanos, donde identificamos 62 genes compartidos por

W/DEN y HC/DEN, los culaes tienen relevancia clínica y se asocian con un mal pronóstico en los HCC humanos. Se necesitarán más investigaciones para establecer completamente la contribución de cada gen específico. Incluidos cuatro genes (*Slc41a3, Fabp5, Mthfd1l* e *Igdcc4*) con relevancia clínica en la carcinogénesis humana. Estos genes están elevados en las muestras de HCC y se asocian a una baja supervivencia de los pacientes. El gen *Slc41a3* está relacionado con la actividad del transportador transmembrana de cationes. Impulsa la salida de Mg^{2+} particularmente en las mitocondrias. Se ha informado que la sobreexpresión de *Slc41a3* en el cáncer puede ser utilizadó para el transporte de nutrientes y Mg^{2+} para satisfacer las necesidades de proliferación y metabolismo aberrante presente en las células de cancer. Como se ha dicho, las mitocondrias son quizás el organelo más relevante en la célula sobrecargada de colesterol. La sobreexpresión de este sistema transportador podría estar dirigida a compensar la pérdida de fluidez en las mitocondrias, mejorando la extrusión de Mg^{2+}. *Fabp5* codifica la proteína de unión a ácidos grasos 5 (Fabp5). Esta proteína se ha relacionado con el potencial maligno en varios cánceres, incluido el HCC. La tinción positiva de FABP5 en HCC se asocia con mal pronóstico, recurrencia, metástasis e invasión. FABP5 transporta lípidos intracelularmente con fines de almacenamiento, proporcionando bloques de construcción para la construcción de membranas y suministro de energía, ambos muy necesarios en las células en proliferación. *Igdcc4* para la proteína Nope. Es un marcador de células progenitoras, inicialmente identificado en el hígado fetal murino. Anteriormente se ha demostrado que Nope es un marcador confiable de HCC asociado a stemness. Si bien, Nope se detecta escasamente en hepatocitos adultos, el daño podría inducir la

expresión, particularmente en el daño colestásico que se asocia a cambios en la polarización de los hepatocitos. Se ha demostrado que la proteína Nope es un marcador bueno y confiable para el HCC en la clínica porque podría detectarse altamente en tumores AFP positivos y negativos. Mthfd1l, codificada por el gen *Mthfd1l* es una enzima del ciclo del folato. Está involucrado en la generación de formiatos, por lo tanto, en el metabolismo de compuestos monocarbonado, fundamental utilizados en la síntesis de purinas y en la síntesis de proteínas. Por tanto, esta enzima es muy relevante en los tejidos en proliferación, especialmente en el cáncer. La expresión de *Mthfd1l* se ha asociado con un mal pronóstico, sobre todo en el HCC. Nuestra firma genetica propuesta indica claramente una adaptación metabólica, comprometiendo la adaptación mitocondrial y la participación de los macrófagos, particularmente la polarización tipo M2 en un proceso inducido e impulsado por la sobrecarga de colesterol. En conclusión, el consumo de dietas enriquecidas con lípidos, en particular colesterol, podría favorecer el desarrollo de HCC con un fenotipo agresivo y de mal pronóstico.

Abstract

Unbalanced diets, such as those consumed in Western countries, based on high proportions of carbohydrates and lipids, notably cholesterol, greatly contribute to non-alcoholic fatty liver disease (NAFLD), including its progressive form of non-alcoholic steatohepatitis. alcoholic (NASH). Thus, lipid overload is one of the main risk factors for initiation and progression of hepatocellular carcinoma (HCC), the main primary liver cancer, which is associated with a high incidence and mortality worldwide. The present work aimed to characterize the development of HCC in mice fed a Western diet, including the identification of a gene expression signature that defines a subtype of liver cancer raised in a lipid-overloaded liver context. Mice subjected to Western diets with focusing greater interest in high cholesterol content presented a greater number of tumors, of which they present both macroscopically angiogenesis determined by inspection of the tumors and microscopically by detecting CD34, a classic angiogenesis marker. In the same way, it was identified that these tumors under a lipid-overload environment present infiltration characterized through the identification of macrophages, of which we can assume through the detection of specific markers that these myeloid cells present an M2 polarity (pro-tumor polarity). RNA-seq identified a specific gene expression signature that reflected the aforementioned phenotypes. On the other hand, it is noteworthy that four mouse-human orthologous genes of this transcriptomic signature were able to predict survival and prognostic outcome in transcriptional data from patients with HCC. These four genes (*Slc41a3, Fabp5, Mthfd1l* and *Igdcc4*) have clinical relevance in liver carcinogenesis. These genes are

overexpressed in HCC patients and are associated with poor survival. These four genes are widely implicated in metabolic and stem cells processes capacity. Metabolic reprogramming and stem cell capacity are some of the key characteristics of cancer. The transcriptomic signature proposed in this work clearly indicates a metabolic and stem adaptation committed to the adaptation of tumor cells in a process induced and driven by cholesterol overload. In conclusion, the consumption of diets enriched with lipids, in particular cholesterol, could favor the development of HCC with an aggressive phenotype and poor prognosis.

Dramatis Personae

NAFLD. Nonalcoholic fatty liver disease (NAFLD) is an umbrella term for a range of liver conditions affecting people who drink little to no alcohol. As the name implies, the main characteristic of NAFLD is too much fat stored in liver cells. NAFLD is increasingly common around the world, especially in Western nations.

NASH. Nonalcoholic steatohepatitis (NASH) is a liver disease that, until recently, has been underrecognized as a common cause of elevated liver enzymes. Although NASH is generally a benign disorder, it may be progressive, leading to HCC. This pathology is characterized by the accumulation of fat in the liver plus the presence of inflammatory infiltrate in the liver.

HCC. Hepatocellular carcinoma (HCC) is the most common type of primary liver cancer. Hepatocellular carcinoma occurs most often in people with chronic liver diseases, such NAFLD and NASH. The risk of hepatocellular carcinoma, the most common type of liver cancer, is higher in people with long-term liver diseases. It is also higher if the liver is scarred by an accumulation of fat in the liver.

Chapter 1

A historical overview

Non-Alcoholic Fatty Liver Disease (NAFLD) is the fastest growing chronic liver disease (Baffy, Brunt et al. 2012). Although, this condition and its inflammatory progressive form Non-Alcoholic steatohepatitis (NASH) are part of the natural history of liver diseases, it is well-known that changes in dietary behaviors are relevant in the initiation and progression of these lipid-overload conditions, providing an increase in the incidence of liver cancer (Figure 1).

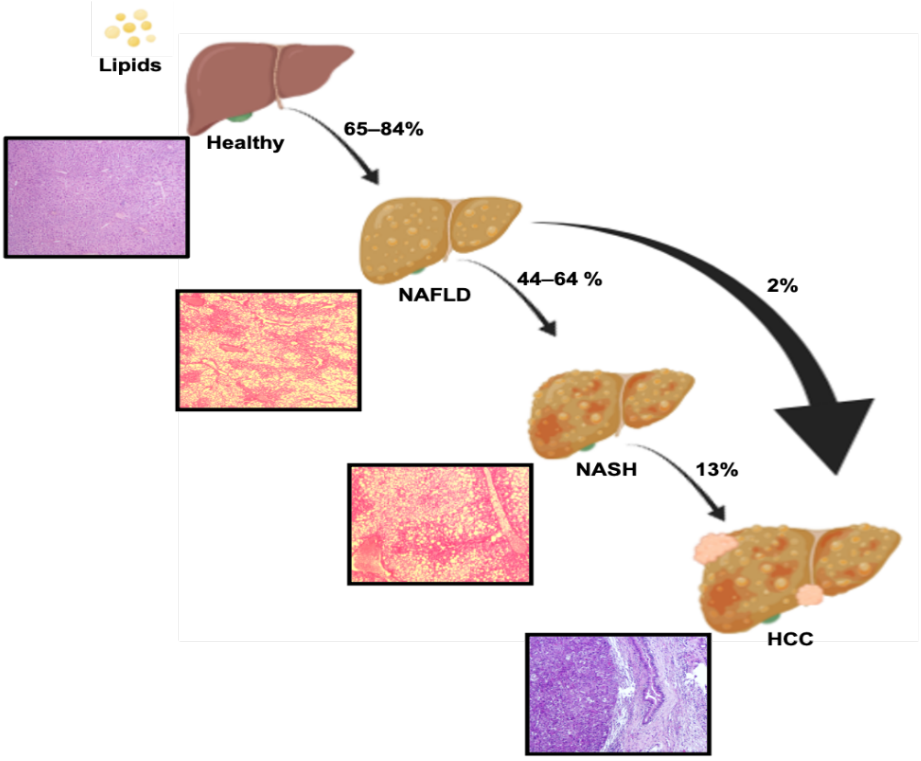


Figure 1. Natural history of liver disease.

The global prevalence of NAFLD is currently estimated in 24% (Younossi, Koenig et al. 2016). Accumulated evidence has suggested a significant association between NAFLD and liver cancer (Enriquez-Cortina, Bello-Monroy et al. 2017).

The first to describe the fatty liver was Dr. Addison in 1836. In 1838, the pathologist Rokitansky documented the accumulation of fat in the liver by autopsies and pointed out that this disorder possibly triggers cirrhosis in this organ. Bartholow in 1885, reported an association between obesity and fatty liver. Decades later, in 1938, Connor described fatty liver infiltration that could lead to the development of cirrhosis in diabetics. Later in 1958, Westwater and Feiner reported the histological findings of fatty infiltration of the liver in obese patients. In 1962, Thaler added an additional clinicopathological description of the disease. Since then, several reports from the 1950s and 1970s pathologically documented the occurrence of fatty liver disease in obese and diabetic subjects (Lonardo, Leoni et al. 2020).

In 1980s the term non-alcoholic steatohepatitis was coined by Dr. Ludwig team. They described the progressive form of fatty liver disease that histologically resembles alcoholic steatohepatitis, although it was observed in patients who denied having abused of alcohol. Most of the patients were obese women and many were diabetic (Armstrong and Marchesini 2019). Histopathological changes included lobular hepatitis, inflammatory infiltrates, Mallory bodies, and focal necrosis with evidence of fibrosis in most samples and cirrhosis in three patients. In 1983, Moran et al., extended these findings to obese children in whom steatohepatitis presented with abnormal activity of liver enzymes and unspecific symptoms (Lonardo, Leoni et al. 2020). There

is general consensus that a constellation of histologic features is required for the histopathologic identification of NASH in adults, including steatosis, ballooning, lobular inflammation, and perisinusoidal fibrosis. By contrast, there is no universal agreement among liver pathologists on the essential criteria for the diagnosis of NASH. Furthermore, compared to other histological features, such as fibrosis, the histological diagnosis of NASH shows great inter-observer and intra-observer variability and sampling error, which is reflected in the prevalence of NASH that varies widely, from 1.4% to 20% liver biopsies (Sanyal 2019). This unreliability of NASH assessment may also affect NASH trials, presenting patients who do not meet inclusion criteria, misclassify fibrosis subgroups, and attenuate the apparent effects of treatment. Future studies should identify reliable non-invasive tests for the prediction of NASH. In this context, a panel of international experts from 22 countries around the world recently proposed to abandon the simple and inaccurate dichotomous classification into "NASH" versus "non-NASH" (Bugianesi, Marzocchi et al. 2004). Interestingly, steatosis may not persist during the progression of NAFLD, and rather may disappear in advanced cases of NAFLD-cirrhosis (Lonardo, Leoni et al. 2020). This can blur the distinction between cryptogenic cirrhosis and NAFLD burn cirrhosis. Unfortunately, this group of patients is often excluded from clinical trials as they lack the key criterion of 'presence of steatosis' (Sanyal 2019).

So, NAFLD reflects a progressive condition in many instances and its prevalence parallels trends in obesity and diabetes. Based on the initial observations of (Marchesini, Suppini et al. 2005), numerous studies from the past 20 years have clearly

illustrated that NAFLD is a metabolic disease representing the hepatic manifestation of a systemic metabolic disorder.

Chapter 2

Non-alcoholic fatty liver disease

NAFLD is becoming the first cause of chronic liver disease in Western countries (Figure 2). This liver disease begins with the excessive accumulation of lipids in the liver tissue, which generates a simple steatosis (Figure 3). Hepatic steatosis develops due to increased lipogenesis or the uptake of lipids from the circulation, which triggers a saturation in the oxidation and elimination capacity of these lipids in the organ (Massoud and Charlton 2018).

As mentioned, NAFLD is characterized by the accumulation of different types of lipids (i.e. triglyceride and cholesterol) in the liver. Particularly, cholesterol overload represents one of the key insults in the organ (Calvisi, Wang et al. 2011), and it has been associated to HCC development as previously proved by our group and others (Enriquez-Cortina, Bello-Monroy et al. 2017, Liu, Wong et al. 2018).

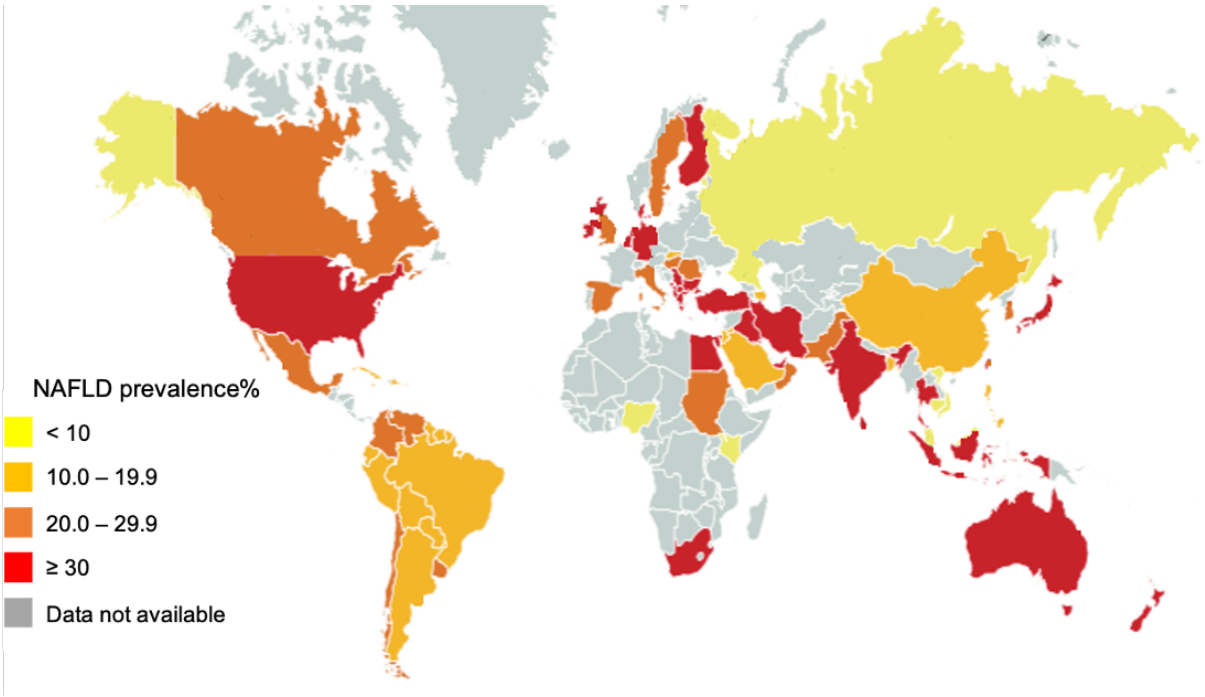


Figure 2. Prevalence of Nonalcoholic fatty liver disease (Zabair Younossi, et. al., 2017)

NAFLD encompasses a wide spectrum of histological severities, from asymptomatic hepatic steatosis to HCC (Che, Paliogiannis et al. 2019). Most patients with NAFLD have simple steatosis, defined by hepatic steatosis in the absence of substantial inflammation or fibrosis. Approximately 10 to 30% of NAFLD patients develop NASH, which is characterized by varying degrees of inflammation and liver fibrosis, in addition to hepatic steatosis. Therefore, NASH is a highly significant histological diagnosis because it can progress to liver failure and HCC in a variable proportion of patients, particulary in those people with other risk factors that could promote the initiation of cellular transformation, such as alcohol consumption, virus infection, drug abuse or the intake of lipid-enriched diets (Massoud and Charlton 2018).

In Western countries, cholesterol represents one of the main lipids consumed in regular diet (Garcia-Ruiz, Conde de la Rosa et al. 2020). It is not fully understood the cholesterol role in the development of NAFLD and its progression to NASH and subsequently to HCC (Sun and Karin 2012).

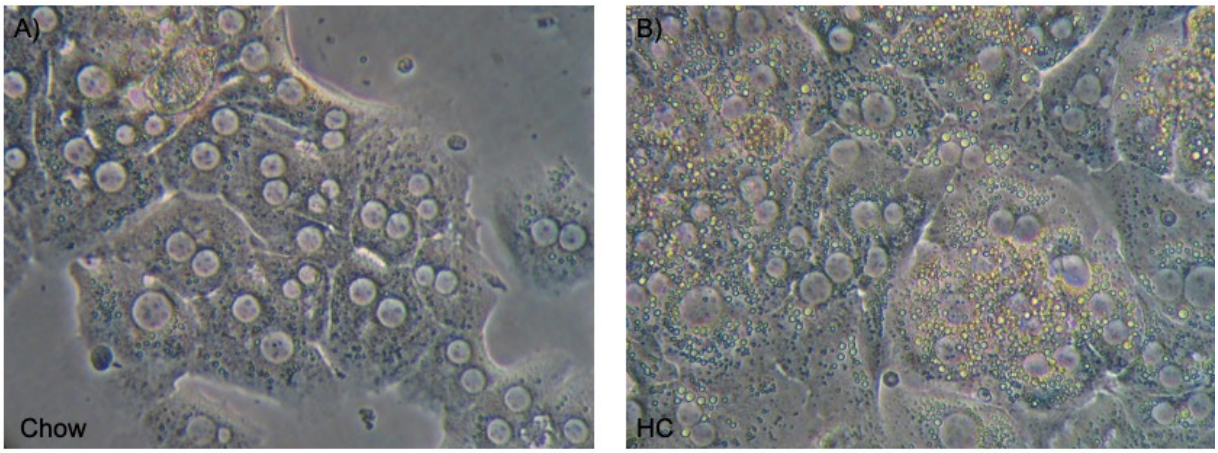


Figure 3. Primary mouse hepatocytes isolated from animals fed A) with a balanced Chow diet and B) with a cholesterol-enriched diet (2% cholesterol), where an excess of lipid drops can be identified.

We have observed a remarkable increment in lipids in hepatocytes from mice fed with a high cholesterol diet (2% cholesterol), indicating that the consumption of this lipid also induces the increment of triglycerides affecting the entire cell (Figure 3). Some studies have reported that cholesterol can affect different cellular organelles, such as the mitochondria, where it is seen that the increase of this lipid in the mitochondrial membranes affects their fluidity (Dominguez-Perez, Simoni-Nieves et al. 2019) and therefore the respiratory chain is affected as a consequence (Garcia-Ruiz, Conde de la Rosa et al. 2020). Another adverse effect of this, is the sequestration of cytochrome C within the mitochondria even in the face of apoptotic signals mediated by said

cytochrome C (Ribas, Garcia-Ruiz et al. 2016). In addition, endoplasmatic reticulum is target of cholesterol presence as previously reported (Maxfield and van Meer 2010). Plasma membrane is also affected since an excessive accumulation of cholesterol in the membrane affects its fluidity and consequently the lipid rafts and the signaling associated to these subdomains of plasma membrane are remarkable impaired. (Goossens, Rodriguez-Vita et al. 2019). Just some references of the remarkable impact of cholesterol overload in the liver tissu have been cited. It is clear that this lipid exerts significant effects in the cell, permitting a variety of adaptations facoring cellular transformation (Enriquez-Cortina, Bello-Monroy et al. 2017, Dominguez-Perez, Simoni-Nieves et al. 2019). The consumption of dietary cholesterol induces DNA oxidative damage, failure of main DNA repair enzymes, and apoptosis resistance (Enriquez-Cortina, Bello-Monroy et al. 2017), these effects strongly conduct to cancer initiation.

Chapter 3

Hepatocellular Carcinoma

Epidemiology

As stated, the HCC is one of the major outcomes of the chronic NAFLD or NASH. HCC is the most common primary liver malignancy, and the fifth and ninth in male and female respectively, cause cancer-related death, and the incidence worldwide according the International Agency for Research on Cancer of World Health Organization (WHO, https://gco.iarc.fr/today/home) (Figure 4). HCC is expected to increase during the next 10-20 years (Cronin, Lake et al. 2018). HCC patients have a highly variable clinical course. The prognostic variability of individuals with HCC supports the notion that HCC comprises several biologically distinct subtypes (Lee, Heo et al. 2006). Compared with viral or alcoholic hepatitis, NAFLD is becoming the major etiology of HCC, compared with hepatropic virus infection or alcoholic liver disease, based on the rising prevalence of obesity on a global scale, and especially in Western countries (Figure 2) (Younes and Bugianesi 2018).

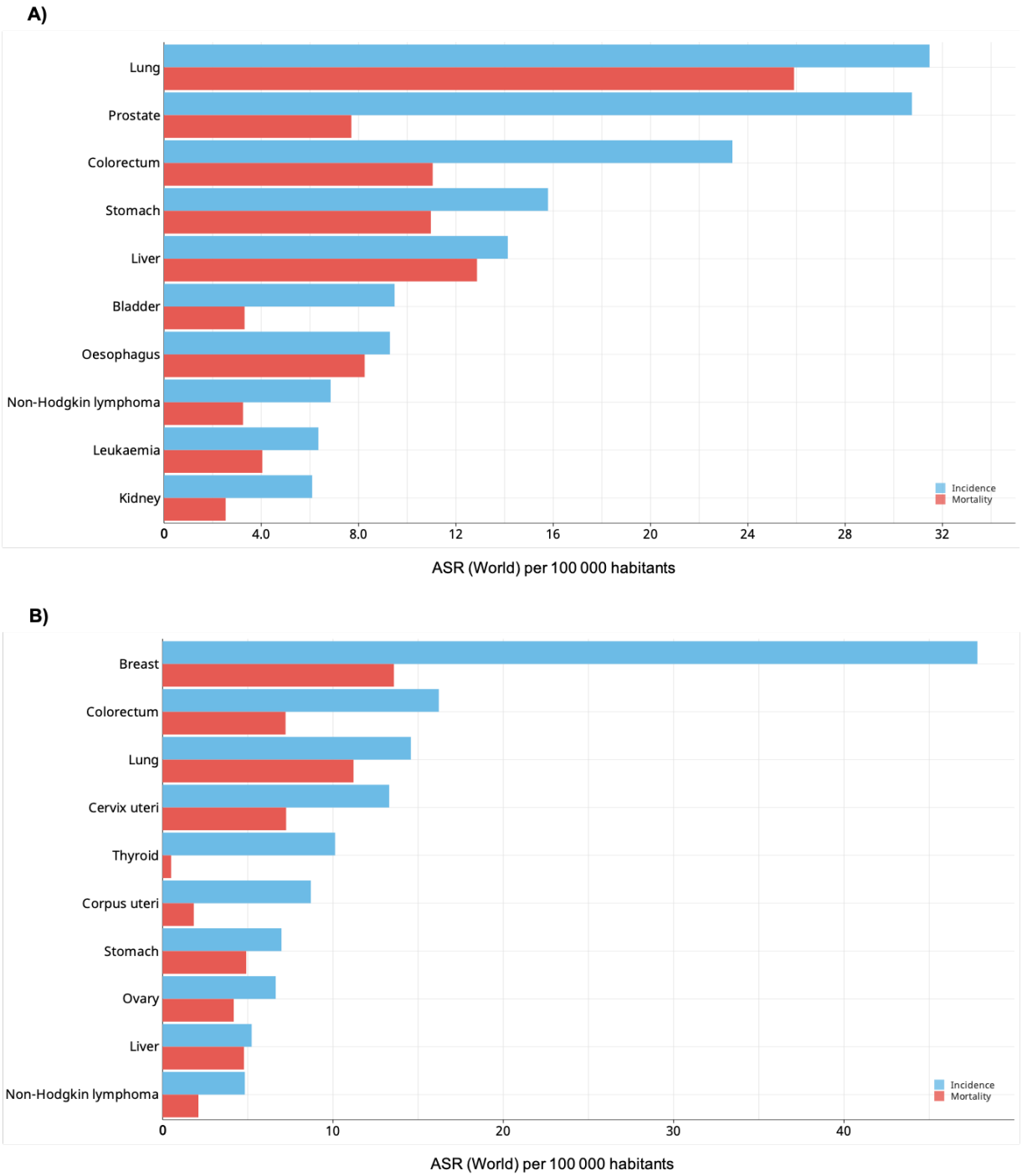


Figure 4. Estimated incidence and mortality world rates 2020 in A) males and B) females. World Health Organization, International Agency for Research on Cancer (https://gco.iarc.fr/today/home).

A large-scale epidemiological study revealed that the obesity is risk factor for HCC (Bhaskaran, Douglas et al. 2014). Moreover, despite the ongoing tendency of cancer declining, the incidence of metabolic syndrome and obesity are widely spreading (Sun and Karin 2012) conditioning the crement of NAFLD- and NASH-related HCC (Figure 5). Consequently, an effective molecular understanding for HCC/NAFLD and HCC/NASH is urgently required. Most patients with NAFLD remain asymptomatic and about 20%-25% progress to develop a more-severe, chronic hepatic inflammatory disease or NASH, and eventually HCC (Sun and Karin 2012). HCC not only develops in the cirrhotic liver, but it can also arise in the non-cirrhotic liver in NASH (Stickel and Hellerbrand 2010). The molecular events involved in NASH progression and development of HCC are not fully understood (Massoud and Charlton 2018). So, more research is required to gain knowledge regarding this particular condition, whichs, as stated, is increasing worldwide.

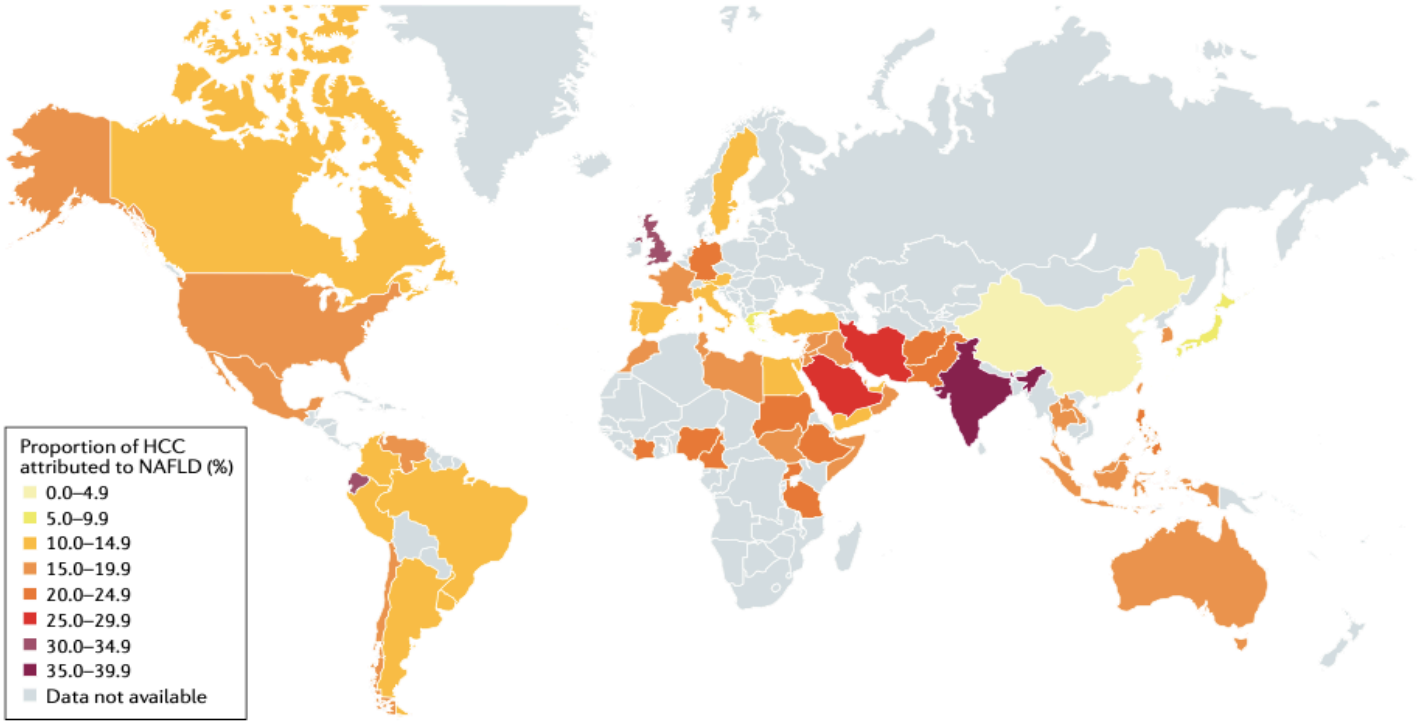


Figure 5. The estimated proportion of HCC attributed to NAFLD (Huang, El-Serag et al. 2020)

The Biology of HCC and cholesterol

HCC is one of the most common cancers due to its association with NAFLD and NASH. HCC cells exhibit significant metabolic changes and are under anabolic pressure for the synthesis lipids to maintain dysregulated cell proliferation (Calvisi, Wang et al. 2011). Cholesterol is fundamental for life. It is precursor of many hormones, and bile salts, which are necessary for a proper digestion. It is a central component of lipid rafts,

so changes in cholesterol levels seriously affects signaling, especially in growth factors or cytokines receptors (Xu, Rychnovsky et al. 2005).

Liver cancer cells tend to accumulate more cholesterol, particularly in organelles, including adapting response to compensate the noxious effects. But cholesterol is not a bad molecule at all. Cholesterol is an important regulator of cell function and plays key roles in the physiological processes. In plasma membrane it is involved in signal transduction, cellullar transport, energy conversion, cell surface recognition, survival and cell differentiation. Therefore, changes in the cholesterol content induce plasma membrane disturbance influecing the structure and fuction.

Cholesterol, is composed of four fused carbon rings, is found alongside phospholipids on the inside of the membrane. Membrane proteins can extend partially within the plasma membrane, cross it completely, or be attached to its inner or outer face. Cholesterol plays relevant roles in the plasma membrane as well as in endo-membranes since it alters the fluidity and the functions of these membranes. In the plasma membrane and other intracellular membranes, cholesterol accumulates in specialized structures known by various names, such as lipid rafts, detergent-resistant membrane domains (DRM), and detergent-soluble glycolipid-enriched complexes (DIG). Lipid rafts appear to serve a number of functions, including intracellular transport and sorting of molecules, down-regulation and recycling of receptors, and targeted export of proteins and lipids. Cells largely satisfy their need for cholesterol through the novo synthesis of acetyl-CoA, and this demand is particularly critical for cancer cells to maintain dysregulated cell proliferation.

It is useful to understand how the concept of the lipid microdomain could explain the phenomenon of signal transmission by proteins anchored to it. It is now well established that proteins anchored to lipid rafts are found together with a number of other signal transduction molecules. According to the postulates of Freeman and Solomon, small, isolated rafts join to form substantially larger rafts (think: island). It is likely that the isolated rafts fuse through the intervention of excess cholesterol present in the cancer cells, which would be reflected in an over-activated signal transduction and this allows the cancer cells to have greater adaptation to their environment.

The cholesterol content of the Western diet is 10-fold higher than Mediterranean geographical zone (Younossi, Koenig et al. 2016). A high cholesterol diet causes accumulation of lipids in the hepatocytes due to it is key component of lipoproteins for exportation (Maxfield and van Meer 2010). Multiple mechanisms may be intervening in the creation of a favorable environment for the formation of tumors in HCC related to NAFLD (Massoud and Charlton 2018). Cholesterol induces liver damage mainly through mitochondrial dysfunction. The accumulation of cholesterol in the mitochondria has diverse cellular implications. One of them is the decrease in the mitochondrial import of GSH, which generates a cellular redox imbalance (Dominguez-Perez, Simoni-Nieves et al. 2019). Previous reports show ROS generation due to cholesterol accumulation in mouse liver increasing DNA oxidation, which causes a faster carcinogenesis process (Enriquez-Cortina, Bello-Monroy et al. 2017).

Similarly, it has been reported that the excess of mitochondrial cholesterol prevents the release of cytochrome C, an important component in the formation of the apoptosome (Mari, Caballero et al. 2006); on the other hand, cholesterol induces the over

expression of antiapototic proteins, such as Mcl-1, which is transcriptionally regulated by the Signal Transducer and Activator Transcription 3 (STAT3) signaling pathway (Dominguez-Perez, Simoni-Nieves et al. 2019).

NAFLD is characterized by a low-grade chronic inflammatory response, which is a risk factor for HCC. When adipose tissue expands it promotes the release of proinflammatory cytokines that can activate pro-oncogenic pathways such as that involving STAT3 (Stickel and Hellerbrand 2010). STAT3 has been highly reported to promotes tumor growth and immune evasion. STAT3 aberrant activation has been found in differents solid tumors, such as bladder, bone, breast, liver, among other. STAT3 activation is correlated with poor prognosis in most of these cancer types. Activated STAT3 prevent p53-mediated growth control allowing tumor progression. STAT3 also induces the expression of vascular endothelial growth factor (VEGF). This stimulates angiogenesis, facilitating invasiveness and/or metastasis. One of the canonical stimulators of the STAT3 signaling pathway is IL-6, which in addition, is a master regulator of inflammation and tumor growth.

Translational oncology and personalized medicine.

Transcriptomics is a system biology-based strategy to decode the behavior of genome expression to determine biological function and gene interaction. The advantage of a transcriptional approach to translational oncology is the improved ability to predict drug

response more accurately and provide information on complex clinical problems. The central hypothesis is that applying a transcriptional approach will be the key to understanding many diseases, such as primary liver cancers, and to future clinical success. It is imperative for future success that these methodologies are adapted to clinical trial designs and practice, particularly in drug-resistant cancers. Transcriptomics is a very useful tool for the generation of gene expression signatures relevant for the diagnostic or therapeutic classification of patients with HCC, it began almost a decade ago and has been extensively reviewed. This strategy has allowed the HCC to be stratified according to the identification of transcriptional signatures, based on different key parameters for liver cancer. Relevant genes in patient survival; Poor and Good prognosis (Lee, Chu et al. 2004), cellular origin of the liver tumor, hepatoblasts or hepatocytes (Lee, Heo et al. 2006), presence or absence of receptor tyrosine kinase (RTK) signaling; c-MET / HGF and TGF-β2 (Coulouarn, Gomez-Quiroz et al. 2006, Kaposi-Novak, Lee et al. 2006). In particular, the application of functional and comparative genomics has advanced greatly in our understanding of HCC and have led to the identification of several relevant genes within the landscape of molecular alterations in HCC. Despite these great efforts, the clinical translation of these findings for everyday medical practice remains to be demonstrated.

Chapter 4

Research Proposal

Justification

Currently, there are a few systematic and wide spectrum studies (physiological, clinical, transcriptomic and molecular) that allow the identification of the differential effect of lipids in the carcinogenic process and the promotion of liver tumors. The study will allow to have the information about genes and signaling routes involved in the processes that will be used to have a molecular panel for the study in patients that will allow a personalized approach. In this lies the difference with what is known in the topic, particularly in terms of the effect of cholesterol.

Research question

Will the consumption of a high cholesterol diet define a liver tumor subtype with greater aggressiveness and a poor prognosis?

Hypothesis

The differential lipid overload in the liver, allows a heterogenous tumor progression, displaying transcriptome alterations, leading to a more aggressiveness tumors.

Objective

- **Main objective**

To determine the differential gene expression profile of NAFLD/NASH-related HCC with emphasis on cholesterol overload.

- **Specific objectives**
    - To determine cellular and physiological parameters of liver tumors induced by the consumption of lipid-enriched diets in mice.
    - To evaluate the transcriptomic differences by RNA-sequencing between tumor tissue from mice subjected to a high cholesterol (HC) diet and a Western diet.
    - To perform the comparative transcriptomic analysis between orthologous genes expression of tumors from mice under different hihg lipid diets, and human HCC.
    - To stablish a gene signature that defines a subtype of HCC raised in the liver with lipid overload to gain prognostic value in patients.

Chapter 5

Experimental Design

Animal model. Sixty-four 14 days-old male mice (strain C57BL/6J) were randomly separated in six groups according to table 1. Briefly, these groups include 1) mice fed with regular chow diet (CW, Purina #5001, PharmaServ, Framingham, MA, USA); 2) mice fed with chow diet and injected with a single dose of *N*-nitrosodiethylamine (DEN, 10 µg/Kg, i.p. Sigma Aldrich, St Louis MO, USA) (CW/DEN); 3) mice fed with western diet (W, catalog #D12089, Research Diets Inc. New Brunswick, USA); 4) mice fed with western diet and injected with a single dose of DEN (W/DEN); 5) mice fed with a high cholesterol diet (HC, 1% cholesterol, #611638, Dyets Inc. Bethlehem, PA, USA); and 6) mice fed with HC diet and injected with a single dose of DEN (HC/DEN). Animals received diet and water *ad libitum*. After 8 months mice were euthanized under Avertin (2-2-2 tribromoethanol) anesthesia. Liver weight was documented, liver tissue, and serum were collected for subsequent analysis (Figure 6) (Enriquez-Cortina, Bello-Monroy et al. 2017). All animals were maintained in specific pathogen-free housing and cared in accordance with the NIH Guide for Care and Use of Laboratory Animals and Universidad Autonoma Metropolitana guidelines for the use of animals.

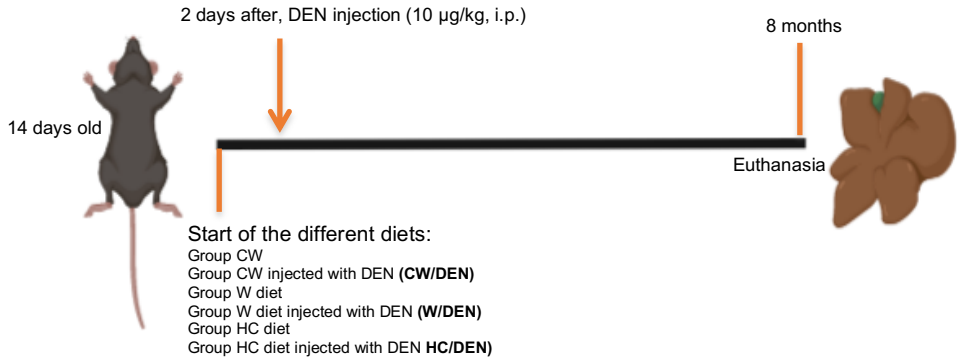


Figure 6. Experimental design overview.

Diet	DEN single dose (10 ug/kg, ip)	Group ID
Regular Chow Diet	-	CW
Regular Chow Diet	+	CW/DEN
Western Diet	-	W
Western Diet	+	W/DEN
High cholesterol 1%	-	HC
High cholesterol 1%	+	HC/DEN

Table 1. Mice groups under different diets and treatments.

Methods

Histology. Microscopic inspection was evaluated by routine Hematoxylin & Eosin (H&E) staining. Fibrosis was assessed by Sirius Red staining as previously reported (Gomez-Quiroz, Seo et al. 2016). Steatohepatitis was defined by the presence of steatosis, inflammation and hepatocellular ballooning (Sanches, Ramalho et al. 2015), as per the FLIP algorithm (Imhof and Aurrand-Lions 2006). The severity of steatosis, lobular inflammation and hepatocellular ballooning were scored using the NASH-Clinical Research Network (CRN) criteria (Lee, Alloosh et al. 2009). Specifically, the amount of steatosis (percentage of hepatocytes containing fat droplets) was scored as 0 (<5%), 1 (5–33%), 2 (>33–66%) and 3 (>66%). Hepatocyte ballooning was classified as 0 (none), 1 (few) or 2 (many cells/prominent ballooning). Foci of lobular inflammation were scored as 0 (no foci), 1 (<2 foci per 200× field), 2 (2–4 foci per 200× field) and 3 (>4 foci per 200× field). The NAFLD activity score (NAS) was computed from the grade of steatosis, inflammation and ballooning (Asgharpour, Cazanave et al. 2016). Paraffin sections of human liver tissue (NASH and HCC patients) were generously provided by Dr. Linda Muñoz-Espinosa, University Hospital, UANL.

Cholesterol determination. Total cholesterol was determined as previously reported (Dominguez-Perez, Simoni-Nieves et al. 2019). Briefly, 10 mg of liver was saponified with alcoholic KOH in a 60ºC heating block for 30 min. After the mixture had cooled, 3 ml of hexane and 600 µl of distilled water were added and shaken to ensure complete mixing. Appropriate aliquots of the hexane layer were evaporated under nitrogen with vacuum (Speed Vac, Savant, Cranbury, NJ) and used for cholesterol measurement with O-phthalaldehyde dissolved in acetic acid (0.5 mg/ml), at 550 nm.

Serum biochemical determination. Blood samples were obtained from the retro-orbital sinus under Avertin anesthesia. Serum total cholesterol, triglycerides, ALT and AST activities were determined by using an automated analyzer for clinical chemistry (SpotChem EZ, ARKRAY, USA Clinical Diagnostics).

RNA extraction, quantification and integrity. Total RNA was extracted using the QIAGEN RNeasy miniKit (Qiagen GMBH, Hilden, Germany) following the manufacturer´s instructions. RNA quantity and purity were estimated using a Nanodrop 2000 Spectrophotometer (Nanodrop Technologies, Wilmington, DE), and integrity was assessed by Agilent 2100 Bioanalyzer (Agilent, Palo Alto, CA)

RNA sequencing. RNA sequencing was performed using Illumina HiSeq4000 and deposited at the Bio-project database (ID: PRJDB10804). Raw reads were filtered by adapter sequences, contamination and low-quality reads. The reads were then mapped with mouse genome reference (GRCm38.p6) using HISAT2 (hisat2-2.0.2-beta) followed by read summarization with featuresCounts (subread-1.5.0-p1). All data

analysis was performed using R programing language and related packages. The output matrix from featureCounts was input into Bioconductor DESeq2 for differential expression analysis with a False Discovery Rate (FDR) of 0.5, and p-value of 0.001 and a log fold change from -1.5 to 1.5. Significance testing was performed using Wald Test statistics. To visualize the data Heatmaps and Principal Components Analysis (PCA) were performance. All plots were generated using the MADE4 package (Castven, Becker et al. 2019).

Enrichment analysis. Gene Set Enrichment analysis (GSEA) was performed using GSEA software provided by Broad Institutes (http://software.broadinstitute.org/gsea/index.jsp). Gene sets from the MSigDB database were tested and gene sets with NOM P-value <0.05 and FDR <0.25 were considered significantly enriched in a priori defined set of genes. We used ingenuity pathway analysis (IPA, Ingenuity Systems, Inc. Redwood City, CA) to investigate the biological pathways and networks associated with model genes using the whole dataset. Genes with their log2-fold change were used as input. We considered disease, biological functions, and upstream regulators to be significant if the absolute value of their activation z-score is > 1.5. The z-score reflects the match between the observed gene expression and the predicted relationship direction. It is used to infer activation states of called functions and regulators (Castven, Becker et al. 2019).

Immunofluorescence. Tissue was either fixed in 4% formaldehyde and preserved in Tissue Tek for cryosections and cut in 3-5 μm sections. Subsequently, these were washed with PBS-tween for 5 min. The specific antibodies (Table 3.) were diluted in

PBS with 0.1% horse serum and incubated overnight at 4 ° C in a humid chamber. The tissues were washed again with PBS, incubated with DAPI for 5 min. Finally, slides were examined using the Carl Zeiss LSM 780 NLO confocal microscope (Carl Zeiss, Inc., USA).

Real-time RT-PCR. After DNase digestion with a DNA-free kit (Ambion Inc.), 500 ng (tissue) and 100 ng (cells) total RNA was reverse transcribed in 20 µl reaction volume with a SuperScript first-strand synthesis kit according to the manufacturer's instructions (Invitrogen Corp.). Real-time quantitative PCR analysis was performed with a CFX96 Touch (Bio-Rad) thermal cycler in a 96-well reaction plate. The 10 µl PCR reaction mix contained 5 µl 2X SYBR Green PCR Master Mix (Bio-Rad), 200 nM of each primer, and 1 µl cDNA template. Reactions were incubated for 10 min at 95°C followed by 40 cycles of 30 sec at 95°C and 60 sec at specific primer temperature. Melting analysis of the PCR products was also conducted to validate the amplification of the specific product. The expression level of mouse rs18 was used as internal reference. Relative gene expression levels were calculated with the 2-ΔΔCT method (Kaposi-Novak, Lee et al. 2006). Primer sequences are listed in Table 2.

Gene name	Ensembl ID	Primer sequence
Ccl2	ENSMUSG00000035385	5´-CCCAATGAGTAGGCTGGAGA-3´ (20)
		5´-TCTGGACCCATTCCTTCTTG-3´ (20)
Cd24	ENSMUSG00000047139	5´-GCTCCTACCCACGCAGATTT-3´ (20)
		5´-TGGTGGTAGCGTTACTTGGA-3´ (20)

Prom1	ENSMUSG00000029086	5′-GAAAAGTTGCTCTGCGAACC-3′ (20)
		5′-TCTCAAGCTGAAAAGCAGCA-3′ (20)
Cd44	ENSMUSG00000005087	5′-TGGATCCGAATTAGCTGGAC-3′ (20)
		5′-AGCTTTTTCTTCTGCCCACA-3′ (20)
Col3α1	ENSMUSG00000026043	5′-GTGTCAAAGGTGAACGTGGC-3′ (20)
		5′-ATCCCAGCAATCCCAAGTGG-3′ (20)
Ccl25	ENSMUSG00000023235	5′-TCTTTGAGGACTGCTGCCTG-3′ (20)
		5′-CGTGTTGTGGTGGAGCTTTG-3′ (20)
Socs3	ENSMUST00000054002	5′-AGCTCCAAAAGCGAGTACCA-3′ (20)
		5′-TGACGCTCAACGTGAAGAAG-3′ (20)
Slc41a3	ENSMUST00000032177	5′-AACAGCCAGACCTTTGTGGTGC-3′ (20)
		5′-GATGCAGTGGTTGTCAGGATCC-3′ (20)
Fabp5	ENSMUST00000029046	5′-GGTGCATTGGTTCAGCATCAGG-3′ (20)
		5′-TCATAGATCCGAGTACAGGTGAC-3′ (20)
Igdcc4	ENSMUST00000035499	5′-CGCACACCTGAATGTCAACTCC-3′ (20)
		5′-CGTGGATGTCTCCAGTCAAGTG-3′ (20)
Mthfd1l	ENSMUST00000043735	5′-GCCATGGATGCCTTAAGTTC-3′ (20)
		5′-AGCCAGGTAAACGAGTGAGC-3′ (20)
Cd36	ENSMUST00000082367	5′-CCTTAAAGGAATCCCCGTGT-3′ (20)
		5′-TGCATTTGCCAATGTCTAGC-3′ (20)
Hmgcs1	ENSMUST00000179869	5′-TTTGATGCAGCTGTTTGAGG-3′ (20)
		5′-CCACCTGTAGGTCTGGCATT-3′ (20)
Abcg8	ENSMUST00000045714	5′-CCTGATCCGTCGTCAGATTT-3′ (20)
		5′-CCATGGCCGTAGTAAAGGAA-3′ (20)
Abcg5	ENSMUST00000066175	5′-CGTCCAGAACAACACGCTAA-3′ (20)
		5′-GCAGCATCTGCCACTTATGA-3′ (20)
Hif1α	ENSMUST00000021530	5′-TCAAGTCAGCAACGTGGAAG-3′ (20)
		5′-TATCGAGGCTGTGTCGACTG-3′ (20)

Rps18	ENST00000414228	5´-TGTGGTGTTGAGGAAAGCAG-3´ (20)
		5´-TCCCATCCTTCACATCCTTC-3´ (20)

Table 2. Primers used in the study

Mouse serum MultiPlex measurements. Cytokines and growth factors were measured in mouse sera using the MOUSE ANGIOGENESIS / GROWTH FACTOR (EGF, FGF-2, Follistatin, HGF, VEGF-A, G-CSF, IL-1β, Il-6, IL-17 and TNF-α) MAGNETIC BEAD PANEL bead assay (EMD Millipore Corporation, Billerica, USA) and a MAGPIX instrument using Luminex xMAP Technology. The analysis was performed according to the manufacturer's instructions.

Data mining. The RNA-seq data level 3 (Counts files) of 371 patients with HCC, and 50 samples of normal liver, were retrieved from The Cancer Genome Atlas (TCGA) database (https://portal.gdc.cancer.gov/) up to January 28, 2018. And 101 microarray data from LEC (Laboratory of Experimental Carcinogenesis) was use. The parameters for the differential expression analysis were FDR equal to 0.5, p-value <0.001 and log fold change from -1.5 to 1.5. And clustering analysis was done using Cluster 3.0 and TreeView 1.6 using uncentered correlation and average linkage options. Integration of genomic data was conducted as previously described using publicly available gene expression data sets downloaded from GEO (Lee, Heo et al. 2006).

Survival analysis. For survival analysis, expression data were categorized using a z-score cutoff of 0. Kaplan–Meier method using the log-rank test was used to estimate

survival curves (Lee, Chu et al. 2004).

Western blot. The Western blot was performed as previously reported (Gerardo-Ramirez, Lazzarini-Lechuga et al. 2019). PVDF membrane (Bio-Rad, USA) was used with the antibodies described in Table 3. The membranes were exposed using Super Signal West Pico Chemiluminescent (Pierce Biotechnology, USA) and observed using a Gel Logic 1500 (Kodak, Rochester, NY, USA). The bands were quantified by densitometry, using the Gel logic 1500 imagine system software.

Antibody	Brand	Catalog number	Dilution
CD34	Abcam	ab81289	1:1000
F4/80	Abcam	ab60343	1:1000
CD206	Santa Cruz	sc-376232	1:250
p-STAT3	Cell Signaling	9134S	1:1000
STAT3	Santa Cruz	sc-483	1:250
Mcl-1	Santa Cruz	Sc74436	1:250
Socs3	Abcam	Ab16030	1:1000
Actin	Sigma Aldrich	A2066	1:10000

Table 3. Antibodies used in the study.

HCC cells lines. Huh7, Hep3B, HepG2, PLC-PRF5 and THLE-3 cell lines were obtained from the American Type Culture Collection (ATCC, Manassas, VA, USA). Cells were cultured in William's medium supplemented with 10% fetal bovine serum (FBS, Hy-Clone, Logan, UT, USA), 100 U/ml ampicillin and 100 µg/ml streptomycin (Thermo Fisher Scientific, Waltham, MA, USA). Cells were maintained at 37°C in a 5%

CO_2 and 90% humidity atmosphere. Cells were plated in plastic culture bottles (Sigma-Aldrich, Saint Louis, MO, USA). All cell lines were mycoplasma free. All experiments were carried out by triplicate in the logarithmic phase of growth.

Cell proliferation and migration. Cell proliferation was addressed by CCK-8 kit (Dojindo Lab, Kumamoto, Japan), following manufacturer's instructions. 5 X 10^3 PLC.PRF5 and HepG2 cells were seeded in 96 well plate. The cultures were supplemented every 24 h with complex cholesterol-cyclodextrin (160 ug/ml) and only cyclodextrin (10 mM). For migration assay HepG2 were grown to 100 % confluence. Cells were maintained in culture medium over night before scratching, and then treatments with cholesterol (160 µg/ml), were supplemented every 24 h. For each condition, at least 3 pictures were taken with an inverted microscope (Carl Zeiss Axiovert 40 CFL) at 0, 24, 48 and 72 h. The wound area was calculated by Fiji Software (ImageJ).

Statical analysis. Each animal and cell experiments were performed at least by triplicate using cells of at least ± 3 different passages. Data are reported as the average ± standard error (SEM). Pearson's correlation analysis was used to assess the correlation between expression of Slc41a3, Fabp5, lgdcc4, mthfd1l and total cholesterol content in human liver cancer cell lines. For the comparison of means of different groups, an analysis of variance (ANOVA) was used, followed by multiple comparisons by the Tukey test. The Prism software was used. The level of significance will be $p \leq 0.05$.

Chapter 6

Results

High lipids diets induce weight gain, liver damage and tumor promotion

Mice fed Western and cholesterol diets for eight months, presented body weight gain (Figures 7A and B), as a consequence of increased visceral fat deposition (Figure 7A, white arrows), comparing with CW fed animals. Increased liver weight was also observed (Figure 7C), but the liver to body weight ratio was unchanged (data not shown) as a result of the obesity observed in animals under this lipid-enriched diet. The phenotype was closely associated to significant increment in AST and ALT serum activities (Figure 8D) in mice under Western diet, indicating that hepatocellular damage persists at eight months of treatment. Interestingly, HC/DEN group did not change AST and ALT values at eight months. No significant difference in liver damage tests was observed in animals treated or not with DEN, but changes were remarkable comparing with animals fed with the regular CW diet.

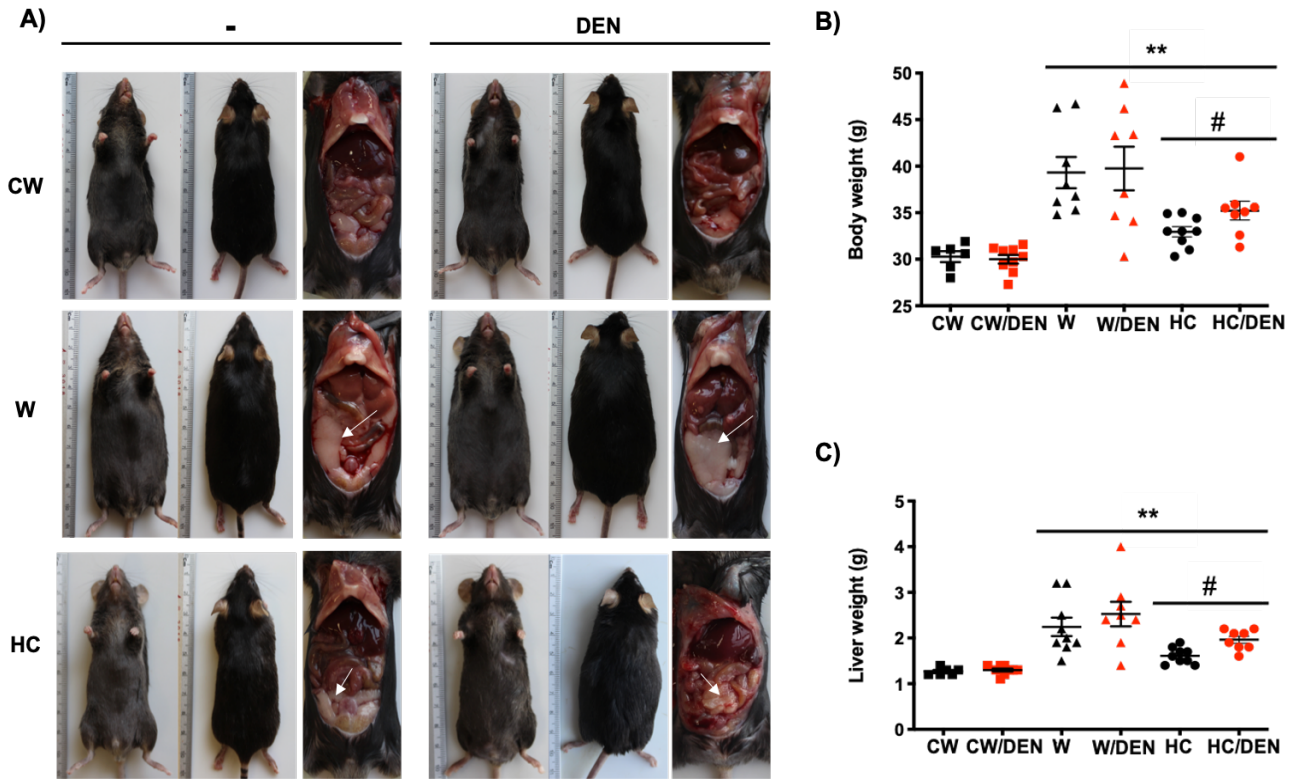


Figure 7. High lipid diets induce weight gain and liver damage in mice. 14 days-old male mice were fed for 8 months with western and high cholesterol diets as stated in Material and Methods. A) Mice under the W and HC diets presented obesity. white arrows show adipose tissue. Representative images of at least eight animals per group. B) body weight, C) liver weight of mice under different diets. Each graph plots the individual data points, the superimpose horizontal line indicates the arithmetic mean and error bars showing ± SEM. ** $p<0.01$ vs CW groups; # $p<0.01$ vs W groups.

In agreement with detected the liver damage, we found the macroscopic changes associated with steatosis including the characteristic yellowish color was observed in the livers, particularly in those under Western diet (Figure 8A) comparing with CW fed animals. Liver lipid overload was biochemically corroborated by testing total cholesterol and triglycerides. Consistently, all experimental groups exhibited increased values of both of lipids (cholesterol and triglycerides) regarding to CW fed mice (Figure 8E).

Next, we proceeded to identified tumors in livers from DEN treated mice. The number of tumors in W/DEN and HC/DEN mice were higher (23.3 ± 10.3 and 9 ± 1.9 tumors, respectively) than in CW/DEN mice (2.7 ± 0.2 tumors) (Figure 8C), suggesting synchronous development of several independent tumors, which is a well-defined characteristic in HCC (Schlageter, Terracciano et al. 2014). Protruding tumors were observed in W/DEN livers (Figure 8A, arrow), comparing with CW/DEN livers, where some pedunculated tumors were identified (Figure 8A, arrowhead), while HC/DEN animals showed the characteristic HCC protruding tumors. In addition, W/DEN tumors exhibited evident increased vascularity (Figure 8B yellow arrow), a distinctive feature of aggressive HCC (Kaposi-Novak, Lee et al. 2006).

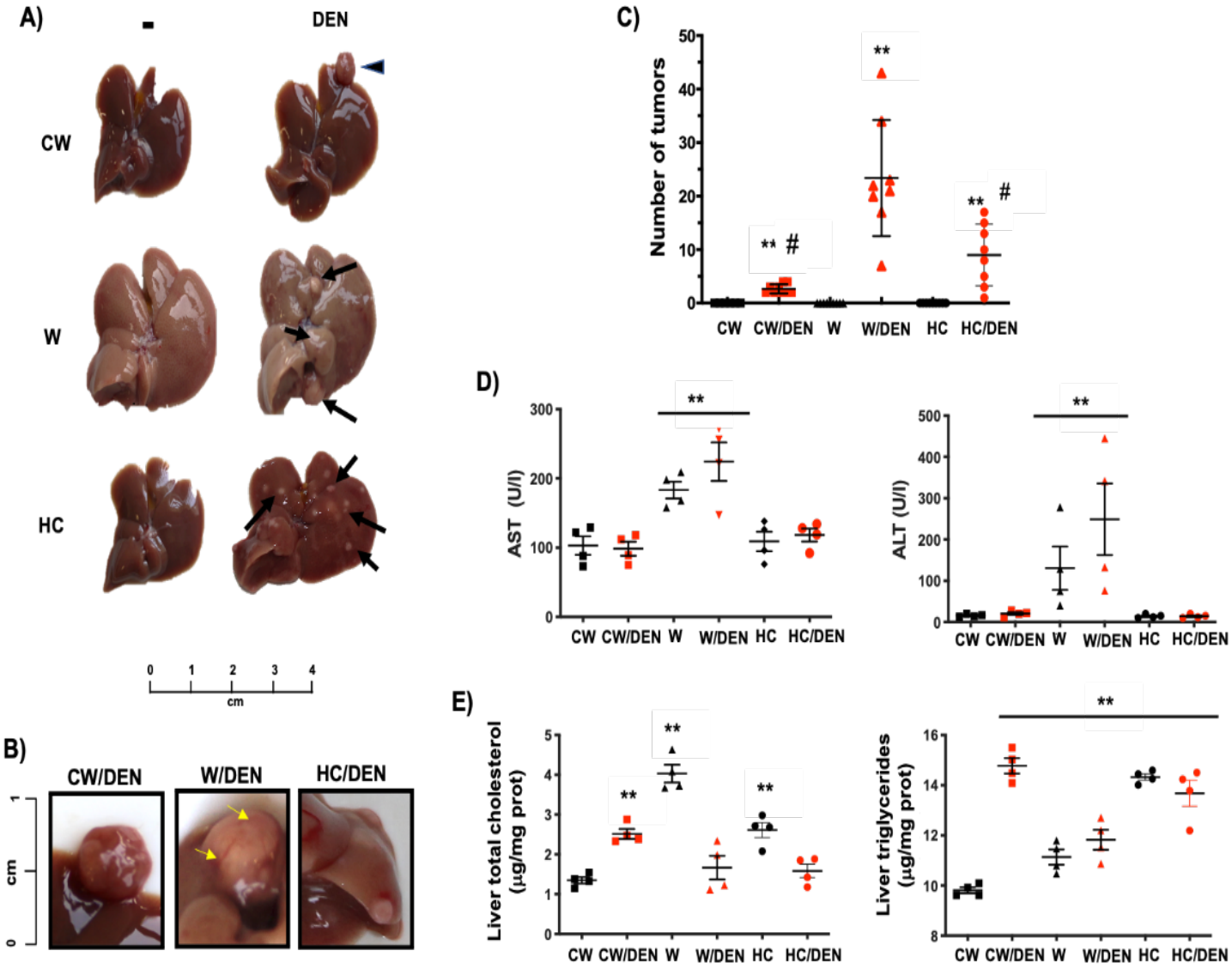


Figure 8. The consumption of a lipid-enriched diets induce lipid liver overload and hepatic tumors. A) Gross inspection of the livers from mice fed with the different diets and treated or not with DEN. Arrows and arrowshead show tumors. B) Tumor gross inspection of mice under different diets. Representative image of at least eight livers, yellow arrows show vascularity. C) Number of tumors in livers from different groups of mice. D) Liver damage addressed by serum activity of aspartate aminotransferase (AST) and alanine aminotransferase (ALT). E) Liver cholesterol and triglycerides content. Each graph plots the individual data points, the superimpose horizontal line indicates the arithmetic mean and error bars showing ± SEM. ** p<0.01 vs CW groups; # p<0.01 vs W groups.

Histological analysis by H&E staining revealed discrete borders and irregular wide trabeculae (>3 cells) in W/DEN tumors. Animals fed with a Western diet presented massive steatosis disrupting normal architecture. Consistently, steatosis (micro and macrovesicular) was most pronounced in surrounding tissue (ST) areas, while lipid content in tumor (T) zones was only marginal and replaced by increased lobular inflammation. Same pattern was also identified in HC/DEN, but the microvesicular steatosis predominated (Figure 9A). Interestingly, liver tissues from NASH and NASH derived HCC patients exhibited a similar histological presentation in comparison with the animal models (Figure 9B). Quantification of the histological findings revealed significant values of steatosis, inflammation and NAFLD activity score in all animals groups comparing with CW control mice (Figure 9C).

Western diet induced mild fibrosis particularly in pericentral zones, but animals in W/DEN group exhibited both pericentral and perisinusoidal zones with bridging fibrosis (Figure 9D) in comparison with HC/DEN and CW/DEN.

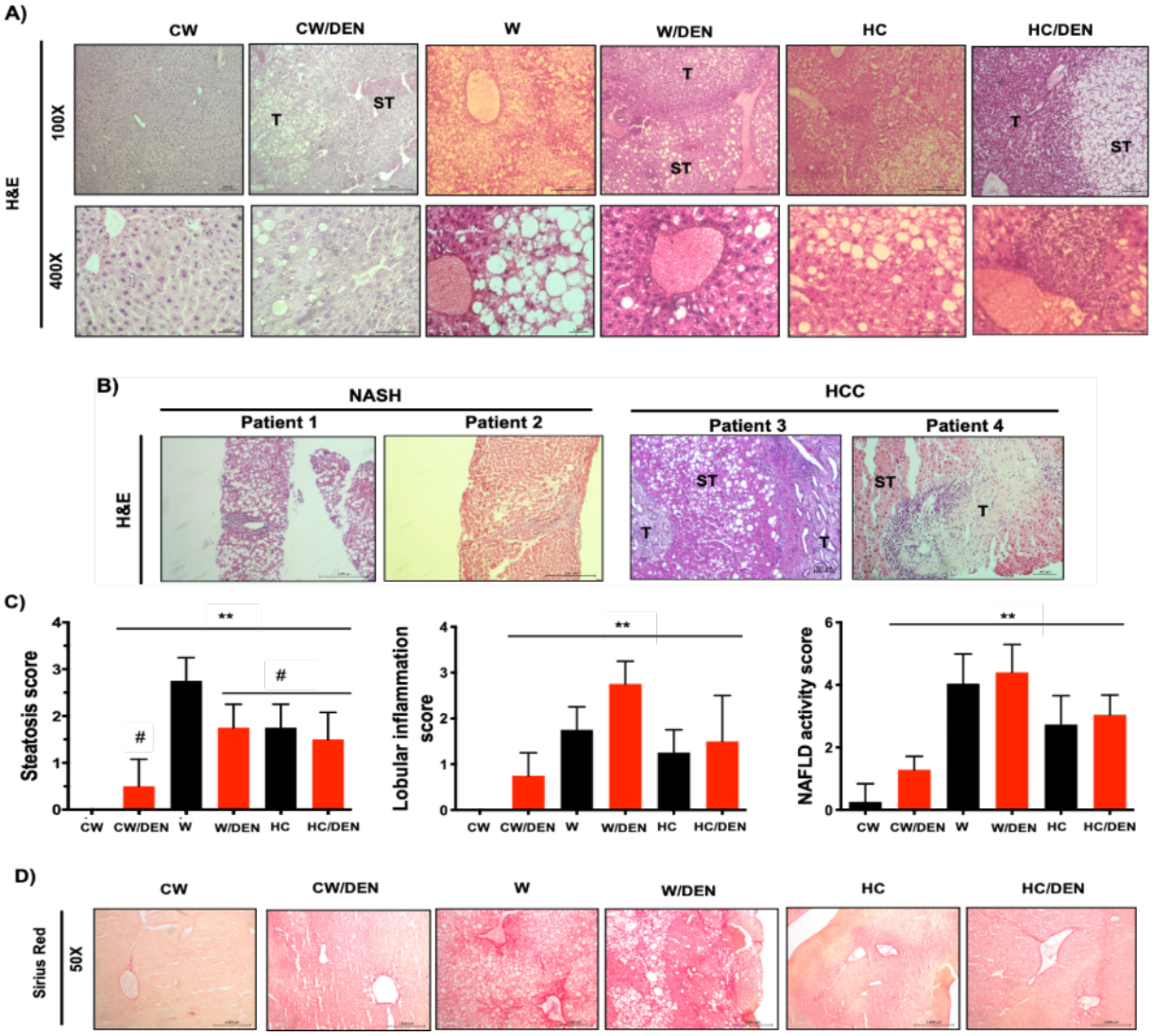


Figure 9. Lost of normal liver architecture. A) mouse and, B) human liver tissue histology assessed by routine H&E. T, tumor; ST, surrounding tissue. C) histological scores. D) Fibrosis determined by Sirius red staining. Each image is representative of at least three animals. Each bar is the mean ± SEM. ** $p<0.01$ vs CW group; # $p<0.05$ vs W diet alone group.

Transcriptional profile of tumors from lipid overloaded livers

To identify the transcriptional alterations in tumors under Western and HC diets consumption, we performed RNA sequencing. Differential expressed genes (DEG) between W/DEN and HC/DEN versus CW/DEN group. The analysis highlighted 671 DEG in W/DEN; and 194 DEG in HC/DEN (adjusted p value below 0.01 and a threshold of 1.5-fold change). In the case of W/DEN analysis we found 217 down-regulated genes and 454 up-regulated genes, and in HC/DEN we found 74 genes significantly down-regulated, and 120 genes were up-regulated when comparing with CW/DEN.

These genes were highly efficient in separating the tumors developed under the high lipids diets versus chow regular diet (Figure 10A and B). To corroborate RNA-sequencing data, we performed real-time RT-PCR to analyze the expression of eight randomly selected genes in samples not included in the RNA-seq, as technical and biological validation, respectively (Figure 10E). For all tested genes, real-time RT-PCR results recapitulate RNA-seq data.

Ingenuity Pathway Analysis (IPA, Figure 10C) of the W/DEN and HC/DEN signatures showed that the dominant functional network up-regulated was involved in IL-6/Stat3 pathway (*Bcl2, Cish, Socs2, Ntrk2, Pdgfb, Csf2rb*), cell cycle/Myc (*Bcl2, Pak1, Rapgef4, App*) and PI3K/Akt signaling *Bcl2, Bcl2l1, Ccnd1, Cdkn1a*). Notably, key tumor-suppressive pathways were down regulated such as p53 (*Bcl2, Bcl2l1, Ccnd1, Cdkn1a*), PTEN (*Ikbke, Itga2, Itga4, Ntrk2*), and apoptosis (*Bcl2, Bcl2l1, Capn11, Capn8*). The involvement of STAT3 and p53 networks (Figure 10D) suggests an aggressive phenotype in tumors generated in a lipid-overloaded environment.

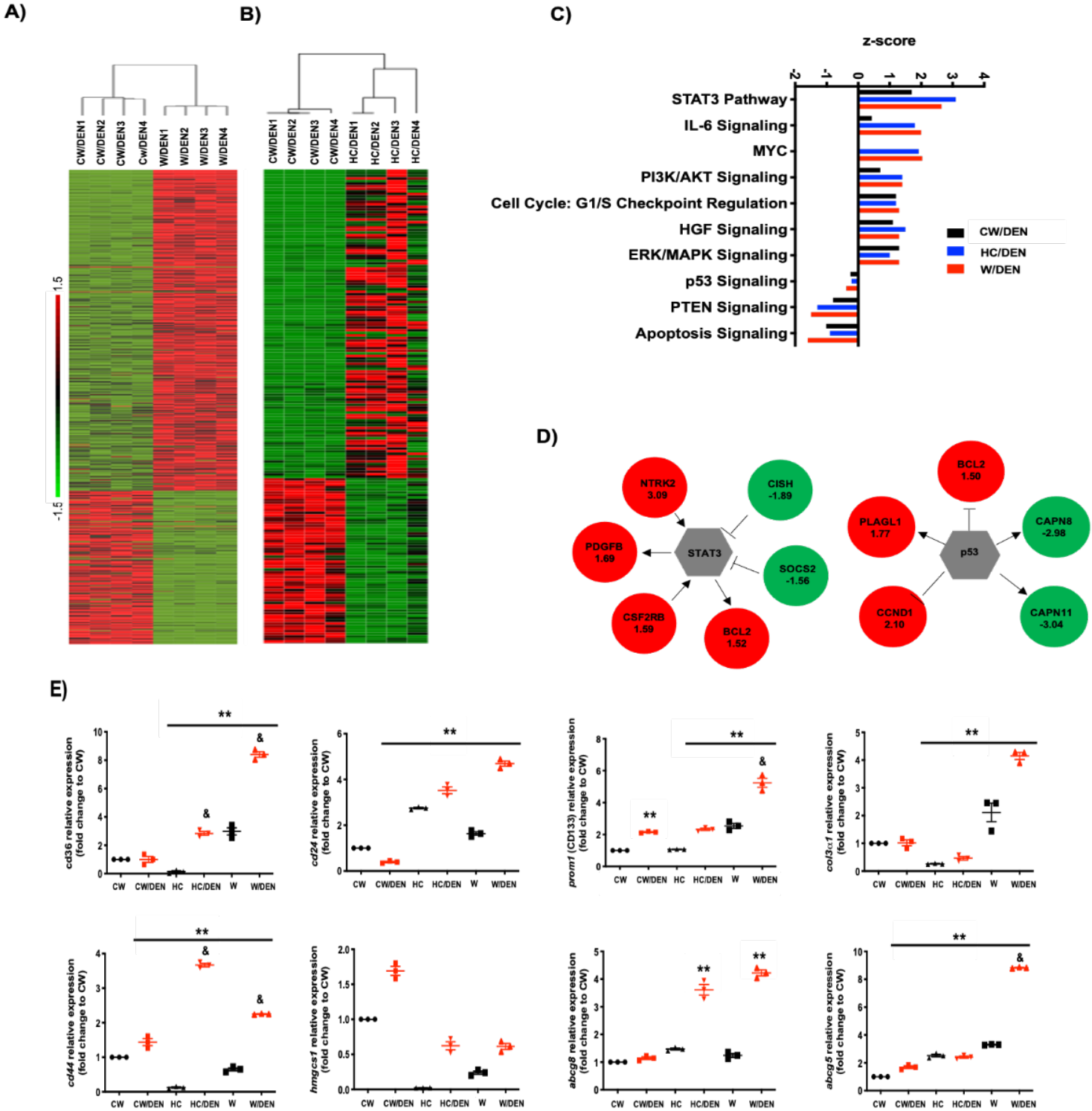
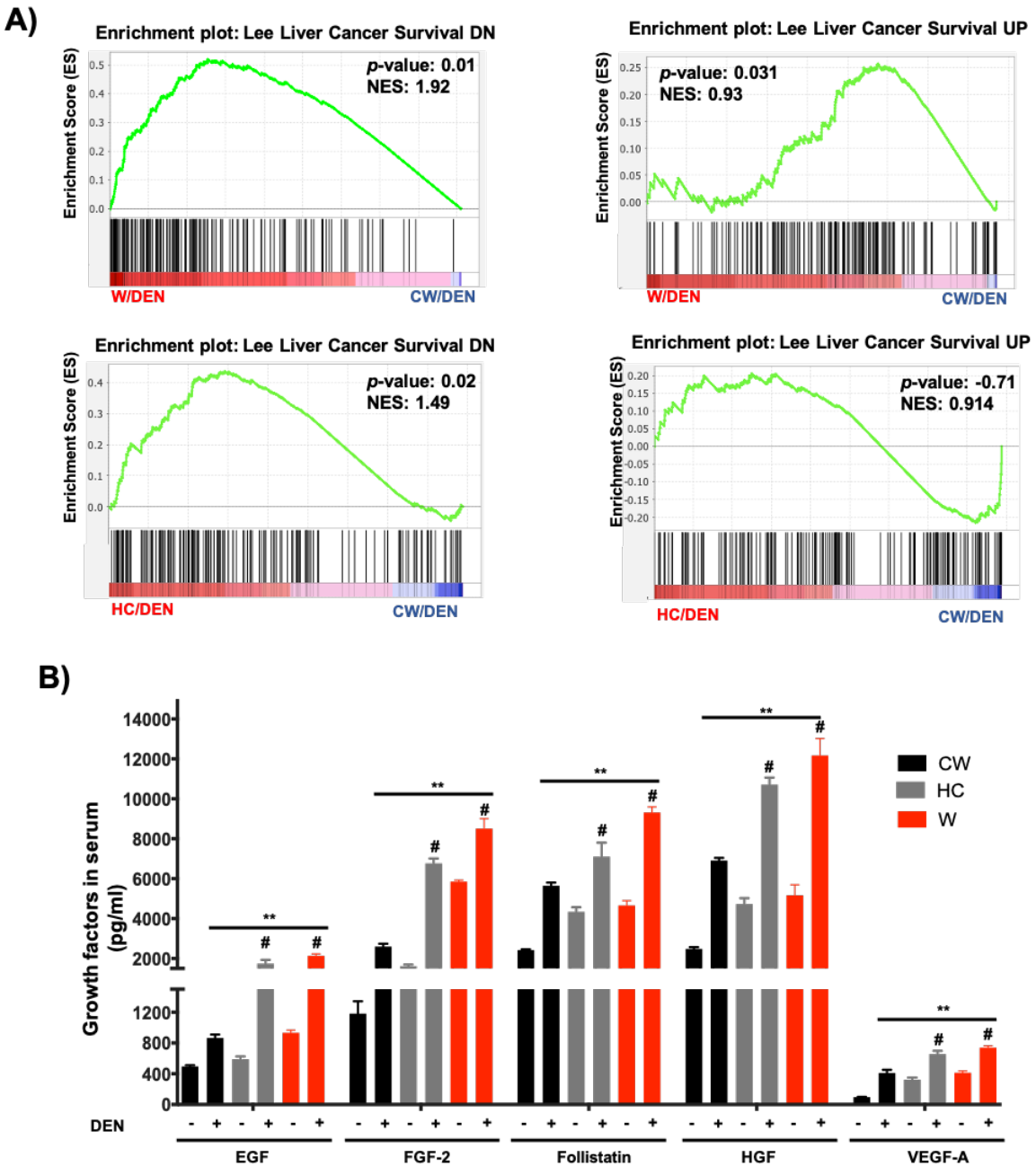

A)
B)
C)
D)
E)
CW/DEN1
CW/DEN2
CW/DEN3
Cw/DEN4
W/DEN1
W/DEN2
W/DEN3
W/DEN4
HC/DEN1
HC/DEN2
HC/DEN3
HC/DEN4
1.5
-1.5
z-score
STAT3 Pathway
IL-6 Signaling
MYC
PI3K/AKT Signaling
Cell Cycle: G1/S Checkpoint Regulation
HGF Signaling
ERK/MAPK Signaling
p53 Signaling
PTEN Signaling
Apoptosis Signaling
CW/DEN
HC/DEN
W/DEN
NTRK2 3.09
CISH -1.89
PDGFB 1.69
STAT3
SOCS2 -1.56
CSF2RB 1.59
BCL2 1.52
BCL2 1.50
PLAGL1 1.77
p53
CAPN8 -2.98
CCND1 2.10
CAPN11 -3.04
cd36 relative expression (fold change to CW)
cd24 relative expression (fold change to CW)
prom1 (CD133) relative expression (fold change to CW)
col3α1 relative expression (fold change to CW)
cd44 relative expression (fold change to CW)
hmgcs1 relative expression (fold change to CW)
abcg8 relative expression (fold change to CW)
abcg5 relative expression (fold change to CW)
CW
CW/DEN
HC
HC/DEN
W
W/DEN

Figure 10. Tumors from high lipids diets exhibit a profound change in gene expression favoring survival and proliferation signaling pathways and decreasing key tumor suppressor routes. Tumor tissues from CW/DEN, W/DEN, HC/DEN were subjected to RNA-sequencing as stated in Material and Methods. A) Heatmaps showing the good separation of A) W/DEN tumors vs CW/DEN and B) HC/DEN tumors vs CW/DEN red and green colors indicate high and low gene expression respectively. C) Process networks analysis in tumors from CW/DEN (black), high cholesterol HC/DEN, (blue) and W/DEN (red). The top rank ordered processes and networks are based on statistical significance ($p<0.01$). D) More representative signalling pathways. E) Expression of eight randomly selected genes in samples not included in the RNA-seq, as technical and biological validation. Each graph plots the individual data points, the superimpose horizontal line indicates the arithmetic mean and error bars showing ± SEM. ** $p<0.01$ vs CW group; & $p<0.05$ vs diet control.

Supporting this hypothesis, gene set enrichment analysis (GSEA) identified an abundance of genes involved in poor prognosis in animals fed with W and HC diets. Accordingly, Lee Liver Cancer Survival DN gene set was significantly enriched in CW/DEN whereas Liver Cancer Survival UP (Lee, Chu et al. 2004) gene set was enriched in W/DEN and HC/DEN tumors indicating worst prognosis in W/DEN and HC/DEN groups compared to CW/DEN (Figure 11A). To corroborate these findings, we performed an immunoassay (MultiPlex) to address the serum content of different growth factors and cytokines associated to unfavorable prognosis in HCC such as EGF, FGF-2, Follistatin, HGF and VEGF-A (Kaposi-Novak, Lee et al. 2006, Tomoda, Nouso et al. 2013, Coleman, Grose et al. 2014, Liu, Chen et al. 2018). An increment in the expression of these soluble factors was observed in the serum of W/DEN and HC/DEN mice comparing with CW/DEN mice (Figure 11B). Interestingly, most of the increased growth factors are related to survival and angiogenesis. To confirm the importance of angiogenesis we assayed the content of CD34, a canonical marker of angiogenesis, highlighted a strong content in W/DEN tumor samples comparing with CW/DEN. No signal was detected in the other groups. Activation of angiogenesis was further corroborated by GSEA demonstrating a significant enrichment of an angiogenesis

related gene set in the expression profiles of tumors derived from W/DEN mice (Figure 11C).



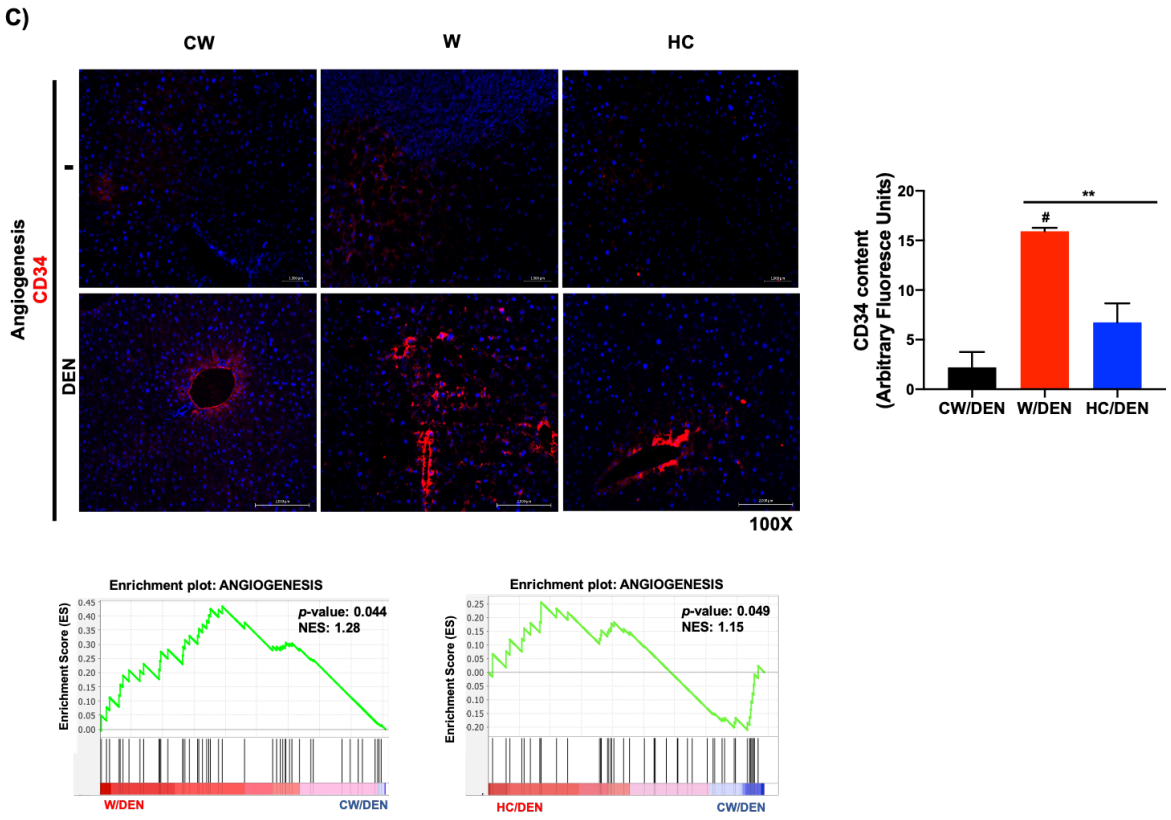


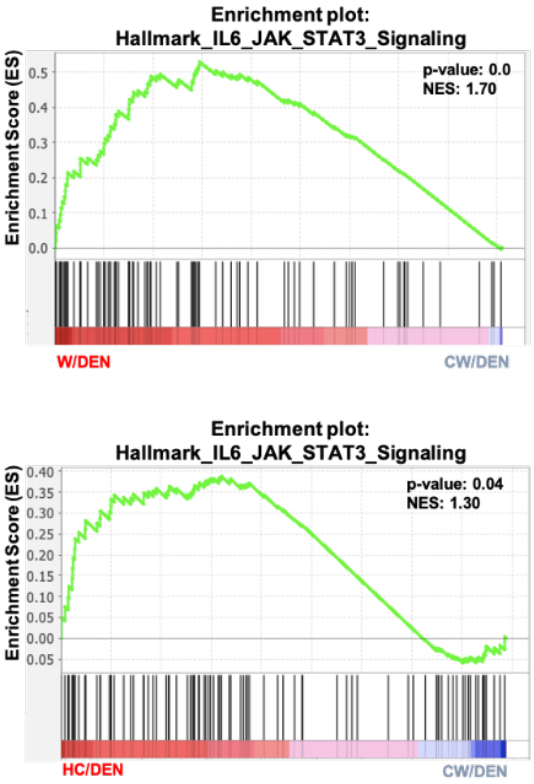
Figure 11. Tumors from high lipids diets exhibit a more aggressive phenotype. A) Gene set enrichment analysis (GSEA) of liver cancer survival (down and up regulated) data sets comparing tumors from W/DEN and HC/DEN to CW/DEN. B) Growth factors serum concentration of all mice groups. Proteins were determined by based multiplex immunoassay. Each bar represents the average ± SEM ** $p<0.01$ vs CW group; # $p<0.05$ vs W diet alone group. C) Angiogenesis judged by immunofluorescence of CD34, representative images of three animals. Original magnification, 100X. Quantification of CD34 fluorescence and GSEA of angiogenesis, data set comparing W/DEN and HC/DEN to CW/DEN

Inflammation present in liver tumors associated to cholesterol consumption

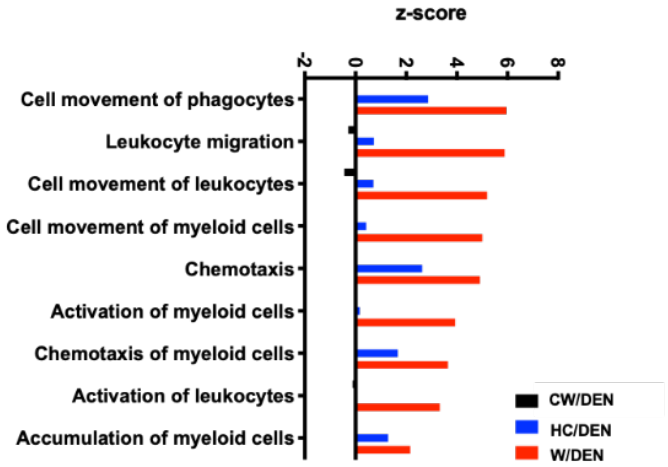
To corroborate the involvement of STAT3 signaling pathway in the phenotype of NAFLD associated HCC in mice, GSEA was performed using the Hallmark_IL6_JAK_STAT3_Signaling gene set (Rebouissou, Amessou et al. 2009). This specific signature was significantly enriched in the expression profiles of tumors derived from mice under high lipids diets, suggesting an activation of the IL6/STAT3 pathway (Figure 12A). STAT3 is a well-known key driver of inflammation. Accordingly, IPA revealed a clear disorder in inflammatory processes in the experimental animal groups judged by the top signaling pathways activated (Figure 12B).

This hypothesis was further confirmed by evaluating Stat3 activation. Western blot analysis demonstrated that tumors developed under steatogenic diets (Western diet or HC diet) presented an increment in Stat3 phosphorylation (Ser 727), which is in agreement with the content of Mcl-1, an antiapoptotic protein highly reported in aggressive tumors and a transcriptional target of Stat3 (Sieghart, Losert et al. 2006) (Figure 12C). To corroborate this hypothesis, macrophage infiltration was evaluated by both F4/80 and the specific M2-macrophages marker CD206 in mouse tissue from experimental groups (Figure 12D). As expected, a massive M2 macrophages infiltration was observed in tumors developed in mice under steatogenic diets (Western diet or HC diet), comparing with liver tissue under diet alone (i.e. without DEN) or in CW/DEN group, which presented a slight positive staining, particular at pericentral vein zone. Further supporting the inflammatory phenotype in animals under the steatogenic diet, a multiplex analysis of the main pro-inflammatory mediators demonstrated an increment in the expression of G-CSF, IL6, IL1β, IL17, and TNF-α (Figure 12E).

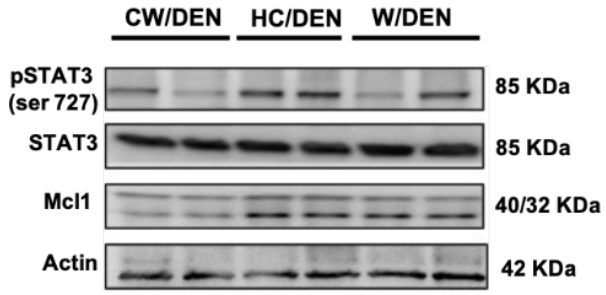
A)


Enrichment plot:
Hallmark_IL6_JAK_STAT3_Signaling
p-value: 0.0
NES: 1.70
Enrichment Score (ES)
W/DEN
CW/DEN
Enrichment plot:
Hallmark_IL6_JAK_STAT3_Signaling
p-value: 0.04
NES: 1.30
Enrichment Score (ES)
HC/DEN
CW/DEN

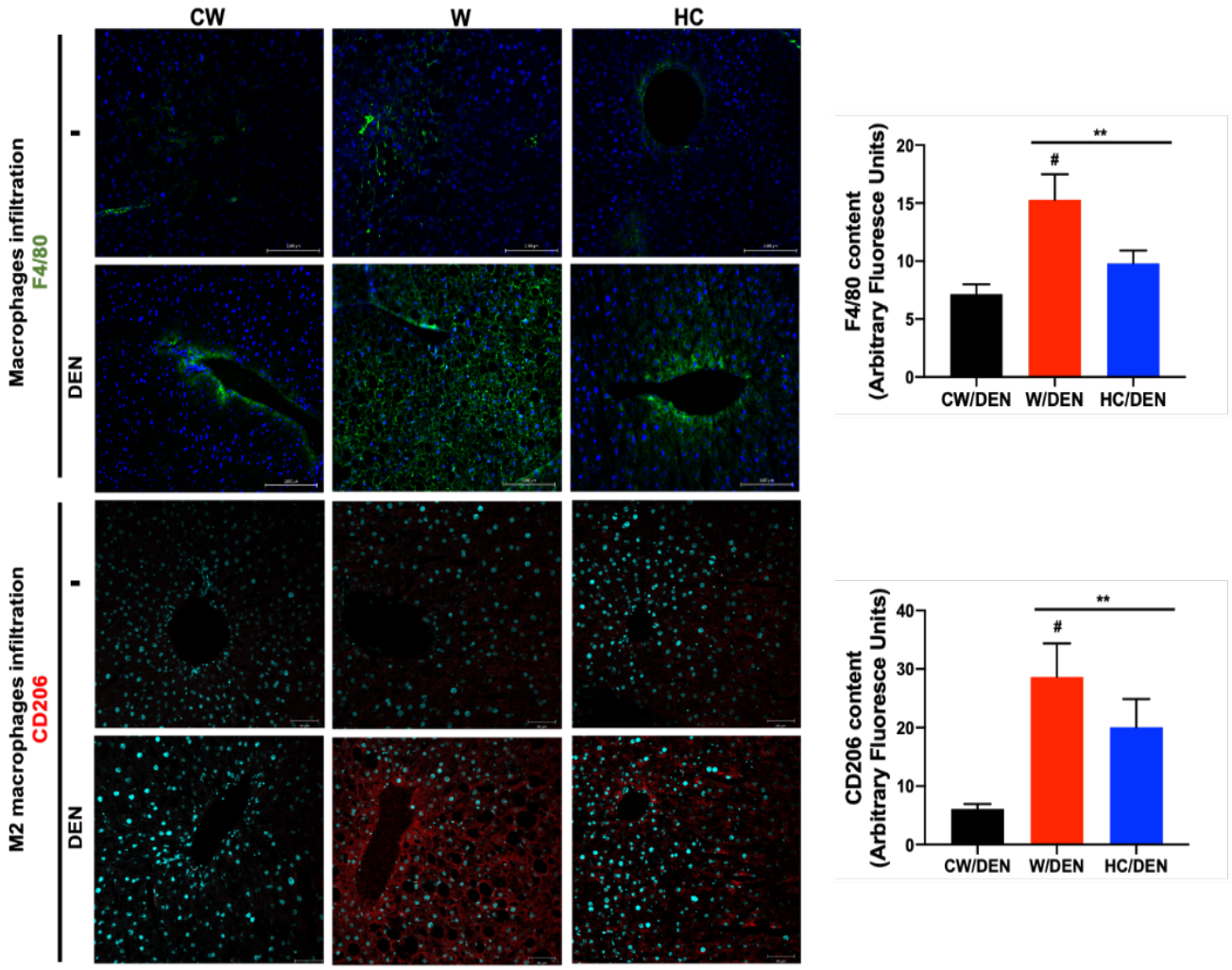
B)


z-score
Cell movement of phagocytes
Leukocyte migration
Cell movement of leukocytes
Cell movement of myeloid cells
Chemotaxis
Activation of myeloid cells
Chemotaxis of myeloid cells
Activation of leukocytes
Accumulation of myeloid cells
CW/DEN
HC/DEN
W/DEN

C)


CW/DEN
HC/DEN
W/DEN
pSTAT3 (ser 727)
85 KDa
STAT3
85 KDa
Mcl1
40/32 KDa
Actin
42 KDa

D)


CW
W
HC
Macrophages infiltration
F4/80
-
DEN
M2 macrophages infiltration
CD206
-
DEN
F4/80 content
(Arbitrary Fluoresce Units)
20
15
10
5
0
#
**
CW/DEN
W/DEN
HC/DEN
CD206 content
(Arbitrary Fluoresce Units)
40
30
20
10
0
#
**
CW/DEN
W/DEN
HC/DEN

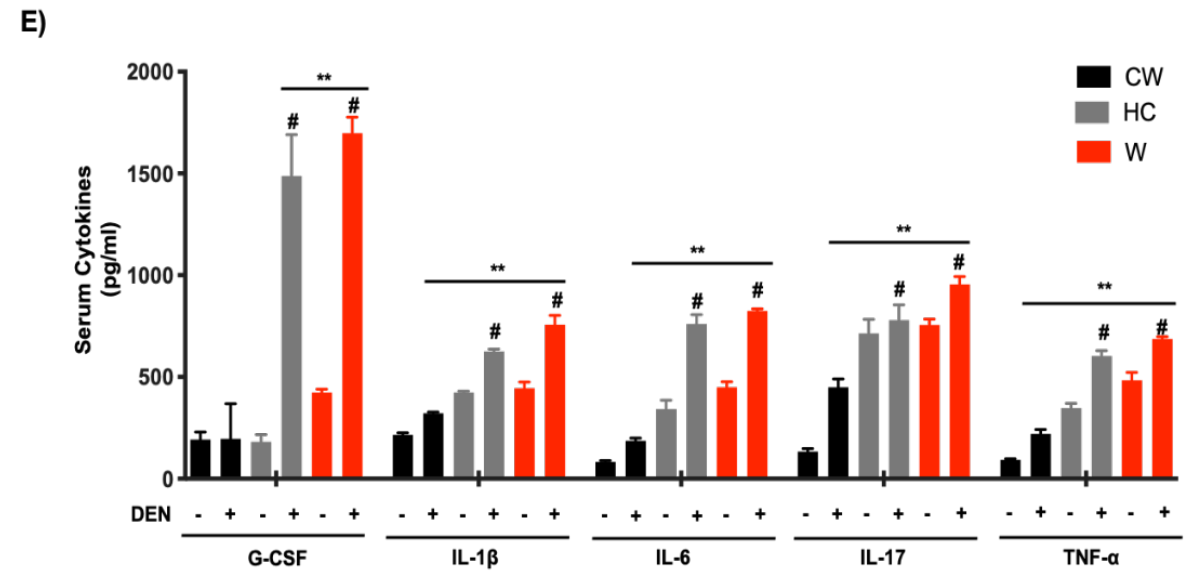
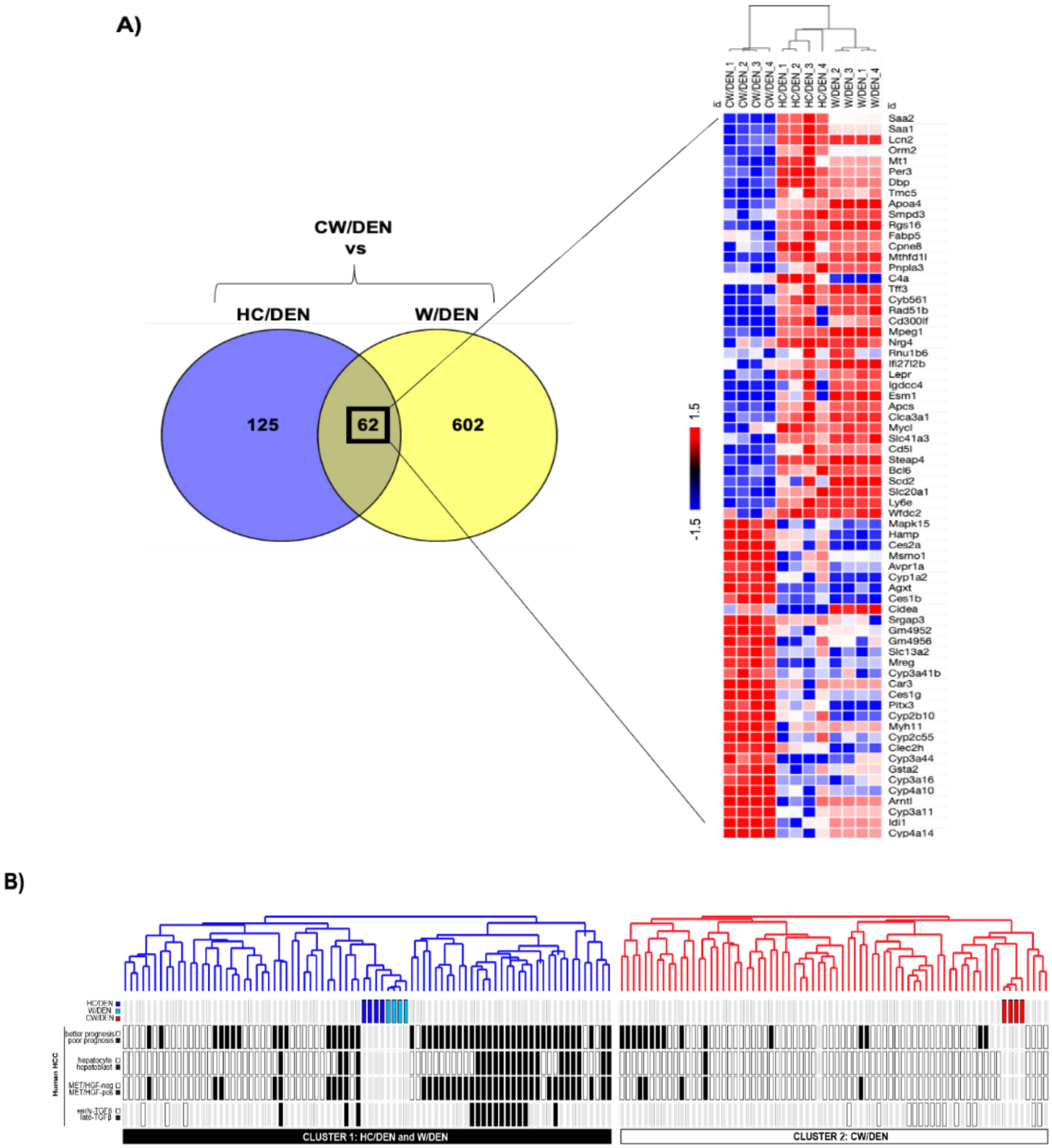


Figure 12. Inflammation as distinctive feature in liver tumors associated to high lipid and cholesterol consumption. A) Gene set enrichment analysis (GSEA) of hallmark IL6-Jak-STAT3 signaling, data set comparing W/DEN and HC/DEN to CW/DEN. B) Process networks analysis related to inflammation in tumors from CW/DEN (black), W/DEN (red) and high cholesterol (HC/DEN, blue). The top rank ordered processes and networks are based on statistical significance ($p<0.01$). C) Western blot against STAT3 signaling pathway D) Macrophages infiltration by immunofluorescence of F4/80 (green fluorescence) and CD206 (M2 phenotype, red fluorescence), representative images of at least three animals per group, original magnification, 100X. Quantification of F4/80 and CD206 fluorescence. E) Pro-inflammatory cytokines serum concentration of all mice groups. Proteins were determined by based multiplex immunoassay. Each bar represents the average ± SEM ** $p<0.01$ vs CW group; # $p<0.05$ vs W diet alone group.

Integrative genomics was next performed to evaluate the clinical relevance of the crosstalk between mouse HCC and human HCC. The cholesterol signature (62 genes shared by W/DEN and HC/DEN) shared by W/DEN and HC/DEN groups in comparison with CW/DEN (Figure 13A) was first integrated with the gene expression profile of 101 cases of human HCCs from LEC cohort, which were extensively characterized (Lee, Chu et al. 2004). Hierarchical clustering analysis of the integrated data set identified 2 robust clusters whose: cluster 1, W/DEN and HC/DEN tumors; cluster 2 CW/DEN tumors (Figure 13B). Strikingly, cluster 1 included significantly tumors, which were

assigned to a poor prognosis group than cluster 2 (Figure 13C-D). As shown in Figure 12C, cluster 1 were defined by a bad survival(Lee, Chu et al. 2004), hepatoblast phenotype, along with the activation of MET/HGF (Kaposi-Novak, Lee et al. 2006) and late TGF-β signaling (Coulouarn, Gomez-Quiroz et al. 2006). Also, we identified signs of vascular invasion in the cluster 1. The percent survival of patients in the cluster 1 was significantly reduced ($p<0.01$) in comparison with the cluster 2 (Figure 13D). The analysis of the 62 orthologous genes in the human TCGA database identified 4 genes differentially overexpressed related to high lipid overload with potential relevance in tumor promotion: *mthfd1l* (W/DEN: 2.74- and HC/DEN: 2.42-fold change), *slc41a3* (W/DEN: 2.67- and HC/DEN: 1.70-fold change), *fabp5* (W/DEN: 2.20- and HC/DEN: 2.70-fold change); and *igdcc4,* (W/DEN: 2.05- and HC/DEN: 1.88-fold change increased) in W/DEN and HC/DEN respectively comparing with CW/DEN. We verified by qRT-PCR the expression of these genes in mouse samples (Figure 14A).


A)
CW/DEN
vs
HC/DEN
W/DEN
125
62
602
CW/DEN_1
CW/DEN_2
CW/DEN_3
CW/DEN_4
HC/DEN_1
HC/DEN_2
HC/DEN_3
HC/DEN_4
W/DEN_2
W/DEN_3
W/DEN_1
W/DEN_4
id
Saa2
Saa1
Lcn2
Orm2
Mt1
Per3
Dbp
Tmc5
Apoa4
Smpd3
Rgs16
Fabp5
Cpne8
Mthfd1l
Pnpla3
C4a
Tff3
Cyb561
Rad51b
Cd300lf
Mpeg1
Nrg4
Rnu1b6
Ifi27l2b
Lepr
Igdcc4
Esm1
Apcs
Clca3a1
Mycl
Slc41a3
Cd5l
Steap4
Bcl6
Scd2
Slc20a1
Ly6e
Wfdc2
Mapk15
Hamp
Ces2a
Msmo1
Avpr1a
Cyp1a2
Agxt
Ces1b
Cidea
Srgap3
Gm4952
Gm4956
Slc13a2
Mreg
Cyp3a41b
Car3
Ces1g
Pitx3
Cyp2b10
Myh11
Cyp2c55
Clec2h
Cyp3a44
Gsta2
Cyp3a16
Cyp4a10
Arntl
Cyp3a11
Idi1
Cyp4a14
1.5
-1.5
B)
HC/DEN
W/DEN
CW/DEN
better prognosis
poor prognosis
hepatocyte
hepatoblast
MET/HGF-neg
MET/HGF-pos
early-TGFβ
late-TGFβ
Human HCC
CLUSTER 1: HC/DEN and W/DEN
CLUSTER 2: CW/DEN

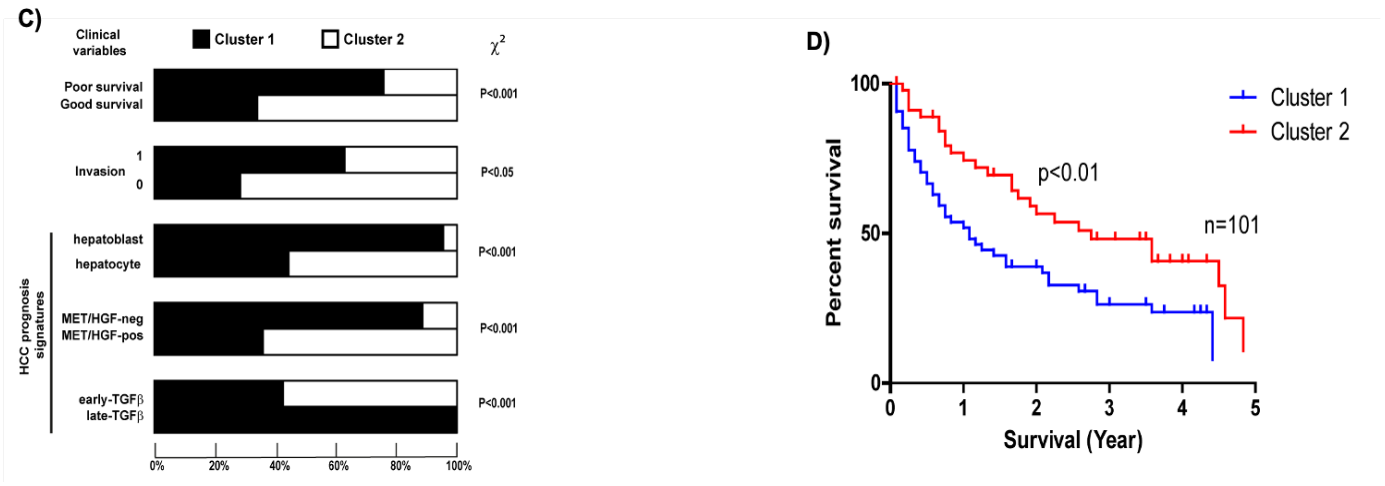
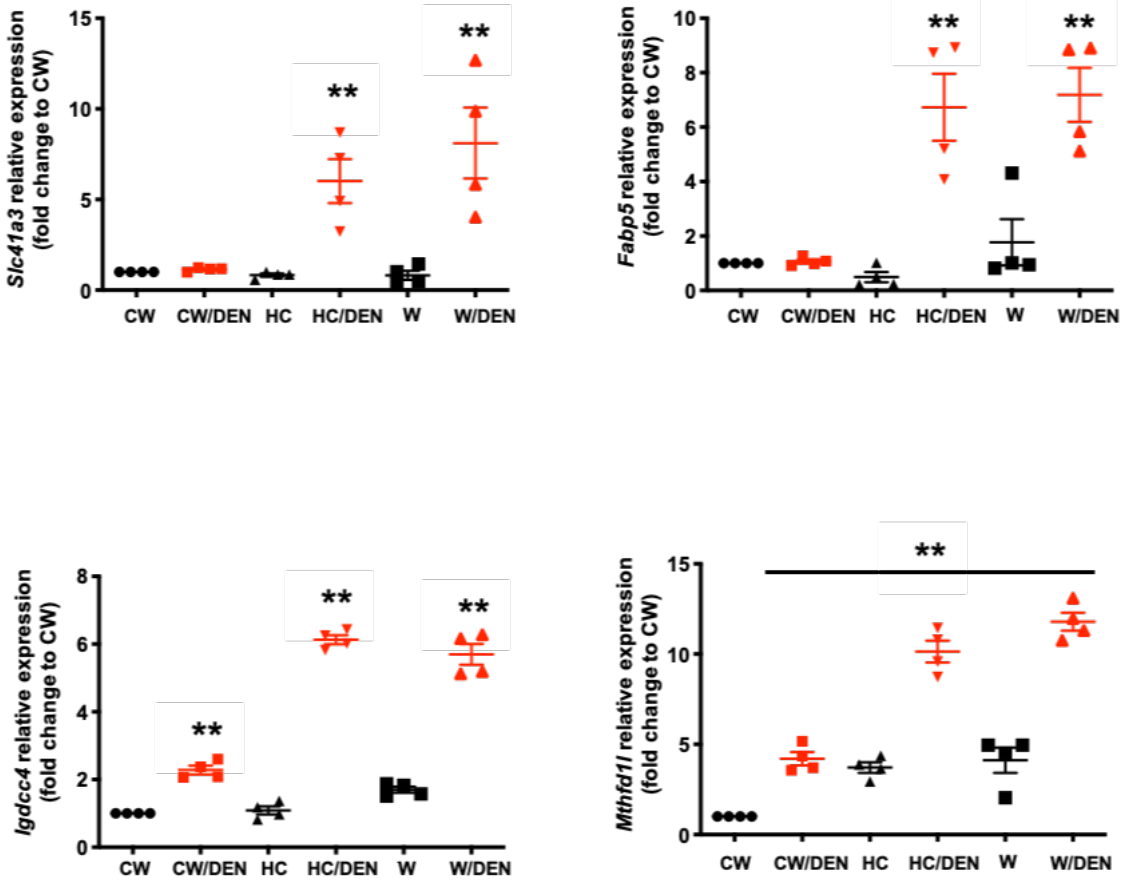


Figure 13. High cholesterol diet consumption promotes specific gene signature. A) Venn diagram depicting differentially expressed common genes between HC/DEN and W/DEN groups. Heatmap shows the common 62 genes indicating the fold change value. B) Dendrogram overview of mice tumors integrated with 101 cases of human HCC. Clustering analysis was based on the expression of 62 ortholog genes in W/DEN and HC/DEN. Two clusters (1 and 2) were identified. C) Distribution of human HCC samples between previously described subgroups with respect to survival (better vs. poorprognosis), cell origin (hepatoblast vs. hepatocytes), activation of MET/HGF, and TGF-β signaling pathway (early vs. late) is indicated on the left. B, statistical analysis of HCC distribution between clusters 1 and 2 based on previous gene signatures and clinical parameters. Cluster 1, which is defined by the W/DEN and HC/DEN signature, shows a significant enrichment in HCCs with the following features: bad survival, hepatoblast traits, activation of MET/HGF, and late TGF-β pathways. D) Kaplan–Meier plots and log-rank statistics analysis revealed a significant decrease in overall survival for patients included in cluster 1.

Then, we explored the correlation between the expression of these genes and cholesterol content in four well-known human HCC cell lines using, as a control, of non-cancerous hepatocyte-like THLE-3 cell line. Figure 14B depicts the differences in cholesterol content in the different cell lines. We determined the expression of the four genes in those cell lines and a statistically significant correlation between gene expression and cholesterol content was observed for all genes analyzed (Figure 14C-D).

A)


Slc41a3 relative expression (fold change to CW)
15
10
5
0
**
**
CW
CW/DEN
HC
HC/DEN
W
W/DEN
Fabp5 relative expression (fold change to CW)
10
8
6
4
2
0
**
**
CW
CW/DEN
HC
HC/DEN
W
W/DEN
Igdcc4 relative expression (fold change to CW)
8
6
4
2
0
**
**
CW
CW/DEN
HC
HC/DEN
W
W/DEN
Mthfd1l relative expression (fold change to CW)
15
10
5
0
**
CW
CW/DEN
HC
HC/DEN
W
W/DEN

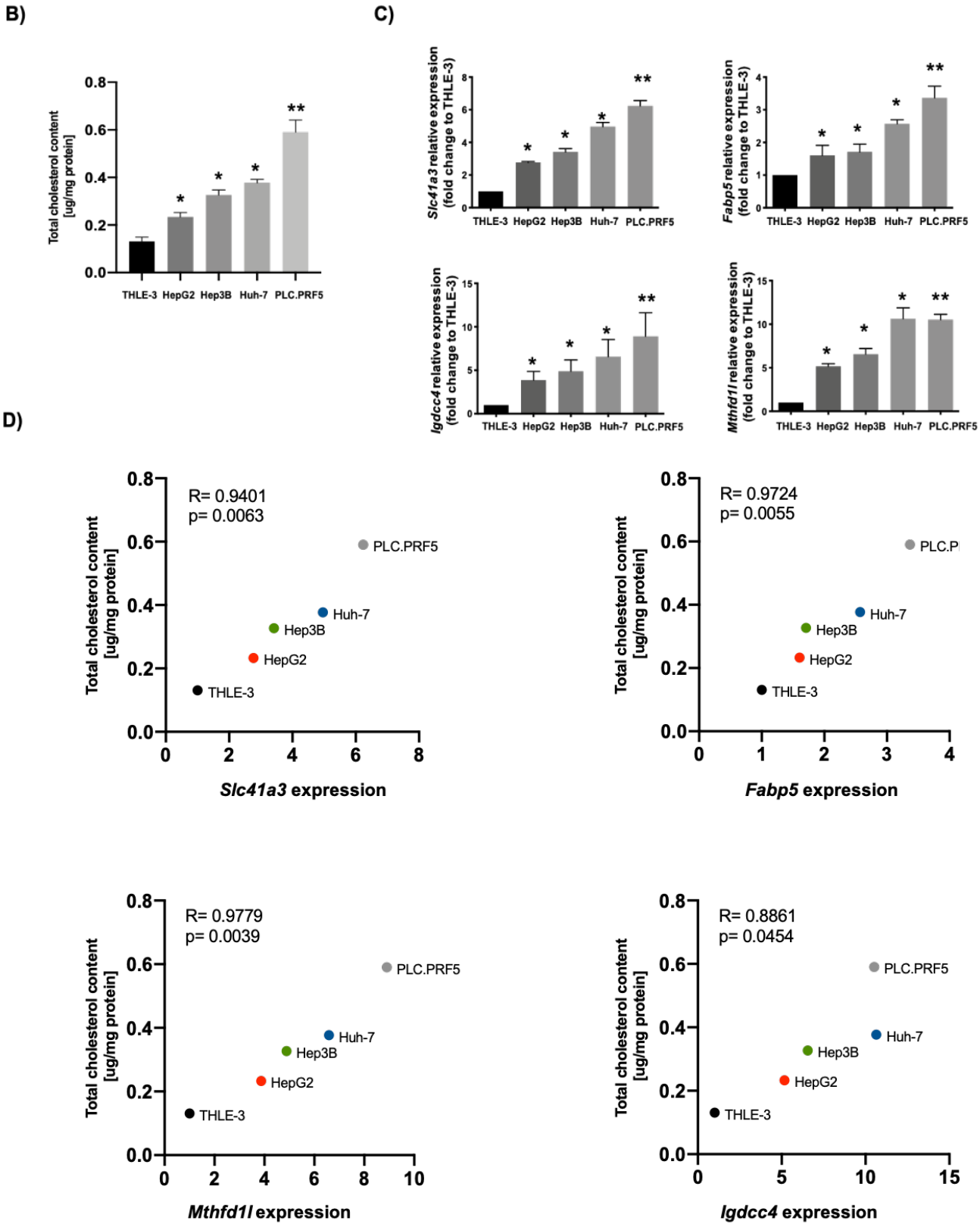
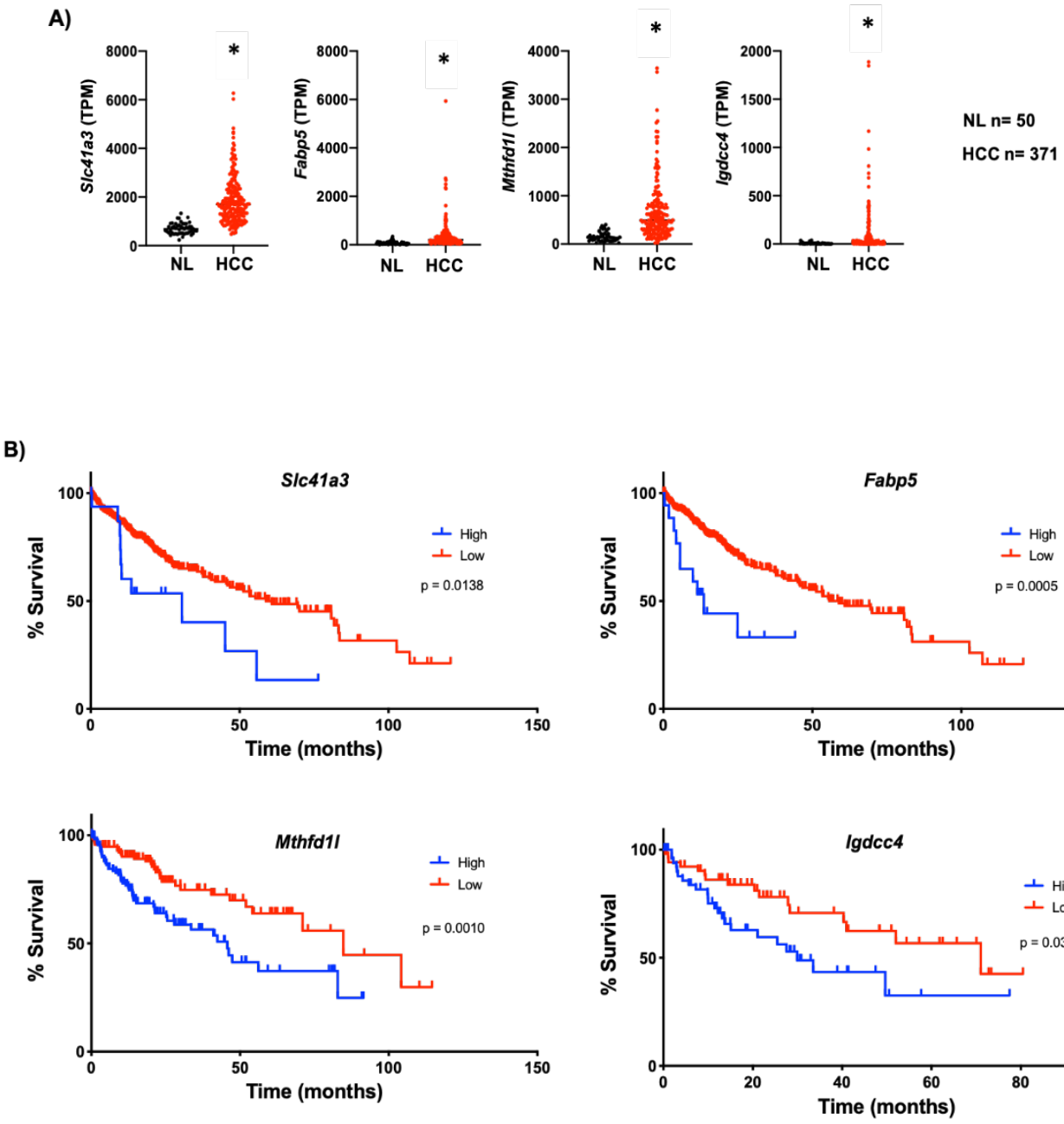
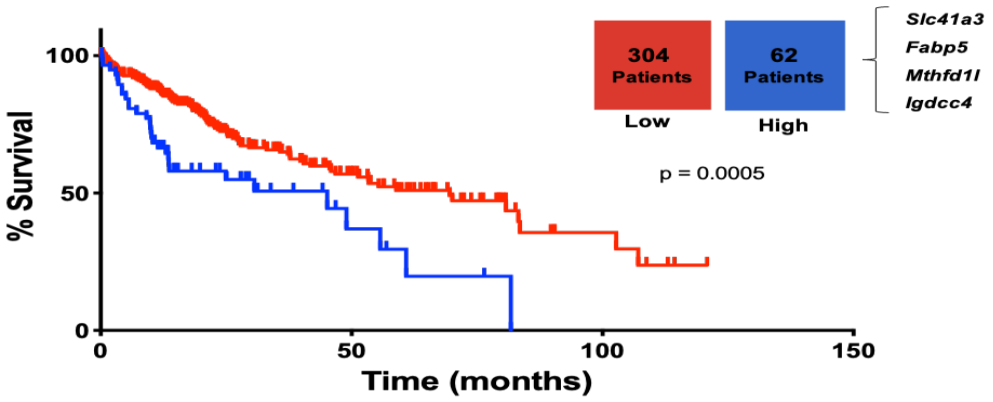

B)
C)
D)
Total cholesterol content [ug/mg protein]
THLE-3 HepG2 Hep3B Huh-7 PLC.PRF5
Slc41a3 relative expression (fold change to THLE-3)
Fabp5 relative expression (fold change to THLE-3)
Igdcc4 relative expression (fold change to THLE-3)
Mthfd1l relative expression (fold change to THLE-3)
R= 0.9401
p= 0.0063
Slc41a3 expression
R= 0.9724
p= 0.0055
Fabp5 expression
R= 0.9779
p= 0.0039
Mthfd1l expression
R= 0.8861
p= 0.0454
Igdcc4 expression

Figure 14. Lipid-associated four gene signature of HCC correlates with cholesterol overload in human cancer cell lines. A) Expression of the 4 genes differentially overexpressed related to high lipid overload with potential relevance in tumor promotion: *mthfd1*, *slc41a3*, *fabp5*, *igdcc4*. B) Total cholesterol biochemical quantification in different human HCC-derived cell lines. C) Slc41a3, Fabp5, Igdcc4 and Mthfd1l gene expression addressed by quantitative RT-PCR in different HCC-derived human cell lines. THLE-3 cells were used as control not transformed cells. Each bar represents the average ± SEM * $p<0.05$; ** $p<0.01$ vs THLE-3 cells. D) Pearson correlation analysis between total cholesterol content and gene expression of Slc41a3, Fabp5, Igdcc4 and Mthfd1l.

The clinical relevance of mouse data in human liver carcinogenesis was determined by analyzing the expression of the 4 genes in the TCGA dataset, including 50 non-tumor liver tissue (NL) and 371 HCC samples (LIHC, Liver Hepatocellular Carcinoma). The four-gene signature associated to NASH was increased in HCC (Figure 15A). Next, we evaluated the capacity of these genes to predict survival in the 371 human HCC. For all genes analyzed, high expression was associated to a poor outcome (Figure 15B). Finally, we grouped the four genes and performed the analysis between patients with altered (n=62) vs unaltered (n=304) gene expression. As expected, Kaplan-Meier plot and log-rank testing demonstrated a reduced overall survival for patients included in the altered gene group ($p<0.001$) (Figure 15C). Thus, the molecular differences between these two subclasses of HCC were associate with a remarkable difference in the clinical outcome.


A)
Slc41a3 (TPM)
Fabp5 (TPM)
Mthfd1l (TPM)
Igdcc4 (TPM)
NL
HCC
*
NL n= 50
HCC n= 371
B)
Slc41a3
Fabp5
Mthfd1l
Igdcc4
% Survival
Time (months)
High
Low
p = 0.0138
p = 0.0005
p = 0.0010
p = 0.0328

C)



	No. of cases (Total)	No. of Cases (Deceased)	Median Months Overall
Cluster 1	62	30	45.11
Cluster 2	304	99	69.57

Figure 14. Lipid-associated four gene signature defines a subtype of human liver cancer with poor prognosis. A) Plots charts showing higher expression of *Slc41a3*, *Fabp5*, *Igdcc4* and *Mthfd1l* in human HCC (n=371) compared to no-tumor liver tissue (NL, n=50) according to the TCGA data base (https://www.cbioportal.org/). TPM, transcripts per million. * p<0.01 vs normal liver (NL). B) Kaplan-Meier curves of overall survival in HCC patients. Patients with HCC were separated into two groups, high (blue) and low (red) expression of *Slc41a3* (p=0.0138), *Fabp5* (p=0.0005), *Igdcc4* (p=0.0010), and *Mthfd1l* (p=0.0328). C) HCC data set from the TCGA was divided in unaltered and altered groups regarding the four gene signature and the overall survival in HCC patients was addressed and plotted in a Kaplan-Meier curve, (red altered or low group) and low (blue unaltered or high group).

Chapter 7

Discussion

Previously, we demonstrated the liver tumor promotion properties elicited by the consumption of a high cholesterol diet in mice. Tumors generated presented an aggressive phenotype, including lung metastasis, comparing with animals fed with regular chow diet (Enriquez-Cortina, Bello-Monroy et al. 2017). This outcome was strongly associated to oxidative stress-mediated DNA damage, failure in the activation of the main DNA repair protein machinery and apoptosis resistance. The main objectives of the present work were to characterize the HCC progression in NASH induced by the consumption of high lipid diets, particularly the contribution of cholesterol and to identify the gene expression profile associated to this particular feature. Thus, we fed animals up to 8 months with a commercial and well-studied Western diet (high lipid, cholesterol and carbohydrates). Then, mice received a single dose of DEN to induce liver carcinogenesis, as we previously reported (Takami, Kaposi-Novak et al. 2007, Enriquez-Cortina, Bello-Monroy et al. 2017).

Under Western diet, mice exhibited signs of obesity with a gain of weight and accumulation of visceral fat, together with the presence of liver damage. These findings are in agreement with those observed in humans under an occidental (western) pattern diet (Sun and Karin 2012), and in others well-characterized mouse models of NASH (Asgharpour, Cazanave et al. 2016, Tsuchida, Lee et al. 2018). The co-treatment with DEN efficiently induced a higher burden of HCC comparing with CW/DEN groups

clearly suggesting that lipid overload acts as a tumor promoter. One of the key components of Western diet is high cholesterol. We and others have published that this lipid, in addition to the well-recognized fundamental properties for life, displays noxious effects when excessively accumulated in cells, particularly as a result of mitochondrial dysfunction and impairment of signal transduction through altering cellular membrane fluidity (Mari, Caballero et al. 2006, Gomez-Quiroz, Seo et al. 2016, Dominguez-Perez, Simoni-Nieves et al. 2019). When accumulated in the liver, we previously demonstrated that cholesterol definitively increases tumor burden and aggressivity (Enriquez-Cortina, Bello-Monroy et al. 2017, Garcia-Ruiz, de la Rosa et al. 2020). However, the exact molecular mechanisms by which cholesterol favors tumor development are not completed understood, yet.

The transcriptomic analysis carried out by RNA-seq shows a well separation between CW/DEN and HC/DEN, W/DEN groups. GSEA revealed a noticeable inflammatory phenotype, particularly driven by IL-6/STAT3 signaling, in addition to other pathways related to growth factors such as HGF, including PI3K/AKT and ERK pathways. Very interestingly is the abrogation of key tumor suppressive signals such as p53, PTEN and apoptosis signaling in this model. Our previous work identified a remarkable mechanistic effect induced by cholesterol overload in the liver, including down-regulation of the main DNA repair proteins such as ATM, ATR, CHK1 and 2, and p53 (Enriquez-Cortina, Bello-Monroy et al. 2017). In the present work, IPA confirmed this effect in terms of signaling pathways controlled by p53. Even more, an interesting crosstalk between p53 and STAT3 signaling pathways by the intervention of PI3K and MAPK pathways has been recently reported in ovarian cancer (Liang, Ren et al. 2019),

and linked to an aggressive phenotype mediated by epithelial-mesenchymal transition, resulting in cell metastasis and chemoresistance.

Since early 2000´s some reports pointed out the transcriptional repression of p53 by STAT3 (Niu, Wright et al. 2005). P53 loss of function has been also related to STAT3 activation in pancreatic cancer (Wormann, Song et al. 2016). Our previously published work reported that cholesterol overload in the liver of mice fed with a high cholesterol diet for 30 days presented a remarkable activation of STAT3 and the increment in the expression of key target genes such as Mcl-1 (Dominguez-Perez, Simoni-Nieves et al. 2019). It is clear that cholesterol takes control of these relevant signaling pathways in preparation for tumor promotion. Contrary, it has been observed that dephosphorylation of STAT3 could stabilize p53 and leads to apoptosis (Sainz-Perez, Gary-Gouy et al. 2008).

In agreement with RNA-seq analysis, we found poor survival according to Lee and collaborators (Lee, Chu et al. 2004, Lee, Chu et al. 2004). The main cytokines and growth factors associated to proliferation and inflammation (e.g. IL-6, IL-17, HGF, VEGF-A, among others) were significantly elevated in mice under W/DEN treatment, F4/80 and CD206 IF corroborated a significant inflammatory infiltration when comparing with CW/DEN tumoral, once again STAT3 as a key driver in NASH and HCC inflammation as reported (Min, Mirshahi et al. 2015, Grohmann, Wiede et al. 2018).

The modulation of the immune response promoting the recruitment and the activation of macrophages has been previously reported in tumors raised under the consumption of high lipid/cholesterol diets (Shono, Habu et al. 2011). The close contact of macrophages and tumor cells is associated to M2-like macrophages polarization

increasing the aggressiveness of the tumors (Yang, Ye et al. 2018). In agreement with these previous findings, we observed a prominent F4/80 (canonical macrophage market) and CD206 (M2 macrophage marker) signal in high lipids diets particularly in Western diet. Interestingly, it has been observed that M2 macrophages could provide cholesterol to tumor cells, making a cholesterol co-dependence between these cells in the tumor microenvironment (Goossens, Rodriguez-Vita et al. 2019). Recently, Bao and collaborators reported that high M2 macrophages infiltration is associated with a poorer survival and increase in the cancer recurrence (Bao, Zhao et al. 2019).

In addition to a well-defined macrophages infiltration, we also observed an increase in pro-angiogenic response, judged by the increment in VEGF-A and HGF expression, and confirmed by CD34 IF, supporting the aggressive phenotype. Accordingly, we reported that HGF/Met-regulated expression signature was associated to an increment in angiogenesis and was able to define a subset of human HCC with poor prognosis and aggressive phenotype (Kaposi-Novak, Lee et al. 2006). Another characteristic observed in this signature was the prominent decompensation of lipogenesis and oxidative stress.

To gain more mechanistic evidence of the relevance of tumor development in lipid-overloaded livers, we studied another group of mice fed with a high cholesterol diet (carbohydrates and other lipids in standard contents). Gene expression analysis in this tumorigenic process, identified 194 differentially expressed genes relating to CW/DEN. Comparison between HC/DEN vs W/DEN identified 62 commonly regulated genes. Supporting these findings, we established an integrative genomics between mice high cholesterol tumors and human HCCs, where these 62 genes shared by W/DEN and

HC/DEN had clinical relevance and is associated with poor prognosis in human HCCs. More investigations will be needed to fully establish the contribution of each specific genes.

Including four genes (*Slc41a3, Fabp5, Mthfd1l* and *Igdcc4*) with clinical relevance in human carcinogenesis. These genes are elevated in HCC samples and are associated to a poor survival in patients. Clustering these four genes and separating human HCC in those with altered expression (n=62) regarding patients with unaltered expression (n= 304), we clearly observed a significant decrement in survival.

The solute carrier (Slc) family 41 comprises three members including the Slc41a3. It is related to cation transmembrane transporter activity. It drives the efflux of Mg^{2+} particularly in mitochondria rather than plasma membrane (Mastrototaro, Smorodchenko et al. 2016). Slc41a3 overexpression has been reported in cancer playing a role for nutrient and Mg^{2+} transport to meet the needs for aberrant metabolism and proliferation (Trapani and Wolf 2019). As we have stated, mitochondria are perhaps the most relevant organelle target in the cholesterol overloaded cell. Overexpression of this transporter system could be directed to compensate the loss of fluidity in the mitochondria, improving the extrusion of Mg^{2+}. *Fabp5* encodes for the fatty acid-binding protein 5 (Fabp5). This protein has been related to malignant potential in several cancers, including HCC. Positive staining of FABP5 in HCC is associated with poor prognosis, recurrence, metastasis and vascular invasion (Ohata, Yokoo et al. 2017). FABP5 transports lipids intracellularly for storage purposes, providing building blocks for membrane construction and energy supply, both highly required in the proliferating cells (Furuhashi and Hotamisligil 2008). *Igdcc4* encodes the neighbor of

Punc E11, also known as Nope. It is a plasma membrane oncofetal stem/progenitor cell marker, initially identified in the murine fetal liver (Bowe, Zweerink et al. 2018). It is barely detected in the adult liver. It has been previously showed that Nope is a sensitive marker of HCC (Marquardt, Quasdorff et al. 2011) associated to stemness resembling early postnatal hepatocytes. Although Nope is scarcely detected in adult hepatocytes, the damage could induce their expression, particularly in the cholestatic damage which is associated to changes in hepatocyte polarization (Bowe, Zweerink et al. 2018). Nope protein has been demonstrated to be a good and confident marker for HCC in the clinic because it could be highly detected in AFP-positive and -negative tumors (Marquardt, Quasdorff et al. 2011). The methylenetetrahydrofolate dehydrogenase 1 like (Mthfd1l), encoded by *Mthfd1l* gene is an enzyme of the folate cycle. It is involved in formate generation, therefore in the metabolism of mono carbon compound fundamental in both, purine synthesis and protein synthesis initiation. Thus, this enzyme is highly relevant in the proliferating tissues, particularly in cancer (Agarwal, Behring et al. 2019, He, Wang et al. 2020). Mthfd1l expression has been associated with poor prognosis, notably in HCC (Lee, Xu et al. 2017). In normal conditions MTHFD1L is expressed in mitochondria in embryonic tissues (Pike, Rajendra et al. 2010), once again the mitochondria as an important target in our model. Interestingly, MTHFD1L has been also associated to redox homeostasis in cancer and, as we have proved, one of the main consequences in cancer development in the lipid overloaded liver is the disruption of redox balance (Enriquez-Cortina, Bello-Monroy et al. 2017).

Metabolic reprograming is one of the key features in cancer. Our proposed signature clearly indicates a metabolic adaptation, compromising mitochondrial adaptation and

macrophages participation, particularly the M2-like polarization in a process induced and driven by cholesterol overload.

Conclusions

The overall incidence of liver cancer in non-alcoholic fatty liver disease has not yet been quantified, but in the present work, we have characterized an animal model of NASH-derived HCC that recapitulates the human disease, with a clear inflammatory and angiogenic component. RNA-seq analysis identified a specific gene expression profile defining a four-gene signature with potential prognostic applications in the clinic, predicting poor survival in patients with HCC.

Dietary intervention controlling the kind of lipid rather than the amount ingested could decrease the incidence of aggressive liver cancer.

Chapter 8

Perspectives

The present work opened many new questions. One of them is to determine the role of cholesterol in the aberrant signaling present in HCC. Cholesterol plays a very important role in the plasma membrane as well as in the endo-membranes since it alters the fluidity and the functions of these membranes. In the plasma membrane and other intracellular membranes, cholesterol accumulates in specialized structures known by various names, such as lipid rafts, detergent-resistant membrane domains (DRM), and detergent-soluble glycolipid-enriched complexes (DIG). Lipid rafts appear to serve a number of functions, including intracellular transport and sorting of molecules, down-regulation and recycling of receptors, and targeted export of proteins and lipids. Cancer incidence is one of the leading causes of death in the world and has become a global health problem. HCC is one of the most common cancers due to its association with obesity. And since HCC celsl has an excessive accumulation of cholesterol, this could be affecting the composition and structure of these lipid rafts (microdomains). It is useful to understand how the concept of the lipid microdomain could explain the phenomenon of signal transmission by proteins anchored to it. It is now well established that proteins anchored to lipid rafts are found together with a number of other signal transduction molecules.

So atomic force microscopy (AFM) allows for nano-scale research of cells and molecules. Recent advances have allowed its application in cancer research and diagnosis. The physicochemical properties of living cells undergo changes when their physiological conditions are altered. These physicochemical properties can therefore reflect complex physiological processes that occur in cells. When cells are in the process of carcinogenesis and stimulated by external stimuli, their morphology, elasticity and adhesion properties can change. AFM can perform surface imaging and ultrastructural observation of living cells with atomic resolution under almost physiological conditions, collecting information from force spectroscopy that allows the study of the mechanical properties of cells. For this reason, AFM has the potential to be used as a tool for high resolution research on the ultrastructure and mechanical properties of tumor cells (Deng, Xiong et al. 2018).

Because the molecular characterization of HCC and cancer in general represents a promising opportunity to improve the treatment of patients with cancer, due to the identification of subtypes of HCC, as is the case in the present work, in which we were able to establish a gene signature which occurs in tumors with an etiology of NAFLD (specifically caused by excess dietary cholesterol) which from the clinical perspective the main goal to deal with the results obtained in this work is to acquire more evidence of the implications and relevance of the transcriptomic signature obtained from the RNA-seq (*Slc41a3, Fabp5, Mthfd1l* and *Igdcc4*). The first approach for the study of these four genes involved in the aggressiveness of HCC under an environment of lipid

overload is using the crispr cas9 technique. since this technique, allows us to silence and overexpress these genes in cell lines (*in vitro*) and in animals (*in vivo*).

References.

Agarwal, S., M. Behring, K. Hale, S. Al Diffalha, K. Wang, U. Manne and S. Varambally (2019). "MTHFD1L, A Folate Cycle Enzyme, Is Involved in Progression of Colorectal Cancer." Transl Oncol **12**(11): 1461-1467.

Asgharpour, A., S. C. Cazanave, T. Pacana, M. Seneshaw, R. Vincent, B. A. Banini, D. P. Kumar, K. Daita, H. K. Min, F. Mirshahi, P. Bedossa, X. Sun, Y. Hoshida, S. V. Koduru, D. Contaifer, Jr., U. O. Warncke, D. S. Wijesinghe and A. J. Sanyal (2016). "A diet-induced animal model of non-alcoholic fatty liver disease and hepatocellular cancer." J Hepatol **65**(3): 579-588.

Baffy, G., E. M. Brunt and S. H. Caldwell (2012). "Hepatocellular carcinoma in non-alcoholic fatty liver disease: an emerging menace." J Hepatol **56**(6): 1384-1391.

Bao, D., J. Zhao, X. Zhou, Q. Yang, Y. Chen, J. Zhu, P. Yuan, J. Yang, T. Qin, S. Wan and J. Xing (2019). "Mitochondrial fission-induced mtDNA stress promotes tumor-associated macrophage infiltration and HCC progression." Oncogene **38**(25): 5007-5020.

Bello-Monroy, O., D. Mata-Espinosa, C. Enriquez-Cortina, V. Souza, R. U. Miranda, L. Bucio, J. Barrios-Payan, B. Marquina-Castillo, I. Rodriguez-Ochoa, P. Rosales, M. C. Gutierrez-Ruiz, R. Hernandez-Pando and L. E. Gomez-Quiroz (2020). "Hepatocyte growth factor enhances the clearance of a multidrug-resistant Mycobacterium tuberculosis strain by high doses of conventional chemotherapy, preserving liver function." J Cell Physiol **235**(2): 1637-1648.

Bhaskaran, K., I. Douglas, H. Forbes, I. dos-Santos-Silva, D. A. Leon and L. Smeeth (2014). "Body-mass index and risk of 22 specific cancers: a population-based cohort study of 5.24 million UK adults." Lancet **384**(9945): 755-765.

Bowe, A., S. Zweerink, V. Muck, V. Kondylis, S. Schulte, T. Goeser and D. Nierhoff (2018). "Depolarized Hepatocytes Express the Stem/Progenitor Cell Marker Neighbor of Punc E11 After Bile Duct Ligation in Mice." J Histochem Cytochem **66**(8): 563-576.

Calvisi, D. F., C. Wang, C. Ho, S. Ladu, S. A. Lee, S. Mattu, G. Destefanis, S. Delogu, A. Zimmermann, J. Ericsson, S. Brozzetti, T. Staniscia, X. Chen, F. Dombrowski and M. Evert (2011). "Increased lipogenesis, induced by AKT-mTORC1-RPS6 signaling, promotes development of human hepatocellular carcinoma." Gastroenterology **140**(3): 1071-1083.

Castven, D., D. Becker, C. Czauderna, D. Wilhelm, J. B. Andersen, S. Strand, M. Hartmann, S. Heilmann-Heimbach, W. Roth, N. Hartmann, B. K. Straub, F. L. Mahn, S. Franck, S. Pereira, A. Haupts, A. Vogel, M. A. Worns, A. Weinmann, S. Heinrich, H. Lang, S. S. Thorgeirsson, P. R. Galle and J. U. Marquardt (2019). "Application of patient-derived liver cancer cells for phenotypic characterization and therapeutic target identification." Int J Cancer **144**(11): 2782-2794.
Charbonneau, M. E., K. D. Passalacqua, S. E. Hagen, H. D. Showalter, C. E. Wobus and M. X. D. O'Riordan (2019). "Perturbation of ubiquitin homeostasis promotes macrophage oxidative defenses." Sci Rep **9**(1): 10245.
Cho, M. L., S. Y. Min, S. H. Chang, K. W. Kim, S. B. Heo, S. H. Lee, S. H. Park, C. S. Cho and H. Y. Kim (2006). "Transforming growth factor beta 1(TGF-beta1) down-regulates TNFalpha-induced RANTES production in rheumatoid synovial fibroblasts through NF-kappaB-mediated transcriptional repression." Immunol Lett **105**(2): 159-166.
Clavijo-Cornejo, D., C. Enriquez-Cortina, A. Lopez-Reyes, M. Dominguez-Perez, N. Nuno, M. Dominguez-Meraz, L. Bucio, V. Souza, V. M. Factor, S. S. Thorgeirsson, M. C. Gutierrez-Ruiz and L. E. Gomez-Quiroz (2013). "Biphasic regulation of the NADPH oxidase by HGF/c-Met signaling pathway in primary mouse hepatocytes." Biochimie **95**(6): 1177-1184.
Coleman, S. J., R. P. Grose and H. M. Kocher (2014). "Fibroblast growth factor family as a potential target in the treatment of hepatocellular carcinoma." J Hepatocell Carcinoma **1**: 43-54.
Conrotto, P., S. Corso, S. Gamberini, P. M. Comoglio and S. Giordano (2004). "Interplay between scatter factor receptors and B plexins controls invasive growth." Oncogene **23**(30): 5131-5137.
Coulouarn, C., L. E. Gomez-Quiroz, J. S. Lee, P. Kaposi-Novak, E. A. Conner, T. A. Goldina, G. E. Onishchenko, V. M. Factor and S. S. Thorgeirsson (2006). "Oncogene-specific gene expression signatures at preneoplastic stage in mice define distinct mechanisms of hepatocarcinogenesis." Hepatology **44**(4): 1003-1011.
Cronin, K. A., A. J. Lake, S. Scott, R. L. Sherman, A. M. Noone, N. Howlader, S. J. Henley, R. N. Anderson, A. U. Firth, J. Ma, B. A. Kohler and A. Jemal (2018). "Annual Report to the Nation on the Status of Cancer, part I: National cancer statistics." Cancer **124**(13): 2785-2800.
Datta De, D., A. Datta, S. Bhattacharjya and S. Roychoudhury (2013). "NF-kappaB mediated transcriptional repression of acid modifying hormone gastrin." PLoS One **8**(8): e73409.
Deng, X., F. Xiong, X. Li, B. Xiang, Z. Li, X. Wu, C. Guo, X. Li, Y. Li, G. Li, W. Xiong and Z. Zeng (2018). "Application of atomic force microscopy in cancer research." J Nanobiotechnology **16**(1): 102.
Dominguez-Perez, M., N. Nuno-Lambarri, D. Clavijo-Cornejo, A. Luna-Lopez, V. Souza, L. Bucio, R. U. Miranda, L. Munoz, L. E. Gomez-Quiroz, S. Uribe-Carvajal and M. C. Gutierrez-Ruiz (2016). "Hepatocyte Growth Factor Reduces Free Cholesterol-Mediated Lipotoxicity in Primary Hepatocytes by Countering Oxidative Stress." Oxid Med Cell Longev **2016**: 7960386.

Dominguez-Perez, M., A. Simoni-Nieves, P. Rosales, N. Nuno-Lambarri, M. Rosas-Lemus, V. Souza, R. U. Miranda, L. Bucio, S. Uribe Carvajal, J. U. Marquardt, D. Seo, L. E. Gomez-Quiroz and M. C. Gutierrez-Ruiz (2019). "Cholesterol burden in the liver induces mitochondrial dynamic changes and resistance to apoptosis." J Cell Physiol **234**(5): 7213-7223.
Enriquez-Cortina, C., M. Almonte-Becerril, D. Clavijo-Cornejo, M. Palestino-Dominguez, O. Bello-Monroy, N. Nuno, A. Lopez, L. Bucio, V. Souza, R. Hernandez-Pando, L. Munoz, M. C. Gutierrez-Ruiz and L. E. Gomez-Quiroz (2013). "Hepatocyte growth factor protects against isoniazid/rifampicin-induced oxidative liver damage." Toxicol Sci **135**(1): 26-36.
Enriquez-Cortina, C., O. Bello-Monroy, P. Rosales-Cruz, V. Souza, R. U. Miranda, R. Toledo-Perez, A. Luna-Lopez, A. Simoni-Nieves, R. Hernandez-Pando, M. C. Gutierrez-Ruiz, D. F. Calvisi, J. U. Marquardt, L. Bucio and L. E. Gomez-Quiroz (2017). "Cholesterol overload in the liver aggravates oxidative stress-mediated DNA damage and accelerates hepatocarcinogenesis." Oncotarget **8**(61): 104136-104148.
Furuhashi, M. and G. S. Hotamisligil (2008). "Fatty acid-binding proteins: role in metabolic diseases and potential as drug targets." Nat Rev Drug Discov **7**(6): 489-503.
Garcia-Ruiz, C., L. Conde de la Rosa, V. Ribas and J. C. Fernandez-Checa (2020). "Mitochondrial Cholesterol and Cancer." Semin Cancer Biol.
Garcia-Ruiz, C., L. C. de la Rosa, V. Ribas and J. C. Fernandez-Checa (2020). "Mitochondrial Cholesterol and Cancer." Semin Cancer Biol.
Gerardo-Ramirez, M., R. Lazzarini-Lechuga, S. Hernandez-Rizo, J. E. Jimenez-Salazar, A. Simoni-Nieves, C. Garcia-Ruiz, J. C. Fernandez-Checa, J. U. Marquardt, C. Coulouarn, M. C. Gutierrez-Ruiz, B. Perez-Aguilar and L. E. Gomez-Quiroz (2019). "GDF11 exhibits tumor suppressive properties in hepatocellular carcinoma cells by restricting clonal expansion and invasion." Biochim Biophys Acta Mol Basis Dis **1865**(6): 1540-1554.
Gomez-Quiroz, L. E., V. M. Factor, P. Kaposi-Novak, C. Coulouarn, E. A. Conner and S. S. Thorgeirsson (2008). "Hepatocyte-specific c-Met deletion disrupts redox homeostasis and sensitizes to Fas-mediated apoptosis." J Biol Chem **283**(21): 14581-14589.
Gomez-Quiroz, L. E., D. Seo, Y. H. Lee, M. Kitade, T. Gaiser, M. Gillen, S. B. Lee, M. C. Gutierrez-Ruiz, E. A. Conner, V. M. Factor, S. S. Thorgeirsson and J. U. Marquardt (2016). "Loss of c-Met signaling sensitizes hepatocytes to lipotoxicity and induces cholestatic liver damage by aggravating oxidative stress." Toxicology **361-362**: 39-48.
Goossens, P., J. Rodriguez-Vita, A. Etzerodt, M. Masse, O. Rastoin, V. Gouirand, T. Ulas, O. Papantonopoulou, M. Van Eck, N. Auphan-Anezin, M. Bebien, C. Verthuy, T. P. Vu Manh, M. Turner, M. Dalod, J. L. Schultze and T. Lawrence (2019). "Membrane Cholesterol Efflux Drives Tumor-Associated Macrophage Reprogramming and Tumor Progression." Cell Metab **29**(6): 1376-1389 e1374.
Grohmann, M., F. Wiede, G. T. Dodd, E. N. Gurzov, G. J. Ooi, T. Butt, A. A. Rasmiena, S. Kaur, T. Gulati, P. K. Goh, A. E. Treloar, S. Archer, W. A. Brown, M. Muller, M. J. Watt, O. Ohara, C. A. McLean and T. Tiganis (2018). "Obesity Drives STAT-1-Dependent NASH and STAT-3-Dependent HCC." Cell **175**(5): 1289-1306 e1220.

He, Z., X. Wang, H. Zhang, B. Liang, J. Zhang, Z. Zhang and Y. Yang (2020). "High expression of folate cycle enzyme MTHFD1L correlates with poor prognosis and increased proliferation and migration in colorectal cancer." J Cancer **11**(14): 4213-4221.
Huang, D. Q., H. B. El-Serag and R. Loomba (2020). "Global epidemiology of NAFLD-related HCC: trends, predictions, risk factors and prevention." Nat Rev Gastroenterol Hepatol.
Imhof, B. A. and M. Aurrand-Lions (2006). "Angiogenesis and inflammation face off." Nat Med **12**(2): 171-172.
Kaposi-Novak, P., J. S. Lee, L. Gomez-Quiroz, C. Coulouarn, V. M. Factor and S. S. Thorgeirsson (2006). "Met-regulated expression signature defines a subset of human hepatocellular carcinomas with poor prognosis and aggressive phenotype." J Clin Invest **116**(6): 1582-1595.
Lambeth, J. D. (2004). "NOX enzymes and the biology of reactive oxygen." Nat Rev Immunol **4**(3): 181-189.
Lee, D., I. M. Xu, D. K. Chiu, R. K. Lai, A. P. Tse, L. Lan Li, C. T. Law, F. H. Tsang, L. L. Wei, C. Y. Chan, C. M. Wong, I. O. Ng and C. C. Wong (2017). "Folate cycle enzyme MTHFD1L confers metabolic advantages in hepatocellular carcinoma." J Clin Invest **127**(5): 1856-1872.
Lee, J. S., I. S. Chu, J. Heo, D. F. Calvisi, Z. Sun, T. Roskams, A. Durnez, A. J. Demetris and S. S. Thorgeirsson (2004). "Classification and prediction of survival in hepatocellular carcinoma by gene expression profiling." Hepatology **40**(3): 667-676.
Lee, J. S., I. S. Chu, A. Mikaelyan, D. F. Calvisi, J. Heo, J. K. Reddy and S. S. Thorgeirsson (2004). "Application of comparative functional genomics to identify best-fit mouse models to study human cancer." Nat Genet **36**(12): 1306-1311.
Lee, J. S., J. Heo, L. Libbrecht, I. S. Chu, P. Kaposi-Novak, D. F. Calvisi, A. Mikaelyan, L. R. Roberts, A. J. Demetris, Z. Sun, F. Nevens, T. Roskams and S. S. Thorgeirsson (2006). "A novel prognostic subtype of human hepatocellular carcinoma derived from hepatic progenitor cells." Nat Med **12**(4): 410-416.
Lee, L., M. Alloosh, R. Saxena, W. Van Alstine, B. A. Watkins, J. E. Klaunig, M. Sturek and N. Chalasani (2009). "Nutritional model of steatohepatitis and metabolic syndrome in the Ossabaw miniature swine." Hepatology **50**(1): 56-67.
Liang, F., C. Ren, J. Wang, S. Wang, L. Yang, X. Han, Y. Chen, G. Tong and G. Yang (2019). "The crosstalk between STAT3 and p53/RAS signaling controls cancer cell metastasis and cisplatin resistance via the Slug/MAPK/PI3K/AKT-mediated regulation of EMT and autophagy." Oncogenesis **8**(10): 59.
Liu, D., C. C. Wong, L. Fu, H. Chen, L. Zhao, C. Li, Y. Zhou, Y. Zhang, W. Xu, Y. Yang, B. Wu, G. Cheng, P. B. Lai, N. Wong, J. J. Y. Sung and J. Yu (2018). "Squalene epoxidase drives NAFLD-induced hepatocellular carcinoma and is a pharmaceutical target." Sci Transl Med **10**(437).
Liu, Z., D. Chen, F. Ning, J. Du and H. Wang (2018). "EGF is highly expressed in hepatocellular carcinoma (HCC) and promotes motility of HCC cells via fibronectin." J Cell Biochem **119**(5): 4170-4183.
Lonardo, A., S. Leoni, K. A. Alswat and Y. Fouad (2020). "History of Nonalcoholic Fatty Liver Disease." Int J Mol Sci **21**(16).

Marchesini, G., A. Suppini and G. Forlani (2005). "NAFLD treatment: cognitive-behavioral therapy has entered the arena." J Hepatol **43**(6): 926-928.
Mari, M., F. Caballero, A. Colell, A. Morales, J. Caballeria, A. Fernandez, C. Enrich, J. C. Fernandez-Checa and C. Garcia-Ruiz (2006). "Mitochondrial free cholesterol loading sensitizes to TNF- and Fas-mediated steatohepatitis." Cell Metab **4**(3): 185-198.
Marquardt, J. U., M. Quasdorff, H. Varnholt, H. M. Curth, S. Mesghenna, U. Protzer, T. Goeser and D. Nierhoff (2011). "Neighbor of Punc E11, a novel oncofetal marker for hepatocellular carcinoma." Int J Cancer **128**(10): 2353-2363.
Marquardt, J. U., D. Seo, L. E. Gomez-Quiroz, K. Uchida, M. C. Gillen, M. Kitade, P. Kaposi-Novak, E. A. Conner, V. M. Factor and S. S. Thorgeirsson (2012). "Loss of c-Met accelerates development of liver fibrosis in response to CCl(4) exposure through deregulation of multiple molecular pathways." Biochim Biophys Acta **1822**(6): 942-951.
Massoud, O. and M. Charlton (2018). "Nonalcoholic Fatty Liver Disease/Nonalcoholic Steatohepatitis and Hepatocellular Carcinoma." Clin Liver Dis **22**(1): 201-211.
Mastrototaro, L., A. Smorodchenko, J. R. Aschenbach, M. Kolisek and G. Sponder (2016). "Solute carrier 41A3 encodes for a mitochondrial Mg(2+) efflux system." Sci Rep **6**: 27999.
Maxfield, F. R. and G. van Meer (2010). "Cholesterol, the central lipid of mammalian cells." Curr Opin Cell Biol **22**(4): 422-429.
Min, H. K., F. Mirshahi, A. Verdianelli, T. Pacana, V. Patel, C. G. Park, A. Choi, J. H. Lee, C. B. Park, S. Ren and A. J. Sanyal (2015). "Activation of the GP130-STAT3 axis and its potential implications in nonalcoholic fatty liver disease." Am J Physiol Gastrointest Liver Physiol **308**(9): G794-803.
Niu, G., K. L. Wright, Y. Ma, G. M. Wright, M. Huang, R. Irby, J. Briggs, J. Karras, W. D. Cress, D. Pardoll, R. Jove, J. Chen and H. Yu (2005). "Role of Stat3 in regulating p53 expression and function." Mol Cell Biol **25**(17): 7432-7440.
Nowak, T., P. Niemiec, T. Iwanicki, A. Balcerzyk, J. Krauze, A. Ochalska-Tyka and I. Zak (2018). "Analysis of selected promoter polymorphisms and haplotypes of the CYBA gene encoding the p22phox, subunit of NADPH oxidases, in patients with coronary artery disease." Free Radic Res **52**(10): 1132-1139.
Ohata, T., H. Yokoo, T. Kamiyama, M. Fukai, T. Aiyama, Y. Hatanaka, K. Hatanaka, K. Wakayama, T. Orimo, T. Kakisaka, N. Kobayashi, Y. Matsuno and A. Taketomi (2017). "Fatty acid-binding protein 5 function in hepatocellular carcinoma through induction of epithelial-mesenchymal transition." Cancer Med **6**(5): 1049-1061.
Orian-Rousseau, V., L. Chen, J. P. Sleeman, P. Herrlich and H. Ponta (2002). "CD44 is required for two consecutive steps in HGF/c-Met signaling." Genes Dev **16**(23): 3074-3086.
Ozaki, M., S. Haga, H. Q. Zhang, K. Irani and S. Suzuki (2003). "Inhibition of hypoxia/reoxygenation-induced oxidative stress in HGF-stimulated antiapoptotic signaling: role of PI3-K and Akt kinase upon rac1." Cell Death Differ **10**(5): 508-515.
Palestino-Dominguez, M., M. Pelaez-Luna, R. Lazzarini-Lechuga, I. Rodriguez-Ochoa, V. Souza, R. U. Miranda, B. Perez-Aguilar, L. Bucio, J. U. Marquardt, L. E. Gomez-Quiroz and M. C. Gutierrez-Ruiz (2018). "Recombinant human hepatocyte growth

factor provides protective effects in cerulein-induced acute pancreatitis in mice." J Cell Physiol **233**(12): 9354-9364.
Pike, S. T., R. Rajendra, K. Artzt and D. R. Appling (2010). "Mitochondrial C1-tetrahydrofolate synthase (MTHFD1L) supports the flow of mitochondrial one-carbon units into the methyl cycle in embryos." J Biol Chem **285**(7): 4612-4620.
Rebouissou, S., M. Amessou, G. Couchy, K. Poussin, S. Imbeaud, C. Pilati, T. Izard, C. Balabaud, P. Bioulac-Sage and J. Zucman-Rossi (2009). "Frequent in-frame somatic deletions activate gp130 in inflammatory hepatocellular tumours." Nature **457**(7226): 200-204.
Ribas, V., C. Garcia-Ruiz and J. C. Fernandez-Checa (2016). "Mitochondria, cholesterol and cancer cell metabolism." Clin Transl Med **5**(1): 22.
Sainz-Perez, A., H. Gary-Gouy, F. Gaudin, G. Maarof, A. Marfaing-Koka, T. de Revel and A. Dalloul (2008). "IL-24 induces apoptosis of chronic lymphocytic leukemia B cells engaged into the cell cycle through dephosphorylation of STAT3 and stabilization of p53 expression." J Immunol **181**(9): 6051-6060.
Salas-Silva, S., A. Simoni-Nieves, M. V. Razori, J. Lopez-Ramirez, J. Barrera-Chimal, R. Lazzarini, O. Bello, V. Souza, R. U. Miranda-Labra, M. C. Gutierrez-Ruiz, L. E. Gomez-Quiroz, M. G. Roma and L. Bucio-Ortiz (2020). "HGF induces protective effects in alpha-naphthylisothiocyanate-induced intrahepatic cholestasis by counteracting oxidative stress." Biochem Pharmacol **174**: 113812.
Sanches, S. C., L. N. Ramalho, M. J. Augusto, D. M. da Silva and F. S. Ramalho (2015). "Nonalcoholic Steatohepatitis: A Search for Factual Animal Models." Biomed Res Int **2015**: 574832.
Sanyal, A. J. (2019). "Past, present and future perspectives in nonalcoholic fatty liver disease." Nat Rev Gastroenterol Hepatol **16**(6): 377-386.
Schlageter, M., L. M. Terracciano, S. D'Angelo and P. Sorrentino (2014). "Histopathology of hepatocellular carcinoma." World J Gastroenterol **20**(43): 15955-15964.
Schroder, K., S. Schutz, I. Schloffel, S. Batz, I. Takac, N. Weissmann, U. R. Michaelis, M. Koyanagi and R. P. Brandes (2011). "Hepatocyte growth factor induces a proangiogenic phenotype and mobilizes endothelial progenitor cells by activating Nox2." Antioxid Redox Signal **15**(4): 915-923.
Shono, S., Y. Habu, M. Nakashima, A. Sato, H. Nakashima, H. Miyazaki, M. Kinoshita, G. Tsumatori, N. Shinomiya and S. Seki (2011). "The immunologic outcome of enhanced function of mouse liver lymphocytes and Kupffer cells by high-fat and high-cholesterol diet." Shock **36**(5): 484-493.
Sieghart, W., D. Losert, S. Strommer, D. Cejka, K. Schmid, S. Rasoul-Rockenschaub, M. Bodingbauer, R. Crevenna, B. P. Monia, M. Peck-Radosavljevic and V. Wacheck (2006). "Mcl-1 overexpression in hepatocellular carcinoma: a potential target for antisense therapy." J Hepatol **44**(1): 151-157.
Starley, B. Q., C. J. Calcagno and S. A. Harrison (2010). "Nonalcoholic fatty liver disease and hepatocellular carcinoma: a weighty connection." Hepatology **51**(5): 1820-1832.

Stasia, M. J. (2016). "CYBA encoding p22(phox), the cytochrome b558 alpha polypeptide: gene structure, expression, role and physiopathology." Gene **586**(1): 27-35.
Stickel, F. and C. Hellerbrand (2010). "Non-alcoholic fatty liver disease as a risk factor for hepatocellular carcinoma: mechanisms and implications." Gut **59**(10): 1303-1307.
Sun, B. and M. Karin (2012). "Obesity, inflammation, and liver cancer." J Hepatol **56**(3): 704-713.
Takami, T., P. Kaposi-Novak, K. Uchida, L. E. Gomez-Quiroz, E. A. Conner, V. M. Factor and S. S. Thorgeirsson (2007). "Loss of hepatocyte growth factor/c-Met signaling pathway accelerates early stages of N-nitrosodiethylamine induced hepatocarcinogenesis." Cancer Res **67**(20): 9844-9851.
Tomoda, T., K. Nouso, K. Miyahara, S. Kobayashi, H. Kinugasa, J. Toyosawa, H. Hagihara, K. Kuwaki, H. Onishi, S. Nakamura, F. Ikeda, Y. Miyake, H. Shiraha, A. Takaki and K. Yamamoto (2013). "Prognotic impact of serum follistatin in patients with hepatocellular carcinoma." J Gastroenterol Hepatol **28**(8): 1391-1396.
Trapani, V. and F. I. Wolf (2019). "Dysregulation of Mg(2+) homeostasis contributes to acquisition of cancer hallmarks." Cell Calcium **83**: 102078.
Tsuchida, T., Y. A. Lee, N. Fujiwara, M. Ybanez, B. Allen, S. Martins, M. I. Fiel, N. Goossens, H. I. Chou, Y. Hoshida and S. L. Friedman (2018). "A simple diet- and chemical-induced murine NASH model with rapid progression of steatohepatitis, fibrosis and liver cancer." J Hepatol **69**(2): 385-395.
Usatyuk, P. V., P. Fu, V. Mohan, Y. Epshtein, J. R. Jacobson, J. Gomez-Cambronero, K. K. Wary, V. Bindokas, S. M. Dudek, R. Salgia, J. G. Garcia and V. Natarajan (2014). "Role of c-Met/phosphatidylinositol 3-kinase (PI3k)/Akt signaling in hepatocyte growth factor (HGF)-mediated lamellipodia formation, reactive oxygen species (ROS) generation, and motility of lung endothelial cells." J Biol Chem **289**(19): 13476-13491.
Valdes-Arzate, A., A. Luna, L. Bucio, C. Licona, D. L. Clemens, V. Souza, E. Hernandez, D. Kershenobich, M. C. Gutierrez-Ruiz and L. E. Gomez-Quiroz (2009). "Hepatocyte growth factor protects hepatocytes against oxidative injury induced by ethanol metabolism." Free Radic Biol Med **47**(4): 424-430.
Viticchie, G. and P. A. J. Muller (2015). "c-Met and Other Cell Surface Molecules: Interaction, Activation and Functional Consequences." Biomedicines **3**(1): 46-70.
Wang, X., M. C. DeFrances, Y. Dai, P. Pediaditakis, C. Johnson, A. Bell, G. K. Michalopoulos and R. Zarnegar (2002). "A mechanism of cell survival: sequestration of Fas by the HGF receptor Met." Mol Cell **9**(2): 411-421.
Wormann, S. M., L. Song, J. Ai, K. N. Diakopoulos, M. U. Kurkowski, K. Gorgulu, D. Ruess, A. Campbell, C. Doglioni, D. Jodrell, A. Neesse, I. E. Demir, A. P. Karpathaki, M. Barenboim, T. Hagemann, S. Rose-John, O. Sansom, R. M. Schmid, M. P. Protti, M. Lesina and H. Algul (2016). "Loss of P53 Function Activates JAK2-STAT3 Signaling to Promote Pancreatic Tumor Growth, Stroma Modification, and Gemcitabine Resistance in Mice and Is Associated With Patient Survival." Gastroenterology **151**(1): 180-193 e112.
Xu, F., S. D. Rychnovsky, J. D. Belani, H. H. Hobbs, J. C. Cohen and R. B. Rawson (2005). "Dual roles for cholesterol in mammalian cells." Proc Natl Acad Sci U S A **102**(41): 14551-14556.

Yang, Y., Y. C. Ye, Y. Chen, J. L. Zhao, C. C. Gao, H. Han, W. C. Liu and H. Y. Qin (2018). "Crosstalk between hepatic tumor cells and macrophages via Wnt/beta-catenin signaling promotes M2-like macrophage polarization and reinforces tumor malignant behaviors." Cell Death Dis **9**(8): 793.
Younes, R. and E. Bugianesi (2018). "Should we undertake surveillance for HCC in patients with NAFLD?" J Hepatol **68**(2): 326-334.
Younossi, Z. M., A. B. Koenig, D. Abdelatif, Y. Fazel, L. Henry and M. Wymer (2016). "Global epidemiology of nonalcoholic fatty liver disease-Meta-analytic assessment of prevalence, incidence, and outcomes." Hepatology **64**(1): 73-84.

Annexed I.

HGF/c-Met regulates p22^{phox} subunit of the NADPH oxidase complex in primary mouse hepatocytes by transcriptional and post-translational mechanisms.

Our group has proved that HGF and its receptor c-Met are regulators of cellular redox status in the liver (Kaposi-Novak, Lee et al. 2006), particularly regulating the activity of the multiprotein NADPH oxidase complex as we previously reported (Gomez-Quiroz, Factor et al. 2008, Clavijo-Cornejo, Enriquez-Cortina et al. 2013). In the present work, we were aimed to gain mechanistic information about this regulation. Previously, we observed a decrease in the content of the main protein components of the system induced by the signaling of HGF, mainly the p22^{phox} subunit encoded by *cyba* gene. p22^{phox} which is a conserved subunit in the different complexes of NADPH oxidase, (NOX1-4) (Lambeth 2004).

Figure 1A shows that HGF treatment in primary mouse hepatocytes significantly decreases the expression of *cyba* gene at 12 h of treatment, data consistent with our previous finding at the protein level. In order to gain mechanistic evidence of the *cyba* repression we constructed and cloned different *cyba* promoter sections (Figure 1B) by using the promotorless pmCherry vector. Figure 1C shows the different *cyba* promotor activity (judged by mCherry reporter fluorescence) induced by HGF treatment,

indicating that the segment A-E (-1 to -500 bp) owns the transcriptional repression of *cyba* gene, remaining segments of the promotor exhibited no changes.

Interestingly, this *cyba* promoter section contains a NF-κB (p65 subunit) consensus sequence determined by JASPAR software (Supplementary figure 1 and 2), it has been reported that NF-κB could exert gene repression in some genes (Cho, Min et al. 2006, Datta De, Datta et al. 2013).

In order to address whether the *cyba* transcriptional repression could be instigated by NF-κB we used the well-known specific NF-κB peptide inhibitor SN50 (Gomez-Quiroz, Factor et al. 2008), figure 2A shows that the decrement in the expression of the gene induced by HGF treatment is abrogated by the SN50, similar data were observed by the NF-κB chemical inhibitor sulfasalazine (Figure 2B). The decrement of the *cyba* gene is evaded by the inhibition of the transcription factor, clarifying that NF-κB drives the repressive activity exerted by HGF over the $p22^{phox}$ gene in hepatocytes.

To gain confidence we performed a competitive assay transfecting NF-κB consensus sequence (ODS) at high concentration (100 nM) in order to compete with natural sequence in the genome, figure 2C shows that NF-κB sequence abrogated the effect of HGF, confirming previous results obtained in figure 2A and B. As a control we used AP-1 transcription factor consensus sequence, which had no effect, corroborating the irrelevance of AP-1 in the repression of *cyba* in hepatocytes.

HGF induces proteasome 26S- dependent degradation of $p22^{phox}$

As we previously reported, HGF effect on *cyba* gene is also observed at the protein level at 12 h of treatment, addressed by both Western blot and immunofluorescence of

p22^{phox} (Figure 3A and B, respectively). The overlapping of *cyba* mRNA and p22^{phox} protein decrement at 12 h suggests different mechanism of regulation. Data suggest that the decrement in protein content is driven by a post-translational mechanism. Then, we decided to address the involvement of the proteasome 26S in degradation of p22^{phox}. Hepatocytes were pretreated with epox for 30 min, after that, cells were treated with HGF for 12 h, Figure 4 shows the decrement of p22^{phox}, determined by Western blot (Figure 4A) and IF (Figure 4B). To gain more confidence we studied the ubiquitination of p22^{phox} induced by HGF treatment. Figure 4C shows that ubiquitination of the protein was time-dependent manner, peaking at 12 h of treatment.

c-Met interacts with p22^{phox}

It has been reported the peculiar mechanism of regulation exerted by c-Met over some key membrane proteins such as FAS (Wang, DeFrances et al. 2002), plexin B1, CD44, among others (Viticchie and Muller 2015), by physical interaction each other. We explored the possible interaction between c-Met and p22^{phox} by IP, identifying an interaction between both proteins at basal levels (NT) being stable up to 30 min after treatment with HGF, presenting a decrease in the interaction at later times, reaching its maximum point at 60 min (Figure 5A). To validate these results, we performed the reverse IP (Figure 5B) corroborating the interaction of both proteins and its decrement at 60 min. To gain further insight into the mechanism of c-Met-p22^{phox} interaction or association, chemical crosslinking was performed. Hepatocytes culture was subjected to the cell-impermeable thiol-cleavable crosslinking agent DSSTP, which only crosslinks proteins on the extracellular space and previously proved in other c-Met interactions (Wang, DeFrances et al. 2002). Figure 5C shows the detection of a strong

band consisting of c-Met plus $p22^{phox}$, in the not treated cells (basal interaction) which was decreased with HGF treatment for 60 min. The use of DTT as agent of crosslinking reversion, induced the disappearance of such band indicating that the band was product of the crosslinking. No detectable bands were observed by using the cell-permeable DSP crosslinker agent (Figure 5D) clearly indicating that c-Met and $p22^{phox}$ interaction is on the cell membrane.

Interestingly, we could not identify the interaction of c-Met and $p22^{phox}$ by regular immuno-colocalization using fluorescence antibodies. The first antibody used impeded the attachment of the second one (data not shown), we decided to construct plasmids encoding sequences for the production of chimeric proteins coupled to fluorescence markers eCFP/$p22^{phox}$ and eYFP/c-Met, as stated under material and methods section. HepG2 cells were co-transfected with both plasmids and after verification of proper production of fluorescent proteins, were treated with HGF. Figure 6A shows the basal co-localization (green fluorescence, arrows) in no treated cells, which disappears after 60 min of HGF treatment, confirming the c-Met and $p22^{phox}$ interaction.

We selected eCFP/$p22^{phox}$ and eYFP/c-Met because both fluorescent proteins allow FRET studies. Figure 6B shows the percentage of FRET efficiency in a time course study, where significant change was observed since 30 min and peaked at 60 min, confirming the IP and crosslinking results in figure 5.

Finally, the ROS content in hepatocytes treated with TGF-β, pretreated or not with HGF was addressed. Figure 7 shows that TGF-β increases ROS production, judged by DHE fluorescence, and the treatment with HGF significantly decreased the content of ROS,

indicating that $p22^{phox}$ repression certainly decreases ROS derived from NADPH oxidase, as previously we published (Clavijo-Cornejo, Enriquez-Cortina et al. 2013).

Discussion

We have previously published that HGF/c-Met is key regulator of cellular redox status and oxidative stress in many systems such as liver (Kaposi-Novak, Lee et al. 2006, Gomez-Quiroz, Seo et al. 2016), pancreas (Palestino-Dominguez, Pelaez-Luna et al. 2018), lungs (Bello-Monroy, Mata-Espinosa et al. 2020), biliary tree(Salas-Silva, Simoni-Nieves et al. 2020), among others. Particularly, in the liver, HGF/c-Met has demonstrated to influence the initiation, progression or treatment of alcoholic liver disease (Valdes-Arzate, Luna et al. 2009), cholestasis (Salas-Silva, Simoni-Nieves et al. 2020), hepatocellular carcinoma (Kaposi-Novak, Lee et al. 2006, Takami, Kaposi-Novak et al. 2007), fibrosis (Marquardt, Seo et al. 2012) , drug-induced liver injury (Enriquez-Cortina, Almonte-Becerril et al. 2013, Bello-Monroy, Mata-Espinosa et al. 2020), and NASH (Dominguez-Perez, Nuno-Lambarri et al. 2016, Gomez-Quiroz, Seo et al. 2016). Data published have provided mechanistic insights indicating that HGF/c-Met could exert these antioxidant/protective responses by multiples mechanisms, such as the activation of antioxidant-related transcription factors such as Nrf2 or NF-κB which, in addition express antioxidant enzymes like catalase, superoxide dismutase 1 and 2, and glutathione-related enzymes (Gomez-Quiroz, Factor et al. 2008, Valdes-Arzate, Luna et al. 2009). Another mechanism of action is directed to eliminate

xenobiotics, which are potentially inducers of oxidative stress as we recently reported in cholestasis (Salas-Silva, Simoni-Nieves et al. 2020).

In the present work we are characterizing another mechanism of antioxidant action elicited by HGF/c-Met, which is directed to control the ROS-generating systems driven by the NADPH oxidases. The conserved membrane-resident component of the NADPH oxidases $p22^{phox}$, which is used by at least four complexes (NADPH oxidase 1-4), is particularly affected by HGF signaling, as we previously reported in wild-type primary mouse hepatocytes (Clavijo-Cornejo, Enriquez-Cortina et al. 2013) and in c-Met KO hepatocytes, where we observed a profound oxidative stress in untreated hepatocytes. In fact, this ROS control is key component of the HGF/c-Met signature defining an new aggressive phenotype tumor subtype with poor prognosis as we previously reported (Kaposi-Novak, Lee et al. 2006, Takami, Kaposi-Novak et al. 2007).

Previously we showed the downregulation of some components of the NADPH oxidase by HGF signaling, including the catalytic subunit Nox2; contrary, in c-Met KO hepatocytes we observed the over activation of the enzyme and a prominent oxidative stress (Kaposi-Novak, Lee et al. 2006). Although, we reported that HGF exerts gene expression repression in NADPH oxidase components, in the present work we found that NF-κB is part of the gene repression machinery since the inhibition of its activity abolished the downregulation of $p22^{phox}$ maintaining basal protein content (Figure 2), suggesting that this transcription factor is key regulator of the NADPH oxidase, since abrogation was not complete. NF-κB consensus sequence was identified downstream near to the transcription start site. Our current data support previous works reporting a

profound effects induced by HGF in downregulation of NADPH oxidase at the transcriptional level, we have now advanced in the knowledge pointing out the relevance of NF-κB in the repressive stimulus of the pro-oxidant systems and in the expression of antioxidant and protective machinery (Gomez-Quiroz, Factor et al. 2008, Valdes-Arzate, Luna et al. 2009).

The second mechanism of HGF/c-Met-mediated regulation of NADPH oxidase, particularly in $p22^{phox}$, is post-translational. In this case, data show a fast decrease in the $p22^{phox}$ content since 3 h of HGF treatment in primary mouse hepatocytes. This effect continued in a time-dependent manner peaking at 12 h (Clavijo-Cornejo, Enriquez-Cortina et al. 2013), so we decided to explore whether this effect could be related to $p22^{phox}$ degradation by proteosome 26S. Our results clearly indicate the polyubiquitination of $p22^{phox}$ induced by HGF, epox, inhibitor of the proteasome activity, avoided the degradation of the target protein. Data suggest that ubiquitin/proteasome 26S system is key determinant in NADPH oxidase activity, recently it has been published that perturbation of ubiquitin homeostasis led to a rapid and transient ROS generation in macrophages cell line (Charbonneau, Passalacqua et al. 2019), supporting this mechanism of regulation of the system, at least partially characterized in hepatocytes in terms of $p22^{phox}$ regulatory subunit.

The relevance of $p22^{phox}$ goes beyond of being a simple scaffolding protein, it displays regulatory functions, particularly at the level of $p47^{phox}$ (Stasia 2016), in fact some polymorphism has been identified in *cyba* resulting in a significant risk factor for

coronary artery disease (Nowak, Niemiec et al. 2018), but the relationship of this polymorphisms remains uncharacterized in liver diseases.

The physical interaction of c-Met with multiple membrane proteins has been positioned as a key regulatory mechanism (Viticchie and Muller 2015). It is particularly relevant the interaction or sequestration with FAS, which is a remarkable mechanism of HGF-induced anti-apoptosis response (Wang, DeFrances et al. 2002), in addition, c-Met interacts with CD44 (Orian-Rousseau, Chen et al. 2002) acting each other as coactivators of signaling; plexin B1 (Conrotto, Corso et al. 2004) is another membrane protein that interacts with c-Met, in this case antagonizing each other (Conrotto, Corso et al. 2004). Our research provides evidence that c-Met is capable to interact with $p22^{phox}$ and repress the NADPH oxidase activity, at least partially, as we previously published (Clavijo-Cornejo, Enriquez-Cortina et al. 2013) and supported in this work (Figure 5 and 6). In addition, we are reporting that this interaction is intracellular, and after HGF treatment this protein-protein binding is lost, judged by FRET analysis, in order to increase ROS production at early times, for Nrf2 signaling (Clavijo-Cornejo, Enriquez-Cortina et al. 2013).

The relationship of HGF/c-Met and NADPH oxidase has been corroborated by another mechanism, the control of Rac1, a prominent regulator of the oxidase. Ozaki and collaborators proved that HGF and its canonical signaling mediated by PI3K/Akt is necessary and sufficient to suppress intracellular ROS generation and apoptosis by inhibiting Rac1 in a model of hypoxia/reoxygenation in the liver (Ozaki, Haga et al. 2003), supporting the broad range of action induced by HGF on the modulation of cellular redox state driven by NADPH oxidase in the liver.

This regulation has been observed in other cell types. It has been reported that HGF increases the NADPH oxidase-mediated ROS formation in endothelial progenitor cells and in human umbilical vein cells, thereby inducing cell migration and angiogenesis, a phenomenon not observed in NOX2-deficient cells (Schroder, Schutz et al. 2011). Similar findings have been found in the lung endothelial cells, where c-Met signaling induced the NADPH oxidase activation particularly in motile cells; this effect was mediated by $p47^{phox}$, cortactin, and Rac1 translocation to lamellipodia. The NADPH oxidase inhibition by apocynin, or the siRNA-mediated inactivation of $p47^{phox}$, or cortactin, significantly decreased the lamellipodia formation and cell migration promoted by HGF (Usatyuk, Fu et al. 2014).

Conclusion

In conclusion, in the present work we gained mechanistic evidence regarding the regulation of the NADPH oxidase by HGF/c-Met, particularly interfering with the regulatory subunit $p22^{phox}$ that supports the previous relevant physiological findings in many liver diseases (Supplementary figure 3), and this positions the axis HGF/c-Met/NADPH oxidase/ROS as a key mechanism of HGF singling in the liver.

References

Agarwal, S., M. Behring, K. Hale, S. Al Diffalha, K. Wang, U. Manne and S. Varambally (2019). "MTHFD1L, A Folate Cycle Enzyme, Is Involved in Progression of Colorectal Cancer." Transl Oncol **12**(11): 1461-1467.
Armstrong, M. J. and G. Marchesini (2019). "Referral pathways for NAFLD fibrosis in primary care - No longer a 'needle in a haystack'." J Hepatol **71**(2): 246-248.
Asgharpour, A., S. C. Cazanave, T. Pacana, M. Seneshaw, R. Vincent, B. A. Banini, D. P. Kumar, K. Daita, H. K. Min, F. Mirshahi, P. Bedossa, X. Sun, Y. Hoshida, S. V. Koduru, D. Contaifer, Jr., U. O. Warncke, D. S. Wijesinghe and A. J. Sanyal (2016). "A diet-induced animal model of non-alcoholic fatty liver disease and hepatocellular cancer." J Hepatol **65**(3): 579-588.
Baffy, G., E. M. Brunt and S. H. Caldwell (2012). "Hepatocellular carcinoma in non-alcoholic fatty liver disease: an emerging menace." J Hepatol **56**(6): 1384-1391.
Bao, D., J. Zhao, X. Zhou, Q. Yang, Y. Chen, J. Zhu, P. Yuan, J. Yang, T. Qin, S. Wan and J. Xing (2019). "Mitochondrial fission-induced mtDNA stress promotes tumor-associated macrophage infiltration and HCC progression." Oncogene **38**(25): 5007-5020.
Bello-Monroy, O., D. Mata-Espinosa, C. Enriquez-Cortina, V. Souza, R. U. Miranda, L. Bucio, J. Barrios-Payan, B. Marquina-Castillo, I. Rodriguez-Ochoa, P. Rosales, M. C. Gutierrez-Ruiz, R. Hernandez-Pando and L. E. Gomez-Quiroz (2020). "Hepatocyte growth factor enhances the clearance of a multidrug-resistant Mycobacterium tuberculosis strain by high doses of conventional chemotherapy, preserving liver function." J Cell Physiol **235**(2): 1637-1648.
Bhaskaran, K., I. Douglas, H. Forbes, I. dos-Santos-Silva, D. A. Leon and L. Smeeth (2014). "Body-mass index and risk of 22 specific cancers: a population-based cohort study of 5.24 million UK adults." Lancet **384**(9945): 755-765.
Bowe, A., S. Zweerink, V. Muck, V. Kondylis, S. Schulte, T. Goeser and D. Nierhoff (2018). "Depolarized Hepatocytes Express the Stem/Progenitor Cell Marker Neighbor of Punc E11 After Bile Duct Ligation in Mice." J Histochem Cytochem **66**(8): 563-576.
Bugianesi, E., R. Marzocchi, N. Villanova and G. Marchesini (2004). "Non-alcoholic fatty liver disease/non-alcoholic steatohepatitis (NAFLD/NASH): treatment." Best Pract Res Clin Gastroenterol **18**(6): 1105-1116.
Calvisi, D. F., C. Wang, C. Ho, S. Ladu, S. A. Lee, S. Mattu, G. Destefanis, S. Delogu, A. Zimmermann, J. Ericsson, S. Brozzetti, T. Staniscia, X. Chen, F. Dombrowski and M. Evert (2011). "Increased lipogenesis, induced by AKT-mTORC1-RPS6 signaling, promotes development of human hepatocellular carcinoma." Gastroenterology **140**(3): 1071-1083.
Castven, D., D. Becker, C. Czauderna, D. Wilhelm, J. B. Andersen, S. Strand, M. Hartmann, S. Heilmann-Heimbach, W. Roth, N. Hartmann, B. K. Straub, F. L. Mahn, S. Franck, S. Pereira, A. Haupts, A. Vogel, M. A. Worns, A. Weinmann, S. Heinrich, H. Lang, S. S. Thorgeirsson, P. R. Galle and J. U. Marquardt (2019). "Application of patient-derived liver cancer cells for phenotypic characterization and therapeutic target identification." Int J Cancer **144**(11): 2782-2794.
Charbonneau, M. E., K. D. Passalacqua, S. E. Hagen, H. D. Showalter, C. E. Wobus and M. X. D. O'Riordan (2019). "Perturbation of ubiquitin homeostasis promotes macrophage oxidative defenses." Sci Rep **9**(1): 10245.
Che, L., P. Paliogiannis, A. Cigliano, M. G. Pilo, X. Chen and D. F. Calvisi (2019). "Pathogenetic, Prognostic, and Therapeutic Role of Fatty Acid Synthase in Human Hepatocellular Carcinoma." Front Oncol **9**: 1412.

Cho, M. L., S. Y. Min, S. H. Chang, K. W. Kim, S. B. Heo, S. H. Lee, S. H. Park, C. S. Cho and H. Y. Kim (2006). "Transforming growth factor beta 1(TGF-beta1) down-regulates TNFalpha-induced RANTES production in rheumatoid synovial fibroblasts through NF-kappaB-mediated transcriptional repression." Immunol Lett **105**(2): 159-166.
Clavijo-Cornejo, D., C. Enriquez-Cortina, A. Lopez-Reyes, M. Dominguez-Perez, N. Nuno, M. Dominguez-Meraz, L. Bucio, V. Souza, V. M. Factor, S. S. Thorgeirsson, M. C. Gutierrez-Ruiz and L. E. Gomez-Quiroz (2013). "Biphasic regulation of the NADPH oxidase by HGF/c-Met signaling pathway in primary mouse hepatocytes." Biochimie **95**(6): 1177-1184.
Coleman, S. J., R. P. Grose and H. M. Kocher (2014). "Fibroblast growth factor family as a potential target in the treatment of hepatocellular carcinoma." J Hepatocell Carcinoma **1**: 43-54.
Conrotto, P., S. Corso, S. Gamberini, P. M. Comoglio and S. Giordano (2004). "Interplay between scatter factor receptors and B plexins controls invasive growth." Oncogene **23**(30): 5131-5137.
Coulouarn, C., L. E. Gomez-Quiroz, J. S. Lee, P. Kaposi-Novak, E. A. Conner, T. A. Goldina, G. E. Onishchenko, V. M. Factor and S. S. Thorgeirsson (2006). "Oncogene-specific gene expression signatures at preneoplastic stage in mice define distinct mechanisms of hepatocarcinogenesis." Hepatology **44**(4): 1003-1011.
Cronin, K. A., A. J. Lake, S. Scott, R. L. Sherman, A. M. Noone, N. Howlader, S. J. Henley, R. N. Anderson, A. U. Firth, J. Ma, B. A. Kohler and A. Jemal (2018). "Annual Report to the Nation on the Status of Cancer, part I: National cancer statistics." Cancer **124**(13): 2785-2800.
Datta De, D., A. Datta, S. Bhattacharjya and S. Roychoudhury (2013). "NF-kappaB mediated transcriptional repression of acid modifying hormone gastrin." PLoS One **8**(8): e73409.
Deng, X., F. Xiong, X. Li, B. Xiang, Z. Li, X. Wu, C. Guo, X. Li, Y. Li, G. Li, W. Xiong and Z. Zeng (2018). "Application of atomic force microscopy in cancer research." J Nanobiotechnology **16**(1): 102.
Dominguez-Perez, M., N. Nuno-Lambarri, D. Clavijo-Cornejo, A. Luna-Lopez, V. Souza, L. Bucio, R. U. Miranda, L. Munoz, L. E. Gomez-Quiroz, S. Uribe-Carvajal and M. C. Gutierrez-Ruiz (2016). "Hepatocyte Growth Factor Reduces Free Cholesterol-Mediated Lipotoxicity in Primary Hepatocytes by Countering Oxidative Stress." Oxid Med Cell Longev **2016**: 7960386.
Dominguez-Perez, M., A. Simoni-Nieves, P. Rosales, N. Nuno-Lambarri, M. Rosas-Lemus, V. Souza, R. U. Miranda, L. Bucio, S. Uribe Carvajal, J. U. Marquardt, D. Seo, L. E. Gomez-Quiroz and M. C. Gutierrez-Ruiz (2019). "Cholesterol burden in the liver induces mitochondrial dynamic changes and resistance to apoptosis." J Cell Physiol **234**(5): 7213-7223.
Enriquez-Cortina, C., M. Almonte-Becerril, D. Clavijo-Cornejo, M. Palestino-Dominguez, O. Bello-Monroy, N. Nuno, A. Lopez, L. Bucio, V. Souza, R. Hernandez-Pando, L. Munoz, M. C. Gutierrez-Ruiz and L. E. Gomez-Quiroz (2013). "Hepatocyte growth factor protects against isoniazid/rifampicin-induced oxidative liver damage." Toxicol Sci **135**(1): 26-36.
Enriquez-Cortina, C., O. Bello-Monroy, P. Rosales-Cruz, V. Souza, R. U. Miranda, R. Toledo-Perez, A. Luna-Lopez, A. Simoni-Nieves, R. Hernandez-Pando, M. C. Gutierrez-Ruiz, D. F. Calvisi, J. U. Marquardt, L. Bucio and L. E. Gomez-Quiroz (2017). "Cholesterol overload in the liver aggravates oxidative stress-mediated DNA damage and accelerates hepatocarcinogenesis." Oncotarget **8**(61): 104136-104148.
Furuhashi, M. and G. S. Hotamisligil (2008). "Fatty acid-binding proteins: role in metabolic diseases and potential as drug targets." Nat Rev Drug Discov **7**(6): 489-503.

Garcia-Ruiz, C., L. Conde de la Rosa, V. Ribas and J. C. Fernandez-Checa (2020). "Mitochondrial Cholesterol and Cancer." Semin Cancer Biol.
Garcia-Ruiz, C., L. C. de la Rosa, V. Ribas and J. C. Fernandez-Checa (2020). "Mitochondrial Cholesterol and Cancer." Semin Cancer Biol.
Gerardo-Ramirez, M., R. Lazzarini-Lechuga, S. Hernandez-Rizo, J. E. Jimenez-Salazar, A. Simoni-Nieves, C. Garcia-Ruiz, J. C. Fernandez-Checa, J. U. Marquardt, C. Coulouarn, M. C. Gutierrez-Ruiz, B. Perez-Aguilar and L. E. Gomez-Quiroz (2019). "GDF11 exhibits tumor suppressive properties in hepatocellular carcinoma cells by restricting clonal expansion and invasion." Biochim Biophys Acta Mol Basis Dis **1865**(6): 1540-1554.
Gomez-Quiroz, L. E., V. M. Factor, P. Kaposi-Novak, C. Coulouarn, E. A. Conner and S. S. Thorgeirsson (2008). "Hepatocyte-specific c-Met deletion disrupts redox homeostasis and sensitizes to Fas-mediated apoptosis." J Biol Chem **283**(21): 14581-14589.
Gomez-Quiroz, L. E., D. Seo, Y. H. Lee, M. Kitade, T. Gaiser, M. Gillen, S. B. Lee, M. C. Gutierrez-Ruiz, E. A. Conner, V. M. Factor, S. S. Thorgeirsson and J. U. Marquardt (2016). "Loss of c-Met signaling sensitizes hepatocytes to lipotoxicity and induces cholestatic liver damage by aggravating oxidative stress." Toxicology **361-362**: 39-48.
Goossens, P., J. Rodriguez-Vita, A. Etzerodt, M. Masse, O. Rastoin, V. Gouirand, T. Ulas, O. Papantonopoulou, M. Van Eck, N. Auphan-Anezin, M. Bebien, C. Verthuy, T. P. Vu Manh, M. Turner, M. Dalod, J. L. Schultze and T. Lawrence (2019). "Membrane Cholesterol Efflux Drives Tumor-Associated Macrophage Reprogramming and Tumor Progression." Cell Metab **29**(6): 1376-1389 e1374.
Grohmann, M., F. Wiede, G. T. Dodd, E. N. Gurzov, G. J. Ooi, T. Butt, A. A. Rasmiena, S. Kaur, T. Gulati, P. K. Goh, A. E. Treloar, S. Archer, W. A. Brown, M. Muller, M. J. Watt, O. Ohara, C. A. McLean and T. Tiganis (2018). "Obesity Drives STAT-1-Dependent NASH and STAT-3-Dependent HCC." Cell **175**(5): 1289-1306 e1220.
He, Z., X. Wang, H. Zhang, B. Liang, J. Zhang, Z. Zhang and Y. Yang (2020). "High expression of folate cycle enzyme MTHFD1L correlates with poor prognosis and increased proliferation and migration in colorectal cancer." J Cancer **11**(14): 4213-4221.
Huang, D. Q., H. B. El-Serag and R. Loomba (2020). "Global epidemiology of NAFLD-related HCC: trends, predictions, risk factors and prevention." Nat Rev Gastroenterol Hepatol.
Imhof, B. A. and M. Aurrand-Lions (2006). "Angiogenesis and inflammation face off." Nat Med **12**(2): 171-172.
Kaposi-Novak, P., J. S. Lee, L. Gomez-Quiroz, C. Coulouarn, V. M. Factor and S. S. Thorgeirsson (2006). "Met-regulated expression signature defines a subset of human hepatocellular carcinomas with poor prognosis and aggressive phenotype." J Clin Invest **116**(6): 1582-1595.
Lambeth, J. D. (2004). "NOX enzymes and the biology of reactive oxygen." Nat Rev Immunol **4**(3): 181-189.
Lee, D., I. M. Xu, D. K. Chiu, R. K. Lai, A. P. Tse, L. Lan Li, C. T. Law, F. H. Tsang, L. L. Wei, C. Y. Chan, C. M. Wong, I. O. Ng and C. C. Wong (2017). "Folate cycle enzyme MTHFD1L confers metabolic advantages in hepatocellular carcinoma." J Clin Invest **127**(5): 1856-1872.
Lee, J. S., I. S. Chu, J. Heo, D. F. Calvisi, Z. Sun, T. Roskams, A. Durnez, A. J. Demetris and S. S. Thorgeirsson (2004). "Classification and prediction of survival in hepatocellular carcinoma by gene expression profiling." Hepatology **40**(3): 667-676.

Lee, J. S., I. S. Chu, A. Mikaelyan, D. F. Calvisi, J. Heo, J. K. Reddy and S. S. Thorgeirsson (2004). "Application of comparative functional genomics to identify best-fit mouse models to study human cancer." Nat Genet **36**(12): 1306-1311.
Lee, J. S., J. Heo, L. Libbrecht, I. S. Chu, P. Kaposi-Novak, D. F. Calvisi, A. Mikaelyan, L. R. Roberts, A. J. Demetris, Z. Sun, F. Nevens, T. Roskams and S. S. Thorgeirsson (2006). "A novel prognostic subtype of human hepatocellular carcinoma derived from hepatic progenitor cells." Nat Med **12**(4): 410-416.
Lee, L., M. Alloosh, R. Saxena, W. Van Alstine, B. A. Watkins, J. E. Klaunig, M. Sturek and N. Chalasani (2009). "Nutritional model of steatohepatitis and metabolic syndrome in the Ossabaw miniature swine." Hepatology **50**(1): 56-67.
Liang, F., C. Ren, J. Wang, S. Wang, L. Yang, X. Han, Y. Chen, G. Tong and G. Yang (2019). "The crosstalk between STAT3 and p53/RAS signaling controls cancer cell metastasis and cisplatin resistance via the Slug/MAPK/PI3K/AKT-mediated regulation of EMT and autophagy." Oncogenesis **8**(10): 59.
Liu, D., C. C. Wong, L. Fu, H. Chen, L. Zhao, C. Li, Y. Zhou, Y. Zhang, W. Xu, Y. Yang, B. Wu, G. Cheng, P. B. Lai, N. Wong, J. J. Y. Sung and J. Yu (2018). "Squalene epoxidase drives NAFLD-induced hepatocellular carcinoma and is a pharmaceutical target." Sci Transl Med **10**(437).
Liu, Z., D. Chen, F. Ning, J. Du and H. Wang (2018). "EGF is highly expressed in hepatocellular carcinoma (HCC) and promotes motility of HCC cells via fibronectin." J Cell Biochem **119**(5): 4170-4183.
Lonardo, A., S. Leoni, K. A. Alswat and Y. Fouad (2020). "History of Nonalcoholic Fatty Liver Disease." Int J Mol Sci **21**(16).
Marchesini, G., A. Suppini and G. Forlani (2005). "NAFLD treatment: cognitive-behavioral therapy has entered the arena." J Hepatol **43**(6): 926-928.
Mari, M., F. Caballero, A. Colell, A. Morales, J. Caballeria, A. Fernandez, C. Enrich, J. C. Fernandez-Checa and C. Garcia-Ruiz (2006). "Mitochondrial free cholesterol loading sensitizes to TNF- and Fas-mediated steatohepatitis." Cell Metab **4**(3): 185-198.
Marquardt, J. U., M. Quasdorff, H. Varnholt, H. M. Curth, S. Mesghenna, U. Protzer, T. Goeser and D. Nierhoff (2011). "Neighbor of Punc E11, a novel oncofetal marker for hepatocellular carcinoma." Int J Cancer **128**(10): 2353-2363.
Marquardt, J. U., D. Seo, L. E. Gomez-Quiroz, K. Uchida, M. C. Gillen, M. Kitade, P. Kaposi-Novak, E. A. Conner, V. M. Factor and S. S. Thorgeirsson (2012). "Loss of c-Met accelerates development of liver fibrosis in response to CCl(4) exposure through deregulation of multiple molecular pathways." Biochim Biophys Acta **1822**(6): 942-951.
Massoud, O. and M. Charlton (2018). "Nonalcoholic Fatty Liver Disease/Nonalcoholic Steatohepatitis and Hepatocellular Carcinoma." Clin Liver Dis **22**(1): 201-211.
Mastrototaro, L., A. Smorodchenko, J. R. Aschenbach, M. Kolisek and G. Sponder (2016). "Solute carrier 41A3 encodes for a mitochondrial Mg(2+) efflux system." Sci Rep **6**: 27999.
Maxfield, F. R. and G. van Meer (2010). "Cholesterol, the central lipid of mammalian cells." Curr Opin Cell Biol **22**(4): 422-429.
Min, H. K., F. Mirshahi, A. Verdianelli, T. Pacana, V. Patel, C. G. Park, A. Choi, J. H. Lee, C. B. Park, S. Ren and A. J. Sanyal (2015). "Activation of the GP130-STAT3 axis and its potential implications in nonalcoholic fatty liver disease." Am J Physiol Gastrointest Liver Physiol **308**(9): G794-803.

Niu, G., K. L. Wright, Y. Ma, G. M. Wright, M. Huang, R. Irby, J. Briggs, J. Karras, W. D. Cress, D. Pardoll, R. Jove, J. Chen and H. Yu (2005). "Role of Stat3 in regulating p53 expression and function." Mol Cell Biol **25**(17): 7432-7440.
Nowak, T., P. Niemiec, T. Iwanicki, A. Balcerzyk, J. Krauze, A. Ochalska-Tyka and I. Zak (2018). "Analysis of selected promoter polymorphisms and haplotypes of the CYBA gene encoding the p22phox, subunit of NADPH oxidases, in patients with coronary artery disease." Free Radic Res **52**(10): 1132-1139.
Ohata, T., H. Yokoo, T. Kamiyama, M. Fukai, T. Aiyama, Y. Hatanaka, K. Hatanaka, K. Wakayama, T. Orimo, T. Kakisaka, N. Kobayashi, Y. Matsuno and A. Taketomi (2017). "Fatty acid-binding protein 5 function in hepatocellular carcinoma through induction of epithelial-mesenchymal transition." Cancer Med **6**(5): 1049-1061.
Orian-Rousseau, V., L. Chen, J. P. Sleeman, P. Herrlich and H. Ponta (2002). "CD44 is required for two consecutive steps in HGF/c-Met signaling." Genes Dev **16**(23): 3074-3086.
Ozaki, M., S. Haga, H. Q. Zhang, K. Irani and S. Suzuki (2003). "Inhibition of hypoxia/reoxygenation-induced oxidative stress in HGF-stimulated antiapoptotic signaling: role of PI3-K and Akt kinase upon rac1." Cell Death Differ **10**(5): 508-515.
Palestino-Dominguez, M., M. Pelaez-Luna, R. Lazzarini-Lechuga, I. Rodriguez-Ochoa, V. Souza, R. U. Miranda, B. Perez-Aguilar, L. Bucio, J. U. Marquardt, L. E. Gomez-Quiroz and M. C. Gutierrez-Ruiz (2018). "Recombinant human hepatocyte growth factor provides protective effects in cerulein-induced acute pancreatitis in mice." J Cell Physiol **233**(12): 9354-9364.
Pike, S. T., R. Rajendra, K. Artzt and D. R. Appling (2010). "Mitochondrial C1-tetrahydrofolate synthase (MTHFD1L) supports the flow of mitochondrial one-carbon units into the methyl cycle in embryos." J Biol Chem **285**(7): 4612-4620.
Rebouissou, S., M. Amessou, G. Couchy, K. Poussin, S. Imbeaud, C. Pilati, T. Izard, C. Balabaud, P. Bioulac-Sage and J. Zucman-Rossi (2009). "Frequent in-frame somatic deletions activate gp130 in inflammatory hepatocellular tumours." Nature **457**(7226): 200-204.
Ribas, V., C. Garcia-Ruiz and J. C. Fernandez-Checa (2016). "Mitochondria, cholesterol and cancer cell metabolism." Clin Transl Med **5**(1): 22.
Sainz-Perez, A., H. Gary-Gouy, F. Gaudin, G. Maarof, A. Marfaing-Koka, T. de Revel and A. Dalloul (2008). "IL-24 induces apoptosis of chronic lymphocytic leukemia B cells engaged into the cell cycle through dephosphorylation of STAT3 and stabilization of p53 expression." J Immunol **181**(9): 6051-6060.
Salas-Silva, S., A. Simoni-Nieves, M. V. Razori, J. Lopez-Ramirez, J. Barrera-Chimal, R. Lazzarini, O. Bello, V. Souza, R. U. Miranda-Labra, M. C. Gutierrez-Ruiz, L. E. Gomez-Quiroz, M. G. Roma and L. Bucio-Ortiz (2020). "HGF induces protective effects in alpha-naphthylisothiocyanate-induced intrahepatic cholestasis by counteracting oxidative stress." Biochem Pharmacol **174**: 113812.
Sanches, S. C., L. N. Ramalho, M. J. Augusto, D. M. da Silva and F. S. Ramalho (2015). "Nonalcoholic Steatohepatitis: A Search for Factual Animal Models." Biomed Res Int **2015**: 574832.
Sanyal, A. J. (2019). "Past, present and future perspectives in nonalcoholic fatty liver disease." Nat Rev Gastroenterol Hepatol **16**(6): 377-386.
Schlageter, M., L. M. Terracciano, S. D'Angelo and P. Sorrentino (2014). "Histopathology of hepatocellular carcinoma." World J Gastroenterol **20**(43): 15955-15964.

Schroder, K., S. Schutz, I. Schloffel, S. Batz, I. Takac, N. Weissmann, U. R. Michaelis, M. Koyanagi and R. P. Brandes (2011). "Hepatocyte growth factor induces a proangiogenic phenotype and mobilizes endothelial progenitor cells by activating Nox2." Antioxid Redox Signal **15**(4): 915-923.
Shono, S., Y. Habu, M. Nakashima, A. Sato, H. Nakashima, H. Miyazaki, M. Kinoshita, G. Tsumatori, N. Shinomiya and S. Seki (2011). "The immunologic outcome of enhanced function of mouse liver lymphocytes and Kupffer cells by high-fat and high-cholesterol diet." Shock **36**(5): 484-493.
Sieghart, W., D. Losert, S. Strommer, D. Cejka, K. Schmid, S. Rasoul-Rockenschaub, M. Bodingbauer, R. Crevenna, B. P. Monia, M. Peck-Radosavljevic and V. Wacheck (2006). "Mcl-1 overexpression in hepatocellular carcinoma: a potential target for antisense therapy." J Hepatol **44**(1): 151-157.
Stasia, M. J. (2016). "CYBA encoding p22(phox), the cytochrome b558 alpha polypeptide: gene structure, expression, role and physiopathology." Gene **586**(1): 27-35.
Stickel, F. and C. Hellerbrand (2010). "Non-alcoholic fatty liver disease as a risk factor for hepatocellular carcinoma: mechanisms and implications." Gut **59**(10): 1303-1307.
Sun, B. and M. Karin (2012). "Obesity, inflammation, and liver cancer." J Hepatol **56**(3): 704-713.
Takami, T., P. Kaposi-Novak, K. Uchida, L. E. Gomez-Quiroz, E. A. Conner, V. M. Factor and S. S. Thorgeirsson (2007). "Loss of hepatocyte growth factor/c-Met signaling pathway accelerates early stages of N-nitrosodiethylamine induced hepatocarcinogenesis." Cancer Res **67**(20): 9844-9851.
Tomoda, T., K. Nouso, K. Miyahara, S. Kobayashi, H. Kinugasa, J. Toyosawa, H. Hagihara, K. Kuwaki, H. Onishi, S. Nakamura, F. Ikeda, Y. Miyake, H. Shiraha, A. Takaki and K. Yamamoto (2013). "Prognotic impact of serum follistatin in patients with hepatocellular carcinoma." J Gastroenterol Hepatol **28**(8): 1391-1396.
Trapani, V. and F. I. Wolf (2019). "Dysregulation of Mg(2+) homeostasis contributes to acquisition of cancer hallmarks." Cell Calcium **83**: 102078.
Tsuchida, T., Y. A. Lee, N. Fujiwara, M. Ybanez, B. Allen, S. Martins, M. I. Fiel, N. Goossens, H. I. Chou, Y. Hoshida and S. L. Friedman (2018). "A simple diet- and chemical-induced murine NASH model with rapid progression of steatohepatitis, fibrosis and liver cancer." J Hepatol **69**(2): 385-395.
Usatyuk, P. V., P. Fu, V. Mohan, Y. Epshtein, J. R. Jacobson, J. Gomez-Cambronero, K. K. Wary, V. Bindokas, S. M. Dudek, R. Salgia, J. G. Garcia and V. Natarajan (2014). "Role of c-Met/phosphatidylinositol 3-kinase (PI3k)/Akt signaling in hepatocyte growth factor (HGF)-mediated lamellipodia formation, reactive oxygen species (ROS) generation, and motility of lung endothelial cells." J Biol Chem **289**(19): 13476-13491.
Valdes-Arzate, A., A. Luna, L. Bucio, C. Licona, D. L. Clemens, V. Souza, E. Hernandez, D. Kershenobich, M. C. Gutierrez-Ruiz and L. E. Gomez-Quiroz (2009). "Hepatocyte growth factor protects hepatocytes against oxidative injury induced by ethanol metabolism." Free Radic Biol Med **47**(4): 424-430.
Viticchie, G. and P. A. J. Muller (2015). "c-Met and Other Cell Surface Molecules: Interaction, Activation and Functional Consequences." Biomedicines **3**(1): 46-70.

Wang, X., M. C. DeFrances, Y. Dai, P. Pediaditakis, C. Johnson, A. Bell, G. K. Michalopoulos and R. Zarnegar (2002). "A mechanism of cell survival: sequestration of Fas by the HGF receptor Met." Mol Cell **9**(2): 411-421.
Wormann, S. M., L. Song, J. Ai, K. N. Diakopoulos, M. U. Kurkowski, K. Gorgulu, D. Ruess, A. Campbell, C. Doglioni, D. Jodrell, A. Neesse, I. E. Demir, A. P. Karpathaki, M. Barenboim, T. Hagemann, S. Rose-John, O. Sansom, R. M. Schmid, M. P. Protti, M. Lesina and H. Algul (2016). "Loss of P53 Function Activates JAK2-STAT3 Signaling to Promote Pancreatic Tumor Growth, Stroma Modification, and Gemcitabine Resistance in Mice and Is Associated With Patient Survival." Gastroenterology **151**(1): 180-193 e112.
Xu, F., S. D. Rychnovsky, J. D. Belani, H. H. Hobbs, J. C. Cohen and R. B. Rawson (2005). "Dual roles for cholesterol in mammalian cells." Proc Natl Acad Sci U S A **102**(41): 14551-14556.
Yang, Y., Y. C. Ye, Y. Chen, J. L. Zhao, C. C. Gao, H. Han, W. C. Liu and H. Y. Qin (2018). "Crosstalk between hepatic tumor cells and macrophages via Wnt/beta-catenin signaling promotes M2-like macrophage polarization and reinforces tumor malignant behaviors." Cell Death Dis **9**(8): 793.
Younes, R. and E. Bugianesi (2018). "Should we undertake surveillance for HCC in patients with NAFLD?" J Hepatol **68**(2): 326-334.
Younossi, Z. M., A. B. Koenig, D. Abdelatif, Y. Fazel, L. Henry and M. Wymer (2016). "Global epidemiology of nonalcoholic fatty liver disease-Meta-analytic assessment of prevalence, incidence, and outcomes." Hepatology **64**(1): 73-84.

Annexed II.
Publications generated during the Doctorate

[Cancers] Manuscript ID: cancers-1097922 - Accepted for Publication
1 mensaje

Cancers Editorial Office <cancers@mdpi.com> 8 de marzo de 2021 a las 19:06
Responder a: Cancers Editorial Office <cancers@mdpi.com>
Para: Luis Enrique Gomez <legq@xanum.uam.mx>
CC: Arturo Simoni-Nieves <bioexpp22@gmail.com>, Soraya Salas-Silva <esss2491@gmail.com>, Lisette Chavez-Rodríguez <lisettechavez23@gmail.com>, Oscar Escobedo-Calvario <escobedocoa@hotmail.com>, Matthis Desoteux <desoteux.matthis@hotmail.fr>, Leticia Bucio <lebo@xanum.uam.mx>, Veronica Souza <veso@xanum.uam.mx>, Roxana Miranda-Labra <roxml@xanum.uam.mx>, Linda Muñoz-Espinosa <linda_uanl@hotmail.com>, Cédric Coulouarn <cedric.coulouarn@inserm.fr>, Maria C Gutierrez-Ruiz <mcgr@xanum.uam.mx>, Jens-Uwe Marquardt <Jens.Marquardt@uksh.de>, Cancers Editorial Office <cancers@mdpi.com>

Dear Dr. Gomez,

We are pleased to inform you that the following paper has been officially accepted for publication:

Manuscript ID: cancers-1097922
Type of manuscript: Article
Title: The consumption of high cholesterol diets conditions the development of a subtype of HCC with high aggressiveness and poor prognosis
Authors: Arturo Simoni-Nieves, Soraya Salas-Silva, Lisette Chavez-Rodríguez, Oscar Escobedo-Calvario, Matthis Desoteux, Leticia Bucio, Veronica Souza, Roxana Miranda-Labra, Linda Muñoz-Espinosa, Cédric Coulouarn, Maria C Gutierrez-Ruiz, Jens-Uwe Marquardt, Luis E. Gomez-Quiroz *
Received: 24 January 2021
E-mails: bioexpp22@gmail.com, esss2491@gmail.com, lisettechavez23@gmail.com, escobedocoa@hotmail.com, desoteux.matthis@hotmail.fr, lebo@xanum.uam.mx, veso@xanum.uam.mx, roxml@xanum.uam.mx, linda_uanl@hotmail.com, cedric.coulouarn@inserm.fr, mcgr@xanum.uam.mx, Jens.Marquardt@uksh.de, legq@xanum.uam.mx
Submitted to section: Cancer Causes, Screening and Diagnosis, https://www.mdpi.com/journal/cancers/sections/Cancer_Causes_Screening_Diagnosis
The Mechanisms of Physical Activity, Diet, and Body Composition in Cancer Prevention and Control
https://www.mdpi.com/journal/cancers/special_issues/MPADBC
https://susy.mdpi.com/user/manuscripts/review_info/f0181e24baf832e33be3fc8745b2b2ae

We will now make the final preparations for publication, then return the manuscript to you for your approval.

If, however, extensive English edits are required to your manuscript, we will need to return the paper requesting improvements throughout.

We encourage you to set up your profile at SciProfiles.com, MDPI's researcher network platform. Articles you publish with MDPI will be linked to your SciProfiles page, where colleagues and peers will be able to see all of your publications, citations, as well as your other academic contributions.

We also invite you to contribute to Encyclopedia (https://encyclopedia.pub), a scholarly platform providing accurate information about the latest research results. You can adapt parts of your paper to provide valuable reference information for others in the field.

Kind regards,
Ms. Wendy Shao
Assistant Editor

cancers

MDPI

Article

The consumption of cholesterol-enriched diets conditions the development of a subtype of HCC with high aggressiveness and poor prognosis.

Arturo Simoni-Nieves[1,2], Soraya Salas-Silva[1,2], Lisette Chávez-Rodríguez[1,2], Oscar Alejandro Escobedo-Calvario[1,2], Matthis Desoteux[3], Leticia Bucio[2,4], Verónica Souza[2,4], Roxana U. Miranda-Labra[2,4], Linda E. Muñoz-Espinosa[5], Cédric Coulouarn[3], María Concepción Gutiérrez-Ruiz[2,4], Jens U. Marquardt[6, #], Luis E. Gomez-Quiroz[2,4, # *]

1 Posgrado en Biología Experimental, DCBS, Universidad Autónoma Metropolitana Iztapalapa, Mexico City, Mexico; bioexpp22@gmail.com (A.S.-N.); esss2491@gmail.com (S.S.-S.); lisettechavez23@gmail.com (L.C.-R.); escobedocoa@hotmail.com (O.A.E.-C.)

2 Área de Medicina Experimental y Traslacional, Departamento de Ciencias de la Salud, Universidad Autónoma Metropolitana-Iztapalapa, Mexico City, Mexico; bioexpp22@gmail.com (A.S.-N.); esss2491@gmail.com (S.S.-S.); lisettechavez23@gmail.com (L.C.-R.); escobedocoa@hotmail.com (O.A.E.-C.); lebo@xanum.uam.mx (L.B.); veso@xanum.uam.mx (V.S.); roxml@xanum.uam.mx (R.U.M.-L.); mcgr@xanum.uam.mx (M.C.G.-R.); legq@xanum.uam.mx (L.E.G.-Q.)

3. Inserm, Univ Rennes, COSS (Chemistry, Oncogenesis Stress Signaling), UMR_S 1242, Centre de Lutte contre le Cancer Eugène Marquis, Rennes, France; desoteux.matthis@hotmail.fr (M.D.); cedric.coulouarn@inserm.fr (C.C.)

4. Laboratorio de Medicina Experimental, Unidad de Medicina Traslacional, IIB, UNAM/ Instituto Nacional de Cardiología Ignacio Chavez, Mexico City, Mexico; lebo@xanum.uam.mx (L.B.); veso@xanum.uam.mx (V.S.); roxml@xanum.uam.mx (R.U.M.-L.); mcgr@xanum.uam.mx (M.C.G.-R.); legq@xanum.uam.mx (L.E.G.-Q.)

5 Liver Unit, Department of Internal Medicine, "Dr. José E. González" University Hospital, Universidad Autónoma de Nuevo León, Monterrey, NL, Mexico; linda_uanl@hotmail.com (L.E.M.-E.)

6. Department of Medicine I, University Hospital Schleswig-Holstein, Lübeck, Germany; Jens.Marquardt@uksh.de (J.U.M.)

Shared Senior authorship

* Corresponding author: legq@xanum.uam.mx; Tel/Fax: 55-58044730. Departamento de Ciencias de la Salud, Universidad Autónoma Metropolitana Iztapalapa. Av. San Rafael Atlixco 186, Col. Vicentina, 09340, Iztapalapa. Mexico City, Mexico.

Citation: XXXXXXXXXXXX.. https://doi.org/10.3390/xxxxx

Academic Editor: Firstname Lastname
Received: date
Accepted: date
Published: date

Publisher's Note: MDPI stays neutral with regard to jurisdictional claims in published maps and institutional affiliations.

Simple Summary: It is well known that non-alcoholic fatty liver disease is an important risk factor in the development of hepatocellular carcinoma, but the implication of cholesterol in this subject remains unclear, especially in western countries where its consumption is particularly elevated. This work provides evidence of a cholesterol-related transcriptional fingerprint and its implications in the progression and aggressiveness of hepatocellular carcinoma with remarkable interest in the clinical practice.

Copyright: © 2021 by the authors. Submitted for possible open access publication under the terms and conditions of the Creative Commons Attribution (CC BY) license (http://creativecommons.org/licenses/by/4.0/).

Abstract: Non-alcoholic fatty liver disease (NAFLD) and progression to non-alcoholic steatohepatitis (NASH) results as a consequence of diverse conditions, mainly unbalanced diets. Particularly, high fat and cholesterol content as well as carbohydrates, such as those commonly ingested in Western countries, frequently drive adverse metabolic alterations in the liver and promotes NAFLD development. Lipid liver overload is also one of the main risk factors for initiation and progression of hepatocellular carcinoma (HCC), but detailed knowledge on the relevance of high nutritional cholesterol remains elusive. We were aimed to characterize HCC development in mice fed with a western diet (high in lipids and cholesterol) and to identify molecular alterations that define a subtype of liver cancer induced by lipid overload. Mice under western or high cholesterol diets more frequently developed tumors with a more aggressive phenotype than animals fed with a chow diet. Associated changes involved macrophage infiltration, angiogenesis and stemness features. RNA-seq revealed a specific gene expression signature (*Slc41a, Fabp5, Igdcc4* and *Mthfd1l)* resembling the adverse phenotypic features and poor clinical outcome that seen in patients with HCC. In conclusion, consumption of lipid enriched diets, particularly cholesterol, could accelerate HCC development with an aggressive phenotype and poor prognosis.

Keywords: NAFLD; NASH; HCC; Cholesterol; Western diet

1. Introduction

Non-alcoholic fatty liver disease (NAFLD) is the fastest growing chronic liver disease [1]. NAFLD and its inflammatory progressive form non-alcoholic steatohepatitis (NASH) are part of the natural history of hepatic diseases. It is well-known that changes in dietary behaviors contribute to the initiation and progression of these lipid-overload condition, increasing the incidence of liver cancer. The global prevalence of NAFLD is currently estimated as 24% [2]. Accumulated evidence has suggested a significant association between NAFLD and liver cancer [3, 4]. Hepatocellular carcinoma (HCC) is the main primary liver cancer, it represents the fifth and ninth cause of cancer-related death in male and female, respectively [5]. A global increase in the incidence of HCC is expected in the next 10-20 years [6]. HCC exhibits highly variable clinical outcomes, the prognostic variability of individuals with HCC supports the notion that HCC comprises several biologically distinct subtypes [7]. Compared with viral or alcoholic hepatitis, NAFLD is becoming major etiology for HCC, based on the increasing prevalence of obesity, especially in Western countries [8]. A large-scale epidemiological study revealed that obesity could represent the main risk factor in cancer such as HCC [9]. The effective molecular understanding of NASH-related HCC is urgently required for a better management of patients with HCC, including early diagnosis and more accurate prognosis, along with the design of optimized treatments. Most patients with NAFLD remain asymptomatic and about 20-25% progress to develop a more-severe chronic hepatic inflammatory disease, defined as NASH, and eventually 2.6% of those patients develop HCC [5, 10]. HCC not only develops on a background of liver cirrhosis, but also on non-cirrhotic liver in NASH. The molecular events involved in NASH progression and HCC development are not fully understood [11]. Among the biochemical determinants characterizing the NAFLD are the accumulation of triglycerides and cholesterol. Particularly, cholesterol overload represents a key insult in the liver as we and others have reported [12], and it has been associated to HCC development [3, 4, 13, 14]. Although the relationship between NAFLD and HCC has been extensively reported [15], the particular contribution of cholesterol in HCC onset and progression has been poorly studied, espe-

cially in populations where dietary cholesterol intake is important. The cholesterol content in western diet is 10-fold higher than in Mediterranean geographical zone [2]. Cholesterol is fundamental for life, it is precursor of many hormones, and bile salts, which are necessary for a proper digestion. It is a remarkable component of lipid rafts, so changes in cholesterol levels seriously affect cell signaling, especially for growth factors or cytokine receptors [16]. A high cholesterol diet causes an accumulation of lipids in the hepatocytes which are key components of lipoproteins used for lipid exportation [17]. Multiple mechanisms contribute to create a favorable environment for the development of NAFLD-related HCC tumors [11]. Obesity is characterized by a low-grade chronic inflammatory response, which is a risk factor for HCC. Adipose tissue expansion promotes the release of proinflammatory cytokines that can activate pro-oncogenic pathways such as STAT3 [18], which has been widely reported to promote tumor growth and immune evasion. STAT3 overactivation has been found in different solid tumors, such as bladder, bone, breast, liver, among others [19], correlating with poor prognosis in most of these cancer [20]. Activated STAT3 prevents p53-mediated growth control, thus allowing tumor progression. STAT3 also induces the expression of vascular endothelial growth factor (VEGF), stimulating angiogenesis that favors invasion and metastasis [21]. The canonical inducer of STAT3 activation is IL-6 which is also a master regulator of inflammation and tumor growth [20, 22]. In the present work, we aimed at i) characterizing HCC onset and progression in a background of lipid overload, particularly in cholesterol, and, ii) identifying the clinical relevance of a gene expression signature established from this HCC. Notably, we hypothesized that this gene signature could predict the clinical outcome of patients with HCC by defining a subtype of tumors with high aggressiveness and poor prognosis.

2. Materials and Methods

Animals. Sixty-four 14 days-old male mice (strain C57BL/6) were randomly separated in six groups according to supplementary table 1. Briefly, these groups include 1) mice fed with regular chow diet (CW); 2) mice fed with chow diet and injected with a single dose of *N*-nitrosodiethylamine (DEN, 10 μg/Kg, i.p.) (CW/DEN); 3) mice fed with Western diet (W, catalog #D12089, Research Diets Inc. New Brunswick, USA); 4) mice fed with Western diet and injected with a single dose of DEN (W/DEN). Later we added two additional groups: 5) mice fed with a high cholesterol diet (HC, 1% cholesterol, #611638, Dyets Inc. Bethlehem, PA, USA); and 6) mice fed with HC diet and injected with a single dose of DEN (HC/DEN). Animals received diet and water *ad libitum*. After 8 months mice were euthanized under Avertin (2-2-2 tribromoethanol) anesthesia. Liver weight was documented, liver tissue, and serum were collected for subsequent analysis [3]. All animals were maintained in specific pathogen-free housing and cared in accordance with the NIH Guide for Care and Use of Laboratory Animals and Universidad Autonoma Metropolitana guidelines for the use of animals.

Diet composition, in terms of main components are as follows: CW diet (fat 5%, cholesterol 0.01%, carbohydrates 23.30% and protein 17.10%); western diet (fat 5%, cholesterol 1.0%, carbohydrates 33.00% and protein 17.50%); and HC diet (fat 5%, cholesterol 1.0%, carbohydrates 23.00% and protein 17.50%).

Histology. Microscopic inspection was evaluated by routine Hematoxylin & Eosin (H&E) staining. Fibrosis was assessed by Sirius Red staining as previously reported [23]. Steatohepatitis was defined by the presence of steatosis, inflammation and hepatocellular ballooning [24], as per the FLIP algorithm [25]. The severity of steatosis, lobular inflammation and hepatocellular ballooning were scored using the NASH-Clinical Re-

search Network (CRN) criteria [26]. Specifically, the amount of steatosis (percentage of hepatocytes containing fat droplets) was scored as 0 (<5%), 1 (5–33%), 2 (>33–66%) and 3 (>66%). Hepatocyte ballooning was classified as 0 (none), 1 (few) or 2 (many cells/prominent ballooning). Foci of lobular inflammation were scored as 0 (no foci), 1 (<2 foci per 200× field), 2 (2–4 foci per 200× field) and 3 (>4 foci per 200× field). The NAFLD activity score (NAS) was computed from the grade of steatosis, inflammation and ballooning [27]. Paraffin sections of human liver tissue (NASH and HCC patients) were generously provided by Dr. Linda Muñoz-Espinosa, University Hospital, UANL.

Cell lines culture. Huh7, Hep3B, HepG2 and THLE-3 cell lines were obtained from the American Type Culture Collection (ATCC, Manassas, VA, USA) and PLC-PRF5 cell line was provided by Dr. Jens U. Marquardt. Cells were cultured in William's medium supplemented with 10% fetal bovine serum (FBS, Hy-Clone, Logan, UT, USA), 100 U/ml ampicillin and 100 μg/ml streptomycin (Thermo Fisher Scientific, Waltham, MA, USA). Cells were maintained at 37°C in a 5% CO_2 and 90% humidity atmosphere. Cells were plated in plastic culture bottles (Sigma-Aldrich, Saint Louis, MO, USA). All cell lines were mycoplasma free. All experiments were carried out by triplicate in the logarithmic phase of growth.

Cholesterol determination. Total cholesterol was determined as previously reported [28]. Briefly, 10 mg of liver was saponified with alcoholic KOH in a 60ºC heating block for 30 min. After the mixture had cooled, 3 ml of hexane and 600 μl of distilled water were added and shaken to ensure complete mixing. Appropriate aliquots of the hexane layer were evaporated under nitrogen with vacuum (Speed Vac, Savant, Cranbury, NJ) and used for cholesterol measurement with O-phthalaldehyde dissolved in acetic acid (0.5 mg/ml), at 550 nm.

Serum biochemical determinations. Blood samples were obtained from the retro-orbital sinus under avertin anesthesia. Serum total cholesterol, triglycerides, ALT and AST activities were determined by using an automated analyzer for clinical chemistry (SpotChem EZ, ARKRAY, USA Clinical Diagnostics).

RNA extraction, quantification and integrity. Total RNA was extracted using the QIAGEN RNeasy mini-Kit (Qiagen GMBH, Hilden, Germany) following the manufacturer´s instructions. RNA quantity and purity were estimated using a Nanodrop 2000 Spectrophotometer (Nanodrop Technologies, Wilmington, DE), and integrity was assessed by Agilent 2100 Bioanalyzer (Agilent, Palo Alto, CA).

RNA Sequencing. RNA sequencing was performed using Illumina HiSeq4000 and deposited at the Bio-project database (ID: PRJDB10804). Raw reads were filtered by adapter sequences, contamination and low-quality reads. The reads were then mapped with mouse genome reference (GRCm38.p6) using HISAT2 (hisat2-2.0.2-beta) followed by read summarization with featuresCounts (subread-1.5.0-p1). All data analysis was performed using R programing language and related packages. The output matrix from featureCounts was input into Bioconductor DESeq2 for differential expression analysis with a False Discovery Rate (FDR) of 0.5, and *p*-value of 0.001 and a log fold change from -1.5 to 1.5. Significance testing was performed using Wald Test statistics. To visualize the data Heatmaps and Principal Components Analysis (PCA) were performance. All plots were generated using the MADE4 package [29].

Enrichment Analysis. Gene Set Enrichment analysis (GSEA) was performed using GSEA software provided by Broad Institutes (http://software.broadinstitute.org/gsea/index.jsp). Gene sets from the MSigDB database were tested and gene sets with NOM *p*-value <0.05 and FDR <0.25 were considered significantly enriched in a priori defined set of genes. We used ingenuity pathway analysis (IPA, Ingenuity Systems, Inc. Redwood City, CA) to investigate the biological pathways and networks associated with model genes using the whole dataset. Genes with their

log2-fold change were used as input. We considered disease, biological functions, and upstream regulators to be significant if the absolute value of their activation *z*-score is >1.5. The *z*-score reflects the match between the observed gene expression and the predicted relationship direction. It is used to infer activation states of called functions and regulators [29].

Immunofluorescence (IF). Tissue was either fixed in 4% formaldehyde and preserved in Tissue Tek for cryosections and cut in 3-5 µm sections. Subsequently, these were washed with PBS-tween for 5 min. The specific antibodies (Supplementary Table 3.) were diluted in PBS with 0.1% horse serum and incubated overnight at 4 ° C in a humid chamber. The tissues were washed again with PBS, incubated with DAPI for 5 min. Finally, slides were examined using the Carl Zeiss LSM 780 NLO confocal microscope (Carl Zeiss, Inc., USA).

Quantitative RT-PCR. After DNase digestion with a DNA-free kit (Ambion Inc.), 500 ng (tissue) and 100 ng (cells) total RNA was reverse transcribed in 20 µl reaction volume with a SuperScript first-strand synthesis kit according to the manufacturer's instructions (Invitrogen Corp.). Real-time quantitative PCR analysis was performed with a CFX96 Touch (Bio-Rad) thermal cycler in a 96-well reaction plate. The 10 µl PCR reaction mix contained 5 µl 2X SYBR Green PCR Master Mix (Bio-Rad), 200 nM of each primer, and 1 µl cDNA template. Reactions were incubated for 10 min at 95°C followed by 40 cycles of 30 sec at 95°C and 60 sec at specific primer temperature. Melting analysis of the PCR products was also conducted to validate the amplification of the specific product. The expression level of mouse rs18 was used as an internal reference. Relative gene expression levels were calculated with the $2^{-\Delta\Delta CT}$ method [30]. Primer sequences are listed in supplementary table 2.

Mouse Serum MultiPlex Measurements. Cytokines and growth factors were measured in mouse sera using the MOUSE ANGIOGENESIS / GROWTH FACTOR MAGNETIC BEAD PANEL bead assay (EMD Millipore Corporation, Billerica, USA) and a MAGPIX instrument using Luminex xMAP Technology. The analysis was performed according to the manufacturer's instructions.

Data mining. The RNA-seq data level 3 (Counts files) of 371 patients with HCC, and 50 samples of normal liver, were retrieved from The Cancer Genome Atlas (TCGA) database (https://portal.gdc.cancer.gov/) up to January 28, 2018. And 101 microarray data from LEC (Laboratory of Experimental Carcinogenesis) was use. The parameters for the differential expression analysis were False Discovery Rate (FDR) equal to 0.5, *p*-value <0.001 and log fold change from -1.5 to 1.5. And clustering analysis was done using Cluster 3.0 and TreeView 1.6 using uncentered correla- tion and average linkage options. Integration of genomic data was conducted as previously described using publicly available gene expression data sets downloaded from GEO [7].

Survival analysis. For survival analysis, expression data were categorized using a *z*-score cutoff of 0. Kaplan–Meier method using the log-rank test was used to estimate survival curves [31].

Statistical analysis. Each animal and cell experiments were performed at least by triplicate using cells of at least ± 3 different passages. Data are reported as the average ± standard error (SEM). Pearson's correlation analysis was used to assess the correlation between expression of Slc41a3, Fabp5, Igdcc4, mthfd1l and total cholesterol content in human liver cancer cell lines. For the comparison of means of different groups, an analysis of variance (ANOVA) was used, followed by multiple comparisons by the Tukey test. The GraphPad prism software (v. 8.2.1) was used. Differences were considered significant at $p \leq 0.05$.

3. Results

3.1. High lipid diets induce weight gain, liver damage and tumor promotion.

Mice fed western and cholesterol diets for eight months (Figure 1A), presented body weight gain (Figures 1B and C), as a consequence of increased visceral fat deposition (Supplementary Figure 1A, white arrows), comparing with CW fed animals. Increased liver weight was also observed (Figure 1D), but the liver to body weight ratio was unchanged (data not shown) as a result of the obesity observed in animals under this lipid-enriched diet (Supplementary Figure 1A). The phenotype was closely associated to significant increment in AST and ALT serum activities (Figure 1E) in mice under western diet, indicating that hepatocellular damage persists at eight months of treatment. Interestingly, HC/DEN group did not change AST and ALT values at eight months. No significant difference in liver damage tests was observed in animals treated or not with DEN, but changes were remarkable comparing with animals fed with the regular CW diet.

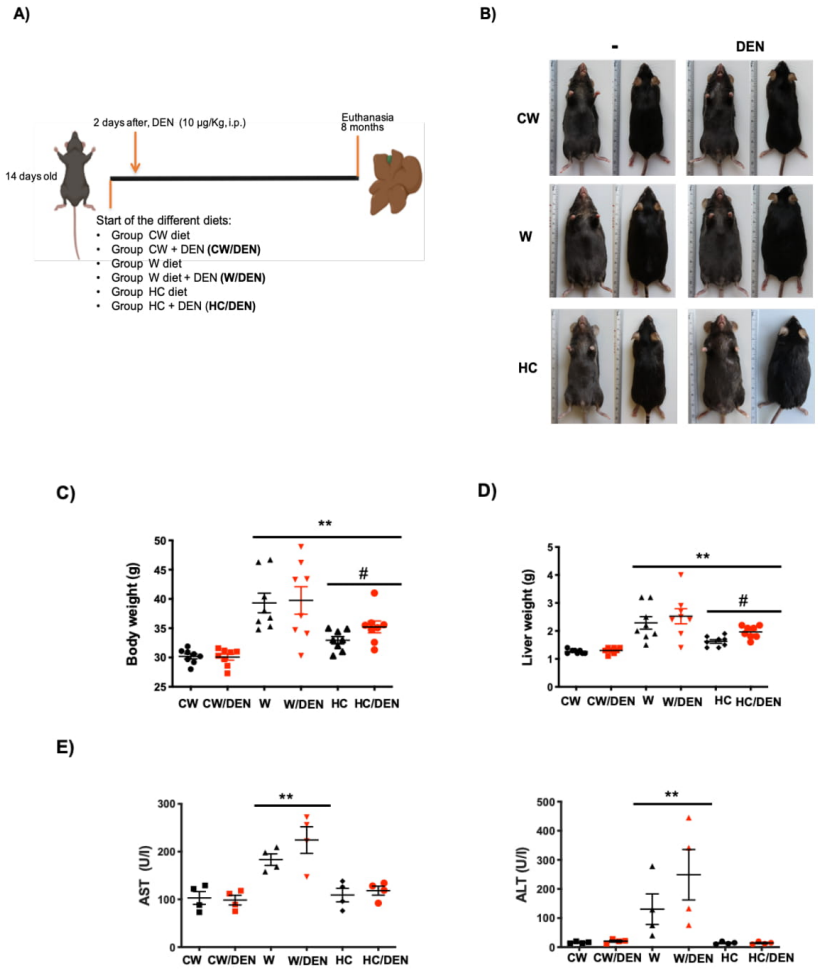
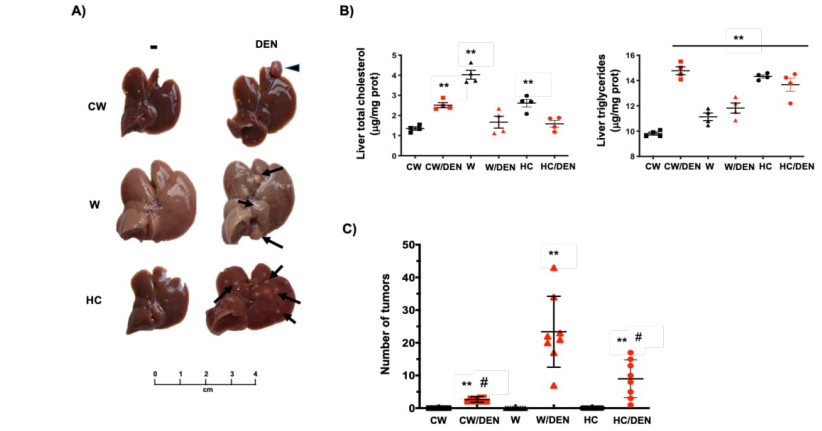


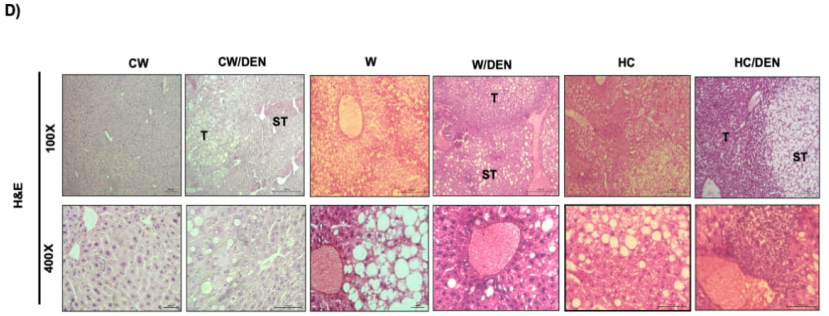
Figure 1. Lipid-enriched diets induce weight gain and liver damage. 14 days-old male mice were fed for 8 months with western and high cholesterol diets as stated in Material and Methods. A) Experimental design. CW, chow standard diet; W, western diet; HC, high cholesterol; DEN, *N*-nitrosodiethylamine. B) Mice under the W and HC diets presented obesity. Representative images (n=8). C) body weight (n=8) and, D) liver weight (n=8), of mice under different diets. E) Liver damage addressed by serum activity of aspartate aminotransferase (AST) and alanine aminotransferase (ALT) (n=4). Each graph plots the individual data points, the superimpose horizontal line indicates the arithmetic mean and error bar shows ± SEM. ** p<0.01 vs CW groups; # p<0.01 vs W groups.

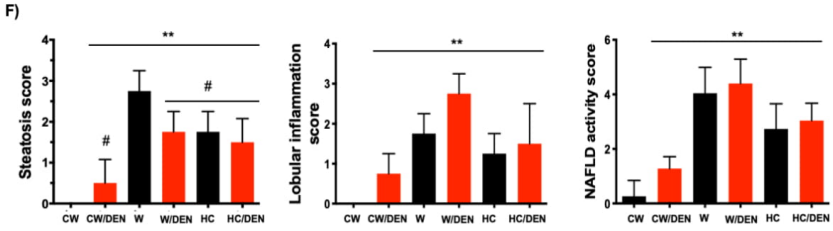
In agreement with liver damage, we found the macroscopic changes associated with steatosis including the characteristic yellowish color in the livers, particularly in those under western diet (Figure 2A) comparing with CW fed animals. Liver lipid overload was biochemically corroborated by testing total cholesterol and triglycerides. Consistently, all experimental groups exhibited increased values of both of lipids regarding to CW fed mice (Figure 2B). Next, we proceeded to identified tumors in livers from DEN treated mice. The number of tumors in W/DEN and HC/DEN mice were higher (23.3 ± 10.3 and 9 ± 1.9 tumors, respectively) than in CW/DEN mice (2.7 ± 0.2 tumors) (Figure 2C), suggesting synchronous development of several independent tumors, which is a well-defined characteristic in HCC [32]. Protruding tumors were observed in W/DEN livers (Figure 2A, arrow), comparing with CW/DEN livers, where some pedunculated tumors were identified (Figure 2A, arrowhead), while HC/DEN animals showed the characteristic HCC protruding tumors. In addition, W/DEN tumors exhibited increased vascularity (Supplementary figure 1B yellow arrow), a distinctive feature of aggressive HCC [30].

Histological analysis by H&E staining revealed discrete borders and irregular wide trabeculae (>3 cells) in W/DEN tumors. Animals fed with a western diet presented massive steatosis disrupting normal architecture. Consistently, steatosis (micro and macrovesicular) was most pronounced in surrounding tissue (ST) areas, while lipid content in tumor (T) zones was only marginal and replaced by increased lobular inflammation. Same pattern was also identified in HC/DEN, but the microsteatosis predominated (Figure 2D). Interestingly, liver tissues from NASH and NASH derived HCC patients exhibited a similar histological presentation in comparison with the animal models (Figure 2E). Quantification of the histological findings revealed significant values of steatosis, inflammation and NAFLD activity score in all animals' groups comparing with CW control mice (Figure 2F).

Western diet induced mild fibrosis particularly in pericentral zones, but animals in W/DEN group exhibited both pericentral and perisinusoidal zones with bridging fibrosis (Figure 2G) in comparison with HC/DEN and CW/DEN.


A)
-
DEN
CW
W
HC
0 1 2 3 4
cm
B)
Liver total cholesterol (µg/mg prot)
Liver triglycerides (µg/mg prot)
CW CW/DEN W W/DEN HC HC/DEN
C)
Number of tumors
CW CW/DEN W W/DEN HC HC/DEN


D)
CW
CW/DEN
W
W/DEN
HC
HC/DEN
H&E
100X
400X
T
ST


F)
Steatosis score
Lobular inflammation score
NAFLD activity score
CW CW/DEN W W/DEN HC HC/DEN

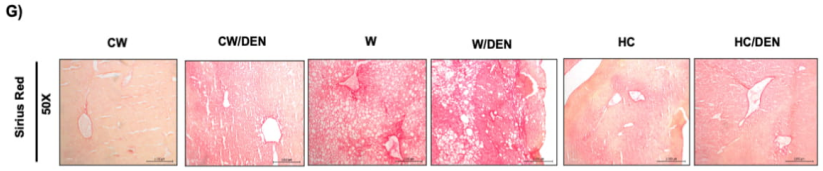

G)
CW
CW/DEN
W
W/DEN
HC
HC/DEN
Sirius Red
50X

Figure 2. The consumption of a western diet induces lipid liver overload and hepatic tumors. A) Gross inspection of the livers from mice fed with the different diets and treated or not with DEN. Arrows and arrowshead show tumors. Representative images of at least eight animals per group. B) Liver cholesterol and triglycerides content (n=4). C) Number of tumors in livers from different groups of mice. Each graph plots the individual data points, the superimpose horizontal line indicates the arithmetic mean and error bars showing ± SEM (n=8). D) mouse and, E) human liver tissue histology assessed by routine H&E. Each mouse image is representative of four animals. T, tumor; ST, surrounding tissue. F) histological scores. G) Fibrosis determined by Sirius red staining. Each image is representative of four animals. Each bar is the mean ± SEM. ** p<0.01 vs CW group; # p<0.05 vs W diet alone group

3.2. Transcriptional profile of tumors from lipid overloaded livers.

To identify the transcriptional alterations in tumors under western and HC diets consumption, we performed RNA-sequencing. Differentially expressed genes (DEG) between W/DEN and HC/DEN versus CW/DEN group. The analysis highlighted 671 DEG in W/DEN; and 194 DEG in HC/DEN (adjusted p value below 0.01 and a threshold of 1.5-fold change). In the case of W/DEN analysis we found 217 down-regulated genes and 454 up-regulated genes (supplementary table 4), and in HC/DEN we found 74 genes significantly down-regulated, and 120 genes were up-regulated when comparing with CW/DEN (Supplementary table 5). These genes were highly efficient in separating the tumors developed under the lipid-enriched diets versus chow regular diet (Figure 3A and B). To corroborate RNA-sequencing data, we performed real-time RT-PCR to analyze the expression of eight genes in samples not included in the RNA-seq, as technical and biological validation, respectively (Supplementary Figure 2). For all tested genes, real-time RT-PCR results recapitulated the RNA-seq data.

Ingenuity Pathway Analysis (IPA, Figure 3C) of the W/DEN and HC/DEN signatures showed that the dominant functional network up-regulated was involved in IL-6/Stat3 pathway (Bcl2, Cish, Socs2, Ntrk2, Pdgfb, Csf2rb), cell cycle/Myc (Bcl2, Pak1, Rapgef4, App), PI3K/Akt signaling Bcl2, Bcl2l1, Ccnd1, Cdkn1a). Notably, key tumor-suppressive pathways were down regulated such as p53 (Bcl2, Bcl2l1, Ccnd1, Cdkn1a), PTEN (Ikbke, Iitga2, Iitga4, Ntrk2), and apoptosis (Bcl2, Bcl2l1, Capn11, Capn8). The involvement of STAT3 and p53 networks (Figure 3D) suggests an aggressive

phenotype in tumors generated in a lipid overloaded environment. Supporting this hypothesis, gene set enrichment analysis (GSEA) identified an abundance of genes involved in poor prognosis in animals fed with W and HC diets. Accordingly, Lee Liver Cancer Survival DN gene set was significantly enriched in CW/DEN whereas Liver Cancer Survival UP [31] gene set was enriched in W/DEN and HC/DEN tumors indicating worst prognosis in W/DEN and HC/DEN groups compared to CW/DEN (Figure 3E). To corroborate these findings, we performed an immunoassay (MultiPlex) to address the serum content of different growth factors and cytokines associated to unfavorable prognosis in HCC such as EGF, FGF-2, Follistatin, HGF and VEGF-A [30, 33-35]. An increment in the expression of these soluble factors was observed in the serum of W/DEN mice comparing with CW/DEN mice (Figure 3F). Interestingly, most of the increased growth factors are related to survival and angiogenesis. To confirm the relevance of angiogenesis we assayed the content of CD34, a canonical marker of angiogenesis, highlighted a strong content in W/DEN tumor samples comparing with CW/DEN. No signal was detected in the other groups. Activation of angiogenesis was further corroborated by GSEA demonstrating a significant enrichment of an angiogenesis related gene set in the expression profiles of tumors derived from W/DEN mice (Figure 3G).

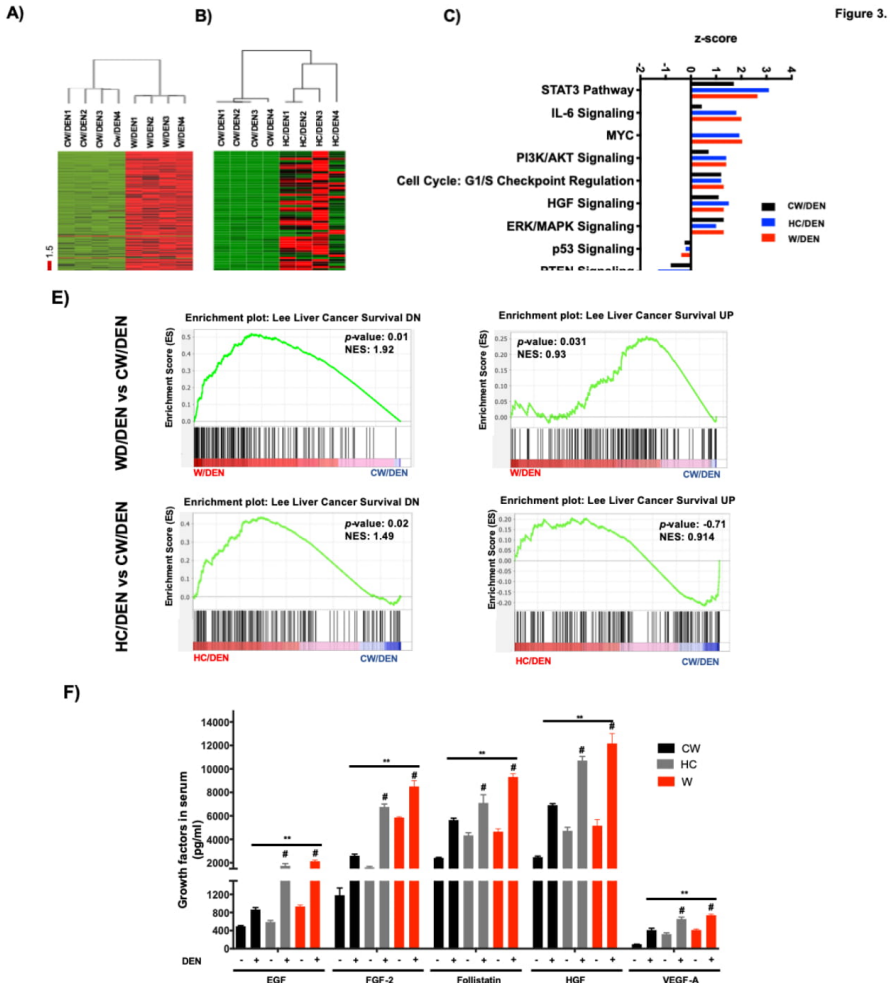


Figure 3.

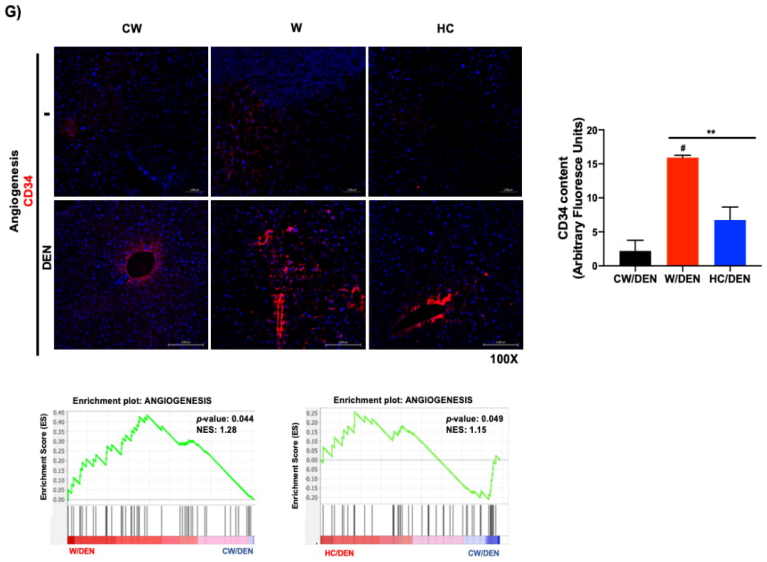
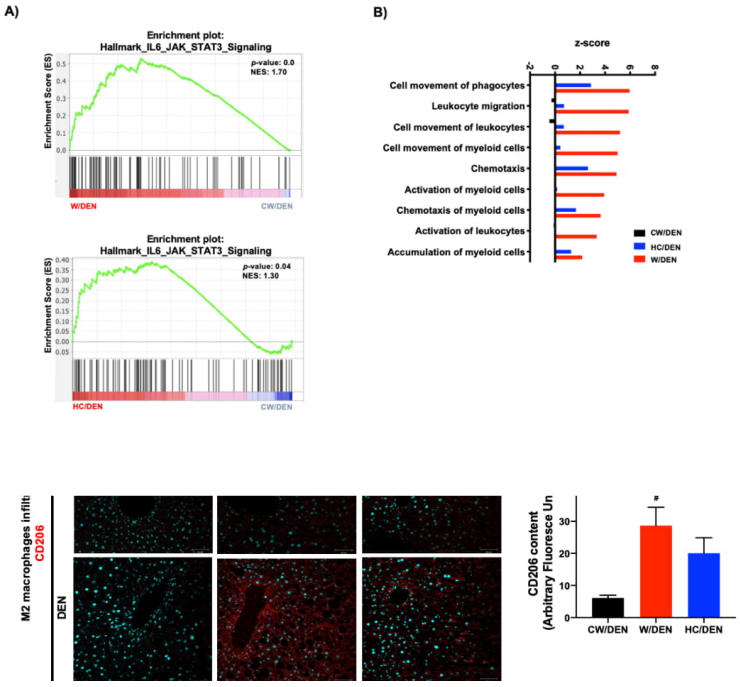


Figure 3. Tumors from lipid-enriched diets exhibit a profound change in gene expression favoring survival and proliferation signaling pathways and decreasing key tumor suppressor routes. Tumor tissues from CW/DEN, W/DEN, HC/DEN were subjected to RNA-sequencing as stated in Material and Methods. A) Heatmaps showing the good separation of A) W/DEN tumors vs CW/DEN and B) HC/DEN tumors vs CW/DEN red and green colors indicate high and low gene

expression respectively (*n*=4). C) Process networks analysis in tumors from CW/DEN (black), high cholesterol HC/DEN, (blue) and W/DEN (red) (*n*=4). The top rank ordered processes and networks are based on statistical significance (p<0.01). D) Expression targets of Stat3 and p53 in tumors signature. E) Gene set enrichment analysis (GSEA) of liver cancer survival (down and up regulated) data sets comparing tumors from W/DEN and HC/DEN to CW/DEN. F) Growth factors serum concentration of all mice groups. Proteins were determined by based multiplex immunoassay (*n*=4). Each bar represents the average ± SEM ** p<0.01 vs CW group; # p<0.05 vs W diet alone group. G) Angiogenesis judged by immunofluorescence of CD34, representative images of four animals. Original magnification, 100X. Quantification of CD34 fluorescence and GSEA of angiogenesis, data set comparing W/DEN and HC/DEN to CW/DEN (*n*=4).

3.3. *Inflammation* present in liver tumors associated to cholesterol consumption.

To corroborate the involvement of STAT3 signaling pathway in the phenotype of NAFLD-associated HCC in mice, GSEA was performed using the Hallmark_IL6_JAK_STAT3_Signaling gene set [36]. This specific signature was significantly enriched in the expression profiles of tumors derived from mice under lipid-enriched diets, suggesting an activation of the IL6/STAT3 pathway (Figure 4A). STAT3 is a well-known key driver of inflammation. Accordingly, IPA revealed a clear inflammatory disorder judged by the top signaling pathways activated (Figure 4B). To corroborate this hypothesis, macrophage infiltration was evaluated by both F4/80 and the specific M2-macrophages marker CD206 in mouse tissue from experimental groups (Figure 4C). As expected, a massive M2 macrophages infiltration was observed in tumors developed in mice under steatogenic diets (W or HC diet), comparing with liver tissue under the diets alone (i.e. without DEN) or in CW/DEN group, which presented a slight positive staining, particularly in pericentral zone. To support further the inflammatory phenotype, a multiplex analysis of the main pro-inflammatory mediators demonstrated an increment in the expression of G-CSF, IL6, IL1β, IL17, and TNF-α (Figure 4D).



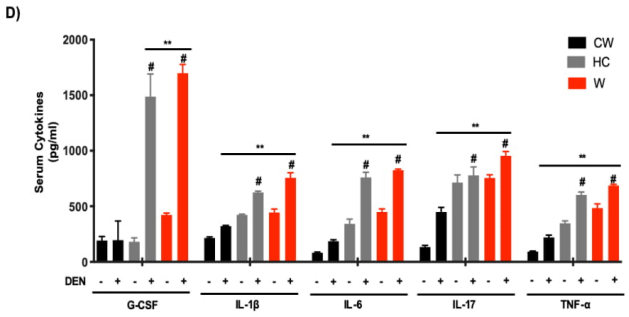
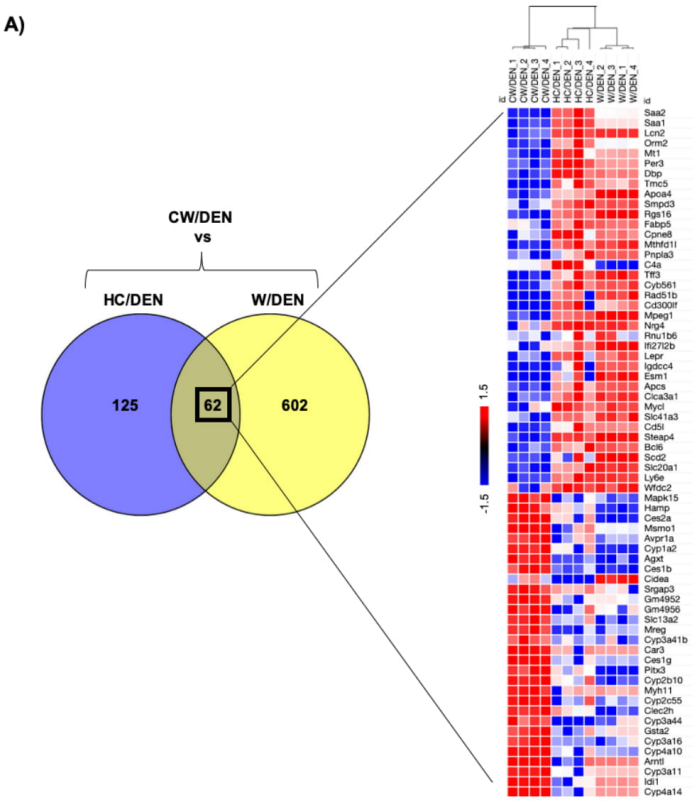


Figure 4. Inflammation as distinctive feature in liver tumors associated to lipid-enriched and cholesterol diets consumption. A) Gene set enrichment analysis (GSEA) of hallmark IL6-Jak-STAT3 signaling, data set comparing W/DEN and HC/DEN to CW/DEN (*n*=4). B) Process networks analysis related to inflammation in tumors from CW/DEN (black), W/DEN (red) and HC/DEN, (blue) (*n*=4). The top rank ordered processes and networks are based on statistical significance ($p<0.01$). C) Macrophages infiltration by immunofluorescence of F4/80 (green fluorescence) and CD206 (M2 phenotype, red fluorescence), representative images of four animals per group, original magnification, 100X. Quantification of F4/80 and CD206 fluorescence. D) Pro-inflammatory cytokines serum concentration of all mice groups. Proteins were determined by based multiplex immunoassay (*n*=4). Each bar represents the average ± SEM ** $p<0.01$ vs CW group; # $p<0.05$ vs W diet alone group.

Integrative genomics was performed to evaluate the clinical relevance of the crosstalk between mouse HCC and human HCC. The cholesterol signature (62 genes shared by W/DEN and HC/DEN) shared by W/DEN and HC/DEN groups in comparison with CW/DEN (Figure 5A) was first integrated with the gene expression profile of 101 cases of human HCCs from LEC cohort, which were extensively characterized [37]. Hierarchical clustering analysis of the integrated data set identified 2 robust clusters whose: cluster 1, W/DEN and HC/DEN tumors; cluster 2 CW/DEN tumors (Figure 5B). Strikingly, cluster 1 included significantly tumors, which were assigned to a poor prognosis group than cluster 2 (Figure 5C-D). As shown in Figure 5C, cluster 1 were defined by a bad survival[31], hepatoblast traits, along with the activation of MET/HGF [30] and late TGF-β signaling [38]. Also, we identified signs of vascular invasion in the cluster 1. The percent survival of patients in the cluster 1 was significantly reduced (p<0.01) in comparison with the cluster 2 (Figure 5D).



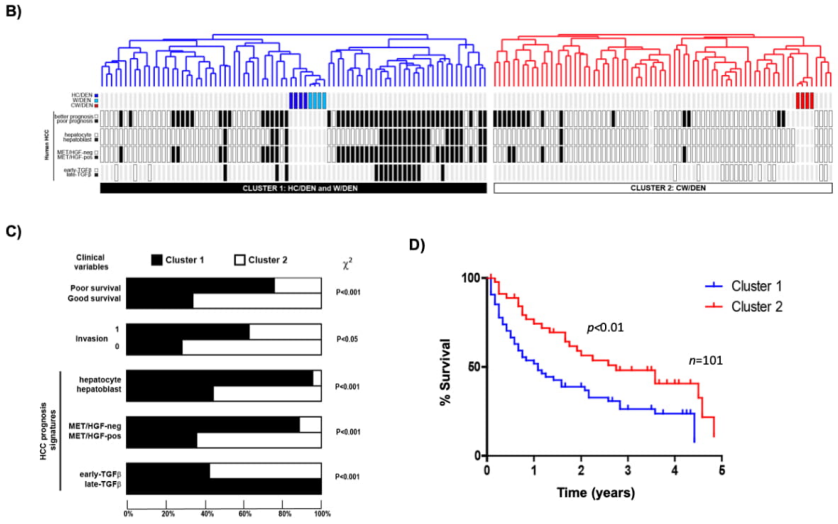


Figure 5. Cholesterol-enriched diet consumption promotes liver tumors. A) Venn diagram depicting differentially expressed common genes between HC/DEN and W/DEN groups (*n*=4). Heatmap shows the common 62 genes indicating the fold change value. B) Dendrogram overview of mice tumors integrated with 101 cases of human HCC. Clustering analysis was based on the expression of 62 ortholog genes in W/DEN and HC/DEN. Two clusters (1 and 2) were identified. C) Distribution of human HCC samples between previously described subgroups with respect to survival (better vs. poorprognosis), cell origin (hepatoblast vs. hepatocytes), activation of MET/HGF), and TGF-β signaling pathway (early vs late) is indicated on the left. F, statistical analysis of HCC distribution between clusters 1 and 2 based on previous gene signatures and clinical parameters. Cluster 1, which is defined by the W/DEN and HC/DEN signature, shows a significant enrichment in HCCs with the following features: bad survival, hepatoblast traits,

activation of MET/HGF, and late TGF-β pathways. D) Kaplan–Meier plots and log-rank statistics analysis revealed a significant decrease in overall survival for patients included in cluster 1.

The analysis of the 62 orthologous genes in the human TCGA database identified 4 genes differentially overexpressed related to high lipid overload with potential relevance in tumor promotion: Mthfd1l, (W/DEN: 2.74- and HC/DEN: 2.42-fold change) Slc41a3, (W/DEN: 2.67- and HC/DEN: 1.70-fold change), Fabp5 (W/DEN: 2.20- and HC/DEN: 2.70-fold change); and Igdcc4, (W/DEN: 2.05- and HC/DEN: 1.88-fold change increased) in W/DEN and HC/DEN respectively comparing with CW/DEN. We verified by qRT-PCR the expression of these genes in mouse samples (supplementary Figure 3).

Then, we explored the correlation between the expression of these genes and cholesterol content in four well-known human HCC cell lines using, as a control, the non-cancerous hepatocyte-like THLE-3 cell line. Figure 6A depicts the differences in cholesterol content in the different cell lines. We determined the expression of the four genes in those cell lines and a significant correlation between gene expression and cholesterol content was observed for all genes examined (Figure 6B-C).

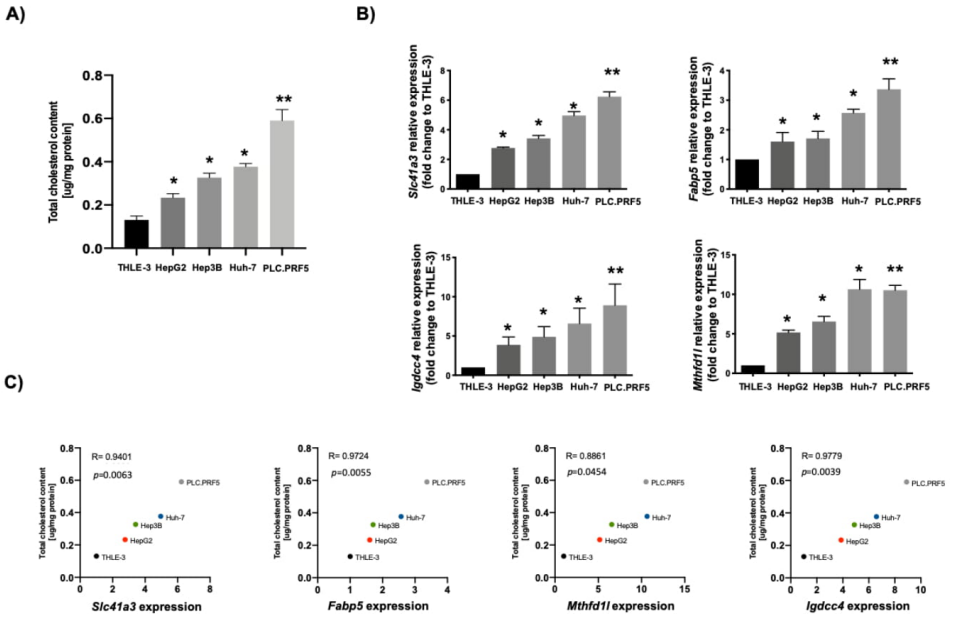
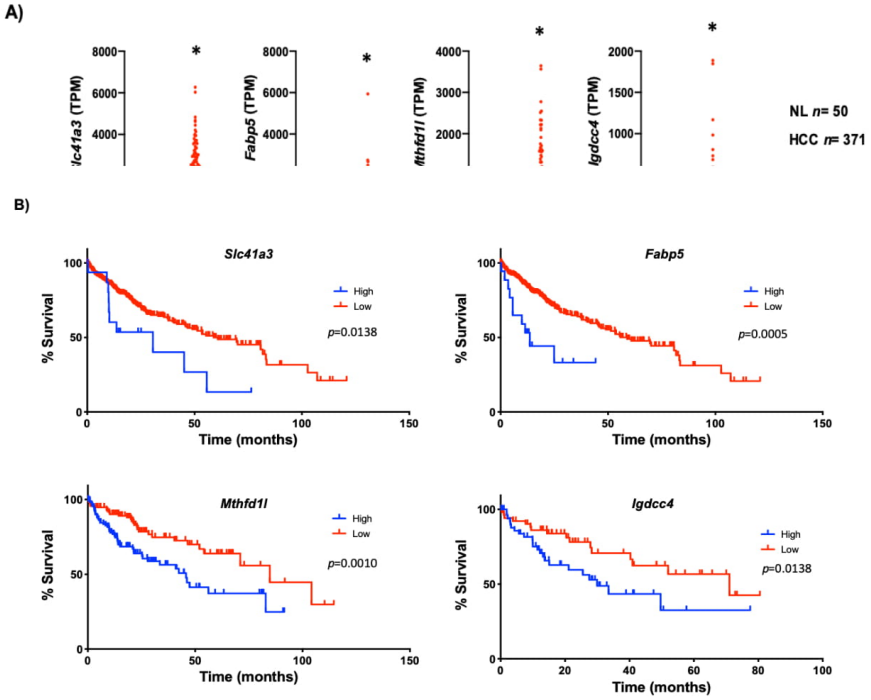


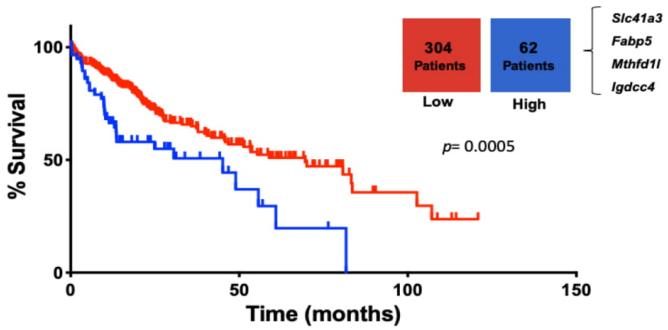
Figure 6. Lipid-associated four gene signature of HCC correlates with cholesterol overload in human cancer cell lines. A) Total cholesterol quantification in different human HCC-derived cell lines (*n*=4). B) *Slc41a3, Fabp5, Igdcc4* and *Mthfd1l* gene expression addressed by qRT-PCR in different HCC-derived human cell lines. THLE-3 cells were used as control (*n*=4). Each bar

represents the average ± SEM * p<0.05; ** *p*<0.01 vs THLE-3 cells. C) Pearson correlation analysis between total cholesterol content and gene expression of *Slc41a3, Fabp5, Igdcc4* and *Mthfd1l* (*n*=4).

The clinical relevance of mouse data in human liver cancer was determined by analyzing the expression of the four genes in the TCGA dataset, including 50 non-tumor liver tissue (NL) and 371 HCC samples (LIHC, Liver Hepatocellular Carcinoma). The four-gene signature associated to mouse NASH was increased in human HCC (Figure 7A). Next, we evaluated the capacity of these genes to predict survival in the 371 human HCC. For all genes analyzed, high expression was associated to a poor outcome (Figure 7B). Finally, we grouped the four genes and performed the analysis between patients with altered (*n*=62) vs unaltered (*n*=304) gene expression. As expected, Kaplan-Meier plot and log-rank testing demonstrated a reduced overall survival for patients included in the altered gene group (*p*<0.001) (Figure 7C). Thus, the molecular differences between these two subclasses of HCC were associated with a remarkable difference in the clinical outcome.



C)



	No. of cases (Total)	No. of Cases (Deceased)	Median Months Overall
Cluster 1	62	30	45.11
Cluster 2	304	99	69.57

Figure 7. Lipid-associated four-gene signature defines a subtype of human liver cancer with poor prognosis. A) Plots chart showing higher expression of Slc41a3, *Fabp5*, Igdcc4 and *Mthfd1l* in human HCC (n=371) compared to no-tumor liver tissue (NL, n=50) according to the TCGA data base (https://www.cbioportal.org/). TPM, transcripts per million. * p<0.01 vs normal liver (NL). B) Kaplan-Meier curves of overall survival in HCC patients. Patients with HCC were separated into two groups, high (red) and low (black) expression of *Slc41a3* (p=0.0138), *Fabp5* (p=0.0005), *Igdcc4* (p=0.0010), and *Mthfd1l* (p=0.0328). C) HCC data set from the TCGA was divided in unaltered and altered groups regarding the four gene signature and the overall survival in HCC patients was addressed and plotted in a Kaplan-Meier curve, (red altered group) and low (black unaltered group).

4. Discussion

Previously, we demonstrated the liver tumor promotion properties elicited by the consumption of a cholesterol-enriched diet in mice. Tumors presented an aggressive phenotype, including lung metastasis, comparing with animals fed regular chow diet [3]. This outcome was strongly associated to reactive oxygen species (ROS)-induced DNA damage, failure in the activation of the major DNA repair machinery and apoptosis resistance. The main objectives of the present work were to characterize the HCC progression in NASH induced by the consumption of lipid-enriched diets, particularly the contribution of cholesterol and, to identify the gene expression profile associated to this particular feature. Thus, we fed animals up to 8 months with a commercial and well-studied western diet (high lipid, cholesterol and carbohydrates). Then, mice received a single dose of DEN to induce liver carcinogenesis, as we previously reported [3, 39].

Under western diet, mice exhibited obesity, body weight gain due to accumulation of visceral fat, and the presence of liver damage. These findings are in agreement with those observed in humans under an occidental (western) pattern diet [10], and in others well-characterized mouse models of NASH [27, 40]. The co-treatment with DEN efficiently induced higher burden of HCC comparing with CW/DEN groups clearly sug-

gesting that lipid overload in the liver acts as a tumor promoter. One of the key components of western diet is high cholesterol. We and others have published that this lipid, in addition to the well-recognized fundamental properties for life, displays noxious effects when it is excessively accumulated in cells, particularly as a result of mitochondrial dysfunction and impairment of signal transduction through altering cellular membrane fluidity [12, 23, 28]. We previously demonstrated that cholesterol definitively increases tumor burden and aggressivity [3, 14]. However, the exact molecular mechanism by which cholesterol promotes tumor development is not fully understood.

The transcriptomic analysis carried out by RNA-seq shows a well separation between CW/DEN and lipid-enriched diets (W/DEN, HC/DEN) groups (Figure 3A-B). GSEA revealed a noticeable inflammatory phenotype, particularly associated to IL-6/STAT3 signaling, in addition to other pathways related to growth factors such as HGF, including PI3K/AKT and ERK pathways. It was interesting the abrogation of key tumor suppressive signals such as p53, PTEN and apoptosis signaling observed in the model (Figure 3C). Our previous work identified a remarkable mechanistic effect induced by cholesterol overload in the liver, including down-regulation of the main DNA repair proteins such as ATM, ATR, CHK1 and 2, and p53 [3]. In the present work, IPA confirmed this effect in terms of signaling pathways controlled by p53. Even more, an interesting crosstalk between p53 and STAT3 signaling pathways, by the intervention of PI3K and MAPK signaling, has been recently reported in ovarian cancer [41], and linked to an aggressive phenotype mediated by epithelial-mesenchymal transition, resulting in cell metastasis and chemoresistance.

Since early 2000´s some reports pointed out the transcriptional repression of p53 by STAT3 [42]. p53 loss of function has been also associated to STAT3 activation in pancreatic cancer [43]. We previously reported that cholesterol overload in the liver, due to consumption of cholesterol-enriched diet for 30 days, presented a remarkable activation of STAT3 and the increment in the expression of key target genes such as Mcl-1, these was associated to apoptosis resistance [28]. It is clear that cholesterol controls these relevant signaling pathways in preparation for tumor promotion from the beginning of the process. Contrary, it has been observed that dephosphorylation of STAT3 could stabilize p53 and leads to apoptosis [44].

The modulation of the immune response that promotes macrophage recruitment and activation has been previously reported in tumors reared under the consumption of cholesterol-enriched diet [45]. The close contact of macrophages and tumor cells is associated to M2-like macrophages polarization increasing the aggressiveness of the tumors [46]. In agreement with these previous findings, we observed a prominent F4/80 (canonical macrophage marker) and CD206 (M2-macrophage marker) signals in tissues from mice fed lipid-enriched diets particularly in western diet (Figure 5C). Interestingly, it has been observed that M2-macrophages could provide cholesterol to tumor cells, making a cholesterol co-dependence between these cells in the tumor microenvironment [47]. Recently, Bao and collaborators reported that a high M2-macrophages infiltration is associated with a poorer survival and increase in the cancer recurrence [48].

In addition to a well-defined macrophages infiltration, we also observed an increase in pro-angiogenic response, judged by the increment in VEGF-A and HGF content, and confirmed by CD34 IF, supporting the aggressive phenotype. Accordingly, we reported that HGF/Met-regulated expression signature was associated to an increment in angiogenesis and was able to define a subset of human HCC with poor prognosis and aggressive phenotype [30]. Another characteristic observed in this signature was the prominent decompensation of lipogenesis and oxidative stress.

To gain more mechanistic evidence of the relevance of tumor development in the liver with lipid overload, we studied another group of mice fed with a high cholesterol

diet (carbohydrates and other lipids in standard contents). Gene expression analysis in this tumorigenic process, identified 194 differentially expressed genes relating to CW/DEN. Comparison between HC/DEN vs W/DEN identified 62 commonly regulated genes (Figure 5A). Supporting these findings, we established an integrative genomics between tumors from mice fed cholesterol-enriched diets and human HCC, where these 62 genes shared by W/DEN and HC/DEN had clinical relevance and is associated with poor prognosis in human HCC. Further research is required to fully establish the contribution of each specific genes, including four outstanding genes (*Slc41a3, Fabp5, Mthfd1l* and *Igdcc4*) with clinical relevance in human cancer. These genes are elevated in HCC samples and are associated to poor survival. Clustering these four genes and separating human HCC in those with altered expression (n=62) regarding patients with unaltered expression (*n*= 304) observed a significant decrement in survival (Figure 7C).

The solute carrier (Slc) family 41 comprises three members including the Slc41a3. It is related to cation transmembrane transporter activity, driving the efflux of Mg^{2+} particularly in mitochondria rather than plasma membrane [49]. Slc41a3 overexpression has been reported in cancer for nutrient and Mg^{2+} transport to meet the needs for aberrant metabolism and proliferation [50]. As we have mentioned, mitochondria are the main target of excess of cholesterol. Overexpression of this transporter system could be directed to compensate the loss of fluidity in the mitochondria, improving the extrusion of Mg^{2+}.

Fabp5 encodes for the fatty acid-binding protein 5 (Fabp5). This protein has been related to malignant potential in several cancers, including HCC. Positive staining of Fabp5 in HCC is associated with poor prognosis, recurrence, metastasis and vascular invasion [51]. Fabp5 transports lipids intracellularly for storage purposes, providing building blocks for membrane construction and energy supply, both highly required in the proliferating cells [52].

Igdcc4 encodes the neighbor of Punc E11, also known as Nope. It is a plasma membrane oncofetal stem/progenitor cell marker, initially identified in the murine fetal liver [53]. It is barely detected in the adult liver. It has been previously showed that Nope is a sensitive marker of HCC [54] associated to stemness resembling early postnatal hepatocytes. Although Nope is scarcely detected in adult hepatocytes, the damage could induce the expression, particularly in the cholestatic damage which is associated to changes in hepatocyte polarization [53]. Nope protein has been demonstrated to be a good and confident marker for HCC in the clinic because it could be highly detected in AFP-positive and -negative tumors [54].

The methylenetetrahydrofolate dehydrogenase 1 like (Mthfd1l), encoded by *Mthfd1l* gene is an enzyme of the folate cycle. It is involved in formate generation, therefore in the metabolism of mono carbon compound fundamental in both, purine synthesis and protein synthesis initiation. Consequently, this enzyme is highly relevant in the proliferating tissues, particularly in cancer [55, 56]. *Mthfd1l* expression has been associated with poor prognosis, notably in HCC [57]. In normal conditions MTHFD1L is expressed in mitochondria in embryonic tissues [58], once again the mitochondria as an important target in our model. Interestingly, MTHFD1L has been also associated to redox homeostasis in cancer and, as we have demonstrated, one of the main consequences in cancer development in the liver with lipid overloaded is the disruption of redox balance [3]. Metabolic reprograming is one of the key features in cancer. The proposed four-gene signature clearly indicates a metabolic adaptation, compromising mitochondrial adaptation and macrophages participation, particularly the M2-like polarization in a process induced and driven by cholesterol overload.

5. Conclusions

In conclusion, we have characterized an animal model of NASH-derived HCC that recapitulates the human disease, with a clear inflammatory and angiogenic component. RNA-seq analysis identified a specific gene expression profile defining a four-gene signature with potential prognostic applications in the clinical practice, predicting poor survival in patients with HCC. Dietary interventions controlling the quantity and, even more importantly, the quality of dietary lipids could decrease the incidence of aggressive liver cancers.

Supplementary Materials: The following are available online at www.mdpi.com/xxx/s1, …

Author Contributions: "Conceptualization, L.E.G.-Q. and J.U.M.; methodology, A.S.-N., S.S.-S.; software, A.S.-N., M.D.; validation, S.S.-S., L.C.-R. and O.A.E.-C.; formal analysis, L.E.G.-Q., J.U.M. and A.S.-N.; investigation, L.E.G.-Q. and A.S.-N..; resources, L.E.G.-Q. and A.S.-N.; data curation, A.S.-N., M.D. and C.C.; writing—original draft preparation, L.E.G.-Q. and A.S.-N.; writing—review and editing, L.E.G.-Q., J.U.M., C.C. and A.S.-N.; visualization, L.E.G.-Q. and A.S.-N.; supervision, L.E.G.-Q. and J.U.M..; project administration, L.E.G.-Q. and J.U.M.; funding acquisition, L.E.G.-Q. and J.U.M. All authors have read and agreed to the published version of the manuscript.

Funding: This research was funded by a grant from the Consejo Nacional de Ciencia y Tecnología (CONACYT): Fronteras de la Ciencia #1320, CB-252942. The German Research Foundation (MA 4443/2-2; SFB1292), the Volkswagen Foundation (Lichtenberg program), the Wilhelm-Sander Foundation (2017.007.1), and Universidad Autónoma Metropolitana Iztapalapa. ASN, SSS, LCR, AEC were Conacyt scholarship holders.

Institutional Review Board Statement: The study was conducted according to the guidelines of the Declaration of Helsinki, and approved by the Ethics Committee of Universidad Autonoma Metropolitana, Unidad Iztapalapa.

Informed Consent Statement: "Informed consent was obtained from all subjects involved in the study."

Data Availability Statement: Data available on request from the authors

Acknowledgments: This work was partially funded by a grant from the Consejo Nacional de Ciencia y Tecnología (CONACYT): Fronteras de la Ciencia #1320, CB-252942. The German Research Foundation (MA 4443/2-2; SFB1292), the Volkswagen Foundation (Lichtenberg program), the Wilhelm-Sander Foundation (2017.007.1), and Universidad Autónoma Metropolitana Iztapalapa. ASN, SSS, LCR, AEC were Conacyt scholarship holders. We thank Confocal microscopy core unit and Dr. Roberto Lazzarini. Universidad Autónoma Metropolitana Iztapalapa.

Conflicts of Interest: The authors declare no conflict of interest.

References

1. Baffy, G., E. M. Brunt, and S. H. Caldwell. "Hepatocellular Carcinoma in Non-Alcoholic Fatty Liver Disease: An Emerging Menace." *J Hepatol* 56, no. 6 (2012): 1384-91.
2. Younossi, Z. M., A. B. Koenig, D. Abdelatif, Y. Fazel, L. Henry, and M. Wymer. "Global Epidemiology of Nonalcoholic Fatty Liver Disease-Meta-Analytic Assessment of Prevalence, Incidence, and Outcomes." *Hepatology* 64, no. 1 (2016): 73-84.
3. Enriquez-Cortina, C., O. Bello-Monroy, P. Rosales-Cruz, V. Souza, R. U. Miranda, R. Toledo-Perez, A. Luna-Lopez, A. Simoni-Nieves, R. Hernandez-Pando, M. C. Gutierrez-Ruiz, D. F. Calvisi, J. U. Marquardt, L. Bucio, and L. E. Gomez-Quiroz. "Cholesterol Overload in the Liver Aggravates

Oxidative Stress-Mediated DNA Damage and Accelerates Hepatocarcinogenesis." *Oncotarget* 8, no. 61 (2017): 104136-48.

4. Calvisi, D. F., C. Wang, C. Ho, S. Ladu, S. A. Lee, S. Mattu, G. Destefanis, S. Delogu, A. Zimmermann, J. Ericsson, S. Brozzetti, T. Staniscia, X. Chen, F. Dombrowski, and M. Evert. "Increased Lipogenesis, Induced by Akt-Mtorc1-Rps6 Signaling, Promotes Development of Human Hepatocellular Carcinoma." *Gastroenterology* 140, no. 3 (2011): 1071-83.
5. Huang, D. Q., H. B. El-Serag, and R. Loomba. "Global Epidemiology of Nafld-Related Hcc: Trends, Predictions, Risk Factors and Prevention." *Nat Rev Gastroenterol Hepatol* (2020).
6. Cronin, K. A., A. J. Lake, S. Scott, R. L. Sherman, A. M. Noone, N. Howlader, S. J. Henley, R. N. Anderson, A. U. Firth, J. Ma, B. A. Kohler, and A. Jemal. "Annual Report to the Nation on the Status of Cancer, Part I: National Cancer Statistics." *Cancer* 124, no. 13 (2018): 2785-800.
7. Lee, J. S., J. Heo, L. Libbrecht, I. S. Chu, P. Kaposi-Novak, D. F. Calvisi, A. Mikaelyan, L. R. Roberts, A. J. Demetris, Z. Sun, F. Nevens, T. Roskams, and S. S. Thorgeirsson. "A Novel Prognostic Subtype of Human Hepatocellular Carcinoma Derived from Hepatic Progenitor Cells." *Nat Med* 12, no. 4 (2006): 410-6.
8. Younes, R., and E. Bugianesi. "Should We Undertake Surveillance for Hcc in Patients with Nafld?" *J Hepatol* 68, no. 2 (2018): 326-34.
9. Bhaskaran, K., I. Douglas, H. Forbes, I. dos-Santos-Silva, D. A. Leon, and L. Smeeth. "Body-Mass Index and Risk of 22 Specific Cancers: A Population-Based Cohort Study of 5.24 Million Uk Adults." *Lancet* 384, no. 9945 (2014): 755-65.
10. Sun, B., and M. Karin. "Obesity, Inflammation, and Liver Cancer." *J Hepatol* 56, no. 3 (2012): 704-13.
11. Massoud, O., and M. Charlton. "Nonalcoholic Fatty Liver Disease/Nonalcoholic Steatohepatitis and Hepatocellular Carcinoma." *Clin Liver Dis* 22, no. 1 (2018): 201-11.
12. Mari, M., F. Caballero, A. Colell, A. Morales, J. Caballeria, A. Fernandez, C. Enrich, J. C. Fernandez-Checa, and C. Garcia-Ruiz. "Mitochondrial Free Cholesterol Loading Sensitizes to Tnf- and Fas-Mediated Steatohepatitis." *Cell Metab* 4, no. 3 (2006): 185-98.
13. Liu, D., C. C. Wong, L. Fu, H. Chen, L. Zhao, C. Li, Y. Zhou, Y. Zhang, W. Xu, Y. Yang, B. Wu, G. Cheng, P. B. Lai, N. Wong, J. J. Y. Sung, and J. Yu. "Squalene Epoxidase Drives Nafld-Induced Hepatocellular Carcinoma and Is a Pharmaceutical Target." *Sci Transl Med* 10, no. 437 (2018).
14. Garcia-Ruiz, C., L. C. de la Rosa, V. Ribas, and J. C. Fernandez-Checa. "Mitochondrial Cholesterol and Cancer." *Semin Cancer Biol* (2020).
15. Starley, B. Q., C. J. Calcagno, and S. A. Harrison. "Nonalcoholic Fatty Liver Disease and Hepatocellular Carcinoma: A Weighty Connection." *Hepatology* 51, no. 5 (2010): 1820-32.
16. Xu, F., S. D. Rychnovsky, J. D. Belani, H. H. Hobbs, J. C. Cohen, and R. B. Rawson. "Dual Roles for Cholesterol in Mammalian Cells." *Proc Natl Acad Sci U S A* 102, no. 41 (2005): 14551-6.
17. Maxfield, F. R., and G. van Meer. "Cholesterol, the Central Lipid of Mammalian Cells." *Curr Opin Cell Biol* 22, no. 4 (2010): 422-9.
18. Stickel, F., and C. Hellerbrand. "Non-Alcoholic Fatty Liver Disease as a Risk Factor for Hepatocellular Carcinoma: Mechanisms and Implications." *Gut* 59, no. 10 (2010): 1303-7.
19. Lee, C., and S. T. Cheung. "Stat3: An Emerging Therapeutic Target for Hepatocellular Carcinoma." *Cancers (Basel)* 11, no. 11 (2019).

20. Wang, Y., Y. Shen, S. Wang, Q. Shen, and X. Zhou. "The Role of Stat3 in Leading the Crosstalk between Human Cancers and the Immune System." *Cancer Lett* 415 (2018): 117-28.
21. Luo, Y., J. He, X. Tao, H. Wang, Q. Fang, S. Guo, and C. Song. "Mir20b Negatively Regulates Vegf Expression by Targeting Stat3 in H22 Hepatocellular Carcinoma Cells." *Oncol Rep* 40, no. 5 (2018): 2806-13.
22. Hodge, D. R., E. M. Hurt, and W. L. Farrar. "The Role of Il-6 and Stat3 in Inflammation and Cancer." *Eur J Cancer* 41, no. 16 (2005): 2502-12.
23. Gomez-Quiroz, L. E., D. Seo, Y. H. Lee, M. Kitade, T. Gaiser, M. Gillen, S. B. Lee, M. C. Gutierrez-Ruiz, E. A. Conner, V. M. Factor, S. S. Thorgeirsson, and J. U. Marquardt. "Loss of C-Met Signaling Sensitizes Hepatocytes to Lipotoxicity and Induces Cholestatic Liver Damage by Aggravating Oxidative Stress." *Toxicology* 361-362 (2016): 39-48.
24. Sanches, S. C., L. N. Ramalho, M. J. Augusto, D. M. da Silva, and F. S. Ramalho. "Nonalcoholic Steatohepatitis: A Search for Factual Animal Models." *Biomed Res Int* 2015 (2015): 574832.
25. Imhof, B. A., and M. Aurrand-Lions. "Angiogenesis and Inflammation Face Off." *Nat Med* 12, no. 2 (2006): 171-2.
26. Lee, L., M. Alloosh, R. Saxena, W. Van Alstine, B. A. Watkins, J. E. Klaunig, M. Sturek, and N. Chalasani. "Nutritional Model of Steatohepatitis and Metabolic Syndrome in the Ossabaw Miniature Swine." *Hepatology* 50, no. 1 (2009): 56-67.
27. Asgharpour, A., S. C. Cazanave, T. Pacana, M. Seneshaw, R. Vincent, B. A. Banini, D. P. Kumar, K. Daita, H. K. Min, F. Mirshahi, P. Bedossa, X. Sun, Y. Hoshida, S. V. Koduru, D. Contaifer, Jr., U. O. Warncke, D. S. Wijesinghe, and A. J. Sanyal. "A Diet-Induced Animal Model of Non-Alcoholic Fatty Liver Disease and Hepatocellular Cancer." *J Hepatol* 65, no. 3 (2016): 579-88.
28. Dominguez-Perez, M., A. Simoni-Nieves, P. Rosales, N. Nuno-Lambarri, M. Rosas-Lemus, V. Souza, R. U. Miranda, L. Bucio, S. Uribe Carvajal, J. U. Marquardt, D. Seo, L. E. Gomez-Quiroz, and M. C. Gutierrez-Ruiz. "Cholesterol Burden in the Liver Induces Mitochondrial Dynamic Changes and Resistance to Apoptosis." *J Cell Physiol* 234, no. 5 (2019): 7213-23.
29. Castven, D., D. Becker, C. Czauderna, D. Wilhelm, J. B. Andersen, S. Strand, M. Hartmann, S. Heilmann-Heimbach, W. Roth, N. Hartmann, B. K. Straub, F. L. Mahn, S. Franck, S. Pereira, A. Haupts, A. Vogel, M. A. Worns, A. Weinmann, S. Heinrich, H. Lang, S. S. Thorgeirsson, P. R. Galle, and J. U. Marquardt. "Application of Patient-Derived Liver Cancer Cells for Phenotypic Characterization and Therapeutic Target Identification." *Int J Cancer* 144, no. 11 (2019): 2782-94.
30. Kaposi-Novak, P., J. S. Lee, L. Gomez-Quiroz, C. Coulouarn, V. M. Factor, and S. S. Thorgeirsson. "Met-Regulated Expression Signature Defines a Subset of Human Hepatocellular Carcinomas with Poor Prognosis and Aggressive Phenotype." *J Clin Invest* 116, no. 6 (2006): 1582-95.
31. Lee, J. S., I. S. Chu, J. Heo, D. F. Calvisi, Z. Sun, T. Roskams, A. Durnez, A. J. Demetris, and S. S. Thorgeirsson. "Classification and Prediction of Survival in Hepatocellular Carcinoma by Gene Expression Profiling." *Hepatology* 40, no. 3 (2004): 667-76.
32. Schlageter, M., L. M. Terracciano, S. D'Angelo, and P. Sorrentino. "Histopathology of Hepatocellular Carcinoma." *World J Gastroenterol* 20, no. 43 (2014): 15955-64.

33. Liu, Z., D. Chen, F. Ning, J. Du, and H. Wang. "Egf Is Highly Expressed in Hepatocellular Carcinoma (Hcc) and Promotes Motility of Hcc Cells Via Fibronectin." *J Cell Biochem* 119, no. 5 (2018): 4170-83.
34. Coleman, S. J., R. P. Grose, and H. M. Kocher. "Fibroblast Growth Factor Family as a Potential Target in the Treatment of Hepatocellular Carcinoma." *J Hepatocell Carcinoma* 1 (2014): 43-54.
35. Tomoda, T., K. Nouso, K. Miyahara, S. Kobayashi, H. Kinugasa, J. Toyosawa, H. Hagihara, K. Kuwaki, H. Onishi, S. Nakamura, F. Ikeda, Y. Miyake, H. Shiraha, A. Takaki, and K. Yamamoto. "Prognotic Impact of Serum Follistatin in Patients with Hepatocellular Carcinoma." *J Gastroenterol Hepatol* 28, no. 8 (2013): 1391-6.
36. Rebouissou, S., M. Amessou, G. Couchy, K. Poussin, S. Imbeaud, C. Pilati, T. Izard, C. Balabaud, P. Bioulac-Sage, and J. Zucman-Rossi. "Frequent in-Frame Somatic Deletions Activate Gp130 in Inflammatory Hepatocellular Tumours." *Nature* 457, no. 7226 (2009): 200-4.
37. Lee, J. S., I. S. Chu, A. Mikaelyan, D. F. Calvisi, J. Heo, J. K. Reddy, and S. S. Thorgeirsson. "Application of Comparative Functional Genomics to Identify Best-Fit Mouse Models to Study Human Cancer." *Nat Genet* 36, no. 12 (2004): 1306-11.
38. Coulouarn, C., L. E. Gomez-Quiroz, J. S. Lee, P. Kaposi-Novak, E. A. Conner, T. A. Goldina, G. E. Onishchenko, V. M. Factor, and S. S. Thorgeirsson. "Oncogene-Specific Gene Expression Signatures at Preneoplastic Stage in Mice Define Distinct Mechanisms of Hepatocarcinogenesis." *Hepatology* 44, no. 4 (2006): 1003-11.
39. Takami, T., P. Kaposi-Novak, K. Uchida, L. E. Gomez-Quiroz, E. A. Conner, V. M. Factor, and S. S. Thorgeirsson. "Loss of Hepatocyte Growth Factor/C-Met Signaling Pathway Accelerates Early Stages of N-Nitrosodiethylamine Induced Hepatocarcinogenesis." *Cancer Res* 67, no. 20 (2007): 9844-51.
40. Tsuchida, T., Y. A. Lee, N. Fujiwara, M. Ybanez, B. Allen, S. Martins, M. I. Fiel, N. Goossens, H. I. Chou, Y. Hoshida, and S. L. Friedman. "A Simple Diet- and Chemical-Induced Murine Nash Model with Rapid Progression of Steatohepatitis, Fibrosis and Liver Cancer." *J Hepatol* 69, no. 2 (2018): 385-95.
41. Liang, F., C. Ren, J. Wang, S. Wang, L. Yang, X. Han, Y. Chen, G. Tong, and G. Yang. "The Crosstalk between Stat3 and P53/Ras Signaling Controls Cancer Cell Metastasis and Cisplatin Resistance Via the Slug/Mapk/Pi3k/Akt-Mediated Regulation of Emt and Autophagy." *Oncogenesis* 8, no. 10 (2019): 59.
42. Niu, G., K. L. Wright, Y. Ma, G. M. Wright, M. Huang, R. Irby, J. Briggs, J. Karras, W. D. Cress, D. Pardoll, R. Jove, J. Chen, and H. Yu. "Role of Stat3 in Regulating P53 Expression and Function." *Mol Cell Biol* 25, no. 17 (2005): 7432-40.
43. Wormann, S. M., L. Song, J. Ai, K. N. Diakopoulos, M. U. Kurkowski, K. Gorgulu, D. Ruess, A. Campbell, C. Doglioni, D. Jodrell, A. Neesse, I. E. Demir, A. P. Karpathaki, M. Barenboim, T. Hagemann, S. Rose-John, O. Sansom, R. M. Schmid, M. P. Protti, M. Lesina, and H. Algul. "Loss of P53 Function Activates Jak2-Stat3 Signaling to Promote Pancreatic Tumor Growth, Stroma Modification, and Gemcitabine Resistance in Mice and Is Associated with Patient Survival." *Gastroenterology* 151, no. 1 (2016): 180-93 e12.
44. Sainz-Perez, A., H. Gary-Gouy, F. Gaudin, G. Maarof, A. Marfaing-Koka, T. de Revel, and A. Dalloul. "Il-24 Induces Apoptosis of Chronic Lymphocytic Leukemia B Cells Engaged into the

Cell Cycle through Dephosphorylation of Stat3 and Stabilization of P53 Expression." *J Immunol* 181, no. 9 (2008): 6051-60.

45. Shono, S., Y. Habu, M. Nakashima, A. Sato, H. Nakashima, H. Miyazaki, M. Kinoshita, G. Tsumatori, N. Shinomiya, and S. Seki. "The Immunologic Outcome of Enhanced Function of Mouse Liver Lymphocytes and Kupffer Cells by High-Fat and High-Cholesterol Diet." *Shock* 36, no. 5 (2011): 484-93.
46. Yang, Y., Y. C. Ye, Y. Chen, J. L. Zhao, C. C. Gao, H. Han, W. C. Liu, and H. Y. Qin. "Crosstalk between Hepatic Tumor Cells and Macrophages Via Wnt/Beta-Catenin Signaling Promotes M2-Like Macrophage Polarization and Reinforces Tumor Malignant Behaviors." *Cell Death Dis* 9, no. 8 (2018): 793.
47. Goossens, P., J. Rodriguez-Vita, A. Etzerodt, M. Masse, O. Rastoin, V. Gouirand, T. Ulas, O. Papantonopoulou, M. Van Eck, N. Auphan-Anezin, M. Bebien, C. Verthuy, T. P. Vu Manh, M. Turner, M. Dalod, J. L. Schultze, and T. Lawrence. "Membrane Cholesterol Efflux Drives Tumor-Associated Macrophage Reprogramming and Tumor Progression." *Cell Metab* 29, no. 6 (2019): 1376-89 e4.
48. Bao, D., J. Zhao, X. Zhou, Q. Yang, Y. Chen, J. Zhu, P. Yuan, J. Yang, T. Qin, S. Wan, and J. Xing. "Mitochondrial Fission-Induced Mtdna Stress Promotes Tumor-Associated Macrophage Infiltration and Hcc Progression." *Oncogene* 38, no. 25 (2019): 5007-20.
49. Mastrototaro, L., A. Smorodchenko, J. R. Aschenbach, M. Kolisek, and G. Sponder. "Solute Carrier 41a3 Encodes for a Mitochondrial Mg(2+) Efflux System." *Sci Rep* 6 (2016): 27999.
50. Trapani, V., and F. I. Wolf. "Dysregulation of Mg(2+) Homeostasis Contributes to Acquisition of Cancer Hallmarks." *Cell Calcium* 83 (2019): 102078.
51. Ohata, T., H. Yokoo, T. Kamiyama, M. Fukai, T. Aiyama, Y. Hatanaka, K. Hatanaka, K. Wakayama, T. Orimo, T. Kakisaka, N. Kobayashi, Y. Matsuno, and A. Taketomi. "Fatty Acid-Binding Protein 5 Function in Hepatocellular Carcinoma through Induction of Epithelial-Mesenchymal Transition." *Cancer Med* 6, no. 5 (2017): 1049-61.
52. Furuhashi, M., and G. S. Hotamisligil. "Fatty Acid-Binding Proteins: Role in Metabolic Diseases and Potential as Drug Targets." *Nat Rev Drug Discov* 7, no. 6 (2008): 489-503.
53. Bowe, A., S. Zweerink, V. Muck, V. Kondylis, S. Schulte, T. Goeser, and D. Nierhoff. "Depolarized Hepatocytes Express the Stem/Progenitor Cell Marker Neighbor of Punc E11 after Bile Duct Ligation in Mice." *J Histochem Cytochem* 66, no. 8 (2018): 563-76.
54. Marquardt, J. U., M. Quasdorff, H. Varnholt, H. M. Curth, S. Mesghenna, U. Protzer, T. Goeser, and D. Nierhoff. "Neighbor of Punc E11, a Novel Oncofetal Marker for Hepatocellular Carcinoma." *Int J Cancer* 128, no. 10 (2011): 2353-63.
55. He, Z., X. Wang, H. Zhang, B. Liang, J. Zhang, Z. Zhang, and Y. Yang. "High Expression of Folate Cycle Enzyme Mthfd1l Correlates with Poor Prognosis and Increased Proliferation and Migration in Colorectal Cancer." *J Cancer* 11, no. 14 (2020): 4213-21.
56. Agarwal, S., M. Behring, K. Hale, S. Al Diffalha, K. Wang, U. Manne, and S. Varambally. "Mthfd1l, a Folate Cycle Enzyme, Is Involved in Progression of Colorectal Cancer." *Transl Oncol* 12, no. 11 (2019): 1461-67.

57. Lee, D., I. M. Xu, D. K. Chiu, R. K. Lai, A. P. Tse, L. Lan Li, C. T. Law, F. H. Tsang, L. L. Wei, C. Y. Chan, C. M. Wong, I. O. Ng, and C. C. Wong. "Folate Cycle Enzyme Mthfd1l Confers Metabolic Advantages in Hepatocellular Carcinoma." *J Clin Invest* 127, no. 5 (2017): 1856-72.
58. Pike, S. T., R. Rajendra, K. Artzt, and D. R. Appling. "Mitochondrial C1-Tetrahydrofolate Synthase (Mthfd1l) Supports the Flow of Mitochondrial One-Carbon Units into the Methyl Cycle in Embryos." *J Biol Chem* 285, no. 7 (2010): 4612-20.

Supplementary information were uploaded: Supp Figures 1-3, Tables 1-6

Annals of Hepatology xxx (xxxx) 100339

Contents lists available at ScienceDirect

Annals of Hepatology

journal homepage: http://ees.elsevier.com

Original article

HGF/c-Met regulates p22^{phox} subunit of the NADPH oxidase complex in primary mouse hepatocytes by transcriptional and post-translational mechanisms

Arturo Simoni-Nieves [a,b], Denise Clavijo-Cornejo [c], Soraya Salas-Silva [a,b], Oscar Alejandro Escobedo-Calvario [a,b], Leticia Bucio [b,d], Verónica Souza [b,d], María Concepción Gutiérrez-Ruiz [b,d], Roxana U. Miranda-Labra [b,d,1,*], Luis Enrique Gomez-Quiroz [b,d,1,*]

[a] Posgrado en Biología Experimental, DCBS, Universidad Autónoma Metropolitana-Iztapalapa, Mexico City, Mexico
[b] Área de Medicina Experimental y Traslacional, Departamento de Ciencias de la Salud, Universidad Autónoma Metropolitana-Iztapalapa, Mexico City, Mexico
[c] División de Enfermedades Musculoesqueléticas y Reumáticas, Instituto Nacional de Rehabilitación Luis Guillermo Ibarra Ibarra, Mexico City, Mexico
[d] Laboratorio de Medicina Experimental, Unidad de Medicina Traslacional, IIB, UNAM/Instituto Nacional de Cardiología Ignacio Chavez, Mexico City, Mexico

ARTICLE INFO

Article history:
Received 23 January 2021
Accepted 18 February 2021
Available online xxx

Keywords:
p22^{phox}
NADPH oxidase
HGF
Hepatocytes
c-Met

ABSTRACT

Introduction and objectives: It is well-known that signaling mediated by the hepatocyte growth factor (HGF) and its receptor c-Met in the liver is involved in the control of cellular redox status and oxidative stress, particularly through its ability to induce hepatoprotective gene expression by activating survival pathways in hepatocytes. It has been reported that HGF can regulate the expression of some members of the NADPH oxidase family in liver cells, particularly the catalytic subunits and p22^{phox}. In the present work we were focused to characterize the mechanism of regulation of p22^{phox} by HGF and its receptor c-Met in primary mouse hepatocytes as a key determinant for cellular redox regulation.

Materials and methods: Primary mouse hepatocytes were treated with HGF (50 ng/mL) for different times. *cyba* expression (gene encoding p22^{phox}) or protein content were addressed by real time RT-PCR, Western blot or immunofluorescence. Protein interactions were explored by immunoprecipitation and FRET analysis.

Results: Our results provided mechanistic information supporting the transcriptional repression of*cyba* induced by HGF in a mechanism dependent of NF-κB activity. We identified a post-translational regulation mechanism directed by p22^{phox} degradation by proteasome 26S, and a second mechanism mediated by p22^{phox} sequestration by c-Met in plasma membrane.

Conclusion: Our data clearly show that HGF/c-Met exerts regulation of the NADPH oxidase by a wide-range of molecular mechanisms. NADPH oxidase-derived reactive oxygen species regulated by HGF/c-Met represents one of the main mechanisms of signal transduction elicited by this growth factor.

© 2021

1. Introduction

The liver is perhaps the major organ capable to efficiently handling profound changes in cellular redox status and oxidative stress [1]. In fact, hepatocytes have gained advantages using reactive oxygen species (ROS) generated as by-products in many metabolic and biotransformation processes [2]. But some ROS-generating systems function exclusively for ROS production, particularly for cell signaling or in the respiratory burst in phagocytic cells. The nicotinamide adenine dinucleotide phosphate (NADPH) oxidase is a remarkable system dedicated to the production of ROS. This system is ubiquitously distributed, not only in phagocytic cells, but in practically all cell types in mammals [3].

In the liver the NADPH oxidase plays outstanding function in normal physiology and its dysfunction is involved in virtually all liver diseases [4]. A system with these characteristics must be adequately regulated, particularly since NADPH oxidases play a role in signal transduction in non-phagocytic cells as we and others have reported [2,3,5].

The hepatocyte growth factor (HGF) is a multitask receptor tyrosine kinase that in addition of its well-known antiapoptotic and mitogenic properties, has the ability to exerts other functions such as motogenesis, morphogenesis, and metabolic control. In all cases its function is regulated by a fine-tuned ROS production [6–8].

HGF and its receptor c-Met display protective effects in the liver regulating the cellular redox status in apoptosis [2], fibrosis [9],

* Corresponding authors.
E-mail addresses: roxml@xanum.uam.mx (R.U. Miranda-Labra); legq@xanum.uam.mx (L.E. Gomez-Quiroz)
[1] Shared senior authorship.

https://doi.org/10.1016/j.aohep.2021.100339
1665-2681/© 2021.

UNCORRECTED PROOF

cancer [7,10], drug-induced liver injury [11,12], NASH [6,13], cholestasis [14], and alcoholic liver disease [15], even more this protective response has been observed in the pancreas [16], lungs [12], among other organs.

We have previously reported that HGF/c-Met exerts regulatory properties in the NADPH oxidase complex in hepatocytes. The liver from the c-Met KO mouse exhibits oxidative stress at basal conditions [7], and even sublethal dose of FAS agonist such as Jo2 antibody induces massive apoptosis in the liver of these animals [1]. Hepatocytes from c-Met KO mice are susceptible to apoptosis due to the oxidative stress produced by the overactivation of the NADPH oxidase, in fact, treatment of wild type hepatocytes with HGF induces the downregulation of at least the catalytic subunit Nox2 and the regulatory subunit $p22^{phox}$. The $p22^{phox}$ subunit of the oxidase complex is a key regulatory protein which permanently resides in membranes, and it is a common member of at least four members of the NADPH oxidase family [17,18]. HGF/c-Met as a master regulator of the cellular redox state in the liver, takes control of the pro-oxidative system by regulating $p22^{phox}$. In the present work we provide mechanistic evidence regarding the regulation of $p22^{phox}$ by HGF/c-Met in primary mouse hepatocytes, particularly related to the transcriptional and post-translational regulation of this relevant subunit of the NADPH oxidases.

2. Materials and methods

2.1. Materials

All reagents were purchased from Sigma-Aldrich Inc. (Saint Louis, MO, USA) except where noted. The human recombinant hepatocyte growth factor (HGF) and transforming growth factor beta (TGF-β) were obtained from PeproTech (Rocky Hill, NJ, USA).

2.2. Primary mouse hepatocytes isolation, purification and culture

8–10-weeks-old C57BL/6 J male mice were obtained from the Universidad Autonoma Metropolitana Iztapalapa (UAM-I) animal facility and were maintained in pathogen-free conditions with controlled temperature and humidity on a 12 h light-dark cycle in the same facility. The experimental protocols used were approved and carried out in accordance with the UAM-I experimental animal guidelines and NIH Guide for the Care and Use of Laboratory Animals. Hepatocytes were isolated by a two-step collagenase perfusion, as we previously described [5]. The viability was >90% as assessed by trypan blue exclusion test. Hepatocytes were seeded at 2.13×10^5 cells/cm^2 in 10-cm dishes (Thermo Scientific, Waltham, MA, USA) in the Ham´s F-12/Dulbecco´s modified Eagle´s basal hepatocyte growth medium supplemented with 10% fetal bovine serum. After 4 h of attachment, the medium was replaced to a serum-free basal hepatocyte growth medium. The following day, cells were treated with 50 ng/mL HGF, 10 ng/mL TGF-β, 200 nM epoxomicin (epox, 30 min before HGF treatment), 30 μM of SN50 (Merck and Co., Kenilworth, NJ, USA. 30 min before HGF treatment) or 2.5 mM Sulfasalazine (30 min before HGF treatment). Time of treatment was according to each experiment.

2.3. HepG2 cell line culture

HepG2 cell line was obtained from American Type Culture Collection, cells were grown in DMEM media supplemented with 10% heat-inactivated fetal bovine serum, 100 U/mL penicillin and 100 μg/mL streptomycin, at 37 °C in a 5% CO_2 atmosphere as previously published [19].

2.4. Real-time RT-PCR

After treatments, cells were subjected to RNA isolation, and DNase digestion with a DNA-free kit (Ambion, Inc, Austin TX, USA), 1 μg of total RNA was reverse transcribed in 20 μL reaction volume with a SuperScript (Invitrogen Corp, Carlsbad CA, USA) first-strand synthesis kit according to the manufacturer's instructions. The qRT-PCR analysis was performed with a CFX96 Touch (Bio-Rad, Hercules, CA, USA) thermal cycler in a 96-wells reaction plate. The 10 μL PCR reaction mix contained 5 μL 2X SYBR Green PCR Master Mix (Bio-Rad), 200 nM of each primer, and 1 μL cDNA template. Reactions were incubated for 10 min at 95 °C followed by 40 cycles of 30 s at 95 °C and 60 s at specific primer temperature. Melting analysis of the PCR products was also conducted to validate the amplification of the specific product. The expression level of mouse rps18 was used as an internal reference. Relative gene expression level was calculated with the $2^{-\Delta\Delta CT}$ method. Primer sequences are listed in Supplementary Table 1.

2.5. In silico analysis of cyba gene promoter

For the identification of canonical bindings sites for transcription factors (TFs) in the *cyba* promoter (2000 base pairs upstream of the start of transcription), the JASPAR platform was used (http://jaspar.genereg.net) with a relative profile score threshold of 95%.

2.6. cyba promoter analysis

For the amplification of the different segments of the *cyba* promoter, we used the oligonucleotides listed in Supplementary Table 2 which have cut-off sequences for restriction enzymes (HindIII in the forward oligonucleotides; and EcoRI in the reverse oligonucleotides). Products were cloned in the promoterless pmCherry plasmid (Life Technologies, CA, US). Plasmid were transfected as stated below in HepG2 cells. mCherry fluorescence was recorded in a DTX800 Multimode detector microplate reader (Beckman Coulter, Brea, CA, USA) at 587 nm of excitation and 610 nm of emission. Data are reported as absolute fluorescence.

2.7. Transfection with decoy oligodeoxynucleotides (ODN)

HepG2 cells were seeded in 24-wells plates at a density of 3×10^5 cells/cm^2 and transfected with ODN 100 nM. (NF-κB: 5′-AGA GGA ATT TCC ACG ATT-3′. AP-1: 5′-TGT GAT GAC TCA GGT TTG-3′, Mock 5′-CAC AAA GTG TAA CAG TCT-3′) using the cationic liposome vector Lipofectamine 2000 (Invitrogen) according to the manufacturer's instructions [20]. After 6 h incubation, cells were washed twice with serum-free culture medium and left at 37 °C and 5% CO_2 for at least 4 h before HGF treatment (50 ng/mL) for a further 12 h.

2.8. Immunofluorescence

Immunofluorescence was performed as previously published [6,9]. Slides were examined using the Carl Zeiss LSM 780 NLO confocal microscope (Carl Zeiss, Oberkochen, Germany).

2.9. Plasmids transfection

Plasmids were transfected by using Lipofectamine 2000 (Invitrogen Inc.) in HepG2 cells at 60% of confluence. We transfected adherent cells with 100 ng of DNA according to the manufacturer's in-

UNCORRECTED PROOF

structions. After transfection, the cells were incubated for further 2–3 days.

2.10. Western blot

Western blotting was performed following the protocol previously reported [2,21], using different antibodies as shown in Supplementary Table 3.

2.11. Immunoprecipitation

1−2 mg of whole cell lysate were subjected to immunoprecipitation (IP), as previously reported [5], SDS-PAGE, using anti-$p22^{phox}$, anti-c-Met or anti-polyUb antibodies (Supplementary Table 3).

2.12. Chemical crosslinking

To determine spatial protein association between $p22^{phox}$ and c-Met, isolated mice hepatocytes were exposed to crosslinking reagents. Chemical crosslinker stock solutions were freshly prepared before use. The 3,3-dithiobis (sulfosuccinimidyl propionate) (DTSSP) cell permeable crosslinker agent and the dithiobis (succinimidyl propionate) (DSP) cell impermeable crosslinker agent were added to 3×10^6 hepatocytes to a final concentration of 1 mM and 0.5 mM respectively. Crosslinking was performed for 25 min at room temperature. The reaction was terminated by the addition of ice-cold 50 mM Tris/HCl. Next the samples were immunoprecipitated as mention above. Dithiothreitol (DTT) was used to reverse the crosslinking as control.

2.13. Chimeric fluorescent proteins production

The $p22^{phox}$ and c-Met-containing plasmids were generated by PCR based amplification of $p22^{phox}$ and c-Met ORF from mouse cDNA by using primers listed in Supplementary table 4, which have cut-off sequences for restriction enzymes (XhoI in forward oligonucleotide and EcoRI in the reverse oligonucleotide) followed by enhancer Cyan Fluorescence Protein (eCFP) with an excitation wavelength of 405 nm and emission wavelength of 485 nm and enhancer Yellow Fluorescence Protein (eYFP) with an excitation wavelength of 514 nm and emission wavelength of 527 nm respectively sequence to frame into pcDNA3.1 vector (Life Technologies Co.). Cells transfected with plasmids encoding these chimeric proteins were used for FRET analysis.

FRET measurements by sensitized emission. The Förster resonance energy transfer (FRET) measurements between the $p22^{phox}$ and c-Met were obtained using the sensitized emission (SE) protocol. Briefly, FRET was obtained by measuring the acceptor emission resulting from donor excitation. To avoid overestimation of FRET first we evaluated the bleed-trough between both fluorescence channels for donor and acceptor. After subtracting the bleed-through from the donor emission we calculate FRET by using the following equation:

$$nF = FexD,emA - \alpha FexA,emA - \beta FexD,emD$$

Using an excitation wavelength that excites only the donor, the emission for the acceptor (*FexD,mA*) and donor (*FexD,emD*) channels are obtained. Next, fluorescence is measured in the acceptor channel (*FexA,mA*) at an excitation wavelength that only excites the acceptor. The amount of donor bleed-through into the acceptor channel is determined by a donor-only measurement, which provides the calibration constant $\beta = FexD,mAD|FexD,emDD$. By measuring only the acceptor channel we obtained the constant $\alpha = FexD,mAA|FexA,emAA$ [22].

2.14. Reactive oxygen species determination

Reactive oxygen species (ROS) content was determined by dihydroethidium (DHE, 50 μM) fluorescence as previously reported [14]. DHE-derived fluorescence was recorded in a Multimodal reader (DTX880, Beckman Coulter, Inc. Brea, CA, USA) at 520 nm for excitation and 570 nm for emission. Data are reported in arbitrary fluorescence units (AFU).

2.15. Statistical analysis

Each experiment was performed at least by triplicate. Data are reported as average ± standard error (SEM). Statistical analysis was performed using GraphPad Prism v 8.2.1 software for iOS. Comparisons between groups were made using Student's *t*-test or Mann-Whitney-U test. Differences were considered significant at $p \leq 0.05$.

3. Results

Our group has proved that HGF and its receptor c-Met are regulators of cellular redox status in the liver [7], particularly regulating the activity of the multiprotein NADPH oxidase complex as we previously reported [2,5]. In the present work, we were aimed to gain mechanistic information about this regulation. Previously, we observed a decrease in the content of the main protein components of the system induced by the signaling of HGF, mainly the $p22^{phox}$ subunit encoded by *cyba* gene. $p22^{phox}$ which is a conserved subunit in the different complexes of NADPH oxidase, (NOX1–4) [23].

Fig. 1A shows that HGF treatment in primary mouse hepatocytes significantly decreases the expression of *cyba* gene at 12 h of treatment, data consistent with our previous finding at the protein level. In order to gain mechanistic evidence of the *cyba* repression we constructed and cloned different *cyba* promoter sections (Fig. 1B) by using the promotorless pmCherry vector. Fig. 1C shows the different *cyba* promotor activity (judged by mCherry reporter fluorescence) induced by HGF treatment, indicating that the segment A–E (−1 to −500 bp) owns the transcriptional repression of *cyba* gene, remaining segments of the promotor exhibited no changes.

Interestingly, this *cyba* promoter section contains a NF-κB (p65 subunit) consensus sequence determined by JASPAR software (Supplementary Figs. 1 and 2), it has been reported that NF-κB could exert gene repression in some genes [24,25].

In order to address whether the *cyba* transcriptional repression could be instigated by NF-κB we used the well-known specific NF-κB peptide inhibitor SN50 [2], Fig. 2A shows that the decrement in the expression of the gene induced by HGF treatment is abrogated by the SN50, similar data were observed by the NF-κB chemical inhibitor sulfasalazine (Fig. 2B). The decrement of the *cyba* gene is evaded by the inhibition of the transcription factor, clarifying that NF-κB drives the repressive activity exerted by HGF over the $p22^{phox}$ gene in hepatocytes.

To gain confidence we performed a competitive assay transfecting NF-κB consensus sequence (ODS) at high concentration (100 nM) in order to compete with natural sequence in the genome, Fig. 2C shows that NF-κB sequence abrogated the effect of HGF, confirming previous results obtained in Fig. 2A and B. As a control we used AP-1 transcription factor consensus sequence, which had no effect, corroborating the irrelevance of AP-1 in the repression of *cyba* in hepatocytes.

3.1. HGF induces proteasome 26S-dependent degradation of $p22^{phox}$

As we previously reported, HGF effect on *cyba* gene is also observed at the protein level at 12 h of treatment, addressed by both

UNCORRECTED PROOF

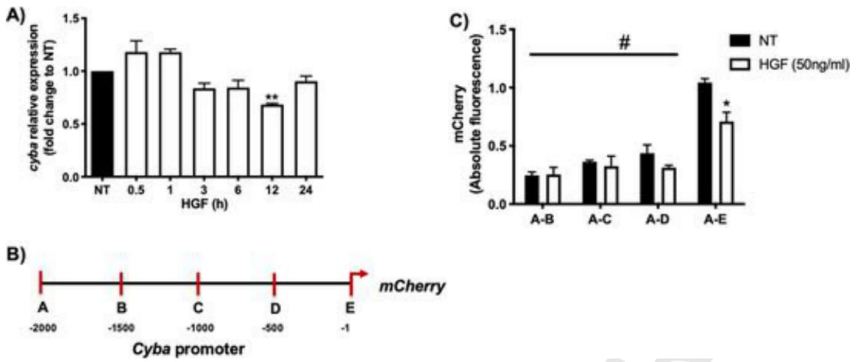


Fig. 1. *cyba* (p22^{phox}) expression is regulated by HGF. A) Primary mouse hepatocytes were treated with HGF (50 ng/mL) for different times. *cyba* expression was addressed by qRT-PCR. B) Graphical representation of cyba promoter and different sections produced for, C) Cloning studies in the promoterless mCherry vector and its activation induced by HGF treatment. Each bar represents the average of at least three independent experiments ± SEM, * $p < 0.05$ vs NT; ** $p < 0.01$ vs NT; # $p < 0.05$ vs A-E promoter section.

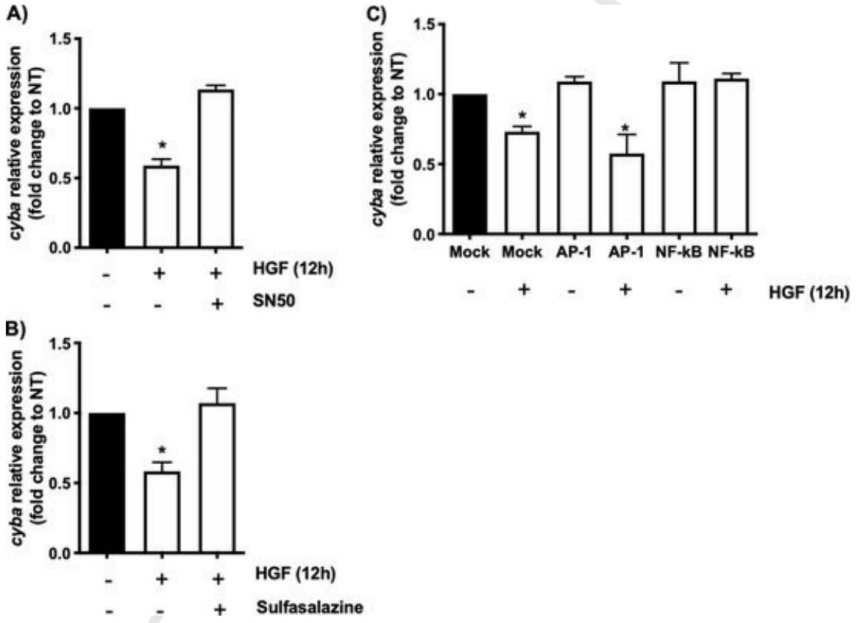


Fig. 2. *cyba* (p22^{phox}) transcriptional repression is driven by NF-κB. Primary mouse hepatocytes were pretreated with A) SN50, NF-κB peptide inhibitor or, B) sulfasalazine, NF-κB chemical inhibitor, for 30 min previous to HGF (50 ng/mL) treatment for 12 h. C) Binding competence of NF-κB by using decoy oligodeoxynucleotides (ODN). Each bar represents the average of at least three independent experiments ± SEM, * $p < 0.05$ vs NT.

Western blot and immunofluorescence of p22^{phox} (Fig. 3A and B, respectively). The overlapping of *cyba* mRNA and p22^{phox} protein decrement at 12 h suggests different mechanism of regulation. Data suggest that the decrement in protein content is driven by a post-translational mechanism. Then, we decided to address the involvement of the proteasome 26S in degradation of p22^{phox}. Hepatocytes were pretreated with epox for 30 min, after that, cells were treated with HGF for 12 h, Fig. 4 shows the decrement of p22^{phox}, determined by Western blot (Fig. 4A) and IF (Fig. 4B). To gain more confidence we studied the ubiquitination of p22^{phox} induced by HGF treatment. Fig. 4C shows that ubiquitination of the protein was time-dependent manner, peaking at 12 h of treatment.

3.2. c-Met interacts with p22^{phox}

It has been reported the peculiar mechanism of regulation exerted by c-Met over some key membrane proteins such as FAS [26], plexin B1, CD44, among others [27], by physical interaction each other. We explored the possible interaction between c-Met and p22^{phox} by IP, identifying an interaction between both proteins at

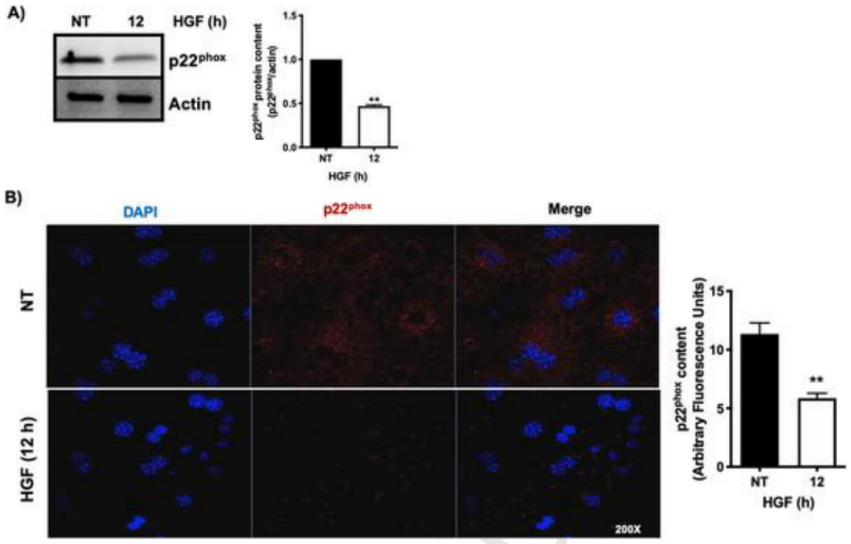


Fig. 3. HGF induces the decrease of the protein content of $p22^{phox}$. Primary mouse hepatocytes were treated for 12 h with HGF (50 ng/mL). A) Western blot of $p22^{phox}$ and densitometric analysis. B) Immunofluorescence of $p22^{phox}$ (in red), nuclei judged by DAPI fluorescence (blue). Images are representative of at least three independent experiments. Each bar represents the average ± SEM, ** $p < 0.01$ vs NT.

basal levels (NT) being stable up to 30 min after treatment with HGF, presenting a decrease in the interaction at later times, reaching its maximum point at 60 min (Fig. 5A). To validate these results, we performed the reverse IP (Fig. 5B) corroborating the interaction of both proteins and its decrement at 60 min. To gain further insight into the mechanism of c-Met-$p22^{phox}$ interaction or association, chemical crosslinking was performed. Hepatocytes culture was subjected to the cell-impermeable thiol-cleavable crosslinking agent DSSTP, which only crosslinks proteins on the extracellular space and previously proved in other c-Met interactions [26]. Fig. 5C shows the detection of a strong band consisting of c-Met plus $p22^{phox}$, in the not treated cells (basal interaction) which was decreased with HGF treatment for 60 min. The use of DTT as agent of crosslinking reversion, induced the disappearance of such band indicating that the band was product of the crosslinking. No detectable bands were observed by using the cell-permeable DSP crosslinker agent (Fig. 5D) clearly indicating that c-Met and $p22^{phox}$ interaction is on the cell membrane.

Interestingly, we could not identify the interaction of c-Met and $p22^{phox}$ by regular immuno-colocalization using fluorescence antibodies. The first antibody used impeded the attachment of the second one (data not shown), we decided to construct plasmids encoding sequences for the production of chimeric proteins coupled to fluorescence markers eCFP/$p22^{phox}$ and eYFP/c-Met, as stated under material and methods section. HepG2 cells were co-transfected with both plasmids and after verification of proper production of fluorescent proteins, were treated with HGF. Fig. 6A shows the basal co-localization (green fluorescence, arrows) in no treated cells, which disappears after 60 min of HGF treatment, confirming the c-Met and $p22^{phox}$ interaction.

We selected eCFP/$p22^{phox}$ and eYFP/c-Met because both fluorescent proteins allow FRET studies. Fig. 6B shows the percentage of FRET efficiency in a time course study, where significant change was observed since 30 min and peaked at 60 min, confirming the IP and crosslinking results in Fig. 5.

Finally, the ROS content in hepatocytes treated with TGF-β, pretreated or not with HGF was addressed. Fig. 7 shows that TGF-β increases ROS production, judged by DHE fluorescence, and the treatment with HGF significantly decreased the content of ROS, indicating that $p22^{phox}$ repression certainly decreases ROS derived from NADPH oxidase, as previously we published [5].

4. Discussion

We have previously published that HGF/c-Met is key regulator of cellular redox status and oxidative stress in many systems such as liver [7,13], pancreas [16], lungs [12], biliary tree [14], among others. Particularly, in the liver, HGF/c-Met has demonstrated to influence the initiation, progression or treatment of alcoholic liver disease [15], cholestasis [14], hepatocellular carcinoma [7,10], fibrosis [9], drug-induced liver injury [11,12], and NASH [6,13]. Data published have provided mechanistic insights indicating that HGF/c-Met could exert these antioxidant/protective responses by multiples mechanisms, such as the activation of antioxidant-related transcription factors such as Nrf2 or NF-κB which, in addition express antioxidant enzymes like catalase, superoxide dismutase 1 and 2, and glutathione-related enzymes [2,15]. Another mechanism of action is directed to eliminate xenobiotics, which are potentially inducers of oxidative stress as we recently reported in cholestasis [14].

In the present work we are characterizing another mechanism of antioxidant action elicited by HGF/c-Met, which is directed to control the ROS-generating systems driven by the NADPH oxidases. The conserved membrane-resident component of the NADPH oxidases $p22^{phox}$, which is used by at least four complexes (NADPH oxidase 1–4), is particularly affected by HGF signaling, as we previously reported in wild-type primary mouse hepatocytes [5] and in c-Met KO hepatocytes, where we observed a profound oxidative stress in untreated hepatocytes. In fact, this ROS control is key component of the HGF/c-Met signature defining an new aggressive phenotype tumor subtype with poor prognosis as we previously reported [7,10].

PROOF

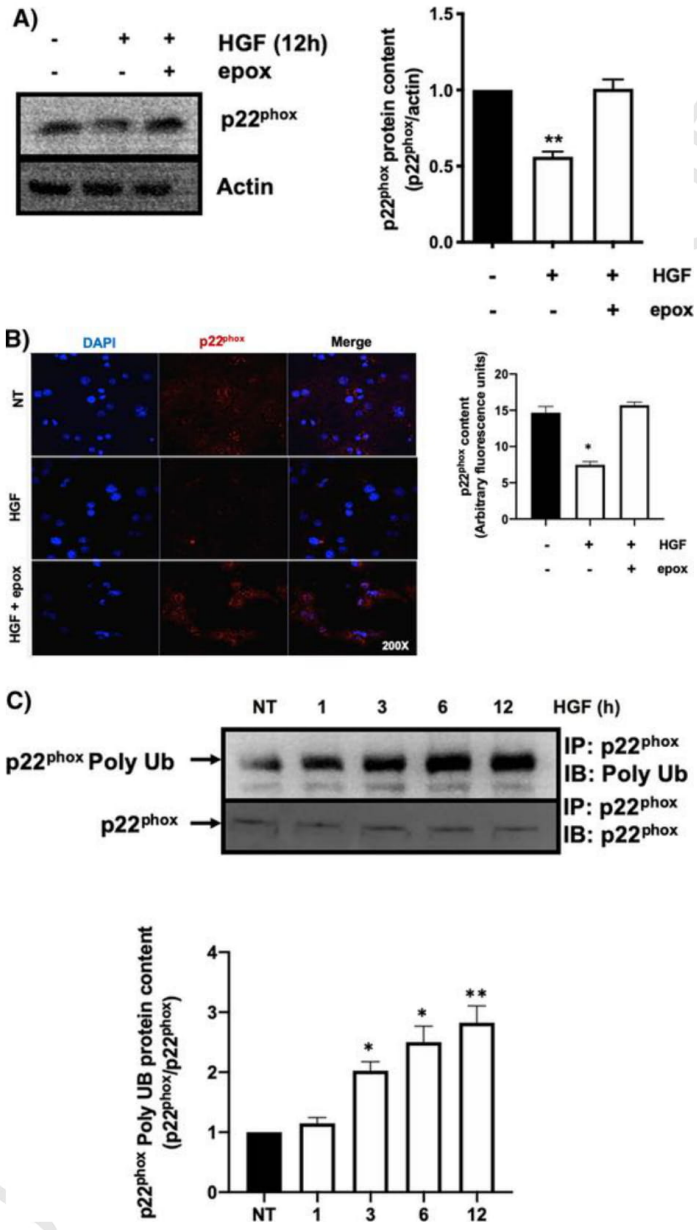


Fig. 4. HGF induces the decrease of $p22^{phox}$ by a mechanism of proteasome 26S. Primary mouse hepatocytes were pretreated with epoxomicin (epox, 200 mM) for 30 min, followed of HGF treatment (50 ng/mL) for 12 h and $p22^{phox}$ was evaluated by A) Western blot and densitometric analysis; B) Immunofluorescence and fluorescence quantification of $p22^{phox}$ (in red), nuclei judged by DAPI fluorescence (blue). Images are representative of at least three independent experiments. Original magnification 200 × . C) Immunoprecipitation of $p22^{phox}$ and immunoblot of poly ubiquitination (poly Ub) and densitometric analysis. Each bar represents the average of at least three independent experiments ± SEM. * $p < 0.05$ vs NT. ** $p < 0.01$ vs NT.

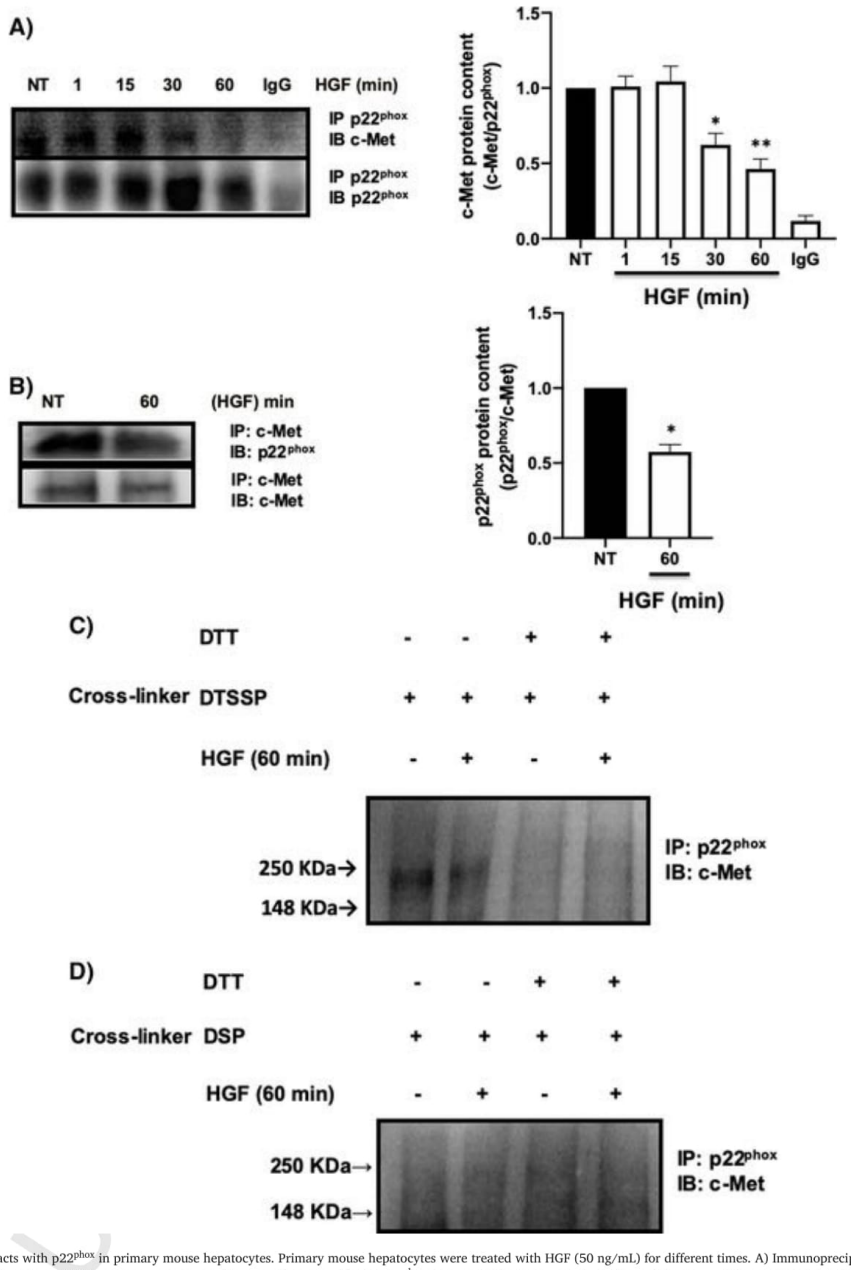


Fig. 5. c-Met interacts with $p22^{phox}$ in primary mouse hepatocytes. Primary mouse hepatocytes were treated with HGF (50 ng/mL) for different times. A) Immunoprecipitation of $p22^{phox}$ and immunoblot of c-Met, and B) Immunoprecipitation of c-Met and immunoblot of $p22^{phox}$. C) Crosslinking using 3,3-dithiobis (sulfosuccinimidyl propionate) (DTSSP, 1 mM) cell permeable crosslinker agent and, D) Crosslinking using the dithiobis (succinimidyl propionate) (DSP, 0.5 mM) cell impermeable crosslinker agent. Crosslinking experiments were subjected to immunoprecipitation of $p22^{phox}$ and immunoblot of c-Met. The product band at 250 KDa represents the molecular weight of c-Met plus $p22^{phox}$. Images representative of at least three independent experiments.

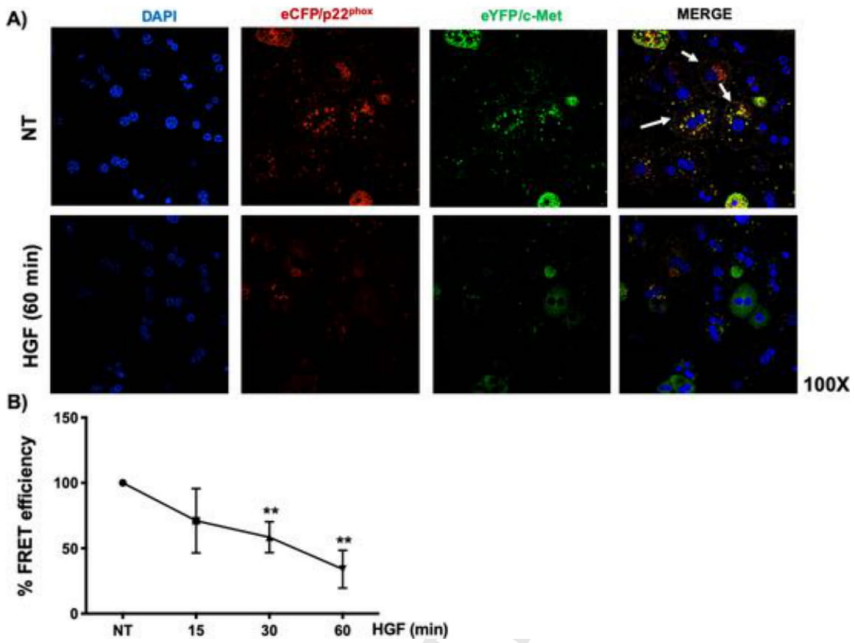


Fig. 6. c-Met interaction with $p22^{phox}$ is disrupted at early times of treatment with HGF in HepG2 cells. HepG2 cells were co-transfected with eCFP/$p22^{phox}$ and eYFP/c-Met chimeric proteins after two days cells were observed by confocal microscopy at different times of incubation with HGF (50 ng/mL). A) representative images of cells treated or not with HGF for 60 min. co-localization of $p22^{phox}$ (red), c-Met (green) and nuclei judged by DAPI fluorescence (blue). Images are representative of at least three independent experiments. Original magnification 200 × . B) Independent experiment for FRET analysis following protocol stated under material and methods section. Cells were treated with HGF for 15, 30 and 60 min. Each point represents the average of at least three independent experiments ± SEM. ** $p < 0.01$ vs NT.

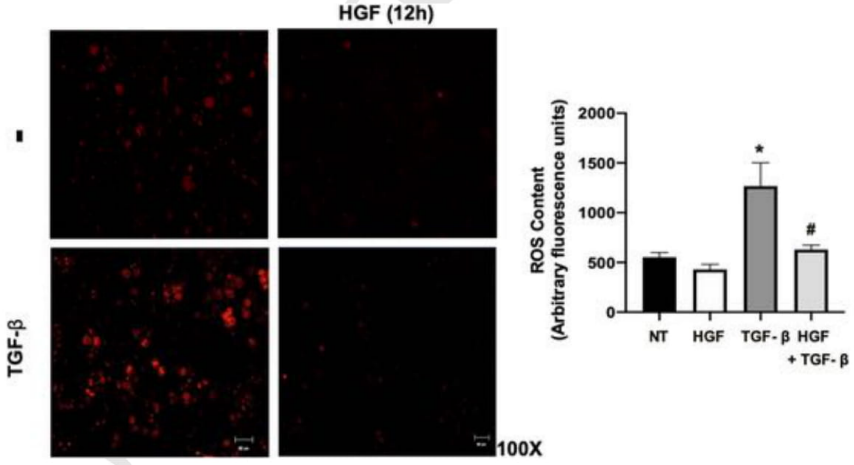


Fig. 7. HGF treatment decreases reactive oxygen species (ROS) induced by transforming growth factor beta (TGF-β). Primary mouse hepatocytes were treated with HGF (50 ng/mL) for 12 h after that cells were treated with TGF-β (10 ng/mL) and ROS were determined using dihydroethidium (DHE, 50 μM) fluorescence (red), for 15 min, in the dark. Images are representative of at least three independent experiments. Each bar represents the average ± SEM, * $p < 0.05$ vs NT; # $p < 0.05$ vs TGF-β.

Previously we showed the downregulation of some components of the NADPH oxidase by HGF signaling, including the catalytic subunit Nox2; contrary, in c-Met KO hepatocytes we observed the over activation of the enzyme and a prominent oxidative stress [7]. Although, we reported that HGF exerts gene expression repression in NADPH oxidase components, in the present work we found that NF-κB is part of the gene repression machinery since the inhibition of its activity abolished the downregulation of $p22^{phox}$ maintaining basal

protein content (Fig. 2), suggesting that this transcription factor is key regulator of the NADPH oxidase, since abrogation was not complete. NF-κB consensus sequence was identified downstream near to the transcription start site. Our current data support previous works reporting a profound effects induced by HGF in downregulation of NADPH oxidase at the transcriptional level, we have now advanced in the knowledge pointing out the relevance of NF-κB in the repressive stimulus of the pro-oxidant systems and in the expression of antioxidant and protective machinery [2,15].

The second mechanism of HGF/c-Met-mediated regulation of NADPH oxidase, particularly in $p22^{phox}$, is post-translational. In this case, data show a fast decrease in the $p22^{phox}$ content since 3 h of HGF treatment in primary mouse hepatocytes. This effect continued in a time-dependent manner peaking at 12 h [5], so we decided to explore whether this effect could be related to $p22^{phox}$ degradation by proteosome 26S. Our results clearly indicate the polyubiquitination of $p22^{phox}$ induced by HGF, epox, inhibitor of the proteasome activity, avoided the degradation of the target protein. Data suggest that ubiquitin/proteasome 26S system is key determinant in NADPH oxidase activity, recently it has been published that perturbation of ubiquitin homeostasis led to a rapid and transient ROS generation in macrophages cell line [28], supporting this mechanism of regulation of the system, at least partially characterized in hepatocytes in terms of $p22^{phox}$ regulatory subunit.

The relevance of $p22^{phox}$ goes beyond of being a simple scaffolding protein, it displays regulatory functions, particularly at the level of $p47^{phox}$ [17], in fact some polymorphism has been identified in *cyba* resulting in a significant risk factor for coronary artery disease [29], but the relationship of this polymorphisms remains uncharacterized in liver diseases.

The physical interaction of c-Met with multiple membrane proteins has been positioned as a key regulatory mechanism [27]. It is particularly relevant the interaction or sequestration with FAS, which is a remarkable mechanism of HGF-induced anti-apoptosis response [26], in addition, c-Met interacts with CD44 [30] acting each other as coactivators of signaling; plexin B1 [31] is another membrane protein that interacts with c-Met, in this case antagonizing each other [31]. Our research provides evidence that c-Met is capable to interact with $p22^{phox}$ and repress the NADPH oxidase activity, at least partially, as we previously published [5] and supported in this work (Figs. 5 and 6). In addition, we are reporting that this interaction is intracellular, and after HGF treatment this protein-protein binding is lost, judged by FRET analysis, in order to increase ROS production at early times, for Nrf2 signaling [5].

The relationship of HGF/c-Met and NADPH oxidase has been corroborated by another mechanism, the control of Rac1, a prominent regulator of the oxidase. Ozaki and collaborators proved that HGF and its canonical signaling mediated by PI3K/Akt is necessary and sufficient to suppress intracellular ROS generation and apoptosis by inhibiting Rac1 in a model of hypoxia/reoxygenation in the liver [32], supporting the broad range of action induced by HGF on the modulation of cellular redox state driven by NADPH oxidase in the liver.

This regulation has been observed in other cell types. It has been reported that HGF increases the NADPH oxidase-mediated ROS formation in endothelial progenitor cells and in human umbilical vein cells, thereby inducing cell migration and angiogenesis, a phenomenon not observed in NOX2-deficient cells [33]. Similar findings have been found in the lung endothelial cells, where c-Met signaling induced the NADPH oxidase activation particularly in motile cells; this effect was mediated by $p47^{phox}$, cortactin, and Rac1 translocation to lamellipodia. The NADPH oxidase inhibition by apocynin, or the siRNA-mediated inactivation of $p47^{phox}$, or cortactin, significantly decreased the lamellipodia formation and cell migration promoted by HGF [34].

5. Conclusion

In conclusion, in the present work we gained mechanistic evidence regarding the regulation of the NADPH oxidase by HGF/c-Met, particularly interfering with the regulatory subunit $p22^{phox}$ that supports the previous relevant physiological findings in many liver diseases (Supplementary Fig. 3), and this positions the axis HGF/c-Met/NADPH oxidase/ROS as a key mechanism of HGF singling in the liver.

Abbreviations

HGF
Hepatocyte growth factor
c-Met
Cellular-mesenchymal epithelial transition factor (HGF receptor)
NADPH
Nicotinamide adenine dinucleotide phosphate
FRET
Förster resonance energy transfer
NF-κB
Nuclear factor-kappa B
ROS
Reactive oxygen species
KO
Knock out
TGF-β
Transforming growth factor beta
Epox
Epoxomicin
DTSSP
3,3-dithiobis sulfosuccinimidyl propionate
DSP
Dithiobis succinimidyl propionate

Conflicts of interest

The authors have no conflicts of interest to declare.

Data availability statement

Data available on request from the authors.

Funding and Acknowledgments

This work was partially funded by grants from CONACYT: CB-252942 granted to Dr. Gomez-Quiroz, and CB-222578 granted to Dr. Miranda-Labra, and Universidad Autónoma Metropolitana-Iztapalapa. ASN, SSS, were Conacyt scholarship holders.

We thank Confocal microscopy core unit and Dr. Roberto Lazzarini. Universidad Autónoma Metropolitana Iztapalapa.

Appendix A. Supplementary data

Supplementary material related to this article can be found, in the online version, at doi:https://doi.org/10.1016/j.aohep.2021.100339.

References

[1] C.G. Huh, V.M. Factor, A. Sanchez, K. Uchida, E.A. Conner, S.S. Thorgeirsson Hepatocyte growth factor/c-met signaling pathway is required for efficient liver regeneration and repair. Proc Natl Acad Sci U S A. 2004;101:4477–4482. doi:10.1073/pnas.0306068101.

[2] L.E. Gomez-Quiroz, V.M. Factor, P. Kaposi-Novak, C. Coulouarn, E.A. Conner, S.S. Thorgeirsson Hepatocyte-specific c-Met deletion disrupts redox homeostasis and sensitizes to Fas-mediated apoptosis. J Biol Chem 2008;283:14581–14589. doi:10.1074/jbc.M707733200.

CORRECTED PROOF

[3] R.P. Brandes, N. Weissmann, K. Schroder Nox family NADPH oxidases: molecular mechanisms of activation. Free Radic Biol Med 2014;76:208–226. doi:10.1016/j.freeradbiomed.2014.07.046.
[4] J.X. Jiang, N.J. Torok NADPH oxidases in chronic liver diseases. Adv Hepatol 2014;2014. doi:10.1155/2014/742931.
[5] D. Clavijo-Cornejo, C. Enriquez-Cortina, A. Lopez-Reyes, M. Dominguez-Perez, N. Nuno, M. Dominguez-Meraz, et al. Biphasic regulation of the NADPH oxidase by HGF/c-Met signaling pathway in primary mouse hepatocytes. Biochimie 2013;95:1177–1184. doi:10.1016/j.biochi.2013.01.005.
[6] M. Dominguez-Perez, N. Nuno-Lambarri, D. Clavijo-Cornejo, A. Luna-Lopez, V. Souza, L. Bucio, et al. Hepatocyte growth factor reduces free cholesterol-mediated lipotoxicity in primary hepatocytes by countering oxidative stress. Oxid Med Cell Longev 2016;2016:7960386. doi:10.1155/2016/7960386.
[7] P. Kaposi-Novak, J.S. Lee, L. Gomez-Quiroz, C. Coulouarn, V.M. Factor, S.S. Thorgeirsson Met-regulated expression signature defines a subset of human hepatocellular carcinomas with poor prognosis and aggressive phenotype. J Clin Invest 2006;116:1582–1595. doi:10.1172/JCI27236.
[8] R. Jagadeeswaran, S. Jagadeeswaran, V.P. Bindokas, R. Salgia Activation of HGF/c-Met pathway contributes to the reactive oxygen species generation and motility of small cell lung cancer cells. Am J Physiol Lung Cell Mol Physiol 2007;292:L1488-1494. doi:10.1152/ajplung.00147.2006.
[9] J.U. Marquardt, D. Seo, L.E. Gomez-Quiroz, K. Uchida, M.C. Gillen, M. Kitade, et al. Loss of c-Met accelerates development of liver fibrosis in response to CCl(4) exposure through deregulation of multiple molecular pathways. Biochim Biophys Acta 2012;1822:942–951. doi:10.1016/j.bbadis.2012.02.012.
[10] T. Takami, P. Kaposi-Novak, K. Uchida, L.E. Gomez-Quiroz, E.A. Conner, V.M. Factor, et al. Loss of hepatocyte growth factor/c-Met signaling pathway accelerates early stages of N-nitrosodiethylamine induced hepatocarcinogenesis. Cancer Res 2007;67:9844–9851. doi:10.1158/0008-5472.CAN-07-1905.
[11] C. Enriquez-Cortina, M. Almonte-Becerril, D. Clavijo-Cornejo, M. Palestino-Dominguez, O. Bello-Monroy, N. Nuno, et al. Hepatocyte growth factor protects against isoniazid/rifampicin-induced oxidative liver damage. Toxicol Sci 2013;135:26–36. doi:10.1093/toxsci/kft134.
[12] O. Bello-Monroy, D. Mata-Espinosa, C. Enriquez-Cortina, V. Souza, R.U. Miranda, L. Bucio, et al. Hepatocyte growth factor enhances the clearance of a multidrug-resistant Mycobacterium tuberculosis strain by high doses of conventional chemotherapy, preserving liver function. J Cell Physiol 2020;235:1637–1648. doi:10.1002/jcp.29082.
[13] L.E. Gomez-Quiroz, D. Seo, Y.H. Lee, M. Kitade, T. Gaiser, M. Gillen, et al. Loss of c-Met signaling sensitizes hepatocytes to lipotoxicity and induces cholestatic liver damage by aggravating oxidative stress. Toxicology 2016;361–362:39–48. doi:10.1016/j.tox.2016.07.004.
[14] S. Salas-Silva, A. Simoni-Nieves, M.V. Razori, J. Lopez-Ramirez, J. Barrera-Chimal, R. Lazzarini, et al. HGF induces protective effects in alpha-naphthylisothiocyanate-induced intrahepatic cholestasis by counteracting oxidative stress. Biochem Pharmacol 2020;174:113812. doi:10.1016/j.bcp.2020.113812.
[15] A. Valdes-Arzate, A. Luna, L. Bucio, C. Licona, D.L. Clemens, V. Souza, et al. Hepatocyte growth factor protects hepatocytes against oxidative injury induced by ethanol metabolism. Free Radic Biol Med 2009;47:424–430. doi:10.1016/j.freeradbiomed.2009.05.014.
[16] M. Palestino-Dominguez, M. Pelaez-Luna, R. Lazzarini-Lechuga, I. Rodriguez-Ochoa, V. Souza, R.U. Miranda, et al. Recombinant human hepatocyte growth factor provides protective effects in cerulein-induced acute pancreatitis in mice. J Cell Physiol 2018;233:9354–9364. doi:10.1002/jcp.26444.
[17] M.J. Stasia CYBA encoding p22(phox), the cytochrome b558 alpha polypeptide: gene structure, expression, role and physiopathology. Gene 2016;586:27–35. doi:10.1016/j.gene.2016.03.050.
[18] K. Belarbi, E. Cuvelier, A. Destee, B. Gressier, M.C. Chartier-Harlin NADPH oxidases in Parkinson's disease: a systematic review. Mol Neurodegener 2017;12:84. doi:10.1186/s13024-017-0225-5.
[19] M. Gerardo-Ramirez, R. Lazzarini-Lechuga, S. Hernandez-Rizo, J.E. Jimenez-Salazar, A. Simoni-Nieves, C. Garcia-Ruiz, et al. GDF11 exhibits tumor suppressive properties in hepatocellular carcinoma cells by restricting clonal expansion and invasion. Biochim Biophys Acta Mol Basis Dis. 2019;1865:1540–1554. doi:10.1016/j.bbadis.2019.03.003.
[20] A. Finotti, M. Borgatti, V. Bezzerri, E. Nicolis, I. Lampronti, M. Dechecchi, et al. Effects of decoy molecules targeting NF-kappaB transcription factors in Cystic fibrosis IB3-1 cells: recruitment of NF-kappaB to the IL-8 gene promoter and transcription of the IL-8 gene. Artif DNA PNA XNA 2012;3:97–296. doi:10.4161/adna.21061.
[21] S. Hernandez, A. Simoni-Nieves, M. Gerardo-Ramirez, S. Torres, R. Fucho, J. Gonzalez, et al. GDF11 restricts aberrant lipogenesis and changes in mitochondrial structure and function in human hepatocellular carcinoma cells. J Cell Physiol 2020. doi:10.1002/jcp.30151.
[22] R. Arteaga-Tlecuitl, A.L. Sanchez-Sandoval, B.E. Ramirez-Cordero, M.J. Rosendo-Pineda, L. Vaca, J.C. Gomora Increase of CaV3 channel activity induced by HVA beta1b-subunit is not mediated by a physical interaction. BMC Res Notes 2018;11:810. doi:10.1186/s13104-018-3917-1.
[23] J.D. Lambeth NOX enzymes and the biology of reactive oxygen. Nat Rev Immunol 2004;4:181–189. doi:10.1038/nri1312.
[24] M.L. Cho, S.Y. Min, S.H. Chang, K.W. Kim, S.B. Heo, S.H. Lee, et al. Transforming growth factor beta 1(TGF-beta1) down-regulates TNFalpha-induced RANTES production in rheumatoid synovial fibroblasts through NF-kappaB-mediated transcriptional repression. Immunol Lett 2006;105:159–166. doi:10.1016/j.imlet.2006.02.003.
[25] D. Datta De, A. Datta, S. Bhattacharjya, S. Roychoudhury NF-kappaB mediated transcriptional repression of acid modifying hormone gastrin. PLoS One 2013;8:e73409. doi:10.1371/journal.pone.0073409.
[26] X. Wang, M.C. DeFrances, Y. Dai, P. Pediaditakis, C. Johnson, A. Bell, et al. A mechanism of cell survival: sequestration of Fas by the HGF receptor Met. Mol Cell 2002;9:411–421. doi:10.1016/s1097-2765(02)00439-2.
[27] G. Viticchie, P.A.J. Muller c-Met and other cell surface molecules: interaction, activation and functional consequences. Biomedicines 2015;3:46–70. doi:10.3390/biomedicines3010046.
[28] M.E. Charbonneau, K.D. Passalacqua, S.E. Hagen, H.D. Showalter, C.E. Wobus, M.X.D. O'Riordan Perturbation of ubiquitin homeostasis promotes macrophage oxidative defenses. Sci Rep 2019;9:10245. doi:10.1038/s41598-019-46526-9.
[29] T. Nowak, P. Niemiec, T. Iwanicki, A. Balcerzyk, J. Krauze, A. Ochalska-Tyka, et al. Analysis of selected promoter polymorphisms and haplotypes of the CYBA gene encoding the p22phox, subunit of NADPH oxidases, in patients with coronary artery disease. Free Radic Res 2018;52:1132–1139. doi:10.1080/10715762.2018.1532569.
[30] V. Orian-Rousseau, L. Chen, J.P. Sleeman, P. Herrlich, H. Ponta CD44 is required for two consecutive steps in HGF/c-Met signaling. Genes Dev 2002;16:3074–3086. doi:10.1101/gad.242602.
[31] P. Conrotto, S. Corso, S. Gamberini, P.M. Comoglio, S. Giordano Interplay between scatter factor receptors and B plexins controls invasive growth. Oncogene 2004;23:5131–5137. doi:10.1038/sj.onc.1207650.
[32] M. Ozaki, S. Haga, H.Q. Zhang, K. Irani, S. Suzuki Inhibition of hypoxia/reoxygenation-induced oxidative stress in HGF-stimulated antiapoptotic signaling: role of PI3-K and Akt kinase upon rac1. Cell Death Differ 2003;10:508–515. doi:10.1038/sj.cdd.4401172.
[33] K. Schroder, S. Schutz, I. Schloffel, S. Batz, I. Takac, N. Weissmann, et al. Hepatocyte growth factor induces a proangiogenic phenotype and mobilizes endothelial progenitor cells by activating Nox2. Antioxid Redox Signal 2011;15:915–923. doi:10.1089/ars.2010.3533.
[34] P.V. Usatyuk, P. Fu, V. Mohan, Y. Epshtein, J.R. Jacobson, J. Gomez-Cambronero, et al. Role of c-Met/phosphatidylinositol 3-kinase (PI3k)/Akt signaling in hepatocyte growth factor (HGF)-mediated lamellipodia formation, reactive oxygen species (ROS) generation, and motility of lung endothelial cells. J Biol Chem 2014;289:13476–13491. doi:10.1074/jbc.M113.527556.

UNCORRECTED PROOF

frontiers in Cell and Developmental Biology

REVIEW
published: 12 January 2021
doi: 10.3389/fcell.2020.622215

Relevance of Membrane Contact Sites in Cancer Progression

*Aurora Gil-Hernández[1], Miguel Arroyo-Campuzano[1], Arturo Simoni-Nieves[2], Cecilia Zazueta[1], Luis Enrique Gomez-Quiroz[2] and Alejandro Silva-Palacios[1]**

[1] Departamento de Biomedicina Cardiovascular, Instituto Nacional de Cardiología Ignacio Chávez, Mexico City, Mexico,
[2] Departamento de Ciencias de la Salud, Universidad Autónoma Metropolitana-Iztapalapa, Mexico City, Mexico

Membrane contact sites (MCS) are typically defined as areas of proximity between heterologous or homologous membranes characterized by specific proteins. The study of MCS is considered as an emergent field that shows how crucial organelle interactions are in cell physiology. MCS regulate a myriad of physiological processes such as apoptosis, calcium, and lipid signaling, just to name a few. The membranal interactions between the endoplasmic reticulum (ER)–mitochondria, the ER–plasma membrane, and the vesicular traffic have received special attention in recent years, particularly in cancer research, in which it has been proposed that MCS regulate tumor metabolism and fate, contributing to their progression. However, as the therapeutic or diagnostic potential of MCS has not been fully revisited, in this review, we provide recent information on MCS relevance on calcium and lipid signaling in cancer cells and on its role in tumor progression. We also describe some proteins associated with MCS, like CERT, STIM1, VDAC, and Orai, that impact on cancer progression and that could be a possible diagnostic marker. Overall, these information might contribute to the understanding of the complex biology of cancer cells.

Keywords: membrane contact sites, metastasis, calcium signaling, lipid signaling, cancer progression

OPEN ACCESS

Edited by:
Simone Patergnani,
University of Ferrara, Italy

Reviewed by:
Youjun Wang,
Beijing Normal University, China
Diego Peretti,
University of Cambridge, United Kingdom

****Correspondence:***
Alejandro Silva-Palacios
alejandro.silva@cardiologia.com;
silpalexuam@gmail.com

Specialty section:
This article was submitted to Signaling, a section of the journal Frontiers in Cell and Developmental Biology

Received: *28 October 2020*
Accepted: *10 December 2020*
Published: *12 January 2021*

Citation:
Gil-Hernández A, Arroyo-Campuzano M, Simoni-Nieves A, Zazueta C, Gomez-Quiroz LE and Silva-Palacios A (2021) Relevance of Membrane Contact Sites in Cancer Progression. Front. Cell Dev. Biol. 8:622215. doi: 10.3389/fcell.2020.622215

INTRODUCTION

Cancer is a serious public health problem worldwide (Henley et al., 2020a); the most common types among women are lung, breast, and colorectal tumor, whereas lung, prostate, and colorectal cancer prevails in men. Globally, 25% of such deaths were from the lung, 9% colorectal, 7% from breast, and 5% from prostate cancer (Henley et al., 2020b).

Breast cancer is the main diagnosis among young women (Rugo, 2019). The risk of recurrence remains latent up to 15 years after adjuvant therapy, as there is an association between progression and risk of metastasis. Breast stages I–III tumors and regional lymph nodes are characterized by 5–10 years survival rates (Liu X. et al., 2019), whereas patients with stage IV metastatic breast cancer have 5 years survival rates below 25%. On average, 5–10% of patients are classified as with stage IV disease at initial diagnosis, but 20–30% of stage I–III patients eventually progress to metastatic disease (Liu X. et al., 2019). Even if the cancer mortality rates decreased by 15% from 2007 to 2017, breast cancer caused 20.7 deaths per 100,000 in women (Henley et al., 2020b), and 1,735,350 new cases were reported in 2018. According to the National Institutes of Health, up to 23.6 million total

cases are expected in 2030; therefore, breast cancer will remain one of the deadliest diseases for individuals[1].

Cancer groups have around 100 highly heterogeneous kinds of diseases, with variable morphological and biological characteristics; hence, the different clinical behaviors and responses to treatment (So et al., 2019) complicate chemoresistance. The classification of cancer is based on its morphology, histological grade (level of differentiation/growth pattern), immunohistochemical subtype, as well as gene expression profiling (Golub et al., 1999; So et al., 2019; Tsang and Tse, 2020). So, to establish the clinical management of cancer in patients, it is essential to understand the underlying biological process that sustains the metabolic and signaling requirements for adequate tumor dynamism, including diffusion or active transport through the cytoplasm, vesicular traffic, and contact site biology (Prinz et al., 2020).

Membrane contact sites (MCS) contribute to maintain the function of the interacting organelles and to preserve cell homeostasis (Prinz et al., 2020). Electron microscopy made these connections evident decades ago (Bernhard and Rouiller, 1956; Copeland and Dalton, 1959), and lately, improved spatial and temporal resolution imaging has led to track organelle dynamics over time, revealing the extent to which many of them are closely related (Wu et al., 2018; **Figure 1**). The best-described membrane contacts involve endoplasmic reticulum (ER)–mitochondria, ER–plasma membrane (PM), ER–Golgi, ER–peroxisome, and ER–lipid droplets (LD) interactions; however, MCS also include LD–peroxisome, mitochondria–vacuole, mitochondria–PM, mitochondria–LD, and mitochondria–peroxisome (Scorrano et al., 2019).

MCS are not only considered as regulatory sites for lipid metabolism and intracellular calcium [$(Ca^{2+})_i$] homeostasis but they also modulate the organelle distribution and structure (Prinz, 2014). Some functions and interactions of MCS have been identified and described to regulate cancer cell metabolism during disease progression. For example, hexokinase 2 overexpression, which is related to the stages of cancer progression, acquisition of invasive and metastatic capabilities, and poor prognosis (Patra et al., 2013), has been located in the mitochondria-associated membranes (MAMs), and its displacement induces mitochondrial Ca^{2+} [$(Ca^{2+})_{mt}$] overload (Ciscato et al., 2020).

In the present work, we reviewed in detail the state-of-the-art of MCS-mediated Ca^{2+} and lipid signaling in cancer, specifically the interactions between ER–PM, ER–mitochondria, and ER–Golgi. Besides this, we describe the involvement of these contact sites in cancer progression, and finally, we address MCS as possible candidates for therapy.

MEMBRANE CONTACT SITES

MCS are defined as areas where two different organelles physically interact without merging, and therefore the identity of each of them is preserved (Jing et al., 2020; Venditti et al., 2020). MCS are dynamic and heterogeneous structures composed of different proteins that act as a bridge between the two membranes, exerting a binding force, that might have additional functions in the cell (Eisenberg-Bord et al., 2016; Peretti et al., 2020). ER, which occupies the largest surface area in the cell, is involved in the formation of many MCS with other organelles (Venditti et al., 2019, 2020). ER contact sites allow the direct exchange of macromolecules and serve as a platform for the recruitment of machinery that regulates biogenesis, division, and trafficking of organelles (Lee et al., 2020). Among the broad processes taking place at such interface are Ca^{2+} homeostasis, lipid signaling, and organelle remodeling (Jing et al., 2020) as well as mitochondrial fusion/fission, autophagy, apoptosis, reactive oxygen species (ROS) signaling, and unfolded protein response (van Vliet et al., 2014; Silva-Palacios et al., 2020).

Endoplasmic Reticulum–Plasma Membrane

ER–PM contacts were first described by electron microscopy in muscle cells (Porter and Palade, 1957) and eventually in many other cell types (Okeke et al., 2016). Their abundance and morphology vary from one cell to another and can be modulated by its functional status. The ER–PM contact sites are represented by both small focal contacts and large cisterns with a gap between ER and PM in the range of 10–30 nm (Orci et al., 2009; Fernández-Busnadiego et al., 2015) that allows the direct interaction of protein and lipid components in both membranes.

Currently, it is well known that the oxysterol-binding protein (OSBP)-related protein (ORP) is the major lipid transporter between ER and PM contacts, specifically of phosphatidylserine (PS) and phosphatidylinositol 4-phosphate (PI4P). Similarly, OSBP counteracts the transport of sterols and PI4P in the ER–Golgi contact (see below), while Osh3 (OSBP homolog in yeast) regulates the metabolism of phosphoinositol (PI) (Fernández-Busnadiego, 2016). Recently, it was reported that a robust exchange of sterols at the ER–PM contact site in yeasts lacking tether proteins (including E-synaptotagmin and the vesicle-associated membrane protein, VAMP). These sites act as an interface for the regulation and integration of lipid synthesis pathways to maintain plasma membrane composition and integrity. Loss of ER–PM contacts in yeast has been associated with low levels of PS, phosphatidylcholine, and phosphatidic acid and with the disruption of membrane dynamics (Quon and Beh, 2016; Quon et al., 2018). The vesicle-associated protein (VAP) in mammals neither appears to be strictly necessary for the maintenance of ER–PM contact, probably because other transmembrane proteins of the endoplasmic reticulum are involved in the tethering complex (Chung et al., 2015; Lees et al., 2017). The ER–PM contact sites in non-muscular cells remained poorly described until recently, when the discovery of the stromal interaction molecule 1 system (STIM/Orai1) revealed that these contacts mediate calcium input through the store-operated Ca^{2+} entry system (SOCE) (see below) into all metazoan cells (Collado and Fernández-Busnadiego, 2017). In addition, inositol 1,4,5-trisphosphate receptor (IP_3R) might form a complex with STIM1 and improve the SOCE pathway cation input (Paknejad and Hite, 2018; Sampieri et al., 2018).

[1]https://www.cancer.gov/

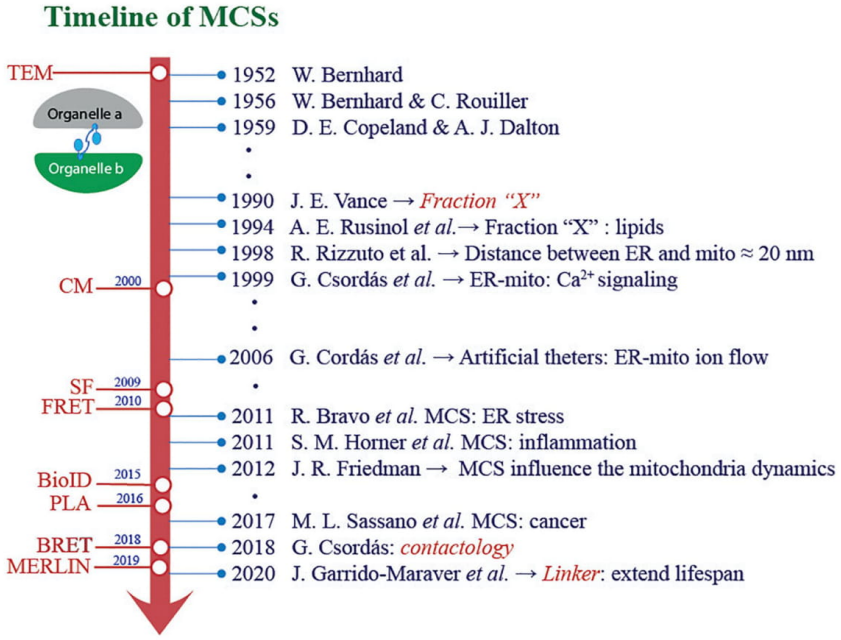


FIGURE 1 | Scientific and technological advances in the study of membrane contact sites. The knowledge about organelle contacts and their role in different pathophysiological conditions has experienced a great "boom." In harmony with these advances, significant progress has been made in optimizing methodology strategies to study and comprehend the interaction between organelles. TEM, transmission electronic microscopy; CM, confocal microscopy; SF, subcellular fractionation; FRET, fluorescence resonance assembly transfer; BioID, proximity-dependent biotin identification; PLA, proximity ligation assay; BRET, bioluminescence resonance energy transfer; MERLIN, mitochondria–endoplasmic reticulum length indicator nanosensor.

Endoplasmic Reticulum–Mitochondria

MAMs are specific MCS between the ER and the mitochondria, which participate in different cellular functions (Peretti et al., 2020). The average distance between both organelles varies from 10 to 60 nm. In this sense, several studies indicate that 9–16 nm is enough distance to tether the outer mitochondrial membrane (OMM) to the smooth ER, while a space of 20 nm has been observed between the OMM and the rough ER (Achleitner et al., 1999; Csordás et al., 2006; Giacomello and Pellegrini, 2016; Simmen and Herrera-Cruz, 2018; Wu et al., 2018).

It has been reported that distances between MAMs greater than 30 nm are required for Ca^{2+} transport in cardiomyocytes (Sharma et al., 2000). The MAM tethering axis includes the IP_3R in the ER which is pivotal for communication and interaction with the voltage-dependent anion channel (VDAC), which is located at the OMM and is responsible for the release of adenosine triphosphate (ATP) from the mitochondria to the cytosol (Fang and Maldonado, 2018). It is relevant to note that isoform 1 of IP_3R is crucial for calcium exchange with the mitochondria (Bartok et al., 2019).

The interaction between IP_3R and VDAC is mediated by glucose-regulated protein 75 (Grp75), which participates in calcium exchange and stabilizes the membrane contact site (Szabadkai et al., 2006; Patergnani et al., 2011). Mitofusin 2 (Mfn2), mostly located in MAM (de Brito and Scorrano, 2008), also regulates calcium transport in ER–mitochondria contacts. MAMs convey calcium signaling between the IP_3R and the mitochondrial calcium uniporter (MCU), the channel responsible for Ca^{2+} uptake into the mitochondrial matrix. Other recently described proteins that maintain MAM integrity are DJ-1 (oncoprotein encoded in PARK7 gene) (Xu et al., 2018; Liu Y. et al., 2019; Basso et al., 2020) and PDZ domain-containing protein 8 (a synaptotagmin-like mitochondrial lipid-binding protein domain-containing ER transmembrane protein) that has been implicated in ER-dependent mitochondrial calcium homeostasis (Hirabayashi et al., 2017; Elbaz-Alon et al., 2020), while pannexin 2 has been reported to sensitize cancer cells to apoptotic stimuli (Le Vasseur et al., 2019). In triple-negative breast cancer (TNBC), MCU silencing disturbs calcium uptake, enhancing alternative pathways such as SOCE, whereas the reduction of mitochondrial calcium levels inhibits cell migration in cancer cell lines. Depletion of MCU expression also reduces ROS production and deregulates hypoxia-inducible factor 1 alpha, diminishing cancer progression (Tosatto et al., 2016).

Endoplasmic Reticulum–Trans Golgi Network

The Golgi complex is part of the cytoplasmic endomembrane system, which is normally found adjacent to the nucleus (Li et al., 2019). Transmission electron microscopy analysis revealed that the Golgi forms stacks consisting of eight-storey cisterns placed parallel to each other (Donizy and Marczuk, 2019). The Golgi complex is divided into three compartments: (1) the *cis*-Golgi network (near the ER and receiving its output), (2) the middle part, and (3) the *trans*-Golgi network (TGN, near the PM that sends vesicle-dependent and vesicle-independent molecules to different destinations) (Witkos and Lowe, 2016). This peculiar structure actively participates in the traffic of proteins and lipids into the cell and regulates post-translational modification (De Matteis and Rega, 2015; Howley and Howe, 2018). The phospholipid composition of the ER and the *trans*-Golgi membrane differ significantly, the cytosolic side of the ER membrane is slightly charged, and phospholipids are enriched in monounsaturated chains, while the TGN membrane is enriched with sphingolipids and with negatively charged lipids such as PS, PI, and PI4P on its cytosolic side (Mesmin et al., 2019).

The ER and Golgi network is related to the molecular traffic of vesicular and non-vesicular routes (Lev, 2010, 2012; Wu et al., 2018). Specifically, the VAMP-associated protein is involved in the formation of MCS between ER and almost all organelles (Murphy and Levine, 2016). At ER–Golgi sites, VAPs provide contacts with FFAT motifs [two phenylalanine (FF) in an acid tract] of three different proteins involved in lipid transfer such as Nir2 (important for PI transfer from the ER to the PM), ceramide transferase (CERT, responsible for ceramide transfer between ER and TGN) (Hanada et al., 2003), and ORP protein, which exclusively transfers cholesterol and PI4P but also acts as tethers agent (De Matteis and Rega, 2015).

REGULATED CELLULAR PROCESSES AT CONTACT SITES AND THEIR RELATION TO CANCER PROGRESSION

Calcium Signaling

MCSs allows the efficient transfer of metabolites between compartments, particularly of calcium. The cytosol calcium concentrations are ∼100 nM (Marchi et al., 2020), whereas in the ER lumen [$(Ca^{2+})_{ER}$], it reaches 100–800 μM (Burdakov et al., 2005; Zhai et al., 2020).

The role of calcium signaling in cancer progression has been discussed in detail recently (Marchi and Pinton, 2016; Bong and Monteith, 2018). Calcium regulates cellular processes such as proliferation, migration, and resistance (among others), contributing to the development of a malignant phenotype that is essential and continuously rewired at all stages of carcinogenesis (Morciano et al., 2018). This scenario seems to be caused by the uneven regulation of pumps and channels and to the consequent alteration in calcium concentration (Dang et al., 2017; So et al., 2019; Makena and Rao, 2020; Yang et al., 2020). It has been proposed that changes in the distance and morphology of the mitochondrial tether can dramatically alter calcium homeostasis and cell function (Simoes et al., 2020); therefore, it is imperative to understand the regulation of this cation by MCS in cancer.

Store-Operated Ca^{2+} Entry

Store-operated Ca^{2+} entry (SOCE) is an ancient and ubiquitous Ca^{2+} signaling pathway discovered decades ago (PutneyJr., 1986), the main components of which are the stromal interaction molecule 1 (STIM1) and Orai1 (Roos et al., 2005; Zhang et al., 2005; Feske et al., 2006). The depletion of the Ca^{2+} store directly results in the activation of the Ca^{2+} channel in the plasma membrane (PutneyJr., 1986), whereas SOCE is activated by membrane receptors or by pharmacological manipulations that empty the ER intracellular Ca^{2+} stores (Xie J. et al., 2016).

STIM proteins (in humans 1 and 2) are single-pass membrane proteins located in the ER membrane that, after ER Ca^{2+} depletion, regulate the Orai channel (Hou et al., 2020). Structurally, all STIM1 monomers contain an N-terminal signal peptide, a canonical Ca^{2+}-binding EF 1 hand, a non-Ca^{2+}-binding EF 2 hand, and a sterile α-motif (SAM) domain in the ER luminal region (known as ER-SAM) (Dziadek and Johnstone, 2007; Schober et al., 2019). The C-terminus domain located in the cytosolic side of the ER membrane is characterized by the coiled-coil 1 (CC1) segments, a STIM-Orai-activating region (SOAR) or calcium release-activated calcium (CRAC) activation domain (CAD), and the motif S/TxIP which are the components of the Orai1 activation small fragment (Chen Y. T. et al., 2013; Stathopulos et al., 2013; Rathner et al., 2018; **Figure 2**).

When the $[Ca^{2+}]_{ER}$ decreases, the cation dissociates from the different binding sites in the EF-SAM, producing a conformational change in this region (Zheng et al., 2011). That this, at rest, the EF-SAM region of STIM1 is monomers, while the cytosolic region of STIM1 are dimers. After activation, EF-SAM oligomerizes, which leads to conformational changes in its cytosolic region, elongating the SOAR/CAD segments (extended state) and the S/TxIP motif (Gudlur et al., 2018; Hirve et al., 2018). Thanks to this and its positively charged polybasic tail, STIM1 moves along the microtubules network interacting with the EB1 protein, generating clusters and elongation of the ER near the PM and favoring its union with Orai1 (Grigoriev et al., 2008) (reviewed in Ma et al., 2020).

Calcium Release-Activated Calcium Channel

Orai is the pore-forming protein of the calcium release-activated calcium (CRAC) channel; there are three human Orai (Orai1-3) proteins which consist of four transmembrane (TM) helices (TM1–4) with cytoplasmic N- and C-terminal domains (Hou et al., 2012; Stathopulos et al., 2013). The channel structure consists of six Orai subunits arranged as a hexamer with a central pore (Hou et al., 2012; Cai et al., 2016). TM2–4 forms concentric rings around the ion-conducting pore, surrounding the TM1 helices located at the boundary of the ion pore. A TM4 extension binds with a SOAR, promoting coupling between PM and ER and mediating intracellular Ca^{2+} mobilization

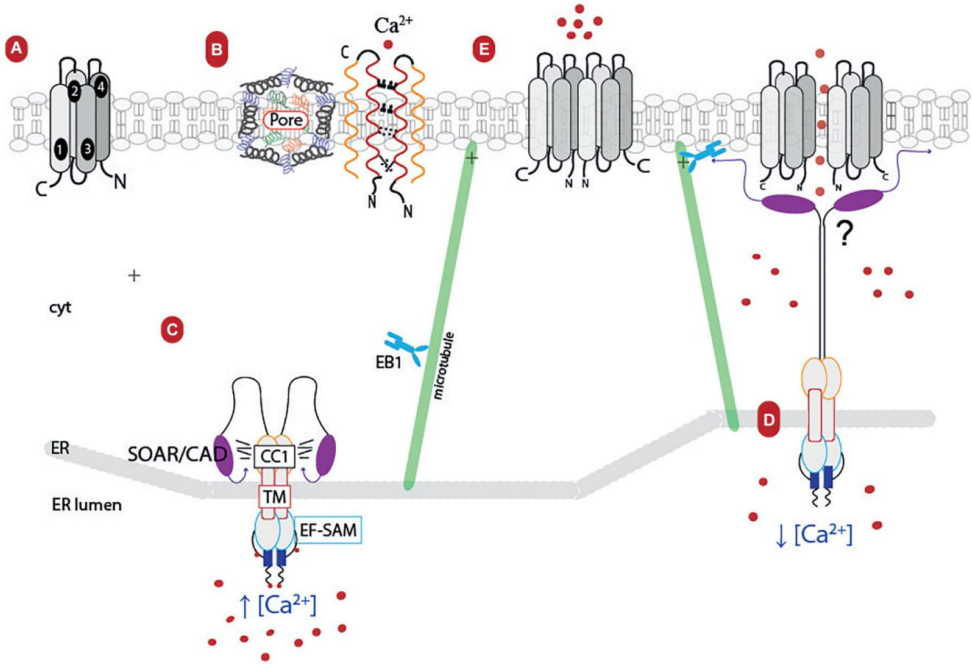


FIGURE 2 | Cartoon model of ER–PM junction (store-operated Ca^{2+} entry system pathway). **(A)** Orai's monomeric structure: TM1-4 and its C- and N-terminal endings facing the cytosol. **(B)** Orai channel structure: The channel is conformed by six subunits (monomers) which interact with each other due to the hydrophobic cluster (E106, V102, F99, R91) in their respective TM1. These interactions leave the ion pore at the center of the channel, and it is also stabilized by the TM1–TM2 turret, causing the channel's selectivity. **(C)** STIM1 resting state: This protein seems to dimerize in basal conditions. STIM1 monomer's structure consists of the EF-SAM calcium sensor, facing the ER-lumen, the TM domain, and the CC1, SOAR/CAD segments oriented to the cytosol. The STIM1 monomer in the presence of calcium is folded into the cytosol domain due to hydrophobic interactions between the coiled coils. **(D)** STIM1 extended state: STIM1 interacts with EB1 protein, helping to remodel the ER and forming STIM1 clusters near the PM; its polybasic tail also seems to interact with the PM. When there is a Ca^{2+} depletion in the ER lumen, STIM1 suffers a conformational change, and both monomers release its SOAR/CAD segments, which, in turn, interact with Orai. **(E)** Possible activation of Orai: STIM1 could contribute to either rotate Orai's helices or help the subunits' outward movement. Orai loses its high permeability and allows the entry of extracellular calcium. TM, transmembrane helices; EF-SAM, EF hand 1, non-canonical ER hand 2, and sterile alfa motile; CC1, coiled coil 1; SOAR/CAD, Stim1-Orai1 activating region/CRAC activation domain; EB1, microtubule plus-end tracking of end binding protein 1; cyt, cytosol; ER, endoplasmic reticulum; PM, plasma membrane.

(Park et al., 2009; Cai et al., 2018). Orai's selectivity for calcium is determined by the mainly electronegative charged TM1–TM2 turret structure, which is stabilized by a VQLD motif and a lysine residue from the TM3 (K270 in *D. melanogaster*) and by the narrowing of the region near the Ca^{2+} binding site formed by the E106 residue (Yeung et al., 2018; Bulla et al., 2019; Hou et al., 2020).

It has been proposed that, after Ca^{2+} store depletion in ER, the CRAC channels interact both at their cytoplasmic N- and C-termini with the ER Ca^{2+} sensor protein STIM1, resulting in close coupling in the apposed sites at the ER–plasma membrane junctions (**Figure 2**). Specifically, the SOAR/CAD segment interacts with the Orai1 hexamer, producing the pore helix, which displaces six F99 residues and disrupts the V102-F99 hydrophobic segment that closes the channel, increasing port hydration and calcium conduction (Yamashita et al., 2017, 2020). Another hypothesis, derived from cryo-electron microscopy (3.3 Å resolution) studies in *D. melanogaster*'s mutant protein, suggests that Orai subunits are displaced, causing the repositioning of F171 (F99 in human Orai), widening the hydrophobic región, and promoting channel opening (Hou et al., 2020).

The SOCE pathway involvement in cancer progression is undeniable and might be a target for the study and treatment of this disease. Flourakis et al. (2010) demonstrated that SOCE is the main source of Ca^{2+} influx that triggers apoptotic cell death in human prostate cancer cells. Orai1 *knockdown* in cancer cells inhibits SOCE and protects these cells from apoptotic death

(Flourakis et al., 2010). Also, the inhibition of STIM1 and Orai1 reduces cell migration and tumor metastasis in breast cancer cells by down-regulating the calcium-dependent focal adhesion pathway (Yang et al., 2009), an effect also seen in cervical cancer (Chen Y. F. et al., 2011, 2013) and hepatocarcinoma cells (Yang et al., 2013).

It has been shown that pharmacological upregulation of the SOCE pathway decreases glioblastoma tumor cell growth, activating Ca^{2+} entry and inhibiting the YAP/TAZ pathway (a key transcription factor that regulates tumor cell proliferation and aggressiveness) (Enzo et al., 2015). On the other hand, SOCE activates the extracellular signal-regulated kinase (ERK) signaling pathway, promoting cell proliferation and migration in melanoma cells (Umemura et al., 2014), while Orai1/STIM1 enhances Akt activity, contributing to *cis*-platin resistance in ovarian carcinoma cells (Schmidt et al., 2014). Recently, it was reported that the inhibition of STIM1/Orai1 interactions in TNBC cell lines with NO1, a fluorescent ligand for Sigma-2R (initially described as a cholesterol transport regulator), causes an alteration of the SOCE pathway, increasing apoptotic cell death and reducing the proliferation and migration rate of these cells (Cantonero et al., 2020).

Ineffective epithelial–mesenchymal transition (EMT) and metastasis suppression were observed in MDA-MB-231 and MCF-7 cell lines treated with transforming growth factor-β (TGF-β) in which STIM1 was *knocked-down*, proving a clue of the role of SOCE in TGF-β-induced cancer progression (Zhang et al., 2017). Furthermore, in very aggressive cancer cell lines (such as MDA-MB-231), STIM1 is overexpressed as compared to the MCF-7 cell line (Kulkarni et al., 2019).

On the other hand, deregulation of Orai by siRNA inhibition in cancer cell lines promotes deregulation of proteins involved in the cell cycle such as cyclin-D1 and cyclin-E, as well as overexpression of p53 and p21, together with an increase in $[Ca^{2+}]_i$, which collectively favor apoptosis (Faouzi et al., 2011). Besides these, Orai3 produces resistance to chemotherapeutic drugs through increased free calcium uptake, which leads to p53 inactivation (Hasna et al., 2018). In turn, silencing of Orai1 and 2 with SOCE chemical inhibitors and siRNAs inhibits calcium uptake and suppresses cancer cell proliferation, colony formation, and migration in association with inhibition of the Akt/mammalian target of rapamycin (mTOR)/nuclear factor κB (NF-κB) pathway (Singh et al., 2020). Orai can be inactivated through phosphorylation in its Ser-27, -30, or -34 residues. In MDA-MB-231 cell lines, it has been reported that overexpression of Orai1, as well as calcium–calmodulin-activated adenylyl cyclase type 8 (which interacts at phosphorylation sites), prevents the inactivation of Orai1, increasing calcium signaling and promoting cancer cell migration (Sanchez-Collado et al., 2019). In summary, these examples highlight the relevance of the ER–PM contact site both in calcium signaling and in other physiological pathways.

Clinically, STIM1 has been correlated with poor prognosis in breast (Yang et al., 2017), colorectal (Wang et al., 2015), and lung carcinoma (Zhan et al., 2015) because its overexpression in patients' tissues is associated with increased tumor size, lymphatic metastases, and other factors. Orai3 is also overexpressed in several types of cancer such as esophageal and gastric carcinoma among others (Zhu et al., 2014; Xia et al., 2016; Wang L. et al., 2017).

In conclusion, $[Ca^{2+}]_i$ modulated by SOCE is a master physiological regulator that contributes to uncontrolled proliferation and malignant tumor progression (Sharma and Elble, 2020). We must recall that mitochondrial Ca^{2+} activates the Krebs cycle, apoptosis, and mitochondrial fission (Harper et al., 2020). In particular, the activity of α-ketoglutarate, isocitrate, and pyruvate dehydrogenases is controlled by the cation, increasing the ATP synthesis. However, cancer cells require a high glycolytic rate (Warburg effect) to maintain growth and tumor progression. Such metabolic switch has been associated with alterations in calcium signaling in MAMs (Bittremieux et al., 2016). Therefore, deregulation of Ca^{2+} import via MAMs could affect tumorigenesis through metabolism and cell death (Peretti et al., 2020).

Further information of the expression profile of some MCS protein-related genes is included in the cancer genomic database The Cancer Genome Atlas (TCGA), which is integrated with clinical characteristics, including patient outcome in common cancer types. For example, the *Stim1* gene was shown to be elevated in many solid tumors (**Figure 3A**), but the gene product is not considered as prognostic. Interestingly, the expression of the *Stim1* gene is diminished in breast cancer (**Figure 3B**) and is practically comparable to normal tissue levels at all stages (**Figure 3C**). Regarding Orai, its expression increases (**Figure 3D**), particularly in breast (**Figure 3E**) and renal cancer (**Figure 3F**). These changes could be easily addressed by conventional methods such as qRT-PCR to confirm their prognostic relevance.

IP_3R

Overexpression of $IP_3$1 and 2 receptors has been related to apoptosis in different tissues and cancer cells (Assefa et al., 2004; Kopacek et al., 2009; Akl et al., 2013; Hudecova et al., 2016) and to compromised cell metabolism (particularly glycolytic and the mitochondrial bioenergetic) (Singh et al., 2017). Recently, it has been reported that down-regulation of IP_3R3 correlates with a lower migration rate due to the modulation of Ca^{2+} signaling. Accordingly, overexpression of IP_3R in cancer cells improves free calcium fluctuation and promotes efficient migration (Mound et al., 2017). Migration is also associated with cell morphology, i.e., when IP_3R3 is silenced, a rounded shape is produced in highly invasive cancer cell lines, resulting in a low rate of adhesion and migration, as a consequence of Ca^{2+} oscillation and cytoskeletal changes driven through the ARHGAP18/RhoA/mDia1/FAK signaling pathway (Vautrin-Glabik et al., 2018). This silencing is also related to the induction of apoptosis in different cancer cell lines such as colorectal, ovarian, and clear cell renal carcinoma tumors (Rezuchova et al., 2019).

VDAC

On the other hand, the role of the mitochondrial protein VDAC in cancer is debated. For example, VDAC1 *knockdown* has been related to proliferation inhibition. Also, the VDAC inhibitor, JQ1, prevents the activity of bromodomain-containing proteins

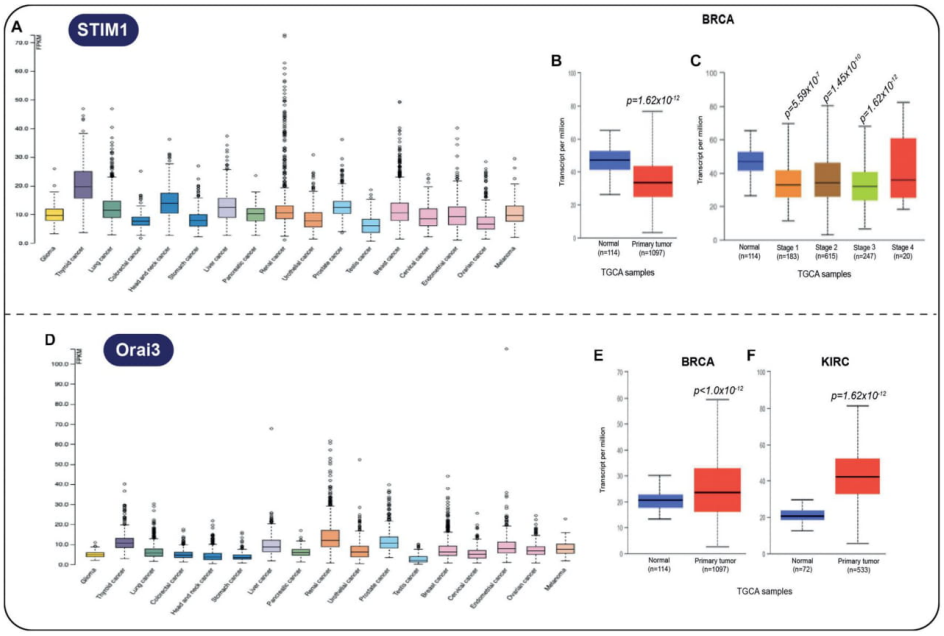


FIGURE 3 | (A) *Stim1* gene product is elevated in several solid tumors. **(B)** *Stim1* gene expression in breast cancer (BRCA) vs. tissue samples ($p = 1.62 \times 10^{-12}$) and **(C)** *Stim1* gene expression in all stages of BRCA vs. normal samples. **(D)** *Orai3* gene overexpression is associated with many cancers, in particular with **(E)** BRCA ($p < 1.0 \times 10^{-12}$) and with **(F)** KIRC ($p = 1.62 \times 10^{-12}$). All data were taken by UALCAN cancer database (Chandrashekar et al., 2017).

(BRD), including BRD4, that is enriched in patients with basal luminal breast cancer (Qi, 2014), suggesting that VDAC1 is relevant in cancer cell progression and is a hallmark of poor prognosis (Yang et al., 2019).

In this regard, Dr. Lev's group recently identified that the combination of the synthetic drug JQ1 and the proteasome inhibitor bortezomib induces ferroptosis in multiple TNBC cells line *in vitro* and *in vivo*. The findings of this group indicate that combination therapies effectively decrease the size of the tumor and significantly prolong the survival of mice up to 80 days. Mechanistically, these therapies induce ferroptosis in correlation with the reduction of glutathione peroxidase 4, nuclear factor erythroid 2-related factor 2 (Nrf2), and glutathione metabolism. Therefore, drug combination might be a new therapeutic option for patients with triple-negative breast cancer, highlighting ferroptosis as a promising avenue for the treatment of TNBC (Verma et al., 2020). Relevant to this issue is the finding that progesterone induces VDAC and sarco(endo)plasmic reticulum Ca^{2+}-ATPase (SERCA) expression, inhibiting the growth of MCF-7 cells (Azeez et al., 2018).

Using the TCGA database, we also detect VDAC overexpression in several solid tumors (**Figure 4A**). Notably, in breast cancer (**Figure 4B**), lung adenocarcinoma (**Figure 4C**), and head and neck carcinoma (**Figure 4D**), a close relationship exists between gene expression and poor survival outcome. By using the extraordinary resources based on "omics" data, more MCS-associated protein could be relevant in the clinical context; some of them might be useful for outcome prediction, particularly in the emerging "contactology science."

Grp75

Grp75 (also known as mortalin or HSPA9) interacts with p53 (the master regulator of multiple cellular physiological processes such as apoptosis, senescence, cell cycle arrest, etc.), preventing its activation and therefore promoting cancer cell survival. In human breast cancer cells, treatment with the molecule embelin inhibits Grp75-p53 interaction, leading to the downregulation of Grp75 as long as metastatic signaling occurs, inhibiting mitochondrial fission and arresting growth (Nigam et al., 2015). Grp75 is also a metastatic hallmark in cancer. Interestingly, mortalin also increases in adjacent non-tumor cells, suggesting that such enrichment could be detected at the early stages of cancer (Jin et al., 2016).

PERK

The protein kinase RNA like ER kinase (PERK) is another tether in MAM extensions that could promote or suppress tumor progression in cancer cells. PERK triggers multiple steps

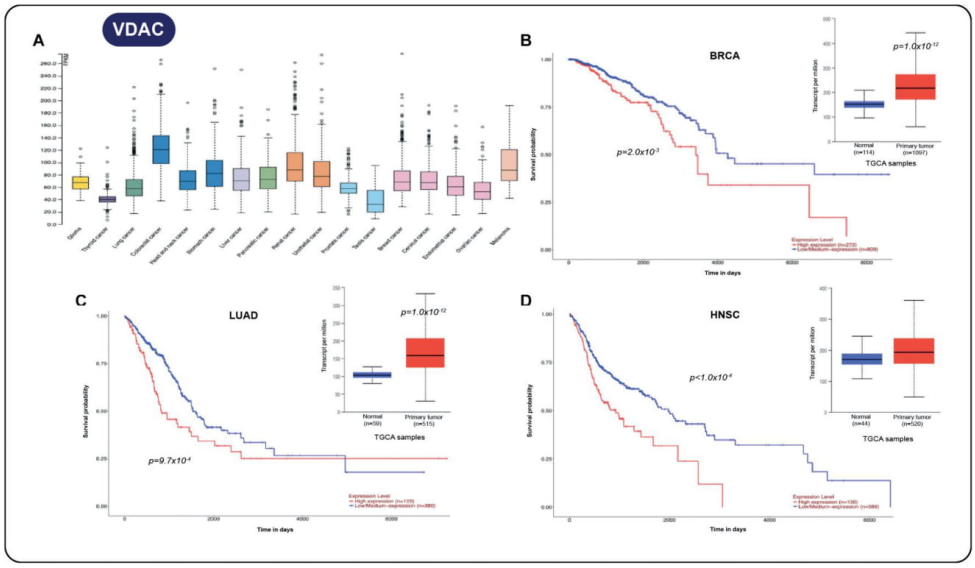


FIGURE 4 | (A) Increment in voltage-dependent anion channel (VDAC) in several solid tumors. **(B)** Survival analysis for the *VDAC* gene and expression in breast cancer samples vs. normal tissue ($p = 1.0 \times 10^{-12}$). **(C)** Survival analysis of VDAC gene and expression in lung adenocarcinoma vs. normal tissue samples ($p = 1.0 \times 10^{-12}$). **(D)** Survival analysis and expression of VDAC in head and neck carcinoma samples vs. normal tissue samples ($p = 1.0 \times 10^{-12}$). All data were taken from the UALCAN cancer database (Chandrashekar et al., 2017).

in the metastatic cascade, including angiogenesis, migration, survival, and colonization at secondary organ sites. It is also required for the metastatic dissemination of cancer cells that have undergone EMT (Feng et al., 2017), and its absence inhibits tumor growth in animal models by disrupting redox homeostasis (Bobrovnikova-Marjon et al., 2010; Salaroglio et al., 2017). In this regard, Raturi et al. (2016) described that cancer cells with low levels of thioredoxin-related transmembrane protein 1 (TMX1) show increased Ca^{2+} release from the ER with a concomitant decrease in mitochondrial cation levels that results in reduction of respiration and glycolytic energy-based tumor growth (Ganapathy-Kanniappan and Geschwind, 2013). TMX1 requires thioredoxin and palmitoylation motifs to target MAM and to participate in calcium flow between ER and mitochondria contact sites (Raturi et al., 2016). Recently, the expression of FUN14 domain-containing protein 1 was positively correlated with breast cancer metastasis and the Ca^{2+}/NFATC1/BMI1 axis, suggesting that inhibition of this protein could represent a therapeutic target for breast cancer (Wu et al., 2019). From the above-mentioned description, it is clear that calcium regulation is essential in carcinogenesis and tumor development. Last but not least, other MAM-tethering proteins are the mitochondrial proteins Mfn1 and Mfn2, which have been reported to be anti-proliferative and pro-apoptotic in cancer cells. Overexpression of both mitofusins in cancer cells has been demonstrated, as well as their interactions with phosphatidylinositol 3-kinase (PI3K)/Akt and P21Ras pathways, which are involved in cell proliferation, metastasis, and invasion processes (Ma et al., 2015; Li et al., 2018; Moghaddam et al., 2020).

Lipid Exchange and Signaling in Cancer

Lipidomic remodeling, including alteration in fatty acid transport, *de novo* lipogenesis, β-oxidation, and storage as lipid droplets, is a metabolic hallmark of cancer cells (Blücher and Stadler, 2017; Enríquez-Cortina et al., 2017; Diaz-Aragon et al., 2019).

Under basal conditions, cells store fatty acids as an energy reserve to ensure their survival. They are located in bodies called *lipid droplets*, whose function is to transport lipids to all organelles (mainly to the mitochondria) (Cohen et al., 2018). Lipid transport is coupled to membrane vesicle trafficking of the secretory pathway and also supplied to different compartments through *non-vesicular traffic* (Urbani and Simoni, 1990; Lev, 2010, 2012). Lipid transfer proteins (LTPs) facilitate lipid traffic from a donor to a receptor compartment (Lev, 2010; Wong et al., 2019). Most intracellular LTPs are anchored to the MCS, whereas domains containing the lipid-binding cavity transfers the lipid cargo from one organelle to the others (Wong et al., 2017, Hanada, 2018; Wong et al., 2019). LTP dysfunction may contribute to cancer development, as it has been suggested that these proteins are involved in both migration and cell growth (Sassano et al., 2017) and that their deregulation could lead

to disease progression (Peretti et al., 2020), making them an attractive target in cancer research.

LTPs acting at the ER–Golgi interface are as follows: (1) CERT, which transports the newly synthesized ceramide from the ER to the trans-Golgi network *via* the MCS (Scheffer et al., 2011; Kumagai and Hanada, 2019), (2) the four-phosphate adaptor protein 2 involved in the transport of glucosylceramide to the TGN (Mesmin et al., 2019), and (3) OSBP, which is engaged in the direct transfer of cholesterol from the ER to the TGN *via* PI4P-coupled countertransport (Mesmin et al., 2017). All LTPs share structural characteristics that allow them to bind to the Golgi and ER simultaneously, acting as a bridge. Most relevant are the N-terminal pleckstrin homology (PH) domain that is selective for PI4P in the TGN and a central motif of FFAT that binds to the VAPA and VAPB proteins located in the ER (Loewen et al., 2003; Kawano et al., 2006). In the following sections, we describe current information on the relevance of some LTPs in cancer migration and progression; in particular, we will refer to CERTs and OSBPs.

Ceramide Transfer Protein

CERT (encoded by *COL4A3BP*) contains a steroidogenic regulatory protein-related lipid transfer (START) terminal carboxylic domain responsible for ceramide binding and intermembrane transfer that also shows high specificity with natural C_{14-20} ceramide, but not with longer acyl chains (Hanada et al., 2003; Kumagai et al., 2005).

It has been observed that stress stimuli, such as those exerted by chemotherapeutic drugs, cause an increase in ceramide levels by stimulating *de novo* ceramide synthesis, sphingomyelin hydrolysis, or both (Alphonse et al., 2004; Mesicek et al., 2010). In this sense, some tumor models are associated with impaired ceramide signaling, suggesting that this molecule plays a key role in tumor development and progression (Norris et al., 2006; Kim et al., 2008; Ruckhäberle et al., 2008). Specifically, its decrease results in resistance to cell death stimuli (Bonnaud et al., 2007), while its restoration increases sensitivity (Morales et al., 2007), which supports the central role of ceramide signaling in cell death. Swanton et al. (2007) also observed that downregulation of *COL4A3BP*, besides sensitizing cancer cells to multiple cytotoxic agents, enhances ER stress, proposing *COL4A3BP* as a possible target in chemotherapy-resistant cancers.

CERT represents the main ceramide gateway from the endoplasmic reticulum and might increase its levels in the mitochondria (Scheffer et al., 2011). In light of this, Dadsena et al. (2019) identified VDAC1 and VDAC2 channels as binding proteins to mitochondrial ceramide by using a photoactivatable ceramide probe. On the other hand, VDAC2 loss or the replacement of a membrane-facing residue of glutamate with glutamine makes human colon cancer cells resistant to ceramide-induced apoptosis (Dadsena et al., 2019). To reinforce the premise that deregulation of ceramide levels in ER is linked to mitochondrial apoptosis, Jain et al. (2017) demonstrated that mitoCERT (a ceramide transfer protein equipped with an OMM anchor) triggers mitochondrial Bax-dependent apoptosis HeLa cells.

The regulation of CERT differs between different types of cancer. For instance, CERT is overexpressed in ovarian cancer cells (Juul et al., 2010) and HER^+ cells (Lee et al., 2012); its silencing exerts enhanced sensitivity to multi-drug treatment in several cancer cell lines (Swanton et al., 2007) and also induces changes in the levels of lysosome-associated membrane protein 2, which increases the autophagosome–lysosome flux in colorectal and breast cancer cell lines (Lee et al., 2012). On the other hand, the downward regulation of CERT improved ErbB1 mobility, ligand autophosphorylation, internalization, and chemotaxis that eventually contribute to TNBC cell progression (Heering et al., 2012). CERT decrease is also related to alterations in the activity of phospholipase D2, which facilitate the activation of HER1 (Heering et al., 2012). In this context, the activity of PLD increases in different types of cancer; for instance, it was shown that this phospholipase is dispensable for tumorigenesis and growth of breast tumors, but it is essential for lung metastasis of mammary cancer cells (Wang Z. et al., 2017).

As mentioned above, CERT1 displays a profound impact on human cancers. The survival analysis of the prediction outcome in the TCGA data set in cancer patients with high and low expression of *COL4A3BP* gene (**Figure 5A**) also reveals that its high expression was associated with a poor outcome in renal cancer (**Figure 5A**) and cholangiocarcinoma (CHOL, **Figure 5B**). Furthermore, cholangiocarcinoma primary tumors exhibited a higher expression of *COL4A3BP* gene as compared with normal liver (**Figure 5C**), according to the UALCAN database[2] (Chandrashekar et al., 2017). The genomic findings regarding this gene in TCGA data point to it as a noteworthy target for future research, particularly in CHOL, which is the second liver primary tumor with higher mortality (Banales et al., 2020).

Nir

On the other hand, the Nir2 protein (which contains a PI transfer domain and transfer phosphatidic acid) (Kim et al., 2015) mediates the interactions with ER through a VAP binding site located in the Golgi. It works in coordination with CERT and OSBP in the ER–Golgi contact sites to regulate the transport of ceramide (Amarilio et al., 2005; Peretti et al., 2008). Nir2-mediated MSC allows the regulation of lipids involved in the activation of the mitogen-activated protein kinase and PI3K signaling pathways, which, in turn, play an important role in the initiation and progression of breast cancer and with EMT activation (Keinan et al., 2014; Ellis and Ma, 2019). Expression of Nir2 in MDA-MB-231 cells correlates with a poor prognosis in breast cancer. By contrast, depletion of Nir2 expression in MDA-MB-231 cells reduces metastasis in number and size (Keinan et al., 2014).

In the cell lines of colorectal adenocarcinoma SW48, the participation of Nir1 and Nir2 genes has been investigated as key regulators of cell morphogenesis. Under normal conditions, the regulation of both genes is differential, i.e., Nir1 is regulated downward, while Nir2 is regulated upward. However, these scenarios are modified with tumor suppressors such as the TGFβ-induced factor 2-linked X (TGIF2LX). In the

[2]http://ualcan.path.uab.edu

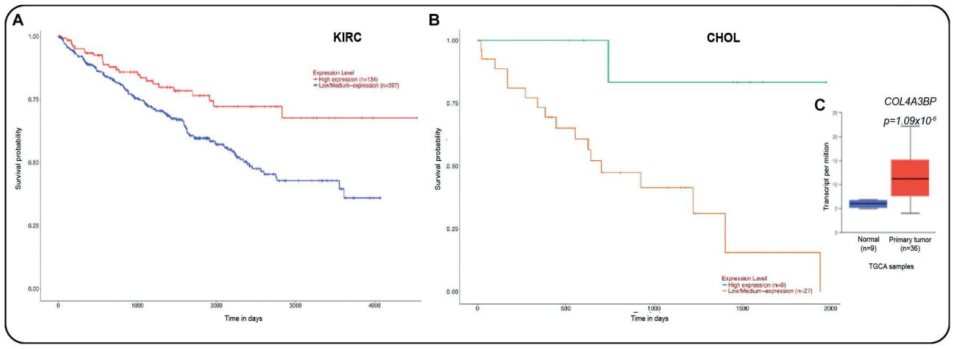


FIGURE 5 | (A) Survival analysis for the *COL4A3BP* gene (CERT protein) in kidney renal clear carcinoma and in **(B)** in cholangiocarcinoma (CHOL). **(C)** *COL4A3BP* gene expression in CHOL samples against normal liver ($p = 1.09 \times 10^{-6}$). All data were taken from the UALCAN cancer database (Chandrashekar et al., 2017).

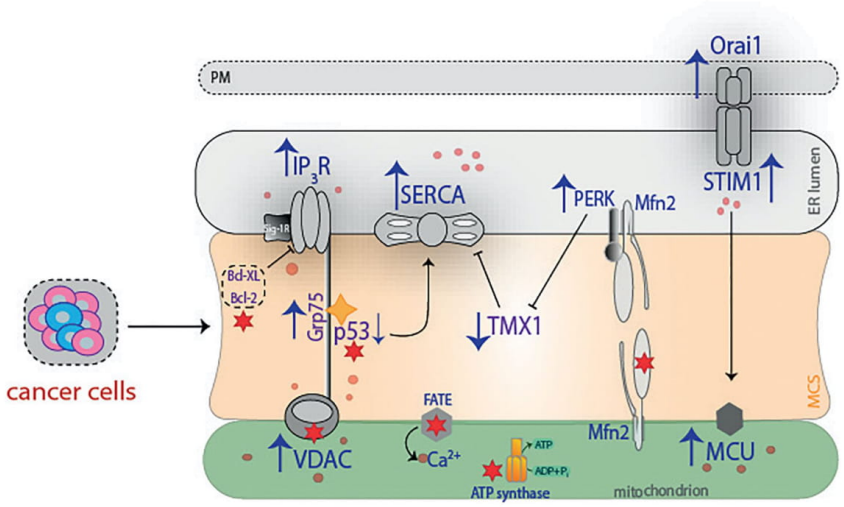


FIGURE 6 | Summary of proteins with relevance in cancer. The progression and metastasis of cancer cells benefit is associated with an overexpression of different proteins. To mention a few examples, IP_3 overexpression favors cancer migration, with a concomitant increase in Ca^{2+} concentrations, while VDAC and SERCA increase is related with poor prognosis. Grp75 interacts with p53 and promotes cancer cell survival, whereas Orai1 and STIM1 boost Ca^{2+} and allow cancer cell migration. On the other hand, PERK increases invasion and metastasis by limiting redox homeostasis through TMX1, which is decreased in cancer. Ultimately, red stars illustrate the effect that different therapies exert on cancer. PM, plasma membrane; STIM1, stromal interaction molecule 1; IP_3R, inositol 1,4,5-triphosphate receptor; SERCA, sarco(endo)plasmic reticulum Ca^{2+}-ATPase; PERK, protein kinase RNA-like ER kinase; Mfn2, mitofusin 2; Bcl-XL, B-cell lymphoma—extra large; Bcl-2, B cell lymphoma-2; Grp75, glucose-related protein 75; p53, tumor suppressor protein; TMX1, thioredoxin-related transmembrane protein 1; VDAC, voltage-dependent anion channel; ATP, adenosine triphosphate; ADP, adenosine diphosphate; MCU, mitochondrial calcium uniporter; MCS, membrane contact sites.

presence/absence of TGIF2LX, Nir2 acts as a tumor suppressor and Nir1 acts as a proto-oncogene, respectively (Mobini et al., 2016). Interestingly, overexpression of TGIF2LX in C57BL/6 nude mice induced a different effect in Nir1 and Nir2, suggesting that the regulation of these genes would help suppress the progression of colorectal carcinoma (Mobini et al., 2018). Speaking of Nir1, it has been shown that its binding to chemokine ligand 18 induces the progression and metastasis of invasive ductal breast carcinoma to the lung through the LIMK/cofilin and PI3K/Akt/GSK3β/Snail signaling cascade, promoting EMT

(Zhang et al., 2013). These results suggest that direct intervention on Nir1 could serve as a potential target in cancer progression, and the study of Nir2 may be useful to understand some LTP-mediated mechanisms that regulate key cellular processes and contribute to cancer metastasis.

Oxysterol-Binding Protein

As already mentioned, ORP proteins contain double-targeting determinants for ER and associated organelles, such as an FFAT motif that binds to VAP proteins located in the ER and PH domain that allow their interactions with different non-ER organelle membranes (Olkkonen and Li, 2013). Galmes et al. (2016) showed in HeLa cells that OPR5 and OPR8 are located in ER–mitochondria MCS, in addition to mitochondrial protein tyrosine phosphatase-interacting protein-51 that interacts with ER–PM contacts. Interestingly, the depletion of ORP5 and ORP8 leads to defects in mitochondrial morphology and respiratory function (Galmes et al., 2016).

Cholesterol has acquired great relevance thanks to its participation in carcinogenic signaling pathways (Huang et al., 2020). In this sense, it has been described that hypercholesterolemia represents a risk factor in the development of some types of cancer such as breast, prostate, liver, and colorectal cancer. At the cellular level, cholesterol is an important component of cell membranes and lipid rafts (Ding et al., 2019; Huang et al., 2020), while tumor cells use it for membrane formation during cell growth and division (Vassilev et al., 2015).

The location of cholesterol in cell membranes favors its interaction with membrane proteins. In terms of cholesterol trafficking, it has been reported that the START domain 3 (StARD3, steroidogenic acute regulatory protein-related lipid transfer domain-3) creates endosome–ER contact sites, promoting cholesterol accumulation in endosomes at the expense of the plasma membrane (Wilhelm et al., 2017). STARD3 has an N-terminal MLN64 domain (MENTAL) with four transmembrane subunits anchored to the endosome membrane, a central FFAT region, and a hydrophobic START C-terminal domain in which cholesterol binds (Voilquin et al., 2019). This process is favored by the interaction with ER-anchored VAP protein, generating a highly efficient cholesterol transport (Wilhelm et al., 2017). Overexpression of StARD3 was identified in at least 14 of 93 invasive breast carcinomas, which also expressed high levels of HER2 mRNA, and may increase oncogenic signaling through membrane-associated kinases such as proto-oncogene tyrosine-protein kinase Src (Vassilev et al., 2015). In this regard, Zhang et al. (2011) evaluated the activation of Src in primary breast tumor samples of patients treated with trastuzumab (an anti-HER2 monoclonal antibody indicated for the treatment of tumors that overexpress HER2) by immunohistochemical staining and demonstrated a strong correlation between patients expressing high levels of Src activity and low survival as well as high survival in those patients with low Src activity (Zhang et al., 2011), suggesting that STARD3 may contribute to the aggressive behavior of patients' resistance to trastuzumab.

It has also been described that STARD3, when overexpressed, generates rigid endosome and a static ER–endosome contact site, preventing the late maturation of endosome to lysosome and consequently blocking lysosomal degradation of cell surface receptors (including HER2 and other growth factors). In turn, the receptors are recycled back to the plasma membrane, favoring the spread of cell signals of uncontrolled cell growth. Thus, STARD3 increases the progression of HER2-positive cancer (Peretti et al., 2020). Qiu et al. (2014) reported a strong expression of STARD3 in tubular adenocarcinoma cells, positively associated with a high mitochondria number. In this sense, alterations in mitochondrial cholesterol trafficking have been associated with inhibition of cell death by inhibiting the release of cytochrome c and Smac/Diablo, facilitating the survival of tumor cells (Smith and Land, 2012). Interestingly, even in non-cancerous cells, cholesterol accumulation in hepatocytes is strongly associated to apoptosis resistance and mitochondrial dynamic changes (Domínguez-Pérez et al., 2019). Mitochondrial cholesterol is also associated with resistance to chemotherapy. Montero et al. (2008) found that StART silencing in H35 and HepG2 cells significantly decreases cholesterol levels in the mitochondria as a result of cholesterol delivery reduction from extramitochondrial sources into the mitochondria. Additionally, over-accumulation of cholesterol in tumor tissues is strongly associated with low serum cholesterol levels in patients diagnosed with cancer (Strasak et al., 2009; Benn et al., 2011; Smith and Land, 2012). Finally, it has been reported that mitochondrial cholesterol overload is directly associated with aggressive liver cancer phenotype with poor prognosis (Enríquez-Cortina et al., 2017). In brief, LTPs impact cancer progression and metastasis; however, more studies are needed to understand the specific function of LTPs.

In the next section, we tackle the effect of cancer chemotherapy and its relationship with MCS, with greater emphasis on ER–mitochondria contact sites and calcium management, which are the most reported players in cancer progression and metastasis.

MCS AS POSSIBLE THERAPEUTIC TARGETS IN CANCER

Although pioneering studies by Howatson and Ham (1955) reported a limited number of contacts between the ER and the mitochondria in rat liver cancer compared to normal tissue, it was the first evidence of the relationship between organelles and their importance in tumorigenesis. As it is known, organelles sense stress in the cellular microenvironment and modify their structure and function according to cellular demand for survival; however, deterioration of the signaling cascades might lead to oncogene activation. In this regard, oncoproteins located in the MAM, such as AKT (Betz et al., 2013), PERK (Fels and Koumenis, 2006; Bu and Diehl, 2016), Grp75 (Wadhwa et al., 2006), and VDAC (Pernemalm et al., 2013; Shoshan-Barmatz et al., 2015) as well as tumor suppressors such as p53 (Giorgi et al., 2015), the phosphatase tensin homolog (Bononi et al., 2013), and the promyelocytic leukemia (Giorgi et al., 2010; Missiroli et al., 2016), interact with Ca^{2+} handling proteins, modulating their activity and promoting tumorigenesis (Morciano et al., 2018; Xia et al., 2019).

Anti-cancer drugs have multiple modes of action; in this regard, much attention has been paid to calcium signaling, as its deregulation in MAMs has been identified as a hallmark of cancer cells. Ca^{2+} ions shift cancer metabolism toward glycolytic metabolism and increase their resistance to cell death (Bittremieux et al., 2016). These also support mesenchymal transformation, migration, invasion, and metastasis (Ren et al., 2017). However, changes in Ca^{2+} signaling depend on the type of cancer cell and the chemotherapeutic treatment used. For instance, *cis*-platin (used for solid tumors) in rat dorsal root ganglion neurons blocks VDAC at high concentrations (Tomaszewski and Büsselberg, 2007), while in prostate cancer it promotes calcium uptake through other channels (Chen et al., 2014) and in lung carcinoma it favors its liberation *via* SOCE (Gualdani et al., 2019). Therefore, management of Ca^{2+} signaling is a major complication in chemotherapeutic treatments (Varghese et al., 2019).

There is a growing number of reports on Ca^{2+} signaling alterations in MCS research, but the information in this area still remains scarce. The following sections present current evidence on the role of conventional chemotherapeutic strategies and their relevance in MCS as a study target in cancer treatment.

Chemotherapeutic Compounds and Their Role in MCS

Some compounds used in chemotherapy have been shown to indirectly modulate interactions between the ER and the mitochondria. However, there are no conclusive studies that demonstrate their direct participation. It has been suggested that these drugs could act on some of the MCS's interaction proteins. For example, the expression of Mfn2 (which controls the stability of the ER–mitochondria interaction and the transfer of Ca^{2+} and lipids) decreases in neonatal cardiomyocytes exposed to doxorubicin (Dox) (Tang et al., 2017). Other reports indicate that p53, located in the ER, MAM, and cytosol under basal conditions, is accumulated in the ER–mitochondria interface in response to Dox in $p53^{+/+}$ HTC-116 cells, modulating Ca^{2+} homeostasis. In this sense, p53 interacts with SERCA, promoting the accumulation of calcium in the ER and its subsequent transfer to the mitochondria, triggering apoptosis (Giorgi et al., 2015). Betz et al. (2013) showed that mTORC2 is detected in the contacts of the mitochondria with the ER where it phosphorylates and activates the Akt after growth factor stimulation. In turn, mTORC2–Akt signaling regulates MAM integrity, Ca^{2+} flux in the ER–mitochondria contacts, and energy metabolism. Nevertheless, some of the side effects of Dox are related to Ca^{2+}. Aziz et al. (2019) reported that calcium derived from the ER increases significantly as compared to cytosolic calcium via Src kinase activation in rat ovarian follicles (Aziz et al., 2019).

cis-Platin can also affect MCS homeostasis. Studies in the A549 cell lines resistant to *cis*-platin show elevated concentrations of free intracellular Ca^{2+} (Liang and Huang, 2000). Other studies showed that the IP_3R gene is deregulated in the drug-resistant cell, explaining in part the bladder cancer cells' resistance to apoptosis (Tsunoda et al., 2005). Xu et al. (2015) also revealed that *cis*-platinum causes the pro-apoptotic release of Ca^{2+} from the ER in the cytosol and the mitochondria, leading to cationic overload in both compartments and ultimately contributing to ER- and mitochondria-mediated apoptosis in *cis*-platin-sensitive SKOV3 cells (Xu et al., 2015). The same group demonstrated that ABT737 (a pharmacological Bcl-2 inhibitor that interacts with IP_3R and suppresses Ca^{2+} signaling) (Akl et al., 2014) increases *cis*-platinum cytotoxicity in chemically resistant SKOV3 cells. Interestingly, ABT737 increased the free calcium levels both in the cytosol and the mitochondria, accentuating apoptosis mediated by the ER–mitochondria contacts (Xie Q. et al., 2016). On the other hand, BIRD2 inhibits Bcl-2/IP_3R interaction by attenuating Bcl-2 control after Ca^{2+} elevation and calcium-mediated apoptosis in different types of cancer *in vitro* and *in vivo* (Distelhorst, 2018). Bittremieux et al. (2019) recently showed that BIRD2 changes calcium signals from pro-survival to pro-death in the cancer cell, that is, IP_3R-mediated calcium release from the ER causes a marked increase in intracellular Ca^{2+}, leading to calcium mitochondrial overload and apoptosis triggering (Bittremieux et al., 2019).

In addition, chemotherapeutic compounds are related to some of the cellular processes that take place at the MCS interface. For instance, in pancreatic cancer cells, *cis*-platin stimulates ER stress and interacts with bortezomib (a potent and selective proteome inhibitor for the treatment of solid neoplasias) by increasing ER dilatation, $[Ca^{2+}]_i$ levels, and cell death. It is important to note that combination therapy (bortezomib plus *cis*-platin) induces JNK activation and apoptosis in these cells, resulting in a reduction in tumor burden and suggesting that this combination increases the anti-cancer activity of *cis*-platin (Nawrocki et al., 2005). On the other hand, oxaliplatin (a platinum-based drug) acts as a mediator of Ca^{2+} signaling and plays a role in peripheral neuropathy. It has been described that prolonged exposure to the drug induces changes in ER loading and IP_3R-mediated Ca^{2+} signaling in SH-SY5Y neuroblastoma cells (Schulze et al., 2011).

Most of the works cited here refer to different cancer cell lines, where the protection mechanism of pharmacological compounds is associated with calcium management. However, the relevance of these molecules at the interface of the ER–mitochondria contact sites, as well as in other interactions in cancer, is still scarce; we believe that it is paramount to study not only the management of Ca^{2+} but also other processes carried out in the MCS that could be modulated by some of the molecules already described.

CONCLUSION AND PERSPECTIVES

The identification of new targets that provide better prognosis in cancer is necessary due to the increase in the number of new cases in the world. In particular, the increased interest in the study of contact sites in different physiopathological conditions suggests that they could be placed as novel targets in cancer studies. However, even though several working groups are actively studying the role of MCS in cancer (as well as in other pathological conditions), there are missing links that must be incorporated to understand their function in an integrated way.

The nutraceutical compounds' effect on contact sites is also an interesting issue to be explored. The relevance of these molecules lies in their ability to regulate some of the proteins that conform with the MCS machinery, such as Mfn2, IP_3R, VDAC1, but they could also function as adjuvant therapy to improve the beneficial effects of conventional therapy (**Figure 6**). It is clear that a considerable number of proteins that regulate membrane contacts have been "discovered" in recent years, but it has to be determined which of them might have the potential to reduce cancer progression. Overall, one of the most attractive and immediate perspectives in the field of "contactology" (Csordás et al., 2018) would be to elucidate and/or describe what other types of organelle interactions occur in cancer as well as to detail how they would favor and/or inhibit cancer progression. Undoubtedly, it remains a real challenge to limit the progression of cancer, but great advances in this area have been made. We believe that understanding the MCS mode of action could improve the management of several diseases.

Finally, we believe that more studies of MCS might position them as novel relevant markers for diagnostic and prognostic purposes in cancer.

AUTHOR CONTRIBUTIONS

AG-H, MA-C, CZ, LEG-Q, and AS-P have made a substantial, direct, and intellectual contribution to the work. AS-N and LEG-Q have made the bioinformatic analysis used in this manuscript. AS-P authorized and reviewed the drafts of the document. All authors approved its publication.

ACKNOWLEDGMENTS

We would like to apologize to colleagues whose outstanding work on the role of contactology in cancer could not be included due to space limitations.

REFERENCES

Achleitner, G., Gaigg, B., Krasser, A., Kainersdorfer, E., Kohlwein, S. D., Perktold, A., et al. (1999). Association between the endoplasmic reticulum and mitochondria of yeast facilitates interorganelle transport of phospholipids through membrane contact. *Eur. J. Biochem.* 264, 545–553. doi: 10.1046/j.1432-1327.1999.0012/26/2020

Akl, H., Monaco, G., La Rovere, R., Welkenhuyzen, K., Kiviluoto, S., Vervliet, T., et al. (2013). IP3R2 levels dictate the apoptotic sensitivity of diffuse large B-cell lymphoma cells to an IP3R-derived peptide targeting the BH4 domain of Bcl-2. ***Cell Death Dis***. 4:e632. doi: 10.1038/cddis.2013.140

Akl, H., Vervloessem, T., Kiviluoto, S., Bittremieux, M., Parys, J. B., De Smedt, H., et al. (2014). A dual role for the anti-apoptotic Bcl-2 protein in cancer: mitochondria versus endoplasmic reticulum. ***Biochim. Biophys. Acta***. 1843, 2240–2252. doi: 10.1016/j.bbamcr.2014.04.017

Alphonse, G., Bionda, C., Aloy, M. T., Ardail, D., Rousson, R., and Rodriguez-Lafrasse, C. (2004). Overcoming resistance to gamma-rays in squamous carcinoma cells by poly-drug elevation of ceramide levels. ***Oncogene*** 23, 2703–2715. doi: 10.1038/sj.onc.1207357

Amarilio, R., Ramachandran, S., Sabanay, H., and Lev, S. (2005). Differential regulation of endoplasmic reticulum structure through VAP-Nir protein interaction. *J. Biol. Chem.* 280, 5934–5944. doi: 10.1074/jbc.M409566200

Assefa, Z., Bultynck, G., Szlufcik, K., Nadif Kasri, N., Vermassen, E., Goris, J., et al. (2004). Caspase-3-induced truncation of type 1 inositol trisphosphate receptor accelerates apoptotic cell death and induces inositol trisphosphate-independent calcium release during apoptosis. *J. Biol. Chem.* 279, 43227–43236. doi: 10.1074/jbc.M403872200

Azeez, J. M., Vini, R., Remadevi, V., Surendran, A., Jaleel, A., Santhosh Kumar, T. R., et al. (2018). VDAC1 and SERCA3 mediate progesterone-triggered Ca2+ signaling in breast cancer cells. *J. Proteome Res.* 17, 698–709. doi: 10.1021/acs.jproteome.7b00754

Aziz, A. U. R., Geng, C., Li, W., Yu, X., Qin, K. R., Wang, H., et al. (2019). Doxorubicin induces ER calcium release via Src in rat ovarian follicles. *Toxicol Sci.* 168, 171–178. doi: 10.1093/toxsci/kfy284

Banales, J. M., Marin, J. J. G., Lamarca, A., Rodrigues, P. M., Khan, S. A., Roberts, L. R., et al. (2020). Cholangiocarcinoma 2020: the next horizon in mechanisms and management. *Nat. Rev. Gastroenterol. Hepatol.* 17, 557–588. doi: 10.1038/s41575-020-0310-z

Bartok, A., Weaver, D., Golenár, T., Nichtova, Z., Katona, M., Bánsághi, S., et al. (2019). IP3 receptor isoforms differently regulate ER-mitochondrial contacts and local calcium transfer. *Nat. Commun.* 10:3726. doi: 10.1038/s41467-019-11646-3

Basso, V., Marchesan, E., and Ziviani, E. (2020). A trio has turned into a quartet: DJ-1 interacts with the IP3R-Grp75-VDAC complex to control ER-mitochondria interaction. *Cell Calcium.* 87:102186. doi: 10.1016/j.ceca.2020.102186

Benn, M., Tybjærg-Hansen, A., Stender, S., Frikke-Schmidt, R., and Nordestgaard, B. G. (2011). Low-density lipoprotein cholesterol and the risk of cancer: a mendelian randomization study. *J. Natl. Cancer Inst.* 103, 508–519. doi: 10.1093/jnci/djr008

Bernhard, W., and Rouiller, C. (1956). Close topographical relationship between mitochondria and ergastoplasm of liver cells in a definite phase of cellular activity. *J. Biophys. Biochem. Cytol.* 2, 73–78. doi: 10.1083/jcb.2.4.73

Betz, C., Stracka, D., Prescianotto-Baschong, C., Frieden, M., Demaurex, N., and Hall, M. N. (2013). Feature article: mTOR complex 2-Akt signaling at mitochondria-associated endoplasmic reticulum membranes (MAM) regulates mitochondrial physiology. *Proc. Natl. Acad. Sci. U S A* 110, 12526–12534. doi: 10.1073/ pnas.1302455110

Bittremieux, M., La Rovere, R. M., Akl, H., Martines, C., Welkenhuyzen, K., Dubron, K., et al. (2019). Constitutive IP3 signaling underlies the sensitivity of B-cell cancers to the Bcl-2/IP3 receptor disruptor BIRD-2. *Cell Death Differ* 26, 531–547. doi: 10.1038/s41418-018-0142-3

Bittremieux, M., Parys, J. B., Pinton, P., and Bultynck, G. (2016). ER functions of oncogenes and tumor suppressors: Modulators of intracellular Ca(2+) signaling. ***Biochim. Biophys. Acta*** 1863, 1364–1378. doi: 10.1016/j.bbamcr.2016.01.002

Blücher, C., and Stadler, S. C. (2017). Obesity and breast cancer: Current insights on the role of fatty acids and lipid metabolism in promoting breast cancer growth and progression. *Front. Endocrinol.* 8:293. doi: 10.3389/fendo.2017.00293

Bobrovnikova-Marjon, E., Grigoriadou, C., Pytel, D., Zhang, F., Ye, J., Koumenis, C., et al. (2010). PERK promotes cancer cell proliferation and tumor growth by limiting oxidative DNA damage. *Oncogene* 29, 3881–3895. doi: 10.1038/onc.2010.153

Bong, A., and Monteith, G. R. (2018). Calcium signaling and the therapeutic targeting of cancer cells. *Biochim. Biophys. Acta Mol. Cell Res.* 1865, 1786–1794. doi: 10.1016/j.bbamcr.2018.05.015

Bonnaud, S., Niaudet, C., Pottier, G., Gaugler, M. H., Millour, J., Barbet, J., et al. (2007). Sphingosine-1-phosphate protects proliferating endothelial cells from ceramide-induced apoptosis but not from DNA damage-induced mitotic death. *Cancer Res.* 67, 1803–1811. doi: 10.1158/0008-5472.CAN-06-2802

Bononi, A., Bonora, M., Marchi, S., Missiroli, S., Poletti, F., Giorgi, C., et al. (2013). Identification of PTEN at the ER and MAMs and its regulation of Ca(2+) signaling and apoptosis in a protein phosphatase-dependent manner. *Cell Death Differ.* 20, 1631–1643. doi: 10.1038/cdd.2013.77

Bu, Y., and Diehl, J. A. (2016). PERK integrates oncogenic signaling and cell survival during cancer development. *J. Cell Physiol.* 231, 2088–2096. doi: 10.1002/ jcp.25336

Bulla, M., Gyimesi, G., Kim, J. H., Bhardwaj, R., Hediger, M. A., Frieden, M., et al. (2019). ORAI1 channel gating and selectivity is differentially altered by natural mutations in the first or third transmembrane domain. *J. Physiol.* 597, 561–582. doi: 10.1113/JP277079

Burdakov, D., Petersen, O. H., and Verkhratsky, A. (2005). Intraluminal calcium as a primary regulator of endoplasmic reticulum function. *Cell Calcium.* 38, 303–310. doi: 10.1016/j.ceca.2005.06.010

Cai, X., Nwokonko, R. M., Loktionova, N. A., Abdulqadir, R., Baraniak, J. H. Jr., Wang, Y., et al. (2018). Pore properties of Orai1 calcium channel dimers and their activation by the STIM1 ER calcium sensor. *J. Biol. Chem.* 293, 12962–12974. doi: 10.1074/jbc.RA118.003424

Cai, X., Zhou, Y., Nwokonko, R. M., Loktionova, N. A., Wang, X., Xin, P., et al. (2016). The Orai1 store-operated calcium channel functions as a hexamer. *J. Biol. Chem.* 291, 25764–25775. doi: 10.1074/jbc.M116.758813

Cantonero, C., Camello, P. J., Abate, C., Berardi, F., Salido, G. M., Rosado, J. A., et al. (2020). NO1, a new Sigma 2 Receptor/TMEM97 fluorescent ligand, downregulates SOCE and promotes apoptosis in the triple negative breast cancer cell lines. *Cancers* 12:257. doi: 10.3390/cancers12020257

Chandrashekar, D. S., Bashel, B., Balasubramanya, S. A. H., Creighton, C. J., Rodriguez, I. P., Chakravarthi, B. V. S. K., et al. (2017). UALCAN: A portal for facilitating tumor subgroup gene expression and survival analyses. *Neoplasia* 19, 649–658. doi: 10.1016/j.neo.2017.05.002

Chen, R., Zeng, X., Zhang, R., Huang, J., Kuang, X., Yang, J., et al. (2014). Cav1.3 channel α1D protein is overexpressed and modulates androgen receptor transactivation in prostate cancers. *Urol. Oncol.* 32, 524–536. doi: 10.1016/j.urolonc.2013.05.011

Chen, Y. F., Chen, Y. T., Chiu, W. T., and Shen, M. R. (2013). Remodeling of calcium signaling in tumor progression. *J. Biomed. Sci.* 20:23. doi: 10.1186/1423-0127-20-23

Chen, Y. F., Chiu, W. T., Chen, Y. T., Lin, P. Y., Huang, H. J., Chou, C. Y., et al. (2011). Calcium store sensor stromal-interaction molecule 1-dependent signaling plays an important role in cervical cancer growth, migration, and angiogenesis. *Proc. Natl. Acad. Sci. U S A.* 108, 15225–15230. doi: 10.1073/pnas.1103315108

Chen, Y. T., Chen, Y. F., Chiu, W. T., Wang, Y. K., Chang, H. C., and Shen, M. R. (2013). The ER Ca^{2+} sensor STIM1 regulates actomyosin contractility of migratory cells. *J. Cell Sci.* 126, 1260–1267. doi: 10.1242/jcs.121129

Chung, J., Torta, F., Masai, K., Lucast, L., Czapla, H., Tanner, L. B., et al. (2015). PI4P/phosphatidylserine countertransport at ORP5-and ORP8-mediated ER-plasma membrane contacts. *Science* 349, 428–432. doi: 10.1126/science.aab1370

Ciscato, F., Filadi, R., Masgras, I., Pizzi, M., Marin, O., Damiano, N., et al. (2020). Hexokinase 2 displacement from mitochondria-associated membranes prompts Ca2+-dependent death of cancer cells. *EMBO Rep.* 21:e49117. doi: 10.15252/embr.201949117

Cohen, S., Rambold, A. S., and Lippincott-Schwartz, J. (2018). Mitochondrial and lipid droplet dynamics regulate intra- and intercellular fatty acid trafficking. *Mol. Cell Oncol.* 5:e1043038. doi: 10.1080/23723556.2015.1043038

Collado, J., and Fernández-Busnadiego, R. (2017). Deciphering the molecular architecture of membrane contact sites by cryo-electron tomography. *Biochim. Biophys. Acta Mol. Cell Res.* 1864, 1507–1512. doi: 10.1016/j.bbamcr.2017.03.009

Copeland, D. E., and Dalton, A. J. (1959). An association between mitochondria and the endoplasmic reticulum in cells of the pseudobranch gland of a teleost. *J. Biophys. Biochem. Cytol.* 5, 393–396. doi: 10.1083/jcb.5.3.393

Csordás, G., Renken, C., Várnai, P., Walter, L., Weaver, D., Buttle, K. F., et al. (2006). Structural and functional features and significance of the physical linkage between ER and mitochondria. *J. Cell Biol.* 174, 915–921. doi: 10.1083/jcb.200604016

Csordás, G., Weaver, D., and Hajnóczky, G. (2018). Endoplasmic reticulum-mitochondrial contactology: Structure and signaling functions. *Trends Cell Biol.* 28, 523–540. doi: 10.1016/j.tcb.2018.02.009

Dadsena, S., Bockelmann, S., Mina, J. G. M., Hassan, D. G., Korneev, S., Razzera, G., et al. (2019). Ceramides bind VDAC2 to trigger mitochondrial apoptosis. *Nat. Commun.* 10:1832. doi: 10.1038/s41467-019-09654-4

Dang, D., Prasad, H., and Rao, R. (2017). Secretory pathway Ca2+ -ATPases promote in vitro microcalcifications in breast cancer cells. *Mol. Carcinog.* 56, 2474–2485. doi: 10.1002/mc.22695

de Brito, O. M., and Scorrano, L. (2008). Mitofusin 2 tethers endoplasmic reticulum to mitochondria. *Nature* 456, 605–610. doi: 10.1038/nature07534

De Matteis, M. A., and Rega, L. R. (2015). Endoplasmic reticulum-Golgi complex membrane contact sites. *Curr. Opin. Cell Biol.* 35, 43–50. doi: 10.1016/j.ceb.2015.04.001

Diaz-Aragon, R., Ramirez-Ricardo, J., Cortes-Reynosa, P., Simoni-Nieves, A., Gomez-Quiroz, L. E., and Perez Salazar, E. (2019). Role of phospholipase D in migration and invasion induced by linoleic acid in breast cancer cells. *Mol. Cell Biochem.* 457, 119–132. doi: 10.1007/s11010-019-03517-8

Ding, X., Zhang, W., Li, S., and Yang, H. (2019). The role of cholesterol metabolism in cancer. *Am. J. Cancer Res.* 9, 219–227.

Distelhorst, C. W. (2018). Targeting Bcl-2-IP3 receptor interaction to treat cancer: A novel approach inspired by nearly a century treating cancer with adrenal corticosteroid hormones. *Biochim. Biophys. Acta Mol. Cell Res.* 1865, 1795–1804. doi: 10.1016/j.bbamcr.2018.07.020

Domínguez-Pérez, M., Simoni-Nieves, A., Rosales, P., Nuño-Lámbarri, N., Rosas-Lemus, M., Souza, V., et al. (2019). Cholesterol burden in the liver induces mitochondrial dynamic changes and resistance to apoptosis. *J. Cell Physiol.* 234, 7213–7223. doi: 10.1002/jcp.27474

Donizy, P., and Marczuk, J. (2019). Selected Golgi-localized proteins and carcinogenesis: What do we know? *Results Probl. Cell Differ.* 67, 487–529. doi: 10.1007/978-3-030-23173-6_20

Dziadek, M. A., and Johnstone, L. S. (2007). Biochemical properties and cellular localisation of STIM proteins. *Cell Calcium.* 42, 123–132. doi: 10.1016/j.ceca.2007.02.006

Eisenberg-Bord, M., Shai, N., Schuldiner, M., and Bohnert, M. (2016). A tether as a tether is a tether: tethering at membrane contact sites. *Dev. Cell.* 39, 395–409. doi: 10.1016/j.devcel.2016.10.022

Elbaz-Alon, Y., Guo, Y., Segev, N., Harel, M., Quinnell, D. E., Geiger, T., et al. (2020). PDZD8 interacts with Protrudin and Rab7 at ER-late endosome membrane contact sites associated with mitochondria. *Nat. Commun.* 11:3645. doi: 10.1038/s41467-020-17451-7

Ellis, H., and Ma, C. X. (2019). PI3K inhibitors in breast cancer therapy. *Curr. Oncol. Rep.* 21:110. doi: 10.1007/s11912-019-0846-7

Enríquez-Cortina, C., Bello-Monroy, O., Rosales-Cruz, P., Souza, V., Miranda, R. U., Toledo-Pérez, R., et al. (2017). Cholesterol overload in the liver aggravates oxidative stress-mediated DNA damage and accelerates hepatocarcinogenesis. *Oncotarget* 8, 104136–104148. doi: 10.18632/oncotarget.22024

Enzo, E., Santinon, G., Pocaterra, A., Aragona, M., Bresolin, S., Forcato, M., et al. (2015). Aerobic glycolysis tunes YAP/TAZ transcriptional activity. *EMBO J.* 34, 1349–1370. doi: 10.15252/embj.201490379

Fang, D., and Maldonado, E. N. (2018). VDAC regulation: A mitochondrial target to stop cell proliferation. *Adv. Cancer Res.* 138, 41–69. doi: 10.1016/bs.acr.2018.02.002

Faouzi, M., Hague, F., Potier, M., Ahidouch, A., Sevestre, H., and Ouadid-Ahidouch, H. (2011). Down-regulation of Orai3 arrests cell-cycle progression and induces apoptosis in breast cancer cells but not in normal breast epithelial cells. *J. Cell Physiol.* 226, 542–551. doi: 10.1002/jcp.22363

Fels, D. R., and Koumenis, C. (2006). The PERK/eIF2alpha/ATF4 module of the UPR in hypoxia resistance and tumor growth. *Cancer Biol. Ther.* 5, 723–728. doi: 10.4161/cbt.5.7.2967

Feng, Y. X., Jin, D. X., Sokol, E. S., Reinhardt, F., Miller, D. H., and Gupta, P. B. (2017). Cancer-specific PERK signaling drives invasion and metastasis through CREB3L1. *Nat. Commun.* 8:1079. doi: 10.1038/s41467-017-01052-y

Fernández-Busnadiego, R., Saheki, Y., and De Camilli, P. (2015). Three-dimensional architecture of extended synaptotagmin-mediated endoplasmic reticulum–plasma membrane contact sites. *Proc. Natl. Acad. Sci. U S A.* 112, E2004–E2013. doi: 10.1073/pnas.1503191112

Fernández-Busnadiego, R. (2016). Supramolecular architecture of endoplasmic reticulum-plasma membrane contact sites. *Biochem. Soc. Trans.* 44, 534–540. doi: 10.1042/BST20150279

Feske, S., Gwack, Y., Prakriya, M., Srikanth, S., Puppel, S. H., Tanasa, B., et al. (2006). A mutation in Orai1 causes immune deficiency by abrogating CRAC channel function. *Nature* 441, 179–185. doi: 10.1038/nature04702

Flourakis, M., Lehen'kyi, V., Beck, B., Raphaël, M., Vandenberghe, M., Abeele, F. V., et al. (2010). Orai1 contributes to the establishment of an apoptosis-resistant phenotype in prostate cancer cells. *Cell Death Dis.* 1:e75. doi: 10.1038/cddis.2010.52

Galmes, R., Houcine, A., van Vliet, A. R., Agostinis, P., Jackson, C. L., and Giordano, F. (2016). ORP5/ORP8 localize to endoplasmic reticulum-mitochondria contacts and are involved in mitochondrial function. *EMBO Rep.* 17, 800–810. doi: 10.15252/embr.201541108

Ganapathy-Kanniappan, S., and Geschwind, J. F. (2013). Tumor glycolysis as a target for cancer therapy: progress and prospects. *Mol. Cancer.* 12:152. doi: 10.1186/1476-4598-12-152

Giacomello, M., and Pellegrini, L. (2016). The coming of age of the mitochondria-ER contact: a matter of thickness. *Cell Death Differ.* 23, 1417–1427. doi: 10.1038/cdd.2016.52

Giorgi, C., Bonora, M., Sorrentino, G., Missiroli, S., Poletti, F., Suski, J. M., et al. (2015). p53 at the endoplasmic reticulum regulates apoptosis in a Ca2+-dependent manner. *Proc. Natl. Acad. Sci. U S A.* 112, 1779–1784. doi: 10.1073/pnas.1410723112

Giorgi, C., Ito, K., Lin, H. K., Santangelo, C., Wieckowski, M. R., Lebiedzinska, M., et al. (2010). PML regulates apoptosis at endoplasmic reticulum by modulating calcium release. *Science* 330, 1247–1251. doi: 10.1126/science.1189157

Golub, T. R., Slonim, D. K., Tamayo, P., Huard, C., Gaasenbeek, M., Mesirov, J. P., et al. (1999). Molecular classification of cancer: class discovery and class prediction by gene expression monitoring. *Science* 286, 531–537. doi: 10.1126/science.286.5439.531

Grigoriev, I., Gouveia, S. M., van der Vaart, B., Demmers, J., Smyth, J. T., Honnappa, S., et al. (2008). STIM1 is a MT-plus-end-tracking protein involved in remodeling of the ER. *Curr. Biol.* 18, 177–182. doi: 10.1016/j.cub.2007.12.050

Gualdani, R., de Clippele, M., Ratbi, I., Gailly, P., and Tajeddine, N. (2019). Store-operated calcium entry contributes to cisplatin-induced cell death in non-small cell lung carcinoma. ***Cancers*** 11:430. doi: 10.3390/cancers11030430

Gudlur, A., Zeraik, A. E., Hirve, N., Rajanikanth, V., Bobkov, A. A., Ma, G., et al. (2018). Calcium sensing by the STIM1 ER-luminal domain. *Nat. Commun.* 9:4536. doi: 10.1038/s41467-018-06816-8

Hanada, K. (2018). Lipid transfer proteins rectify inter-organelle flux and accurately deliver lipids at membrane contact sites. *J. Lipid Res.* 59, 1341–1366. doi: 10.1194/jlr.R085324

Hanada, K., Kumagai, K., Yasuda, S., Miura, Y., Kawano, M., Fukasawa, M., et al. (2003). Molecular machinery for non-vesicular trafficking of ceramide. *Nature* 426, 803–809. doi: 10.1038/nature02188

Harper, C. S., White, A. J., and Lackner, L. L. (2020). The multifunctional nature of mitochondrial contact site proteins. *Curr. Opin. Cell Biol.* 65, 58–65. doi: 10.1016/j.ceb.2020.02.010

Hasna, J., Hague, F., Rodat-Despoix, L., Geerts, D., Leroy, C., and Tulasne, D. (2018). Orai3 calcium channel and resistance to chemotherapy in breast cancer cells: the p53 connection. *Cell Death Differ.* 25, 693–707. doi: 10.1038/s41418-017-0007-1

Heering, J., Weis, N., Holeiter, M., Neugart, F., Staebler, A., Fehm, T. N., et al. (2012). Loss of the ceramide transfer protein augments EGF receptor signaling in breast cancer. *Cancer Res.* 72, 2855–2866. doi: 10.1158/0008-5472.CAN-11-3069

Henley, S. J., Thomas, C. C., Lewis, D. R., Ward, E. M., Islami, F., Wu, M., et al. (2020b). Annual report to the nation on the status of cancer, part II: Progress toward healthy people 2020 objectives for 4 common cancers. *Cancer* 126, 2250–2266. doi: 10.1002/cncr.32801

Henley, S. J., Ward, E. M., Scott, S., Ma, J., Anderson, R. N., Firth, A. U., et al. (2020a). Annual report to the nation on the status of cancer, part I: National cancer statistics. *Cancer* 126, 2225–2249. doi: 10.1002/cncr.32802

Hirabayashi, Y., Kwon, S. K., Paek, H., Pernice, W. M., Paul, M. A., Lee, J., et al. (2017). ER-mitochondria tethering by PDZD8 regulates Ca2+ dynamics in mammalian neurons. *Science* 358, 623–630. doi: 10.1126/science.aan6009

Hirve, N., Rajanikanth, V., Hogan, P. G., and Gudlur, A. (2018). Coiled-coil formation conveys a STIM1 signal from ER lumen to cytoplasm. *Cell Rep.* 22, 72–83. doi: 10.1016/j.celrep.2017.12.030

Hou, X., Pedi, L., Diver, M. M., and Long, S. B. (2012). Crystal structure of the calcium release-activated calcium channel Orai. *Science* 338, 1308–1313. doi: 10.1126/science.1228757

Hou, X. R., Outhwaite, I. R., Pedi, L., and Long, S. B. (2020). Cryo-EM structure of the calcium release-activated calcium channel Orai in an open conformation. *eLife* 9:e627772. doi: 10.7554/e.Life.62772

Howatson, A. F., and Ham, A. W. (1955). Electron microscope study of sections of two rat liver tumors. *Cancer Res.* 15, 62–69.

Howley, B. V., and Howe, P. H. (2018). Metastasis-associated upregulation of ER-Golgi trafficking kinetics: regulation of cancer progression via the Golgi apparatus. *Oncoscience* 5, 142–143. doi: 10.18632/oncoscience.426

Huang, B., Song, B. L., and Xu, C. (2020). Cholesterol metabolism in cancer: mechanisms and therapeutic opportunities. *Nat. Metab.* 2, 132–141. doi: 10.1038/s42255-020-0174-0

Hudecova, S., Markova, J., Simko, V., Csaderova, L., Stracina, T., Sirova, M., et al. (2016). Sulforaphane-induced apoptosis involves the type 1 IP3 receptor. *Oncotarget* 7, 61403–61418. doi: 10.18632/oncotarget.8968

Jain, A., Beutel, O., Ebell, K., Korneev, S., and Holthuis, J. C. (2017). Diverting CERT-mediated ceramide transport to mitochondria triggers Bax-dependent apoptosis. *J. Cell Sci.* 130, 360–371. doi: 10.1242/jcs.194191

Jin, H., Ji, M., Chen, L., Liu, Q., Che, S., Xu, M., et al. (2016). The clinicopathological significance of Mortalin overexpression in invasive ductal carcinoma of breast. *J. Exp. Clin. Cancer Res.* 35:42. doi: 10.1186/s13046-016-0316-0

Jing, J., Liu, G., Huang, Y., and Zhou, Y. (2020). A molecular toolbox for interrogation of membrane contact sites. *J. Physiol.* 598, 1725–1739. doi: 10.1113/JP277761

Juul, N., Szallasi, Z., Eklund, A. C., Li, Q., Burrell, R. A., Gerlinger, M., et al. (2010). Assessment of an RNA interference screen-derived mitotic and ceramide pathway metagene as a predictor of response to neoadjuvant paclitaxel for primary triple-negative breast cancer: a retrospective analysis of five clinical trials. *Lancet Oncol.* 11, 358–365. doi: 10.1016/S1470-2045(10)70018-8

Kawano, M., Kumagai, K., Nishijima, M., and Hanada, K. (2006). Efficient trafficking of ceramide from the endoplasmic reticulum to the Golgi apparatus requires a VAMP-associated protein-interacting FFAT motif of CERT. *J. Biol. Chem.* 281, 30279–30288. doi: 10.1074/jbc.M605032200

Keinan, O., Kedan, A., Gavert, N., Selitrennik, M., Kim, S., Karn, T., et al. (2014). The lipid-transfer protein Nir2 enhances epithelial-mesenchymal transition and facilitates breast cancer metastasis. *J. Cell Sci.* 127, 4740–4749. doi: 10.1242/jcs.155721

Kim, W. J., Okimoto, R. A., Purton, L. E., Goodwin, M., Haserlat, S. M., and Dayyani, F. (2008). Mutations in the neutral sphingomyelinase gene SMPD3 implicate the ceramide pathway in human leukemias. *Blood* 111, 4716–4472. doi: 10.1182/blood-2007-10-113068

Kim, Y. J., Guzman-Hernandez, M. L., Wisniewski, E., and Balla, T. (2015). Phosphatidylinositol-phosphatidic acid exchange by Nir2 at ER-PM contact sites maintains phosphoinositide signaling competence. *Dev. Cell.* 33, 549–561. doi: 10.1016/j.devcel.2015.04.028

Kopacek, J., Ondrias, K., Sedlakova, B., Tomaskova, J., Zahradnikova, L., Sedlak, J., et al. (2009). Type 2 IP(3) receptors are involved in uranyl acetate induced apoptosis in HEK 293 cells. *Toxicology* 262, 73–79. doi: 10.1016/j.tox.2009.05.006

Kulkarni, R. P., Elmi, A., Alcantara-Adap, E., Hubrack, S., Nader, N., and Yu, F. (2019). miRNA-dependent regulation of STIM1 expression in breast cancer. *Sci. Rep.* 9:13076. doi: 10.1038/s41598-019-49629-5

Kumagai, K., and Hanada, K. (2019). Structure, functions and regulation of CERT, a lipid-transfer protein for the delivery of ceramide at the ER-Golgi membrane contact sites. *FEBS Lett.* 593, 2366–2377. doi: 10.1002/1873-3468.13511

Kumagai, K., Yasuda, S., Okemoto, K., Nishijima, M., Kobayashi, S., and Hanada, K. (2005). CERT mediates intermembrane transfer of various molecular species of ceramides. *J. Biol. Chem.* 280, 6488–6495. doi: 10.1074/jbc.M409290200

Le Vasseur, M., Chen, V. C., Huang, K., Vogl, W. A., and Naus, C. C. (2019). Pannexin 2 localizes at ER-Mitochondria contact sites. *Cancers* 11:343. doi: 10.3390/cancers11030343

Lee, A. J., Roylance, R., Sander, J., Gorman, P., Endesfelder, D., Kschischo, M., et al. (2012). CERT depletion predicts chemotherapy benefit and mediates cytotoxic and polyploid-specific cancer cell death through autophagy induction. *J. Pathol.* 226, 482–494. doi: 10.1002/path.2998

Lee, J. E., Cathey, P. I., Wu, H., Parker, R., and Voeltz, G. K. (2020). Endoplasmic reticulum contact sites regulate the dynamics of membraneless organelles. *Science* 367:eaay7108. doi: 10.1126/science.aay7108

Lees, J. A., Messa, M., Sun, E. W., Wheeler, H., Torta, F., Wenk, M. R., et al. (2017). Lipid transport by TMEM24 at ER–plasma membrane contacts regulates pulsatile insulin secretion. *Science* 355:eaah6171. doi: 10.1126/science.aah6171

Lev, S. (2010). Non-vesicular lipid transport by lipid-transfer proteins and beyond. *Nat. Rev. Mol. Cell Biol.* 11, 739–750. doi: 10.1038/nrm2971

Lev, S. (2012). Nonvesicular lipid transfer from the endoplasmic reticulum. ***Cold Spring Harb. Perspect. Biol***. 4:a013300. doi: 10.1101/cshperspect.a013300

Li, J., Ahat, E., and Wang, Y. (2019). Golgi structure and function in health, stress, and diseases. *Results Probl. Cell Differ.* 67, 441–485. doi: 10.1007/978-3-030-23173-6_19

Li, Y., Dong, W., Shan, X., Hong, H., Liu, Y., Liu, Y., et al. (2018). The anti-tumor effects of Mfn2 in breast cancer are dependent on promoter DNA methylation, the P21Ras motif and PKA phosphorylation site. *Oncol. Lett.* 15, 8011–8018. doi: 10.3892/ol.2018.8314

Liang, X., and Huang, Y. (2000). Intracellular free calcium concentration and cisplatin resistance in human lung adenocarcinoma A549 cells. *Biosci. Rep.* 20, 129–138. doi: 10.1023/a:1005530501137

Liu, X., Li, J., Cadilha, B. L., Markota, A., Voigt, C., Huang, Z., et al. (2019). Epithelial-type systemic breast carcinoma cells with a restricted mesenchymal transition are a major source of metastasis. *Sci. Adv.* 5:eaav4275. doi: 10.1126/sciadv.aav4275

Liu, Y., Ma, X., Fujioka, H., Liu, J., Chen, S., and Zhu, X. (2019). DJ-1 regulates the integrity and function of ER-mitochondria association through interaction with IP3R3-Grp75-VDAC1. *Proc. Natl. Acad. Sci. U S A.* 116, 25322–25328. doi: 10.1073/pnas.1906565116

Loewen, C. J., Roy, A., and Levine, T. P. (2003). A conserved ER targeting motif in three families of lipid binding proteins and in Opi1p binds VAP. *EMBO J.* 22, 2025–2035. doi: 10.1093/emboj/cdg201

Ma, G., He, L., Liu, S., Xie, J., Huang, Z., Jing, J., et al. (2020). Optogenetic engineering to probe the molecular choreography of STIM1-mediated cell signaling. *Nat. Commun.* 11:1039. doi: 10.1038/s41467-020-14841-9

Ma, L. I., Chang, Y., Yu, L., He, W., and Liu, Y. (2015). Pro-apoptotic and anti-proliferative effects of mitofusin-2 via PI3K/Akt signaling in breast cancer cells. *Oncol. Lett.* 10, 3816–3822. doi: 10.3892/ol.2015.3748

Makena, M. R., and Rao, R. (2020). Subtype specific targeting of calcium signaling in breast cancer. *Cell Calcium.* 85:102109. doi: 10.1016/j.ceca.2019.102109

Marchi, S., and Pinton, P. (2016). Alterations of calcium homeostasis in cancer cells. *Curr. Opin. Pharmacol.* 29, 1–6. doi: 10.1016/j.coph.2016.03.002

Marchi, S., Giorgi, C., Galluzzi, L., and Pinton, P. (2020). Ca2+ fluxes and cancer. *Mol. Cell.* 78, 1055–1069. doi: 10.1016/j.molcel.2020.04.017

Mesicek, J., Lee, H., Feldman, T., Jiang, X., Skobeleva, A., Berdyshev, E. V., et al. (2010). Ceramide synthases 2, 5, and 6 confer distinct roles in radiation-induced apoptosis in HeLa cells. *Cell Signal.* 22, 1300–1307. doi: 10.1016/j.cellsig.2010.04.006

Mesmin, B., Bigay, J., Polidori, J., Jamecna, D., Lacas-Gervais, S., and Antonny, B. (2017). Sterol transfer, PI4P consumption, and control of membrane lipid order by endogenous OSBP. *EMBO J.* 36, 3156–3174. doi: 10.15252/embj.201796687

Mesmin, B., Kovacs, D., and D'Angelo, G. (2019). Lipid exchange and signaling at ER-Golgi contact sites. *Curr. Opin. Cell Biol.* 57, 8–15. doi: 10.1016/j.ceb.2018.10.002

Missiroli, S., Bonora, M., Patergnani, S., Poletti, F., Perrone, M., Gafa, R., et al. (2016). PML at mitochondria-associated membranes is critical for the repression of autophagy and cancer development. *Cell Rep.* 16, 2415–2427. doi: 10.1016/j celrep.2016.07.082

Mobini, G. R., Ghafari, A., Amanpour, S., Fateh, R., Ghahremani, M. H., Muhammadnejad, S., et al. (2018). In vivo identification of novel TGIF2LX target genes in colorectal adenocarcinoma using the cDNA-AFLP method. *Arab. J. Gastroenterol.* 19, 65–70. doi: 10.1016/j.ajg.2018.05.001

Mobini, G. R., Ghahremani, M. H., Amanpour, S., Dehpour, A. R., Akbari, A., Hoseiniharouni, S. M., et al. (2016). Transforming growth factor beta-induced factor 2-linked X (TGIF2LX) regulates two morphogenesis genes, Nir1 and Nir2 in human colorectal. *Acta Med. Iran.* 54, 302–307.

Moghaddam, F. D., Mortazavi, P., Hamedi, S., Nabiuni, M., and Roodbari, N. H. (2020). Apoptotic effects of melittin on 4T1 breast cancer cell line is associated with up regulation of Mfn1 and Drp1 mRNA expression. *Anticancer Agents Med. Chem.* 20, 790–799. doi: 10.2174/1871520620666200211091451

Montero, J., Morales, A., Llacuna, L., Lluis, J. M., Terrones, O., Basañez, G., et al. (2008). Mitochondrial cholesterol contributes to chemotherapy resistance in hepatocellular carcinoma. *Cancer Res.* 68, 5246–5256. doi: 10.1158/0008-5472.CAN-07-6161

Morales, A., París, R., Villanueva, A., Llacuna, L., García-Ruiz, C., and Fernández-Checa, J. C. (2007). Pharmacological inhibition or small interfering RNA targeting acid ceramidase sensitizes hepatoma cells to chemotherapy and reduces tumor growth in vivo. *Oncogene* 26, 905–916. doi: 10.1038/sj.onc.1209834

Morciano, G., Marchi, S., Morganti, C., Sbano, L., Bittremieux, M., Kerkhofs, M., et al. (2018). Role of mitochondria-associated ER membranes in calcium regulation in cancer-specific settings. *Neoplasia* 20, 510–523. doi: 10.1016/j.neo.2018.03.005

Mound, A., Vautrin-Glabik, A., Foulon, A., Botia, B., Hague, F., Parys, J. B., et al. (2017). Downregulation of type 3 inositol (1,4,5)-trisphosphate receptor decreases breast cancer cell migration through an oscillatory Ca2+ signal. *Oncotarget* 8, 72324–72341. doi: 10.18632/oncotarget.20327

Murphy, S. E., and Levine, T. P. (2016). VAP, a versatile access point for the endoplasmic reticulum: review and analysis of FFAT-like motifs in the VAPome. *Biochim. Biophys. Acta.* 1861, 952–961. doi: 10.1016/j.bbalip.2016.02.009

Nawrocki, S. T., Carew, J. S., Pino, M. S., Highshaw, R. A., Dunner, K. Jr., Huang, P., et al. (2005). Bortezomib sensitizes pancreatic cancer cells to endoplasmic reticulum stress-mediated apoptosis. ***Cancer Res***. 65, 11658–11666. doi: 10.1158/0008-5472.CAN-05-2370

Nigam, N., Grover, A., Goyal, S., Katiyar, S. P., Bhargava, P., Wang, P. C., et al. (2015). Targeting mortalin by embelin causes activation of tumor suppressor p53 and deactivation of metastatic signaling in human breast cancer cells. *PLoS One.* 10:e0138192. doi: 10.1371/journal.pone.0138192

Norris, J. S., Bielawska, A., Day, T., El-Zawahri, A., ElOjeimy, S., Hannun, Y., et al. (2006). Combined therapeutic use of AdGFPFasL and small molecule inhibitors of ceramide metabolism in prostate and head and neck cancers: a status report. *Cancer Gene Ther.* 13, 1045–1051. doi: 10.1038/sj.cgt.7700965

Okeke, E., Dingsdale, H., Parker, T., Voronina, S., and Tepikin, A. V. (2016). Endoplasmic reticulum-plasma membrane junctions: structure, function and dynamics. *J. Physiol.* 594, 2837–2847. doi: 10.1113/JP271142

Olkkonen, V. M., and Li, S. (2013). Oxysterol-binding proteins: sterol and phosphoinositide sensors coordinating transport, signaling and metabolism. *Prog. Lipid Res.* 52, 529–538. doi: 10.1016/j.plipres.2013.06.004

Orci, L., Ravazzola, M., Le Coadic, M., Shen, W. W., Demaurex, N., and Cosson, P. (2009). STIM1-induced pre- cortical and cortical subdomains of the endoplasmic reticulum. *Proc. Natl. Acad. Sci. U S A.* 106, 19358–19362. doi: 10.1073/pnas.0911280106

Paknejad, N., and Hite, R. K. (2018). Structural basis for the regulation of inositol trisphosphate receptors by Ca2+ and IP3. *Nat. Struct. Mol. Biol.* 25, 660–668. doi: 10.1038/s41594-018-0089-6

Park, C. Y., Hoover, P. J., Mullins, F. M., Bachhawat, P., Covington, E. D., Raunser, S., et al. (2009). STIM1 clusters and activates CRAC channels via direct binding of a cytosolic domain to Orai1. *Cell* 136, 876–890. doi: 10.1016/j.cell.2009.02.014

Patergnani, S., Suski, J. M., Agnoletto, C., Bononi, A., Bonora, M., De Marchi, E., et al. (2011). Calcium signaling around mitochondria associated membranes (MAMs). *Cell Commun. Signal.* 9:19. doi: 10.1186/1478-811X-9-19

Patra, K. C., Wang, Q., Bhaskar, P. T., Miller, L., Wang, Z., Wheaton, W., et al. (2013). Hexokinase 2 is required for tumor initiation and maintenance and its systemic deletion is therapeutic in mouse models of cancer. *Cancer Cell* 24, 213–228. doi: 10.1016/j.ccr.2013.06.014

Peretti, D., Dahan, N., Shimoni, E., Hirschberg, K., and Lev, S. (2008). Coordinated lipid transfer between the endoplasmic reticulum and the Golgi complex requires the VAP proteins and is essential for Golgi-mediated transport. *Mol. Biol. Cell.* 19, 3871–3884. doi: 10.1091/mbc.e08-05-0498

Peretti, D., Kim, S., Tufi, R., and Lev, S. (2020). Lipid transfer proteins and membrane contact sites in human cancer. *Front. Cell Dev. Biol.* 7:371. doi: 10.3389/fcell.2019.00371

Pernemalm, M., De Petris, L., Branca, R. M., Forshed, J., Kanter, L., Soria, J. C., et al. (2013). Quantitative proteomics profiling of primary lung adenocarcinoma tumors reveals functional perturbations in tumor metabolism. *J. Proteome Res.* 12, 3934–3943. doi: 10.1021/pr4002096

Porter, K. R., and Palade, G. E. (1957). Studies on the endoplasmic reticulum: III. Its form and distribution in striated muscle cells. *J. Biophys. Biochem. Cytol.* 3, 269–300. doi: 10.1083/jcb.3.2.269

Prinz, W. A. (2014). Bridging the gap: membrane contact sites in signaling, metabolism, and organelle dynamics. *J. Cell Biol.* 205, 759–769. doi: 10.1083/jcb.201401126

Prinz, W. A., Toulmay, A., and Balla, T. (2020). The functional universe of membrane contact sites. *Nat. Rev. Mol. Cell Biol.* 21, 7–24. doi: 10.1038/s41580-019-0180-9

Putney, J. W. Jr. (1986). A model for receptor-regulated calcium entry. *Cell Calcium.* 7, 1–12. doi: 10.1016/0143-4160(86)90026-6

Qi, J. (2014). Bromodomain and extraterminal domain inhibitors (BETi) for cancer therapy: chemical modulation of chromatin structure. *Cold Spring Harb. Perspect Biol.* 6:a018663. doi: 10.1101/cshperspect.a018663

Qiu, Y., Zhang, Z. Y., Du, W. D., Ye, L., Xu, S., Zuo, X. B., et al. (2014). Association analysis of ERBB2 amplicon genetic polymorphisms and STARD3 expression with risk of gastric cancer in the Chinese population. *Gene* 535, 225–232. doi: 10.1016/j.gene.2013.11.030

Quon, E., and Beh, C. T. (2016). Membrane contact sites: Complex zones for membrane association and lipid exchange. ***Lipid Insights*** 8, 55–63. doi: 10.4137/LPI.S37190

Quon, E., Sere, Y. Y., Chauhan, N., Johansen, J., Sullivan, D. P., Dittman, J. S., et al. (2018). Endoplasmic reticulum-plasma membrane contact sites integrate sterol and phospholipid regulation. *PLoS Biol.* 16:e2003864. doi: 10.1371/journal.pbio.2003864

Rathner, P., Stadlbauer, M., Romanin, C., Fahrner, M., Derler, I., and Müller, N. (2018). Rapid NMR-scale purification of 15N,13C isotope-labeled recombinant human STIM1 coiled coil fragments. *Protein Expr. Purif.* 146, 45–50. doi: 10.1016/j.pep.2018.01.013

Raturi, A., Gutiérrez, T., Ortiz-Sandoval, C., Ruangkittisakul, A., Herrera-Cruz, M. S., Rockley, J. P., et al. (2016). TMX1 determines cancer cell metabolism as a thiol-based modulator of ER-mitochondria Ca2+ flux. *J. Cell Biol.* 214, 433–444. doi: 10.1083/jcb.201512077

Ren, T., Zhang, H., Wang, J., Zhu, J., Jin, M., Wu, Y., et al. (2017). MCU-dependent mitochondrial Ca2+ inhibits NAD+/SIRT3/SOD2 pathway to promote ROS production and metastasis of HCC cells. *Oncogene* 36, 5897–5909. doi: 10.1038/onc.2017.167

Rezuchova, I., Hudecova, S., Soltysova, A., Matuskova, M., Durinikova, E., Chovancova, B., et al. (2019). Type 3 inositol 1,4,5-trisphosphate receptor has antiapoptotic and proliferative role in cancer cells. *Cell Death Dis.* 10:186. doi: 10.1038/s41419-019-1433-4

Roos, J., DiGregorio, P. J., Yeromin, A. V., Ohlsen, K., Lioudyno, M., Zhang, S., et al. (2005). STIM1, an essential and conserved component of store-operated Ca2+ channel function. *J. Cell Biol.* 169, 435–445. doi: 10.1083/jcb.200502019

Ruckhäberle, E., Rody, A., Engels, K., Gaetje, R., von Minckwitz, G., Schiffmann, S., et al. (2008). Microarray analysis of altered sphingolipid metabolism reveals prognostic significance of sphingosine kinase 1 in breast cancer. *Breast Cancer Res Treat.* 112, 41–52. doi: 10.1007/s10549-007-9836-9

Rugo, H. S. (2019). Achieving improved survival outcomes in advanced breast cancer. *N. Engl. J. Med.* 381, 371–372. doi: 10.1056/NEJMe1906236

Salaroglio, I. C., Panada, E., Moiso, E., Buondonno, I., Provero, P., Rubinstein, M., et al. (2017). PERK induces resistance to cell death elicited by endoplasmic reticulum stress and chemotherapy. *Mol. Cancer.* 16, 91. doi: 10.1186/s12943-017-0657-0

Sampieri, A., Santoyo, K., Asanov, A., and And Vaca, L. (2018). Association of the IP3R to STIM1 provides a reduced intraluminal calcium microenvironment, resulting in enhanced store-operated calcium entry. *Sci. Rep.* 8:13252. doi: 10.1038/s41598-018-31621-0

Sanchez-Collado, J., Lopez, J. J., Jardin, I., Camello, P. J., Falcon, D., Regodon, S., et al. (2019). Adenylyl cyclase type 8 overexpression impairs phosphorylation-dependent Orai1 inactivation and promotes migration in MDA-MB-231 breast cancer cells. *Cancers* 11:1624. doi: 10.3390/cancers11111624

Sassano, M. L., van Vliet, A. R., and Agostinis, P. (2017). Mitochondria-associated membranes as networking platforms and regulators of cancer cell fate. *Front. Oncol.* 7:174. doi: 10.3389/fonc.2017.00174

Scheffer, L., Raghavendra, P. R., Ma, J., and Acharya, J. K. (2011). Ceramide transfer protein and cancer. *Anticancer Agents Med. Chem.* 11, 904–910. doi: 10.2174/187152011797655087

Schmidt, S., Liu, G., Liu, G., Yang, W., Honisch, S., Pantelakos, S., et al. (2014). Enhanced Orai1 and STIM1 expression as well as store operated Ca2+ entry in therapy resistant ovary carcinoma cells. *Oncotarget* 5, 4799–4810. doi: 10.18632/oncotarget.2035

Schober, R., Bonhenry, D., Lunz, V., Zhu, J., Krizova, A., Frischauf, I., et al. (2019). Sequential activation of STIM1 links Ca2+ with luminal domain unfolding. *Sci. Signal.* 12:eaax3194. doi: 10.1126/scisignal.aax3194

Schulze, C., McGowan, M., Jordt, S. E., and Ehrlich, B. E. (2011). Prolonged oxaliplatin exposure alters intracellular calcium signaling: a new mechanism to explain oxaliplatin-associated peripheral neuropathy. *Clin. Colorectal. Cancer* 10, 126–133. doi: 10.1016/j.clcc.2011.03.010

Scorrano, L., De Matteis, M. A., Emr, S., Giordano, F., Hajnóczky, G., Kornmann, B., et al. (2019). Coming together to define membrane contact sites. *Nat. Commun.* 10:1287. doi: 10.1038/s41467-019-09253-3

Sharma, A., and Elble, R. C. (2020). From Orai to E-Cadherin: subversion of calcium trafficking in cancer to drive proliferation, anoikis-resistance, and metastasis. *Biomedicines* 8:169. doi: 10.3390/biomedicines8060169

Sharma, V. K., Ramesh, V., Franzini-Armstrong, C., and Sheu, S. S. (2000). Transport of Ca2+ from sarcoplasmic reticulum to mitochondria in rat ventricular myocytes. *J. Bioenerg. Biomembr.* 32, 97–104. doi: 10.1023/a:1005520714221

Shoshan-Barmatz, V., Ben-Hail, D., Admoni, L., Krelin, Y., and Tripathi, S. S. (2015). The mitochondrial voltage-dependent anion channel 1 in tumor cells. *Biochim. Biophys. Acta.* 1848, 2547–2575. doi: 10.1016/j.bbamem.2014.10.04

Silva-Palacios, A., Zazueta, C., and Pedraza-Chaverri, J. (2020). ER membranes associated with mitochondria: Possible therapeutic targets in heart-associated diseases. *Pharmacol. Res.* 156:104758. doi: 10.1016/j.phrs.2020.104758

Simmen, T., and Herrera-Cruz, M. S. (2018). Plastic mitochondria-endoplasmic reticulum (ER) contacts use chaperones and tethers to mould their structure and signaling. *Curr. Opin. Cell Biol.* 53, 61–69. doi: 10.1016/j.ceb.2018.04.014

Simoes, I. C. M., Morciano, G., Lebiedzinska-Arciszewska, M., Aguiari, G., Pinton, P., Potes, Y., et al. (2020). The mystery of mitochondria-ER contact sites in physiology and pathology: A cancer perspective. *Biochim. Biophys. Acta Mol. Basis Dis.* 1866:165834. doi: 10.1016/j.bbadis.2020.165834

Singh, A. K., Roy, N. K., Bordoloi, D., Padmavathi, G., Banik, K., Khwairakpam, A. D., et al. (2020). Orai-1 and Orai-2 regulate oral cancer cell migration and colonisation by suppressing Akt/mTOR/NF-κB signalling. *Life Sci.* 261:118372. doi: 10.1016/j.lfs.2020.118372

Singh, A., Sharma, R. K., Chagtoo, M., Agarwal, G., George, N., Sinha, N., et al. (2017). 1H NMR metabolomics reveals association of high expression of inositol 1, 4, 5 trisphosphate receptor and metabolites in breast cancer patients. *PLoS One* 12:e0169330. doi: 10.1371/journal.pone.0169330

Smith, B., and Land, H. (2012). Anticancer activity of the cholesterol exporter ABCA1 gene. *Cell Rep.* 2, 580–590. doi: 10.1016/j.celrep.2012.08.011

So, C. L., Saunus, J. M., Roberts-Thomson, S. J., and Monteith, G. R. (2019). Calcium signalling and breast cancer. *Semin. Cell Dev. Biol.* 94, 74–83. doi: 10.1016/j.semcdb.2018.11.001

Stathopulos, P. B., Schindl, R., Fahrner, M., Zheng, L., Gasmi-Seabrook, G. M., Muik, M., et al. (2013). STIM1/Orai1 coiled-coil interplay in the regulation of store-operated calcium entry. *Nat. Commun.* 4:2963. doi: 10.1038/ncomms3963

Strasak, A. M., Pfeiffer, R. M., Brant, L. J., Rapp, K., Hilbe, W., Oberaigner, W., et al. (2009). Time-dependent association of total serum cholesterol and cancer incidence in a cohort of 172,210 men and women: a prospective 19-year follow-up study. *Ann. Oncol.* 20, 1113–1120. doi: 10.1093/annonc/mdn736

Swanton, C., Marani, M., Pardo, O., Warne, P. H., Kelly, G., Sahai, E., et al. (2007). Regulators of mitotic arrest and ceramide metabolism are determinants of sensitivity to paclitaxel and other chemotherapeutic drugs. *Cancer Cell.* 11, 498–512. doi: 10.1016/j.ccr.2007.04.011

Szabadkai, G., Bianchi, K., Várnai, P., De Stefani, D., Wieckowski, M. R., Cavagna, D., et al. (2006). Chaperone-mediated coupling of endoplasmic reticulum and mitochondrial Ca2+ channels. *J. Cell Biol.* 175, 901–911. doi: 10.1083/jcb.200608073

Tang, H., Tao, A., Song, J., Liu, Q., Wang, H., and Rui, T. (2017). Doxorubicin-induced cardiomyocyte apoptosis: Role of mitofusin 2. *Int. J. Biochem. Cell Biol.* 88, 55–59. doi: 10.1016/j.biocel.2017.05.006

Tomaszewski, A., and Büsselberg, D. (2007). Cisplatin modulates voltage gated channel currents of dorsal root ganglion neurons of rats. *Neurotoxicology* 28, 49–58. doi: 10.1016/j.neuro.2006.07.005

Tosatto, A., Sommaggio, R., Kummerow, C., Bentham, R. B., Blacker, T. S., Berecz, T., et al. (2016). The mitochondrial calcium uniporter regulates breast cancer

progression via HIF-1α. *EMBO Mol. Med.* 8, 569–585. doi: 10.15252/emmm.201606255

Tsang, J. Y. S., and Tse, G. M. (2020). Molecular classification of breast cancer. *Adv. Anat. Pathol.* 27, 27–35. doi: 10.1097/PAP.0000000000000232

Tsunoda, T., Koga, H., Yokomizo, A., Tatsugami, K., Eto, M., Inokuchi, J., et al. (2005). Inositol 1,4,5-trisphosphate (IP3) receptor type1 (IP3R1) modulates the acquisition of cisplatin resistance in bladder cancer cell lines. *Oncogene* 24, 1396–1402. doi: 10.1038/sj.onc.1208313

Umemura, M., Baljinnyam, E., Feske, S., De Lorenzo, M. S., Xie, L. H., Feng, X., et al. (2014). Store-operated Ca2+ entry (SOCE) regulates melanoma proliferation and cell migration. *PLoS One* 9:e89292. doi: 10.1371/journal.pone.0089292

Urbani, L., and Simoni, R. D. (1990). Cholesterol and vesicular stomatitis virus G protein take separate routes from the endoplasmic reticulum to the plasma membrane. *J. Biol. Chem.* 265, 1919–1923.

van Vliet, A. R., Verfaillie, T., and Agostinis, P. (2014). New functions of mitochondria associated membranes in cellular signaling. *Biochim. Biophys. Acta.* 1843, 2253–2262. doi: 10.1016/j.bbamcr.2014.03.009

Varghese, E., Samuel, S. M., Sadiq, Z., Kubatka, P., Liskova, A., Benacka, J., et al. (2019). Anti-cancer agents in proliferation and cell death: The calcium connection. *Int. J. Mol. Sci.* 20:3017. doi: 10.3390/ijms20123017

Vassilev, B., Sihto, H., Li, S., Hölttä-Vuori, M., Ilola, J., Lundin, J., et al. (2015). Elevated levels of StAR-related lipid transfer protein 3 alter cholesterol balance and adhesiveness of breast cancer cells: potential mechanisms contributing to progression of HER2-positive breast cancers. *Am. J. Pathol.* 185, 987–1000. doi: 10.1016/j.ajpath.2014.12.018

Vautrin-Glabik, A., Botia, B., Kischel, P., Ouadid-Ahidouch, H., and Rodat-Despoix, L. (2018). IP3R3 silencing induced actin cytoskeletal reorganization through ARHGAP18/RhoA/mDia1/FAK pathway in breast cancer cell lines. *Biochim. Biophys. Acta Mol. Cell Res.* 1865, 945–958. doi: 10.1016/j.bbamcr.2018.04.002

Venditti, R., Masone, M. C., and De Matteis, M. A. (2020). ER-Golgi membrane contact sites. *Biochem. Soc. Trans.* 48, 187–197. doi: 10.1042/BST20190537

Venditti, R., Rega, L. R., Masone, M. C., Santoro, M., Polishchuk, E., Sarnataro, D., et al. (2019). Molecular determinants of ER-Golgi contacts identified through a new FRET-FLIM system. *J. Cell Biol.* 218, 1055–1065. doi: 10.1083/jcb.201812020

Verma, N., Vinik, Y., Saroha, A., Nair, N. U., Ruppin, E., Mills, G., et al. (2020). Synthetic lethal combination targeting BET uncovered intrinsic susceptibility of TNBC to ferroptosis. *Sci. Adv.* 6:eaba8968. doi: 10.1126/sciadv.aba8968

Voilquin, L., Lodi, M., Di Mattia, T., Chenard, M.-P., Mathelin, C., Alpy, F., et al. (2019). *STARD3: A swiss army knife for intracellular cholesterol transport. **Contact***. Thousand Oaks, CA: Sage, doi: 10.1177/2515256419856730

Wadhwa, R., Takano, S., Kaur, K., Deocaris, C. C., Pereira-Smith, O. M., Reddel, R. R., et al. (2006). Upregulation of mortalin/mthsp70/Grp75 contributes to human carcinogenesis. *Int. J. Cancer* 118, 2973–2980. doi: 10.1002/ijc.21773

Wang, J. Y., Sun, J., Huang, M. Y., Wang, Y. S., Hou, M. F., Sun, Y., et al. (2015). STIM1 overexpression promotes colorectal cancer progression, cell motility and COX-2 expression. *Oncogene* 34, 4358–4367. doi: 10.1038/onc.2014.366

Wang, L., Hao, J., Zhang, Y., Yang, Z., Cao, Y., Lu, W., et al. (2017). Orai1 mediates tumor-promoting store-operated Ca2+ entry in human gastrointestinal stromal tumors via c-KIT and the extracellular signal-regulated kinase pathway. *Tumour Biol.* 39:1010428317691426. doi: 10.1177/1010428317691426

Wang, Z., Zhang, F., He, J., Wu, P., Tay, L., Cai, M., et al. (2017). Binding of PLD2-generated phosphatidic acid to KIF5B promotes MT1-MMP surface trafficking and lung metastasis of mouse breast cancer cells. *Dev. Cell.* 43, 186.e–197.e. doi: 10.1016/j.devcel.2017.09.012

Wilhelm, L. P., Wendling, C., Védie, B., Kobayashi, T., Chenard, M. P., Tomasetto, C., et al. (2017). STARD3 mediates endoplasmic reticulum-to-endosome cholesterol transport at membrane contact sites. *EMBO J.* 36, 1412–1433. doi: 10.15252/embj.201695917

Witkos, T. M., and Lowe, M. (2016). The golgin family of coiled-coil tethering proteins. *Front Cell Dev Biol.* 3:86. doi: 10.3389/fcell.2015.00086

Wong, L. H., Gatta, A. T., and Levine, T. P. (2019). Lipid transfer proteins: the lipid commute via shuttles, bridges and tubes. *Nat. Rev. Mol. Cell Biol.* 20, 85–101. doi: 10.1038/s41580-018-0071-5

Wong, L. H., Čopič, A., and Levine, T. P. (2017). Advances on the transfer of lipids by lipid transfer proteins. *Trends Biochem. Sci.* 18, 886–893. doi: 10.1016/j.tibs.2017.05.001

Wu, H., Carvalho, P., and Voeltz, G. K. (2018). Here, there, and everywhere: the importance of ER membrane contact sites. *Science* 361:eaan5835. doi: 10.1126/science.aan5835

Wu, L., Zhang, D., Zhou, L., Pei, Y., Zhuang, Y., Cui, W., et al. (2019). FUN14 domain-containing 1 promotes breast cancer proliferation and migration by activating calcium-NFATC1-BMI1 axis. *EBioMedicine* 41, 384–394. doi: 10.1016/j.ebiom.2019.02.032

Xia, J., Wang, H., Huang, H., Sun, L., Dong, S., Huang, N., et al. (2016). Elevated Orai1 and STIM1 expressions upregulate MACC1 expression to promote tumor cell proliferation, metabolism, migration, and invasion in human gastric cancer. *Cancer Lett.* 381, 31–40. doi: 10.1016/j.canlet.2016.07.014

Xia, M., Zhang, Y., Jin, K., Lu, Z., Zeng, Z., and Xiong, W. (2019). Communication between mitochondria and other organelles: a brand-new perspective on mitochondria in cancer. *Cell Biosci.* 9:27. doi: 10.1186/s13578-019-0289-8

Xie, J., Pan, H., Yao, J., Zhou, Y., and Han, W. (2016). SOCE and cancer: Recent progress and new perspectives. *Int. J. Cancer.* 138, 2067–2077. doi: 10.1002/ijc.29840

Xie, Q., Su, J., Jiao, B., Shen, L., Ma, L., Qu, X., et al. (2016). ABT737 reverses cisplatin resistance by regulating ER-mitochondria Ca2+ signal transduction in human ovarian cancer cells. *Int. J. Oncol.* 49, 2507–2519. doi: 10.3892/ijo.2016.3733

Xu, H., Guan, N., Ren, Y. L., Wei, Q. J., Tao, Y. H., Yang, G. S., et al. (2018). IP3R-Grp75-VDAC1-MCU calcium regulation axis antagonists protect podocytes from apoptosis and decrease proteinuria in an Adriamycin nephropathy rat model. *BMC Nephrol.* 19:140. doi: 10.1186/s12882-018-0940-3

Xu, Y., Wang, C., Su, J., Xie, Q., Ma, L., Zeng, L., et al. (2015). Tolerance to endoplasmic reticulum stress mediates cisplatin resistance in human ovarian cancer cells by maintaining endoplasmic reticulum and mitochondrial homeostasis. *Oncol. Rep.* 34, 3051–3060. doi: 10.3892/or.2015.4283

Yamashita, M., Ing, C. E., Yeung, P. S., Maneshi, M. M., Pomès, R., and Prakriya, M. (2020). The basic residues in the Orai1 channel inner pore promote opening of the outer hydrophobic gate. *J. Gen. Physiol.* 152, e201912397. doi: 10.1085/jgp.201912397

Yamashita, M., Yeung, P. S., Ing, C. E., McNally, B. A., Pomès, R., and Prakriya, M. (2017). STIM1 activates CRAC channels through rotation of the pore helix to open a hydrophobic gate. *Nat. Commun.* 8:14512. doi: 10.1038/ncomms14512

Yang, G., Zhou, D., Li, J., Wang, W., Zhong, W., Fan, W., et al. (2019). VDAC1 is regulated by BRD4 and contributes to JQ1 resistance in breast cancer. *Oncol. Lett.* 18, 2340–2347. doi: 10.3892/ol.2019.10534

Yang, N., Tang, Y., Wang, F., Zhang, H., Xu, D., Shen, Y., et al. (2013). Blockade of store-operated Ca(2+) entry inhibits hepatocarcinoma cell migration and invasion by regulating focal adhesion turnover. *Cancer Lett.* 330, 163–169. doi: 10.1016/j.canlet.2012.11.040

Yang, S., Zhang, J. J., and Huang, X. Y. (2009). Orai1 and STIM1 are critical for breast tumor cell migration and metastasis. *Cancer Cell.* 15, 124–134. doi: 10.1016/j.ccr.2008.12.019

Yang, Y., Jiang, Z., Wang, B., Chang, L., Liu, J., Zhang, L., et al. (2017). Expression of STIM1 is associated with tumor aggressiveness and poor prognosis in breast cancer. *Pathol. Res. Pract.* 213, 1043–1047. doi: 10.1016/j.prp.2017.08.006

Yang, Z., Yue, Z., Ma, X., and Xu, Z. (2020). Calcium homeostasis: A potential vicious cycle of bone metastasis in breast cancers. *Front. Oncol.* 10:293. doi: 10.3389/fonc.2020.00293

Yeung, P. S., Yamashita, M., Ing, C. E., Pomès, R., Freymann, D. M., and Prakriya, M. (2018). Mapping the functional anatomy of Orai1 transmembrane domains for CRAC channel gating. *Proc. Natl. Acad. Sci. U S A.* 115, E5193–E5202. doi: 10.1073/pnas.1718373115

Zhai, X., Sterea, A. M., and El Hiani, Y. (2020). Lessons from the endoplasmic reticulum transporters-a cancer connection. *Cells* 9:1536. doi: 10.3390/cells9061536

Zhan, Z. Y., Zhong, L. X., Feng, M., Wang, J. F., Liu, D. B., and Xiong, J. P. (2015). Over-expression of Orai1 mediates cell proliferation and associates with poor prognosis in human non-small cell lung carcinoma. *Int. J. Clin. Exp. Pathol.* 8, 5080–5088.

Zhang, B., Yin, C., Li, H., Shi, L., Liu, N., Sun, Y., et al. (2013). Nir1 promotes invasion of breast cancer cells by binding to chemokine (C-C motif) ligand 18 through the PI3K/Akt/GSK3β/Snail signalling pathway. ***Eur. J. Cancer***. 49, 3900–3913. doi: 10.1016/j.ejca.2013.07.146

Zhang, S. L., Yu, Y., Roos, J., Kozak, J. A., Deerinck, T. J., Ellisman, M. H., et al. (2005). STIM1 is a Ca2+ sensor that activates CRAC channels and migrates from the Ca2+ store to the plasma membrane. *Nature* 437, 902–905. doi: 10.1038/nature04147

Zhang, S., Huang, W. C., Li, P., Guo, H., Poh, S. B., Brady, S. W., et al. (2011). Combating trastuzumab resistance by targeting SRC, a common node downstream of multiple resistance pathways. *Nat. Med.* 17, 461–469. doi: 10.1038/nm.2309

Zhang, S., Miao, Y., Zheng, X., Gong, Y., Zhang, J., Zou, F., et al. (2017). STIM1 and STIM2 differently regulate endogenous Ca2+ entry and promote TGF-β-induced EMT in breast cancer cells. *Biochem. Biophys. Res. Commun.* 488, 74–80. doi: 10.1016/j.bbrc.2017.05.009

Zheng, L., Stathopulos, P. B., Schindl, R., Li, G. Y., Romanin, C., and Ikura, M. (2011). Auto-inhibitory role of the EF-SAM domain of STIM proteins in store-operated calcium entry. *Proc. Natl. Acad. Sci. U S A.* 108, 1337–1342. doi: 10.1073/pnas.1015125108

Zhu, H., Zhang, H., Jin, F., Fang, M., Huang, M., Yang, C. S., et al. (2014). Elevated Orai1 expression mediates tumor- promoting intracellular Ca2+ oscillations in human esophageal squamous cell carcinoma. *Oncotarget* 5, 3455–3471. doi: 10.18632/oncotarget.1903

Conflict of Interest: The authors declare that the research was conducted in the absence of any commercial or financial relationships that could be construed as a potential conflict of interest.

Copyright © 2021 Gil-Hernández, Arroyo-Campuzano, Simoni-Nieves, Zazueta, Gomez-Quiroz and Silva-Palacios. This is an open-access article distributed under the terms of the Creative Commons Attribution License (CC BY). The use, distribution or reproduction in other forums is permitted, provided the original author(s) and the copyright owner(s) are credited and that the original publication in this journal is cited, in accordance with accepted academic practice. No use, distribution or reproduction is permitted which does not comply with these terms.

Received: 19 September 2020 | Revised: 28 October 2020 | Accepted: 29 October 2020

DOI: 10.1002/jcp.30151

ORIGINAL RESEARCH ARTICLE

Journal of Cellular Physiology WILEY

GDF11 restricts aberrant lipogenesis and changes in mitochondrial structure and function in human hepatocellular carcinoma cells

Sharik Hernandez[1] | Arturo Simoni-Nieves[1,2] | Monserrat Gerardo-Ramírez[1,2] | Sandra Torres[3,4] | Raquel Fucho[3,4] | Jonathan Gonzalez[1] | Lyssia Castellanos-Tapia[5] | Rogelio Hernández-Pando[6] | Elizabeth Tejero-Barrera[5] | Leticia Bucio[2,7] | Verónica Souza[2,7] | Roxana Miranda-Labra[2,7] | José C. Fernández-Checa[3,4] | Jens U. Marquardt[8] | Luis E. Gomez-Quiroz[2,7] | Carmen García-Ruiz[3,4] | María C. Gutiérrez-Ruiz[2,7]

[1]Posgrado en Biología Experimental, División de Ciencias Biológicas y de la Salud, Universidad Autónoma Metropolitana-Iztapalapa, Mexico City, Mexico

[2]Departamento de Ciencias de la Salud, Universidad Autónoma Metropolitana-Iztapalapa, Mexico City, Mexico

[3]Department of Cell Death and Proliferation, Instituto de Investigaciones Biomédicas de Barcelona, CSIC, Liver Unit Hospital Clinic, IDIBAPS and CIBERehd, Barcelona, Spain, Southern California Research Center for ALPD and Cirrhosis, KECK School of Medicine, USC, Los Angeles, USA

[4]Southern California Research Center for ALPD and Cirrhosis, KECK School of Medicine, USC, Los Angeles, USA

[5]Laboratorio de Nutrigenomica, Instituto Nacional de Medicina Genómica, Mexico City, Mexico

[6]Departamento de Patología Experimental, INCMNSZ, Mexico City, Mexico

[7]Laboratorio de Medicina Experimental, Unidad de Medicina Translacional, Instituto de Investigaciones Biomédicas, UNAM/Instituto Nacional de Cardiología Ignacio Chavez, Mexico City, Mexico

[8]Department of Medicine I, University Hospital Schleswig-Holstein, Lübeck, Germany

Correspondence
Luis E. Gomez-Quiroz, Departamento de Ciencias de la Salud, Universidad Autónoma Metropolitana Iztapalapa, Av. San Rafael Atlixco 186, Col. Vicentina, 09340, Iztapalapa, Mexico City, Mexico.
Email: legq@xanum.uam.mx

Carmen García-Ruiz, Department of Cell Death and Proliferation, Instituto de Investigaciones Biomédicas de Barcelona-CSIC, C/Roselló 161 7 floor, 08036-Barcelona, Spain.
Email: carmen.garcia@iibb.csic.es

María C. Gutiérrez-Ruiz, Departamento de Ciencias de la Salud, Universidad Autónoma Metropolitana Iztapalapa, Av. San Rafael Atlixco 186, Col. Vicentina, 09340, Iztapalapa, Mexico City, Mexico.
Email: mcgr@xanum.uam.mx

Funding information
National Institute on Alcohol Abuse and Alcoholism/National Institutes of Health,

Abstract

Growth differentiation factor 11 (GDF11) has been characterized as a key regulator of differentiation in cells that retain stemness features. Recently, it has been reported that GDF11 exerts tumor-suppressive properties in hepatocellular carcinoma cells, decreasing clonogenicity, proliferation, spheroid formation, and cellular function, all associated with a decrement in stemness features, resulting in mesenchymal to epithelial transition and loss of aggressiveness. The aim of the present work was to investigate the mechanism associated with the tumor-suppressive properties displayed by GDF11 in liver cancer cells. Hepatocellular carcinoma-derived cell lines were exposed to GDF11 (50 ng/ml), RNA-seq analysis in Huh7 cell line revealed that GDF11 exerted profound transcriptomic impact, which involved regulation of cholesterol metabolic process, steroid metabolic process as well as key signaling pathways, resembling endoplasmic reticulum-related functions. Cholesterol and triglycerides determination in Huh7 and Hep3B cells treated with GDF11 exhibited

Sharik Hernandez and Arturo Simoni-Nieves collaborated equally in the work.
Luis E. Gomez-Quiroz and Carmen García-Ruiz shared Senior authorship.

 © 2020 Wiley Periodicals LLC

Grant/Award Number: P50AA011999; Consejo Nacional de Ciencia y Tecnología, Grant/Award Number: CB-252942; CIBEREHD, Grant/Award Number: SAF-2015–Q469944R

a significant decrement in the content of these lipids. The mTOR signaling pathway was downregulated, and this was associated with a reduction in key proteins involved in the mevalonate pathway. In addition, real-time metabolism assessed by Seahorse technology showed abridged glycolysis as well as glycolytic capacity, closely related to an impaired oxygen consumption rate and decrement in adenosine triphosphate production. Finally, transmission electron microscopy revealed mitochondrial abnormalities, such as cristae disarrangement, consistent with metabolic changes. Results provide evidence that GDF11 impairs cancer cell metabolism targeting lipid homeostasis, glycolysis, and mitochondria function and morphology.

KEYWORDS

cholesterol, GDF11, HCC, Huh7 cells, metabolism, mitochondria

1 | INTRODUCTION

Liver diseases have been positioned as one of the main concerns in public health worldwide. Changes in human habits increase the prevalence of severe liver diseases, such as alcoholic and nonalcoholic liver diseases, viral hepatitis, and liver cancer (Ferlay et al., 2015; Méndez-Sánchez et al., 2010). Hepatocellular carcinoma (HCC) is one of the most prevalent and aggressive tumors worldwide with a high rate of postsurgical recurrence (Ferlay et al., 2015; Forner et al., 2012; Kaposi-Novak et al., 2006). It is a complex disease with multiple axes that must be considered in basic and clinical studies, including differentiation, drug-resistant, aberrant metabolism, increased cell survival, among others.

Recently, we have reported that the growth differentiation factor 11 (GDF11), a member of the subfamily of the bone morphogenic proteins (Walker et al., 2016), displays tumor-suppressive properties in HCC-derived cell lines ranging from cell cycle arrest to mesenchymal to epithelial transition, and decrease in invasion capacity (Gerardo-Ramirez et al., 2019). Interestingly, this response was closely associated with the loss in mitochondrial function, suggesting cell metabolism contribution.

Cancer cells take advantage of manipulating their metabolism, which must be optimized for survival, high proliferation, and drug resistance (Zhu & Thompson, 2019). Aberrant lipogenesis represents one of the main adaptive response, increasing the synthesis of free fatty acids, and particularly, cholesterol (Gong et al., 2019), by enhancing the activity of crucial transcription factors, such as SREBP1 and 2, driving the expression of enzymes, such as fatty acid synthase (FASN), acetyl-CoA carboxylase, 3-hydroxy-3-methylglutaryl-CoA reductase (HMGCR), mevalonate kinase (MVK), among others. The overexpression of these proteins has been associated with high aggressiveness and poor prognosis in human liver tumors (Calvisi et al., 2011; Montero et al., 2008).

The Akt/mTOR signaling pathway is one of the key drivers of cell metabolism. In addition, it is involved in cell survival, cytoskeleton reorganization, and cell proliferation (Manning & Toker, 2017; Papa & Pandolfi, 2019), placing this pathway as a determinant in cancer biology, even more, the aberrant activation of Akt in mice livers, rises liver tumors resembling the human HCC with high aggressiveness (Calvisi et al., 2011).

Another important metabolic adaptation is the relationship between glycolysis and energetic mitochondrial metabolism. Although doctor Warburg reported that impairment of mitochondrial function could lead to the aerobic glycolysis or Warburg effect (Warburg, 1956), which is indeed true under some conditions, new evidence has been gained supporting that mitochondrial proficient function could occur under Warburg effect and lactate production (Wallace, 2012). Efficient mitochondrial functionality is required for a competent cancer cell function, including respiration and adenosine triphosphate (ATP) production, and also other mitochondria activities are essential, such as signal transduction, cellular redox control, survival, or building blocks production, particularly those derived from tricarboxylic acids cycle (Baulies et al., 2018; Vyas et al., 2016; Wallace, 2012).

The metabolic axis in cancer cells is then confirmed by the connection of aberrant lipogenesis, the Warburg effect, and the mitochondria functionality, raising a well-implemented adaptive response, leading to an aggressive phenotype.

In the present work, we aimed to address the metabolic changes induced by GDF11 in HCC-derived human cell lines. Our data show a profound impact in aberrant lipogenesis and in mitochondrial energetic metabolism, positioning GDF11 as a good alternative for cancer metabolic control in HCC treatment.

2 | MATERIALS AND METHODS

2.1 | Cell culture

Huh7, Hep3B, HepG2, and SNU-387 cell lines were obtained from the American Type Culture Collection (ATCC). Cells were cultured in William's medium supplemented with 10% fetal bovine serum

(FBS, Hy-Clone), 100 U/ml ampicillin and 100 µg/ml streptomycin (Thermo Fisher Scientific). Cells were maintained at 37°C in a 5% CO_2 and 90% humidity atmosphere. Cells were plated in plastic culture bottles (Sigma-Aldrich). All cell lines were mycoplasma free.

2.2 | Main experimental design

Cells were exposed to 50 ng/ml GDF11 (Gerardo-Ramirez et al., 2019; Williams et al., 2013) for different times. GDF11 was added to the culture media every 24 h and cells were recovered after 72 h of treatment for all experiments.

2.3 | RNA-sequencing (RNA-seq)

RNA-seq was performed as previously reported (Castven et al., 2019). Briefly, total RNA was extracted using the TRIzol Reagent (Thermo Fisher Scientific) following the manufacturer's instructions. RNA quantity and purity were estimated using a Nanodrop ND-2000c Spectrophotometer (NanoDrop Technologies), and integrity was assessed by Agilent 2100 Bioanalyzer (Agilent). RNA sequencing was performed using Illumina HiSeq4000 and deposited at the Bioproject database (ID: PRJNA596004). Raw reads were filtered by removing adapter sequences, contamination, and low-quality reads. The reads were then mapped with the human genome reference sequence (GRCh37.82) using HISAT2 (hisat2-2.0.2-beta) followed by read summarization with featureCounts (subread-1.5.0-p1). The parameters for the differential expression analysis were false discovery rate (FDR) equal to 0.5, $p < .001$ and log fold change from −1.5 to 1.5. All data analysis was performed using R programing language and related packages. The output matrix from featureCounts was input into the Bioconductor package DESeq2 for differential expression analysis.

2.4 | Enrichment analysis

Gene Set Enrichment Analysis (GSEA) was performed using GSEA software provided by Broad Institutes (http://software.broadinstitute.org/gsea/index.jsp). Gene sets from the MSigDB database were tested and gene sets with NOM $p < .05$ and FDR < 0.25 were considered significantly enriched in a priori defined set of genes. We used ingenuity pathway analysis (IPA; Ingenuity Systems, Inc.) software to figure out the biological pathways and networks associated with model genes using the whole data set. Genes with log2-fold change were used as input. We considered a disease, biological functions, and upstream regulators to be significant if the absolute value of their activation z-score > 1.5. The z-score reflects the match between the observed gene expression and the predicted relationship direction. It is used to infer activation states of called functions and regulators (Castven et al., 2019).

2.5 | Western blot analysis

Western blot was conducted as we previously reported (Enriquez-Cortina et al., 2013). Polyvinylidene fluoride membranes were probed with specific antibodies as described in Table S1. Horseradish peroxidase-conjugated antibodies were used according to the primary antibodies. Blots were exposed using Super Signal West Pico Chemiluminescent substrate (Pierce Biotechnology). Signal was detected using Gel Logic 2500 (Kodak).

2.6 | Immunofluorescence assays

Immunofluorescence was conducted as previously reported (Marquardt et al., 2012). Briefly, the cells were treated for 72 h with GDF11, and then fixed with 4% paraformaldehyde in phosphate-buffered saline (PBS). Samples were permeabilized with 0.01% (v/v) Triton-X 100 for 30 min and blocked with 3% (w/v) bovine serum albumin (BSA) in PBS for 30 min and subsequently incubated with primary antibodies anti-TOM 20 (sc-11415, dilution 1:250; Santa Cruz Biotechnology), conjugated with alexa flour 488 (Molecular Probes, Thermo Fisher Scientific), and filipin (Sigma-Aldrich). Ki67 was addressed by using anti-Ki67 antibody (15580; dilution 1:100; Abcam) as previously reported (Gerardo-Ramírez et al., 2019). Nuclei were counterstained with 1 µg/ml 4′,6-diamidino-2-phenylindole (DAPI; Sigma-Aldrich). Images were obtained using a multi-photon confocal microscope (LSM-780 NLO; Carl Zeiss).

2.7 | Cholesterol determination

Total cholesterol determination was measured as previously reported (Domínguez-Pérez et al., 2019). Briefly, 10 mg of cell lysate was saponified with alcoholic KOH in a 60°C heating block for 30 min, 3 ml of hexane and 600 µl of distilled water were added and shaken to ensure complete mixing. After evaporation, the samples were used for cholesterol measurement with *O*-phthalaldehyde dissolved in acetic acid (0.5 mg/ml). After that, sulfuric acid (1 ml) was added and then read at 550 nm in a spectrophotometer.

2.8 | Triglycerides (TGs) determination

TG content was determined using the triglyceride determination kit (Sigma-Aldrich) following the manufacturer's instructions.

2.9 | Oil red O staining

Intracellular neutral lipids were determined by oil red O. Cells were seeded into 24-well chambers. After treatment, the cells were washed with ice-cold PBS and then fixed with 4% paraformaldehyde for

15 min. The cells were stained with freshly diluted 0.5% Oil red O solution for 1 h; after that, we proceeded to microphotography.

2.10 | Real-time cellular metabolism determination by Seahorse

In vivo real-time oxygen consumption rate (OCR) and extracellular acidification rate (ECAR) were monitored with the Seahorse XF^{e}24 Flux Analyzer (Seahorse Bioscience) according to the manufacturer's instructions. Briefly, Hep3B and Huh7 cells were treated with 50 ng/ml rhGDF11 every 24 h for 2 days in free FBS media. After incubation, the cells were harvested immediately by trypsinization and replated at 50,000 and 40,000 cells/well density in an XF^{e}24-well plate in a complete medium (10% FBS, 1% P/S) to allow adherence to the plate. After adherence, the cells were treated with rhGDF11 (50 ng/ml) every 24 h until completing 72 h of treatment. For assessment of the real-time ECAR, cells were incubated with unbuffered assay media (XF Base Media containing 2 mM L-glutamine), followed by sequential injection of 10 mM glucose, 2 μM oligomycin, and 50 mM 2-deoxy-glucose (2-DG). For OCR, the cells were incubated with unbuffered assay media (XF Base Media with 10 mM glucose, 2 mM L-glutamine, and 1 mM pyruvate) followed by a sequential injection of 1 μM oligomycin, 1 μM carbonyl cyanide-4 (trifluoromethoxy) phenylhydrazone (FCCP), and 0.5 μM antimycin A plus Rotenone (XF Cell Mito Stress kit). Both ECAR and OCR measurements were normalized with total protein.

2.11 | Transmission electron microscopy (TEM)

TEM was performed according to a recently published study (Domínguez-Pérez et al., 2019). Briefly, cells were fixed with 2% glutaraldehyde in 0.1 M phosphate buffer (pH 7.4), followed by 1% OsO_4. After dehydration, thin sections were stained with uranyl acetate and lead citrate for observation under a JEOL JEM 12000 EII transmission electron microscope (Peabody).

2.12 | Mitochondrial network complexity analysis

Mitochondrial network complexity analysis was performed as reported (Baulies et al., 2018). Immunofluorescence for the mitochondrial marker TOM 20 was performed and analyzed using the ImageJ software (NIH).

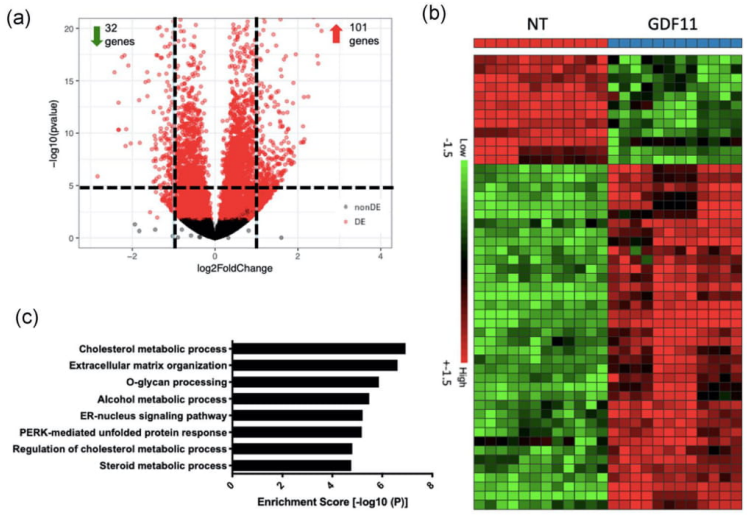


FIGURE 1 Molecular profile of GDF11-treated cells. (a) Volcano plot representing the RNA-seq data of GDF11-treated cells. DE, different statistical red dots, and non-DE in black dots. (b) Unsupervised hierarchical cluster analysis of GDF11-treated and not treated cells. A total of 133 differentially expressed genes in which 32 were downregulated (in green) and 101 upregulated (in red). (c) Top signaling pathways in GDF11-treated cells as determined by ingenuity pathway analysis. (d) Gene Set Enrichment Analysis (GSEA) of Huh7 cell line treated with GDF11 for 72 h was performed. Normalized enrichment score (NES) reflects the degree of overrepresentation at the peak of the entire set. Statistical significance calculated by nominal *p* value of the ES by using an empirical phenotype-based permutation test. (e) Validation of the RNA-seq data. Seven randomly selected genes from the RNA-seq analysis were corroborated by qRT-PCR according to protocol depicted under the material and methods section. Each column represents the mean ± *SEM* of at least four independent experiments carried out by triplicate. ***$p \leq .001$, ****$p \leq .0001$ versus NT cells. GDF11, growth differentiation factor 11; qRT-PCR, reverse-transcriptase polymerase chain reaction; RNA-seq, RNA-sequencing; *SEM*, standard error of mean

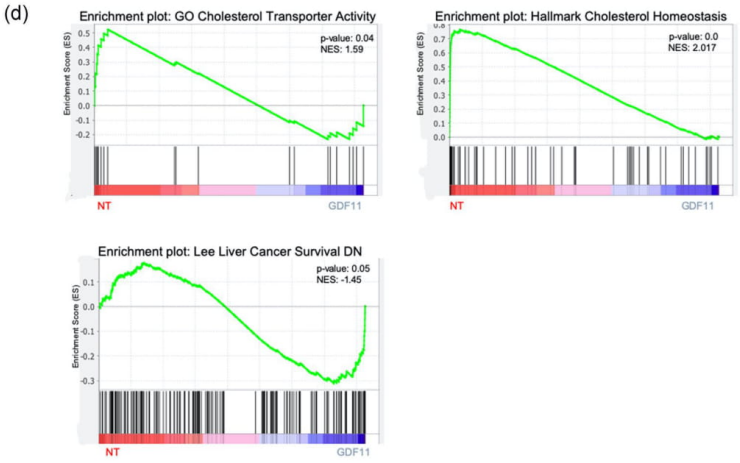


FIGURE 1 (Continued)

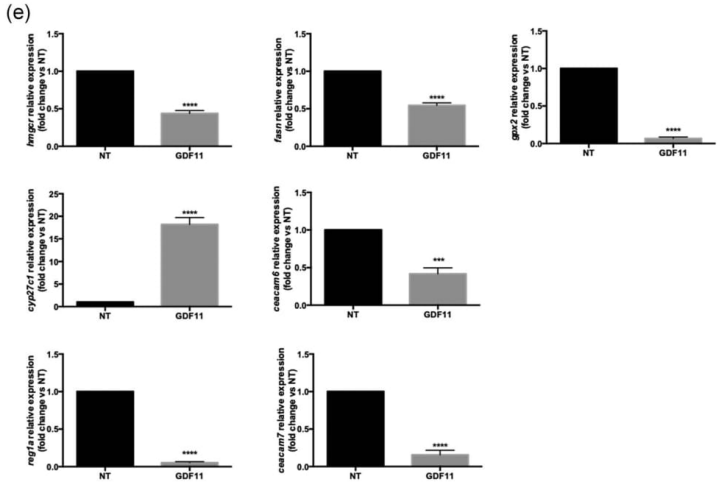


FIGURE 1 (Continued)

2.13 | Real-time quantitative reverse-transcriptase polymerase chain reaction (qRT-PCR)

One μg of total RNA was reverse-transcribed in 20 μl reaction volume with a SuperScript (Invitrogen Corp.) first-strand synthesis kit according to the manufacturer's instructions. Oligonucleotide primers were designed using Primer3 v.0.4.0 (http://frodo.wi.mit.edu/primer3/) as described earlier (Czauderna et al., 2018). The qRT-PCR analysis was performed with a CFX96 Touch (Bio-Rad) thermal cycler in a 96-well reaction plate. The 10 μl PCR reaction mix contained 5 μl 2X SYBR Green PCR Master Mix (Bio-Rad), 200 nM of each primer, and 1 μl complementary DNA template. Reactions were incubated for 10 min at 95°C, followed by 40 cycles of 30 s at 95°C and 60 s at specific primer temperature. The expression level of ribosomal protein S18 (rs18) was used as a reference. Relative gene expression levels were calculated using the formula $2^{-\Delta\Delta C_t}$. Primer sequences are listed in Table S2.

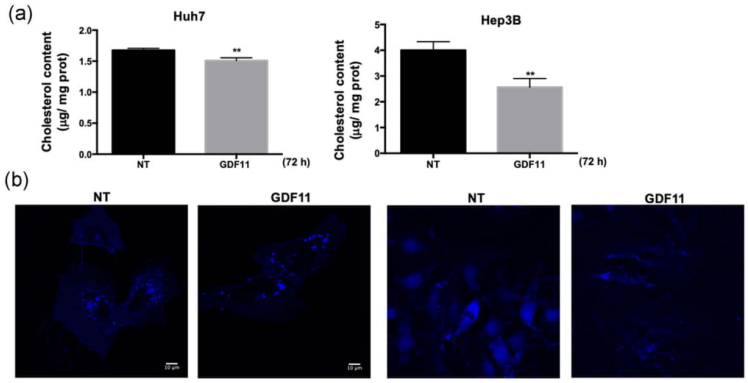


FIGURE 2 GDF11 decreases aberrant lipogenesis. Huh7 and Hep3B cells were treated for 72 h with GDF11 (50 ng/ml). (a) Cholesterol content was determined biochemically as described under material and methods. (b) Free cholesterol visualized by filipin staining and confocal microscopy. (c) Triglycerides content was determined biochemically. (d) Neutral lipids determined by Oil Red O staining. Original magnification ×400. Each column represents the mean ± *SEM* of at least four independent experiments carried out by triplicate. $^{*}p \leq .05$, $^{**}p \leq .01$, $^{****}p \leq .0001$ versus NT cells at 72 h. Representative images of at least four independent experiments. GDF11, growth differentiation factor 11; NT, not treated; *SEM*, standard error of mean

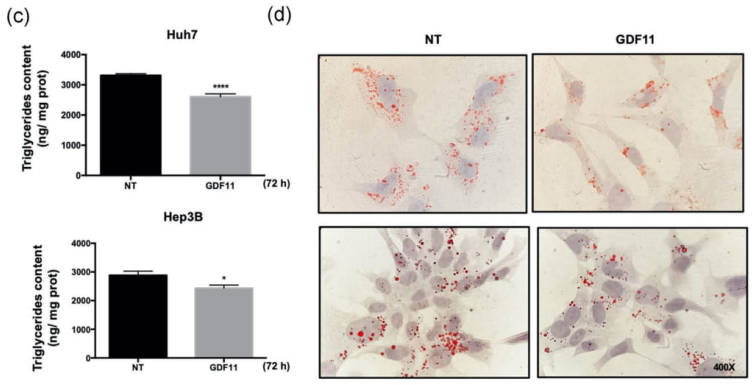


FIGURE 2 (Continued)

2.14 | Protein quantification

The protein content was determined by using the bicinchoninic acid method (BCA; Pierce, Thermo Fisher Scientific), following the manufacturer's instructions.

2.15 | Statistical analysis

The results are presented as the average of at least three independent experiments. A two-way analysis of variance (ANOVA) followed by Tukey's posttest was performed for the analysis of cell proliferation and one-way ANOVA followed by Tukey's posttest was performed for mitochondrial functionality by 3-(4,5-dimethylthiazol-2-yl)-2,5-diphenyltetrazolium bromide (MTT). A two-tailed *t* test was performed for the analysis of cholesterol, TGs, OCR, ECAR, and mitochondrial morphology.

3 | RESULTS

3.1 | GDF11 decreases cell proliferation and induces cellular dysfunction

Recently, we demonstrated that GDF11 exerts antitumorigenic effects in human HCC-derived cell lines. This response was closely

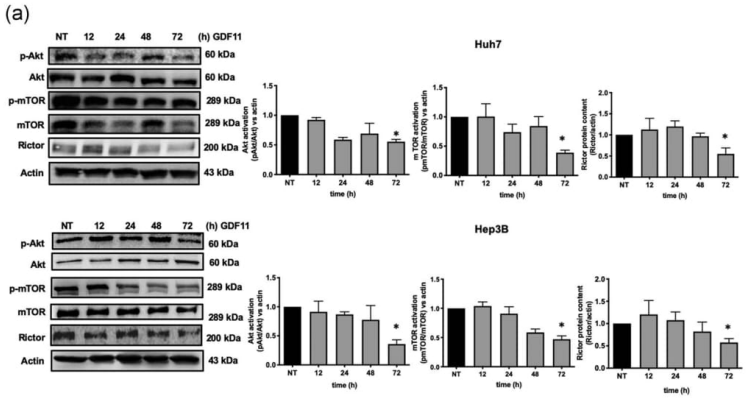


FIGURE 3 GDF11 downregulates Akt/mTOR signaling pathway and repress key proteins involved in aberrant lipogenesis. Cells were treated at different times with GDF11 (50 ng/ml), the whole-cell lysate was extracted, and western blot analysis was performed (a) Akt/mTOR signaling pathway determined by western blot analysis and densitometric analysis. (b) Lipogenesis-related proteins determined by western blot analysis and densitometric analysis. Representative images of at least three independent experiments. Each column represents the mean ± *SEM* of at least four independent experiments carried out by triplicate. *$p \leq .05$ versus NT cells. GDF11, growth differentiation factor 11; NT, not treated; *SEM*, standard error of mean

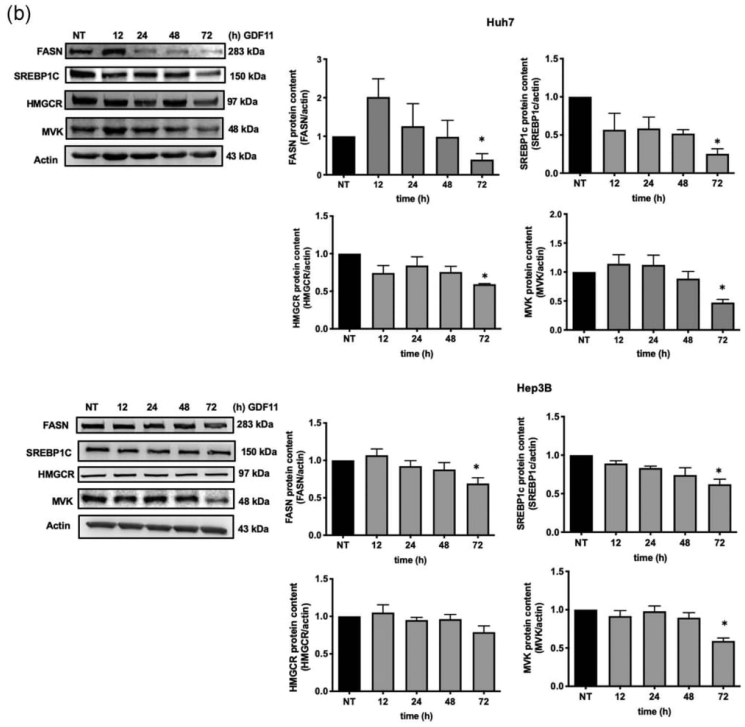


FIGURE 3 (Continued)

related to the stemness feature of the cells. It was outstanding that the main stemness and aggressiveness of the markers were significantly repressed by GDF11, influencing the proliferation and invasion capacity (Gerardo-Ramirez et al., 2019) consistently; we did not find significant changes in cell morphology, addressed by bright field microscopy (Figure S1a) or in cell viability at 72 h of GDF11 treatment (Figure S1b). GDF11 significantly suppressed cell proliferation in Hep3B, Huh7, SNU387, and HepG2 (Figure S1c) with no relevant effects by the presence or absence of FBS in the culture media, which is consistent with our previous report (Gerardo-Ramirez et al., 2019). In addition, Ki67 immunofluorescence in Huh-7 cell line exhibited a decrease in positive cells (Figure S1d). Mitochondrial functionality, judged by MTT assay, decreased in a time-dependent manner, in Huh7, Hep3B, HepG2, and SNU387 cell lines (Figure S1e), and the wound-healing response was also diminished by GDF11 treatment (Figure S1f).

3.2 | Aberrant lipogenesis in HCC cells is impaired by GDF11 treatment

The transcriptomic analysis performed by RNA-seq in Huh7 cell line treated with GDF11 (50 ng/ml) for 72 h revealed 133 differentially expressed genes in which 101 genes were upregulated and 32 genes downregulated (Figure 1a and Table S3). Unsupervised hierarchical clustering confirmed that identified genes were highly efficient in separating untreated from treated cells (Figure 1b). Gene ontology (GO) enrichment analysis addressed by IPA revealed that main pathways affected by GDF11 were involved in the cholesterol process, particularly those related to the downregulation of its metabolism (Hmgcs1, Insig1, Cyp27c1, Fasn, Dhcr7, Lamp1, and Abca5), extracellular matrix organization (Comp, adamts16, Npnt, Dpysl3, Pcdh20, and Lgals14), proliferation (Rasgrf1, Reg1a, and Ramp1), endoplasmic reticulum-nucleus signaling (insig1, Cyp27c1, Hmgcs1, and Hspa5), among others (Figure 1c).

GSEA further confirmed that the set of genes associated to cholesterol transport and its homeostasis is certainly affected and related to a decrease in cell survival (Figure 1d).

Some genes were selected to corroborate the sequencing data by qRT-PCR. Figure 1e shows the relative expression of those genes validating the RNA-seq results and confirming the deep impact in lipid homeostasis.

Consistent with RNA-seq analysis, the cells exposed to GDF11 for 72 h, significantly decreased cholesterol content in both, Huh7 and Hep3B cell lines (Figure 2a), these were corroborated by filipin staining (Figure 2b). Interestingly, less cytoplasmic distribution of

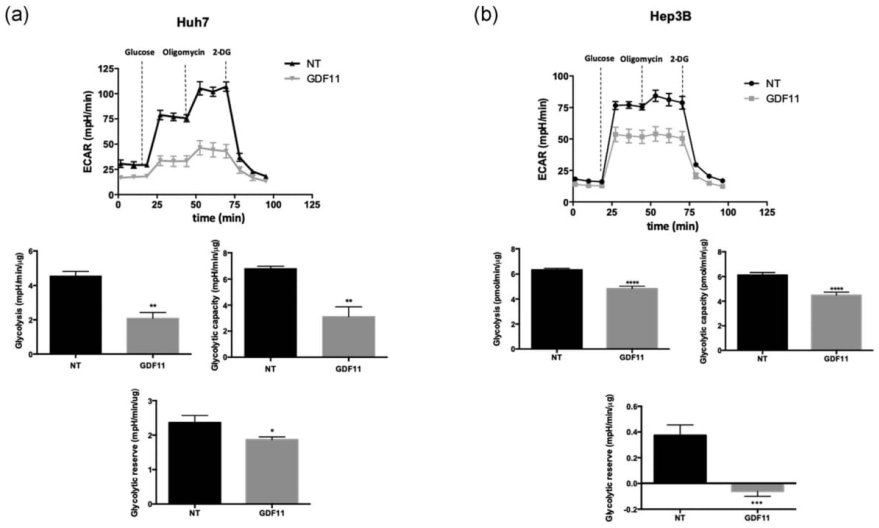


FIGURE 4 GDF11 restricts cell metabolism by decreasing the extracellular acidification rate (ECAR) and oxygen consumption rate (OCR). Cells were treated for 72 h with GDF11 (50 ng/ml). ECAR, a measure of lactate production and glycolysis in (a) Huh7 cell line; (b) Hep3B cell line. OCR, a measure of oxidative phosphorylation in (c) Huh7 cell line; (d) Hep3B cell line; (e) Defective metabolic profile (based on relative values of OCR and ECAR) of GDF11-treated cells. Using Seahorse XFe24 Flux Analyzer. Dashed lines indicate the addition of glucose, oligomycin (an inhibitor of the ATP synthase), 2-deoxyglucose (2-DG), carbonilcyanide *p*-triflouromethoxyphenylhydrazone (FCCP, a mitochondria protonophore), antimycin A (AA, a mitochondrial complex III inhibitor), and Rotenone (R, a mitochondrial complex I inhibitor). $^{*}p \leq .05$, $^{**}p \leq .01$, $^{****}p \leq .0001$ versus NT cells. ATP, adenosine triphosphate; GDF11, growth differentiation factor 11; NT, not treated

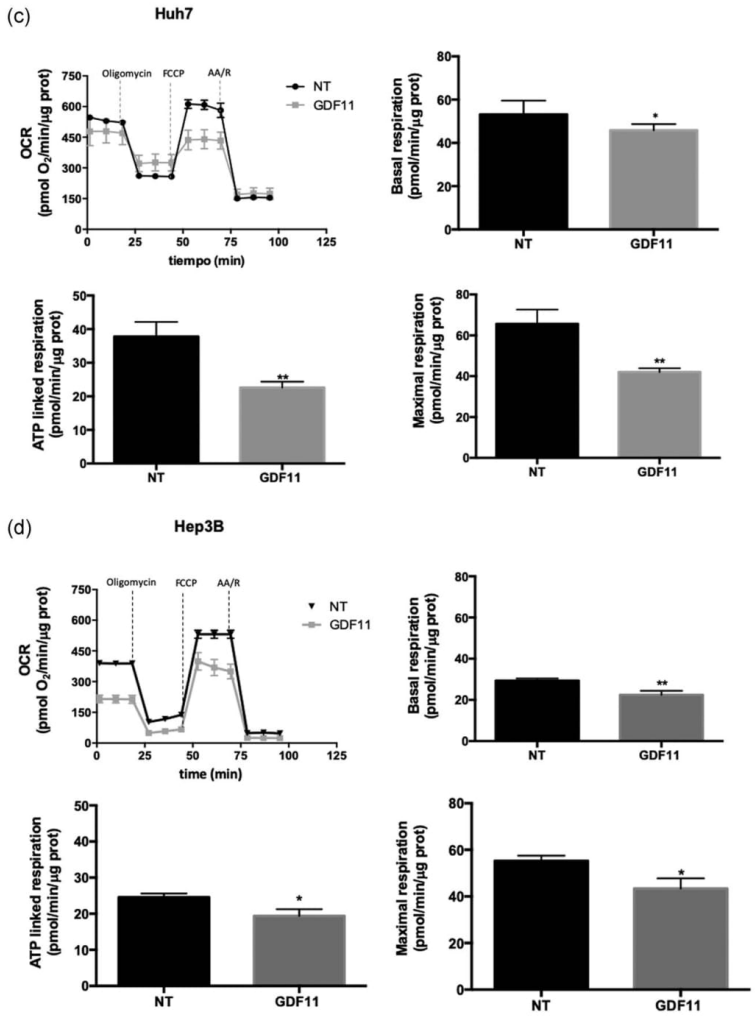


FIGURE 4 (Continued)

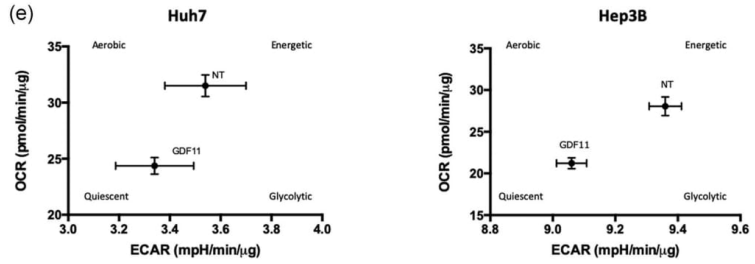


FIGURE 4 (Continued)

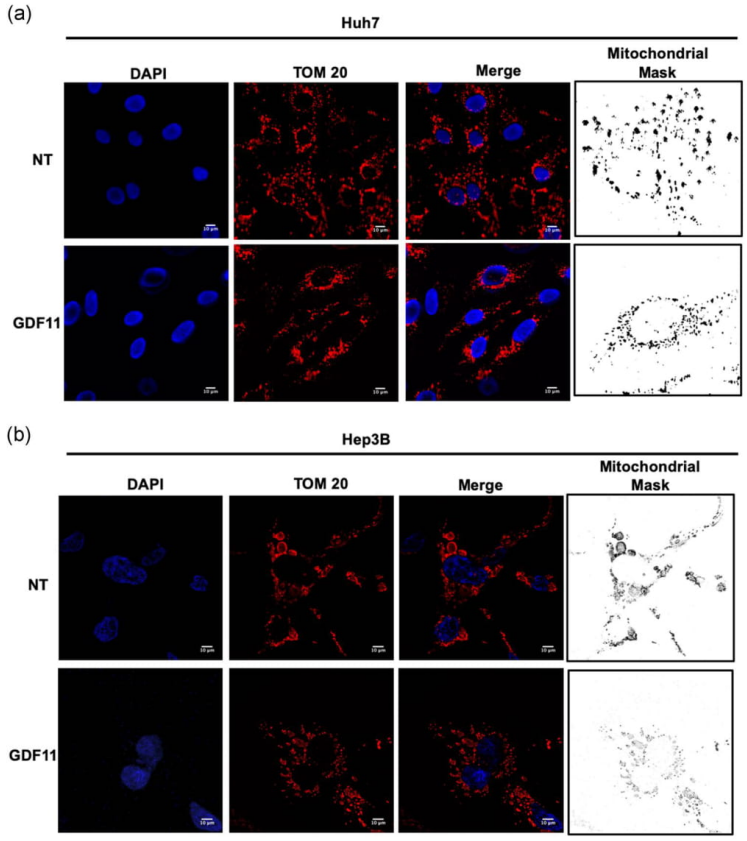


FIGURE 5 Mitochondrial network complexity is affected by GDF11 treatment. Determination of mitochondrial network complexity determined from TOM 20-labeled mitochondria and examined by confocal microscopy in (a) Huh7 cell line; (b) Hep3B cell line. (c) Analysis by ImageJ software to determine area and perimeter in both cell lines. Each column represents the mean ± *SEM* of at least four independent experiments carried out in triplicate. $^{*}p \leq .05$, $^{**}p \leq .01$ versus NT cells. DAPI, 4′,6-diamidino-2-phenylindole; GDF11, growth differentiation factor 11; NT, not treated; *SEM*, standard error of mean

cholesterol was found in GDF11-treated cells. As expected, neutral lipids were significantly decreased in cells under GDF11 treatment judged by biochemical quantification of TGs (Figure 2c) and oil red O staining (Figure 2d), data are in agreement with *Fasn* downregulation observed in RNA-seq and corroborated by qRT-PCR (Figure 1d) and western blot analysis (Figure 3b).

To gain mechanistic support, we evaluated, by western blot analysis, some relevant components of the Akt/mTOR pathway, the main signaling driver of lipid homeostasis, particularly in liver cancer (Calvisi et al., 2011). Figure 3a clearly shows the downregulation of Akt, and mTOR activation, and Rictor content at 72 h of treatment, in both cell lines. The expression of main target proteins of this signaling pathway, particularly those related to lipogenesis, such as FASN, SREBP1, HMGCR, MVK, were also diminished, most of them since 48 h, peaking maximal repression at 72 h (Figure 3b). Interestingly, we could not find significant changes in HMGCR in the Hep3B cell line, but MVK was deeply downregulated, significantly impacting the cholesterol content.

3.3 | GDF11 impairs glycolysis and oxygen consumption

Indirect mitochondrial functionality evaluated by MTT assay (Figure S1d) strongly suggests a defective energetic metabolism. To gain more evidence of the bioenergetics status of cells treated with GDF11, we proceeded to analyze the ECAR, a measure of lactate production and glycolysis, and the OCR, a measure of oxidative

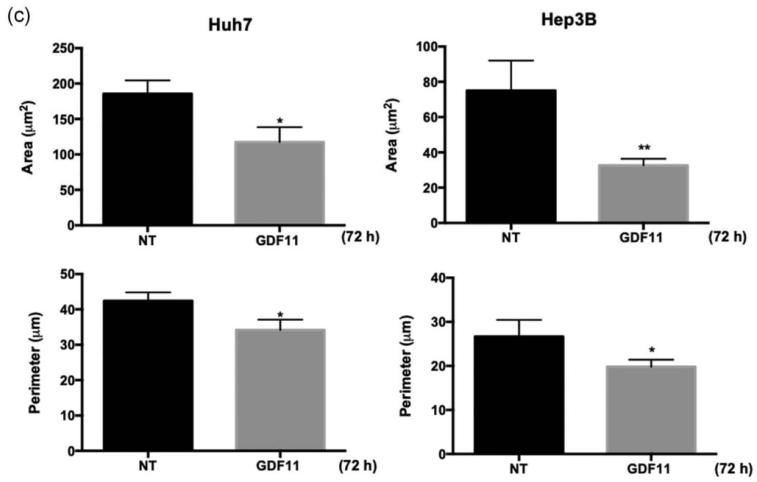


FIGURE 5 (Continued)

phosphorylation, by using Seahorse technology as previously reported (Baulies et al., 2018), after 72 h of GDF11 treatment. Figure 4a,b shows the decrement in ECAR in GDF11-treated cells and a low response to glucose, resulting in glycolysis, glycolytic capacity, and glycolytic reserve reduction in both cell lines (Figure 4a,b). Not treated cells showed a robust glycolytic activity, which is reliable with the high proliferation of cancer cells.

Interestingly, the basal and maximal OCR of GDF11-treated cells were significantly lower compared with not treated cells. Basal mitochondrial respiration (Figure 4c,d) were normalized by subtracting nonmitochondrial OCR in the presence of oligomycin A inhibition, which was significantly decreased in GDF11-treated cells. Maximal respiration was determined by the effect induced by the protonophore FCCP to uncouple mitochondrial ATP generation to oxygen intake. -Figure 4 shows that untreated cells responded to FCCP by increasing their OCR to maximal rates; GDF11-treated cells did not have an appreciable respiratory reserve capacity, these were narrowly related to a decrement in ATP-linked respiration (Figure 4c,d). The increase was considered as respiratory reserve capability, maximal OCR minus basal OCR. This implies that at basal levels, the GDF11-treated cells were operating closer to maximal OCR capacity, which resulted in a lower reserve capacity. Lower respiratory reserve capacity is linked to lower mitochondrial fidelity. GDF11 promoted defective mitochondrial function, indicated by low basal OCR and a slight response to FCCP.

To obtain an overview of the metabolic profiles of both cell lines studied, basal ECAR against mitochondrial OCR were plotted in response to 72 h treatment of GDF11 (Figure 4e); revealing thoughtful differences, cell lines fall into two groups of cellular bioenergetics profiles. Control cells clearly represent highly energetic cells with high respiration and glycolysis, while GDF11-treated cells presented OCR and ECAR decrement in both cell lines, supporting that GDF11 induces a profound change in metabolic profile.

3.4 | GDF11 alters mitochondria structure and network complexity

An overview of the mitochondria status revealed reflective changes in morphology and cell distribution in both cell lines, judged by TOM 20 immunofluorescence and confocal microscopy inspection (Figure 5a,b), in fact, the analysis of the overall area and perimeter of mitochondria, performed by ImageJ software (Baulies et al., 2018; Valente et al., 2017) showed a decrement in both parameters (Figure 5c), indicating a deep impact in mitochondrial morphology and network in both cell lines.

Finally, TEM was performed to assess the ultrastructure of cellular components, particularly mitochondria. GDF11-treated cells showed disarrangement of cristae, exhibiting partial cristolysis (Arismendi-Morillo, 2009), an electro-lucent matrix, reduced size (Figure 6a–d), and round-shaped morphology. Mitochondrial counting revealed a small difference, but a significantly smaller number of mitochondria in GDF11-treated cells (Figure 6e,f). Electro-dense structures resembling mitochondrial degeneration, particularly mitochondrial ghost (Ampawong et al., 2018) were predominant (Mg). Interestingly, an increment of lysosomes (L) was observed in GDF11-treated cells.

4 | DISCUSSION

HCC accounts for 90% of primary liver cancer, with increasing new cases every year, raising a warning worldwide (Jemal et al., 2017). It is imperative to seek new therapeutic approaches aimed at controlling cancer strengths points that could provide adaptive benefits.

It has been extensively reported that liver cancer aggressiveness is closely associated with aberrant lipogenesis (Calvisi et al., 2011;

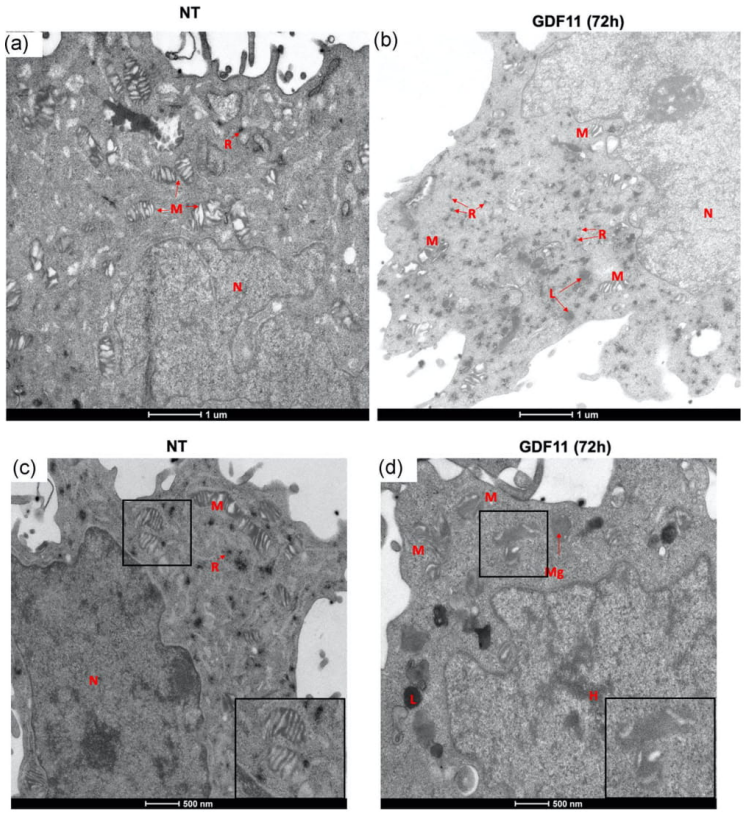


FIGURE 6 GDF11 induces changes in mitochondrial structure. Representative ultrastructure images of Hep3B cells being treated (b, d) and not treated (NT), (a, c). L, lysosomes; M, mitochondria; Mg, the mitochondrial ghost (advance mitochondrial degeneration); N, nucleus; R, ribosomes. Representative images, of at least four independent experiments. Morphometric analysis of TEM, (e) mitochondrial length, (f) mitochondria per field. Each column represents the mean ± *SEM* of at least four independent experiments carried out in triplicate. $^{**}p \leq .01$, $^{****}p \leq .0001$ versus NT cells. GDF11, growth differentiation factor 11; *SEM*, standard error of mean; TEM, transmission electron microscopy

Marí et al., 2006; Montero et al., 2008), particularly cholesterol has been positioned as a key determinant lipid in HCC playing remarkable roles as a tumor promoter. Cholesterol overload has been practically linked to all HCC stages, from the initiation to the tumor promotion, invasion, and metastasis (Chimento et al., 2018; Enríquez-Cortina et al., 2017); we have reported that high cholesterol diet induces DNA damage and promotes the development of HCC with an aggressive phenotype, including apoptosis resistance, and lung metastasis (Enríquez-Cortina et al., 2017). Recently, Che et al. (2019) reported that cholesterol supports the HCC lesions depleted of FASN; even more, the inhibition of this enzyme increases the nuclear localization and activation of SREBP2, a main transcription factor in the mevalonate pathway, and the expression of HMGCR in human HCC cell lines, supporting the hypothesis that cholesterol is more relevant than free fatty acids in cancer. Recently, it was reported that the mevalonate pathway is coordinating energy input and cell proliferation in colon cancer cells (Gong et al., 2019), clearly indicating the well-preserved and extraordinarily role of this pathway in cancer diversity.

We recently described that GDF11 displays functions directed to suppress aggressiveness properties in liver cancer cells, such as high proliferation, migration, invasion, and clonogenicity (Gerardo-Ramirez et al., 2019), in the present work we were aimed to figure out the mechanism associated with these antitumorigenic properties elicited by GDF11. To have a complete overview of the influence of GDF11 in HCC cells, we performed RNA-seq analysis in Huh7 cell line, we applied a strong statistical cutoff ($p < .001$ and log fold change from −1.5 to 1.5) resulting in 133 genes differentially expressed; it was

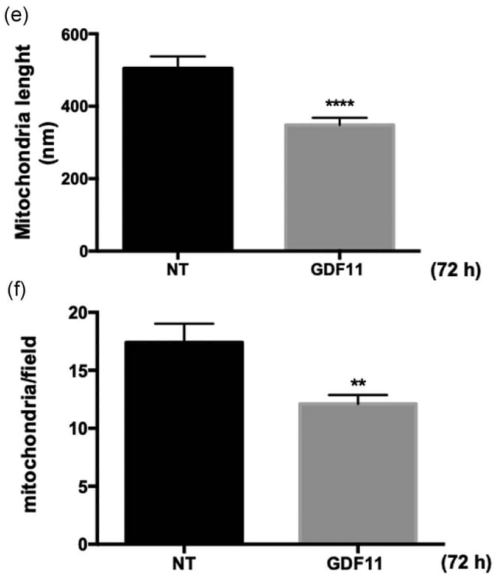


FIGURE 6 (Continued)

remarkable that the cholesterol-related process and metabolism, resulted as the central affected pathways (Figure 1c); the analysis of the Akt/mTOR pathway and target genes involved in lipogenesis undoubtedly confirms the sequencing data. Interestingly, GDF11 induced a better survival phenotype (Figure 1d), according to Lee et al. (2004), comparing with not treated cells, confirming that GDF11 lessens aggressiveness in HCC cell lines.

GDF11 induced the decrement of MVK and HMGCR, judged by western blot analysis (Figure 3b), in both cell lines, but with an outstanding effect in the Huh7 cell line, and this was corroborated by biochemical and confocal determination of cholesterol. It is known that the overexpression of enzymes, such as HMGCR, MVK, SQS, is closely associated with poor prognosis in HCC patients (Calvisi et al., 2011).

The mevalonate pathway is not the only lipid-related route affected; fatty acids homeostasis was seriously touched judged by a decrement of *Fasn* expression, confirmed by TG content determination and oil red O staining (Figure 2). It is widely reported that aberrant lipogenesis represents one of the main advantages for the cancer cell because lipids are necessary for new membranes construction in proliferating cells, posttranslational modifications of oncoproteins, such as Ras, and energy source (Calvisi et al., 2011). GDF11 treatment significantly decreases both, cholesterol and TG, and these were associated with a decrement in proliferation, migration, and invasion as we previously reported (Gerardo-Ramirez et al., 2019) and Figure S1 shows.

The effect of GDF11 in metabolism expands beyond lipogenesis, encompassing the bioenergetics level.

The high proliferative capacity of cancer cells requires efficient mitochondrial function; it is important to be clear about that, although cancer cells have partially impeded the mitochondria to avoid cytochrome *C* release favoring apoptosis. Mitochondria must be in a physiological steady-state because high proliferation also requires mitochondrial biogenesis, it has been proved that the knockdown of TOP1mt gene, which encodes for the mitochondrial topoisomerase 1B, induces an impairment of liver regeneration (Khiati et al., 2015), and the overexpression in liver cancer is associated with tumor promotion and carcinogenesis (Baechler et al., 2019). Mitochondria are essential for cancer cells, revisiting the initial Warburg conclusions (Wallace, 2012), sustaining that aerobic glycolysis is favored when mitochondria are impaired; in this regard, our data provide evidence showing the central role of mitochondrial function for liver cancer cells. GDF11 treatment considerably decreased both glycolysis and oxidative phosphorylation (Figure 4a–d), inducing a quiescent state, with very low proliferation and with the loss of tumorigenic properties; the metabolic profile confirms the significant change in GDF11-treated cells compared with not treated (Figure 4e).

The loss in mitochondrial function was closely related to profound morphological changes in these organelles observed by transmission electron and confocal microscopy. GDF11-treated cells exhibited a decrease in the number of mitochondria and mitochondrial size and shape; the mitochondria became smaller and more rounded. These data suggest that GDF11 induce morphological transitions related to cell metabolism.

The identification of this metabolic axis, the targeting of this as a unique entity, could allow much better therapeutic approaches against diverse cancers, particularly in the liver.

ACKNOWLEDGMENTS

This study was partially funded by a grant from the Consejo Nacional de Ciencia y Tecnología (CONACYT): CB-252942, Fronteras de la Ciencia-1320, Apoyo al Fortalecimiento y Desarrollo de la Infra-estructura 2013-205941 and 2017-280788, and Universidad Autonoma Metropolitana. We thank the confocal core unit of the Universidad Autonoma Metropolitana Iztapalapa. SH, MGR, ASN are scholarship holders from Conacyt. We acknowledge the support from grants: PID2019-111669RB, and SAF2017-85877R from Plan Nacional de IþD, Spain, and by the CIBEREHD; the center grant P50AA011999 Southern California Research Center for ALPD and Cirrhosis funded by the National Institute on Alcohol Abuse and Alcoholism/National Institutes of Health (NIH); as well as support from AGAUR of the Generalitat de Catalunya SGR-2017-1112, European Cooperation in Science & Technology (COST) ACTION CA17112 Prospective European Drug-Induced Liver Injury Network, and the Fundación BBVA. RED Nacional 2018-102799-T de enfermedades metabólicas y Cáncer y Proyecto 201916/31 De Fundacion Marató TV3.

CONFLICT OF INTERESTS

The authors declare that there are no conflict of interests.

DATA AVAILABILITY STATEMENT

Data are available on request from the authors.

ORCID

Luis E. Gomez-Quiroz https://orcid.org/0000-0002-5704-5985
María C. Gutiérrez-Ruiz https://orcid.org/0000-0003-0501-7226

REFERENCES

Ampawong, S., Isarangkul, D., Reamtong, O., & Aramwit, P. (2018). Adaptive effect of sericin on hepatic mitochondrial conformation through its regulation of apoptosis, autophagy and energy maintenance: A proteomics approach. *Scientific Reports*, *8*(1), 14943. https://doi.org/10.1038/s41598-018-33372-4

Arismendi-Morillo, G. (2009). Electron microscopy morphology of the mitochondrial network in human cancer. *International Journal of Biochemistry and Cell Biology*, *41*(10), 2062–2068. https://doi.org/10.1016/j.biocel.2009.02.002

Baechler, S. A., Factor, V. M., Dalla Rosa, I., Ravji, A., Becker, D., Khiati, S., Miller Jenkins, L. M., Lang, M., Sourbier, C., Michaels, S. A., Neckers, L. M., Zhang, H. L., Spinazzola, A., Huang, S. N., Marquardt, J. U., & Pommier, Y. (2019). The mitochondrial type IB topoisomerase drives mitochondrial translation and carcinogenesis. *Nature Communications*, *10*(1), 83. https://doi.org/10.1038/s41467-018-07922-3

Baulies, A., Montero, J., Matías, N., Insausti, N., Terrones, O., Basañez, G., Vallejo, C., Conde de La Rosa, L., Martinez, L., Robles, D., Morales, A., Abian, J., Carrascal, M., Machida, K., Kumar, D. B. U., Tsukamoto, H., Kaplowitz, N., Garcia-Ruiz, C., & Fernández-Checa, J. C. (2018). The 2-oxoglutarate carrier promotes liver cancer by sustaining mitochondrial GSH despite cholesterol loading. *Redox Biology*, *14*, 164–177. https://doi.org/10.1016/j.redox.2017.08.022

Calvisi, D. F., Wang, C., Ho, C., Ladu, S., Lee, S. A., Mattu, S., Destefanis, G., Delogu, S., Zimmermann, A., & Ericsson, J. (2011). Increased lipogenesis, induced by AKT-mTORC1-RPS6 signaling, promotes development of human hepatocellular carcinoma. *Gastroenterology*, *140*(3), 1071–1083. https://doi.org/10.1053/j.gastro.2010.12.006

Castven, D., Becker, D., Czauderna, C., Wilhelm, D., Andersen, J. B., Strand, S., Hartmann, M., Heilmann-Heimbach, S., Roth, W., Hartmann, N., Straub, B. K., Mahn, F. L., Franck, S., Pereira, S., Haupts, A., Vogel, A., Wörns, M. A., Weinmann, A., Heinrich, S., … Marquardt, J. U. (2019). Application of patient-derived liver cancer cells for phenotypic characterization and therapeutic target identification. *International Journal of Cancer*, *144*(11), 2782–2794. https://doi.org/10.1002/ijc.32026

Che, L., Chi, W., Qiao, Y., Zhang, J., Song, X., Liu, Y., & Chen, L. (2019). Cholesterol biosynthesis supports the growth of hepatocarcinoma lesions depleted of fatty acid synthase in mice and humans. *Gut*, *69*(1), 177–186. https://doi.org/10.1136/gutjnl-2018-317581

Chimento, A., Casaburi, I., Avena, P., Trotta, F., De Luca, A., Rago, V., Pezzi, V., & Sirianni, R. (2018). Cholesterol and its metabolites in tumor growth: Therapeutic potential of statins in cancer treatment. *Front Endocrinol (Lausanne)*, *9*, 807. https://doi.org/10.3389/fendo.2018.00807

Czauderna, C., Palestino-Dominguez, M., Castven, D., Becker, D., Zanon-Rodriguez, L., Hajduk, J., Mahn, F. L., Herr, M., Strand, D., Strand, S., Heilmann-Heimbach, S., Gomez-Quiroz, L. E., Wörns, M. A., Galle, P. R., & Marquardt, J. U. (2018). Ginkgo biloba induces different gene expression signatures and oncogenic pathways in malignant and non-malignant cells of the liver. *PLOS One*, *13*(12), e0209067. https://doi.org/10.1371/journal.pone.0209067

Domínguez-Pérez, M., Simoni-Nieves, A., Rosales, P., Nuño-Lámbarri, N., Rosas-Lemus, M., Souza, V., Miranda, R. U., Bucio, L., Uribe Carvajal, S., Marquardt, J. U., Seo, D., Gomez-Quiroz, L. E., & Gutiérrez-Ruiz, M. C. (2019). Cholesterol burden in the liver induces mitochondrial dynamic changes and resistance to apoptosis. *Journal of Cellular Physiology*, *234*(5), 7213–7223. https://doi.org/10.1002/jcp.27474

Enriquez-Cortina, C., Almonte-Becerril, M., Clavijo-Cornejo, D., Palestino-Domínguez, M., Bello-Monroy, O., Nuño, N., López, A., Bucio, L., Souza, V., Hernández-Pando, R., Muñoz, L., Gutiérrez-Ruiz, M. C., & Gómez-Quiroz, L. E. (2013). Hepatocyte growth factor protects against isoniazid/rifampicin-induced oxidative liver damage. *Toxicological Sciences*, *135*(1), 26–36. https://doi.org/10.1093/toxsci/kft134

Enríquez-Cortina, C., Bello-Monroy, O., Rosales-Cruz, P., Souza, V., Miranda, R. U., Toledo-Pérez, R., Luna-López, A., Simoni-Nieves, A., Hernández-Pando, R., Gutiérrez-Ruiz, M. C., Calvisi, D. F., Marquardt, J. U., Bucio, L., & Gomez-Quiroz, L. E. (2017). Cholesterol overload in the liver aggravates oxidative stress-mediated DNA damage and accelerates hepatocarcinogenesis. *Oncotarget*, *8*(61), 104136–104148. https://doi.org/10.18632/oncotarget.22024

Ferlay, J., Soerjomataram, I., Dikshit, R., Eser, S., Mathers, C., Rebelo, M., Parkin, D. M., Forman, D., & Bray, F. (2015). Cancer incidence and mortality worldwide: Sources, methods and major patterns in GLOBOCAN 2012. *International Journal of Cancer*, *136*(5), E359–E386. https://doi.org/10.1002/ijc.29210

Forner, A., Llovet, J. M., & Bruix, J. (2012). Hepatocellular carcinoma. *Lancet*, *379*(9822), 1245–1255. https://doi.org/10.1016/S0140-6736(11)61347-0

Gerardo-Ramírez, M., Lazzarini-Lechuga, R., Hernández-Rizo, S., Jiménez-Salazar, J. E., Simoni-Nieves, A., García-Ruiz, C., Fernández-Checa, J. C., Marquardt, J. U., Coulouarn, C., Gutiérrez-Ruiz, M. C., Pérez-Aguilar, B., & Gomez-Quiroz, L. E. (2019). GDF11 exhibits tumor suppressive properties in hepatocellular carcinoma cells by restricting clonal expansion and invasion. *Biochimica et Biophysica Acta, Molecular Basis of Disease*, *1865*(6), 1540–1554. https://doi.org/10.1016/j.bbadis.2019.03.003

Gong, L., Xiao, Y., Xia, F., Wu, P., Zhao, T., Xie, S., Wang, R., Wen, Q., Zhou, W., Xu, H., Zhu, L., Zheng, Z., Yang, T., Chen, Z., & Duan, Q. (2019). The mevalonate coordinates energy input and cell proliferation. *Cell Death & Disease*, *10*(4), 327. https://doi.org/10.1038/s41419-019-1544-y

Jemal, A., Ward, E. M., Johnson, C. J., Cronin, K. A., Ma, J., Ryerson, A. B., Mariotto, A., Lake, A. J., Wilson, R., Sherman, R. L., Anderson, R. N., Henley, S. J., Kohler, B. A., Penberthy, L., Feuer, E. J., & Weir, H. K. (2017). Annual report to the nation on the status of cancer, 1975-2014, featuring survival. *Journal of the National Cancer Institute*, *109*(9), djx030. https://doi.org/10.1093/jnci/djx030

Kaposi-Novak, P., Lee, J. S., Gomez-Quiroz, L., Coulouarn, C., Factor, V. M., & Thorgeirsson, S. S. (2006). Met-regulated expression signature defines a subset of human hepatocellular carcinomas with poor prognosis and aggressive phenotype. *Journal of Clinical Investigation*, *116*(6), 1582–1595. https://doi.org/10.1172/JCI27236

Khiati, S., Baechler, S. A., Factor, V. M., Zhang, H., Huang, S. N., Dalla Rosa, I., Sourbier, C., Neckers, L., Thorgeirsson, S. S., & Pommier, Y. (2015). Lack of mitochondrial topoisomerase I (TOP1mt) impairs liver regeneration. *Proceedings of the National Academy of Sciences of the United States of America*, *112*(36), 11282–11287. https://doi.org/10.1073/pnas.1511016112

Lee, J. S., Chu, I. S., Heo, J., Calvisi, D. F., Sun, Z., Roskams, T., Durnez, A., Demetris, A. J., & Thorgeirsson, S. S. (2004). Classification and prediction of survival in hepatocellular carcinoma by gene expression profiling. *Hepatology*, *40*(3), 667–676. https://doi.org/10.1002/hep.20375

Manning, B. D., & Toker, A. (2017). AKT/PKB signaling: Navigating the network. *Cell*, *169*(3), 381–405. https://doi.org/10.1016/j.cell.2017.04.001

Marí, M., Caballero, F., Colell, A., Morales, A., Caballeria, J., Fernandez, A., Enrich, C., Fernandez-Checa, J. C., & García-Ruiz, C. (2006). Mitochondrial free cholesterol loading sensitizes to TNF- and Fas-mediated steatohepatitis. *Cell Metabolism*, *4*(3), 185–198. https://doi.org/10.1016/j.cmet.2006.07.006

Marquardt, J. U., Seo, D., Gómez-Quiroz, L. E., Uchida, K., Gillen, M. C., Kitade, M., Kaposi-Novak, P., Conner, E. A., Factor, V. M., & Thorgeirsson, S. S. (2012). Loss of c-Met accelerates development of liver fibrosis in response to CCl(4) exposure through deregulation of multiple molecular pathways. *Biochimica et Biophysica Acta/General Subjects*, *1822*(6), 942–951. https://doi.org/10.1016/j.bbadis.2012.02.012

Méndez-Sánchez, N., García-Villegas, E., Merino-Zeferino, B., Ochoa-Cruz, S., Villa, A. R., Madrigal, H., Kobashi-Margáin, R. A., Gutiérrez-Grobe, Y., Chávez-Tapia, N., Ponciano-Rodríguez, G., & Uribe, M. (2010). Liver diseases in Mexico and their associated mortality trends from 2000 to 2007: A retrospective study of the nation and the federal states. *Annals of Hepatology*, *9*(4), 428–438.

Montero, J., Morales, A., Llacuna, L., Lluis, J. M., Terrones, O., Basanez, G., Antonsson, B., Prieto, J., Garcia-Ruiz, C., Colell, A., & Fernandez-Checa, J. C. (2008). Mitochondrial cholesterol contributes to chemotherapy resistance in hepatocellular carcinoma. *Cancer Research*, *68*(13), 5246–5256. https://doi.org/10.1158/0008-5472.CAN-07-6161

Papa, A., & Pandolfi, P. P. (2019). The PTEN(-)PI3K axis in cancer. *Biomolecules*, *9*(4), 153. https://doi.org/10.3390/biom9040153

Valente, A. J., Maddalena, L. A., Robb, E. L., Moradi, F., & Stuart, J. A. (2017). A simple ImageJ macro tool for analyzing mitochondrial network morphology in mammalian cell culture. *Acta Histochemica*, *119*(3), 315–326. https://doi.org/10.1016/j.acthis.2017.03.001

Vyas, S., Zaganjor, E., & Haigis, M. C. (2016). Mitochondria and cancer. *Cell*, *166*(3), 555–566. https://doi.org/10.1016/j.cell.2016.07.002

Walker, R. G., Poggioli, T., Katsimpardi, L., Buchanan, S. M., Oh, J., Wattrus, S., Heidecker, B., Fong, Y. W., Rubin, L. L., Ganz, P., Thompson, T. B., Wagers, A. J., & Lee, R. T. (2016). Biochemistry and biology of GDF11 and myostatin: Similarities, differences, and questions for future investigation. *Circulation Research*, *118*(7), 1125–1141. https://doi.org/10.1161/CIRCRESAHA.116.308391

Wallace, D. C. (2012). Mitochondria and cancer. *Nature Reviews Cancer*, *12*(10), 685–698. https://doi.org/10.1038/nrc3365

Warburg, O. (1956). On the origin of cancer cells. *Science*, *123*(3191), 309–314.

Williams, G., Zentar, M. P., Gajendra, S., Sonego, M., Doherty, P., & Lalli, G. (2013). Transcriptional basis for the inhibition of neural stem cell proliferation and migration by the TGFbeta-family member GDF11. *PLOS One*, *8*(11), e78478. https://doi.org/10.1371/journal.pone.0078478

Zhu, J., & Thompson, C. B. (2019). Metabolic regulation of cell growth and proliferation. *Nature Reviews Molecular Cell Biology*, *20*, 436–450. https://doi.org/10.1038/s41580-019-0123-5

SUPPORTING INFORMATION

Additional supporting information may be found online in the Supporting Information section.

How to cite this article: Hernandez S, Simoni-Nieves A, Gerardo-Ramírez M, et al. GDF11 restricts aberrant lipogenesis and changes in mitochondrial structure and function in human hepatocellular carcinoma cells. *J Cell Physiol*. 2020;1–15. https://doi.org/10.1002/jcp.30151

frontiers in Oncology

REVIEW
published: 15 October 2019
doi: 10.3389/fonc.2019.01039

GDF11 Implications in Cancer Biology and Metabolism. Facts and Controversies

Arturo Simoni-Nieves[1,2], *Monserrat Gerardo-Ramírez*[1,2], *Gibrán Pedraza-Vázquez*[1,2], *Lisette Chávez-Rodríguez*[1,2], *Leticia Bucio*[2,3], *Verónica Souza*[2,3], *Roxana U. Miranda-Labra*[2,3], *Luis E. Gomez-Quiroz*[2,3]* and *María Concepción Gutiérrez-Ruiz*[2,3]*

[1] Posgrado en Biología Experimental, DCBS, Universidad Autónoma Metropolitana-Iztapalapa, Mexico City, Mexico, [2] Laboratorio de Fisiología Celular y Biología Molecular, Departamento de Ciencias de la Salud, Universidad Autónoma Metropolitana-Iztapalapa, Mexico City, Mexico, [3] Laboratorio de Medicina Experimental, Unidad de Medicina Translacional, Instituto de Investigaciones Biomédicas, UNAM/Instituto Nacional de Cardiología Ignacio Chavez, Mexico City, Mexico

OPEN ACCESS

Edited by:
Antonio Giuseppe Naccarato, University of Pisa, Italy

Reviewed by:
Prospero Civita, Brain Tumor Research Center, United Kingdom
Sujit Kumar Bhutia, National Institute of Technology Rourkela, India

***Correspondence:**
Luis E. Gomez-Quiroz
legq@xanum.uam.mx
María Concepción Gutiérrez-Ruiz
mcgr@xanum.uam.mx

Specialty section:
This article was submitted to Cancer Metabolism, a section of the journal Frontiers in Oncology

Received: 10 August 2019
Accepted: 24 September 2019
Published: 15 October 2019

Citation:
Simoni-Nieves A, Gerardo-Ramírez M, Pedraza-Vázquez G, Chávez-Rodríguez L, Bucio L, Souza V, Miranda-Labra RU, Gomez-Quiroz LE and Gutiérrez-Ruiz MC (2019) GDF11 Implications in Cancer Biology and Metabolism. Facts and Controversies. Front. Oncol. 9:1039. doi: 10.3389/fonc.2019.01039

Growth Differentiation Factor 11 (GDF11), a member of the super family of the Transforming Growth Factor β, has gained more attention in the last few years due to numerous reports regarding its functions in other systems, which are different to those related to differentiation and embryonic development, such as age-related muscle dysfunction, skin biology, metabolism, and cancer. GDF11 is expressed in many tissues, including skeletal muscle, pancreas, kidney, nervous system, and retina, among others. GDF11 circulating levels and protein content in tissues are quite variable and are affected by pathological conditions or age. Although, GDF11 biology had a lot of controversies, must of them are only misunderstandings regarding the variability of its responses, which are independent of the tissue, grade of cellular differentiation or pathologies. A blunt fact regarding GDF11 biology is that its target cells have stemness feature, a property that could be found in certain adult cells in health and in disease, such as cancer cells. This review is focused to present and analyze the recent findings in the emerging research field of GDF11 function in cancer and metabolism, and discusses the controversies surrounding the biology of this atypical growth factor.

Keywords: GDF11, PCSK5, cancer, liver, HCC, metabolism

INTRODUCTION

On May 2013 the research groups, led by doctors Amy J. Wagers and Richard T. Lee, published outstanding work suggesting that the growth differentiation factor 11 (GDF11) could be a good candidate for the age-related heart hypertrophy reversion observed in the model of heterochronic parabiosis (1). One year later, on May 2014, Science journal published a couple of works by the same research team at Harvard University, unveiling that systemic injection of the GDF11 reverses age-related dysfunction in skeletal muscle (2) and vascular and neurogenic function in the brain (3). Both reports were astonishing, particularly because myostatin, also known as GDF8, shares high structural homology with GDF11, but GDF8 induces exactly the contrary effect, muscle growth inhibition (4). At that moment, GDF11 was called "the rejuvenation factor," a term taken by a commentary note published by Jocelyn Kaiser in the same number of the Science journal (5), and Karoline E. Brun published another similar commentary in Cell journal entitle "GDF11 and the Mythical Fountain of Youth" (6).

The findings, beyond this unfortunate motto, revealed that GDF11 could exert functions in adult systems, in addition of those characterized in embryonic and fetal tissues. The works by the groups of doctors Wagers and Lee provided evidence that the main target cells are those with certain stemness phenotype, such as the satellite cells in the muscle, which are the progenitor ones for new functional muscle cells.

If GDF11 targets cells with stemness capacity, then many cancer cells should be targeted by this growth factor.

Many cancer cells gain stemness capacity and this correlates with aggressiveness and poor prognosis. The findings raised by the group of doctors, Wagers and Lee, position cancer cells as a target of GDF11 since they proved that stemness is a key condition for GDF11 effect. However, the results could be opposite depending of the cancer cell origin, metabolic status, or the stage of the cancer. We must wait for incoming works in the next few years, perhaps months, revealing a more precise mechanism regarding these apparent controversies in cancer and metabolism.

This work is focused to review the general knowledge of GDF11, and its functions in cancer biology and metabolism, taking into consideration recent findings in the specialized literature and in the public databases and scientific on-line resources.

GDF11 AN ATYPICAL TGF-β FAMILY MEMBER

GDF11 (also known as Bone Morphogenetic Protein, BMP11), is a member of the super family of the Transforming Growth Factor beta (TGF-β) and a subfamily of the BMP which is widely secreted in many species, including mouse, rat and human, and it is accepted as a key factor in embryo development, particularly in the anterior/posterior patterning (7–9).

GDF11 was identified by McPherron et al. in 1999, who cloned the human and mouse GDF11 and characterized its function in pattering the axial skeleton (9). Two years prior, the same group also discovered and characterized the GDF8 (10).

In humans, GDF11 gene is located in chromosome 12 (12q13.2, forward strand, Ensembl accession number: ENSG00000135414). Two splice variants products have been identified, according to Ensembl (**Figure 1**), the first one, GDF11-201 is a 8657 bp RNA, formed by three coding exons, generating a 407 amino acids protein, and the second one, GDF11-202, is a 1,258 bp, formed by three exons generating a 380 amino acids protein (11). Jeanplong (12) reported another RNA splice variant determined as GDF-11ΔEx11, characterized by the absence of exon 1, and composed for exon 2 and 3 with transcriptional initiation in intron 1 (4,701 bp). It is predicted this variant could be regulated by transcription factors, such as some myogenic factors (MRF, Myf5, MyoD, Myogenin, and MRF4), Pax3, NF1, AP1, among others (12), suggesting that it could be involved in muscle development and/or repair as reported in other work (2). Interestingly, the promoter of GDF11 could also be activated by trichostatin A (13), an inhibitor of histone deacetylases (HDAC), suggesting a clear epigenetic regulation of the GDF11 gene expression; HDAC3 regulates zebrafish liver development by modulating GDF11. The overexpression of HDAC3 increases liver size, while the increase of GDF11 expression induces a small size liver; interestingly, the knockdown of GDF11 did not induce any relevant change in liver morphology. The role of HDAC3 in GDF11 function in liver development is likely a direct control over the hepatocyte precursor (hepatoblast) proliferation, as observed in HCC-derived cells (14), but this must be deeply addressed.

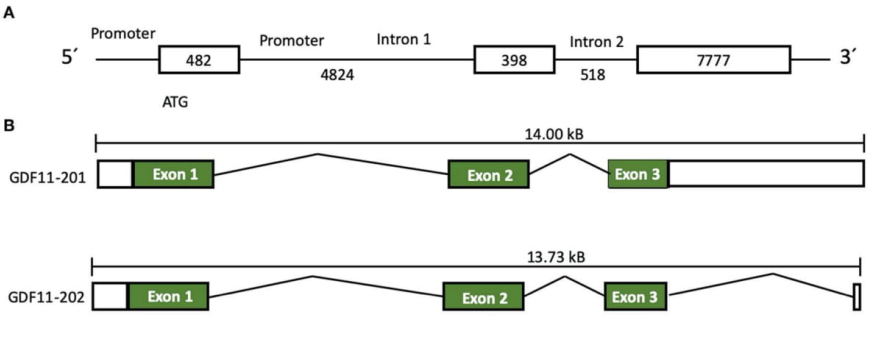
GDF11 mRNA is translated in a precursor protein (**Figure 2**), which is processed by specific proteases generating the mature GDF11 (C-terminal, 12.5 kDa) and the pro-domain (N-terminal, 30.1 kDa). GDF11 shares 89% amino acid sequence homology with GDF8, however GDF8 expression in human tissues is restricted to cardiac and skeletal muscle (1), while GDF11 is practically expressed in all tissues (15). Although there is high homology between mature GDF8 and GDF11, the pro-domains of both proteins share only 54% homology. The pro-domain is fundamental for proper protein folding, disulfide bond formation and exportation of the homodimers (16), suggesting differences in post-translational process.

The protein convertase subtilisin/kexin 5 (PCSK5) is one of the main acting proteins on GDF11, activating the mature GDF11 by proteolytic process at basic sites of the pro-domain (17). The elimination of PCSK5 in the mouse embryo was associated with abnormal expression of Hlxb9 and Hox genes, two well-known GDF11 target genes, generating defects in the anteroposterior patterning and strongly proposing a relationship with GDF11 functions (7, 8).

In humans, GDF11 is expressed in practically all tissues, but is particularly relevant in the brain (hippocampus), the kidneys, the endometrium, and the heart muscle; while the liver is the organ with the lowest expression (1, 15, 18).

THE SIGNAL TRANSDUCTION

As a member of the BMP family, GDF11 uses the canonical receptors and the SMAD proteins for signaling. The GDF11 dimer (a disulfide-linked homodimer of carboxy-terminal fragments) binds the activin receptors type II A or B (ActRIIA, ActRIIB), proteins with serine/threonine kinase activity; leading to the recruitment and transphosphorylation of two type I serine/threonine kinase receptors, also known as activin-like kinase receptors (ALK), particularly the 4, 5, or 7 (19, 20). The activated ALK receptor phosphorylates and activates the receptor-regulated SMAD (R-SAMD). GDF11 particularly transduces by using SMAD2 and 3 (14, 21), and some reports also propose the participation of SMAD1, 5 and 8 (22). The R-SMAD dimer recruits the co-SMAD, SMAD4, to form a trimeric complex, which eventually translocates to the nucleus for gene expression regulation (23). Although the signal transduction of the TGF-β family might seem simple, it is highly regulated by extracellular and intracellular mechanisms. Inside the cell, the regulation can occur at the membrane or in the cytosol, during nuclear translocation and DNA biding, at this level, is a



Name Splice Variant	Ensambl trasncript number	bp	Protein	Ensambl protein number	Biotype
GDF11-201	ENST00000257868.9	8657	407aa 45.1 KDa	ENSP00000257868.5	Protein coding
GDF11-202	ENST00000546799.1	1258	380aa 42.2 KDa	ENSP00000448390.1	Protein coding

FIGURE 1 | Schematic representation of GDF11 gene and mRNA. **(A)** Gdf11 gene and **(B)** Gdf11 transcripts and table with the two transcripts specifications according to Ensembl (www.ensembl.org, ENSG00000135414.9) and Jeanplog 2014.

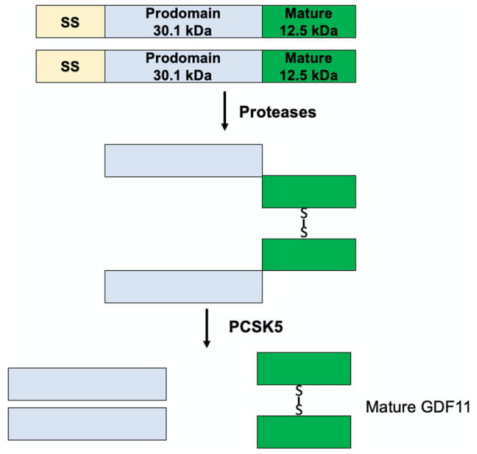


FIGURE 2 | Maturation process of GDF11.

tetrameric complex because the interaction with a fourth protein component or partner (24) (**Figure 3**).

GDF11 can also transduce by non-canonical pathways. Mitogen activated protein kinase (MAPK) is perhaps the main non-SMAD pathway controlled by the growth factor, activating routes such as p38, AKT, and JNK (25, 26), however, in some cases, inhibiting the activation of JNK or NF-κB (27) depending of the cell lineage. Further, it has been described that the family can also transduce by MAPKKK7 [also known as TGF-β activated kinase 1 (TAK1)] via MEK6 (28–30). TAK1 is part of a signaling complex formed by TAK1 binding protein 1 (TAB1) and with either TAB2 or TAB3 (31). TAK1 complex follows an intricate mechanism of activation involving the tumor necrosis factor receptor-associated factor (TRAF) 2 or 6, adaptor proteins with non-conventional activity of E3 ubiquitin ligase. TRAF proteins exert regulation over TAB2 or 3. Finally, the autophosphorylation of TAK1 leads to the activation of its downstream targets, particularly members of the MAPK and NF-κB signaling pathways (32).

Negative regulation of the GDF11-mediated signaling can also occur at different levels. Extracellularly, GDF11 can be negatively regulated by the interaction with many proteins such as follistatin (33, 34), GDF-associated serum protein-1 (GASP-1), GASP-2 (35), decorin and follistatin-like 3, among others (4). Follistatin, a secreted glycoprotein, binds GDF11 and inhibits its interaction with ActRIIB. Follistatin is the main extracellular inhibitor of GDF11, and is transcriptionally regulated by the same GDF11 signaling, indicating that the signal transduction is restricted by a negative feedback mechanism (36).

The BMP and activin membrane-bound inhibitor (BAMBI), a co-receptor that is not functional due to it lacks cytosolic domain, has been suggested to be another negative regulator in plasma membrane, but that still remains to be confirmed (19).

In the cytosol, GDF11 follows the canonical negative regulation of the family. It has been reported that GDF11 is regulated by SMAD7 (37) and SMAD6 (19). The SMAD specific E3 ubiquitin protein ligase 2 (SMURF2) also displays negative regulation of the signaling pathway (28). Negative-regulation

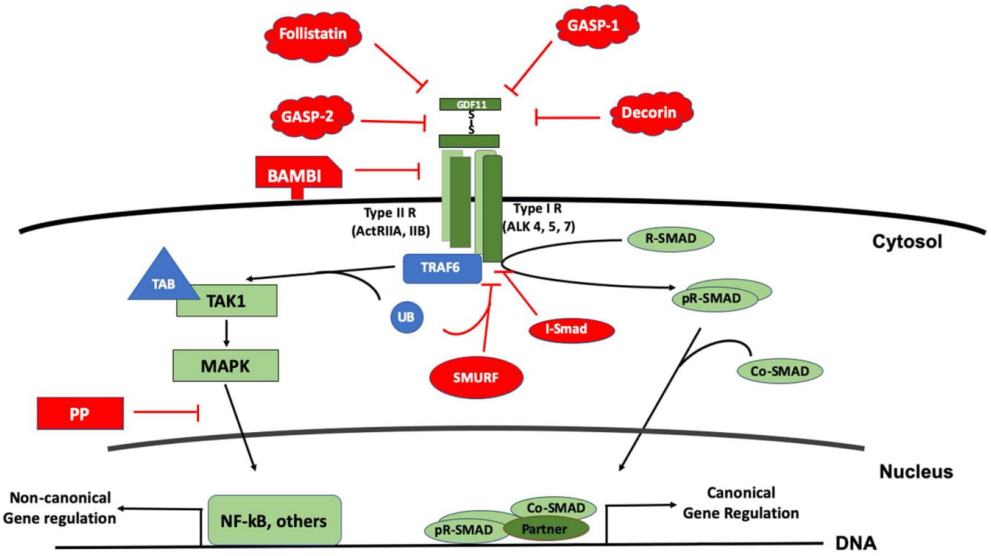


FIGURE 3 | The signal transduction of GDF11. The figure displays the canonical signal transduction mediated by R-SMAD (SMAD 2/3, SMAD 1,5,8), assisted by the Co-SMAD (SMAD4). The signal could inhibited by inhibitory SMAD (I-SMAD) 6 or 7 or by the SMAD specific E3 ubiquitin protein ligase (SMURF). Extracellularly, GDF11 could be inhibited by the BMP and activin membrane-bound inhibitor (BAMBI), or the action of proteins such as Follistatin, Decorin, and GDF-associated serum protein-1 (GASP-1) and GASP-2. The non-canonical pathway is driven particularly by the Mitogen Activated Proteins Kinases (MAPK), signaling continues to the tumor necrosis factor receptor-associated factor (TRAF) 2 or 6; and TGF-β activated kinase 1 (TAK1), which in addition uses the TAK1 binding protein (TAB) 1 and one of both 2 or 3. Non-canonical regulation could influence the nuclear factor kappa B (NF-kB) among others, and the inhibition of this pathway could be blocked by protein phosphatases (PP).

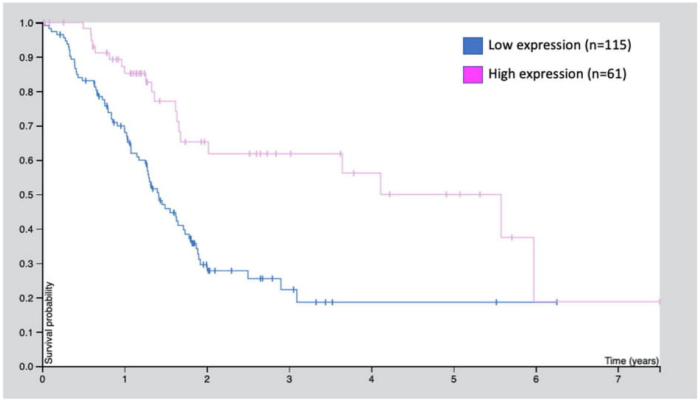


FIGURE 4 | Kaplan-Meier survival curve of 176 patients with pancreatic cancer. Patients were classified as low GDF11 expression and high GDF11 expression, $p < 0.001$, according to the human protein atlas (www.proteinatlas.org/ENSG00000135414-GDF11/pathology).

of the non-canonical pathway is driven by specific protein phosphatases (PP), such as PPC1, among others.

DEVELOPMENT AND AGED-RELATED FUNCTION

Although GDF11 was identified in 1999 (9), as previously mentioned, in 2014 the growth factor was transiently located in the "*Sancta sanctorum*" of the "miraculous" molecule, when the laboratory of Amy Wagers (2) reported that GDF11 was responsible for the skeletal muscle regeneration in mice heterochronic parabiosis. A profound controversy arose regarding the rejuvenating property of GDF11; some groups stated that this property is displayed by the growth factor (1–3, 38), while others reported the opposite effect (39–42), as previously mentioned. To have a good point of view regarding this debate, we suggest a deep view of cited works and commentaries regarding the controversy (3, 5, 6, 19, 42, 43).

Regardless of this disagreement, there is no doubt about the GDF11 function in differentiation and embryonic development, particularly in anterior/posterior axial skeleton (9) and brain function (44), which are nicely reviewed elsewhere (19, 45, 46).

GDF11 VS. GDF8 AND THE RACE FOR THE DISCOVERY OF THE REJUVENATION PROPERTIES

GDF11 and GDF8 are close related members of the activins subclass in the TGF-β superfamily. Sharing 90% of their amino acid sequence (38, 47), these two proteins have been a technical challenge for antibody manufacturers and, therefore, protagonists of one of the most controversial studies in recent years (29, 39, 48–50), regarding to the issue of GDF11 being the protein responsible for "rejuvenation" of aged organisms (1, 2), as previously mentioned.

The race from the discovery of the rejuvenation properties of GDF11 to the following debate of the antibody specificity led to a deeper structural analysis of these proteins and the interaction with their receptor. Due to the similarities of ∼90% of sequence identity of the C-terminal signaling domain between GDF11 and GDF8, their mature form is nearly identical, which causes these proteins to share the same activin type II receptor (38).

Although they are indeed similar in their monomeric form, in fact these proteins are thought to have opposite functions, where GDF11 works as a muscle generator in embryogenesis (9) but GDF8 acts as a muscle mass inhibitor (10, 51), which may be the result of the final homodimer structure. Thus, it is important to understand that the GDF11 and GDF8 homodimer formation leads to a different conformation that allows them to interact with the same receptor in a unique and specific way. It is reported that both homodimers are linked by a single disulfide bond in an antiparallel conformation, but the flexibility in the relative orientations generated by the differences in their structure are determinant for the quaternary structure variations that lead to a distinctive biological response (47, 52).

It has also been reported that GDF11 has a stronger affinity for the receptor than GDF8 (38) and that it is more dependent on direct receptor contacts (53), but there is also an issue with crystal structures of both proteins. Human myostatin alone has not been reported and the available structures are bound to extracellular antagonists (follistatin and follistatin-like 3) (54, 55), which have been compared to a small-angle X-ray scattering (SAXS) analysis to determine the mechanism of activation (52). On the other hand, human GDF11 structure has been resolved in recent years (47), thus, it is possible to discover the real impact of the structure of both proteins in future, at which point we can begin to uncover exactly what makes the responses so different.

GDF11 EFFECTS IN CANCER BIOLOGY

An emerging field of research is the impact of GDF11 in cancer biology. Most of the cancer cells, particularly those with high aggressiveness, retain or recover stemness capacity, placing them as a potential target of GDF11 (14, 23).

There exist some controversies in cancer biology as well; in some cases GDF11 induces clear tumor suppressive properties (14, 23), and in others it is the opposite (56, 57). Once again, the versatility displayed by this growth factor depends of cell progeny, grade of differentiation or transformation.

LIVER CANCER

We recently published work describing how GDF11 induces tumor suppressive properties in human hepatocellular carcinoma-derived cells, Huh7 and Hep3B cell lines, restricting spheroid formation and clonogenic capacity, an effect that is also observed in other liver cancer cell lines (SNU-182, Hepa1-6, and HepG2), decreasing proliferation, motogenesis, and invasion. These characteristics were associated with transcriptional repression of cyclin D1 and A, and the overexpression of p27 (14). GDF11 effects, on hepatic cell proliferation, have been found in liver development, where GDF11 targets the hepatoblast, the hepatocyte precursor (13, 58).

Remarkably, the invasion experiments using the chick embryo chorioallantoic membrane (CAM) model (14, 59) revealed a static phenotype in Huh7 cells treated for 72 h with GDF11 (50 ng/ml), an outcome well-correlated with a decrease in cell migration and proliferation. Furthermore, GDF11 treated cells were incapable of sustaining colony and sphere capacity in the absence of GDF11, up to 5 days, indicating that the effect of GDF11 on self-renewal capacity is not transient, suggesting a reprogramming effect.

Similar results were obtained in the hepatoblastoma cell lines, HepG2 and SMMC-7721: the treatment with GDF11 up to 72 h reduced cell viability. Although SMMC-7721 cells are probably a HELA-derivative cell line, the effect was also present (60). This report also provides preliminary evidence that the expression of GDF11 was significantly lower in cancerous tissue rather than in normal liver.

Outstandingly, GDF11 was capable of decreasing aggressiveness-associated markers in Huh7 and Hep3B cells,

producing a deregulation in the expression of *Epcam, promo1* (CD133), *cd24, and ck19*, that was associated with the repression of Snail and N-cadherin, and the overexpression of occluding and E-cadherin, strongly indicating a mesenchymal to epithelial transition (14).

It is interesting that, under normal conditions, liver cells, which are the poorest in GDF11 production, are highly responsive to GDF11 in the context of cancer could be relevant in terms of a possible use of GDF11 for treatment. The work by Gerardo-Ramírez clearly showed that all HCC cells used in the study responded to the exogenous GDF11 treatment, decreasing all aggressiveness-associated markers. Interestingly, the effects in HCC cells were differentiated, and it was dependent of the stemness capacity, being more responsive to Hep3B cells, which express fewer stemness markers compared to Huh7 cells. Supporting this statement, in liver development GDF11 has been related to inhibition of liver growth, mainly targeting proliferation of hepatoblast, the cell precursor or mature hepatocytes by a mechanism involving HDAC3, which inhibits the expression of GDF11 as proven by Farooq and collaborators (58). This work clearly demonstrates that GDF11 targets hepatic cells with stemness features, not necessarily those observed in cancer, but in the normal liver, particularly in development.

BREAST CANCER

Similarly, Bajikar et al. (23) identified a tumor-suppressive role of GDF11 in a triple-negative breast cancer (TNBC). These cells, under 3D culture, heterogeneously express GDF11 and very low levels of GDF8, as well as the main canonical receptors, such as ALK4, and ALK5, among other protein machinery required for a proper signal transduction. This clearly indicates that breast epithelial cells express the required components to recognize GDF11 as an autocrine or paracrine stimulus (23). GDF11 also induced a decrease in number and size of the spheroids and generated more-compacted structures by the increment in E-cadherin, as observed in liver cancer cell lines, and GDF11 treatment induces a cell-cell adhesion preventing metastasis phenomena (14, 23).

Authors also found a defective GDF11 maturation and secretion in seven of nine studied TNBC cell lines. The linker was the convertase PCSK5, in which a deficiency was found in the TNBC cells, inducing the extracellular accumulation of the immature proGDF11 and, for instance, loss in the bioactivity of GDF11. This mechanism was also observed in mice; the lack of Pcsk5 in $Apc^{min/+}$ animals (61) increases adenocarcinoma formation in the small intestine, decreasing the survival (23, 62), which demonstrates a clear function in tandem of GDF11 and PCSK5 to induce the tumor suppressive properties. In fact, the restoration of the PCSK5 activity in the TNBC cells suppresses lung metastasis (23).

Another work by Wallner et al. (63) revealed that super-physiological levels of GDF11 (2 μg/ml) could provide advantages in chemotherapy in breast adenocarcinoma, inducing a decrement in the migrative capacity of MCF-7 cells in a scratch assay. Similar findings were observed in the presence of follistatin (2 μg/ml), while GDF8 (2 μg/ml) induced cell death at the same time. This study also showed that GDF11 is expressed in low grade adenocarcinoma tissue (G1), but lower levels in G3 tissue were found, and it was correlated with high expression of follistatin in G1, suggesting an inhibitory effect of GDF11 at higher levels of differentiation, which is consistent with the idea that high aggressiveness in cancer associates with less GDF11 function, confirming the tumor suppressive capacity of GDF11.

PANCREATIC CANCER

Pancreatic cancer (PC) represents one of the most lethal cancers worldwide (64). It has been reported that GDF11 is down-regulated in PC tissue, compared with surrounding tissue, and pancreatic cell lines exhibit a low expression of the growth factor (65). This group also reported that, in a cohort of 63 PC patients, those with high GDF11 expression had significantly better survival rates in comparison with those with low GDF11 expression. These effects were related to decreased proliferation, migration and invasion, and these observations are in agreement with those reported in HCC and TNBC. GDF11 is also capable of inducing apoptosis in PC cell lines (65).

Similarly, the human protein atlas (https://www.proteinatlas.org) provides evidence from 176 patients: those with high GDF11 expression ($n = 61$) exhibited better survival rates, compared with those with low expression ($n = 115$, $p < 0.001$) (**Figure 4**). These observations strongly suggest that GDF11 could also exert tumor suppressive properties that should be deeply addressed to gain confidence, particularly the effect of exogenous active GDF11 (18).

Interestingly, another member of the family GDF15 is directly correlated with poor survival in PC patients, and it is proposed as a better marker than CA-125 (66), again raising the atypical functions of this growth factor.

As observed in HCC, in PC, the targets of GDF11 are poorly differentiated cells. In the mouse embryo, GDF11 is expressed in the pancreatic epithelium, at embryonic day E12-E14 (67), as it happens in the liver, but in $GDF11^{-/-}$ animals the pancreas size are 2-fold smaller than wild type.

In the context of the educated guess that cells with some stemness phenotype respond to GDF11, even in cancer, it has been proven that GDF11 negatively regulates $NGN3^{+}$ progenitor cells and GDF11 induces β-cell differentiation (68), supporting the role of GDF11 in metabolism. Under this context, GDF11 exerts its functions in pancreatic cells with stemness phenotype.

COLORECTAL CANCER

In 130 patients with colorectal cancer (CRC), the expression of GDF11 was significantly higher compared with normal tissue (56). The classification of the patient cohort in low and high GDF11 expression revealed that those patients with high levels of GDF11 showed a higher frequency of lymph node metastasis, more deaths and lower survival. The study suggests that GDF11 could be a prognostic biomarker in patients with this disease.

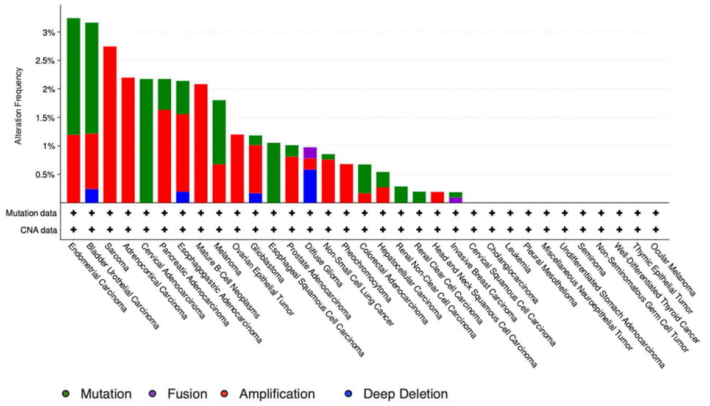


FIGURE 5 | Genomic alterations in Gdf11 gene. Alteration frequency by type of cancer according to cBioportal for cancer genomics (https://www.cbioportal.org).

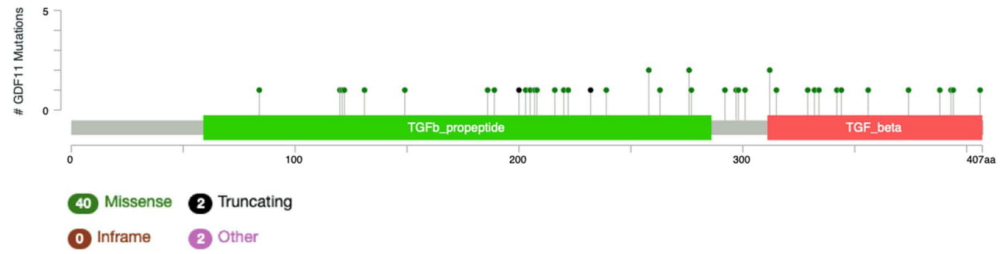


FIGURE 6 | Number of mutations in Gdf11 gene. According to cBioportal for cancer genomics (https://www.cbioportal.org). RefSeq: NM_005811. Ensembl ENST00000257868. CCDS: CCDS8891. UniProt:GDF11_HUMAN. Somatic Mutations Frequency: 0.4%. Forty missense mutations. Two truncating, 0 inframe, 2 other.

It is known that lymphangiogenesis is a fundamental phenomenon for colorectal cancer dissemination (69). Recently, Ungaro and collaborators reported that the microenvironment in the lymphatic vessels provides support to the tumor-derived cells by manipulating the production of extracellular matrix proteins and soluble factors, such as cytokines and growth factors (70). Whole transcriptomic analysis addressed by RNA-seq of isolated human intestinal lymphatic endothelial cells (HILEC) from surgically resected CRC and healthy corresponding controls, revealed that among those genes differentially expressed, GDF11 was observed as a significant increment with high statistical confidence. CACO-2 cells demonstrated high proliferation in co-culture with CRC-HILEC, but the GDF11 silencing by siRNA abrogated this effect indicating a tumor promotion role of GDF11 in CRC. Interestingly, GDF11 was expressed not only in lymphatic vessels in CRC, but also in normal tissue (69). The study also provides evidence of a direct correlation of GDF11 expression and tumor stage, confirming in this particular cancer that GDF11 expression could be a marker of tumor progression (70), and also raises mechanistic evidence that microenvironment in the lymphatic vessel could play a pivotal role in metastasis by local production of GDF11.

OTHER TYPES OF CANCER

Some reports have pointed to the pro-tumorigenic properties of GDF11, with major or minor confidence of rigorous scientific approach.

In oral squamous cell carcinoma, Qin and coauthors (57) showed that in a small patient cohort GDF11 expression is positively correlated with aggressiveness, finding a higher expression in metastatic oral cancer ($n = 19$) in comparison with non-metastatic oral cancer ($n = 15$). Authors also sustain that GDF11 induced epithelial to mesenchymal transition by downregulating epithelial markers such as E-cadherin, and the overexpression of vimentin or metalloproteinase 9.

In uveal melanoma, GDF11 expression was significantly upregulated compared with surrounding tissue, the expression

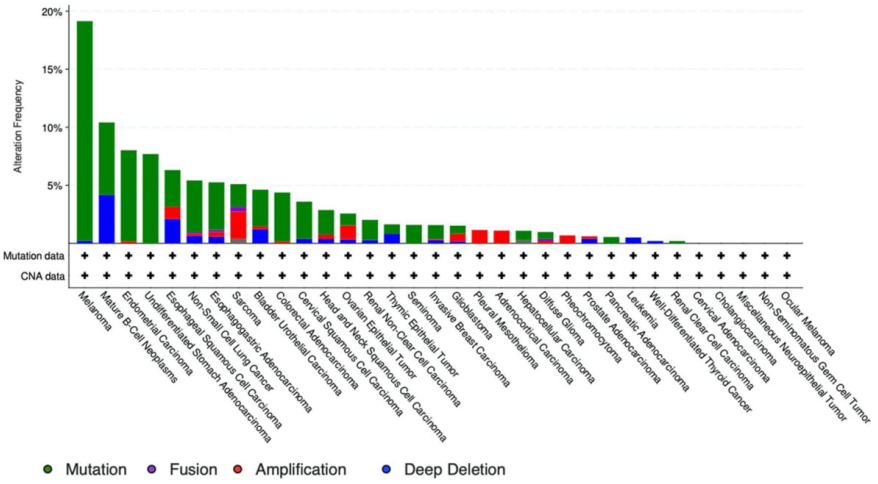


FIGURE 7 | Genomic alterations in Pcsk5 gene. Alteration frequency by type of cancer according to cBioportal for cancer genomics (https://www.cbioportal.org).

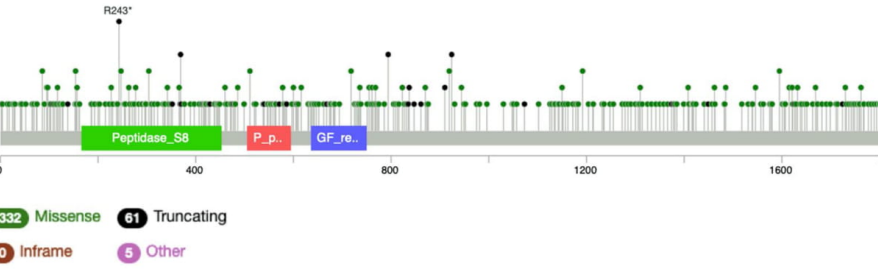


FIGURE 8 | Number of mutations in Pcsk5 gene. According to cBioportal for cancer genomics (https://www.cbioportal.org). RefSeq: NM_001190482. Ensembl ENST00000545128. CCDS: CCDS55320. UniProt: PCSK5_HUMAN. Somatic Mutations Frequency: 2.8%. Three hundred thirty-two missense mutations, 61 truncating, 0 inframe, 5 others.

was higher in stage IV and substantially greater in the deceased cases regarding living cases (71). The multivariate analysis confirmed that GDF11 is an independent prognostic indicator of unfavorable overall survival.

GDF11 AND PCSK MUTATIONS

The study by Liu et al. (71) also showed that no relevant mutations were observed in the GDF11 gene in fact. The cBioportal for cancer genomics web site (https://www.cbioportal.org) indicates that GDF11 is altered in 1% of database patients. **Figure 4** shows the alteration frequency in *Gdf11* gene in some cancers, and **Figure 5** depicts the number of somatic mutations, most of which are missense (72). It seems that mutations in the Gdf11 gene are not the main consequence in those cancers where GDF11 is a prognostic factor, which increases research interest in transcriptional and post-translational regulation.

It is particularly relevant to consider the convertase PCSK5, a key regulator of GDF11 activity. Pcsk5 gene presents a high frequency of genomic alterations in 3% of the patients, according to cBioportal, being particularly relevant in melanoma, endometrial carcinoma, and stomach adenocarcinoma, among others (**Figure 6**). Missense mutations are particularly observed in the peptidase transcript (**Figure 7**) (72). As proven remarkably by the team of doctor Kevin A. Janes (23), maturation of bioactive GDF11 is defective in TNBC due to insufficient PCSK5 activity but, as shown, the frequency of mutations appear not to be related with the flaw (**Figure 8**). Once again, transcriptional and post-translational regulation should be considered in future research.

TABLE 1 | Overview of cancer cell lines or tissue from patients with differential effect of GDF11, as tumor suppressive or tumor promotion protein.

Cancer	Cell/Tissue	Tumor suppressive	Tumor promotion	References
Liver	Huh7 Hep3B SNU-182 Hepa1-6 HepG2	X		(14)
Liver	HepG2 SMMC-7721 and tissue	X		(60)
Breast	MDA-MB-231 MDA-MB-468 and tissue	X		(23)
Breast	MCF-7	X		(63)
Pancreas	PANC-1 CFPAC-1 Tissue	X		(65)
Colorectal	Tissue		X	(56)
Colorectal	Tissue		X	(70)
Colorectal	CACO-2		X	(69)
Oral squamous cell carcinoma	Tissue		X	(57)
Uveal melanoma	Tissue		X	(71)

EFFECTS OF GDF11 AS METABOLISM REGULATOR

The impact of GDF11 in the development of pancreas implies that the growth factor could exert some metabolic regulation on this organ in the adult, particularly in the endocrine pancreas (67). Dichmann and coauthors found that in the gdf11$^{-/-}$ mouse, the maturation and number of β- and α-cells are normal, however, another group led by Harmon reported that the gdf11$^{-/-}$ mouse exhibited impairment maturation of β-cells and an increment in α-cells, which could produce glucagon in comparison with the wild type mouse (68). This controversy, which is not unusual, must be addressed, but makes it clear that GDF11 could be inducing effects in the metabolism mediated by the pancreas.

Recently, a work by Anon-Hidalgo et al. (73) reported a convincing study associating the circulating levels of GDF11 with thyroid-stimulating hormone (TSH) in humans. The study showed subjects with high or normal levels of TSH present high level contents of GDF11, compared with patients with low levels of TSH. This finding could be due to the fact that other members of the family, such as GDF8 and GDF15, are regulators of the energy homeostasis (74, 75). Anon-Hidalgo team states that it could be related to a regulation of TSH by GDF11, or GDF11 could be positively regulated by TSH or any other thyroid hormones (73).

Luo et al. published that GDF11 decreased lipid content in human mesenchymal stem cells and the mouse 3T3-L1 cell line. This was associated with the repression of adipogenic genes, such as the transcription factors *Pparg, Cebpa*, and the executer proteins *Plp, Cd36, Plin1, Adipoq*, among others, in a mechanism associated to the canonical signal transduction mediated by SMAD2/3 (76). The report provides evidence that GDF11 could exert control over lipid content in unclear fashion. The role of GDF11 in lipid homeostasis could be directed to lipid uptake or efflux, intervening in lipogenic or lipolysis pathways, or lipid removal by autophagy, but data provided by Luo et al. suggest an intervention in lipogenesis. Interestingly, obese mice fed with a high lipid diet present significantly decreased circulating GDF11 levels, compared with mice under low fat diet (77). The mRNA and protein content of GDF11 in skeletal muscle from mice under the high fat diet correlated with the serum content of the growth factor, exhibiting lower expression and protein content, compared with animals under low fat diet. Furthermore, palmitate treatment in the mouse-derived myoblast cell line, C2C12, decreases GDF11 expression. However, the GDF11 did not ameliorate the palmitate-induced insulin resistance and GDF11 treatment did not change expression of Glut4 or Irs-1.

The evidence sustains the metabolic intervention by GDF11, at least in terms of lipid homeostasis, and again in cells with stemness features. This could be relevant in cancer, since lipid overload is one of the main characteristics required for a proper cancer cell proliferation (78, 79). In fact, it is reported that GDF11 impairs mitochondrial function in cancer cell lines, particularly in HCC-derived cells (14). The impact of GDF11 in the central metabolic organelle could explain the tumor suppressive properties exerted by the growth factor. Mitochondria provide essential intermediaries required for cell proliferation: driving redox and calcium homeostasis, coordinating energy supply and mediating cell survival; all of which are fundamental for all cells, and particularly for transformed ones (80). A report by Hernandez-Rizo and collaborators states that GDF11 restricts cell proliferation in hepatic tumor cells through glycolysis and lipid metabolism impairment (81). In agreement with these findings, Garrido-Moreno et al. (82) recently reported that GDF11 prevents cardiomyocyte hypertrophy by preserving the communication between the mitochondria and sarcoplasmic reticulum and calcium mobility, preserving oxidative mitochondria metabolism by a mechanism mediated by the maintenance of mitochondrial cytosolic calcium buffering capacity.

Although the evidence of GDF11 regulation of the energetic and lipid metabolism is limited, it clearly indicates an effect tending to maintain the cellular energetic homeostasis. More research is required to characterize the mechanism underlying metabolic regulation by the growth factor, particularly in cancer cells.

CONCLUDING REMARKS AND FUTURE PROSPECTIVE

GDF11 is an intriguing non-conventional growth factor, perhaps the most fascinating new member of the TGF-β superfamily. It transduces, as practically all members, by the canonical

SMAD and non-canonical MAPK pathways, but its functions can be quite variable, even contradictory, depending of the cell lineage, tissue (**Table 1**), or even age. This raises a complex body of physiological control, which could also differ in health or disease. GDF11 displays a versatile response that must be fully characterized, due to it representing an interesting point of intervention in many diseases or physiological conditions, particularly in cancer. It is remarkable that one of the main characteristics in GDF11 target cells, in normal or pathological conditions, is the stemness capacity. The effects exerted by the growth factor in cancer have begun to be characterized with greater scientific rigor and mechanistic approaches.

Perhaps it is time that GDF11, due to its diverse functionality, constitutes its own subfamily as an atypical and versatile member of the TGF-β family.

We must be cautious to oversimplify its functions. The controversies found clearly indicate that GDF11 displays particular activities depending of cell type, grade of differentiation, and pathological or normal conditions. This remarkable atypical member of the TGF-β family must be carefully studied in clear and well-controlled biological systems. The knowledge, regarding GDF11, will surely be increased in the next few years. The mechanism of action in each particular cancer or cell type must be elucidated to clarify these controversies, and perhaps they will stop being such, thanks to the mechanistic enlightenments obtained in the incoming research in the field.

AUTHOR CONTRIBUTIONS

AS-N, MG-R, GP-V, and LC-R conception and preparation of the manuscript. LB, VS, and RM-L reviewed and corrected the manuscript. MCG-R and LG-Q final review of the manuscript and financial support.

FUNDING

This work was partially funded by a grant from the Consejo Nacional de Ciencia y Tecnología (CONACYT): CB-252942; Fronteras de la Ciencia 1320; Apoyo al Fortalecimiento y Desarrollo de la Infraestructura 2017-280788, and Universidad Autonoma Metropolitana. We thank Frida Gomez-Cuevas for the assistance in the preparation of the manuscript.

REFERENCES

1. Loffredo FS, Steinhauser ML, Jay SM, Gannon J, Pancoast JR, Yalamanchi P, et al. Growth differentiation factor 11 is a circulating factor that reverses age-related cardiac hypertrophy. *Cell*. (2013) 153:828–39. doi: 10.1016/j.cell.2013.04.015
2. Sinha M, Jang YC, Oh J, Khong D, Wu EY, Manohar R, et al. Restoring systemic GDF11 levels reverses age-related dysfunction in mouse skeletal muscle. *Science*. (2014) 344:649–52. doi: 10.1126/science.1251152
3. Katsimpardi L, Litterman NK, Schein PA, Miller CM, Loffredo FS, Wojtkiewicz GR, et al. Vascular and neurogenic rejuvenation of the aging mouse brain by young systemic factors. *Science*. (2014) 344:630–4. doi: 10.1126/science.1251141
4. Walker RG, Poggioli T, Katsimpardi L, Buchanan SM, Oh J, Wattrus S, et al. Biochemistry and biology of GDF11 and myostatin: similarities, differences, and questions for future investigation. *Circ Res*. (2016) 118:1125–41; discussion 1142. doi: 10.1161/CIRCRESAHA.116.308391
5. Kaiser J. Aging. 'Rejuvenation factor' in blood turns back the clock in old mice. *Science*. (2014) 344:570–1. doi: 10.1126/science.344.6184.570
6. Brun CE, Rudnicki MA. GDF11 and the mythical fountain of youth. *Cell Metab*. (2015) 22:54–6. doi: 10.1016/j.cmet.2015.05.009
7. Lee YJ, McPherron A, Choe S, Sakai Y, Chandraratna RA, Lee SJ, et al. Growth differentiation factor 11 signaling controls retinoic acid activity for axial vertebral development. *Dev Biol*. (2010) 347:195–203. doi: 10.1016/j.ydbio.2010.08.022
8. Tsuda T, Iwai N, Deguchi E, Kimura O, Ono S, Furukawa T, et al. PCSK5 and GDF11 expression in the hindgut region of mouse embryos with anorectal malformations. *Eur J Pediatr Surg*. (2011) 21:238–41. doi: 10.1055/s-0031-1273691
9. McPherron AC, Lawler AM, Lee SJ. Regulation of anterior/posterior patterning of the axial skeleton by growth/differentiation factor 11. *Nat Genet*. (1999) 22:260–4. doi: 10.1038/10320
10. McPherron AC, Lawler AM, Lee SJ. Regulation of skeletal muscle mass in mice by a new TGF-beta superfamily member. *Nature*. (1997) 387:83–90. doi: 10.1038/387083a0
11. Hunt SE, McLaren W, Gil L, Thormann A, Schuilenburg H, Sheppard D, et al. Ensembl variation resources. *Database*. (2018) 2018:bay119. doi: 10.1093/database/bay119
12. Jeanplong F, Falconer SJ, Oldham JM, Maqbool NJ, Thomas M, Hennebry A, et al. Identification and expression of a novel transcript of the growth and differentiation factor-11 gene. *Mol Cell Biochem*. (2014) 390:9–18. doi: 10.1007/s11010-013-1949-3
13. Zhang X, Wharton W, Yuan Z, Tsai SC, Olashaw N, Seto E. Activation of the growth-differentiation factor 11 gene by the histone deacetylase (HDAC) inhibitor trichostatin A and repression by HDAC3. *Mol Cell Biol*. (2004) 24:5106–18. doi: 10.1128/MCB.24.12.5106-5118.2004
14. Gerardo-Ramirez M, Lazzarini-Lechuga R, Hernandez-Rizo S, Jimenez-Salazar JE, Simoni-Nieves A, Garcia-Ruiz C, et al. GDF11 exhibits tumor suppressive properties in hepatocellular carcinoma cells by restricting clonal expansion and invasion. *Biochim Biophys Acta Mol Basis Dis*. (2019) 1865:1540–54. doi: 10.1016/j.bbadis.2019.03.003
15. Uhlen M, Fagerberg L, Hallstrom BM, Lindskog C, Oksvold P, Mardinoglu A, et al. Proteomics. Tissue-based map of the human proteome. *Science*. (2015) 347:1260419. doi: 10.1126/science.1260419
16. Gray AM, Mason AJ. Requirement for activin A and transforming growth factor–beta 1 pro-regions in homodimer assembly. *Science*. (1990) 247:1328–30. doi: 10.1126/science.2315700
17. Essalmani R, Zaid A, Marcinkiewicz J, Chamberland A, Pasquato A, Seidah NG, et al. *In vivo* functions of the proprotein convertase PC5/6 during mouse development: Gdf11 is a likely substrate. *Proc Natl Acad Sci USA*. (2008) 105:5750–5. doi: 10.1073/pnas.0709428105
18. Uhlen M, Zhang C, Lee S, Sjostedt E, Fagerberg L, Bidkhori G, et al. A pathology atlas of the human cancer transcriptome. *Science*. (2017) 357:eaan2507. doi: 10.1126/science.aan2507
19. Jamaiyar A, Wan W, Janota DM, Enrick MK, Chilian WM, Yin L. The versatility and paradox of GDF 11. *Pharmacol Ther*. (2017) 175:28–34. doi: 10.1016/j.pharmthera.2017.02.032
20. Andersson O, Reissmann E, Ibanez CF. Growth differentiation factor 11 signals through the transforming growth factor-beta receptor ALK5 to regionalize the anterior-posterior axis. *EMBO Rep*. (2006) 7:831–7. doi: 10.1038/sj.embor.7400752
21. Gaunt SJ, George M, Paul YL. Direct activation of a mouse Hoxd11 axial expression enhancer by Gdf11/Smad signalling. *Dev Biol*. (2013) 383:52–60. doi: 10.1016/j.ydbio.2013.08.025
22. Zhang YH, Cheng F, Du XT, Gao JL, Xiao XL, Li N, et al. GDF11/BMP11 activates both smad1/5/8 and smad2/3 signals but shows no significant effect on proliferation and migration of human umbilical vein endothelial cells. *Oncotarget*. (2016) 7:12063–74. doi: 10.18632/oncotarget.10664

23. Bajikar SS, Wang CC, Borten MA, Pereira EJ, Atkins KA, Janes KA. Tumor-suppressor inactivation of GDF11 occurs by precursor sequestration in triple-negative breast cancer. *Dev Cell*. (2017) 43:418–35 e13. doi: 10.1016/j.devcel.2017.10.027
24. Hata A, Chen YG. TGF-beta signaling from receptors to smads. *Cold Spring Harb Perspect Biol*. (2016) 8:a022061. doi: 10.1101/cshperspect.a022061
25. Wang Z, Dou M, Liu F, Jiang P, Ye S, Ma L, et al. GDF11 induces differentiation and apoptosis and inhibits migration of C17.2 neural stem cells via modulating MAPK signaling pathway. *PeerJ*. (2018) 6:e5524. doi: 10.7717/peerj.5524
26. Demontis F, Patel VK, Swindell WR, Perrimon N. Intertissue control of the nucleolus via a myokine-dependent longevity pathway. *Cell Rep*. (2014) 7:1481–94. doi: 10.1016/j.celrep.2014.05.001
27. Mei W, Xiang G, Li Y, Li H, Xiang L, Lu J, et al. GDF11 protects against endothelial injury and reduces atherosclerotic lesion formation in apolipoprotein e-null mice. *Mol Ther*. (2016) 24:1926–38. doi: 10.1038/mt.2016.160
28. van Wijk B, Moorman AF, van den Hoff MJ. Role of bone morphogenetic proteins in cardiac differentiation. *Cardiovasc Res*. (2007) 74:244–55. doi: 10.1016/j.cardiores.2006.11.022
29. Hammers DW, Merscham-Banda M, Hsiao JY, Engst S, Hartman JJ, Sweeney HL. Supraphysiological levels of GDF11 induce striated muscle atrophy. *EMBO Mol Med*. (2017) 9:531–44. doi: 10.15252/emmm.201607231
30. Hindi SM, Sato S, Xiong G, Bohnert KR, Gibb AA, Gallot YS, et al. TAK1 regulates skeletal muscle mass and mitochondrial function. *JCI Insight*. (2018) 3:98441. doi: 10.1172/jci.insight.98441
31. Mihaly SR, Ninomiya-Tsuji J, Morioka S. TAK1 control of cell death. *Cell Death Differ*. (2014) 21:1667–76. doi: 10.1038/cdd.2014.123
32. Wang C, Deng L, Hong M, Akkaraju GR, Inoue J, Chen ZJ. TAK1 is a ubiquitin-dependent kinase of MKK and IKK. *Nature*. (2001) 412:346–51. doi: 10.1038/35085597
33. Fife E, Kostka J, Kroc L, Guligowska A, Piglowska M, Soltysik B, et al. Relationship of muscle function to circulating myostatin, follistatin and GDF11 in older women and men. *BMC Geriatr*. (2018) 18:200. doi: 10.1186/s12877-018-0888-y
34. Schneyer AL, Sidis Y, Gulati A, Sun JL, Keutmann H, Krasney PA. Differential antagonism of activin, myostatin and growth and differentiation factor 11 by wild-type and mutant follistatin. *Endocrinology*. (2008) 149:4589–95. doi: 10.1210/en.2008-0259
35. Lee YS, Lee SJ. Regulation of GDF-11 and myostatin activity by GASP-1 and GASP-2. *Proc Natl Acad Sci USA*. (2013) 110:E3713–22. doi: 10.1073/pnas.1309907110
36. Gamer LW, Cox KA, Small C, Rosen V. Gdf11 is a negative regulator of chondrogenesis and myogenesis in the developing chick limb. *Dev Biol*. (2001) 229:407–20. doi: 10.1006/dbio.2000.9981
37. Smart NG, Apelqvist AA, Gu X, Harmon EB, Topper JN, MacDonald RJ, et al. Conditional expression of Smad7 in pancreatic beta cells disrupts TGF-beta signaling and induces reversible diabetes mellitus. *PLoS Biol*. (2006) 4:e39. doi: 10.1371/journal.pbio.0040039
38. Walker RG, Czepnik M, Goebel EJ, McCoy JC, Vujic A, Cho M, et al. Structural basis for potency differences between GDF8 and GDF11. *BMC Biol*. (2017) 15:19. doi: 10.1186/s12915-017-0350-1
39. Egerman MA, Cadena SM, Gilbert JA, Meyer A, Nelson HN, Swalley SE, et al. GDF11 increases with age and inhibits skeletal muscle regeneration. *Cell Metab*. (2015) 22:164–74. doi: 10.1016/j.cmet.2015.05.010
40. Glass DJ. Elevated GDF11 is a risk factor for age-related frailty and disease in humans. *Cell Metab*. (2016) 24:7–8. doi: 10.1016/j.cmet.2016.06.017
41. Zhao L, Zhang S, Cui J, Huang W, Wang J, Su F, et al. TERT assists GDF11 to rejuvenate senescent VEGFR2(+)/CD133(+) cells in elderly patients with myocardial infarction. *Lab Invest*. (2019). doi: 10.1038/s41374-019-0290-1. [Epub ahead of print].
42. Egerman MA, Glass DJ. The role of GDF11 in aging and skeletal muscle, cardiac and bone homeostasis. *Crit Rev Biochem Mol Biol*. (2019) 54:174–83. doi: 10.1080/10409238.2019.1610722
43. Fan X, Gaur U, Sun L, Yang D, Yang M. The growth differentiation factor 11 (GDF11) and myostatin (MSTN) in tissue specific aging. *Mech Ageing Dev*. (2017) 164:108–12. doi: 10.1016/j.mad.2017.04.009
44. Gokoffski KK, Wu HH, Beites CL, Kim J, Kim EJ, Matzuk MM, et al. Activin and GDF11 collaborate in feedback control of neuroepithelial stem cell proliferation and fate. *Development*. (2011) 138:4131–42. doi: 10.1242/dev.065870
45. Zhang Y, Wei Y, Liu D, Liu F, Li X, Pan L, et al. Role of growth differentiation factor 11 in development, physiology and disease. *Oncotarget*. (2017) 8:81604–16. doi: 10.18632/oncotarget.20258
46. Gad JM, Tam PP. Axis development: the mouse becomes a dachshund. *Curr Biol*. (1999) 9:R783–6. doi: 10.1016/S0960-9822(00)80013-5
47. Padyana AK, Vaidialingam B, Hayes DB, Gupta P, Franti M, Farrow NA. Crystal structure of human GDF11. *Acta Crystallogr F Struct Biol Commun*. (2016) 72:160–4. doi: 10.1107/S2053230X16001588
48. Jones JE, Cadena SM, Gong C, Wang X, Chen Z, Wang SX, et al. Supraphysiologic administration of GDF11 induces cachexia in part by upregulating GDF15. *Cell Rep*. (2018) 22:1522–30. doi: 10.1016/j.celrep.2018.01.044
49. Zimmers TA, Jiang Y, Wang M, Liang TW, Rupert JE, Au ED, et al. Exogenous GDF11 induces cardiac and skeletal muscle dysfunction and wasting. *Basic Res Cardiol*. (2017) 112:48. doi: 10.1007/s00395-017-0642-1
50. Hinken AC, Powers JM, Luo G, Holt JA, Billin AN, Russell AJ. Lack of evidence for GDF11 as a rejuvenator of aged skeletal muscle satellite cells. *Aging Cell*. (2016) 15:582–4. doi: 10.1111/acel.12475
51. McPherron AC, Lee SJ. Double muscling in cattle due to mutations in the myostatin gene. *Proc Natl Acad Sci USA*. (1997) 94:12457–61. doi: 10.1073/pnas.94.23.12457
52. Walker RG, McCoy JC, Czepnik M, Mills MJ, Hagg A, Walton KL, et al. Molecular characterization of latent GDF8 reveals mechanisms of activation. *Proc Natl Acad Sci USA*. (2018) 115:E866–75. doi: 10.1073/pnas.1714622115
53. Goebel EJ, Corpina RA, Hinck CS, Czepnik M, Castonguay R, Grenha R, et al. Structural characterization of an activin class ternary receptor complex reveals a third paradigm for receptor specificity. *Proc Natl Acad Sci USA*. (2019) 116:15505–13. doi: 10.1073/pnas.1906253116
54. Cash JN, Angerman EB, Kattamuri C, Nolan K, Zhao H, Sidis Y, et al. Structure of myostatin.follistatin-like 3: N-terminal domains of follistatin-type molecules exhibit alternate modes of binding. *J Biol Chem*. (2012) 287:1043–53. doi: 10.1074/jbc.M111.270801
55. Cash JN, Rejon CA, McPherron AC, Bernard DJ, Thompson TB. The structure of myostatin:follistatin 288: insights into receptor utilization and heparin binding. *EMBO J*. (2009) 28:2662–76. doi: 10.1038/emboj.2009.205
56. Yokoe T, Ohmachi T, Inoue H, Mimori K, Tanaka F, Kusunoki M, et al. Clinical significance of growth differentiation factor 11 in colorectal cancer. *Int J Oncol*. (2007) 31:1097–101. doi: 10.3892/ijo.31.5.1097
57. Qin X, Kuang H, Chen L, Wei S, Yu D, Liang F. Coexpression of growth differentiation factor 11 and reactive oxygen species in metastatic oral cancer and its role in inducing the epithelial to mesenchymal transition. *Oral Surg Oral Med Oral Pathol Oral Radiol*. (2017) 123:697–706. doi: 10.1016/j.oooo.2017.03.010
58. Farooq M, Sulochana KN, Pan X, To J, Sheng D, Gong Z, et al. Histone deacetylase 3 (hdac3) is specifically required for liver development in zebrafish. *Dev Biol*. (2008) 317:336–53. doi: 10.1016/j.ydbio.2008.02.034
59. Lazzarini-Lechuga R, Alcantar-Ramirez O, Jaime-Cruz R, Gómez-Quiroz L. Efecto teratogénico de nanopartículas de oro de 20 nm durante la septación cardiaca. *Mundo Nano*. (2014) 7:69–77. doi: 10.22201/ceiich.24485691e.2014.13.48710
60. Zhang YH, Pan LH, Pang Y, Yang JX, Lv MJ, Liu F, et al. GDF11/BMP11 as a novel tumor marker for liver cancer. *Exp Ther Med*. (2018) 15:3495–500. doi: 10.3892/etm.2018.5861
61. Su LK, Kinzler KW, Vogelstein B, Preisinger AC, Moser AR, Luongo C, et al. Multiple intestinal neoplasia caused by a mutation in the murine homolog of the APC gene. *Science*. (1992) 256:668–70. doi: 10.1126/science.1350108
62. Sun X, Essalmani R, Seidah NG, Prat A. The proprotein convertase PC5/6 is protective against intestinal tumorigenesis: *in vivo* mouse model. *Mol Cancer*. (2009) 8:73. doi: 10.1186/1476-4598-8-73
63. Wallner C, Drysch M, Becerikli M, Jaurich H, Wagner JM, Dittfeld S, et al. Interaction with the GDF8/11 pathway reveals treatment options for adenocarcinoma of the breast. *Breast*. (2018) 37:134–41. doi: 10.1016/j.breast.2017.11.010

64. Jemal A, Ward EM, Johnson CJ, Cronin KA, Ma J, Ryerson B, et al. Annual report to the nation on the status of cancer, 1975-2014, featuring survival. *J Natl Cancer Inst*. (2017) 109:djx030. doi: 10.1093/jnci/djx030
65. Liu Y, Shao L, Chen K, Wang Z, Wang J, Jing W, et al. GDF11 restrains tumor growth by promoting apoptosis in pancreatic cancer. *Onco Targets Ther*. (2018) 11:8371–9. doi: 10.2147/OTT.S181792
66. Hogendorf P, Durczynski A, Skulimowski A, Kumor A, Poznanska G, Strzelczyk J. Growth differentiation factor (GDF-15) concentration combined with Ca125 levels in serum is superior to commonly used cancer biomarkers in differentiation of pancreatic mass. *Cancer Biomark*. (2018) 21:505–11. doi: 10.3233/CBM-170203
67. Dichmann DS, Yassin H, Serup P. Analysis of pancreatic endocrine development in GDF11-deficient mice. *Dev Dyn*. (2006) 235:3016–25. doi: 10.1002/dvdy.20953
68. Harmon EB, Apelqvist AA, Smart NG, Gu X, Osborne DH, Kim SK. GDF11 modulates NGN3+ islet progenitor cell number and promotes beta-cell differentiation in pancreas development. *Development*. (2004) 131:6163–74. doi: 10.1242/dev.01535
69. Barresi V, Reggiani-Bonetti L, Di Gregorio C, De Leon MP, Barresi G. Lymphatic vessel density and its prognostic value in stage I colorectal carcinoma. *J Clin Pathol*. (2011) 64:6–12. doi: 10.1136/jcp.2010.083550
70. Ungaro F, Colombo P, Massimino L, Ugolini GS, Correale C, Rasponi M, et al. Lymphatic endothelium contributes to colorectal cancer growth via the soluble matrisome component GDF11. *Int J Cancer*. (2019) 145:1913–20. doi: 10.1002/ijc.32286
71. Liu X, Zhang Q, Fan C, Tian J, Liu X, Li G. GDF11 upregulation independently predicts shorter overall-survival of uveal melanoma. *PLoS ONE*. (2019) 14:e0214073. doi: 10.1371/journal.pone.0214073
72. Gao J, Aksoy BA, Dogrusoz U, Dresdner G, Gross B, Sumer SO, et al. Integrative analysis of complex cancer genomics and clinical profiles using the cBioPortal. *Sci Signal*. (2013) 6:pl1. doi: 10.1126/scisignal.2004088
73. Anon-Hidalgo J, Catalan V, Rodriguez A, Ramirez B, Idoate-Bayon A, Silva C, et al. Circulating concentrations of GDF11 are positively associated with TSH levels in humans. *J Clin Med*. (2019) 8:E878. doi: 10.3390/jcm8060878
74. Zamani N, Brown CW. Emerging roles for the transforming growth factor-{beta} superfamily in regulating adiposity and energy expenditure. *Endocr Rev*. (2011) 32:387–403. doi: 10.1210/er.2010-0018
75. Hsu JY, Crawley S, Chen M, Ayupova DA, Lindhout DA, Higbee J, et al. Non-homeostatic body weight regulation through a brainstem-restricted receptor for GDF15. *Nature*. (2017) 550:255–9. doi: 10.1038/nature24042
76. Luo H, Guo Y, Liu Y, Wang Y, Zheng R, Ban Y, et al. Growth differentiation factor 11 inhibits adipogenic differentiation by activating TGF-beta/Smad signalling pathway. *Cell Prolif*. (2019) 52:e12631. doi: 10.1111/cpr.12631
77. Jing YY, Li D, Wu F, Gong LL, Li R. GDF11 does not improve the palmitate induced insulin resistance in C2C12. *Eur Rev Med Pharmacol Sci*. (2017) 21:1795–802.
78. Dominguez-Perez M, Simoni-Nieves A, Rosales P, Nuno-Lambarri N, Rosas-Lemus M, Souza V, et al. Cholesterol burden in the liver induces mitochondrial dynamic changes and resistance to apoptosis. *J Cell Physiol*. (2019) 234:7213–23. doi: 10.1002/jcp.27474
79. Calvisi DF, Wang C, Ho C, Ladu S, Lee SA, Mattu S, et al. Increased lipogenesis, induced by AKT-mTORC1-RPS6 signaling, promotes development of human hepatocellular carcinoma. *Gastroenterology*. (2011) 140:1071–83. doi: 10.1053/j.gastro.2010.12.006
80. Porporato PE, Filigheddu N, Pedro JMB, Kroemer G, Galluzzi L. Mitochondrial metabolism and cancer. *Cell Res*. (2018) 28:265–80. doi: 10.1038/cr.2017.155
81. Hernandez-Rizo S, Gerardo-Ramirez M, Fucho R, Perez-Aguilar B, Gomez-Quiroz LE, Fernandez-Checa JC, et al. Growth differentiation factor 11 (GDF11) restricts cell proliferation in hepatic tumor cells through glycolysis and lipid metabolism. *Ann Hepatol*. (2018) 17:683. doi: 10.5604/01.3001.0012.0962
82. Garrido-Moreno V, Diaz-Vegas A, Lopez-Crisosto C, Troncoso MF, Navarro-Marquez M, Garcia L, et al. GDF-11 prevents cardiomyocyte hypertrophy by maintaining the sarcoplasmic reticulum-mitochondria communication. *Pharmacol Res*. (2019) 146:104273. doi: 10.1016/j.phrs.2019.104273

Conflict of Interest: The authors declare that the research was conducted in the absence of any commercial or financial relationships that could be construed as a potential conflict of interest.

Copyright © 2019 Simoni-Nieves, Gerardo-Ramírez, Pedraza-Vázquez, Chávez-Rodríguez, Bucio, Souza, Miranda-Labra, Gomez-Quiroz and Gutiérrez-Ruiz. This is an open-access article distributed under the terms of the Creative Commons Attribution License (CC BY). The use, distribution or reproduction in other forums is permitted, provided the original author(s) and the copyright owner(s) are credited and that the original publication in this journal is cited, in accordance with accepted academic practice. No use, distribution or reproduction is permitted which does not comply with these terms.

Biochemical Pharmacology 174 (2020) 113812

Contents lists available at ScienceDirect

Biochemical Pharmacology

journal homepage: www.elsevier.com/locate/biochempharm

HGF induces protective effects in α-naphthylisothiocyanate-induced intrahepatic cholestasis by counteracting oxidative stress

Soraya Salas-Silva[a,b], Arturo Simoni-Nieves[a,b], María Valeria Razori[c], Jocelyn López-Ramirez[a,b], Jonatan Barrera-Chimal[d,e], Roberto Lazzarini[f], Oscar Bello[a], Verónica Souza[b,e], Roxana U. Miranda-Labra[b,e], María Concepción Gutiérrez-Ruiz[b,e], Luis Enrique Gomez-Quiroz[b,e,1], Marcelo G. Roma[c,1,*], Leticia Bucio-Ortiz[b,e,1,*]

[a] Posgrado en Biología Experimental, DCBS, Universidad Autónoma Metrolitana-Iztapalapa, Ciudad de México, Mexico
[b] Departmento de Ciencias de la Salud, Universidad Autónoma Metropolitana, Unidad Iztapalapa, Ciudad de México, Mexico
[c] Instituto de Fisiología Experimental, Facultad de Ciencias Bioquímicas y Farmacéuticas, Universidad de Rosario, Argentina
[d] Departmento de Medicina Genómica y Toxicología Ambiental, Instituto de Investigaciones Biomédicas, Universidad Nacional Autónoma de México, Ciudad de México, Mexico
[e] Unidad de Medicina Traslacional, Instituto Nacional de Cardiología Ignacio Chávez, Ciudad de México, Mexico
[f] Departamento de Biología de la Reproducción, Universidad Autónoma Metropolitana, Ciudad de México, Mexico

ARTICLE INFO

Keywords:
Cholestasis
HGF
Liver
ANIT
Oxidative stress

ABSTRACT

Cholestasis is a clinical syndrome common to a large number of hepatopathies, in which either bile production or its transit through the biliary tract is impaired due to functional or obstructive causes; the consequent intracellular retention of toxic biliary constituents generates parenchyma damage, largely via oxidative stress-mediated mechanisms. Hepatocyte growth factor (HGF) and its receptor c-Met represent one of the main systems for liver repair damage and defense against hepatotoxic factors, leading to an antioxidant and repair response. In this study, we evaluated the capability of HGF to counteract the damage caused by the model cholestatic agent, α-naphthyl isothiocyanate (ANIT). HGF had clear anti-cholestatic effects, as apparent from the improvement in both bile flow and liver function test. Histology examination revealed a significant reduction of injured areas. HGF also preserved the tight-junctional structure. These anticholestatic effects were associated with the induction of basolateral efflux ABC transporters, which facilitates extrusion of toxic biliary compounds and its further alternative depuration via urine. The biliary epithelium seems to have been also preserved, as suggested by normalization in serum GGT levels, CFTR expression and cholangyocyte primary cilium structure our results clearly show for the first time that HGF protects the liver from a cholestatic injury.

1. Introduction

Cholestasis is a clinical condition common to a large number of liver diseases, originated from impairment in bile production or the bile transit through the biliary tree, thus resulting in a decreased amount of bile reaching the duodenum. The cause of this alteration can be a primary impairment in the capacity of hepatocytes to generate bile (hepatocellular or metabolic cholestasis) or a mechanical obstruction of the bile transit (obstructive cholestasis) [1].

Efflux of solutes by ATP-binding cassette (ABC) transporters is the main determining factor in the general capacity of the liver tissue to secrete bile and to detoxify it from endo and xenobiotics [2]. Bile flow generation is driven mainly by the biliary excretion of bile salts and glutathione, which account for the so called bile salt-dependent and bile salt-independent fraction of bile flow, respectively [2]. The canalicular transporter bile salt export pump (Bsep) is the main bile salt transporter, whereas the human multidrug resistance-associated protein 2 (Mrp2) is the main transporter of glutathione into bile, and also of bilirubin glucuronates and a wide range of glucuronide and glutathione conjugated with endo- and xenobiotics. In addition, other members of this transport family, such as Mrp3 and Mrp4, are located in the basolateral membrane, and mediated the extrusion of numerous bile salts

* Corresponding authors at: Departamento de Ciencias de la Salud, Universidad Autónoma Metropolitana Iztapalapa, Av. San Rafael Atlixco 186, Col. Vicentina, 09340, Iztapalapa, Mexico City, Mexico.
E-mail addresses: mroma@fbioyf.unr.edu.ar (M.G. Roma), lebo@xanum.uam.mx (L. Bucio-Ortiz).
[1] Shared senior authorship.

https://doi.org/10.1016/j.bcp.2020.113812
Received 8 December 2019; Accepted 13 January 2020
Available online 16 January 2020
0006-2952/ © 2020 Elsevier Inc. All rights reserved.

and several glutathione-, glucuronic acid-, and sulfate-conjugates [1]. Cholestatic hepatocytes attempt to limit intracellular accumulation of bile salts and other toxic biliary compounds by inducing these basolateral hepatocellular export pumps, thus allowing their urinary excretion. Also, adaptive changes in the proximal renal tubule occurs, which collectively facilitates their renal elimination at the expense of increasing the bile salt burden for the renal tubular system [3].

α-Naphthyl isothiocyanate (ANIT) is a hepatotoxicant that has been used primarily as a tool to study the pathogenesis of chemical-induced cholestasis, particularly drug-induced cholestasis. Its mechanisms of cholestasis involves impairment of bile salt transporter expression, disruption of hepatic tight junction and, lately, biliary obstruction due to desquamation of the epithelial cells of the bile duct [4]. ANIT also causes death of hepatocytes and cholangiocytes by necrosis and apoptosis, both by direct toxic action and, indirectly, through the generation of an intense inflammation associated with the infiltration of neutrophils around the hepatocytes and bile ducts; this inflammatory state leads to the production of reactive oxygen species (ROS), thus inducing oxidative stress which can also cause death of hepatocytes and cholangiocytes, with the subsequent formation of obstructive cellular debris [5]. Many of these alterations are similar to that occurring in obstructive cholangiopathies such as primary sclerosing cholangitis[6] and this is why ANIT-induced cholestasis has been used as an experimental model to mimic this disease [7].

Hepatocyte growth factor (HGF) and its receptor, cellular-Mesenchyme Epithelium Transition factor (c-Met), represent one of the main system for liver repair damage and defense against different hepatotoxic factors, as extensively proved by our group [8–11]. In addition, HGF is required for repairing process in the kidneys [12], lung [13], and pancreas [14], among other organs. It also affords protective effects on epithelial and non-epithelial organs, such as the heart and the brain [15]. This points c-Met signaling as a critical factor in protecting multiple organs against over-generation of ROS [9,16]. That is why the role of HGF/c-Met has been characterized in the regulation of the cellular redox state and the oxidative stress in the liver [8]. HGF/c-Met regulates the activation of key transcription factors that drive the expression of antioxidant and survival genes, such as nuclear factor kappa B (NF-κB) or the nuclear factor-erythroid 2-related factor 2 (Nrf2), leading to cell survival response under oxidative insults [16].

Nrf2 regulates the expression of a broad range of antioxidant and cytoprotective genes, such as NADPH and γ-glutamylcysteine synthetase, hepatocellular transporters, such as Mrp2, Mrp3, Mrp4, Bsep, OATP, OSTα, and phase I metabolizing enzymes, such as Cyp7a1 and Cyp8b1 [16,17].

Currently, there is no effective treatment for cholestatic diseases due to little knowledge of their pathogenesis. This is why cholestatic diseases are the main cause of liver-associated disease, leading to cirrhosis and progressive liver failure that requires liver transplant for the patient to survive [18]. Although, some limited approaches have been reported regarding the protective effect of HGF in ANIT-induced cholestasis in the rat [19], the mechanism of action remained unclear. For this reason, the aim of this work was to characterize the anti-cholestatic effect of HGF in a mouse model of chemical cholestasis induced by ANIT.

2. Materials and methods

2.1. Animal models

Forty 10-weeks-old CD1 male mice were obtained from the Universidad Autonoma Metropolitana Iztapalapa (UAM-I) animal facility and were maintained in pathogen-free conditions with controlled temperature and humidity on a 12 h light-dark cycle in the same facility. The experimental protocols used were approved and carried out in accordance with the UAM-I experimental animal guidelines and NIH Guide for the Care and Use of Laboratory Animals.

2.2. Experimental design

CD1 mice, placed in metabolic cages, were treated or not with ANIT (60 mg/kg, intragastric, Sigma Aldrich, USA, #N4525 diluted in soy oil) for 48 h. After 24 h of ANIT treatment, HGF (10 μg/kg, intravenous, Peprotech, Rocky Hill, NJ, USA, #100–39) was administrated. Forty-eight hours after ANIT treatment, animals were euthanized under isoflurane anesthesia (2% isoflurane and 2 l/min oxygen). Blood, bile, and liver tissue were obtained. Food and water were given *ad libitum*.

2.3. Serum and urine biochemical determinations

Blood samples were obtained from the orbital venous plexus under Anesthesia (2% isoflurane and 2 l/min oxygen). Aspartate aminotransferase (AST), alanine aminotransferase (ALT), alkaline phosphatase (ALP), and γ-glutamyl transpeptidase (GGT) were determined, by using automated method (SpotChem EZ, ARKRAY, USA).

2.4. Bile salt and bilirubin determination

Serum and tissue bile salts content were assayed by using Total Bile Acid Assay (DIAZYME Laboratories, CA, USA) and bilirubin through Jendrassik-Grof FS kit (DiaSys Inc, Canada), following the manufacturer's instructions.

2.5. Hematoxylin-Eosin staining (H-E)

Histology was performed by routine H-E staining, as previously reported [13].

2.6. Bile flow studies

Bile was collected under isoflurane anesthesia. The common bile duct was cannulated with a polyethylene tubing (PE10). Bile was collected for 30 min, and bile flow was determined gravimetrically, by assuming a density of 1 g/ml, as previously reported [20].

2.7. Bile salts elimination in bile

Total bile salts were determined by the 3α-hydroxysteroid dehydrogenase procedure [21].

2.8. ROS in situ determination

After mice euthanasia, fresh liver tissue was rapidly obtained and sectioned, frozen in liquid nitrogen, and embedded in optimum cutting temperature reagent (OCT, Sakura Finetec, Torrance, CA, USA). Immediately, 8-μm frozen sections were obtained in a cryostat (Leica CM-3050S) at −20 °C, and the slides were then incubated for 15 min with dihydroethidium (DHE, 5 μM #D11347, Invitrogen, CA, USA), in the dark and at room temperature, for determination of superoxide radical detecting ethidium fluorescence. Samples were observed using a confocal microscope (Carl Zeiss 780 LSM-NLO), at excitation and emission wavelengths of 485 and 570 nm, respectively, as we previously reported [8].

2.9. Lipid peroxidation

Lipid peroxidation was assayed by the production of thiobarbituric acid reactive substances (TBARS), using a spectrophotometric method [22].

2.10. Western blot

Western blotting was carried out following the protocol previously reported [23]. Briefly, total proteins were isolated from liver

homogenate with T-PER (Pierce, Invitrogen, CA, USA) extraction reagents, supplemented with protease and phosphatase cocktail inhibitors (Roche Inc, Switzerland). One hundred μg of total protein was separated on precast 4–20% gels (Invitrogen Inc, CA, USA), transferred to polyvinylidene difluoride membrane (PVDF, Invitrogen, CA, USA), and probed with anti-CFTR antibody (Abcam #2784, dilution 1:1000, target protein size 168 KDa) and ZO-1 antibody (Invitrogen #617300, dilution 1:1000, target protein size 195 KDa). Membranes were incubated with anti-mouse/rabbit horseradish peroxidase-conjugated secondary antibody. Immunoreactive band was identified with ECL-Plus Western blotting detection reagents (GE Healthcare). Equal loading was demonstrated by probing the same membrane with actin antibody (Sigma-Aldrich #A2060, dilution 1:10000, target protein size 42 KDa).

2.11. Gene expression determination by real-time RT-PCR

Quantification of mRNA levels for five selected HGF/Met target genes was performed. Total RNA was obtained using TRIzol RNA isolation reagent (# 15596018, Thermo Fisher Scientific, USA) following manufacturer's instruction. After DNase digestion with a DNA-free kit (Ambion Inc, Thermo Fisher Scientific, USA), 1 μg of total RNA was reverse transcribed in 20 μl reaction volume with a SuperScript (#170-8891 Invitrogen, CA, USA) first-strand synthesis kit, according to the manufacturer's instructions. Real-time quantitative PCR analysis was carried out with a CFX96 Touch (Bio-Rad) thermal cycler in a 96-well reaction plate. The 10-μl PCR reaction mix contained 5 μl 2X SYBR Green PCR Master Mix (#172-5016 Bio-Rad Laboratories, USA), 200 nM of each primer, and 1 μl cDNA template. Reactions were incubated for 10 min at 95 °C, followed by 40 cycles of 30 sec at 95 °C and 60 sec at specific primer temperature. Melting analysis of the PCR products was also conducted to validate the amplification of the specific product. The expression level of the mouse ribosomal protein S18 (rps18) was used as an internal reference. Relative gene expression levels were calculated with the $2^{-\Delta\Delta ct}$ method. Primer sequences used in the study are listed in Table 1.

2.12. Canalicular width studies by immunofluorescence and image analysis

To assess the structural status of the paracellular tight junctions that seals the bile canaliculus, immunolocalization of the tight junction-associated protein ZO-1 was studied by confocal microscopy (Zeiss Pascal LSM 5, Carl Zeiss, Germany). For this purpose, a liver lobe was excised, and frozen immediately in isopentane precooled in liquid nitrogen, and stored at −80 °C. The, liver samples were sectioned and fixed, and ZO-1 was labeled with polyclonal antibody (#617300, Invitrogen, CA, USA). Immunostaining was completed by treatment of the preparations with appropriate Cy3-conjugated mouse anti-IgGs (Jackson Immuno Research Laboratory, Inc. West Grove PA). Analysis of images was carried out by using the Image J 1.34 m software (NIH). The average canalicular width of each group was assessed as a first approach to correct for distortions in fluorescence intensity induced by changes in canalicular volume, as a result of the treatments. Assessment of the percentage of 'double rail' canalicular, and canalicular width, in confocal images was also performed. To assess the proportion of canalicular double rail structures, the presence of both single and double canalicular rails was quantified, and then the number of double rail structures was divided by the total (single and double rail) canalicular structures. Alternatively, canalicular structures were addressed in liver tissue from c-MetKO mice using rhodamine-phalloidin reagent (#235138, Abcam) in combination with ZO-1 antibody IF. Liver tissue from c-MetKO mice was generously donated by professor Gomez-Quiroz.

2.13. Bile duct structure by scanning electron microscopy (SEM)

SEM Micrographs were obtained with a scanning electron microscope (JEOL JSM-5900 LV). All samples were fixed in 3% glutaraldehyde for 48 h and incubated with osmium tetraoxide for 2 h and dehydrated in 30–100% ethanol. After drying using the critical point dryer, the samples were coated with gold. The SEM was operated at 15 kV accelerating voltage [24].

2.14. Statistical analysis

Data are presented as mean ± SEM for at least 4 different animals; each experiment was carried out in triplicate. For the comparison of means of different groups, an analysis of variance (ANOVA) was used, followed by multiple comparisons by Tukey test. The Graph Pad Prism version 8 software for MacOS was used. The level of significance considered was $p \leq 0.05$.

3. Results

3.1. ANIT induces time-dependent hepatobiliary damage

In order to confirm the ANIT-induced hepatobiliary damage as reported [25,26], we first evaluated the changes with time of the biochemical liver function test assayed in mice treated with ANIT (60 mg/Kg, intragastric). Fig. 1A shows a remarkably increment in serum activity of AST, and indicator of hepatocellular necrosis, since 12 h of treatment onwards, maintaining this value up to 48 h. Total and direct serum bilirubin levels were elevated later, with increments reaching statistical significance at 48 h of ANIT administration, although a tendency towards increased levels can be seen at 36 h of ANIT exposure. The levels of intracellular bile salt retention was evaluated by assessing serum levels of ALP, a plasma membrane-bound hepatocellular enzyme that is induced and released into blood by the detergent bile salts accumulated in cholestasis [27]. Fig. 1 shows an significant increment of the enzyme since 36 h onwards, reaching a maximal value at 48 h; this correlated with the serum bile salt levels, which increase at 36 h, although they modestly decreased at 48 h, perhaps reflecting induction of renal transporters to improve alternative urinary bile salt excretion [3].

Gross liver examination exhibited macroscopic liver lesions (white arrows) with hepatomegaly (Fig. 1B), consistent with an increment in the liver to body weight ratio (Fig. 1C). The organ also revealed gallbladder swelling and dark coloring (Fig. 1B, black arrow).

The liver histology showed prominent necrotic areas (asterisk) and inflammatory infiltration (black arrows and inset), as compared with livers from not treated animals (Fig. 1D). These data clearly show that ANIT induces hepatobiliary damage, although the evident injury is detected from 36 h onwards.

Since a typical cholestatic phenotype is observed at 48 h, in the

Table 1
PCR Primers used in the study.

Protein name	Acronym	Gene	Foward	Reverse
Bile salt efflux pump	Bsep	*Abcb11*	GGCTTGCTACAGATGCTTCC	GCCAAAAAGGGGAAGAAGAC
Multidrug resistance-associated protein 2	Mrp2	*Abcc2*	CTGAGTGCTTGGACCAGTGA	CCCACAGTCACCATCCTCTT
Multidrug resistance-associated protein 3	Mrp3	*Abcc3*	CCCTGCTCCTGTCTTCTTTG	GCTGAGAGGATCTTGGAACG
Multidrug resistance-associated portein 4	Mrp4	*Abcc4*	CATACCATTGGTTCCGCTCT	GTCAGGAGCTGTTTGATGCA
Ribosomal protein s18	s18	*rps18*	TGTGGTGTTGAGGAAAGCAG	TCCCATCCTTCACATCCTTC

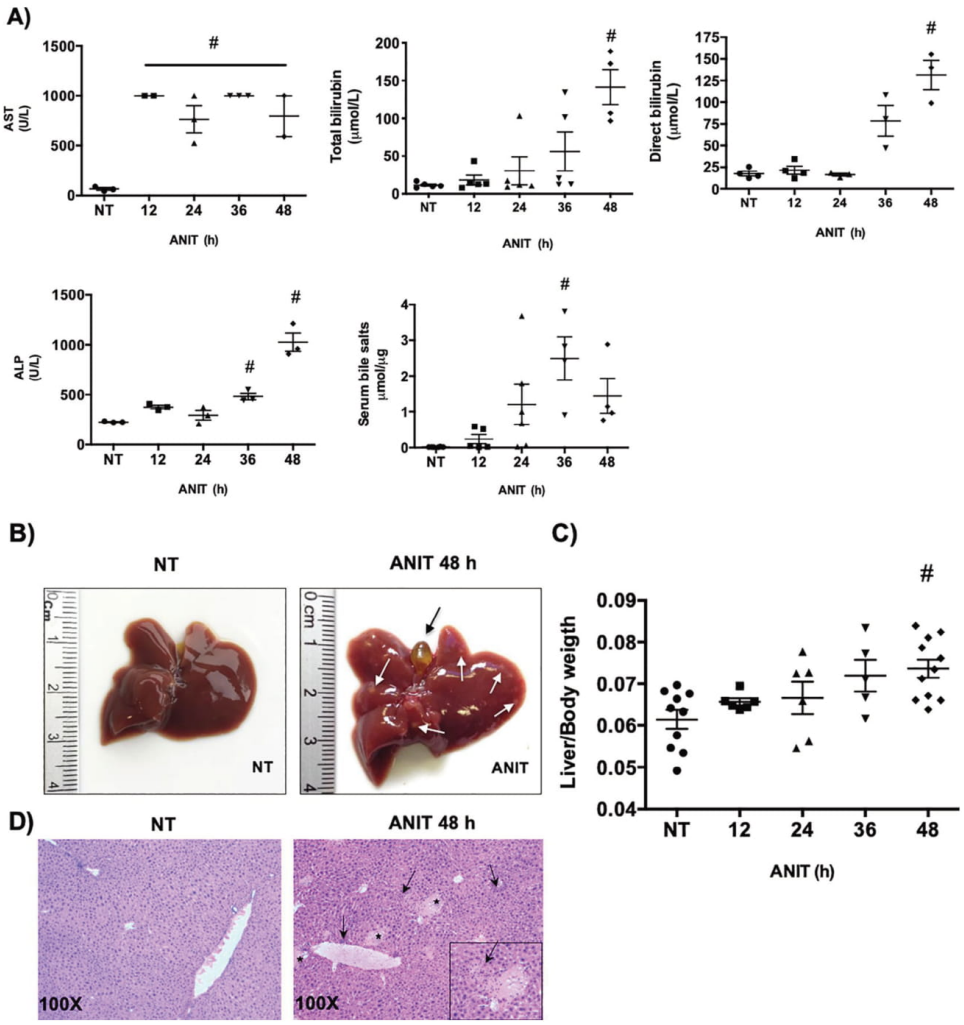


Fig. 1. ANIT induced liver damage determined by liver functional tests. A) Aspartate aminotransferase (AST) activity, Total bilirubin, Direct bilirubin concentration, Alkaline phosphatase (ALP) activity and Serum bile salt content. B) Macroscopic liver inspection of ANIT treatment (white and black arrows show nodulary and gallbladder swelling and dark coloring respectively). C) Liver-to-body weight ratio. D) Histology appearance by H&E staining (black stars indicate areas with necrosis, and arrows show inflammatory infiltrate). The images are representative of at least 3 experimental animals and are shown at 100× the original magnification. Each group represents the median ± SEM in at least four different mice, $^{\#}p < 0.01$ vs NT.

remaining experiments we decided to explore the effects of HGF at this time.

3.2. HGF has anticholestatic properties

As we had previously reported, HGF induces hepatoprotective properties in the liver [8,28]. To ascertain whether this protection could be displayed under a cholestatic condition induced by ANIT, we treated animals with this chemical and we evaluated HGF capability to normalize a number of biochemical liver function tests in mice (Fig. 2A). HGF treatment significantly decreased AST, ALT, ALP, and GGT serum levels (27.6, 7.4, 2.6 and 2.8-fold, respectively). Even more, we observed a significant drop in total (5.4-fold) and direct bilirubin (10.9-fold) in the co-treated group, as compared with mice treated only with ANIT. Similarly, the treatment with HGF fully normalized bile salt levels in both serum and tissue, by improving bile salt levels 19.3-fold and 1.7-fold, respectively.

These data were in agreement with macroscopic inspection of the liver (Fig. 2B). Animals treated with ANIT + HGF presented a significant decrease in tissue lesions, nodularity (white arrows), gallbladder swelling and coloring, and the hepatomegaly decreased to normal values, as shown in Fig. 2C.

The H-E staining showed preservation of the tissue integrity in samples from co-treated animals, as compared to those treated with

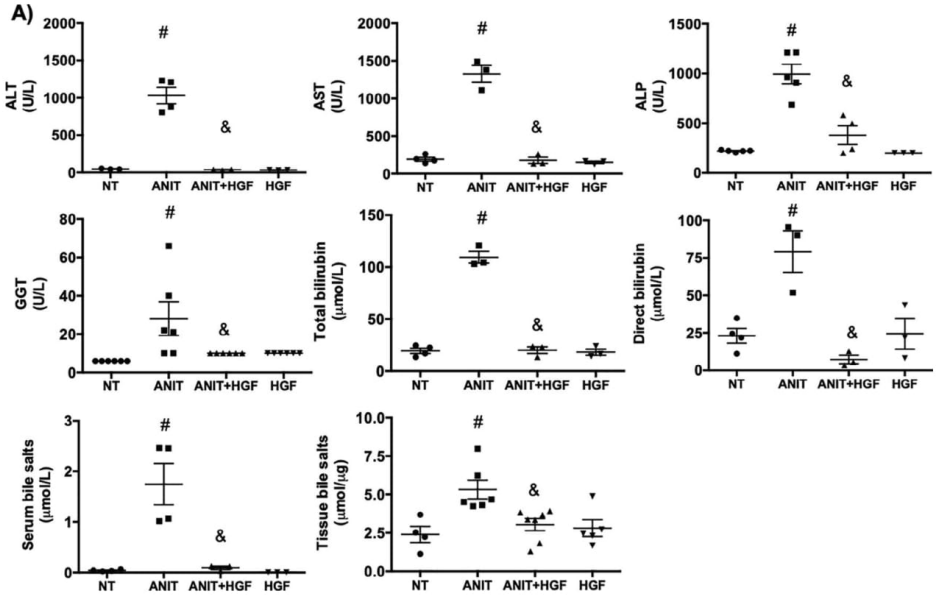


Fig. 2. HGF protects against the cholestatic damage induced by ANIT. A) Alanine aminotransferase (ALT), aspartate transferase (AST), alkaline phosphatase (ALP), γ-glutamil transpeptidase (GGT) activity, total and direct bilirubin concentration, and the serum and tissue levels of bile salts. B) Macroscopic liver inspection of treated groups (white and black arrows show nodulary). C) Liver-to-body weight ratio. D) Histology appearance by H&E staining (black stars indicate areas with necrosis, and arrows show inflammatory infiltrate). The images are representative of at least 4 experimental animals and are shown at 50× and 100× the original magnification. E) Bile flow. Each group represent the median ± SEM in at least four different mice, $^{\#}p < 0.01$ vs NT, $^{\&}p < 0.01$ vs ANIT. F) Bile salts biliary excretion. Each bar represents the median ± SEM in at least four different mice.

ANIT alone; the necrotic areas (asterisk) were significantly decreased by HGF, and inflammatory infiltration was not observed (Fig. 2D).

3.3. HGF restores ANIT-induced bile flow impairment

Bile flow decreased approximately 1.7-fold in ANIT group as compared to the non-treated (NT) group. However, under HGF co-treatment, bile flow was restored to normal values (Fig. 2E), together with a tendency towards increase bile salt output, which did not reach statistical significance (Fig. 2F); this suggests preferential exportation of accumulated bile salts via urine rather than via the biliary route. HGF induced neither choleresis nor increase in bile salt output *per se*.

3.4. HGF diminishes ANIT-induced oxidative stress

To ascertain whether HGF improves the cholestasis by normalizing redox homeostasis, we evaluated the levels of superoxide radical ($O_2^{\cdot-}$) in fresh liver sections in all groups. The confocal images showed that ANIT treatment increased significantly O_2^- cellular content (20-fold) versus the NT group. However, in the co-treated group, this ROS exacerbated levels considerably diminished (Fig. 3A). This was in agreement with the lipid peroxidation data, which were fully normalized by HGF (Fig. 3B), thus confirming that HGF decreases the oxidative damage induced by ANIT exposition.

3.5. HGF preserves the tight-junctional structure disturbed by ANIT

To explore further the possible mechanisms underlying the anticholestatic effects of HGF, and since integrity of tight-junctional complexes that seal the bile canaliculus are required to maintain the bile-to-blood gradients that drive bile formation [29], we analyzed the effect of HGF on the disorganization of these structures, by studying the localization of the tight-junctional protein zonula occludens-1 (ZO-1). To analyze this disorganization at the structural level, we addressed the status of the "double rail" or "train track" [30] canalicular structure by ZO1 immunofluorescence [31]. As shown in Fig. 4A, under normal conditions the bile canaliculus is defined as an intercellular space formed by the apposition of the edges of gutter-like hemicanals delimited by tight junctions, on the facing surfaces of adjacent hepatocytes [32], and this could be identified by a "double rail"-like structure [31], (Fig. 4A, yellow arrow and inset). ANIT treatment induced a decrease in the number of canalicular "double rail" structures (Fig. 4B). Actually, this group predominantly showed a "single rail" feature (white arrow), with a spiral-like structure. HGF cotreatment efficiently preserved the double rail structure similar to that in the NT group (Fig. 4B). Remarkably, HGF alone treatment substantially increased the canalicular width (green arrow) as compared with that of the NT group (1.4-fold) and normalized the decrease in this parameter induced by ANIT (Fig. 4C).

Interestingly, liver tissue from c-MetKO animals [9], (Fig. 4D), presented same abnormalities in the canalicular structure as those observed in both ANIT-treated mice and in the β-catenin KO mouse [30], with no changes in ZO-1 content (Fig. 4E).

These data suggest the HGF involvement in the organization of tight-junctional structures, which are required for normal bile secretion.

3.6. HGF normalize impairment of cystic fibrosis transmembrane conductance regulator (CFTR) induced by ANIT

A common feature in cholangiopathies is the defective ductular secretion of a bicarbonate-rich fluid secretion, which is driven by the

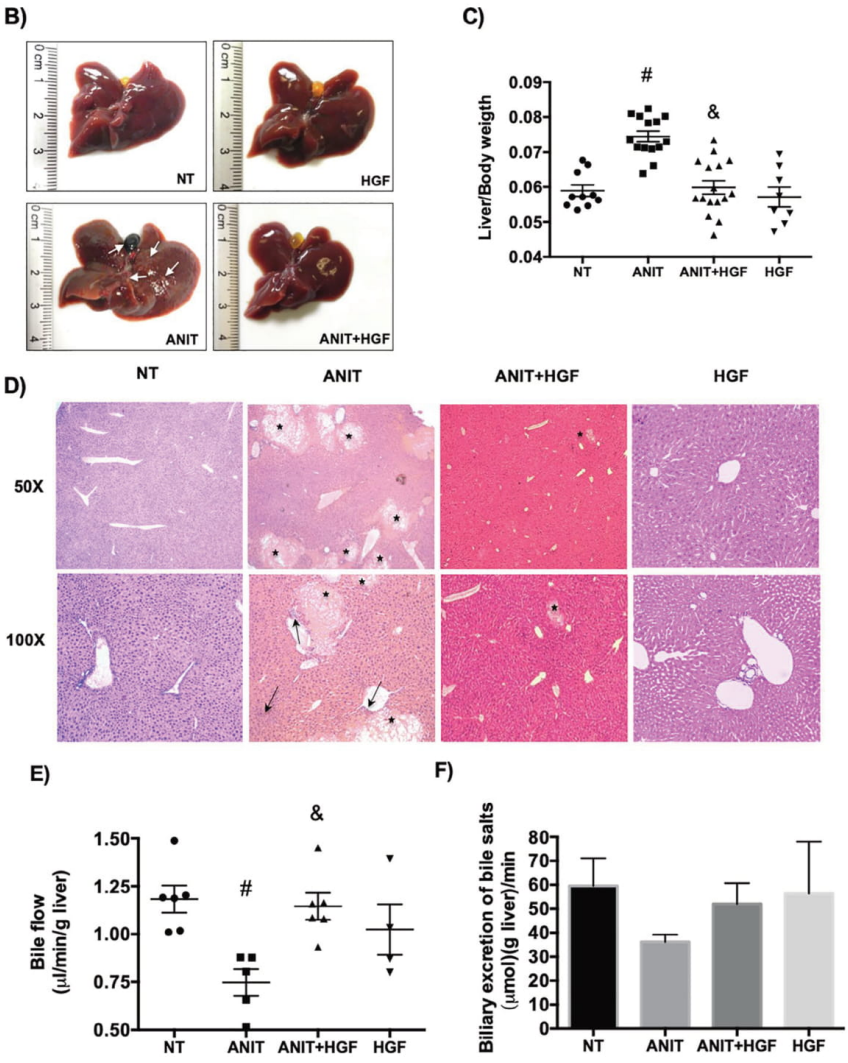


Fig. 2. (*continued*)

ATP-dependent chloride channel, CFTR [33]. Since this ductular bicarbonate-rich secretion has protective effects against bile salt -induced bile duct damage in cholestasis (the so called "bicarbonate umbrella") [34], CFTR function is considered to be a critical factor in protecting the biliary epithelium in cholestatic cholangiopathies. We therefore decided to explore the status of this apical membrane protein in our model. As shown in Fig. 4F, ANIT induced a significant decrease in CFTR expression, and co-treatment with HGF restored this parameter to basal values. Furthermore, HGF had *per se* a stimulatory effect on CFTR expression.

3.7. HGF protects the cholangiocellular cilium from ANIT damage

Cholangiocyte primary cilia are important for normal ductular bile secretion, and defects in its structure and/or function lead to altered ductular fluid secretion [35]. Therefore, we explore the damage caused by ANIT in cholangiocytes, particularly in the primary cilia, at 48 h of exposure. We assessed morphology by scanning electron microscopy (SEM). The primary cilia were shorter and virtually absent, and HGF cotreatment restored the normal cilium morphology (Fig. 5).

3.8. HGF induces basolateral efflux ABC transporters expression

Alterations in ABC transporters play an important role in the cholestatic process [1]. For this reason, we evaluated the genetic expression of the *Abcc2, Abcb11, Abcc3, and Abcc4* genes. *Abcb11*/Bsep is a canalicular transporter that exports bile salts into bile, whereas *Abcc2*/Mrp2 excrete glutathione and endo- and xenobiotics conjugated with

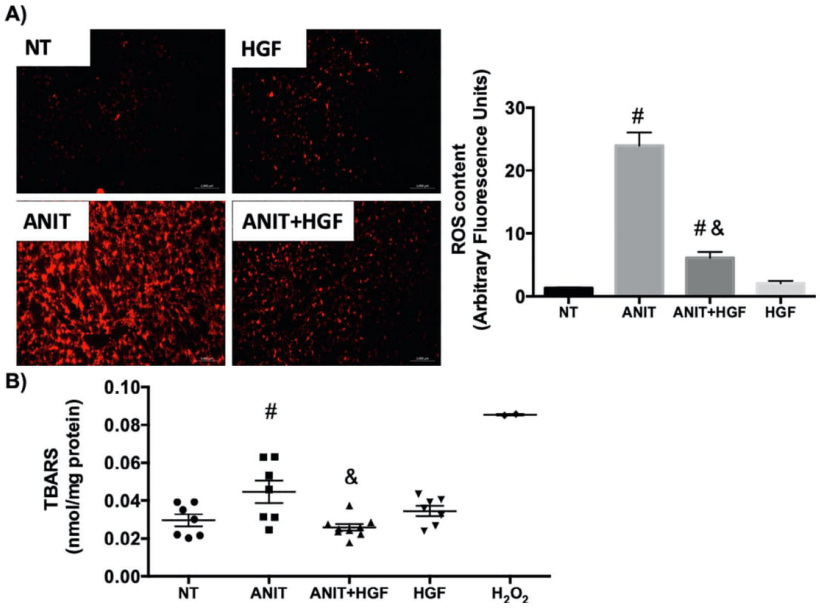


Fig. 3. HGF counteract the alterations in redox homeostasis induced by ANIT. A) Representative images obtained by confocal microscopy (original magnification X100) of superoxide content in liver tissue, as visualized in red with the superoxide probe dihydroethidium (left panel), and the corresponding fluorescence quantification of superoxide tissular levels by densitometric analysis (right panel). B) Lipid peroxidation determination assayed by thiobarbituric acid reactive substances (TBARS). Each group represents median ± SEM in at least five different mice. $^{\#}p < 0.01$ vs NT, $^{\&}p < 0.01$ vs ANIT. (For interpretation of the references to colour in this figure legend, the reader is referred to the web version of this article.)

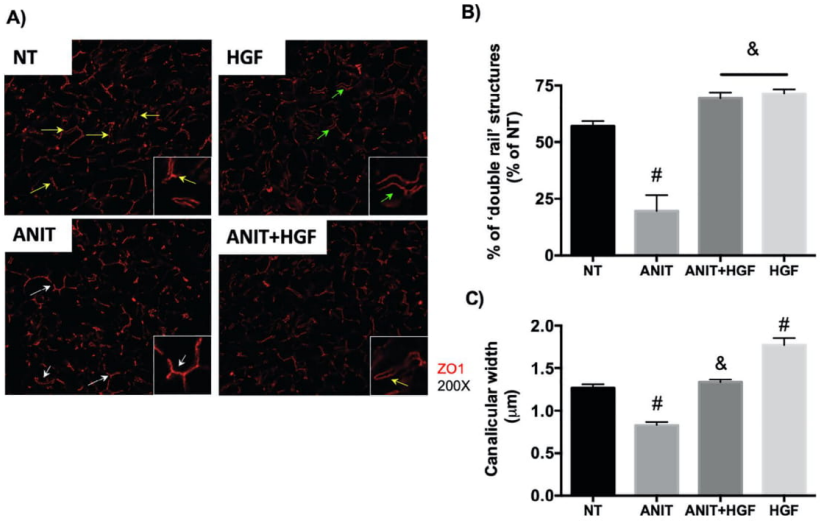


Fig. 4. HGF counteract the structural alterations in tight junctions induced by ANIT. A) Immunofluorescence determined by confocal microscopy of ZO-1 (yellow, white and green arrows show double rail, mono rail, and wider double rail respectively), Original magnification 200×. B) Quantification of the proportion of double rail canalicular structure. C) Canalicular width quantification. D) Representative confocal image composition of immunofluorescences of canalicular structure in liver tissue from untreated wild-type (WT) and c-MetKO. Rhodamine-phalloidin (red), ZO-1 (green). DAPI was used for nuclei identification (blue). E) ZO-1 content addressed by Western blot in liver tissue from c-MetKO and WT mice. The images are representative of at least 4 experimental animals. F) Western blot of CFTR and densitometric analysis. The images are representative of at least 3 experimental animals. Each bar represents median ± SEM, $^{\#}p < 0.01$ vs NT, $^{\&}p < 0.01$ vs ANIT. (For interpretation of the references to colour in this figure legend, the reader is referred to the web version of this article.)

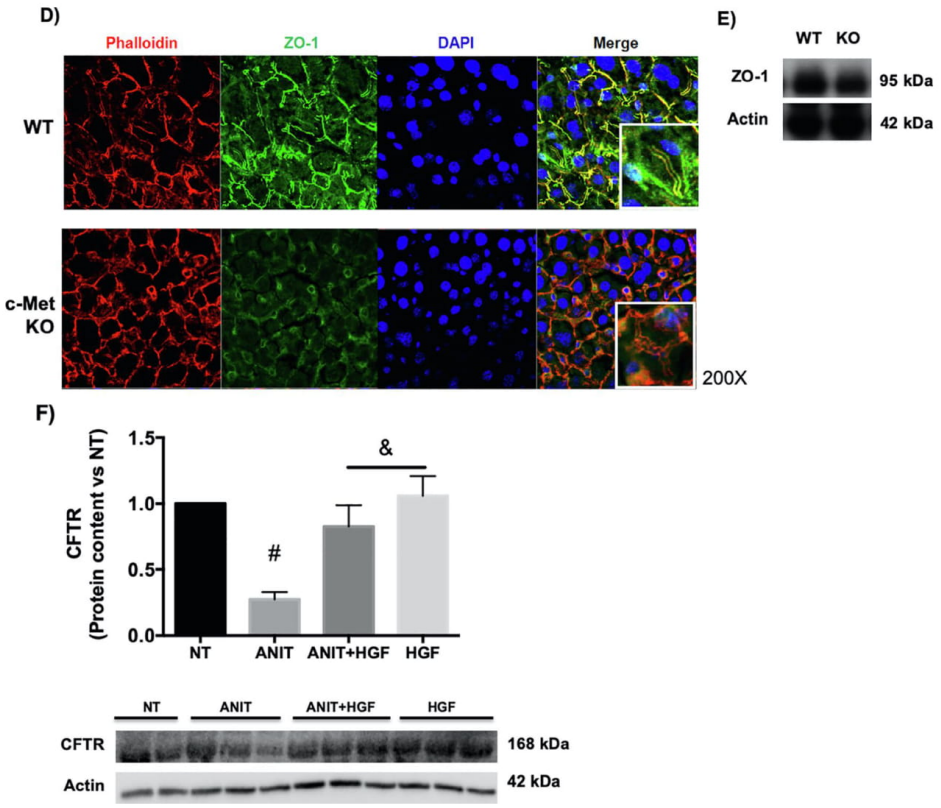


Fig. 4. (*continued*)

glutathione or glucuronic acid, such as glucuronide bilirubin (Fig. 6). *Abcc2*/Mrp2 and *Abcb11*/*Bsep* mRNA levels increased in ANIT alone group, probably as an adaptive mechanism in cholestasis, while the co-treatment with HGF counteracted these changes. On the other hand, the mRNA levels of the basolateral transporter *Abcc3*/Mrp3 and *Abcc4*/Mrp4 increased in co-treated animals (Fig. 6), and interestingly, *Abcc4*/Mrp4 increased as well in HGF alone treatment.

Improvements in the expression of *Abcb11*/Bsep at the canalicular level and that of *Abcc3*/Mrp3 and *Abcc4*/Mrp4 at the basolateral level may help to explain the improved depuration of bile salts and bilirubin in the co-treated group (Fig. 2A), and the lower damage at the histological level (see Fig. 2D).

4. Discussion

HGF exerts protective effects in different liver diseases, such as fibrosis [28], hepatocarcinogenesis [36], and drug-induced hepatotoxicity [8], among others [10]. An improvement in survival response has also been documented in other organs, such as the pancreas [14] and lungs [13], particularly by a mechanism dependent on ROS modulation.

The pathogenesis of cholestatic diseases remains poorly studied, despite the increase in incidence [6,37,38]. Consequently, new therapeutic options are required to counteract these disorders. In the present work, we aimed to evaluate the protective role of HGF in intrahepatic cholestasis by using ANIT as a model of cholestatic hepatobiliary damage.

ANIT-induced cholestasis leads to the accumulation of bile salts in the liver parenchyma, and this represents a second hit that contributes to perpetuation of the disease. Although the mechanism of ANIT-induced cholestasis has not been yet fully elucidated, a recent study showed that ANIT can impair expression of a number of hepatobiliary transporters involved in bile acid hepatic handling in sandwich-cultured rat primary hepatocytes [39], in line with our results here "in vivo". This seems to involve bile salt-dependent AMPK activation via the ERK1/2-LKB pathway, and the further repression of farnesyl X receptor, a master nuclear receptor that regulates bile salt homeostasis [40]. A number of adaptive mechanisms are activated in an attempt to attenuate bile acid accumulation and protect hepatocytes against further injury, mainly induction of basolateral export pumps that extrude these compound to blood, thus allowing their further urinary excretion as an alternative depuration pathway [41]. Oxidative stress seems to play a key role in ANIT-induced cholestasis. In line with our results here, lipid peroxidation, a surrogate marker of oxidative stress, increased rapidly (from 12 h onwards) after "in vivo" ANIT administration, through mechanisms involving, at least in part, a pro-oxidant unbalance by ROS derived from neutrophils infiltrated into the liver tissue [42] and activation of NADPH oxidase 4 expression [43] on one hand, and impairment of antioxidant defenses, including impaired activity of superoxide dismutase and catalase activity [44] on the other hand. Oxidative damage can represents, therefore one of the main first hit that mediates ANIT cholestatic effect on hepatocytes, as oxidative stress rapidly triggers cholestatic mechanisms, including actin

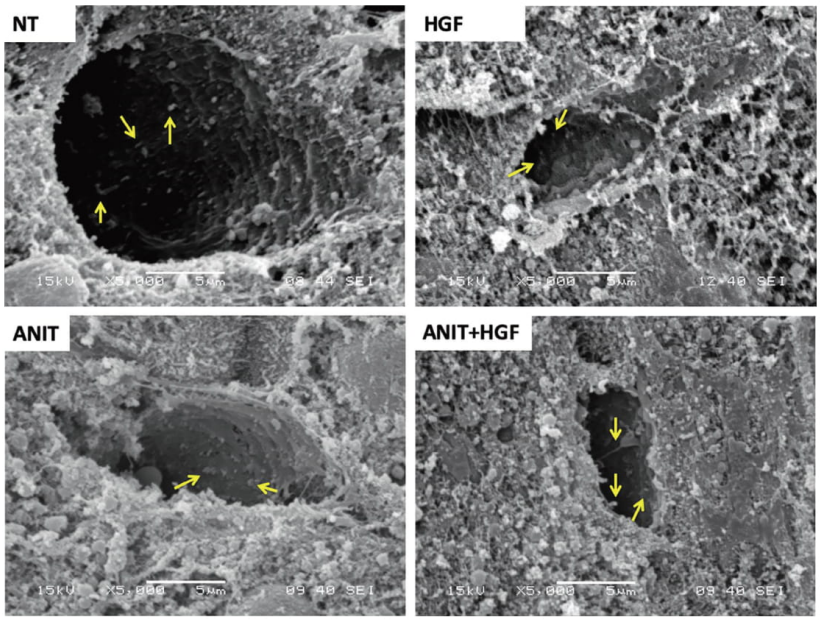


Fig. 5. HGF preserves the cholangiocellular primary cilium. Scanning electron micrograph from livers showing cilia from bile canaliculi (arrows). The images are representative of at least three animals.

disorganization followed by endocytic internalization of the canalicular export pumps Bsep [45], and Mrp2 [46], and thigh-junctional disruption [45]; this leads to a second hit associated with the rapid bile salt accumulation, which may further aggravate oxidative damage, since bile salts are strong pro-oxidant compounds that can promote ROS-mediated hepatocellular apoptosis and necrosis [47], as observed in our cholestatic model. It is therefore not surprising that antioxidants has anticholestatic effects on ANIT-induced cholestasis, as was shown for α-tocopherol [44], paeoniflorin [43], SRT1720 [48], and melatonin [44,49], among many others antioxidant compounds. Interestingly, some of these compounds, such as melatonin [50], SRT1720 [48], 18ß-glycyrrhetinic acid [51], paeoniflorin [52], and dioscin [53], exert antioxidant and anticholestatic effects in ANIT-induced cholestasis and, simultaneously, Nrf2 activation, thus suggesting a causal association between both phenomena. It is therefore highly likely that HGF had exerted anticholestatic effects by activation of Nrf2, since this nuclear receptor is a main downstream mediator of this growth factor [16]. Evidences that a "pure" Nrf2 activation can exert anticholestatic effects are however currently lacking. Oltipraz, a well-known Nrf2 activator, had however anticholestatic effects in Nrf2-null mice [26], thus suggesting that this compound protects livers from ANIT-induced hepatotoxicity via a Nrf2 pathway-independent pathway, perhaps involving constitutive androstane receptor (CAR), a nuclear receptor with anticholestatic properties that is also activated by oltipraz [54]. Therefore, our evidence here on the anticholestatic effects of HGF, a pleiotropic cytokine that selectively activates Nrf2 as we previously reported [16], adds supports to the anticholestaic effects of Nrf2 *per se*.

The possible mechanisms by which HGF would afford anticholestatic effects via Nrf2 in our model are multifactorial. We have shown that HGF as a master regulator of the cellular redox state, since it displays mechanisms mediated by Nrf2 directed to both the induction of antioxidant enzymes [9,10] and the abrogation of pro-oxidant systems, such as NADPH oxidase, which are involved in ANIT-induced cholestasis [43]. Our results clearly show a remarkable increment in ROS content induced by ANIT, and the significant normalization afforded by HGF (Fig. 3), thus suggesting that this cytokine abrogate indeed this pro-oxidant first hit triggering the cholestatic phenotype.

Although this effect likely involved the Nrf2-mediated induction of antioxidant proteins, Nrf2 also induces phase II and III detoxification processes, leading to the elimination of noxious compounds, which, in addition, exerts an indirect antioxidant effect by removing pro-oxidant entities [16,17].

As for phase II detoxification systems, this transcription factor positively modulates the expression of hepatocellular transporters impaired by ANIT, or that of basolateral export pumps that help to maintain low the intracellular levels of bile salts despite the secretory failure; this abrogates the bile salt-mediated second hit, which leads to hepatocellular death, among other deleterious effects. In the present work, we observed an increment in the basolateral bile salts transporter Mrp3 and Mrp4 hepatic expression due to HGF treatment in mice co-treated with ANIT (Fig. 6), thus supporting this content. As shown by studies in Mrp3 and Mrp4 knockout mouse models, bilirubin (mainly as glucuronide conjugates), are the preferred substrate for Mrp3, whereas bile acid conjugates are the preferred substrate for Mrp4 in the cholestatic liver[55]. Both endogenous bile salts [56], and bilirubin [57], particularly in their unconjugated (apolar) form, are highly cytotoxic substances, leading to cell death by necrosis and apoptosis through different mechanisms, involving mitochondrial dysfunction with further oxidative stress generation, disorganization of the plasma membrane, and reticulum endoplasmic stress, among other deleterious effects.

On the other hand, HGF exerts a differential effect on canalicular transporters by transcriptionally decreasing Bsep and Mrp2 expression (Fig. 6), thus suggesting redirection of these compounds to the bloodstream [58,59]. Lack of induction of these transporters and the resulting absence of choleretic effect of HGF may have important positive

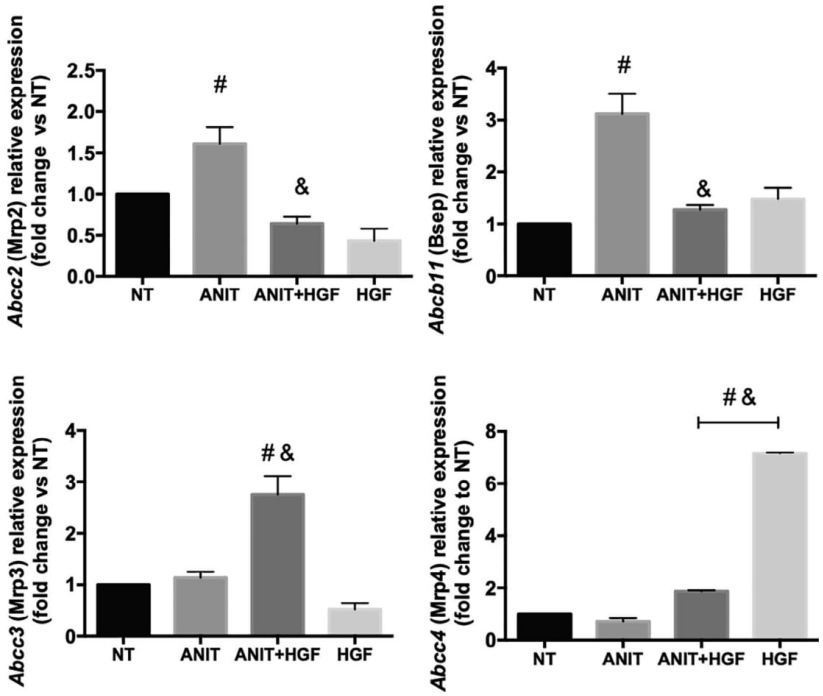


Fig. 6. HGF modulates efflux ABC transporter expression. Messenger RNA levels of the ABC transporters genes Abcc2, Abcb11, Abcc3 and Abcc4. Each bar represents median ± SEM. $^{\#}p < 0.01$ vs NT, $^{\&}p < 0.01$ vs ANIT.

therapeutic implications, particularly under biliary obstruction conditions, as occurs in our model [25], and in obstructive cholangiopathies in humans. This is consistent with findings in the Mrp2-deficient rat which presented protection in ANIT-induced cholestasis [60], it is clear that basolateral elimination of ANIT instead of the biliary route avoids the cholestatic damage as observed in both the HGF-treated mice and the Mrp2-deficient rat.

The choleretic, anticholestatic therapeutic bile acid UDCA, which induced selectively Bsep to increase bile acid-dependent bile flow in ANIT-induced cholestasis, aggravated liver injury when the bile ducts were obstructed [61]. This is most likely a consequence of the biliary infarcts of Hering canals due to the increased intraluminal hydrostatic pressure in obstructed ducts, which leads to extravasation and direct contact of toxic bile with hepatocytes [62]. Suggestively, the clinical benefit of UDCA in the treatment in obstructive cholangiopathies, such as PSC and late-stage primary biliary cholangitis, are limited, when not detrimental [63]. Therefore, therapeutic options that redirects biliary toxic compounds into urine without generating neither choleresis nor increase in bile salt output, as showed here for HGF (Fig. 2 E and F), may be particularly helpful in obstructive cholangiopathies.

HGF seems to have not only favorable functional impact on the cholestatic injury, but also important effects on structural features, such as tight junctional structures, ultimately impact on the secretory function. ANIT is known to alter tight junctional-dependent paracellular permeability as soon as 16 h after ANIT administration [25,64], leading to dissipation of biliary osmotic gradients via the paracellular shunt and, consequently, bile flow impairment. We have shown here that these functional changes in the tight-junctional barrier has a clear structural correlate. Gross alterations in localization of ZO-1, an F-actin–binding protein that localizes to tight junctions and connects them to actin cytoskeleton, were observed, as a loss of its characteristic 'double rail' array (Fig. 4). Since a reduction in actin expression was reported to occur at 48 h of ANIT exposure [65], ZO-1 disorganization can be a direct consequence of the loss of its anchor protein, actin. This does not rule out the possibility that, besides, disorganization of F-actin, a common feature under oxidative stress conditions [45], may have also contributed to ZO-1 disorganization. Even, actin oxidation without actin disorganization may be involved, since oxidative changes in this protein usually inhibits its association with actin-binding proteins, like ZO-1 [66]. Whatever is the underlying mechanism, HGF fully prevented ZO-1 disorganization, opening the possibility that the cytokine also prevents the tight-junction impairment at a functional level.

Our study also provides evidence of cholangiocytes damage, as judged by GGT elevations (Fig. 2A), a cholangiocellular but not hepatocellular enzyme that is induced and removed by biliary bile salts in obstructed ducts [67], the decreased activity of the cholangyocyte chloride channel CFTR (Fig. 4D), and the shortening/disappearance of the primary cilia (Fig. 5). Bile duct damage in ANIT-induced cholestasis occurs by the reversible formation of an unstable glutathione-ANIT conjugate within hepatocytes, which partially dissociates once secreted into bile via Mrp2 due to the alkaline milieu, yielding glutathione and high, toxic levels of unconjugated ANIT in bile [60]. The toxic effects seems to be mediated by highly reactive products formed from the thiocyanate moiety of the molecule after dissociation [68], that can interact with sulfhydryl groups of cholangiocellular surface proteins; damaged proteins are then endocyted and transported to the endoplasmic reticulum, where they initiate of the unfolded protein response and further oxidative stress [68].

The protective effect of HGF at this level may involve accelerated exportation of the glutathione-ANIT conjugate into blood and its further

urinary excretion via induction of Mrp4, which is an efficient glutathione S-conjugate transporter[69], or direct antioxidant effects of HGF on cholangiocytes, thus protecting them from ANIT-induced oxidative stress and cholangiocyte death. In line with this view, the HGF receptor c-Met seems to be expressed in normal cholangiocytes, as inferred for its readily apparent expression in the cell line of normal, immortalized cholangiocytes H69 [70]. Our findings that CFTR is donwregulated in ANIT-intoxicated animals and that its expression is restored by HGF are both novel and may have profound physiopathological and therapeutic implications. As part of its harmful effects on the biliary tree, ANIT induces a strong inflammatory response at this level, and CFTR was shown to be downregulated by proinflammatory cytokines in epithelial cells [71], probably thorough a mechanisms involving oxidative stress [72]. The decrease in CFTR activity may contribute to ANIT-induced cholestasis by impairing the bicarbonate-rich choleresis due to lack of luminal chloride to be exchanged by bicarbonate via the AE2 exchanger, and this may produce *i*) decreased ductular bile flow leading to inspissation and mucus plugging, thus aggravating the obstructive process, and *ii*) lack of the so called "bicarbonate umbrella", which maintain bile salts in their ionic, non-diffusible form, thus impeding cholangiocyte from being attacked by these toxic compounds [73]. In addition, loss of cholangiocyte primary cilium induced by ANIT, as we have shown here (Fig. 5), can contribute to the pathogenesis of the disease. Cholangiocytes proliferate under an obstructive cholestatic condition, as an adaptive response to the liver injury caused by bile salt overload. This adaptive mechanism consistent of expansion of bile ducts and induction of liver progenitors that can differentiate into both hepatocytes and cholangiocytes to replace the damaged cells [74]. The primary cilia are the chemosensors that mediate this adaptive mechanism triggered bile salts, since they express the bile salt receptor TGR5 [74,75]. Therefore, by counteracting cilium damage, HGF would allow bile ducts to trigger this adaptive, reparative process.

In addition, inflammatory infiltrate presented by damaged tissues [76] was not found in ANIT + HGF liver sections (Fig. 2D), suggesting that HGF could also act as a possible immunomodulatory agent, as previously suggested [13,77].

Although all these protective effects were induced by supraphysiological levels of HFG, even physiological levels of HGF seems to afford certain anticholestatic effects. As reported previously by our group [11], mice fed with high cholesterol diet displayed high serum bile salt levels, but the effect was more pronounced in Met KO animals. Indeed, cholesterol-fed Met KO mice had an increased bilirubin and ALP serum levels. Also, they presented a decrease in FXR levels, a key transcription factor for bile salt homeostasis whose impaired expression has been suggested to be a pathogenic factor in many cholestatic diseases, and that foster liver regeneration and growth properties that help to repair liver damage [78].

We also reported that one of the main hepatopathies developed by the lack of c-Met in the c-Met KO mouse was cholestasis. The global transcriptomic analysis of these mice exhibited defective signaling pathways associated to normal hepatobiliary function, such as bile acid biosynthesis, glutathione metabolism, and Nrf2-mediated oxidative stress response [11]. These results further support our contantion that HGF, given at supraphysiological levels for pharmacological purposes, can counteract pathogenic mechanims in cholestatic diseases when their pathomechanisms involves deficit in any of these HGF-regulated pathways, by counteracting this deficiency with an strengthened HGF signaling.

An interesting finding we made was that the absence of c-Met in MetKO animals produced a disruption in the canalicular structure (Fig. 4D). The observed effect is only structural, since no change in the content of ZO-1 was observed (Fig. 4E). These results confirm that HGF/c-Met are of main importance for proper canalicular structure. β-Catenin, one of the canonical efectors of HGF/c-Met signaling, is a key regulator of canalicular morphology and function, and liver-specific loss of this protein is directly associated with imperfect bile canalicular morphology, a physiological dysfunction leading to cholestasis [30].

In conclusion, our study highlights a novel aspect of HGF as anticholestatic agent, which protects the liver against ANIT-induced cholestatic damage. This points HGF and its relevant downstream mediators as a possible therapeutic tool for cholestasis treatment.

CRediT authorship contribution statement

Soraya Salas-Silva: Investigation, Methodology. **Arturo Simoni-Nieves:** Investigation. **María Valeria Razori:** Investigation. **Jocelyn López-Ramirez:** Investigation. **Jonatan Barrera-Chimal:** Data curation. **Roberto Lazzarini:** Investigation. **Oscar Bello:** Investigation, Methodology. **Verónica Souza:** Investigation, Validation. **Roxana U. Miranda-Labra:** Investigation, Validation. **María Concepción Gutiérrez-Ruiz:** Data curation, Validation, Writing - review & editing. **Luis Enrique Gomez-Quiroz:** Methodology, Data curation, Funding acquisition, Writing - original draft, Writing - review & editing. **Marcelo G. Roma:** Data curation, Funding acquisition, Writing - original draft, Writing - review & editing. **Leticia Bucio-Ortiz:** Funding acquisition, Methodology, Writing - original draft, Writing - review & editing.

Declaration of Competing Interest

The authors declare that they have no known competing financial interests or personal relationships that could have appeared to influence the work reported in this paper.

Acknowledgements

This work was partially funded by a grant from the Consejo Nacional de Ciencia y Tecnología (CONACYT), Mexico (CB-A1-S-38154, CB-252942, Infra-2017 280788, Infra-2013 205941), "Estímulo Antonio Ariza Cañadilla 2017" from FUNDHEPA, Mexico. Universidad Autónoma Metropolitana Iztapalapa, Mexico. PUE-CONICET 0089 from Consejo Nacional de Investigaciones Científicas y Tecnologicas, Argentina, and PICT-2016-1613, from Agencia de Promocion Científica y Tecnologica, Argentina.

We thank Dr. Cristina Acosta-Garcia from the Divisional Scanning Electron Microscopy Core Facility, Roberto Lazzarini from the Divisional Confocal Core Facility UAM-I, and Dr. Agustina Cano Martínez, Departamento de Fisiología, Instituto Nacional de Cardiología Ignacio Chávez, for assistance in tissue assays.

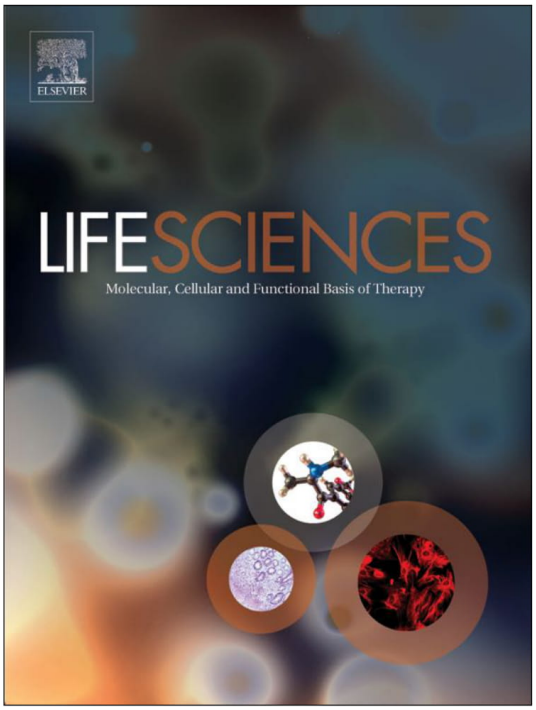
References

[1] M.G. Roma, F.A. Crocenzi, E.A. Sanchez Pozzi, Hepatocellular transport in acquired cholestasis: new insights into functional, regulatory and therapeutic aspects, Clin. Sci. (Lond.) 114 (9) (2008) 567–588.
[2] M.G. Roma, F.A. Crocenzi, A.D. Mottino, Dynamic localization of hepatocellular transporters in health and disease, World J. Gastroenterol. 14 (44) (2008) 6786–6801.
[3] A. Brandoni, M.H. Hazelhoff, R.P. Bulacio, A.M. Torres, Expression and function of renal and hepatic organic anion transporters in extrahepatic cholestasis, World J. Gastroenterol. 18 (44) (2012) 6387–6397.
[4] L.J. Dahm, P.E. Ganey, R.A. Roth, 9.25 – α-Naphthylisothiocyanate A2 – McQueen, Charlene A. In. Comprehensive Toxicology, second ed., Elsevier, Oxford, 2010, pp. 571–579.
[5] P. Kodali, P. Wu, P.A. Lahiji, E.J. Brown, J.J. Maher, ANIT toxicity toward mouse hepatocytes in vivo is mediated primarily by neutrophils via CD18, Am. J. Physiol. Gastrointest. Liver Physiol. 291 (2) (2006) G355–363.
[6] S. Salas-Silva, A. Simoni-Nieves, J. Lopez-Ramirez, L. Bucio, L.E. Gomez-Quiroz, M.C. Gutierrez-Ruiz, et al., Cholangiocyte death in ductopenic cholestatic cholangiopathies: Mechanistic basis and emerging therapeutic strategies, Life Sci. 218 (2019) 324–339.
[7] P. Fickert, M.J. Pollheimer, U. Beuers, C. Lackner, G. Hirschfield, C. Housset, et al., Characterization of animal models for primary sclerosing cholangitis (PSC), J. Hepatol. 60 (6) (2014) 1290–1303.
[8] C. Enriquez-Cortina, M. Almonte-Becerril, D. Clavijo-Cornejo, M. Palestino-Dominguez, O. Bello-Monroy, N. Nuno, et al., Hepatocyte growth factor protects

against isoniazid/rifampicin-induced oxidative liver damage, Toxicol. Sci. 135 (1) (2013) 26–36.
[9] L.E. Gomez-Quiroz, V.M. Factor, P. Kaposi-Novak, C. Coulouarn, E.A. Conner, S.S. Thorgeirsson, Hepatocyte-specific c-Met deletion disrupts redox homeostasis and sensitizes to Fas-mediated apoptosis, J. Biol. Chem. 283 (21) (2008) 14581–14589.
[10] A. Valdes-Arzate, A. Luna, L. Bucio, C. Licona, D.L. Clemens, V. Souza, et al., Hepatocyte growth factor protects hepatocytes against oxidative injury induced by ethanol metabolism, Free Radical Biol. Med. 47 (4) (2009) 424–430.
[11] L.E. Gomez-Quiroz, D. Seo, Y.H. Lee, M. Kitade, T. Gaiser, M. Gillen, et al., Loss of c-Met signaling sensitizes hepatocytes to lipotoxicity and induces cholestatic liver damage by aggravating oxidative stress, Toxicology 361–362 (2016) 39–48.
[12] K. Matsumoto, T. Nakamura, Hepatocyte growth factor: renotropic role and potential therapeutics for renal diseases, Kidney Int. 59 (6) (2001) 2023–2038.
[13] O. Bello-Monroy, D. Mata-Espinosa, C. Enriquez-Cortina, V. Souza, R.U. Miranda, L. Bucio, et al., Hepatocyte growth factor enhances the clearance of a multidrug-resistant Mycobacterium tuberculosis strain by high doses of conventional chemotherapy, preserving liver function, J. Cell. Physiol. (2019).
[14] M. Palestino-Dominguez, M. Pelaez-Luna, R. Lazzarini-Lechuga, I. Rodriguez-Ochoa, V. Souza, R.U. Miranda, et al., Recombinant human hepatocyte growth factor provides protective effects in cerulein-induced acute pancreatitis in mice, J. Cell. Physiol. 233 (12) (2018) 9354–9364.
[15] T. Nakamura, S. Mizuno, K. Matsumoto, Y. Sawa, H. Matsuda, T. Nakamura, Myocardial protection from ischemia/reperfusion injury by endogenous and exogenous HGF, J. Clin. Invest. 106 (12) (2000) 1511–1519.
[16] D. Clavijo-Cornejo, C. Enriquez-Cortina, A. Lopez-Reyes, M. Dominguez-Perez, N. Nuno, M. Dominguez-Meraz, et al., Biphasic regulation of the NADPH oxidase by HGF/c-Met signaling pathway in primary mouse hepatocytes, Biochimie 95 (6) (2013) 1177–1184.
[17] J. Weerachayaphorn, A. Mennone, C.J. Soroka, K. Harry, L.R. Hagey, T.W. Kensler, et al., Nuclear factor-E2-related factor 2 is a major determinant of bile acid homeostasis in the liver and intestine, Am. J. Physiol. Gastrointest. Liver Physiol. 302 (9) (2012) G925–936.
[18] M. Vij, M. Safwan, N.P. Shanmugam, M. Rela, Liver pathology in severe multidrug resistant 3 protein deficiency: a series of 10 pediatric cases, Ann. Diagn. Pathol. 19 (5) (2015) 277–282.
[19] F. Roos, T.G. Terrell, P.J. Godowski, S.M. Chamow, R.H. Schwall, Reduction of alpha-naphthylisothiocyanate-induced hepatotoxicity by recombinant human hepatocyte growth factor, Endocrinology 131 (6) (1992) 2540–2544.
[20] J.E. Manautou, C. Chen, Collection of bile and urine samples for determining the urinary and hepatobiliary disposition of xenobiotics in mice, Curr Protoc Toxicol. (2005) Chapter 5:Unit5 7.
[21] C.L. Basiglio, F.D. Toledo, A.C. Boaglio, S.M. Arriaga, J.E. Ochoa, E.J. Sanchez Pozzi, et al., Physiological concentrations of unconjugated bilirubin prevent oxidative stress-induced hepatocanalicular dysfunction and cholestasis, Arch. Toxicol. 88 (2) (2014) 501–514.
[22] M. Dominguez-Perez, A. Simoni-Nieves, P. Rosales, N. Nuno-Lambarri, M. Rosas-Lemus, V. Souza, et al., Cholesterol burden in the liver induces mitochondrial dynamic changes and resistance to apoptosis, J. Cell. Physiol. (2018).
[23] M. Gerardo-Ramirez, R. Lazzarini-Lechuga, S. Hernandez-Rizo, J.E. Jimenez-Salazar, A. Simoni-Nieves, C. Garcia-Ruiz, et al., GDF11 exhibits tumor suppressive properties in hepatocellular carcinoma cells by restricting clonal expansion and invasion, Biochim. Biophys. Acta, Mol. Basis Dis. 1865 (6) (2019) 1540–1554.
[24] E. Wisse, F. Braet, H. Duimel, C. Vreuls, G. Koek, S.W. Olde Damink, et al., Fixation methods for electron microscopy of human and other liver, World J. Gastroenterol. 16 (23) (2010) 2851–2866.
[25] D.C. Kossor, P.C. Meunier, J.A. Handler, R.S. Sozio, R.S. Goldstein, Temporal relationship of changes in hepatobiliary function and morphology in rats following alpha-naphthylisothiocyanate (ANIT) administration, Toxicol. Appl. Pharmacol. 119 (1) (1993) 108–114.
[26] Y. Tanaka, L.M. Aleksunes, Y.J. Cui, C.D. Klaassen, ANIT-induced intrahepatic cholestasis alters hepatobiliary transporter expression via Nrf2-dependent and independent signaling, Toxicol. Sci. 108 (2) (2009) 247–257.
[27] M.M. Kaplan, A. Righetti, Induction of rat liver alkaline phosphatase: the mechanism of the serum elevation in bile duct obstruction, J. Clin. Invest. 49 (3) (1970) 508–516.
[28] J.U. Marquardt, D. Seo, L.E. Gomez-Quiroz, K. Uchida, M.C. Gillen, M. Kitade, et al., Loss of c-Met accelerates development of liver fibrosis in response to CCl(4) exposure through deregulation of multiple molecular pathways, Biochim. Biophys. Acta, Mol. Basis Dis. 1822 (6) (2012) 942–951.
[29] J.L. Boyer, Tight junctions in normal and cholestatic liver: does the paracellular pathway have functional significance? Hepatology 3 (4) (1983) 614–617.
[30] T.H. Yeh, L. Krauland, V. Singh, B. Zou, P. Devaraj, D.B. Stolz, et al., Liver-specific beta-catenin knockout mice have bile canalicular abnormalities, bile secretory defect, and intrahepatic cholestasis, Hepatology 52 (4) (2010) 1410–1419.
[31] R. Kubitz, A. Helmer, D. Haussinger, Biliary transport systems: short-term regulation, Methods Enzymol. 400 (2005) 542–557.
[32] J. Crawford, P. Bioulac-Sage, P. Hytiroglou, Structure, Function and Responses to Injury, Macsween's Pathology of the Liver, 2018, pp. 1–87.
[33] S. Melero, C. Spirli, A. Zsembery, J.F. Medina, R.E. Joplin, E. Duner, et al., Defective regulation of cholangiocyte Cl-/HCO3(-) and Na+/H+ exchanger activities in primary biliary cirrhosis, Hepatology 35 (6) (2002) 1513–1521.
[34] M. Trauner, P. Fickert, E. Halilbasic, T. Moustafa, Lessons from the toxic bile concept for the pathogenesis and treatment of cholestatic liver diseases, Wien. Med. Wochenschr. 158 (19–20) (2008) 542–548.
[35] A.P. Mansini, E. Peixoto, K.M. Thelen, C. Gaspari, S. Jin, S.A. Gradilone, The cholangiocyte primary cilium in health and disease, Biochim. Biophys. Acta, Mol. Basis Dis. 1864 (4 Pt B) (2018) 1245–1253.
[36] T. Takami, P. Kaposi-Novak, K. Uchida, L.E. Gomez-Quiroz, E.A. Conner, V.M. Factor, et al., Loss of hepatocyte growth factor/c-Met signaling pathway accelerates early stages of N-nitrosodiethylamine induced hepatocarcinogenesis, Cancer Res. 67 (20) (2007) 9844–9851.
[37] European Association for the Study of the L, EASL Clinical Practice Guidelines: management of cholestatic liver diseases, J. Hepatol. 51 (2) (2009) 237–267.
[38] K.D. Nguyen, V. Sundaram, W.S. Ayoub, Atypical causes of cholestasis, World J. Gastroenterol. 20 (28) (2014) 9418–9426.
[39] C. Guo, L. He, D. Yao, A J, B. Cao, J. Ren, et al., Alpha-naphthylisothiocyanate modulates hepatobiliary transporters in sandwich-cultured rat hepatocytes, Toxicol. Lett. 224 (1) (2014) 93–100.
[40] X. Li, R. Liu, L. Yu, Z. Yuan, R. Sun, H. Yang, et al., Alpha-naphthylisothiocyanate impairs bile acid homeostasis through AMPK-FXR pathways in rat primary hepatocytes, Toxicology 370 (2016) 106–115.
[41] Y.J. Cui, L.M. Aleksunes, Y. Tanaka, M.J. Goedken, C.D. Klaassen, Compensatory induction of liver efflux transporters in response to ANIT-induced liver injury is impaired in FXR-null mice, Toxicol. Sci. 110 (1) (2009) 47–60.
[42] M. Kongo, Y. Ohta, K. Nishida, E. Sasaki, N. Harada, I. Ishiguro, An association between lipid peroxidation and alpha-naphthylisothiocyanate-induced liver injury in rats, Toxicol. Lett. 105 (2) (1999) 103–110.
[43] Y. Zhao, G. Zhou, J. Wang, L. Jia, P. Zhang, R. Li, et al., Paeoniflorin protects against ANIT-induced cholestasis by ameliorating oxidative stress in rats, Food Chem. Toxicol. 58 (2013) 242–248.
[44] Y. Ohta, M. Kongo-Nishimura, Y. Imai, T. Matsura, A. Kitagawa, K. Yamada, alpha-Tocopherol protects against alpha-naphthylisothiocyanate-induced hepatotoxicity in rats less effectively than melatonin, Chem. Biol. Interact. 161 (2) (2006) 115–124.
[45] L.M. Perez, P. Milkiewicz, E. Elias, R. Coleman, E.J. Sanchez Pozzi, M.G. Roma, Oxidative stress induces internalization of the bile salt export pump, Bsep, and bile salt secretory failure in isolated rat hepatocyte couplets: a role for protein kinase C and prevention by protein kinase A, Toxicol. Sci. 91 (1) (2006) 150–158.
[46] S. Sekine, K. Ito, T. Horie, Oxidative stress and Mrp2 internalization, Free Radical Biol. Med. 40 (12) (2006) 2166–2174.
[47] R.J. Sokol, M. Devereaux, R. Dahl, E. Gumpricht, "Let there be bile"–understanding hepatic injury in cholestasis, J. Pediatr. Gastroenterol. Nutr. 43 (Suppl 1) (2006) S4–9.
[48] L. Yu, X. Liu, Z. Yuan, X. Li, H. Yang, Z. Yuan, et al., SRT1720 Alleviates ANIT-Induced Cholestasis in a Mouse Model, Front. Pharmacol. 8 (2017) 256.
[49] J.R. Calvo, R.J. Reiter, J.J. Garcia, G.G. Ortiz, D.X. Tan, M. Karbownik, Characterization of the protective effects of melatonin and related indoles against alpha-naphthylisothiocyanate-induced liver injury in rats, J. Cell. Biochem. 80 (4) (2001) 461–470.
[50] Y. Li, H. Yu, Z. Xu, S. Shi, D. Wang, X. Shi, et al., Melatonin ameliorates ANITinduced cholestasis by activating Nrf2 through a PI3K/Aktdependent pathway in rats, Mol. Med. Rep. 19 (2) (2019) 1185–1193.
[51] S.Y. Wu, S.C. Cui, L. Wang, Y.T. Zhang, X.X. Yan, H.L. Lu, et al., 18beta-Glycyrrhetinic acid protects against alpha-naphthylisothiocyanate-induced cholestasis through activation of the Sirt1/FXR signaling pathway, Acta Pharmacol. Sin. 39 (12) (2018) 1865–1873.
[52] Z. Chen, X. Ma, Y. Zhu, Y. Zhao, J. Wang, R. Li, et al., Paeoniflorin ameliorates ANIT-induced cholestasis by activating Nrf2 through an PI3K/Akt-dependent pathway in rats, Phytother. Res. 29 (11) (2015) 1768–1775.
[53] H. Yao, Y. Xu, L. Yin, X. Tao, L. Xu, Y. Qi, et al., Dioscin Protects ANIT-Induced Intrahepatic Cholestasis Through Regulating Transporters, Apoptosis and Oxidative Stress, Front. Pharmacol. 8 (2017) 116.
[54] M.D. Merrell, J.P. Jackson, L.M. Augustine, C.D. Fisher, A.L. Slitt, J.M. Maher, et al., The Nrf2 activator oltipraz also activates the constitutive androstane receptor, Drug Metab. Dispos. 36 (8) (2008) 1716–1721.
[55] A. Mennone, C.J. Soroka, S.Y. Cai, K. Harry, M. Adachi, L. Hagey, et al., Mrp4-/- mice have an impaired cytoprotective response in obstructive cholestasis, Hepatology 43 (5) (2006) 1013–1021.
[56] A.F. Hofmann, Bile Acids: The Good, the Bad, and the Ugly, News Physiol. Sci. 14 (1999) 24–29.
[57] C. Bellarosa, G. Bortolussi, C. Tiribelli, The role of ABC transporters in protecting cells from bilirubin toxicity, Curr. Pharm. Des. 15 (25) (2009) 2884–2892.
[58] G. Zollner, M. Wagner, T. Moustafa, P. Fickert, D. Silbert, J. Gumhold, et al., Coordinated induction of bile acid detoxification and alternative elimination in mice: role of FXR-regulated organic solute transporter-alpha/beta in the adaptive response to bile acids, Am. J. Physiol. Gastrointest. Liver Physiol. 290 (5) (2006) G923–932.
[59] F.G. Russel, J.B. Koenderink, R. Masereeuw, Multidrug resistance protein 4 (MRP4/ABCC4): a versatile efflux transporter for drugs and signalling molecules, Trends Pharmacol. Sci. 29 (4) (2008) 200–207.
[60] C.G. Dietrich, R. Ottenhoff, D.R. de Waart, R.P. Oude Elferink, Role of MRP2 and GSH in intrahepatic cycling of toxins, Toxicology 167 (1) (2001) 73–81.
[61] L. Zhang, H. Su, Y. Li, Y. Fan, Q. Wang, J. Jiang, et al., Different effects of ursodeoxycholic acid on intrahepatic cholestasis in acute and recovery stages induced by alpha-naphthylisothiocyanate in mice, Toxicol. Appl. Pharmacol. 342 (2018) 69–78.
[62] P. Fickert, M.J. Pollheimer, D. Silbert, T. Moustafa, E. Halilbasic, E. Krones, et al., Differential effects of norUDCA and UDCA in obstructive cholestasis in mice, J. Hepatol. 58 (6) (2013) 1201–1208.
[63] M.G. Roma, F.D. Toledo, A.C. Boaglio, C.L. Basiglio, F.A. Crocenzi, E.J. Sanchez Pozzi, Ursodeoxycholic acid in cholestasis: linking action mechanisms to

therapeutic applications, Clin. Sci. (Lond.) 121 (12) (2011) 523–544.
[64] P.J. Lowe, K.S. Kan, S.G. Barnwell, R.K. Sharma, R. Coleman, Transcytosis and paracellular movements of horseradish peroxidase across liver parenchymal tissue from blood to bile. Effects of alpha-naphthylisothiocyanate and colchicine, Biochem. J. 229 (2) (1985) 529–537.
[65] L.I. Hua, L.I. Yiming, L. Lu, Mechanism of α-naphthyl isothiocyanate inducing cholestatic hepatitis: a preliminary study, Linchuang Gandanbing Zazhi 32 (2016) 933–937.
[66] M.E. Farah, V. Sirotkin, B. Haarer, D. Kakhniashvili, D.C. Amberg, Diverse protective roles of the actin cytoskeleton during oxidative stress, Cytoskeleton (Hoboken) 68 (6) (2011) 340–354.
[67] F. Bulle, P. Mavier, E.S. Zafrani, A.M. Preaux, M.C. Lescs, S. Siegrist, et al., Mechanism of gamma-glutamyl transpeptidase release in serum during intrahepatic and extrahepatic cholestasis in the rat: a histochemical, biochemical and molecular approach, Hepatology 11 (4) (1990) 545–550.
[68] J.M. Cullen, J.G. Falls, H.R. Brown, L.W. Yoon, N.F. Cariello, B. Faiola, et al., Time course gene expression using laser capture microscopy-extracted bile ducts, but not hepatic parenchyma, reveals acute alpha-naphthylisothiocyanate toxicity, Toxicol. Pathol. 38 (5) (2010) 715–729.
[69] J. Bai, L. Lai, H.C. Yeo, B.C. Goh, T.M. Tan, Multidrug resistance protein 4 (MRP4/ABCC4) mediates efflux of bimane-glutathione, Int. J. Biochem. Cell Biol. 36 (2) (2004) 247–257.
[70] A. Menakongka, T. Suthiphongchai, Involvement of PI3K and ERK1/2 pathways in hepatocyte growth factor-induced cholangiocarcinoma cell invasion, World J. Gastroenterol. 16 (6) (2010) 713–722.
[71] F. Besancon, G. Przewlocki, I. Baro, A.S. Hongre, D. Escande, A. Edelman, Interferon-gamma downregulates CFTR gene expression in epithelial cells, Am. J. Physiol. 267 (5 Pt 1) (1994) C1398–1404.
[72] F. Qu, X.Q. Qin, Y.R. Cui, Y. Xiang, Y.R. Tan, H.J. Liu, et al., Ozone stress down-regulates the expression of cystic fibrosis transmembrane conductance regulator in human bronchial epithelial cells, Chem. Biol. Interact. 179 (2–3) (2009) 219–226.
[73] F. Freudenberg, A.L. Broderick, B.B. Yu, M.R. Leonard, J.N. Glickman, M.C. Carey, Pathophysiological basis of liver disease in cystic fibrosis employing a DeltaF508 mouse model, Am. J. Physiol. Gastrointest. Liver Physiol. 294 (6) (2008) G1411–1420.
[74] M. Reich, K. Deutschmann, A. Sommerfeld, C. Klindt, S. Kluge, R. Kubitz, et al., TGR5 is essential for bile acid-dependent cholangiocyte proliferation in vivo and in vitro, Gut 65 (3) (2016) 487–501.
[75] V. Keitel, C. Ullmer, D. Haussinger, The membrane-bound bile acid receptor TGR5 (Gpbar-1) is localized in the primary cilium of cholangiocytes, Biol. Chem. 391 (7) (2010) 785–789.
[76] B.L. Copple, H. Jaeschke, C.D. Klaassen, Oxidative stress and the pathogenesis of cholestasis, Semin. Liver Dis. 30 (2) (2010) 195–204.
[77] M. Madrigal, K.S. Rao, N.H. Riordan, A review of therapeutic effects of mesenchymal stem cell secretions and induction of secretory modification by different culture methods, J. Transl. Med. 12 (2014) 260.
[78] M. Cariello, E. Piccinin, O. Garcia-Irigoyen, C. Sabba, A. Moschetta, Nuclear receptor FXR, bile acids and liver damage: Introducing the progressive familial intrahepatic cholestasis with FXR mutations, Biochim. Biophys. Acta, Mol. Basis Dis. 1864 (4 Pt B) (2018) 1308–1318.

Provided for non-commercial research and education use.
Not for reproduction, distribution or commercial use.



(This is a sample cover image for this issue. The actual cover is not yet available at this time.)

This article appeared in a journal published by Elsevier. The attached copy is furnished to the author for internal non-commercial research and education use, including for instruction at the author's institution and sharing with colleagues.

Other uses, including reproduction and distribution, or selling or licensing copies, or posting to personal, institutional or third party websites are prohibited.

In most cases authors are permitted to post their version of the article (e.g. in Word or Tex form) to their personal website or institutional repository. Authors requiring further information regarding Elsevier's archiving and manuscript policies are encouraged to visit:

http://www.elsevier.com/authorsrights

Author's Personal Copy

Life Sciences 218 (2019) 324–339

Contents lists available at ScienceDirect

Life Sciences

journal homepage: www.elsevier.com/locate/lifescie

Review article

Cholangiocyte death in ductopenic cholestatic cholangiopathies: Mechanistic basis and emerging therapeutic strategies

Soraya Salas-Silva[a,b], Arturo Simoni-Nieves[a,b], Jocelyn Lopez-Ramirez[b], Leticia Bucio[b,c], Luis E. Gómez-Quiroz[b,c], María Concepción Gutiérrez-Ruiz[b,c], Marcelo G. Roma[d,*]

[a] Posgrado en Biología Experimental, DCBS, Universidad Autónoma Metropolitana-Iztapalapa, Mexico City, Mexico
[b] Departamento de Ciencias de la Salud, Universidad Autónoma Metropolitana-Iztapalapa, Mexico City, Mexico
[c] Laboratorio de Medicina Experimental, Unidad de Medicina Translacional, Instituto de Investigaciones Biomédicas, UNAM/Instituto Nacional de Cardiología Ignacio Chavez, Mexico City, Mexico
[d] Instituto de Fisiología Experimental (IFISE-CONICET), Facultad de Ciencias Bioquímicas y Farmacéuticas, Universidad Nacional de Rosario (UNR), Suipacha 570, 2000 Rosario, Argentina

ARTICLE INFO

Keywords:
Cholangiopathies
Cholangiocyte death
Cholestasis
Liver

ABSTRACT

Among hepatic diseases, cholestatic ductopenic cholangiopathies are poorly studied, and they are rarely given the importance they deserve, especially considering their high incidence in clinical practice. Although cholestatic ductopenic cholangiopathies have different etiologies and pathogenesis, all have the same target (the cholangiocyte) and similar mechanistic basis of cell death. Cholestatic cholangiopathies are characterized, predominantly, by obstructive or functional damage in the biliary epithelium, resulting in an imbalance between proliferation and cholangiocellular death; this leads to the progressive disappearance of bile ducts, as has been shown to occur in primary sclerosing cholangitis, primary biliary cholangitis, low-phospholipid-associated cholelithiasis syndrome, cystic fibrosis-related liver disease, and drug-induced ductopenia, among other biliary disorders. This review summarizes the features of the more common ductopenic syndromes and the cellular mechanisms involved in cholengiocellular death, with focus on the main forms of cholangiocyte death described so far, namely apoptosis, autophagy, necrosis, and necroptosis. It also emphasizes the importance to study in depth the molecular mechanisms of cholengiocyte death to make possible to counteract them with therapeutic purposes. These therapeutic strategies are limited in number and efficacy at present, and this is why it is important to find complementary, safe strategies to stimulate cholangiocellular proliferation in order favor bile duct replenishment as well. Successful in finding appropriate treatments would prevent the patient from having liver transplantation as the only therapeutic alternative.

1. Introduction

Cholestatic diseases are frequently dismissed as compared to others liver diseases, such as viral hepatitis, nonalcoholic steatohepatitis, and hepatocellular carcinoma, among others. However, most of chronic hepatopathies arise from, or progress towards cholestatic cholangiopathies. In the first three months of 2018, 4798 liver transplants were carried out in USA, with cholestatic cholangiopathies being one of the main causes of this treatment (United Network for Organ Sharin Website; https://unos.org).

Cholagiopathies result from a set of disorders associated with the biliary tract. They represent an actual therapeutic challenge, due to the complex function and anatomy disposition of bile ducts. Actually, there are no appropriate experimental models to study these disorders excluding, perhaps, the bile-duct ligation model [1,2] and the Mdr2-deficiente mouse model [3], which mimic obstructive cholelithiasis and low phospholipid-associated cholestasis secondary leading to sclerosing cholangitis, respectively.

The biliary tree is a highly dynamic structure with cells specialized in bile secretion, bile acid reabsorption, drug metabolism, and immune regulation [4–6]. It is composed of bile ducts, which extend from the small canals of Hering to the large extrahepatic bile duct (Fig. 1) [4].

The biliary epithelial cells form a physical barrier, and act as the first line of defense against the potentially cytotoxic components of bile [7]. Therefore, bile formation and modification require not only functional but also structural integrity of hepatocytes and cholangiocytes [5].

Biliary tree homeostasis is achieved through a balance between cell

* Corresponding author.
E-mail address: mroma@fbioyf.unr.edu.ar (M.G. Roma).

https://doi.org/10.1016/j.lfs.2018.12.044
Received 22 November 2018; Accepted 26 December 2018
Available online 02 January 2019
0024-3205/ © 2019 Elsevier Inc. All rights reserved.

Author's Personal Copy

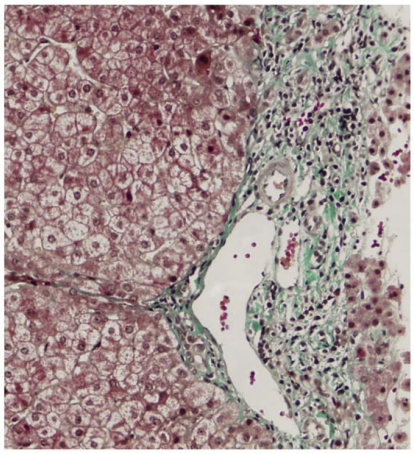


Fig. 1. Liver biopsy specimens of a patient with ductopenia. Portal trial showing absence of interlobular biliary ducts and lymphoplasmocytic infiltrate in a patient with PBC. Piecemeal necrosisis is also observed (right, low corner). Under normal conditions, biliary ducts should be observed in a space lower than two artery diameters. Masson, x40.

death and regeneration [8,9]. When this balance is lost due to exacerbation of cell death or impaired proliferation, the biliary system is affected in several ways that may lead to ductopenia and development of certain hepatopathies, collectively called "ductopenic cholangiopathies". These chronic and progressive liver disorders, characterized by the clinical syndrome of cholestasis due to an affected biliary tree, are responsible for the significant morbidity and mortality rates among pediatric and adult populations.

In this review, we describe the most frequent ductopenic cholestatic cholangiopathies by analyzing their general clinical characteristics and physiopathogenesis mechanisms, and explain in greater detail the mechanisms of cholangiocellular death that lead to these liver diseases. Finally, some hints for therapeutics to limit the ductopenic injury are provided, based either on cholangiocyte protection against these mechanisms of cell death or in the stimulation of cholangiocyte proliferation.

2. Cholestatic cholangiopathies

Cholestasis (literally, "a standing still of bile") is a syndrome originated from a disruption in bile production or flow through the biliary tree, resulting in a decreased amount of bile reaching the duodenum. The cause for this alteration can be a primary impairment in the capacity of hepatocytes or cholangiocytes to generate bile (functional or metabolic cholestasis), or a mechanical impairment hindering or impeding the bile transit (obstructive cholestasis) [10].

Cholestatic cholangiopathies are associated with a functional, obstructive, or mixed damage to the biliary tree, resulting in cholestasis. This disorder is the major determinant of most chronic cholestatic disorders.

All cholestatic cholangiopathies share, either as a primary or a secondary cause, an imbalance between cholangiocyte proliferation and death rate, associated with portal inflammation and fibrosis. Such alterations may be the main primary cause of the cholestatic disorder or a secondary manifestation of a primary hepatocellular dysfunction, which exacerbates the initial cholestatic phenomenon by extending the hepatocellular dysfunction to the cholangiocyte [11].

Cholestasis may arise from a primary obstruction in the bile ducts, but it also develops after the onset of ductopenia [8,9], which may induce loss of functional cholangiocellular mass and a biliary obstruction secondary to cellular detritus build-up and to the fibrosis caused by the inflammatory response thereto [12]. This damage induces the release of cytokines and pro-inflammatory mediators by cholangiocytes or other cell types, which stimulates cell death and proliferation responses, fibrogenesis, and impairment of the biliary epithelium transport function [11].

Chronic cholestatic cholangiopathies are the main cause of liver disease, cirrhosis, and progressive failure, eventually requiring liver transplant for the patient to survive. Some cases of cholestatic diseases are related to mutations in genes encoding proteins that are expressed in the bile canaliculus, and that are important for normal bile flow generation [13].

Cholangiopathies develop when the bile epithelium is damaged, either by infectious agents, autoimmune or genetic disorders, toxic compounds, or ischemia, which gives rise to several abnormalities in the bile duct, as observed in prototypical cholangiopathies such as primary biliary cirrhosis, cystic fibrosis, or biliary atresia [11].

The damage in the bile duct can be attributed to different causes, namely (1) the direct toxic effect of unmetabolized drugs on cholangiocytes (or reactivity of one of their metabolites) [14], (2) the immediate immune response triggered by cholangiocellular damage (e.g., due to an infectious agent or toxin), or autoimmunological causes associated with loss of tolerance to cholangiocellular antigens [6], and (3) a disruption in the protection mechanisms of the cholangiocyte against potentially toxic biliary compounds (e.g., due to a decrease in biliary phospholipids or an alteration in ductular bicarbonate excretion, two protective factors against cytotoxicity of tensioactive bile salts) [7]. Biliary complications, usually of ischemic nature [15], also constitute one of the main causes of morbidity and mortality after liver transplantation [16].

3. Ductopenic cholestatic cholangiopathies

Accelerated chollangiocellular death causes ductopenia, which is defined as the absence of interlobular bile ducts in no less than 50% of the portal triads. Its progression leads to vanishing bile duct syndrome (VBDS) when the bile ducts have virtually disappeared (Fig. 2) [8].

Among the different ductopenic cholestatic cholangiopathies, primary sclerosing cholangitis, primary biliary cirrhosis, biliary atresia, phospholipid decrease-associated cholestasis, cystic fibrosis, and drug-induced cholangiopathy are the more relevant ones [17], and they will be briefly described below.

3.1. Primary sclerosing cholangitis (PSC)

Primary sclerosing cholangitis is a chronic cholestatic autoimmune disease of unknown etiology, in which bile ducts are progressively disorganized due to the permanent presence of fibrosis and dilation of the intrahepatic and extrahepatic bile ducts due to multifocal stenosis, eventually leading to the development of biliary cirrhosis and/or liver failure [18]. It has a prevalence of 0–16.2 cases per 100,000 inhabitants [19].

The characteristic histological changes of PSC are concentric periductal fibrosis (also known as onion skin), and fibro-obliteration of medium-sized or larger bile ducts [6,20]. PSC can develop in 4 stages. At stage 1, or portal stage, lesions are minor; portal edema, lymphocyte infiltration into bile ducts, and non-destructive cholangitis appear in this stage. At stage 2, periportal fibrosis develops. At stage 3, there is septal fibrosis with major damage to the bile ducts, inducing their progressive disappearance (ductopenia). Lastly, cirrhosis is developed at stage 4 [21,22].

PSC etiology is currently unknown, but several pathophysiological mechanisms have been suggested. Defects in the mechanisms that protect against the toxicity of tensioactive bile salts have been proposed

Author's Personal Copy

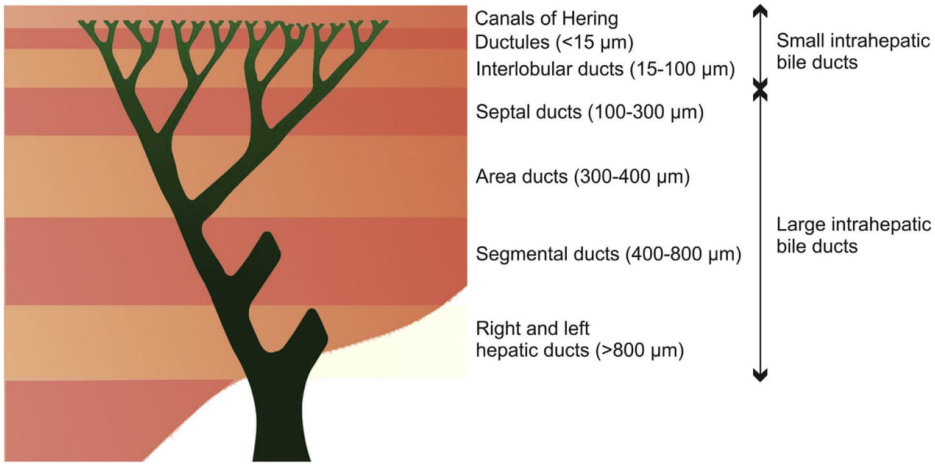


Fig. 2. Schematic representation of the intrahepatic biliary track. The intrahepatic biliary tree is a network of ducts that initiates in the canals of Hering, and gradually merges into an arrangement of interlobular, septal, and major ducts that finally coalesces to form the extrahepatic bile ducts.

as key actors in its development [7]. Release of intestinal pro-inflammatory microbial components into portal circulation (e.g., lipopolysaccharides), capable of triggering an innate immune response, has also been proposed, as well as the possibility of an antigenic factor of intestinal microbial origin [18]. Hepatic recruitment of T lymphocytes derived from intestine, due to overlapping in the pattern of adhesion molecules between intestine and bile ducts, has also been suggested [23]. T cells would then reach the portal area and the peribiliary space, thus inducing focal, fibro-obliterative lesions. Progressive periductal fibrosis, chronic inflammation, and ischemic atrophy of the biliary epithelium cause ductopenia, cholestasis, and obstructive stenosis, thus leading to secondary biliary cirrhosis [24].

Antibodies, such as perinuclear anti-neutrophil cytoplasmic antibodies (pANCA), anti-nuclear antibodies (ANA), and smooth muscle antibodies (SMA) have been reported to be present in this disease [21]. This may reflect, in part, the response of B lymphocytes to antigens of intestinal origin (for pANCA) [25] or genetic causes associated with mutations in the *major histocompatibility complex* (MHC) responsible for antigen presentation, which are predominantly connected to autoimmune diseases related to the adaptive immunologic function; this may also explain the abnormal presence of several other autoantibodies (e.g., ANA and SMA) [26,27].

3.2. Primary biliary cholangitis (PBC)

Formerly known as 'primary biliary cirrhosis', PBC is an autoimmune disease [28] that selectively destroys small, interlobular, and septal bile ducts [6,20,29]; this leads to cholestasis, with increased levels of serum alkaline phosphatase, γ-glutamyltransferase, and bilirubin [30]. This hepatopathy is associated with progressive ductopenia and fibrosis, potentially leading to cirrhosis and, eventually, liver failure [28].

PBC predominantly affects middle aged or elderly women (1:9) [6,28], and it is the leading cause of ductopenia in adults [17]. PBC prevalence rates range from 1.91–40.2 per 100,000 inhabitants, and these values are increasing with time [19].

Histopathologically, PBC destroys intrahepatic bile ducts [6], with focal obliterations of the ducts and granuloma formation [21], inflammation due to infiltration of lymphocytes (CD4+ and CD8+) [17], macrophages, and other inflammatory cells [6]. Vacuolar degeneration and apoptosis of epithelial cells and disruption of the basement membrane is also observed [20]. This leads to the subsequent development of portal fibrosis and, eventually, cirrhosis [31]. More than 40% of PBC patients display ductopenia at their baseline biopsia [32].

Besides PBC, there are other forms of biliary cholangitis, which are secondary in nature. For example, it can represent a late manifestation of extended events of intrahepatic and/or extrahepatic bile duct obstruction (obstructive biliary cirrhosis) [33], or it may be due to other secondary causes of alteration of the bile ducts, e.g., those of infectious or ischemic nature [31], which are usually associated with cholangitis and acute pericholangitis [34].

Regarding pathogenesis, PBC is a prototypical autoimmune liver pathology. It is characterized by the presence of antimitochondrial autoantibodies (AMA) against the E2 subunit of the mitochondrial pyruvate dehydrogenase complex (PDC-E2) [6,35]. These autoantibodies evoke an inflammatory response characterized by infiltration of CD4+ ("helper") and CD8+ ("cytotoxic") T cells specific of mitochondrial antigens, in small and medium-sized bile ducts (i.e., larger interlobular and septal ducts). These autoantibodies are produced as a consequence of the systemic exposure of the PDC-E2 mitochondrial intracellular antigen caused by its release into the extracellular medium after cholangiocyte apoptosis [36]. In most tissues, PDC-E2 conjugates its sulfhydryl groups with glutathione (GSH) during apoptosis, rendering it antigenic in nature. However, the high levels of Bcl2 proapoptotic proteins that constitutively the cholangiocytes express inhibit this conjugation, thus exacerbating its antigenic effects [37,38]. PBC also has high serum IgM levels [28], possibly as a consequence of a decreased commutation of this kind of immunoglobulin into an IgG with similar antigenic specificity [38].

3.3. Biliary atresia (BA)

BA is a severe idiopathic neonatal cholangiopathy characterized by the rapid progression of fibrosis, obliteration, and destruction of the extrahepatic bile ducts during the first weeks of life [6,39–41]. The intrahepatic bile ducts loss their ramifications, a feature of mature ducts, resulting in cholestasis and neonatal hepatitis [42]. Histologically, the extrahepatic bile ducts exhibit extended fibrosis with inflammatory foci, whereas the intrahepatic ducts are hyperplastic, with variable inflammation and fibrosis, surrounded by giant multinucleated

Author's Personal Copy

hepatocytes. Approximately 30% of cases also suffer ductopenia, with narrowed interlobular ducts [43].

This pathology has a female predominance, especially in patients who also have spleen malformation [39]. During the course of the pathology, typical signs and symptoms of cholestasis appear, such as jaundice, pale stools, dark urine, portal hypertension, ascites, splenomegaly and, in certain cases, bleeding [42]. Biliary atresia is the most frequent hepatic cause of child death [44]. The main treatment for atresia is liver transplantation [39], which has improved patient survival [40,41].

Several factors are involved in the development of this disease, such as embryogenesis defects, abnormal fetal or prenatal circulation, viral infections, abnormal inflammatory response, genetic factors, autoimmunity, and environmental toxins [39]. It has been described that, akin to Alagille syndrome (a congenital ductopenic cholestatic cholangiopathy with similar characteristics to BA), a defect in the Notch signaling pathway, which controls transdifferentiation of hepatoblasts and mature hepatocytes into cholangiocytes, alters the expression of hepatic nuclear factor-1β (HNF-1β) [45,46]; this affects the repair mechanisms in postnatal life, due to the absence of reactive ductular cells and accumulation of hepatobiliary cells lacking HNF1β that cannot differentiate into a biliary phenotype [47].

3.4. Low-phospholipid-associated cholelithiasis syndrome (LPAC)

This pathological entity encompasses a group of liver diseases characterized by a variable defect in the biliary excretion of phospholipids. It is causally associated with mutations in the *multidrug resistance protein 3* (MDR3), a floppase encoded by the *ABCB4* gene that enables excretion into bile of phospholipids, such as phosphatidylcholine, by flopping them from the inner to the outer leaflet of the hepatocyte canalicular membrane, from where they are removed by action of luminal detergent bile salts [48–50]. The biliary excretion of phospholipids is crucial to protect both the canalicular membranes of hepatocytes and the apical membranes of cholangiocytes, as the phospholipids present in bile allow for the formation of mixed micelles composed of phospholipids, cholesterol and bile salts, thus protecting the epithelium against the detergent effect of free, monomeric bile salts in the biliary lumen [7,50]. Actually, hydrophobic bile salts have been demonstrated to cause necrosis and apoptosis in immortalized mouse cholangiocytes, and the effect is avoided by luminal phospholipids [51].

Since MDR3 mutations are varied in nature and have different functional impacts, they produce a wide spectrum of severity, depending on the degree of functional alteration [50,52]. In the most benign forms associated with mutations of limited functional impact, bile lithogenicity and cholesterol crystallization increase due to defects in cholesterol micellization, thus inducing obstruction of small bile ducts because of the formation of "biliary sludge"; even in its asymptomatic forms, this entity could be a predisposing factor for cholestatic conditions when potentially harmful factors are added, such as cholestatic hormones (e.g., endogenous estrogens and progesterone in cholestasis of pregnancy) or MDR3-inhibiting drugs (e.g., cyclosporine A, sirolimus, verapamil, and vinblastine) [50,52]. In its more aggressive forms associated with significant functional defects of MDR3, an overt, severe cholestatic disease develops, referred to as "progressive familial intrahepatic cholestasis type 3" (PFIC-3). This hereditary cholestasis occurs at a very young age, with a spectrum ranging from neonatal cholestasis to biliary cirrhosis in young adults. Its progression rate is associated with continuous exposure to detergent bile salt monomers. In homozygotes, a nonsense mutation in the MDR3 gene has been associated with ductopenia [53]. This pathology develops during childhood and adolescence, when the patients show typical cholestasis signs and symptoms, including jaundice, pale stools, hepatomegaly, and pruritus. Gastrointestinal bleedings and cirrhosis with portal hypertension may also occur. It has even been reported that MDR3 deficiency is a high-risk factor for developing hepatocarcinoma (HCC), and cholangiocarcinoma (CCA) has also been described in these patients [7,13,54].

Histologically, portal fibrosis and variable periportal fibrosis may be present, with progression to micronodular biliary cirrhosis, as well as ductular proliferation and infiltration of inflammatory cells, mostly lymphocytes; hepatocellular, canalicular, and ductular bilirubinostasis are also observed [13,54–56].

3.5. Cystic fibrosis (CF)-related liver disease

CF is a recessive autosomal disorder in the gene encoding the *cystic fibrosis transmembrane conductance regulator* (CFTR), an ATP-dependent cholangiocyte Cl^- channel. CFTR insertion into apical membrane of cholangiocytes is mediated by secretin-induced cAMP elevations; the high luminal-to intracelular Cl^- electrochemical gradient thus formed drives HCO_3^- ductular excretion via the *anion exchanger 2* (AE2), which exchange HCO_3^- by Cl^- in an equimolar manner. Since AE2-mediated HCO_3^- excretion is a chief determinant of ductular bile flow, dysfunction of CFTR may induce ultimately a decrease in ductular bile flow. Impairment of ductular bile flow provokes mucus plugging and further luminal obstruction in those bile ducts that cannot be drained normally [57,58]. Bile viscosity has been also verified to increase due to the high mucin content, and this may contribute to cholestasis [59], in part by promoting cholelithiasis [60]. The prevalence of CF-related liver disease ranges from 26% to 45% of CF patients. Portal hypertension without hepatocellular insufficiency is the main presentation of CF-related lived disease, and ductopenia in small portal tracts is observed frequently, in part associated with a diffuse obliterative portal venopathy [61].

In this pathology, production of the "HCO_3^- umbrella," formed by the ductular secretion of HCO_3^- promoted by secretin, is also affected. HCO_3^- provides an alkaline environment along the apical surface of the bile epithelium that maintains bile salts in their ionic forms, thus preventing them from passively entering the cholangiocyte in their acidic, uncharged forms by non-ionic diffusion [7,62]. Since HCO_3^- excretion is also a driving force of the ductular bile flow, failure to excrete this anion in CF also increases the intraluminal concentration of bile salts, thus elevating their cytotoxicity further [7,62]. A deficit of luminal protecting factors leading to cholangiocyte overexposure to bile salts may result in cholangiocellular damage, due to the pronecrotic and proapoptotic effects of these biliary compounds [63]. Actually, it has been proven that extracellular pH is critical for the hydrophobic bile salts to cause the cellular death of immortalized human cholangiocytes; in these cells, bile salts are slightly toxic when exposed to the bile pH (7.4), but the toxicity increases dramatically with small decreases in pH values (from 7.1 to 6.4), which is in the order of that expected to occur after a failure in ductular HCO_3^- excretion [62,64]. In response to the ductular damage induced by these pathological mechanisms, a release of inflammatory cytokines occurs that leads to chronic portal inflammation; depending on the individual's immunogenetic basis and other concurrent factors, this may progress to focal biliary cirrhosis [64].

Neonatal cholestasis is an early manifestation of CF-related liver disease, which results in obstruction of the extrahepatic bile ducts; this could be one of the first manifestations of this pathology [57,58]. Up to 10% of CF patients develop cirrhosis in their first decade of life, progressing from focal biliary cirrhosis of the non-uniform portal tract to multilobular cirrhosis and portal hypertension [65], which could lead to liver failure and encephalopathy [58].

3.6. Drug-induced cholangiopathy

Many toxic drugs or their reactive metabolites can cause ductopenia and VBDS (Table 1).

These compounds may cause ductopenia mainly through the following pathomechanisms:

Author's Personal Copy

Table 1
Drugs that may induce ductopenic cholangiopathies.

Aceprometazine	Co-trimoxazole	Norandrostenolone
Ajmaline	Cromolyn	Phenylbutazone
Amineptine	Cyamemazine Cyclohexyl propionate	Phenytoin
Amitriptyline	Cyproheptadine	Prochlorperazine
Amoxicillin/ clavulanic acid	D-penicillamine	Terbinafine
Ampicillin	Diazepam	Tetracyclines
Azathioprine	Erythromycin	Tiabendazole
Barbiturates	Estradiol	Tiopronin
Carbamazepine	Flucloxacillin	Trifluoperazine
Carbutamide	Glibenclamide	Tolbutamide
Chlorothiazide	Glycyrrhizin	Trimethoprim/ sulfamethoxazole
Chlorpromazine	Haloperidol	Troleandomycin
Cimetidine	Ibuprofen	Xenalamine
Ciprofloxicin	Imipramine	
Clindamycin	Methyltestosterone	

1. Direct attack to cholangiocytes by drugs, or their toxic metabolites, once they have been excreted into bile.
2. Attack to cholangiocytes induced by drugs mediated by immunity, through the formation of immunogenic complexes between the drug (acting as a hapten) and endogenous proteins.

3.6.1. Direct drug attack to cholangiocytes

Toxic drugs or their reactive metabolites can cause ductopenia when they reach the cholangiocyte after being excreted into bile. Frequently, they are electrophilic or nucleophilic chemical products (or even free radicals) capable of promoting a series of chemical reactions that damage the biliary epithelium through multiple mechanisms, such as loss of antioxidant defenses, GSH depletion, and covalent binding to proteins, lipids, and nucleic acids [66].

A prototypical compound that acts via this mechanism is α-naphthylisothiocyanate (ANIT). This cholestatic agent selectively damages cholangiocytes from small and large ducts, thus causing cholangitis and intrahepatic biliary obstruction due to development of biliary sclerosis and progressive destruction of interlobular ducts. Coexistent apoptosis and proliferation are present in small and large ducts [67]. Apoptosis may stimulate cholangiocyte proliferation to compensate for the loss of mass and ductal function, but unlike hepatocytes, the limited proliferative capacity of cholangiocytes is insufficient to prevent ductopenia [68]. The bile duct damage induced by ANIT requires its hepatocellular conjugation with GSH and the subsequent biliary excretion of this metabolite; ANIT forms an adduct of labile GSH within hepatocytes, which dissociates in bile due to the medium alkalinity after being transported by Mrp2 [69]. The bile duct injury is produced mainly through apoptotic mechanisms mediated by ANIT-induced oxidative stress [70].

According to reports with animal models, the hepatotoxic compound carbon tetrachloride (CCl_4) also damages the biliary epithelium through oxidative stress-mediated apoptotic mechanisms, but it affects selectively large cholangiocytes, which produces proliferation of small duct cholangiocytes [71]. In this case, CCl_4 is converted in hepatocytes into the trichloromethyl free radical ($\cdot CC_3$) by the cytochrome P450 isoform CYP2E1, followed by excretion of free radical adducts into bile [72].

Similar mechanisms may apply for several other toxic compounds. For example, flucloxacillin, a ß-lactam antibiotic of the isoxazolyl-penicillin family, causes cholestasis associated with VBDS [73], in which toxic metabolites are generated after CYP3A4-mediated metabolism (e.g., 5′-hydroxymethyl flucloxacillin), which damage cholangiocytes after biliary excretion [74].

3.6.2. Immunologic attack to cholangiocytes by haptenization

As the liver metabolizes the drug, reactive metabolites can be produced, which may react with cellular macromolecules to form stable conjugates that trigger an aberrant immune response against self-proteins, thus forming autoantigens (haptenization) [75,76]. More commonly, haptens become immunogenic by forming adducts with proteins, either on the N-terminal domain (hydroxyalkylation) or on the C-terminal domain (oxoalkylation) [77]. Like in the molecular mimicry phenomenon, this immune response may also lead to reactivity against unmodified self-antigens, leading to immune tolerance breakdown and chronic autoimmunity [78].

4. Immunological mechanisms of ductopenic damage in cholangipathies

The mechanisms of immune-mediated ductular injury in cholangiopaties are common to most cholangiopathies. They are mainly related to the adaptive immune response mediated by CD4+ ("helper") T cells and CD8+ ("cytotoxic") T cells, damaging the cholangiocyte through highly specific T-cell receptors; the latter induce cholangiocellular death through apoptosis, by releasing perforin and granzyme B [79] (Fig. 3). For this immune response to occur, the antigenic moiety of the modified self-antigen needs to be displayed by an antigen-presenting cell (usually a dendritic cells) together with a *class-II MHC* (MHC-II) molecule, leading to a CD4+, T cell-induced immune response. Kupffer, hepatic stellate cells, and liver sinusoidal endothelial cells are all typical antigen-presenting cells in liver [80]. However, cholangiocytes themselves can also act as antigen-presenting cells in the inflammatory context [81], by aberrantly expressing MHC-I, MHC-II, and *intercellular adhesion molecule 1* (ICAM-1). This is due to the transcriptional effects of pro-inflammatory cytokines, such as interpheron-γ (IFN-γ), tumor necrosis factor-α (TNF-α), and interleukin-1 (IL-1) [82], thus increasing the possibility of activating "naïve" T cells, and initiating the cellular immune response [83].

Whatever the antigen-presenting cells are, activation of naïve CD4+, helper T cell after antigen presentation leads to CD4+ release of IL-2, followed by IL-2-induced autocrine clonal expansion. Active CD4+ lymphocytes stimulate, via IL-2 as well, the cell-mediated immunological attack of cholangiocytes by generating, activating, and allowing persistence of CD8+, cytotoxic T lymphocytes and natural killer (NK) cells, two cytolytic effector cells. These T lymphocytes bind to the cholangiocyte plasma membrane via the MHC-II/antigen complex or NKG2D-ligands, respectively [84], and release granzyme B and perforin, which induce apoptosis and necrosis in cholangiocytes [79]. In addition, soluble and plasma-membrane forms of *tumor necrosis factor-related apoptosis-inducing ligand* (TRAIL) and FasL from NK and maprophages interact with their respective receptors, TRAILR and Fas, expressed in cholangiocytes, and reinforce the apoptotic process [85]. Cholangiocytes also express constitutively low levels of leukocyte adhesion molecules, such as *class-I major histocompatibility complex* (MHC-I) and ICAM-1, but these molecules are upregulated during the inflammatory response [82]. Cholangiocytes can also secrete chemokines such as CXCL16 [86] or overexpress *monocyte chemotactic protein-1* (MCP-1) [87], which also promote inflammation by recruiting monocytes and T lymphocytes into portal tracts. MCP-1 upregulation seems to involve the epigenetic effects of micro-RNA miR-873-5p, whose circulating levels are increased in cirrhotic and cholestatic patients [88]; miR-873-5p targets glycine *N*-methyltransferase, the most abundant methyltransferase and master regulator of transmethylation flux involved in global epigenetic changes in liver [88].

Subsequently, an innate immunological response is produced, induced by the extracellular release of *danger-associated molecular patterns* (DAMPs) by the damaged cholangiocytes. DAMPs activate granulocytes and "natural killer" (NK) cells and target directly the cholangiocyte, via TLR receptors present in all these cells, able of recognizing and being activated by DAMPs [82,89]. DAMPs mimic immunological effects of

Author's Personal Copy

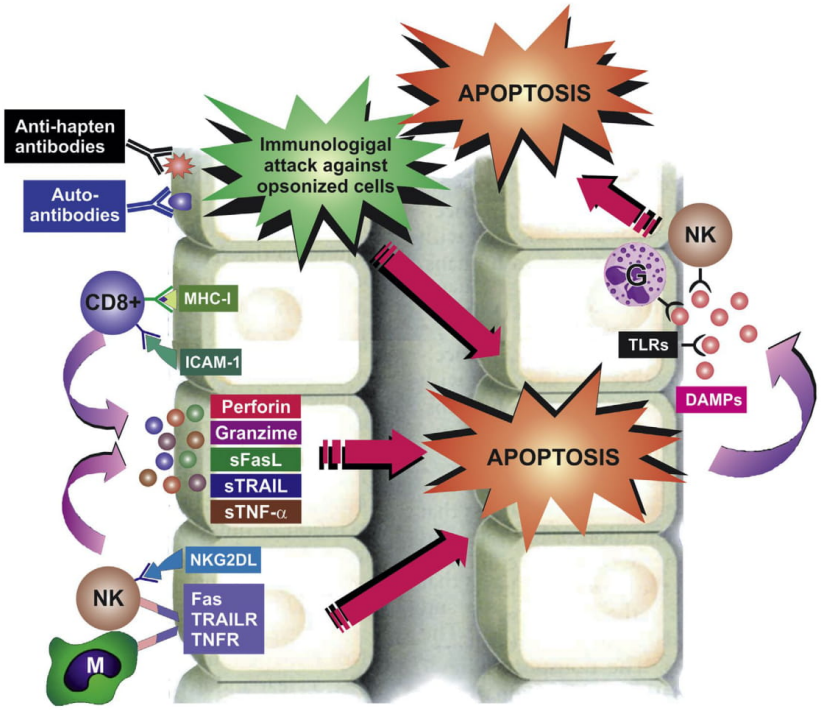


Fig. 3. Immunological mechanisms of ductopenic damage. Cytotoxic T lymphocytes (CD8 +), "natural killer" T cells (NK), and macrophages (M) induce cholangiocyte apoptosis by releasing perforin, granzyme B, and soluble forms of FasL (sFasL), TRAIL (sTRAIL), and TNF-α (sTNF-α), or by binding the membrane-associated forms of these cytokines to their plasma mambrane receptors in cholangiocytes. CD8+ binding to bile ducts is facilitated by the expression in cholangiocytes of the *major histocompatibility complex* (MHC) class I antigen (MHC-I) and T cell adhesion molecules, such as the *intercellular adhesion molecules 1* (ICAM-1). NK bind to the cholangiocyte through the NKG2D ligand. Release of *danger-associated molecular patterns* (DAMPs) by death cholangiocytes activates the innate immunity, which involves DAMP recognition by *toll-like receptors* (TLRs) located in cholangiocytes, NK cells and granulocytes, and the subsequent release of inflammatory/proapoptotic mediators that induce apoptosis in intact cholangiocytes.

pathogen-associated molecular patterns molecules (PAMPs), which alert the immune system against microbial infections. DAMPs are nuclear and cytoplasmic molecules, including nucleosides, uric acid, and the proteins *chromatin-associated protein high-mobility group box 1* (HMGB-1), S100A8/S100A9 and heat shock proteins, among others [90]. Like PAMPs, DAMPs activate NK cells and granulocytes, and the further release of inflammatory/proapoptotic mediators, such as cytokines, chemokines, and reactive oxygen and nitrogen species, thus exacerbating the inflammatory response and contributing significantly to the severity of the cellular injury [91]. Human cholangiocytes express a variety of TLR isoforms, and at least TLR-2 and TLR-4 are functional to mediate the development of a pro-inflammatory phenotype after DAMP release [92]. B cells are hyper-responsive to innate stimuli, and therefore may contribute to the perpetuation of the autoimmune process [93].

In addition to stimulate the immunological cellular response, IL-2 released by CD4+ T cells also stimulates the humoral response, by triggering B-cell proliferation and immunoglobulin synthesis [94]. B cells produce IgG antibodies against either the haptenized proteins (anti-hapten antibodies) or the native ones (auto-antibodies), able to react against cholangiocyte-specific antigens expressed in the bile-duct surface. Opsonization of cholangiocytes may lead to direct attack by immune cells bearing IgG FCγ receptors against the FC moiety of these antibodies, such as NK cells, macrophages, and granulocytes, and to trigger complement-mediated cholangiocellular lysis [78,95].

All this severe inflammation accounts for cholangitis and cholangiolitis, which results in atrophy and progressive periductal fibrosis, bile duct degeneration followed by obstructive cholestasis and, eventually, loss of interlobular bile ducts [96]. This may even coexist with small bile duct proliferation, a phenomenon known as "ductular reaction," due to maturation of intermediate hepatobiliary cells originated from a proliferative behavior in the porto-hepatic interface [97].

5. Mechanisms of cholangiocyte death

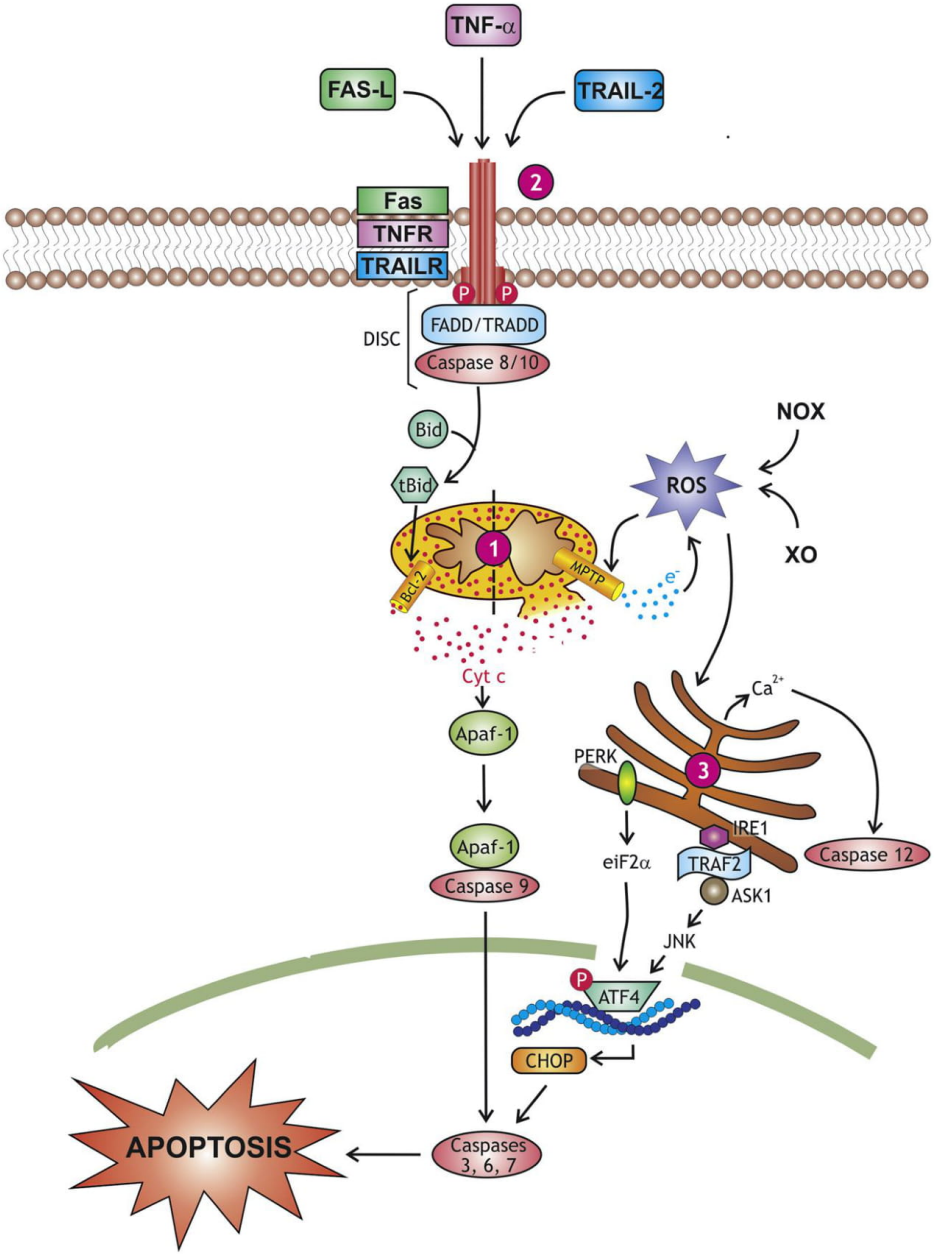
The mechanisms of cell death in cholangiocytes are common to the different ductopenic cholangiopathies. Cholangiocyte death is not as well characterized as hepatocyte death, but we know they comprise the three more important forms of cell death, namely apoptosis (type I), autophagy (type II), and necrosis (type III) [8,9].

The most common death mechanisms in biliary epithelial cells involved in ductopenic cholangiopathies are apoptosis and necrosis [63]. Autophagy and necroapoptosis has not been widely studied, but its role in ductopenic cholangiopathies is emerging [9].

5.1. Apoptosis

Apoptosis is the most widely studied death mechanism in

Author's Personal Copy



(caption on next page)

cholangiopathies, and the main cause of ductopenia associated with them [98]. It results in characteristic morphological changes in cholangiocytes, including decreased cell size, chromatin condensation, and nuclear fragmentation; this leads to formation of apoptotic bodies, which are eliminated by phagocytosis of macrophages or neighboring epithelial cells [99,100]. Apoptosis is carried out through three pathways, namely extrinsic, intrinsic, and endoplasmic reticulum stress pathways (Fig. 4).

Author's Personal Copy

Fig. 4. Mechanisms of apoptosis in cholangiocytes: 1) Intrinsic or mitochondrial pathway of apoptosis, mediated by cytochrome *c* (Cyt *c*) release from the mitochondrial intermembrane space to the cytosol; Cyt *c* interacts with the adaptor protein *apoptotic protease activating factor-1* (APAF-1) to form the "apopsome" complex, which further recruits and activates procaspase-9 by proteolysis; once activated, caspase-9 activates the downstream executioners caspases 3, 6, and 7. Cyt *c* release is facilitated by a) the insertion in the outer mitochondrial membrane of pore-forming proapoptotic proteins of the Bcl-2 family (e.g. Bax, Bad), or b) the formation of mitochondrial permeability transition pores (MPTPs), which is triggered by reactive oxygen species (ROS) from different sources, including the pro-oxidative enzymes NADPH oxidasetrans (NOX) and xanthine oxidase (XO); the mitochondrial permeability transition also exacerbates electron leakage from the respiratory chain, thus promoting the generation of cytosolic ROS from mitochondrial origin. 2) Extrinsic pathway, initiated by a) binding of the pro-inflammatory cytokines *Fas ligand* (Fas-L), *tumor necrosis factor-α* (TNF-α), and *tumor necrosis factor-related apoptosis-inducing ligand-2* (TRAIL-2) to their respective plasma membrane receptors (Fas, TNFR, and TRAILR), b) autophosphorylation of these receptors, c) association of activated receptors with the death domains, *Fas-associating protein with death domain* (FADD) or *TNFR1-associated death domain protein* (TRADD), and with the procaspases 8 and 10 to form the DISC death complex, d) proteolytic activation of these caspases, and e) excision of Bid to truncated Bid (tBid), thus promoting formation of mitochondrial pores dependent of Bcl-2. 3) Endoplasmic reticulum (ER) stress apoptosis, which is induced by a ROS-mediated increase in Ca^{2+} release and executed by caspase 12, or by the activation of the ER stress sensors *inositol-requiring transmembrane kinase/endoribonuclease 1* (IRE1) and *double-stranded RNA-dependent protein kinase* (PKR)-*like eukaryotic initiation factor 2α* (eIF2α) *kinase* (PERK). Both eIF2α, activated by PERK, and *cJUN NH2-terminal kinase* (JNK), activated by *apoptosis signal-regulating kinase 1* (ASK1) after IRE1-induced association of ASK1 with *TNFR-associated factor 2* (TRAF2), induce translocation of the transcription factor *eIF2α-activating transcription factor-4* (ATF4) to the nucleus, and the further expression of the proapoptotic transcription factor *C/EBP homologous protein* (CHOP). Regardless the pathway involved, endoplasmic reticulum stress-related apoptosis is the result of the downstream activation of the executioner caspases 3, 6, and 7 by caspase 12 and CHOP.

Both apoptosis pathways has been reported to be common mechanisms of cholangiocellular death in ductopenic cholangiopathies [29,101,102], either due to an autoimmune or infectious liver disease, or because of permanent exposure of the cholangiocytes to toxic drugs or endogenous damage by bile salts [8]. In the case of PBC, apoptosis of cholangiocytes of small ducts was shown to be secondary to the invasion of inflammatory cells [103]. As for PSC, a role for apoptosis in ductopenia is more controversial. Unlike what happens with PBC, staining for apoptosis was reported to be negative in liver samples of PSC patients [103]. However, further studies demonstrated that patients with PSC increases serum markers of apoptosis [104,105], and that they correlates with disease activity and prognosis [104].

5.1.1. Extrinsic pathway

It is triggered by external activation of death receptors present in the plasma membrane, such as TNFR, Fas, and TRAILR. Activation of these receptors requires binding to their corresponding ligands, i.e., TNF-α, FasL, and TRAIL, all of which have cytokine activity [106]. The aforementioned ligands are transmembane proteins from immune cells, and their soluble forms in plasma are due to the proteolytic cleavage of their extracellular domains by Zn-dependent metalloproteinases (for TNF-α and FasL) [107–109] or cysteine proteases (for TRAIL) [110]. Binding of any of these cytokines is required for apoptosis to take place. First, binding-dependent homo-oligomerization of the receptor is needed. Then, the *death-inducing signaling complex* (DISC) must be formed by association of Fas or TRAILR with the *TNFR-associated death domain* (TRADD) protein. Finally, DISC associates with procaspases 8 and 10 to activate them, and these active caspases activate, in turn, apoptosis executioner caspases, such as 3, 6, and 7 [106].

In the liver, the cytokines capable of activating the extrinsic pathway of apoptosis pathway are mainly produced by Kupffer cells. However, in bile ducts, the major sources of this type of cytokines are inflammatory lymphocytes and macrophages infiltrated in the biliary epithelium [111]. In addition, in several cholangiopathies, cholangiocytes themselves acquire a secretory phenotype associated with senescence, which aberrantly expresses pro-inflammatory receptors, chemokines, cytokines, and other growth factors that may sensitize surrounding cholangiocytes to cell death, as has been shown in PSC [111] and acute post-transplant cellular rejection [112]. Genetic and epigenetic factors may contribute to perpetuate this cholangiocellular phenotype, and the subsequent development of chronic effects, such as fibrosis, cholestasis, VBDS, and even cholangiocellular carcinoma [82].

Fas is a membrane receptor highly expressed in damaged cholangiocytes in PBC [98,113]. It is activated by its ligand, FasL, a cytokine expressed by macrophages and the cytotoxic T lymphocytes surrounding them or localized within the biliary epithelium, as as been shown in PBC [98]. Fas expression has been positively correlated with cholangiocyte apoptosis in PBC [114], with CD68+ monocytes surrounding the damaged bile ducts as a FasL source [115]. Its expression in PSC is much less pronounced, so its proapoptotic role could be considerably less relevant in this cholangiopathy [116].

The TNF-α/TNFR system is commonly involved in immunity-mediated ductopenia, by activating the extrinsic apoptosis pathway [117]. Moreover, cholangiocytes are the main source of TNF-α in the liver, and expression of TNF-α and its receptor are increased in several ductopenic cholangiopathies [118,119]. CD28+-inflammatory T cells located around the liver bile ducts of PSC patients are also an important source of TNF-α [120]. However, antibodies against TNF-α have been inefficient in patients with this pathology [121].

Regarding the TRAILR/TRAIL system, human cholangiocytes constitutively express TRAIL receptor type 2 (TRAILR2). In ductopenic cholangiopathies such as PSC and PBC, expression of this receptor is increased [28,119,122], an effect likely induced by the bile salts accumulated during the cholestatic process [123], via activation of the nuclear factor Sp1 by the *c-Jun N-terminal kinase* (JNK)-dependent pathway [124]. Serum levels of soluble TRAIL are also elevated in patients with PBC [119,125]. Systemic administration of TRAIL to mice induces a sclerosing cholangitis lesion, suggesting that endogenous TRAIL may contribute to human syndromes with these features, e.g., PSC [126,127]. Finally, in patients with BA, TRAIL levels are elevated, in association with an increase in activation of the pro-inflammatory transcription factor-κB (NF-κB) [6]. Nevertheless, none of the inflammatory cells that infiltrate the bile ducts in BA expressed other cytotoxic markers, such as perforin, granzyme B, and FasL [128].

5.1.2. Intrinsic pathway

This apoptotic pathway is activated in response to a large number of cellular stress conditions, such as DNA damage, extracellular matrix detachment, hypoxia, loss of survival factors, and oxidative stress, among others. In this pathway, the mitochondrial internal membrane is permeabilized by formation of *mitochondrial permeability transition pores* (MPTPs), causing colloid-osmotic swelling of the mitochondrial matrix due to entry of small solutes; this causes rupture of the mitochondrial external membrane, release of cytochrome *c* into the cytosol, formation of the apoptosome along with caspase 9 and *apoptosis protease-activating factor-1* (APAF1) and, finally, the apoptosome-mediated activation of the executioner caspases 3, 6, and 7. The mitochondria can also become permeable by assembly into the external mitochondrial membrane of pore-forming proapoptotic proteins of the Bcl-2 family, such as Bax and Bak. These two proteins are also recruited to mitochondria by truncated Bid, originated from to proteolytic excision of a C-terminal fragment of Bid by the extrinsically activated caspases 8 and 10 [129]; this acts as a functional link between intrinsic and extrinsic apoptosis pathways. Nonetheless, these pro-apoptotic stimuli can be avoided by anti-apoptotic proteins of the same family, like Bcl-2, Bc-xL, and Mcl-1, since they sequester proapoptotic proteins of the Bcl-2 family, thus impairing their

Author's Personal Copy

membrane association and insertion, oligomerization, and pore formation [130]. Therefore, change of mitochondrial permeability depends ultimately on the balance between pro- and anti-apoptotic Bcl-2 families of proteins [131]. Loss or reduction of Bcl-2, Mcl-1, and Bcl-XL expression, thus promoting pore formation in the mitochondrial membrane by Bax/Bak, has been observed in small bile ducts upon rejection of a liver allograft [117], and in PBC [103,113,132,133]. In addition, since Bax is expressed throughout the biliary tree and Bcl-2 only in the interlobular bile ducts and bile ductules, susceptibility to pro-apoptotic stimuli is specially selective [134].

The perforin/granzyme B route is the most widely used by CD8+ cytotoxic T cells and NK cells to produce apoptosis in their target cells through the intrinsic pathway. These immune cells release granules containing these two proteins, and perforin forms pores in the plasma membrane of the target cell that enable the diffusion of granzyme B into the cytosol. Once there, granzyme B triggers apoptosis by activating executioner caspase 3, or by excising Bid, which leads to tBid formation and further activation of the intrinsic apoptosis pathway [79,135]. Finally, the immunological cells detaches from the apoptotic cell, and can further interact with another intact target cell [79].

Granzyme B-positive biliary cells are prominent in small bile ducts of PBC patients, and the transcriptional levels of perforin and granzyme B are elevated in liver tissue of these patients [136,137]. Caspase 3 activated by this pathway can potentially generate immunogenic fragments of PDC-E2, so it may contribute to the deposit of autoantigens and the production of antimitochondrial antibodies in this pathology [138].

Oxidative stress is a significant inducer of mitochondrial dysfunction, and as such, a relevant factor in the activation of the intrinsic apoptosis pathway. It has indeed been implicated in cholangiocyte apoptosis and necrosis secondary to immune aggressions, ischemia/ischemia-reperfusion, and exposure to toxic bile salts [139]. Oxidative stress induces drastic changes in the permeability of the plasma membrane, release of mitochondrial components to the cytosol, decreased production of mitochondrial adenosine triphosphate (ATP), and, ultimately, apoptosis or necrosis, depending on the number of mitochondria affected; since apoptosis but not necrosis is an energy-dependent process, the latter predominates when ATP is depleted [140]. Oxidative stress has been shown to be independently associated with more advanced stages of some cholangiopathies as for example PBC [141]. Furthermore, expression of 8-hydroxydeoxyguanosine (8-OHdG), a marker of oxidative DNA damage, was preferentially detected in the nuclei of damaged interlobular bile ducts in this cholangiopathy [142,143]. In response to DNA damage, the gene encoding the cyclin-dependent kinase inhibitor WAF1 (aka p21) is induced by upregulated p53; WAF1 is a potent and reversible inhibitor of cell cycle progression at both the G1 and G2 checkpoints, and upregulated WAF1 induces irreversible G1 arrest and apoptosis. This reactive oxygen species (ROS)-mediated genotoxic mechanism has been shown to be a causal factor of cholangiocyte apoptosis in PBC [144]. In PSC, ductular lesions seem to be secondary to the production of ROS by leukocyte metabolic activation induced by antibodies against the cytoplasm of neutrophils, which is found in the serum of more than 50% of PSC patients [145].

The origin of oxidative stress in cholangiopathies is multifactorial. Once activated, lymphocytes generate an increase in ROS, and this phenomenon is involved in the apoptosis occurring in ductopenic diseases, e.g., in liver allograft rejection [139]. Mitochondrial dysfunction is another source of ROS. Cytochrome *c* release from damaged mitochondria affects the electron flow in the respiratory chain, thus inducing *i*) over-reduction of mitochondrial complexes and electron leakage into the cytosol, with the subsequent formation of ROS, and *ii*) decrease in the electron acceptor NAD^+, which results in ROS emission from the α-ketoglutarate dehydrogenase complex [146]. Oxidative stress can also be produced by enzymes that produce ROS as a consequence of their catalytic activity, such as NADPH oxidase (NOX) and xanthine oxidase (XO). NOX is a membrane-integrated enzyme that transports electrons through the plasma membrane and generates superoxide anion (O_2^-) and hydrogen peroxide (H_2O_2) from molecular oxygen inside the cells, by using NADPH as an electron donor [147]. XO, instead, produces H_2O_2 by catalyzing the oxidation of hypoxanthine to xanthine, and its subsequent oxidation to uric acid [148]. Both pro-oxidative enzymes are involved in ischemic damage to the bile ducts, e.g., in hepatic arterial stenosis, after liver transplantation, or in common bile duct compression after infusion of intra-arterial chemotherapeutic drugs [149]. Finally, the infiltrated eosinophils can be another source of ROS in PBC, since expression of eosinophil peroxidase, an eosinophilic granule protein that produces the powerful oxidant hypochlorous acid (HOCl), is increased within the portal space of PBC patients; macrophages also show evidence of the phagocytized enzyme [150]. The high sensitivity of cholangiocytes to oxidative stress has been attributed to their low GSH content, which is only 1/3 of that of hepatocytes [151], and cholangiocyte GSH levels are further decreased in cholangiopathies, such as PBC [150].

5.1.3. Endoplasmic reticulum stress

This proapoptotic pathway is triggered when the production and transport systems of proteins are altered, leading to accumulation of misfolded proteins, and eventually, apoptosis. Endoplasmic reticulum stress is triggered by several factors, such as oxidative stress, Ca^{2+} accumulation in the organelle, nutrient deprivation, and a large number of toxic aggressions, among others [152].

Endoplasmic reticulum stress is also triggered by loss of Ca^{2+} homeostasis due to its excessive release of the cation from this organelle; under this condition, Ca^{2+}-dependent calpains activate caspase 12, which in turn activates the executioner caspases 3, 6, and 7 [153,154]. Similarly to what happens in mitochondria under pro-apoptotic conditions, Bax and Bak can migrate to the endoplasmic reticulum, where they regulate Ca^{2+} channels and the inositol 1,4,5-trisphosphate receptor, thus potentiating Ca^{2+}-dependent apoptosis. Furthermore, protein misfolding can activate c-Jun through the JNK-dependent proapoptotic route, and induce expression of proapoptotic transcription factor CHOP, which favors apoptosis by modulating activity and expression of members of the Bcl-2 protein family [155].

Although there is no direct evidence of the involvement of endoplasmic reticulum stress as an apoptosis mechanism in ductopenic cholangiopathies, the machinery enabling this pathomechanism is completely functional in cholangiocytes. Furthermore, it can be activated by the high levels of cytotoxic, endogenous bile salts at which they are exposed in obstructive cholangiopathies [35]. Moreover, expression of PDI and GRP78, two endoplasmic reticulum stress markers, was significantly higher in small bile ducts, which are the most affected ones in PBC [9,35].

A possible mechanism accounting for the oxidative and endoplasmic reticulum stress in PBC is the microRNA (miR) dysregulation that occurs in hepatocytes and in immune cells of these patients. miR-506 is overexpressed in cholangiocytes of PBC patients, through a mechanism involving proinflammatory cytokines that are usually found to be elevated in PBC livers, such as IL-8, IL-12, IL-17, IL-18, and TNF-α [156]. Experimental overexpression of miR-506 in cholangiocytes affected mitochondrial energetic metabolism, with increased oxygen consumption, glycolysis, and proton leakage; this indicates uncoupling of respiration, which may have in turn accounted for by the increase in oxidative and endoplasmic reticulum stress [156]. Overexpression of miR-506 also sensitized cholangiocytes to bile acid-induced apoptosis, via a caspase 3-dependent mechanism [156]. Impairment of the HCO_3^- umbrella is a likely mechanism explaining the increased vulnerability to bile acid-induced apoptosis, since overexpression of miR-506 also decreases the Cl^-/HCO_3^- exchanger AE2 expression in cholangiocytes from PBC patients [157], and impaires type III inositol 1,4,5-trisphosphate receptor [158]; this is the major isoform of the receptor in cholangiocytes, where it regulates HCO_3^- and Cl^- secretion into bile [159].

Author's Personal Copy

5.2. Autophagy

Autophagy is regarded as a cellular protective process that eliminates damaged or aged proteins and organelles [9]. It also play a protective role during acute cellular stress (e.g., nutrient deprivation), thus helping surrounding cells to maintain cellular energy homeostasis [35]. Nevertheless, under chronic stress conditions, it represents an alternative mechanism of cell death to apoptosis; actually, these two self-destructive processes share common executer pathways, and are functionally linked [63,160,161]. The first step of autophagy is the nucleation of a membrane of unknown origin, although it seems to come from the endoplasmic reticulum, the Golgi apparatus, or *de novo* synthesis. This initial membrane, referred to as "phagophore", is elongated until the edges are fused, thus producing a double-membrane vacuole, the "autophagosome", that encapsulates the material to be degraded. Once the autophagosome is formed, it fuses with the lysosome, thus creating the autophagolysosome; lysosomal enzymes degrade its content, which allows for the degradation of aged or damaged cell material [162].

There is accumulating evidence that autophagy plays a major role in PBC pathogenesis. Cytoplasmic vesicles containing the autophagy-related marker *microtubule-associated protein-light chain 3* (LC3) has been usually found in injured bile ducts in this hepatopathy [35]. Autophagy seems to be related to the autoimmune process against mitochondrial antigens, by regulating T lymphocytes [63]. In a study where cholangiocytes in culture were exposed to several forms of stress, cells showed LC3 and PDC-E2 co-localization followed by PDC-E2 expression on the cell surface, suggesting that autophagy is responsible for granular expression and subsequent cell surface expression of PDC-E2 [160].

Autophagy may also precede biliary epithelial senescence in cholangiopathies, a process that seems to be involved in bile duct lesions [163]; almost 90% of hepatobiliary cells express senescence markers in cholestatic cholangiopathies [164]. Cholangiocyte senescence can be triggered by different cellular stresses occurring in these hepatopathies, such as oxidative stress and DNA damage [165]. Senescence is a state of irreversible growth arrest in the G1 phase of the cell cycle [166], and therefore, accumulation of senescent cholangiocytes may contribute to loss of functional biliary mass [164]. Furthermore, senescent cholangiocytes express various cytokines and chemokines that may exacerbate the inflammatory microenvironment around bile ducts, thus contributing to pathogenesis [163]. Cholangiocyte senescence during cholestatic liver injury has been linked to the epigenetic regulation of the expression of the positive regulator of biliary development FoxA2, as has been shown for PBC, PSC, and BA [164,167]; the proto-oncogene N-Ras, a known inducer of senescence, has been also causally linked to senescence in PSC cholangiocytes [111].

5.3. Necrosis

Generally, necrosis is a consequence of acute and severe metabolic perturbations, such as those that take place in ischemic cholangiopathies or drug-induced toxicity. This leads to an abrupt increase in the plasma membrane permeability and, eventually, cell lysis. As a consequence, a strong inflammatory response is triggered due to the massive release of DAMPs to the extracellular medium, which activates the innate immune system and initiates a secondary cascade of damage and inflammation against bile ducts [82,89,160].

Necrosis is the main cell death mechanism when there is massive formation of MPTPs, leading to a significant decrease in cellular ATP levels [168,169]. This type of ductopenic lesion predominantly affects the middle third of the bile ducts, leading to hepatic duct confluence, with intrahepatic affectation rarely being present [170]. In PBC, focal lesions display severe inflammatory changes and necrosis around bile ducts, often referred to as "florid duct lesion" [171]. The lymphocytes and mononuclear cells that constitute the inflammatory infiltrate are in close contact with the basal membrane of cholangiocytes undergoing necrosis [171]. In addition, non-anastomotic biliary strictures and bile duct necrosis have been described as frequent complications in liver transplantation related to ischemia-reperfusion injuries [172]. A role for necrosis in PSC ductopenic lesions is doubtful, however, since biochemical markers of necrosis are not elevated in PSC patients [105].

5.4. Necroptosis

Necroptosis, a controlled and genetically regulated form of necrosis that resemble apoptosis regarding its "programmable" trait [173], also occurs in cholangiopathies [174,175]. Necroptosis is similar to necrosis in terms of the kind of cellular alterations observed, as it shows plasma membrane permeation, colloid osmotic swelling (oncosis), mitochondrial dysfunction, and release into the extracellular space of the cytoplasmic content, also inducing inflammatory reactions due to DAMP release [173].

It is induced by similar factors to necrosis (e.g., intracellular ATP depletion, loss of Ca^{2+} homeostasis, mitochondrial depolarization, proteolysis by non-apoptotic proteases, and ROS increase), but it differs in that it can be induced, like apoptosis, by activation of cell surface receptors, mainly TNFR1, although Fas and TRAILR can be involved as well [176]. Caspase 8, the initiator of this process, is normally involved in apoptosis and not necrosis, because it simultaneously inhibits the excision of *receptor-interacting serine/threonine-protein kinase* (RIP)-1 and 3, two molecules that execute necrosis [177]. However, under certain conditions where caspase 8 is inhibited, RIP1 and RIP3 form the "necrosome" with other proteins, and cause necrosis through the *mixed lineage kinase domain-like* (MLKL)-mediated mitochondrial pathway, which involves the recruitment of the mitochondrial protein phosphatases PGAM5L and PGAM5S, and the further *dynamin-related protein-1* (Drp1) activation; this latter protein triggers mitochondrial fission and ROS production, thus causing a cellular damage similar to that observed in necrosis [178].

High expression levels of RIP3 and MLKL have been detected in the liver of PBC patients [175]. Moreover, mice with a RIP3 genetic ablation subjected to obstructive cholestasis by bile duct ligation showed decreased oxidative stress levels, inflammation, and necrosis, suggesting a role of this cell death mechanism in obstructive cholangiopathies [175]. A role for the microRNA miR-21 in cholangiocyte necroptosis has been suggested by studies showing that it is particularly overexpressed in biliary cells in human, as well as in both bile-duct ligated and Mdr2 knockout mice [179]. Finally, although studies of liver transplantation are lacking, necroptosis may play a role in ischemia-reperfusion injuries and also in liver allograft rejection, as inferred from the occurrence of similar injuries after renal transplantation [180].

6. Therapeutic approaches to limit ductopenic injury in cholangiopathies

Since there is a lack of therapeutic strategies to stimulate cholangiocellular proliferation in order to replenish bile duct under ductopenic conditions, current therapeutic strategies are limited to protect cholangiocytes against cell death mechanisms operating via either the exacerbated immunological response or exposure to luminal factors associated with the occurrence of a "toxic bile" in cholangiopathies. The current therapeutic strategies to counteract cholangiocyte death include *i*) the anticholestatic drug ursodesoxycholic acid (UDCA), which may protect these cells from apoptotic and possibly necrotic death induced by deleterious bile salts accumulated during the obstructive process and by cytokines released during the inflammatory process, and *ii*) immunosuppressive and anti-inflammatory agents, when ductopenia is suspected to be predominantly associated with immune-mediated mechanisms.

Author's Personal Copy

6.1. UDCA

This hydrophilic, non-toxic bile salt is used nowadays as the first-choice drug for the treatment of cholestasis in general, and for most cholangiopathies in particular [181]. For example, UDCA has been approved by the Food and Drug Administration for the treatment of PBC [171]. Moderate UDCA doses has been recommended by the European Association for the Study of the Liver for PSC treatment based upon results showing improvement in liver function tests and surrogate markers of prognosis in these patients, although no improved survival was demonstrated so far [21]. As for CF-associated liver disease, even when there is no established therapy for this cholangiopathy, UDCA therapy is highly recommended, since it was suggested to reduce bile viscosity [182,183]. UDCA could be also useful as an adjuvant therapy in BA, where biochemical benefit has been shown in a single crossover trial in older children with the disease after successful surgery [184]. Finally, UDCA could be beneficial even under conditions of complete extrahepatic obstruction, at least when administered at low doses and during a short administration period [185].

A compelling body of experimental and clinical evidences points UDCA as a bile duct-protective agent due to its well recognized capability to counteract bile salt-induced apoptosis and necrosis, and due to its alleged immunosuppressive and immunomodulatory properties.

Its protective mechanisms are as follows:

1) UDCA displaces and replaces highly toxic, endogenous bile salts accumulated in cholestatic hepatopathies; UDCA comprises no more than 4% of the total endogenous bile acid pool, but its value is increased to 40–60% under a conventional UDCA therapy [186]. Since biliary bile salt composition reflects the plasmatic one, the bile salt biliary would be far more harmless to cholangiocytes in patients on UDCA.
2) UDCA may counteract hepatic bile acid-induced cell death in liver. Although there is no direct evidence in cholangiocytes, UDCA have well-documented anti-apoptotic [187] and anti-necrotic [188] properties both in hepatocytes and in other extrahepatic cell types. UDCA has anti-apoptotic effects secondary to mitochondrial injury by blocking MPTP formation induced by both bile salts [189,190] and proinflammatory cytokines, including TNF-α [191], FasL [192], and transforming growth factor-β1 (TGF-β1) [193]. UDCA also reduces the expression of the members of the Bcl-2 family of proteins that form mitochondrial pores (e.g., Bad and Bax) by inhibiting p53, a pro-apoptotic transcription factor that induces Bad and Bax expressions [194]. UDCA also counteracts *t*Bid-induced the mitochondrial pore formation [192], and the upregulation of AP-1, a pro-apoptotic transcription factor activated via the TNFR/TNF-α signaling pathway [195]. Finally, tauroursodeoxycholic acid (TUDCA), a main UDCA metabolite, inhibits endoplasmic reticulum stress-induced apoptosis both by inhibiting caspase-12 activation via modulation of intracellular Ca^{2+} levels [196], and by acting as a chemical chaperone that counteracts endoplasmic reticulum stress itself [197]. Apart from its anti-apoptotic effects, UDCA can activate survival pathways. TUDCA binds to the *epidermal growth factor receptor* (EGFR), which activates the signaling survival pathways mediated by *extracellular signal-regulated kinase* (ERK) and *phosphoinositide 3-kinase* (PI3K)-Akt [198,199]. This mechanism of UDCA protection was confirmed in a rat model of apoptosis-induced ductopenia by combined vagotomy and bile-duct ligation [200].
3) UDCA reinforces adaptive mechanisms that the liver evokes spontaneously in cholestasis to attenuate the damaging effects of accumulated bile salt on hepatocytes and cholangiocytes. This adaptive response involves *i*) decrease of intracellular (and hence intrabiliary) levels of bile salts by repression of Cyp7a1, the rate-limiting enzyme of bile salt synthesis [201]; *ii*) attenuation of bile salt toxicity by promoting formation of less harmful polyhydroxylated bile salts, via induction of sterol hydroxylases [202]; *iii*) downregulation of sinusoidal bile-salt uptake transporters, e.g., *Na^+-taurocholate cotransporting polypeptide* (Ntcp), and upregulation of basolateral bile salt extrusion pumps systems, e.g., *multidrug resistant-associated protein* (Mrp) 3 and 4, which prevents bile salts from building up in liver by diverting them to urine. Patients on UDCA might activate some of these adaptive mechanisms in part by transactivating the nuclear receptor farsenoid X receptor (FXR) [202], but this response can be reinforced by the concomitant administration of the more potent FXR ligand obethicholic acid [203], or by supplementation with rifampicin, which activates pregnane X receptor (PXR), another nuclear receptor with complementary beneficial mechanisms to FXR [204].
4) UDCA restores ductular mechanisms of defense against toxic bile salts, which are frequently altered in ductopenic cholangiopathies [7]. This is accounted for by *i*) stimulation of MDR3-mediated phospholipid biliary excretion [204], an effect that can be reinforced by peroxisome proliferator activated receptor-α (PPAR-α) ligands, such as fibrate drugs [205], and *ii*) stimulation of HCO_3^- ductular excretion, with the concomitant reinforcement of both the "bicarbonate umbrella" and the hypercholeresis-induced dilution of toxic luminal bile salts; this occurs (*1*) by the stimulation of cholangiocyte HCO_3^- secretion via AE2 by transcriptional and post-transcriptional mechanisms [181,206], particularly when combined with glucocorticoids [207], and (*2*) by the ability of unconjugated UDCA to generate luminal HCO_3^- molecules as part of its characteristic cholehepatic recirculation. The UDCA homologue *nor*-UDCA, which suffers cholehepatic shunting even more efficiently than UDCA and has a higher osmotic choleretic efficiency [208], bore better therapeutic effects than UDCA to ameliorate sclerosing cholangitis in Mdr2-knockout mice, which have a complete inability to secrete phospholipid into bile [209]. Furthermore, *nor*UDCA has promising anticholestatic effects in patients with PSC, according to a recent phase II clinical study [210].
5) UDCA bears anti-inflammatory and immunomodulatory properties, in part due to its capability to bind and further activate the glucocorticoid receptor [211]. UDCA may inhibit humoral autoimmunity, as suggested by its ability to inhibit IgM, IgG, and IgA production by B cells exposed to bacteria [212]. UDCA also counteracts the cellular immune response by inhibiting the release of cytokines produced by mononuclear cells, such as IFN-α, IL-2, and IL-4 [212], a finding that was confirmed for IL-2 in a cholangitis experimental model [213]. UDCA may also counteract the overexpression of MHC-II [214] and ICAM-1 [215] in the apical membrane of the biliary epithelial cells, as well as of the ICAM-1 partner receptor in lymphocytes, *lymphocyte function-associated antigen 1* (LFA-1) [215].

6.2. Immunosuppressant agents

Despite many cholangiopathies are considered autoimmune diseases, they not usually respond to conventional immunosuppressive drugs (e.g. azathioprine, chlorambucil, cyclosporine, methotrexate, mycophenolate mofetil), including PBC [216,217] and PSC [218]. These drugs were either only marginally effective, ineffective, or even detrimental, and this is why they are not currently recommended to treat these liver diseases [219]. Similarly, the treatment of PBC with the corticosteroid budesonide is controversial, and should be reserved to non-cirrhotic patients with PBC/autoimmune hepatitis overlap syndrome [21]. A 1-year pilot trial in PBC patients treated with prednisolone showed some improvement in histology and liver function tests, but also a marked increment in bone loss [220]. Finally, a further study combining prednisolone with UDCA showed histological recovery at early PBC stages, but was not superior to UDCA monotherapy [216].

Corticosteroids have been also regarded as mostly ineffective in drug-induced VBDS by some specialists [14]. However, the often association of VBDS with drug-induced hypersensitivity reactions justify the pharmacological induction of immunosuppression as part of the

Author's Personal Copy

general therapeutic strategy for this particular case. Benefits have been supported by anecdotal cases of drug-induced ductopenia in Stevens-Johnson syndrome [221–223], toxic epidermal necrolysis [224–226], erythema multiforme [227], and hemophagocytic lymphohistiocytosis [228]. Corticosteroids are the most common immunosuppresors used in these cases, either alone or together with other immunosuppressive drugs when the patient is unresponsive to corticosteroids. Alternative immunosuppressants applied with some success include mycophenolate moefetil [229], tacrolimus [230], and cyclosporine [225]. Other therapeutic strategies for immunologically mediated diseases, such as administration of infliximab (a monoclonal antibody against human TNFα) and plasmapheresis, have been also successfully employed in these particular cases [224].

6.3. Stimulators of cholangiocyte proliferation

There is no current established therapy to treat ductopenia based upon stimulation of cholangiocyte proliferation.

Cholangiocyte proliferation occurs spontaneously in early stage of the cholangiopathy course as a consequence of the inflammatory process, and the mechanisms involved in this adaptive response may be useful to envisage therapeutic strategies based upon its stimulation. This phenomenon, referred to as "ductular reaction", consist of the formation of small epithelial tubules, with cholangiocytes been produced from hepatic progenitor cells within the Canal of Hering that are activated during liver injury [231,232]. Peribiliary glands that are lined with biliary epithelial cells of large intrahepatic bile ducts and extrahepatic bile duct are also a source of multipotent stem/progenitor cells for cholangiocyte proliferation and renewal [233,234].

Regulatory aspects of this proliferative process have been intensely studied in animal models of biliary hyperplasia, such as bile duct ligation (BDL), partial hepatectomy, chronic bile acid feeding, and more relevant to our issue, in the ductopenic model of administration of CCl_4 to bile-duct ligated rats [71,235,236]. Using these models, several signaling pathways have been identified to regulate proliferation and migration of resident cells in cholangiocyte progenitor niches. After BDL, large cholangiocytes lining larger bile ducts, but not small cholangiocytes lining smaller bile ducts, proliferate through the cAMP-mediated activation of the PKA-Src-MEK-ERK1/2 signaling pathway stimulated by secretin [235,237]; the reason for this difference is that small cholangiocytes do not express secretin receptor, and are normally mitotically dormant [238,239]. However, small cholangiocytes can proliferate via activation of the *Ca^{2+}/calmodulin/calmodulin-dependent protein kinaseI* (CaMKI)/*cAMP-response element binding* (CREB)-dependent signaling pathway by certain stimuli, such as H1 histamine receptor stimulation [240]. In pathologic conditions of large cholangiocyte damage (e.g., after CCl_4 or γ-aminobutyric acid treatment), small cholangiocytes replenish the damaged biliary tree by both amplification of this Ca^{2+}-dependent signaling pathway and transdifferentiation to the large cholangiocyte phenotype [241,242]. These and other hyperproliferative signaling pathway (e.g., the PKCβ-I-dependent one) are evoked by different signaling modulators with potential to be used as coadjuvant agents for ductopenia treatment, including neurotransmitters/neuromodulators (e.g., dopamine, neural growth factor, acetylcholine, epinephrine, calcitonin gene-related peptide, acetylcholine, norepinephrine, anandamide, and histamine) and hormones (e.g., growth hormone, vascular endothelial growth factor, epinephrine, insulin-like growth factor-1, prolactin, melatonin, angiotensin, glucagon-like peptide-1, and different sex hormones) [235,243], acting either from blood and through innervations by the autonomic nervous system, respectively. Alternatively, autocrine/paracrine mechanisms have also been described, which are associated with an increased transdifferentiation of proliferating small cholangiocytes towards a neuroendocrine phenotype able to secrete many of these mediators, and bind them via expression of their receptors [244]. This greater plasticity and proliferative potential of small cholangiocytes as compared to more differentiated, large ones points the former as a functional hepatobiliary progenitor cell population that can be therapeutically targeted to replenish the biliary epithelium in ductopenia. Whatever is its nature, this treatment should be applied early during the ductopenic process, since bile ducts are only rarely reconstructed as complete epithelium-lined tubes once they have been fully destroyed [245].

Caution is warranted when designing these therapeutic strategies, due to putative adverse effects associated with exacerbated cholangiocyte proliferation. First, proliferating cholangiocytes secrete a number of mediators, such as cytokines, chemokines, and other profibrogenic factors, that act via paracrine mechanisms to stimulate myofibroblast activation, migration, and proliferation, thus promoting liver fibrosis [96]. Second, the stimuli needed to activate otherwise quiescent cholangiocytes may trigger uncontrolled cholangiocyte hyperproliferation in susceptible individuals, resulting in liver diseases associated with growth-promoting effects, such as polycystic liver diseases [246] and cholangiocarcinoma [247]. This therapeutic approach may be particularly dangerous in diseases with a high lifetime risk of developing cholangiocarcinoma, such as PSC and CF-associated liver disease, especially if associated with an adjuvant antiapoptotic therapeutic strategy [248]. The crucial question here is whether we will be able to specifically stimulate those pathways that are beneficial for bile duct reconstitution without activating those causing harmful effects, or alternatively, to antagonize the unwanted effects without affecting the beneficial ones. The better comprehension of the signaling pathways that regulate differentiation and proliferation of both stem/progenitor cells and mature cells is clearly needed to develop such novel regenerative therapies.

7. Conclusions

The important advances in understanding cell death mechanisms in general, and the search for evidence of their particular involvement in cholangiopathies, have allowed us to understand in more detail the nature of these liver diseases. This knowledge has allowed us to explain why, under certain conditions or in certain individuals, the cholangiocellular death rate exceeds the cell proliferation rate, thus leading to different degrees of ductopenia. In addition to clearing the main functional cells out of the bile ducts causing both functional and obliterative cholestasis, the exposure of immunological cells to intracellular, potentially antigenic components released by death cholangiocytes is a powerful inflammatory stimulus that perpetuates a vicious cycle by which inflammation leads to cholangiocyte death, which in turn induces even more inflammation. Therefore, to limit this process is critical to improve disease prognosis.

The studies conducted in this field have allowed us to establish that ductopenic disruption is closely related to cholangiocellular death mechanisms, with apoptosis being the major death pathway involved, and the one we know currently in greater detail. However, our knowledge of other less studied cell death mechanisms to which cholangiocytes might be exposed in the context of each cholangiopathy, as well as their mechanisms of initiation and regulation, is still largely insufficient. In this sense, more studies on the role of autophagy and necroptosis, two recently acknowledged cholangiocellular mechanisms of cell death in ductopenic cholangiopathies, are eagerly awaited to better understand their role in the physiopathology of the disease. But at the same time, we must understand more thoroughly the defense mechanisms of the cholangiocyte that allow it to survive, in order to modulate them pharmacologically. Finally, making progress that allows us to envisage repair mechanisms against the damage suffered in each hepatopathy is crucial. Unfortunately, there are no well established therapeutic strategies to stimulate cholangiocellular proliferation in order to counteract ductopenic conditions through bile duct replenishment that lack risks associated with excessive growth-promoting effects. Meanwhile, even more efforts to envisage new modes to counteract the exacerbated cell death must be made, in order to restore

Author's Personal Copy

the balance between cell death and proliferation, by simultaneously improving both sides of the equation. This challenge will also involve answers to the question on how gradients in cholangiocyte phenotypes along the biliary tree will be reconstituted to assure an appropriate ductal structure and function at the organ level.

Conflicts of interest

All authors declare no conflict of interest.

Acknowledgements

This work was partially funded by a grant from the Consejo Nacional de Ciencia y Tecnología (CONACYT), Mexico (CB-252942, Fronteras de la Ciencia-1320, Infra-2017 280788, Infra-2013 205941 and CB-38154), Estímulo Antonio Ariza Cañadilla 2017 from FUNDHEPA, Universidad Autónoma Metropolitana Iztapalapa, Mexico, PUE-CONICET 0089 from Consejo Nacional de Investigaciones Científicas y Tecnológicas, Argentina, and PICT-2016-1613, from Agencia de Promoción Científica y Tecnológica, Argentina.

References

[1] E.A. Rodriguez-Garay, Cholestasis: human disease and experimental animal models, Ann. Hepatol. 2 (2003) 150–158.
[2] N. Nuno-Lambarri, M. Dominguez-Perez, A. Baulies-Domenech, et al., Liver cholesterol overload aggravates obstructive cholestasis by inducing oxidative stress and premature death in mice, Oxidative Med. Cell. Longev. 2016 (2016) 9895176.
[3] P. Fickert, A. Fuchsbichler, M. Wagner, et al., Regurgitation of bile acids from leaky bile ducts causes sclerosing cholangitis in Mdr2 (Abcb4) knockout mice, Gastroenterology 127 (2004) 261–274.
[4] P. Raynaud, R. Carpentier, A. Antoniou, F.P. Lemaigre, Biliary differentiation and bile duct morphogenesis in development and disease, Int. J. Biochem. Cell Biol. 43 (2011) 245–256.
[5] J.H. Tabibian, A.I. Masyuk, T.V. Masyuk, S.P. O'Hara, N.F. LaRusso, Physiology of cholangiocytes, Compr. Physiol. 3 (2013) 541–565.
[6] H. Zhang, P.S.C. Leung, M.E. Gershwin, X. Ma, How the biliary tree maintains immune tolerance? Biochim. Biophys. Acta 2018 (1864) 1367–1373.
[7] M. Trauner, P. Fickert, E. Halilbasic, T. Moustafa, Lessons from the toxic bile concept for the pathogenesis and treatment of cholestatic liver diseases, Wien. Med. Wochenschr. 158 (2008) 542–548.
[8] Y. Nakanuma, K. Tsuneyama, K. Harada, Pathology and pathogenesis of intrahepatic bile duct loss, J. Hepato-Biliary-Pancreat. Surg. 8 (2001) 303–315.
[9] Y. Nakanuma, M. Sasaki, K. Harada, Autophagy and senescence in fibrosing cholangiopathies, J. Hepatol. 62 (2015) 934–945.
[10] M.G. Roma, F.A. Crocenzi, E.A. Sanchez Pozzi, Hepatocellular transport in acquired cholestasis: new insights into functional, regulatory and therapeutic aspects, Clin. Sci. (Lond.) 114 (2008) 567–588.
[11] M. Strazzabosco, Transport systems in cholangiocytes: their role in bile formation and cholestasis, Yale J. Biol. Med. 70 (1997) 427–434.
[12] P. Fickert, M. Wagner, Biliary bile acids in hepatobiliary injury - what is the link? J. Hepatol. 67 (2017) 619–631.
[13] M. Vij, M. Safwan, N.P. Shanmugam, M. Rela, Liver pathology in severe multidrug resistant 3 protein deficiency: a series of 10 pediatric cases, Ann. Diagn. Pathol. 19 (2015) 277–282.
[14] A.P. Geubel, C.L. Sempoux, Drug and toxin-induced bile duct disorders, J. Gastroenterol. Hepatol. 15 (2000) 1232–1238.
[15] C.I. Buis, H. Hoekstra, R.C. Verdonk, R.J. Porte, Causes and consequences of ischemic-type biliary lesions after liver transplantation, J. Hepato-Biliary-Pancreat. Surg. 13 (2006) 517–524.
[16] Y. de V, F.A. von Meijenfeldt, R.J. Porte, Post-transplant cholangiopathy: classification, pathogenesis, and preventive strategies, Biochim. Biophys. Acta 1864 (2018) 1507–1515.
[17] N.S. Reau, D.M. Jensen, Vanishing bile duct syndrome, Clin. Liver Dis. 12 (2008) 203–217.
[18] T.H. Karlsen, E. Schrumpf, K.M. Boberg, Primary sclerosing cholangitis, Best Pract. Res. Clin. Gastroenterol. 24 (2010) 655–666.
[19] K. Boonstra, U. Beuers, C.Y. Ponsioen, Epidemiology of primary sclerosing cholangitis and primary biliary cirrhosis: a systematic review, J. Hepatol. 56 (2012) 1181–1188.
[20] A.D. Burt, Primary biliary cirrhosis and other ductopenic diseases, Clin. Liver Dis. 6 (2002) 363–380.
[21] European Association for the Study of the Liver, EASL clinical practice guidelines: management of cholestatic liver diseases, J. Hepatol. 51 (2009) 237–267.
[22] A.M. Casali, G. Carbone, G. Cavalli, Intrahepatic bile duct loss in primary sclerosing cholangitis: a quantitative study, Histopathology 32 (1998) 449–453.
[23] P.J. Trivedi, D.H. Adams, Mucosal immunity in liver autoimmunity: a comprehensive review, J. Autoimmun. 46 (2013) 97–111.
[24] C.A. O'Mahony, J.M. Vierling, Etiopathogenesis of primary sclerosing cholangitis, Semin. Liver Dis. 26 (2006) 3–21.
[25] B. Terjung, J. Sohne, B. Lechtenberg, et al., p-ANCAs in autoimmune liver disorders recognise human beta-tubulin isotype 5 and cross-react with microbial protein FtsZ, Gut 59 (2010) 808–816.
[26] N.L. Berntsen, B. Fosby, C. Tan, et al., Natural killer T cells mediate inflammation in the bile ducts, Mucosal Immunol. 11 (2018) 1582–1590.
[27] K.K. Farh, A. Marson, J. Zhu, et al., Genetic and epigenetic fine mapping of causal autoimmune disease variants, Nature 518 (2015) 337–343.
[28] A.C. Cheung, N.F. LaRusso, G.J. Gores, K.N. Lazaridis, Epigenetics in the primary biliary cholangitis and primary sclerosing cholangitis, Semin. Liver Dis. 37 (2017) 159–174.
[29] K. Harada, Y. Nakanuma, Molecular mechanisms of cholangiopathy in primary biliary cirrhosis, Med. Mol. Morphol. 39 (2006) 55–61.
[30] J.C. Chang, U. Beuers, R.P. Oude Elferink, The emerging role of soluble adenylyl cyclase in primary biliary cholangitis, Dig. Dis. 35 (2017) 217–223.
[31] J. Ludwig, New concepts in biliary cirrhosis, Semin. Liver Dis. 7 (1987) 293–301.
[32] T. Kumagi, M. Guindi, S.E. Fischer, et al., Baseline ductopenia and treatment response predict long-term histological progression in primary biliary cirrhosis, Am. J. Gastroenterol. 105 (2010) 2186–2194.
[33] H.E. MacMahon, A variant of obstructive biliary cirrhosis, Am. J. Pathol. 60 (1970) 371–384.
[34] Y. Li, G. Ayata, S.P. Baker, B.F. Banner, Cholangitis: a histologic classification based on patterns of injury in liver biopsies, Pathol. Res. Pract. 201 (2005) 565–572.
[35] M. Sasaki, Y. Nakanuma, Bile acids and deregulated cholangiocyte autophagy in primary biliary cholangitis, Dig. Dis. 35 (2017) 210–216.
[36] A. Lleo, P. Invernizzi, I.R. Mackay, H. Prince, R.Q. Zhong, M.E. Gershwin, Etiopathogenesis of primary biliary cirrhosis, World J. Gastroenterol. 14 (2008) 3328–3337.
[37] J.A. Odin, R.C. Huebert, L. Casciola-Rosen, N.F. LaRusso, A. Rosen, Bcl-2-dependent oxidation of pyruvate dehydrogenase-E2, a primary biliary cirrhosis autoantigen, during apoptosis, J. Clin. Invest. 108 (2001) 223–232.
[38] V. Ronca, M. Carbone, F. Bernuzzi, et al., From pathogenesis to novel therapies in the treatment of primary biliary cholangitis, Expert. Rev. Clin. Immunol. 13 (2017) 1121–1131.
[39] A. Asai, A. Miethke, J.A. Bezerra, Pathogenesis of biliary atresia: defining biology to understand clinical phenotypes, Nat. Rev. Gastroenterol. Hepatol. 12 (2015) 342–352.
[40] M. Kasahara, K. Umeshita, S. Sakamoto, A. Fukuda, H. Furukawa, S. Uemoto, Liver transplantation for biliary atresia: a systematic review, Pediatr. Surg. Int. 33 (2017) 1289–1295.
[41] Y. Ye, Z. Li, Q. Feng, et al., Downregulation of microRNA-145 may contribute to liver fibrosis in biliary atresia by targeting ADD3, PLoS One 12 (2017) e0180896.
[42] B. Lakshminarayanan, M. Davenport, Biliary atresia: a comprehensive review, J. Autoimmun. 73 (2016) 1–9.
[43] D.C. Yamaguti, F.R. Patricio, Morphometrical and immunohistochemical study of intrahepatic bile ducts in biliary atresia, Eur. J. Gastroenterol. Hepatol. 23 (2011) 759–765.
[44] A. Matsui, Screening for biliary atresia, Pediatr. Surg. Int. 33 (2017) 1305–1313.
[45] Y. Nishikawa, Y. Doi, H. Watanabe, et al., Transdifferentiation of mature rat hepatocytes into bile duct-like cells in vitro, Am. J. Pathol. 166 (2005) 1077–1088.
[46] N. Tanimizu, A. Miyajima, Notch signaling controls hepatoblast differentiation by altering the expression of liver-enriched transcription factors, J. Cell Sci. 117 (2004) 3165–3174.
[47] R. Fiorotto, C. Spirli, L. Fabris, M. Cadamuro, L. Okolicsanyi, M. Strazzabosco, Ursodeoxycholic acid stimulates cholangiocyte fluid secretion in mice via CFTR-dependent ATP secretion, Gastroenterology 133 (2007) 1603–1613.
[48] S. Ruetz, P. Gros, Phosphatidylcholine translocase: a physiological role for the mdr2 gene, Cell 77 (1994) 1071–1081.
[49] A.J. Smith, J.L. Timmermans-Hereijgers, B. Roelofsen, et al., The human MDR3 P-glycoprotein promotes translocation of phosphatidylcholine through the plasma membrane of fibroblasts from transgenic mice, FEBS Lett. 354 (1994) 263–266.
[50] R.P. Oude Elferink, C.C. Paulusma, Function and pathophysiological importance of ABCB4 (MDR3 P-glycoprotein), Pflugers Arch. 453 (2007) 601–610.
[51] D. Komichi, S. Tazuma, T. Nishioka, H. Hyogo, M. Une, K. Chayama, Unique inhibition of bile salt-induced apoptosis by lecithins and cytoprotective bile salts in immortalized mouse cholangiocytes, Dig. Dis. Sci. 48 (2003) 2315–2322.
[52] A. Davit-Spraul, E. Gonzales, C. Baussan, E. Jacquemin, The spectrum of liver diseases related to ABCB4 gene mutations: pathophysiology and clinical aspects, Semin. Liver Dis. 30 (2010) 134–146.
[53] D. Gotthardt, H. Runz, V. Keitel, et al., A mutation in the canalicular phospholipid transporter gene, ABCB4, is associated with cholestasis, ductopenia, and cirrhosis in adults, Hepatology 48 (2008) 1157–1166.
[54] J. Benzimra, S. Derhy, O. Rosmorduc, Y. Menu, R. Poupon, L. Arrive, Hepatobiliary anomalies associated with ABCB4/MDR3 deficiency in adults: a pictorial essay, Insights Imag. 4 (2013) 331–338.
[55] B. Frider, A. Castillo, R. Gordo-Gilart, et al., Reversal of advanced fibrosis after long-term ursodeoxycholic acid therapy in a patient with residual expression of MDR3, Ann. Hepatol. 14 (2015) 745–751.
[56] M. Vij, N.P. Shanmugam, M.S. Reddy, S. Govil, M. Rela, Hepatocarcinogenesis in multidrug-resistant P-glycoprotein 3 deficiency, Pediatr. Transplant. 21 (2017) e12889.
[57] U. Herrmann, G. Dockter, F. Lammert, Cystic fibrosis-associated liver disease, Best Pract. Res. Clin. Gastroenterol. 24 (2010) 585–592.
[58] L. Leeuwen, A.K. Magoffin, D.A. Fitzgerald, M. Cipolli, K.J. Gaskin, Cholestasis and meconium ileus in infants with cystic fibrosis and their clinical outcomes, Arch.

Author's Personal Copy

Dis. Child. 99 (2014) 443–447.
[59] M. Kappler, C. Espach, A. Schweiger-Kabesch, et al., Ursodeoxycholic acid therapy in cystic fibrosis liver disease–a retrospective long-term follow-up case-control study, Aliment. Pharmacol. Ther. 36 (2012) 266–273.
[60] N. Kobelska-Dubiel, B. Klincewicz, W. Cichy, Liver disease in cystic fibrosis, Przegl. Gastroen. 9 (2014) 136–141.
[61] P. Witters, L. Libbrecht, T. Roskams, et al., Noncirrhotic presinusoidal portal hypertension is common in cystic fibrosis-associated liver disease, Hepatology 53 (2011) 1064–1065.
[62] S. Hohenester, W.L. Maillette de Buy, D.M. Jefferson, R.P. Oude Elferink, U. Beuers, Biliary bicarbonate secretion constitutes a protective mechanism against bile acid-induced injury in man, Dig. Dis. 29 (2011) 62–65.
[63] F. Yang, E. Gaudio, P. Onori, C. Wise, G. Alpini, S.S. Glaser, Mechanisms of biliary damage, J. Cell Death 3 (2010) 13–21.
[64] S. Hohenester, L.M. Wenniger, C.C. Paulusma, et al., A biliary HCO3- umbrella constitutes a protective mechanism against bile acid-induced injury in human cholangiocytes, Hepatology 55 (2012) 173–183.
[65] D.H. Leung, M. Khan, C.G. Minard, et al., Aspartate aminotransferase to platelet ratio and fibrosis-4 as biomarkers in biopsy-validated pediatric cystic fibrosis liver disease, Hepatology 62 (2015) 1576–1583.
[66] M.S. Padda, M. Sanchez, A.J. Akhtar, J.L. Boyer, Drug-induced cholestasis, Hepatology 53 (2011) 1377–1387.
[67] G. Lesage, S. Glaser, Y. Ueno, et al., Regression of cholangiocyte proliferation after cessation of ANIT feeding is coupled with increased apoptosis, Am. J. Physiol. Gastrointest. Liver Physiol. 281 (2001) G182–G190.
[68] Y. Moritoki, Y. Ueno, N. Kanno, et al., Amniotic epithelial cell-derived cholangiocytes in experimental cholestatic ductal hyperplasia, Hepatol. Res. 37 (2007) 286–294.
[69] C.G. Dietrich, R. Ottenhoff, D.R. de Waart, R.P. Oude Elferink, Role of MRP2 and GSH in intrahepatic cycling of toxins, Toxicology 167 (2001) 73–81.
[70] Y. Tanaka, L.M. Aleksunes, Y.J. Cui, C.D. Klaassen, ANIT-induced intrahepatic cholestasis alters hepatobiliary transporter expression via Nrf2-dependent and independent signaling, Toxicol. Sci. 108 (2009) 247–257.
[71] G.D. LeSage, A. Benedetti, S. Glaser, et al., Acute carbon tetrachloride feeding selectively damages large, but not small, cholangiocytes from normal rat liver, Hepatology 29 (1999) 307–319.
[72] K.T. Knecht, R.P. Mason, The detection of halocarbon-derived radical adducts in bile and liver of rats, Drug Metab. Dispos. 19 (1991) 325–331.
[73] M.H. Davies, R.F. Harrison, E. Elias, S.G. Hubscher, Antibiotic-associated acute vanishing bile duct syndrome: a pattern associated with severe, prolonged, intrahepatic cholestasis, J. Hepatol. 20 (1994) 112–116.
[74] F. Lakehal, P.M. Dansette, L. Becquemont, et al., Indirect cytotoxicity of flucloxacillin toward human biliary epithelium via metabolite formation in hepatocytes, Chem. Res. Toxicol. 14 (2001) 694–701.
[75] C. Stephens, R.J. Andrade, M.I. Lucena, Mechanisms of drug-induced liver injury, Curr. Opin. Allergy Clin. Immunol. 14 (2014) 286–292.
[76] J. Uetrecht, Immunoallergic drug-induced liver injury in humans, Semin. Liver Dis. 29 (2009) 383–392.
[77] I. Chipinda, J.M. Hettick, P.D. Siegel, Haptenation: chemical reactivity and protein binding, J. Allergy 2011 (2011) 839682.
[78] Z.X. Liu, N. Kaplowitz, Immune-mediated drug-induced liver disease, Clin. Liver Dis. 6 (2002) 755–774.
[79] I. Voskoboinik, J.C. Whisstock, J.A. Trapani, Perforin and granzymes: function, dysfunction and human pathology, Nat. Rev. Immunol. 15 (2015) 388–400.
[80] M.R. Ebrahimkhani, I. Mohar, I.N. Crispe, Cross-presentation of antigen by diverse subsets of murine liver cells, Hepatology 54 (2011) 1379–1387.
[81] E. Schrumpf, C. Tan, T.H. Karlsen, et al., The biliary epithelium presents antigens to and activates natural killer T cells, Hepatology 62 (2015) 1249–1259.
[82] S.P. O'Hara, J.H. Tabibian, P.L. Splinter, N.F. LaRusso, The dynamic biliary epithelia: molecules, pathways, and disease, J. Hepatol. 58 (2013) 575–582.
[83] I.N. Crispe, Liver antigen-presenting cells, J. Hepatol. 54 (2011) 357–365.
[84] B. Gao, Natural killer group 2 member D, its ligands, and liver disease: good or bad? Hepatology 51 (2010) 8–11.
[85] D.H. Adams, S.C. Afford, The role of cholangiocytes in the development of chronic inflammatory liver disease, Front. Biosci. 7 (2002) e276–e285.
[86] M. Heydtmann, P.F. Lalor, J.A. Eksteen, S.G. Hubscher, M. Briskin, D.H. Adams, CXC chemokine ligand 16 promotes integrin-mediated adhesion of liver-infiltrating lymphocytes to cholangiocytes and hepatocytes within the inflamed human liver, J. Immunol. 174 (2005) 1055–1062.
[87] K. Tsuneyama, K. Harada, M. Yasoshima, et al., Monocyte chemotactic protein-1, −2, and −3 are distinctively expressed in portal tracts and granulomata in primary biliary cirrhosis: implications for pathogenesis, J. Pathol. 193 (2001) 102–109.
[88] D. Fernandez-Ramos, P. Fernandez-Tussy, F. Lopitz-Otsoa, et al., MiR-873-5p acts as an epigenetic regulator in early stages of liver fibrosis and cirrhosis, Cell Death Dis. 9 (2018) 958.
[89] H. Malhi, M.E. Guicciardi, G.J. Gores, Hepatocyte death: a clear and present danger, Physiol. Rev. 90 (2010) 1165–1194.
[90] J.S. Roh, D.H. Sohn, Damage-associated molecular patterns in inflammatory diseases, Immune Netw. 18 (2018) e27.
[91] D. Foell, H. Wittkowski, J. Roth, Mechanisms of disease: a 'DAMP' view of inflammatory arthritis, Nat. Clin. Pract. Rheumatol. 3 (2007) 382–390.
[92] X.M. Chen, S.P. O'Hara, J.B. Nelson, et al., Multiple TLRs are expressed in human cholangiocytes and mediate host epithelial defense responses to *Cryptosporidium parvum* via activation of NF-kappaB, J. Immunol. 175 (2005) 7447–7456.
[93] Y. Moritoki, Z.X. Lian, H. Wulff, et al., AMA production in primary biliary cirrhosis is promoted by the TLR9 ligand CpG and suppressed by potassium channel blockers, Hepatology 45 (2007) 314–322.
[94] T.A. Waldmann, S. Dubois, Y. Tagaya, Contrasting roles of IL-2 and IL-15 in the life and death of lymphocytes: implications for immunotherapy, Immunity 14 (2001) 105–110.
[95] Z.X. Liu, N. Kaplowitz, Immune mechanisms in drug-induced hepatotoxicity, in: M.E. Gershwin, J.M. Vierling, M.P. Manns (Eds.), Liver Immunology - Principles and Practice, Humana Press, 2007, pp. 363–374.
[96] M. Penz-Osterreicher, C.H. Osterreicher, M. Trauner, Fibrosis in autoimmune and cholestatic liver disease, Best Pract. Res. Clin. Gastroenterol. 25 (2011) 245–258.
[97] N.D. Theise, R. Saxena, B.C. Portmann, et al., The canals of Hering and hepatic stem cells in humans, Hepatology 30 (1999) 1425–1433.
[98] K. Harada, S. Ozaki, M.E. Gershwin, Y. Nakanuma, Enhanced apoptosis relates to bile duct loss in primary biliary cirrhosis, Hepatology 26 (1997) 1399–1405.
[99] S. Fulda, K.M. Debatin, Extrinsic versus intrinsic apoptosis pathways in anticancer chemotherapy, Oncogene 25 (2006) 4798–4811.
[100] Z. Jin, W.S. El-Deiry, Overview of cell death signaling pathways, Cancer Biol. Ther. 4 (2005) 139–163.
[101] G. Alpini, J.M. McGill, N.F. LaRusso, The pathobiology of biliary epithelia, Hepatology 35 (2002) 1256–1268.
[102] C.L. Mack, A.G. Feldman, R.J. Sokol, Clues to the etiology of bile duct injury in biliary atresia, Semin. Liver Dis. 32 (2012) 307–316.
[103] J. Tinmouth, M. Lee, I.R. Wanless, F.W. Tsui, R. Inman, E.J. Heathcote, Apoptosis of biliary epithelial cells in primary biliary cirrhosis and primary sclerosing cholangitis, Liver 22 (2002) 228–234.
[104] G. Denk, A.J. Omary, F.P. Reiter, et al., Soluble intracellular adhesion molecule, M30 and M65 as serum markers of disease activity and prognosis in cholestatic liver diseases, Hepatol. Res. 44 (2014) 1286–1298.
[105] H.C. Masuoka, R. Vuppalanchi, R. Deppe, et al., Individuals with primary sclerosing cholangitis have elevated levels of biomarkers for apoptosis but not necrosis, Dig. Dis. Sci. 60 (2015) 3642–3646.
[106] P. Waring, A. Mullbacher, Cell death induced by the Fas/Fas ligand pathway and its role in pathology, Immunol. Cell Biol. 77 (1999) 312–317.
[107] G.M. McGeehan, J.D. Becherer, R.C. Bast Jr.et al., Regulation of tumour necrosis factor-alpha processing by a metalloproteinase inhibitor, Nature 370 (1994) 558–561.
[108] P. Schneider, N. Holler, J.L. Bodmer, et al., Conversion of membrane-bound Fas (CD95) ligand to its soluble form is associated with downregulation of its proapoptotic activity and loss of liver toxicity, J. Exp. Med. 187 (1998) 1205–1213.
[109] N. Kayagaki, A. Kawasaki, T. Ebata, et al., Metalloproteinase-mediated release of human Fas ligand, J. Exp. Med. 182 (1995) 1777–1783.
[110] S.M. Mariani, P.H. Krammer, Surface expression of TRAIL/Apo-2 ligand in activated mouse T and B cells, Eur. J. Immunol. 28 (1998) 1492–1498.
[111] J.H. Tabibian, S.P. O'Hara, P.L. Splinter, C.E. Trussoni, N.F. LaRusso, Cholangiocyte senescence by way of N-ras activation is a characteristic of primary sclerosing cholangitis, Hepatology 59 (2014) 2263–2275.
[112] J.G. Brain, H. Robertson, E. Thompson, et al., Biliary epithelial senescence and plasticity in acute cellular rejection, Am. J. Transplant. 13 (2013) 1688–1702.
[113] T. Kuroki, S. Seki, N. Kawakita, et al., Expression of antigens related to apoptosis and cell proliferation in chronic nonsuppurative destructive cholangitis in primary biliary cirrhosis, Virchows Arch. 429 (1996) 119–129.
[114] A. Tsikrikoni, D.S. Kyriakou, E.I. Rigopoulou, et al., Markers of cell activation and apoptosis in bone marrow mononuclear cells of patients with autoimmune hepatitis type 1 and primary biliary cirrhosis, J. Hepatol. 42 (2005) 393–399.
[115] M. Iwata, K. Harada, K. Hiramatsu, et al., Fas ligand expressing mononuclear cells around intrahepatic bile ducts co-express CD68 in primary biliary cirrhosis, Liver 20 (2000) 129–135.
[116] H.P. Dienes, A.W. Lohse, G. Gerken, et al., Bile duct epithelia as target cells in primary biliary cirrhosis and primary sclerosing cholangitis, Virchows Arch. 431 (1997) 119–124.
[117] C. Gapany, M. Zhao, A. Zimmermann, The apoptosis protector, bcl-2 protein, is downregulated in bile duct epithelial cells of human liver allografts, J. Hepatol. 26 (1997) 535–542.
[118] A. Celli, F.G. Que, Dysregulation of apoptosis in the cholangiopathies and cholangiocarcinoma, Semin. Liver Dis. 18 (1998) 177–185.
[119] Y. Liang, Z. Yang, C. Li, Y. Zhu, L. Zhang, R. Zhong, Characterisation of TNF-related apoptosis-inducing ligand in peripheral blood in patients with primary biliary cirrhosis, Clin. Exp. Med. 8 (2008) 1–7.
[120] E. Liaskou, L.E. Jeffery, P.J. Trivedi, et al., Loss of CD28 expression by liver-infiltrating T cells contributes to pathogenesis of primary sclerosing cholangitis, Gastroenterology 147 (2014) 221–232.
[121] D.W. Hommes, W. Erkelens, C. Ponsioen, et al., A double-blind, placebo-controlled, randomized study of infliximab in primary sclerosing cholangitis, J. Clin. Gastroenterol. 42 (2008) 522–526.
[122] N. Baba, H. Kobashi, K. Yamamoto, et al., Gene expression profiling in biliary epithelial cells of primary biliary cirrhosis using laser capture microdissection and cDNA microarray, Transl. Res. 148 (2006) 103–113.
[123] H. Higuchi, S.F. Bronk, Y. Takikawa, et al., The bile acid glycochenodeoxycholate induces trail-receptor 2/DR5 expression and apoptosis, J. Biol. Chem. 276 (2001) 38610–38618.
[124] H. Higuchi, A. Grambihler, A. Canbay, S.F. Bronk, G.J. Gores, Bile acids up-regulate death receptor 5/TRAIL-receptor 2 expression via a c-Jun N-terminal kinase-dependent pathway involving Sp1, J. Biol. Chem. 279 (2004) 51–60.
[125] N. Pelli, A. Floreani, F. Torre, et al., Soluble apoptosis molecules in primary biliary cirrhosis: analysis and commitment of the Fas and tumour necrosis factor-related apoptosis-inducing ligand systems in comparison with chronic hepatitis C, Clin.

Author's Personal Copy

Exp. Immunol. 148 (2007) 85–89.
[126] M.E. Guicciardi, A. Krishnan, S.F. Bronk, P. Hirsova, T.S. Griffith, G.J. Gores, Biliary tract instillation of a SMAC mimetic induces TRAIL-dependent acute sclerosing cholangitis-like injury in mice, Cell Death Dis. 8 (2017) e2535.
[127] K. Takeda, Y. Kojima, K. Ikejima, et al., Death receptor 5 mediated-apoptosis contributes to cholestatic liver disease, Proc. Natl. Acad. Sci. U. S. A. 105 (2008) 10895–10900.
[128] A.F. Ahmed, H. Ohtani, M. Nio, et al., CD8+ T cells infiltrating into bile ducts in biliary atresia do not appear to function as cytotoxic T cells: a clinicopathological analysis, J. Pathol. 193 (2001) 383–389.
[129] D. Westphal, G. Dewson, P.E. Czabotar, R.M. Kluck, Molecular biology of Bax and Bak activation and action, Biochim. Biophys. Acta 2011 (1813) 521–531.
[130] J.H. Zheng, F.A. Viacava, R.W. Kriwacki, T. Moldoveanu, Discoveries and controversies in BCL-2 protein-mediated apoptosis, FEBS J. 283 (2016) 2690–2700.
[131] R.J. Youle, A. Strasser, The BCL-2 protein family: opposing activities that mediate cell death, Nat. Rev. Mol. Cell Biol. 9 (2008) 47–59.
[132] A.M. Graham, M.M. Dollinger, S.E. Howie, D.J. Harrison, Bile duct cells in primary biliary cirrhosis are 'primed' for apoptosis, Eur. J. Gastroenterol. Hepatol. 10 (1998) 553–557.
[133] M. Iwata, K. Harada, N. Kono, S. Kaneko, K. Kobayashi, Y. Nakanuma, Expression of Bcl-2 familial proteins is reduced in small bile duct lesions of primary biliary cirrhosis, Hum. Pathol. 31 (2000) 179–184.
[134] K. Harada, M. Iwata, N. Kono, W. Koda, T. Shimonishi, Y. Nakanuma, Distribution of apoptotic cells and expression of apoptosis-related proteins along the intrahepatic biliary tree in normal and non-biliary diseased liver, Histopathology 37 (2000) 347–354.
[135] J.A. Trapani, M.J. Smyth, Functional significance of the perforin/granzyme cell death pathway, Nat. Rev. Immunol. 2 (2002) 735–747.
[136] C.K. Fox, A. Furtwaengler, R.R. Nepomuceno, O.M. Martinez, S.M. Krams, Apoptotic pathways in primary biliary cirrhosis and autoimmune hepatitis, Liver 21 (2001) 272–279.
[137] M. Tsuda, Y.M. Ambrosini, W. Zhang, et al., Fine phenotypic and functional characterization of effector cluster of differentiation 8 positive T cells in human patients with primary biliary cirrhosis, Hepatology 54 (2011) 1293–1302.
[138] S. Matsumura, J. Van De Water, H. Kita, et al., Contribution to antimitochondrial antibody production: cleavage of pyruvate dehydrogenase complex-E2 by apoptosis-related proteases, Hepatology 35 (2002) 14–22.
[139] T. Patel, G.J. Gores, Apoptosis and hepatobiliary disease, Hepatology 21 (1995) 1725–1741.
[140] Y. Eguchi, S. Shimizu, Y. Tsujimoto, Intracellular ATP levels determine cell death fate by apoptosis or necrosis, Cancer Res. 57 (1997) 1835–1840.
[141] P. Sorrentino, L. Terracciano, S. D'Angelo, et al., Oxidative stress and steatosis are cofactors of liver injury in primary biliary cirrhosis, J. Gastroenterol. 45 (2010) 1053–1062.
[142] T. Kitada, S. Seki, S. Iwai, T. Yamada, H. Sakaguchi, K. Wakasa, In situ detection of oxidative DNA damage, 8-hydroxydeoxyguanosine, in chronic human liver disease, J. Hepatol. 35 (2001) 613–618.
[143] Y. Kadokawa, K. Ohba, K. Omagari, et al., Intracellular balance of oxidative stress and cytoprotective molecules in damaged interlobular bile ducts in autoimmune hepatitis and primary biliary cirrhosis: in situ detection of 8-hydroxydeoxyguanosine and glutathione-S-transferase-pi, Hepatol. Res. 37 (2007) 620–627.
[144] K. Harada, S. Furubo, S. Ozaki, K. Hiramatsu, Y. Sudo, Y. Nakanuma, Increased expression of WAF1 in intrahepatic bile ducts in primary biliary cirrhosis relates to apoptosis, J. Hepatol. 34 (2001) 500–506.
[145] A. Cecere, L. Tancredi, A. Gattoni, Primary sclerosing cholangitis, Panminerva Med. 44 (2002) 313–323.
[146] C. Chinopoulos, V. dam-Vizi, Calcium, mitochondria and oxidative stress in neuronal pathology. Novel aspects of an enduring theme, FEBS J. 273 (2006) 433–450.
[147] K. Bedard, K.H. Krause, The NOX family of ROS-generating NADPH oxidases: physiology and pathophysiology, Physiol. Rev. 87 (2007) 245–313.
[148] M.G. Battelli, L. Polito, M. Bortolotti, A. Bolognesi, Xanthine oxidoreductase-derived reactive species: physiological and pathological effects, Oxidative Med. Cell. Longev. 2016 (2016) 3527579.
[149] R. Cursio, J. Gugenheim, Ischemia-reperfusion injury and ischemic-type biliary lesions following liver transplantation, J. Transp. Secur. 2012 (2012) 164329.
[150] T.L. Salunga, Z.G. Cui, S. Shimoda, et al., Oxidative stress-induced apoptosis of bile duct cells in primary biliary cirrhosis, J. Autoimmun. 29 (2007) 78–86.
[151] M. Parola, K.H. Cheeseman, M.E. Biocca, M.U. Dianzani, T.F. Slater, Biochemical studies on bile duct epithelial cells isolated from rat liver, J. Hepatol. 10 (1990) 341–345.
[152] A. Kapoor, A.J. Sanyal, Endoplasmic reticulum stress and the unfolded protein response, Clin. Liver Dis. 13 (2009) 581–590.
[153] J. Faitova, D. Krekac, R. Hrstka, B. Vojtesek, Endoplasmic reticulum stress and apoptosis, Cell. Mol. Biol. Lett. 11 (2006) 488–505.
[154] M. Lamkanfi, M. Kalai, P. Vandenabeele, Caspase-12: an overview, Cell Death Differ. 11 (2004) 365–368.
[155] H. Malhi, R.J. Kaufman, Endoplasmic reticulum stress in liver disease, J. Hepatol. 54 (2011) 795–809.
[156] O. Erice, P. Munoz-Garrido, J. Vaquero, et al., MicroRNA-506 promotes primary biliary cholangitis-like features in cholangiocytes and immune activation, Hepatology 67 (2018) 1420–1440.
[157] J.M. Banales, E. Saez, M. Uriz, et al., Up-regulation of microRNA 506 leads to decreased Cl-/HCO3- anion exchanger 2 expression in biliary epithelium of patients with primary biliary cirrhosis, Hepatology 56 (2012) 687–697.
[158] M. Ananthanarayanan, J.M. Banales, M.T. Guerra, et al., Post-translational regulation of the type III inositol 1,4,5-trisphosphate receptor by miRNA-506, J. Biol. Chem. 290 (2015) 184–196.
[159] N. Minagawa, J. Nagata, K. Shibao, et al., Cyclic AMP regulates bicarbonate secretion in cholangiocytes through release of ATP into bile, Gastroenterology 133 (2007) 1592–1602.
[160] K. Harada, Y. Nakanuma, Biliary innate immunity in the pathogenesis of biliary diseases, Inflamm. Allergy Drug Targets 9 (2010) 83–90.
[161] M.C. Maiuri, E. Zalckvar, A. Kimchi, G. Kroemer, Self-eating and self-killing: crosstalk between autophagy and apoptosis, Nat. Rev. Mol. Cell Biol. 8 (2007) 741–752.
[162] D.J. Klionsky, K. Abdelmohsen, A. Abe, et al., Guidelines for the use and interpretation of assays for monitoring autophagy (3rd edition), Autophagy 12 (2016) 1–222.
[163] M. Sasaki, Y. Nakanuma, Novel approach to bile duct damage in primary biliary cirrhosis: participation of cellular senescence and autophagy, Int. J. Hepatol. 2012 (2012) 452143.
[164] K. McDaniel, F. Meng, N. Wu, et al., Forkhead box A2 regulates biliary heterogeneity and senescence during cholestatic liver injury in micedouble dagger, Hepatology 65 (2017) 544–559.
[165] A. Arduini, G. Serviddio, A.M. Tormos, M. Monsalve, J. Sastre, Mitochondrial dysfunction in cholestatic liver diseases, Front. Biosci. (Elite Ed.) 4 (2012) 2233–2252.
[166] F. Rodier, J. Campisi, Four faces of cellular senescence, J. Cell Biol. 192 (2011) 547–556.
[167] L. Meng, M. Quezada, P. Levine, et al., Functional role of cellular senescence in biliary injury, Am. J. Pathol. 185 (2015) 602–609.
[168] J.J. Lemasters, T. Qian, L. He, et al., Role of mitochondrial inner membrane permeabilization in necrotic cell death, apoptosis, and autophagy, Antioxid. Redox Signal. 4 (2002) 769–781.
[169] J.S. Kim, L. He, J.J. Lemasters, Mitochondrial permeability transition: a common pathway to necrosis and apoptosis, Biochem. Biophys. Res. Commun. 304 (2003) 463–470.
[170] X. Xia, S. Demorrow, H. Francis, et al., Cholangiocyte injury and ductopenic syndromes, Semin. Liver Dis. 27 (2007) 401–412.
[171] K.D. Lindor, M.E. Gershwin, R. Poupon, M. Kaplan, N.V. Bergasa, E.J. Heathcote, Primary biliary cirrhosis, Hepatology 50 (2009) 291–308.
[172] P. Deltenre, D.C. Valla, Ischemic cholangiopathy, J. Hepatol. 44 (2006) 806–817.
[173] R. Weinlich, A. Oberst, H.M. Beere, D.R. Green, Necroptosis in development, inflammation and disease, Nat. Rev. Mol. Cell Biol. 18 (2017) 127–136.
[174] M. Sasaki, Y. Nakanuma, Stress-induced cellular responses and cell death mechanisms during inflammatory cholangiopathies, Clin. Res. Hepatol. Gastroenterol. 41 (2017) 129–138.
[175] M.B. Afonso, P.M. Rodrigues, A.L. Simao, et al., Activation of necroptosis in human and experimental cholestasis, Cell Death Dis. 7 (2016) e2390.
[176] W. Zhou, J. Yuan, Necroptosis in health and diseases, Semin. Cell Dev. Biol. 35 (2014) 14–23.
[177] B. Tummers, D.R. Green, Caspase-8: regulating life and death, Immunol. Rev. 277 (2017) 76–89.
[178] K. Moriwaki, F.K. Chan, RIP3: a molecular switch for necrosis and inflammation, Genes Dev. 27 (2013) 1640–1649.
[179] L.L. Kennedy, F. Meng, J.K. Venter, et al., Knockout of microRNA-21 reduces biliary hyperplasia and liver fibrosis in cholestatic bile duct ligated mice, Lab. Investig. 96 (2016) 1256–1267.
[180] A. Lau, S. Wang, J. Jiang, et al., RIPK3-mediated necroptosis promotes donor kidney inflammatory injury and reduces allograft survival, Am. J. Transplant. 13 (2013) 2805–2818.
[181] M.G. Roma, F.D. Toledo, A.C. Boaglio, C.L. Basiglio, F.A. Crocenzi, E.J. Sanchez Pozzi, Ursodeoxycholic acid in cholestasis: linking action mechanisms to therapeutic applications, Clin. Sci. (Lond.) 121 (2011) 523–544.
[182] C. Colombo, P.M. Battezzati, M. Podda, N. Bettinardi, A. Giunta, Ursodeoxycholic acid for liver disease associated with cystic fibrosis: a double-blind multicenter trial. The Italian group for the study of ursodeoxycholic acid in cystic fibrosis, Hepatology 23 (1996) 1484–1490.
[183] C.Y. Ooi, S. Nightingale, P.R. Durie, S.D. Freedman, Ursodeoxycholic acid in cystic fibrosis-associated liver disease, J. Cyst. Fibros. 11 (2012) 72–73.
[184] S. Willot, S. Uhlen, L. Michaud, et al., Effect of ursodeoxycholic acid on liver function in children after successful surgery for biliary atresia, Pediatrics 122 (2008) e1236–e1241.
[185] F. Bessone, M.G. Roma, Is ursodeoxycholic acid detrimental in obstructive cholestasis? A propos of a case of malignant biliary obstruction, Ann. Hepatol. 15 (2016) 442–447.
[186] A.F. Hofmann, Pharmacology of ursodeoxycholic acid, an enterohepatic drug, Scand. J. Gastroenterol. Suppl. 204 (1994) 1–15.
[187] J.D. Amaral, R.J. Viana, R.M. Ramalho, C.J. Steer, C.M. Rodrigues, Bile acids: regulation of apoptosis by ursodeoxycholic acid, J. Lipid Res. 50 (2009) 1721–1734.
[188] C.L. Basiglio, A.D. Mottino, M.G. Roma, Tauroursodeoxycholate counteracts hepatocellular lysis induced by tensioactive bile salts by preventing plasma membrane-micelle transition, Chem. Biol. Interact. 188 (2010) 386–392.
[189] R. Botla, J.R. Spivey, H. Aguilar, S.F. Bronk, G.J. Gores, Ursodeoxycholate (UDCA) inhibits the mitochondrial membrane permeability transition induced by glycochenodeoxycholate: a mechanism of UDCA cytoprotection, J. Pharmacol. Exp. Ther. 272 (1995) 930–938.
[190] C.M. Rodrigues, G. Fan, P.Y. Wong, B.T. Kren, C.J. Steer, Ursodeoxycholic acid may inhibit deoxycholic acid-induced apoptosis by modulating mitochondrial

Author's Personal Copy

transmembrane potential and reactive oxygen species production, Mol. Med. 4 (1998) 165–178.
[191] A. Colell, O. Coll, C. Garcia-Ruiz, et al., Tauroursodeoxycholic acid protects hepatocytes from ethanol-fed rats against tumor necrosis factor-induced cell death by replenishing mitochondrial glutathione, Hepatology 34 (2001) 964–971.
[192] F. Azzaroli, W. Mehal, C.J. Soroka, et al., Ursodeoxycholic acid diminishes Fas-ligand-induced apoptosis in mouse hepatocytes, Hepatology 36 (2002) 49–54.
[193] C.M. Rodrigues, G. Fan, X. Ma, B.T. Kren, C.J. Steer, A novel role for ursodeoxycholic acid in inhibiting apoptosis by modulating mitochondrial membrane perturbation, J. Clin. Invest. 101 (1998) 2790–2799.
[194] J.D. Amaral, R.E. Castro, S. Sola, C.J. Steer, C.M. Rodrigues, p53 is a key molecular target of ursodeoxycholic acid in regulating apoptosis, J. Biol. Chem. 282 (2007) 34250–34259.
[195] K.G. Leong, A. Karsan, Signaling pathways mediated by tumor necrosis factor alpha, Histol. Histopathol. 15 (2000) 1303–1325.
[196] Q. Xie, V.I. Khaoustov, C.C. Chung, et al., Effect of tauroursodeoxycholic acid on endoplasmic reticulum stress-induced caspase-12 activation, Hepatology 36 (2002) 592–601.
[197] U. Ozcan, E. Yilmaz, L. Ozcan, et al., Chemical chaperones reduce ER stress and restore glucose homeostasis in a mouse model of type 2 diabetes, Science 313 (2006) 1137–1140.
[198] M.H. Schoemaker, Conde de la RL, M. Buist-Homan, et al., Tauroursodeoxycholic acid protects rat hepatocytes from bile acid-induced apoptosis via activation of survival pathways, Hepatology 39 (2004) 1563–1573.
[199] E. Im, S. Akare, A. Powell, J.D. Martinez, Ursodeoxycholic acid can suppress deoxycholic acid-induced apoptosis by stimulating Akt/PKB-dependent survival signaling, Nutr. Cancer 51 (2005) 110–116.
[200] M. Marzioni, H. Francis, A. Benedetti, et al., Ca2+-dependent cytoprotective effects of ursodeoxycholic and tauroursodeoxycholic acid on the biliary epithelium in a rat model of cholestasis and loss of bile ducts, Am. J. Pathol. 168 (2006) 398–409.
[201] G. Zollner, M. Wagner, T. Moustafa, et al., Coordinated induction of bile acid detoxification and alternative elimination in mice: role of FXR-regulated organic solute transporter-alpha/beta in the adaptive response to bile acids, Am. J. Physiol. Gastrointest. Liver Physiol. 290 (2006) G923–G932.
[202] E.G. Schuetz, S. Strom, K. Yasuda, et al., Disrupted bile acid homeostasis reveals an unexpected interaction among nuclear hormone receptors, transporters, and cytochrome P450, J. Biol. Chem. 276 (2001) 39411–39418.
[203] R. Poupon, Ursodeoxycholic acid and bile-acid mimetics as therapeutic agents for cholestatic liver diseases: an overview of their mechanisms of action, Clin. Res. Hepatol. Gastroenterol. 36 (Suppl. 1) (2012) S3–12.
[204] H.U. Marschall, M. Wagner, G. Zollner, et al., Complementary stimulation of hepatobiliary transport and detoxification systems by rifampicin and ursodeoxycholic acid in humans, Gastroenterology 129 (2005) 476–485.
[205] N.S. Ghonem, M. Ananthanarayanan, C.J. Soroka, J.L. Boyer, Peroxisome proliferator-activated receptor alpha activates human multidrug resistance transporter 3/ATP-binding cassette protein subfamily B4 transcription and increases rat biliary phosphatidylcholine secretion, Hepatology 59 (2014) 1030–1042.
[206] J. Prieto, N. Garcia, J.M. Marti-Climent, I. Penuelas, J.A. Richter, J.F. Medina, Assessment of biliary bicarbonate secretion in humans by positron emission tomography, Gastroenterology 117 (1999) 167–172.
[207] F. Arenas, I. Hervias, M. Uriz, R. Joplin, J. Prieto, J.F. Medina, Combination of ursodeoxycholic acid and glucocorticoids upregulates the AE2 alternate promoter in human liver cells, J. Clin. Invest. 118 (2008) 695–709.
[208] A.F. Hofmann, S.F. Zakko, M. Lira, et al., Novel biotransformation and physiological properties of norursodeoxycholic acid in humans, Hepatology 42 (2005) 1391–1398.
[209] P. Fickert, M. Wagner, H.U. Marschall, et al., 24-norUrsodeoxycholic acid is superior to ursodeoxycholic acid in the treatment of sclerosing cholangitis in Mdr2 (Abcb4) knockout mice, Gastroenterology 130 (2006) 465–481.
[210] P. Fickert, G.M. Hirschfield, G. Denk, et al., norUrsodeoxycholic acid improves cholestasis in primary sclerosing cholangitis, J. Hepatol. 67 (2017) 549–558.
[211] H. Tanaka, I. Makino, Ursodeoxycholic acid-dependent activation of the glucocorticoid receptor, Biochem. Biophys. Res. Commun. 188 (1992) 942–948.
[212] M. Yoshikawa, T. Tsujii, K. Matsumura, et al., Immunomodulatory effects of ursodeoxycholic acid on immune responses, Hepatology 16 (1992) 358–364.
[213] S. Miyaguchi, M. Mori, Ursodeoxycholic acid (UDCA) suppresses liver interleukin 2 mRNA in the cholangitis model, Hepato-Gastroenterology 52 (2005) 596–602.
[214] S. Terasaki, Y. Nakanuma, H. Ogino, M. Unoura, K. Kobayashi, Hepatocellular and biliary expression of HLA antigens in primary biliary cirrhosis before and after ursodeoxycholic acid therapy, Am. J. Gastroenterol. 86 (1991) 1194–1199.
[215] H. Yokomori, M. Oda, G. Wakabayashi, M. Kitajima, H. Ishii, Ursodeoxycholic acid therapy attenuated expression of adhesion molecule in primary biliary cirrhosis, Intern. Med. 42 (2003) 1259–1261.
[216] M. Leuschner, S. Guldutuna, T. You, K. Hubner, S. Bhatti, U. Leuschner, Ursodeoxycholic acid and prednisolone versus ursodeoxycholic acid and placebo in the treatment of early stages of primary biliary cirrhosis, J. Hepatol. 25 (1996) 49–57.
[217] A. Molinaro, H.U. Marschall, Why doesn't primary biliary cholangitis respond to immunosuppressive medications? Curr. Hepatol. Rep. 16 (2017) 119–123.
[218] X. Peng, X. Luo, J.Y. Hou, et al., Immunosuppressive agents for the treatment of primary sclerosing cholangitis: a systematic review and meta-analysis, Dig. Dis. 35 (2017) 478–485.
[219] T.H. Karlsen, M. Vesterhus, K.M. Boberg, Review article: controversies in the management of primary biliary cirrhosis and primary sclerosing cholangitis, Aliment. Pharmacol. Ther. 39 (2014) 282–301.
[220] H.C. Mitchison, M.F. Bassendine, A.J. Malcolm, A.J. Watson, C.O. Record, James OF, A pilot, double-blind, controlled 1-year trial of prednisolone treatment in primary biliary cirrhosis: hepatic improvement but greater bone loss, Hepatology 10 (1989) 420–429.
[221] D. Juricic, I. Hrstic, D. Radic, et al., Vanishing bile duct syndrome associated with azithromycin in a 62-year-old man, Basic Clin. Pharmacol. Toxicol. 106 (2010) 62–65.
[222] M.S. Morelli, F.X. O'Brien, Stevens-Johnson syndrome and cholestatic hepatitis, Dig. Dis. Sci. 46 (2001) 2385–2388.
[223] H. Tajiri, Y. Etani, S. Mushiake, K. Ozono, M. Nakayama, A favorable response to steroid therapy in a child with drug-associated acute vanishing bile duct syndrome and skin disorder, J. Paediatr. Child Health 44 (2008) 234–236.
[224] J.C. White, S. Appleman, Infliximab/plasmapheresis in vanishing bile duct syndrome secondary to toxic epidermal necrolysis, Pediatrics 134 (2014) e1194–e1198.
[225] W. Karnsakul, T. Arkachaisri, K. Atisook, W. Wisuthsarewong, Y. Sattawatthamrong, P. Aanpreung, Vanishing bile duct syndrome in a child with toxic epidermal necrolysis: an interplay of unbalanced immune regulatory mechanisms, Ann. Hepatol. 5 (2006) 116–119.
[226] H.Y. Kim, H.K. Yang, S.H. Kim, J.H. Park, Ibuprofen associated acute vanishing bile duct syndrome and toxic epidermal necrolysis in an infant, Yonsei Med. J. 55 (2014) 834–837.
[227] J. Takeyama, T. Saito, T. Itagaki, D. Abukawa, Vanishing bile duct syndrome with a history of erythema multiforme, Pediatr. Int. 48 (2006) 651–653.
[228] H. Li, X. Li, X.X. Liao, et al., Drug associated vanishing bile duct syndrome combined with hemophagocytic lymphohistiocytosis, World J. Gastrointest. Endosc. 4 (2012) 376–378.
[229] S.S. Jakab, A.B. West, D.M. Meighan, R.S. Brown Jr., W.B. Hale, Mycophenolate mofetil for drug-induced vanishing bile duct syndrome, World J. Gastroenterol. 13 (2007) 6087–6089.
[230] G. Okan, S. Yaylaci, O. Peker, S. Kaymakoglu, M. Saruc, Vanishing bile duct and Stevens-Johnson syndrome associated with ciprofloxacin treated with tacrolimus, World J. Gastroenterol. 14 (2008) 4697–4700.
[231] T.A. Roskams, N.D. Theise, C. Balabaud, et al., Nomenclature of the finer branches of the biliary tree: canals, ductules, and ductular reactions in human livers, Hepatology 39 (2004) 1739–1745.
[232] A.S. Gouw, A.D. Clouston, N.D. Theise, Ductular reactions in human liver: diversity at the interface, Hepatology 54 (2011) 1853–1863.
[233] G. Lanzoni, V. Cardinale, G. Carpino, The hepatic, biliary, and pancreatic network of stem/progenitor cell niches in humans: a new reference frame for disease and regeneration, Hepatology 64 (2016) 277–286.
[234] I.E.M. de Jong, O.B. van Leeuwen, T. Lisman, A.S.H. Gouw, R.J. Porte, Repopulating the biliary tree from the peribiliary glands, Biochim. Biophys. Acta Mol. basis Dis. 2018 (1864) 1524–1531.
[235] C. Hall, K. Sato, N. Wu, et al., Regulators of cholangiocyte proliferation, Gene Expr. 17 (2017) 155–171.
[236] M. Marzioni, G. Alpini, S. Saccomanno, et al., Glucagon-like peptide-1 and its receptor agonist exendin-4 modulate cholangiocyte adaptive response to cholestasis, Gastroenterology 133 (2007) 244–255.
[237] S. Glaser, I.P. Lam, A. Franchitto, et al., Knockout of secretin receptor reduces large cholangiocyte hyperplasia in mice with extrahepatic cholestasis induced by bile duct ligation, Hepatology 52 (2010) 204–214.
[238] G. Alpini, S.S. Glaser, Y. Ueno, et al., Heterogeneity of the proliferative capacity of rat cholangiocytes after bile duct ligation, Am. J. Phys. 274 (1998) G767–G775.
[239] S.S. Glaser, E. Gaudio, A. Rao, et al., Morphological and functional heterogeneity of the mouse intrahepatic biliary epithelium, Lab. Investig. 89 (2009) 456–469.
[240] H. Francis, S. Glaser, S. Demorrow, et al., Small mouse cholangiocytes proliferate in response to H1 histamine receptor stimulation by activation of the IP3/CaMK I/CREB pathway, Am. J. Physiol. Cell Physiol. 295 (2008) C499–C513.
[241] R. Mancinelli, A. Franchitto, E. Gaudio, et al., After damage of large bile ducts by gamma-aminobutyric acid, small ducts replenish the biliary tree by amplification of calcium-dependent signaling and de novo acquisition of large cholangiocyte phenotypes, Am. J. Pathol. 176 (2010) 1790–1800.
[242] G.D. LeSage, S.S. Glaser, L. Marucci, et al., Acute carbon tetrachloride feeding induces damage of large but not small cholangiocytes from BDL rat liver, Am. J. Phys. 276 (1999) G1289–G1301.
[243] M.K. Munshi, S. Priester, E. Gaudio, et al., Regulation of biliary proliferation by neuroendocrine factors: implications for the pathogenesis of cholestatic liver diseases, Am. J. Pathol. 178 (2011) 472–484.
[244] D. Alvaro, M.G. Mancino, S. Glaser, et al., Proliferating cholangiocytes: a neuroendocrine compartment in the diseased liver, Gastroenterology 132 (2007) 415–431.
[245] S.G. Hubscher, J.A. Buckels, E. Elias, P. McMaster, J. Neuberger, Vanishing bile-duct syndrome following liver transplantation–is it reversible? Transplantation 51 (1991) 1004–1010.
[246] M. Strazzabosco, S. Somlo, Polycystic liver diseases: congenital disorders of cholangiocyte signaling, Gastroenterology 140 (2011) 1855–1859 1859.
[247] A.E. Sirica, M.H. Nathanson, G.J. Gores, LaRusso NF, Pathobiology of biliary epithelia and cholangiocarcinoma: proceedings of the Henry M. and Lillian Stratton basic research single-topic conference, Hepatology 48 (2008) 2040–2046.
[248] U. Beuers, B. Goke, GLP-1 analogues: a new therapeutic approach to prevent ductopenia in cholangiopathies? Gut 58 (2009) 902–903.

Molecular and Cellular Biochemistry
https://doi.org/10.1007/s11010-019-03517-8

Role of phospholipase D in migration and invasion induced by linoleic acid in breast cancer cells

Ricardo Diaz-Aragon[1] · Javier Ramirez-Ricardo[1] · Pedro Cortes-Reynosa[1] · Arturo Simoni-Nieves[2] · Luis-Enrique Gomez-Quiroz[2] · Eduardo Perez Salazar[1]

Received: 28 September 2018 / Accepted: 8 March 2019
© Springer Science+Business Media, LLC, part of Springer Nature 2019

Abstract
Linoleic acid (LA) is an essential and omega-6 polyunsaturated fatty acid that mediates a variety of biological processes, including migration and invasion in breast cancer cells. Phospholipase D (PLD) catalyses the hydrolysis of phosphatidylcholine to produce phosphatidic acid and choline. Increases of expression and activity of PLD are reported in several human cancers, including gastric, colorectal, renal, stomach, lung and breast. In this article, we demonstrate that LA induces an increase of PLD activity in MDA-MB-231 breast cancer cells. Particularly, PLD1 and/or PLD2 mediate migration and invasion induced by LA. Moreover, LA induces increases in number and size of spheroids via PLD activity. FFAR1 also mediates migration and invasion, whereas PLD activation induced by LA requires the activities of FFAR1, FFAR4 and EGFR in MDA-MB-231 cells. In summary, PLD plays a pivotal role in migration and invasion induced by LA in MDA-MB-231 breast cancer cells.

Keywords Breast cancer · Linoleic acid · PLD · Migration · Invasion · Spheroids · FFAR1 · FFAR4

Introduction

Free fatty acids (FFAs) are sources of energy for the body; however, they are also ligands for nuclear peroxisome proliferator-activated receptors, which regulate expression of genes involved in glucose and lipid metabolism [1, 2]. The FFAs induce the activation of signal transduction pathways, which mediate several biological processes including migration and invasion in breast cancer cells [3, 4]. Linoleic acid (LA) is an essential and omega-6 polyunsaturated fatty acid, which is the major fatty acid in occidental diets with an intake of 15–20 g/day/person and a plasma concentration of ~275 μM [5, 6]. Particularly, LA mediates a variety of cell processes in breast cancer cells, including the expression of plasminogen activator inhibitor-1, migration and invasion, whereas it induces an epithelial-to-mesenchymal transition-like process in mammary non-tumourigenic epithelial cells, MCF10A [4, 7–9].

Free fatty acid receptors, 1 (FFAR1) and FFAR4, are G protein-coupled receptors (GPCRs) activated by medium- and long-chain fatty acids, including LA. In contrast, these receptors are not activated by short-chain fatty acids [10, 11]. FFAR1 and FFAR4 are expressed in pancreatic β cells, adipose tissue, breast cancer cell lines (MDA-MB-231 and

Electronic supplementary material The online version of this article (https://doi.org/10.1007/s11010-019-03517-8) contains supplementary material, which is available to authorized users.

✉ Eduardo Perez Salazar
jperez@cell.cinvestav.mx

Ricardo Diaz-Aragon
tarja_diaz@hotmail.com

Javier Ramirez-Ricardo
jarry_725@hotmail.com

Pedro Cortes-Reynosa
pedrocortesr@yahoo.com

Arturo Simoni-Nieves
bioexpp22@gmail.com

Luis-Enrique Gomez-Quiroz
jegq@xanum.uam.mx

[1] Departamento de Biologia Celular, Cinvestav-IPN, Av. IPN # 2508, 07360 Mexico, DF, Mexico

[2] Departamento de Ciencias de la Salud, UAM-Iztapalapa, Mexico City, Mexico

Published online: 15 March 2019

MCF-7) and mammary non-tumourigenic epithelial cells, MCF10A [10, 12, 13]. Particularly, oleic acid induces proliferation via FFAR1 activation, whereas LA induces migration and invasion via FFAR4 activation in MDA-MB-231 cells [4, 14, 15].

Phospholipase D (PLD) is an enzyme that catalyses the hydrolysis of phosphatidylcholine, the major membrane phospholipid, to produce phosphatidic acid (PA) and choline [16]. PA is a second messenger that can be metabolised to other lipid metabolites, such as lyso-PA and diacylglycerol [17, 18]. Two mammalian isoforms of PLD have been described, namely PLD1 and PLD2, which are almost ubiquitous and shared about 50% homology including two highly conserved HDK motifs that define its catalytic activity [19–21]. Particularly, PLD1 and PLD2 are activated by a wide variety of GPCRs and receptor tyrosine kinases (RTKs) in response to a wide range of mitogens. Activation of PLD results in an increase of local concentrations of PA and its involvement in many cellular biological processes, including proliferation, survival, chemiotaxis, vesicular trafficking, secretion, migration and invasion [22–25]. Moreover, increases of expression and activity of PLD are reported in several types of human cancers, including gastric, colorectal, renal, stomach, lung and breast [17, 26, 27].

Previously, we demonstrated that LA induces migration and invasion of MDA-MB-231 breast cancer cells. However, the role of PLD in migration and invasion induced by LA remains to be studied. In this article, we demonstrate that LA induces an increase of PLD activity in MDA-MB-231 breast cancer cells. Particularly, PLD1 and/or PLD2 mediate migration and invasion induced by LA. Moreover, LA induces increases in number and size of spheroids via PLD activity. FFAR1 also mediates migration and invasion, whereas PLD activation induced by LA requires the activity of FFAR1, FFAR4 and EGFR in MDA-MB-231 cells.

Materials and methods

Materials

LA sodium salt, DC260126, phorbol 12,13-dibutyrate (PDB), 1-butanol (BtOH) and *tert*-butanol (*tert*-BtOH) were from Sigma (St. Louis MO). Platelet-derived growth factor (PDGF) and interleukin 1β (IL1β) were from Prepro Tech (Rocky Hill, NJ). AH7614 was from TOCRIS (Minneapolis, MN). Phosphospecific antibody (Ab) to phosphorylated tyrosines PY20 (anti-P-Tyr), VU0155069 and CAY10594 were from Santa Cruz Biotechnology (Santa Cruz, CA). AG1478 was from Calbiochem-Novabiochem (San Diego, CA). Epidermal growth factor receptor (EGFR) Ab was from Cell Signalling Technology (Beverly, MA). Actin Ab was provided for PhD to Manuel Hernandez (Cell Biology Department, Cinvestav-IPN). Basement membrane matrix (BD Matrigel) was from BD Biosciences (Bedford, MA, USA). Type I collagen was from Costar, Corning Inc (NY, USA).

Cell culture

MDA-MB-231 and MCF-7 breast cancer cells were procured from ATCC, and they were cultured in Dulbecco's modified Eagle's medium (DMEM) supplemented with 3.7 g/L sodium bicarbonate, 5% foetal bovine serum (FBS) and antibiotics, in a humidified atmosphere containing 5% CO_2 and 95% air at 37 °C. For experimental purposes, cells were serum-starved for 16 h before treatment with inhibitors and/or LA.

Cell viability assay

After starvation, MDA-MB-231 cells were washed twice with phosphate-buffered saline (PBS). Cells were equilibrated in DMEM without FBS for 30 min at 37 °C, and incubated with inhibitors used in this study for 48 h. After incubation, cells were washed with PBS and reagent WST-1 (Sigma–Aldrich) was added, and then cells were incubated for 2 h at 37 °C. The absorbance was quantified with a microplate reader at 450 nm. Each experiment was repeated three times.

Cell stimulation

Confluent cultures were washed twice with PBS, equilibrated in DMEM at 37 °C for 30 min, and then treated with inhibitors and/or LA for various times. Stimulation was terminated by aspirating the medium, and cells were solubilized in 0.5 mL of ice-cold RIPA buffer (50 mM HEPES pH 7.4, 150 mM NaCl, 1 mM EGTA, 1 mM sodium orthovanadate, 100 mM NaF, 10 mM sodium pyrophosphate, 10% glycerol, 1% Triton X–100, 1% sodium deoxycholate, 1.5 mM MgCl, 0.1% SDS, and 1 mM phenylmethylsulfonyl fluoride).

PLD activity assay

Cells were cultured for 72 h, serum-starved for 16 h, washed with PBS, and lysed by three freeze–thaw cycles in 150 µl ice-cold assay solution (10 mM Tris-HCl pH 8, 10 mM NaCl, 3.2 mM NaF, 0.1% IGEPAL, 0.3% sodium deoxycholate). Next, 50 µl of lysate was incubated for 1 h at 37 °C with choline oxidase (Phospholipase D Activity Assay Kit, Sigma-Aldrich), and activity was estimated by absorbance at 570 nm. A standard curve was generated with different concentrations of choline. All results were normalised with respect to the protein concentration of the lysate.

Immunoprecipitation and Western blotting

Immunoprecipitation (IP) and Western blotting was performed as described previously [9, 28].

Scratch-wound assay

Cells were grown to confluence in 35-mm culture dishes, starved for 16 h in DMEM without FBS, and treated for 2 h with 12 µM mitomycin C to inhibit proliferation during the experiment. Cultures were scratch-wounded using a sterile 200-µl pipette tip, washed twice with PBS and refed with DMEM without FBS in the absence or the presence of inhibitors and/or LA. The progress of cell migration into the wound space was photographed at 48 h using an inverted microscope coupled to a camera. Each experiment was repeated three times. Cell migration was evaluated using the ImageJ software (NIH, USA).

Chemotactic and invasion assays

Chemotactic and invasion assays were performed by the modified Boyden chamber method in 24-well plates containing 12-cell culture inserts of 8 µm pore size (Costar, Corning Inc). For invasion assays, 50 µl matrigel (3 mg/mL) was added into culture inserts and kept for 2 h at 37 °C. Cells were plated at 1×10^5 cells per insert in 100 µl FBS-free DMEM on the top chamber, whereas the lower chamber containing 600 µl DMEM with 90 µM LA and chambers were incubated for 48 h at 37 °C in a 5% CO_2 atmosphere. After incubation, cells and matrigel were removed with cotton swabs, and cells on the lower surface of membrane were washed and fixed with 4% (vol/vol) paraformaldehyde in PBS for 15 min. The number of migrated or invaded cells was estimated by staining of membranes with 0.1% crystal violet in PBS. Membranes were washed three times with PBS, photographed and the resulting dye was eluted with 500 µl 30% acetic acid, and then the absorbance at 600 nm was measured. Background value was obtained from wells without cells.

Spheroid formation assay on low-attachment

Confluent cultures of MDA-MB-231 cells (80%) were harvested with trypsin and gently pipetted to form a single cell suspension. Trypsin was inactivated by addition of FBS-containing medium and the cells were collected by centrifugation. The cells were quantified and seeded at 5,000 cells per well in six-well ultra-low attachment cluster dishes (Costar, Inc). Spheroids were permitted to grow in DMEM with 1% FBS for 5 days, and then spheroids were untreated or treated with 90 µM LA and/or 0.3% BtOH for other 5 days. Spheroid number and area were quantified using an inverted microscope coupled to a camera. The number of spheroids was determined by using the ImageJ software (NIH, USA).

Spheroid formation assay on matrigel and type I collagen

Confluent cultures of MDA-MB-231 cells (80%) were harvested with trypsin and gently pipetted to form a single cell suspension. Trypsin was inactivated by addition of FBS-containing medium and cells were collected by centrifugation and quantified.

A volume of 500 µl of matrigel (3 mg/mL) or 500 µl type I collagen (250 µg/mL) were spread with a pipette tip on the bottom of a 24-well chamber slide. A suspension of MDA-MB-231 single-cells was laid on top of the matrix with a density of 3,000 cells per well and then incubated for 24 h. After incubation, cells were untreated or treated with 90 µM LA and/or 0.3% BtOH and spheroids were permitted to grow in DMEM with 0.1% FBS for 15 days. LA and BtOH were renewed every third day. Spheroid number and area were quantified using an inverted microscope coupled to a camera. The number of spheroids was determined by using the ImageJ software (NIH, USA).

Statistical analysis

Experiments were performed at least three times and results are expressed as mean ± SEM. Data were statistically analysed using one-way ANOVA and Knewman-Keuls's multiple comparison tests. A statistical probability of $P < 0.05$ was considered significant.

Results

LA induces PLD activation in MDA-MB-231 breast cancer cells

We studied whether LA induced activation of PLD. MDA-MB-231 breast cancer cells were treated with 90 µM LA for various times and PLD activity was determined. Our findings showed that LA induced PLD activation at 5 and 60 min of stimulation in MDA-MB-231 cells (Fig. 1a).

Since PDGF, IL1β and PDB induce PLD activation [29, 30], we further substantiate that LA induced the PLD activation by stimulation of MDA-MB-231 cells with 20 ng/ml PDGF, 10 ng/ml IL1β, 1 µM PDB for 30 min or 90 µM LA for 5 min, and then PLD activity was determined. Our findings demonstrated that LA, PDGF, IL1β and PDB induced activation of PLD in MDA-MB-231 cells (Fig. 1b).

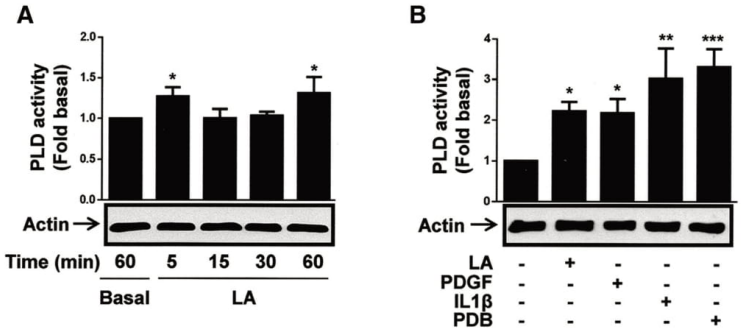


Fig. 1 LA-induced PLD activation in MDA-MB-231 breast cancer cells. **a** MDA-MB-231 cells were stimulated with 90 μM LA for various times, and PLD activity was determined. **b** MDA-MB-231 cells were treated with 90 μM LA for 5 min, 20 ng/ml PDGF, 10 ng/ml IL1β and 1 μM PDB for 30 min, and PLD activity was determined. Actin was included as loading control. Graphs represent the mean ± SEM and are expressed as the fold of PLD activity above unstimulated cells (Basal). Asterisks denote comparisons made to unstimulated cells. $^{*}P<0.05$, $^{**}P<0.01$, $^{***}P<0.001$

LA induces migration and invasion through a PLD-dependent pathway in MDA-MB-231 cells

Since LA induces migration and invasion in breast cancer cells [4, 9], we studied the role of PLD in migration and invasion induced by LA in MDA-MB-231 cells. We first determined whether inhibitors used in these studies were cytotoxic for cells. The MDA-MB-231 cells were treated with different inhibitors to concentrations used in these studies, and viability assays were performed. Our findings showed that inhibitors were not toxic for MDA-MB-231 cells (Fig. 2a).

Next, we studied the role of PLD in migration. Since PLD is able to utilise primary alcohols for a transphosphatidylation reaction to generate phosphatidylalcohols in place of PA, the incubation with BtOH has been used like a PLD inhibitor [31]. Cultures of MDA-MB-231 cells were scratch-wounded and untreated or treated with 0.3% BtOH, 0.3% *tert*-BtOH and 90 μM LA for 48 h. The *tert*-BtOH was included as a negative control of BtOH. As illustrated in Fig. 2b, treatment with BtOH inhibited migration, whereas *tert*-BtOH did not inhibit migration induced by LA in MDA-MB-231 cells.

To further substantiate our findings, we performed cell migration assays using the Boyden chamber method and MDA-MB-231 cells untreated or treated with 0.3% BtOH and stimulated without or with 90 μM LA for 48 h. Our findings showed that treatment with BtOH inhibited migration induced by LA in MDA-MB-231 cells (Fig. 2c).

Next, we studied the role of PLD in the invasion process induced by LA. Invasion assays were performed using the Boyden chamber method and MDA-MB-231 cells untreated or treated with 0.3% BtOH and stimulated without or with 90 μM LA for 48 h. Our findings demonstrated that treatment with BtOH inhibited invasion induced by LA in MDA-MB-231 cells (Fig. 2d).

Roles of PLD1 and PLD2 in migration and invasion induced by LA

We determined whether PLD1 and/or PLD2 mediate migration and invasion induced by LA in MDA-MB-231 cells. Migration assays were performed by using scratch-wound assays and Boyden chamber method with MDA-MB-231 cells untreated or treated for 2 h with 5 μM VU0155069 and 1 μM CAY10594, which are specific inhibitors of PLD1 and PLD2 respectively [32, 33], and stimulated without or with 90 μM LA for 48 h. Our findings demonstrated that inhibition of PLD1 and PLD2 activity inhibited migration induced by LA in MDA-MB-231 cells (Fig. 3a, b).

Invasion assays were performed by the Boyden chamber method and MDA-MB-231 cells untreated or treated for 2 h with 5 μM VU0155069 and 1 μM CAY10594, and stimulated without or with 90 μM LA for 48 h. Our results showed that treatment with VU0155069 completely inhibited invasion, whereas CAY10594 partly inhibited invasion induced by LA in MDA-MB-231 cells (Fig. 3c).

LA induces migration through a PLD-dependent activity in MCF-7 breast cancer cells

To further substantiate the role of PLD in migration induced by LA in breast cancer cells, we studied the role of PLD in migration induced by LA in another breast cancer cell line (MCF-7). First, migration assays were

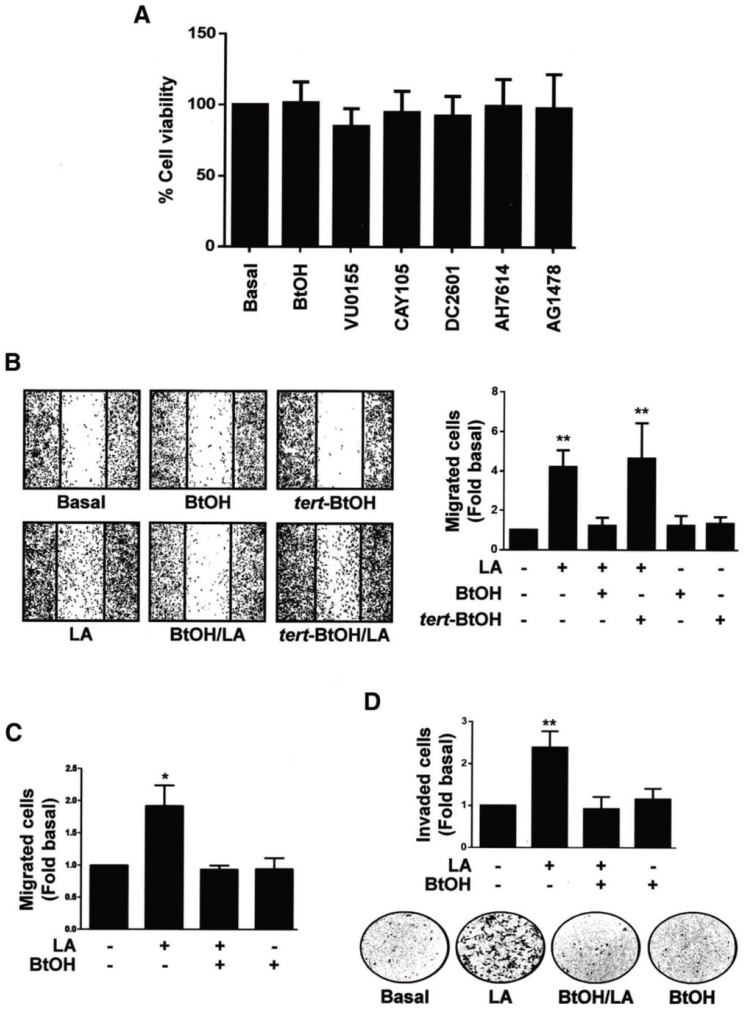


Fig. 2 LA-induced migration and invasion through a PLD-dependent pathway. **a** MDA-MB-231 cells were treated with 0.3% BtOH, 5 μM VU0155069, 1 μM CAY10594, 3 μM DC260126, 20 μM AH7614 and 500 nM AG1478 for 48 h and cytotoxicity assays were performed. Graph represents % cell viability of three independent experiments. **b** Cultures of MDA-MB-231 cells were untreated or treated with 0.3% BtOH or 0.3% *tert*-BtOH for 2 h, scratch-wounded and stimulated with 90 μM LA for 48 h. **c** Migration assays were performed by Boyden chamber method and MDA-MB-231 cells untreated or treated with 0.3% BtOH for 2 h and stimulated with 90 μM LA for 48 h. **d** Invasion assays were performed by Boyden chamber method and MDA-MB-231 cells untreated or treated with 0.3% BtOH for 2 h and stimulated with 90 μM LA for 48 h. Images were taken at 48 h. Graphs represent the mean ± SEM and are expressed as the fold of migrated or invaded cells above unstimulated cells. Asterisks denote comparisons made to unstimulated cells (Basal). $^{*}P < 0.05$, $^{**}P < 0.01$

performed by scratch-wound assays and MCF-7 cells treated with 90 μM LA for various times. Our findings demonstrated that LA induced migration at 72 h of treatment in MCF-7 breast cancer cells (Fig. 4a).

To determine the role of PLD in migration, MCF-7 cells were untreated or treated with 0.3% BtOH and stimulated without or with 90 μM LA for 72 h. Our findings demonstrated that treatment with BtOH inhibited migration induced by LA in MCF-7 cells (Fig. 4b).

LA induces spheroid formation through a PLD-dependent pathway

The three-dimensional cell culture systems mimic better the *in vivo* conditions [34]. We studied the role of PLD in spheroid formation induced by LA. First, we determined whether stimulation of MDA-MB-231 cells with 90 μM LA for 5 days induced spheroids formation and the role of PLD in low-attachment. Our findings demonstrated that treatment

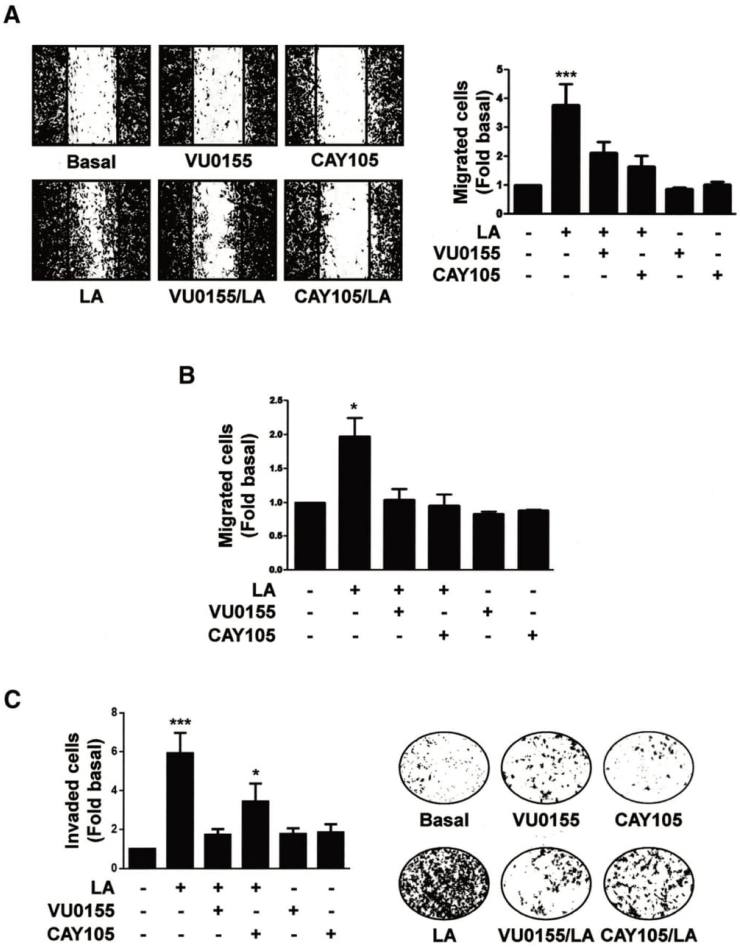


Fig. 3 Roles of PLD1 and PLD2 in migration and invasion induced by LA. **a** and **b**. Migration assays were performed by scratch-wound assays and Boyden chamber method with MDA-MB-231 cells untreated or treated with 5 μM VU0155069 or 1 μM CAY10594 for 2 h and stimulated with 90 μM LA for 48 h. **c**. Invasion assays were performed by Boyden chamber method, and MDA-MB-231 cells untreated or treated with 5 μM VU0155069 or 1 μM CAY10594 for 2 h, and stimulated with 90 μM LA for 48 h. Images were taken at 48 h. Graphs represent the mean ± SEM and are expressed as the fold of migrated or invaded cells above unstimulated cells (basal). Asterisks denote comparisons with unstimulated cells. $*P<0.05$, $***P<0.001$

of MDA-MB-231 cells with LA induced an increase in number of spheroids, and treatment with BtOH inhibited their formation in low-attachment (Fig. 5a). Moreover, treatment of MCF-7 cells with 90 μM LA for 5 days also induced an increase in number of spheroids in low-attachment (Fig. 1S, Panel A).

To further substantiate our findings, we determined whether treatment of MDA-MB-231 cells with 90 μM LA for 15 days induced an increase in the number of spheroids on matrigel and type I collagen and the role of PLD. Our findings demonstrated that stimulation of MDA-MB-231 cells with LA induced increases in number and relative area of spheroids in matrigel and type I collagen, and treatment with BtOH inhibited their formation (Figs. 5b, c, 6a, b). In addition, treatment of MCF-7 cells with 90 μM LA for 15 days also induced increases in the number and relative area of spheroids in matrigel (Fig. 1S, Panel B).

Roles of FFAR1 and FFAR4 in PLD activation

Since LA induces migration and invasion via FFAR4 in MDA-MB-231 cells [4], we studied the role of FFAR1 in migration and invasion induced by LA. Migration, and invasion assays were performed with MDA-MB-231 cells untreated or treated for 1 h with 3 μM DC260126, which is a specific inhibitor of FFAR1 [35], and stimulated without or with 90 μM LA for 48 h. Our findings demonstrated that treatment with DC260126 partly inhibited

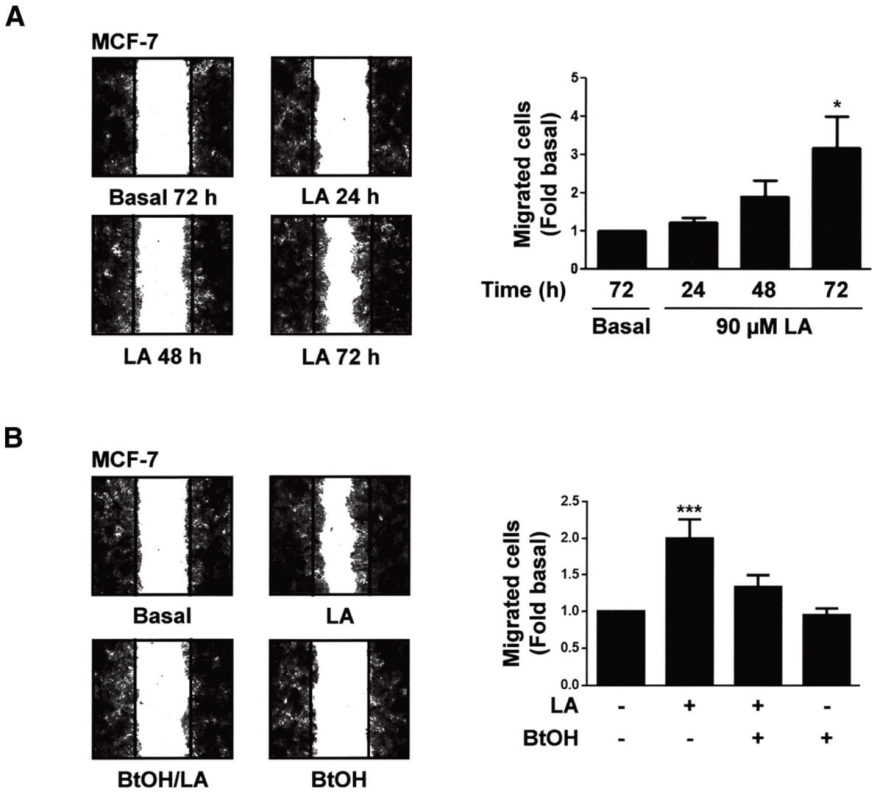


Fig. 4 LA-induced migration via PLD activity in MCF-7 breast cancer cells. **a** Cultures of MCF-7 cells were scratch-wounded and treated with 90 µM LA for various times. **b** Cultures of MCF-7 cells were untreated or treated with 0.3% BtOH for 2 h, scratch-wounded and stimulated without or with 90 µM LA for 72 h. Pictures were taken at 72 h. Graphs represent the mean ± SEM and are expressed as the fold of migrated cells above unstimulated cells (Basal). Asterisks denote comparisons with unstimulated cells. $*P<0.05$, $***P<0.001$

migration, whereas it inhibited the invasion induced by LA in MDA-MB-231 cells (Fig. 7a, b).

Next, we determined the roles of FFAR1 and FFAR4 in PLD activation induced by LA. MDA-MB-231 cells were untreated or treated for 1 h with 3 µM DC260126 and 20 µM AH7614, which are specific inhibitors of FFAR1 and FFAR4, respectively [35, 36], and stimulated without or with 90 µM LA for 5 min, and then PLD activity was analysed. Our findings demonstrated that treatment with DC260126 or AH7614 partly inhibited the PLD activity induced by LA in MDA-MB-231 cells. However, treatment with both DC260126 and AH7614 completely inhibited the PLD activity induced by LA in MDA-MB-231 cells (Fig. 7c).

Role of EGFR in PLD activation

LA induces migration and invasion via EGFR activity in MDA-MB-231 cells [4]. We determined the role of EGFR in PLD activation induced by LA. PLD activity assays were performed with MDA-MB-231 cells untreated or treated for 30 min with 500 nM AG1478, an inhibitor of EGFR [37], and stimulated without or with 90 µM LA for 5 min. Our results showed that PLD activation induced by LA required the activity of EGFR (Fig. 7d).

In order to support our findings, we determined whether LA induced EGFR activation, given by its tyrosine phosphorylation [38]. MDA-MB-231 cells were treated with 90 µM LA for various times and lysed. Lysates were

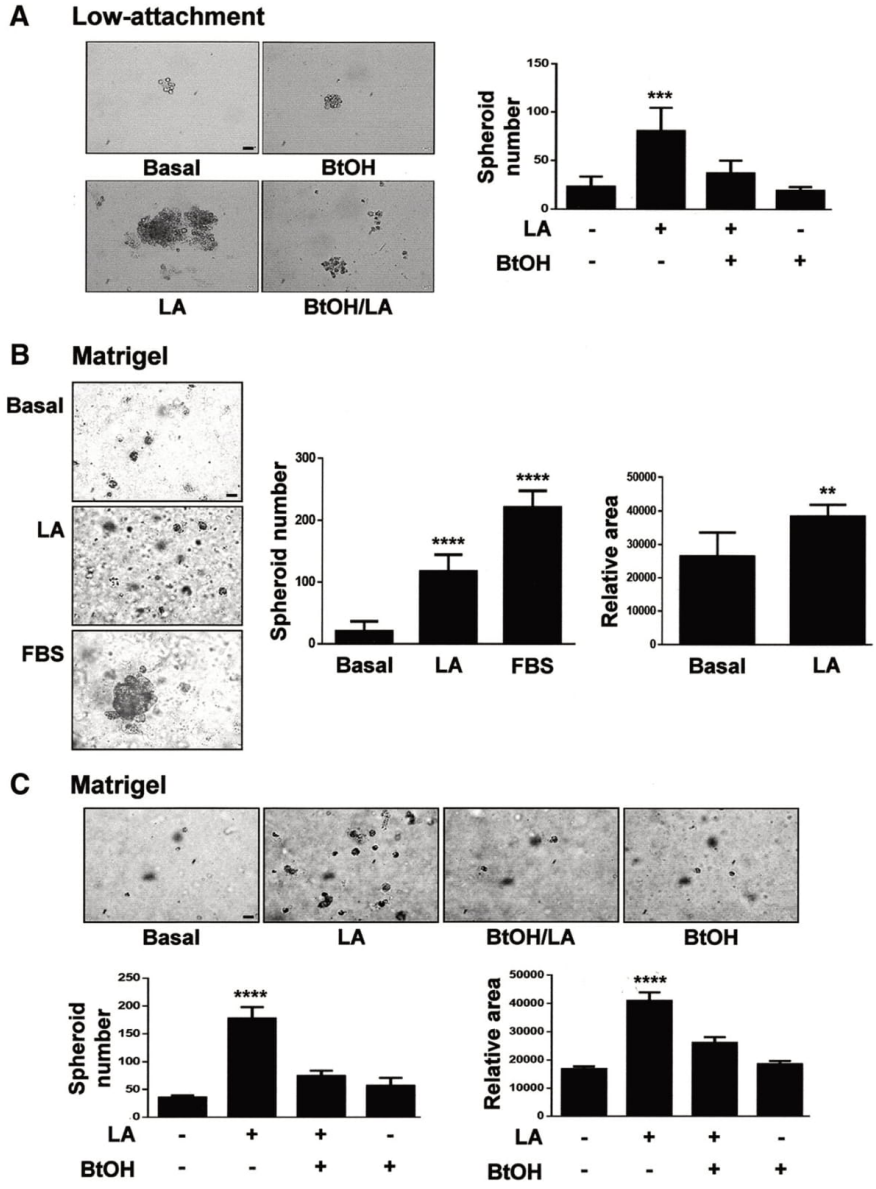


Fig. 5 LA-induces increases in spheroids number and size through a PLD-dependent pathway. **a** MDA-MB-231 cells were untreated or treated with 0.3% BtOH and stimulated with 90 μM LA for 5 days on low-attachment, and spheroid formation was evaluated. **b** and **c**. MDA-MB-231 cells were untreated or treated with 0.3% BtOH and stimulated with 90 μM LA for 15 days on matrigel, and spheroid formation was evaluated. One positive control was included (FBS). Images were acquired and analysed for number and/or size. Representative images are shown. Graphs represent the mean ± SEM of four independent experiments. Scale bar = 300 μm. Asterisks denote comparisons made to unstimulated cells (Basal). $^{**}P < 0.01$, $^{***}P < 0.001$, $^{****}P < 0.0001$

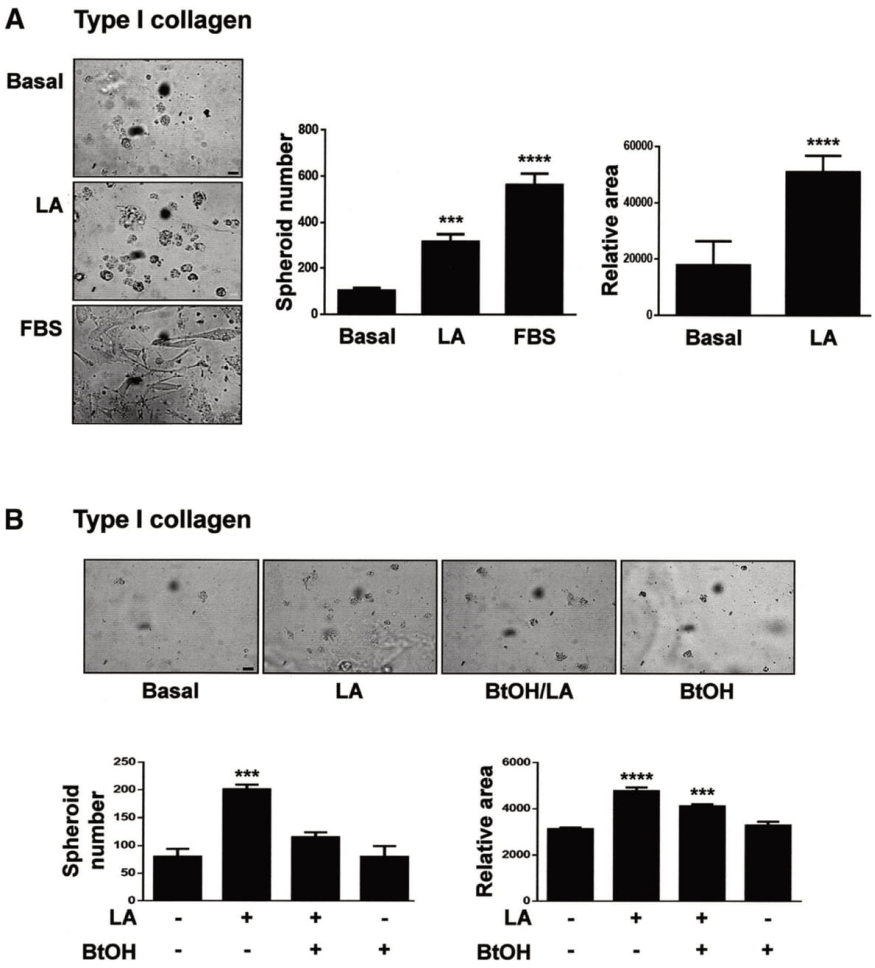


Fig. 6 LA-induced increases in spheroids number and size on type I collagen through a PLD-dependent pathway. **a** MDA-MB-231 cells were untreated or treated with 90 µM LA for 15 days on type I collagen, and spheroid formation was evaluated. One positive control was included (FBS). **b** MDA-MB-231 cells were untreated or treated with 0.3% BtOH and stimulated with 90 µM LA for 15 days on type I collagen, and spheroid formation was evaluated. Images were acquired and analysed for number and size. Representative images are shown. Scale bar = 300 µm. Asterisks denote comparisons made to unstimulated cells (Basal). ***$P < 0.001$, ****$P < 0.0001$

immunoprecipitated with anti-EGFR Ab, and complexes were analysed by Western blotting with anti-P-Tyr Ab. As illustrated in Fig. 7e, LA induced EGFR tyrosine phosphorylation in MDA-MB-231 cells.

Discussion

A strong correlation between a high dietary fat intake and the risk of developing breast cancer has been described previously [39–41]. Particularly, LA is a fatty acid and a

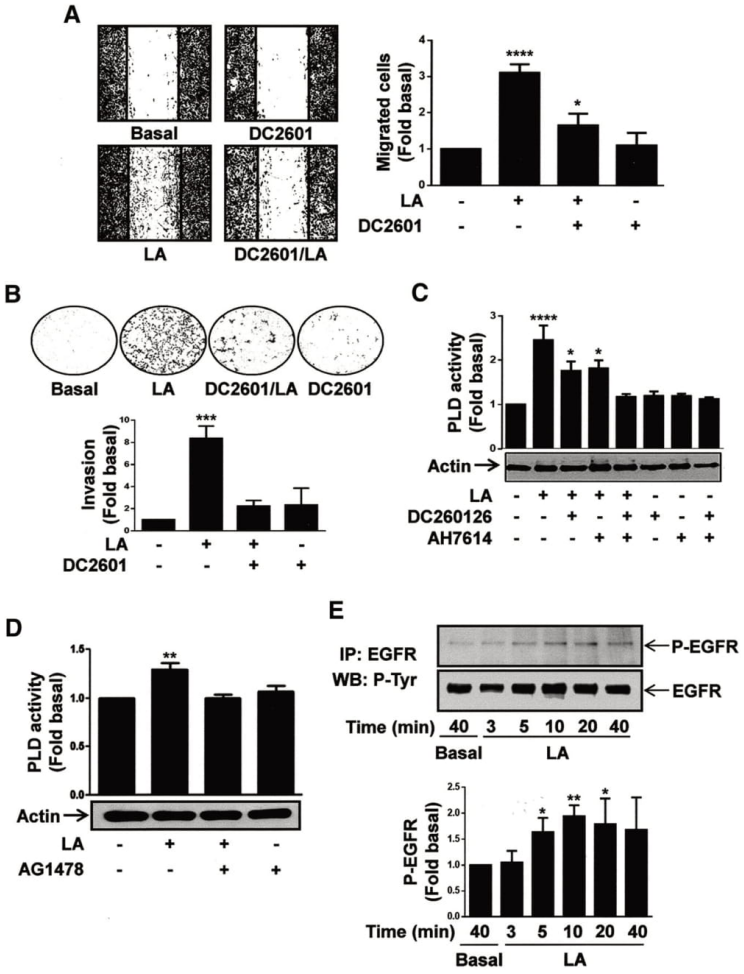


Fig. 7 Roles of FFAR1/FFAR4 and EGFR in migration/invasion and PLD activity induced by LA. **a** and **b**. Migration and invasion assays were performed by scratch-wound assays and Boyden chamber method with MDA-MB-231 cells untreated or treated with 3 μM DC260126 for 1 h and stimulated with 90 μM LA for 48 h. **c** and **d**. MDA-MB-231 cells were untreated or treated with 3 μM DC260126 and 20 μM AH7614 for 1 h or 500 nM AG1478 for 30 min and stimulated with 90 μM LA for 5 min, and PLD activity was determined. Actin was included as loading control. **e**. MDA-MB-231 cells were treated with 90 μM LA for various times and lysed. Lysates were immunoprecipitated (IP) with EGFR Ab followed by Western blotting with anti-P-Tyr Ab. Membranes were analysed further by Western blotting with anti-EGFR Ab. Graphs represent the mean ± SEM and are expressed as the fold of migrated, invaded, PLD activity or P-EGFR above unstimulated cells. Asterisks denote comparisons with unstimulated cells (Basal). $*P<0.05$, $**P<0.01$, $***P<0.001$, $****P<0.0001$

component of vegetable oils, which activates signal transduction pathways that mediate a variety of biological processes including migration and invasion in breast cancer cells, whereas it mediates tumour growth and metastasis in nude mice [4, 7, 9, 42]. However, the capacity of LA to form spheroids and the roles of PLD in spheroids' formation, migration and invasion induced by LA in breast cancer cells have not been studied.

PLD plays a pivotal role in cancer, because the expression and total PLD activity are increased in several human cancers including gastric, colorectal, renal, stomach and breast cancer, and PLD levels correlate with breast cancer grade [17, 26, 27]. We demonstrate here that LA induces a transient PLD activation in MDA-MB-231 cells. Moreover, LA induce migration via PLD activity in MDA-MB-231 and MCF-7 cells, whereas it also mediates invasion via PLD activity in MDA-MB-231 cells.

In agreement with our findings, angiotensin II induces a transient PLD activation in human adrenocortical carcinoma NCI H295R cells, whereas EGF induces also PLD2 activation with two peaks of maximal activity in COS-7 cells expressing PLD2 [43, 44]. Our findings strongly suggest that different ligands induce PLD activation with different kinetics of activity in different cell types. In addition, depriving of serum induces PLD activation and migration through a PLD-dependent pathway in breast cancer cells [45].

PLD1 and PLD2 are expressed differentially and play specific roles in cancer. Particularly, PLD1 is required for secretion of metalloproteinase-9 (MMP-9) and MMP-2 in colorectal cancer cells and glioma cells, respectively [30, 46]. PLD2 activation induces an increase in FAK phosphorylation, Akt activation and invasion in EL4 lymphoma cells, whereas inactivation of PLD2 inhibits metastasis [47]. We demonstrate here that migration induced by LA requires PLD1 and PLD2 activities in MDA-MB-231 cells. Since EGF and PDGF induce PA production, which induces activation of Ras-ERK/PI3K-NFκB signalling pathway and then PLD1 expression, which promote invasion in SK-BR3 breast cancer cells [29]. We propose that LA induces production of PA through PLD2 activation and then activation of a signalling pathway that mediates expression and activation of PLD1, which mediates migration in MDA-MB-231 cells. Supporting our proposal, activation of Wnt pathway induces an increase of PLD1/PLD2 expression, which mediate proliferation and invasion in cancer cells [48].

In addition, we demonstrate that invasion induced by LA requires PLD1 activity in MDA-MB-231 cells. Interestingly, the invasion induced by LA is also partly dependent on PLD2 activity. In agreement with our findings, EGF induces invasion through a PLD2-dependent pathway in MDA-MB-231 cells, whereas invasion induced by PDGF requires PLD1 activity in SK-BR3 breast cancer cells [29, 49]. Taken together these findings, we propose that different ligands mediate invasion through activation of PLD1 and/or PLD2 in breast cancer cells.

In order to mimic in vivo environment, we used spheroid formation assays because it is a 3D culture and is considered a more reliable biological assay [34, 50]. We demonstrate here that LA induces increases in the number and size of spheroids under different conditions, including low-attachment, matrigel and type I collagen, and it requires PLD activity in MDA-MB-231 cells. The 3D tumour spheroids are self-assembled cultures of tumour cells where cell–cell interactions predominate over cell–substrate interactions. It is considered that spheroids resemble avascular tumour nodules, micro-metastasis and intervascular regions of large solid tumours, because they have similar morphological features, microenvironment, volume growth kinetics, and gradients of nutrient distribution, oxygen concentration and cell proliferation [51, 52]. We propose that LA through PLD activation plays a pivotal role in the formation of tumour nodules and micro-metastasis. Supporting our proposal, PLD mediates invasion, tumour growth and metastasis in a human breast cancer xenograph model [49]. Moreover, androgen-insensitive prostate cancer cells, DU145 and PC-3, have a higher PLD activity than androgen-sensitive prostate cancer cells LNCaP, whereas inhibition of PLD activity reduces prostate cancer cell proliferation and colony formation in prostate cancer cell lines and patient-derived prostate cancer cells [53, 54].

Previously, we demonstrated that LA induces migration and invasion via FFAR4 in MDA-MB-231 cells [4, 9]. Moreover, LA induces an elevation of cytosolic Ca^{2+} via FFAR1 and Gi/Go in MCF-7 cells, whereas oleic acid induces proliferation via FFAR1 and Gi/Go in MDA-MB-231 cells [15, 55]. In addition, FFAR4 is expressed in intestine cells and is coupled with Gq/11 [10, 56]. We demonstrate that LA induces PLD activation via FFAR1 and FFAR4 in MDA-MB-231 cells. LA also induces invasion via FFAR1, whereas migration is partly dependent on FFAR1. We propose that LA induces activations of FFAR1 and FFAR4 which activate Gi/Go and/or Gq/11, and then PLD activations which mediate migration and invasion in MDA-MB-231 cells.

GPCRs induce EGFR transactivation via activation of metalloproteinases and then release of EGF-like ligands, such as HB-EGF, from growth factor precursors in plasma membrane [57]. Furthermore, LA induces migration and invasion via FFAR1 and/or FFAR4 and that LA induces migration and invasion through an EGFR-receptor-dependent pathway in MDA-MB-231 cells [4]. Since we demonstrate here that LA induces PLD activation via EGFR, and that LA induces EGFR tyrosine phosphorylation (activation) in MDA-MB-231 cells, we propose that LA induces migration and invasion through activation of FFAR1 and FFAR4 and transactivation of EGFR in MDA-MB-231 cells.

Combining together our above findings, we propose that stimulation of breast cancer cells with LA induces the activation of FFAR1/FFAR4, which promotes EGFR transactivation, and then EGFR signalling promotes PLD1/PLD2 activation, which mediates migration and invasion (Fig. 8).

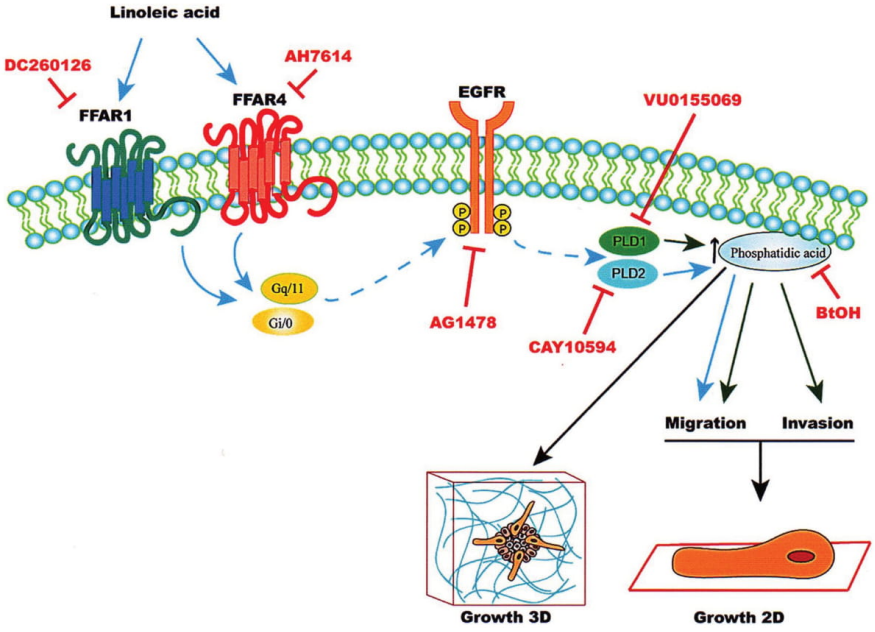


Fig. 8 Model showing roles of PLD1 and PLD2 in migration/invasion induced by LA in MDA-MB-231 breast cancer cells

Acknowledgements R. D.-A. and J. R.-R. are supported by a CONACYT Predoctoral training grant.

Author contributions R. D.-A., J. R.-R. and A. S.-N. performed research and analysed data; L.-E. G.-Q. analysed data; R. D.-A., P. C.-R., and E. P.S. designed the research and analysed data. R. D.-A. and E. P.S. wrote the paper with inputs from all the authors.

Funding This work was supported by a Grant from CONACYT-Mexico (255429) and CONACYT-FOSISS-Mexico (Salud-2015-1-261637).

Compliance with ethical standards

Conflict of interest Authors declare that there is not conflict of interest.

References

1. McArthur MJ, Atshaves BP, Frolov A, Foxworth WD, Kier AB, Schroeder F (1999) Cellular uptake and intracellular trafficking of long chain fatty acids. J Lipid Res 40:1371–1383
2. Ferre P (2004) The biology of peroxisome proliferator-activated receptors: relationship with lipid metabolism and insulin sensitivity. Diabetes 53(Suppl 1):S43–S50
3. Soto-Guzman A, Navarro-Tito N, Castro-Sanchez L, Martinez-Orozco R, Salazar EP (2010) Oleic acid promotes MMP-9 secretion and invasion in breast cancer cells. Clin Exp Metastasis 27:505–515. https://doi.org/10.1007/s10585-010-9340-1
4. Serna-Marquez N, Diaz-Aragon R, Reyes-Uribe E, Cortes-Reynosa P, Salazar EP (2017) Linoleic acid induces migration and invasion through FFAR4- and PI3K-/Akt-dependent pathway in MDA-MB-231 breast cancer cells. Med Oncol 34:111. https://doi.org/10.1007/s12032-017-0969-3
5. Anderson SG, Sanders TA, Cruickshank JK (2009) Plasma fatty acid composition as a predictor of arterial stiffness and mortality. Hypertension 53:839–845. https://doi.org/10.1161/HYPERTENSIONAHA.108.123885
6. Kris-Etherton PM, Taylor DS, Yu-Poth S, Huth P, Moriarty K, Fishell V, Hargrove RL, Zhao G, Etherton TD (2000) Polyunsaturated fatty acids in the food chain in the United States. Am J Clin Nutr 71:179S–179S88S. https://doi.org/10.1093/ajcn/71.1.179S
7. Byon CH, Hardy RW, Ren C, Ponnazhagan S, Welch DR, McDonald JM, Chen Y (2009) Free fatty acids enhance breast cancer cell migration through plasminogen activator inhibitor-1 and SMAD4. Lab Invest 89:1221–1228. https://doi.org/10.1038/labinvest.2009.97
8. Espinosa-Neira R, Mejia-Rangel J, Cortes-Reynosa P, Salazar EP (2011) Linoleic acid induces an EMT-like process in mammary epithelial cells MCF10A. Int J Biochem Cell Biol 43:1782–1791. https://doi.org/10.1016/j.biocel.2011.08.017
9. Serna-Marquez N, Villegas-Comonfort S, Galindo-Hernandez O, Navarro-Tito N, Millan A, Salazar EP (2013) Role of LOXs and COX-2 on FAK activation and cell migration induced by linoleic acid in MDA-MB-231 breast cancer cells. Cell Oncol (Dordr) 36:65–77. https://doi.org/10.1007/s13402-012-0114-4
10. Hirasawa A, Tsumaya K, Awaji T, Katsuma S, Adachi T, Yamada M, Sugimoto Y, Miyazaki S, Tsujimoto G (2005) Free fatty acids regulate gut incretin glucagon-like peptide-1 secretion through GPR120. Nat Med 11:90–94. https://doi.org/10.1038/nm1168

11. Briscoe CP, Tadayyon M, Andrews JL, Benson WG, Chambers JK, Eilert MM, Ellis C, Elshourbagy NA, Goetz AS, Minnick DT, Murdock PR, Sauls HR Jr, Shabon U, Spinage LD, Strum JC, Szekeres PG, Tan KB, Way JM, Ignar DM, Wilson S, Muir AI (2003) The orphan G protein-coupled receptor GPR40 is activated by medium and long chain fatty acids. J Biol Chem 278:11303–11311. https://doi.org/10.1074/jbc.M211495200
12. Soto-Guzman A, Robledo T, Lopez-Perez M, Salazar EP (2008) Oleic acid induces ERK1/2 activation and AP-1 DNA binding activity through a mechanism involving Src kinase and EGFR transactivation in breast cancer cells. Mol Cell Endocrinol 294:81–91. https://doi.org/10.1016/j.mce.2008.08.003
13. Navarro-Tito N, Robledo T, Salazar EP (2008) Arachidonic acid promotes FAK activation and migration in MDA-MB-231 breast cancer cells. Exp Cell Res 314:3340–3355. https://doi.org/10.1016/j.yexcr.2008.08.018
14. Hopkins MM, Zhang Z, Liu Z, Meier KE (2016) Eicosopentaneoic acid and other free fatty acid receptor agonists inhibit lysophosphatidic acid- and epidermal growth factor-induced proliferation of human breast cancer cells. J Clin Med. https://doi.org/10.3390/jcm5020016
15. Hardy S, St-Onge GG, Joly E, Langelier Y, Prentki M (2005) Oleate promotes the proliferation of breast cancer cells via the G protein-coupled receptor GPR40. J Biol Chem 280:13285–13291. https://doi.org/10.1074/jbc.M410922200
16. Exton JH (1999) Regulation of phospholipase D. Biochim Biophys Acta 1439:121–133
17. Gomez-Cambronero J (2014) Phosphatidic acid, phospholipase D and tumorigenesis. Adv Biol Regul 54:197–206. https://doi.org/10.1016/j.jbior.2013.08.006
18. Selvy PE, Lavieri RR, Lindsley CW, Brown HA (2011) Phospholipase D: enzymology, functionality, and chemical modulation. Chem Rev 111:6064–6119. https://doi.org/10.1021/cr200296t
19. Hammond SM, Altshuller YM, Sung TC, Rudge SA, Rose K, Engebrecht J, Morris AJ, Frohman MA (1995) Human ADP-ribosylation factor-activated phosphatidylcholine-specific phospholipase D defines a new and highly conserved gene family. J Biol Chem 270:29640–29643
20. Colley WC, Sung TC, Roll R, Jenco J, Hammond SM, Altshuller Y, Bar-Sagi D, Morris AJ, Frohman MA (1997) Phospholipase D2, a distinct phospholipase D isoform with novel regulatory properties that provokes cytoskeletal reorganization. Curr Biol 7:191–201
21. Kodaki T, Yamashita S (1997) Cloning, expression, and characterization of a novel phospholipase D complementary DNA from rat brain. J Biol Chem 272:11408–11413
22. Cockcroft S (2001) Signalling roles of mammalian phospholipase D1 and D2. Cell Mol Life Sci 58:1674–1687. https://doi.org/10.1007/PL00000805
23. Jang JH, Lee CS, Hwang D, Ryu SH (2012) Understanding of the roles of phospholipase D and phosphatidic acid through their binding partners. Prog Lipid Res 51:71–81. https://doi.org/10.1016/j.plipres.2011.12.003
24. Zhao C, Du G, Skowronek K, Frohman MA, Bar-Sagi D (2007) Phospholipase D2-generated phosphatidic acid couples EGFR stimulation to Ras activation by Sos. Nat Cell Biol 9:706–712. https://doi.org/10.1038/ncb1594
25. Foster DA, Salloum D, Menon D, Frias MA (2014) Phospholipase D and the maintenance of phosphatidic acid levels for regulation of mammalian target of rapamycin (mTOR). J Biol Chem 289:22583–22588. https://doi.org/10.1074/jbc.R114.566091
26. Uchida N, Okamura S, Nagamachi Y, Yamashita S (1997) Increased phospholipase D activity in human breast cancer. J Cancer Res Clin Oncol 123:280–285
27. Uchida N, Okamura S, Kuwano H (1999) Phospholipase D activity in human gastric carcinoma. Anticancer Res 19:671–675
28. Navarro-Tito N, Soto-Guzman A, Castro-Sanchez L, Martinez-Orozco R, Salazar EP (2010) Oleic acid promotes migration on MDA-MB-231 breast cancer cells through an arachidonic acid-dependent pathway. Int J Biochem Cell Biol 42:306–317. https://doi.org/10.1016/j.biocel.2009.11.010
29. Kang DW, Park MH, Lee YJ, Kim HS, Lindsley CW, Alex Brown H, Min do S (2011) Autoregulation of phospholipase D activity is coupled to selective induction of phospholipase D1 expression to promote invasion of breast cancer cells. Int J Cancer 128:805–816. https://doi.org/10.1002/ijc.25402
30. Kang DW, Park MH, Lee YJ, Kim HS, Kwon TK, Park WS, Min do S (2008) Phorbol ester up-regulates phospholipase D1 but not phospholipase D2 expression through a PKC/Ras/ERK/NFkappaB-dependent pathway and enhances matrix metalloproteinase-9 secretion in colon cancer cells. J Biol Chem 283:4094–4104. https://doi.org/10.1074/jbc.M707416200
31. Hu T, Exton JH (2005) 1-Butanol interferes with phospholipase D1 and protein kinase Calpha association and inhibits phospholipase D1 basal activity. Biochem Biophys Res Commun 327:1047–1051. https://doi.org/10.1016/j.bbrc.2004.12.117
32. Scott SA, Selvy PE, Buck JR, Cho HP, Criswell TL, Thomas AL, Armstrong MD, Arteaga CL, Lindsley CW, Brown HA (2009) Design of isoform-selective phospholipase D inhibitors that modulate cancer cell invasiveness. Nat Chem Biol 5:108–117. https://doi.org/10.1038/nchembio.140
33. Lavieri RR, Scott SA, Selvy PE, Kim K, Jadhav S, Morrison RD, Daniels JS, Brown HA, Lindsley CW (2010) Design, synthesis, and biological evaluation of halogenated N-(2-(4-oxo-1-phenyl-1,3,8-triazaspiro[4.5]decan-8-yl)ethyl)benzamides: discovery of an isoform-selective small molecule phospholipase D2 inhibitor. J Med Chem 53:6706–6719. https://doi.org/10.1021/jm100814g
34. Sutherland RM (1988) Cell and environment interactions in tumor microregions: the multicell spheroid model. Science 240:177–184
35. Hu H, He LY, Gong Z, Li N, Lu YN, Zhai QW, Liu H, Jiang HL, Zhu WL, Wang HY (2009) A novel class of antagonists for the FFAs receptor GPR40. Biochem Biophys Res Commun 390:557–563. https://doi.org/10.1016/j.bbrc.2009.10.004
36. Sparks SM, Chen G, Collins JL, Danger D, Dock ST, Jayawickreme C, Jenkinson S, Laudeman C, Leesnitzer MA, Liang X, Maloney P, McCoy DC, Moncol D, Rash V, Rimele T, Vulimiri P, Way JM, Ross S (2014) Identification of diarylsulfonamides as agonists of the free fatty acid receptor 4 (FFA4/GPR120). Bioorg Med Chem Lett 24:3100–3103. https://doi.org/10.1016/j.bmcl.2014.05.012
37. Ward WH, Cook PN, Slater AM, Davies DH, Holdgate GA, Green LR (1994) Epidermal growth factor receptor tyrosine kinase. Investigation of catalytic mechanism, structure-based searching and discovery of a potent inhibitor. Biochem Pharmacol 48:659–666
38. Normanno N, De Luca A, Bianco C, Strizzi L, Mancino M, Maiello MR, Carotenuto A, De Feo G, Caponigro F, Salomon DS (2006) Epidermal growth factor receptor (EGFR) signaling in cancer. Gene 366:2–16. https://doi.org/10.1016/j.gene.2005.10.018
39. Schulz M, Hoffmann K, Weikert C, Nothlings U, Schulze MB, Boeing H (2008) Identification of a dietary pattern characterized by high-fat food choices associated with increased risk of breast cancer: the European Prospective Investigation into Cancer and Nutrition (EPIC)-Potsdam Study. Br J Nutr 100:942–946. https://doi.org/10.1017/S0007114508966149
40. Binukumar B, Mathew A (2005) Dietary fat and risk of breast cancer. World J Surg Oncol 3:45. https://doi.org/10.1186/1477-7819-3-45
41. Abel S, Riedel S, Gelderblom WC (2014) Dietary PUFA and cancer. Proc Nutr Soc 73:361–367. https://doi.org/10.1017/S0029665114000585

42. Rose DP, Connolly JM, Liu XH (1994) Effects of linoleic acid on the growth and metastasis of two human breast cancer cell lines in nude mice and the invasive capacity of these cell lines in vitro. Cancer Res 54:6557–6562
43. Zheng X, Bollag WB (2003) AngII induces transient phospholipase D activity in the H295R glomerulosa cell model. Mol Cell Endocrinol 206:113–122
44. Mahankali M, Henkels KM, Gomez-Cambronero J (2013) A GEF-to-phospholipase molecular switch caused by phosphatidic acid, Rac and JAK tyrosine kinase that explains leukocyte cell migration. J Cell Sci 126:1416–1428. https://doi.org/10.1242/jcs.117960
45. Zheng Y, Rodrik V, Toschi A, Shi M, Hui L, Shen Y, Foster DA (2006) Phospholipase D couples survival and migration signals in stress response of human cancer cells. J Biol Chem 281:15862–15868. https://doi.org/10.1074/jbc.M600660200
46. Park MH, Ahn BH, Hong YK, Min do S (2009) Overexpression of phospholipase D enhances matrix metalloproteinase-2 expression and glioma cell invasion via protein kinase C and protein kinase A/NF-kappaB/Sp1-mediated signaling pathways. Carcinogenesis 30:356–365. https://doi.org/10.1093/carcin/bgn287
47. Knoepp SM, Chahal MS, Xie Y, Zhang Z, Brauner DJ, Hallman MA, Robinson SA, Han S, Imai M, Tomlinson S, Meier KE (2008) Effects of active and inactive phospholipase D2 on signal transduction, adhesion, migration, invasion, and metastasis in EL4 lymphoma cells. Mol Pharmacol 74:574–584. https://doi.org/10.1124/mol.107.040105
48. Kang DW, Choi KY, Min do S (2011) Phospholipase D meets Wnt signaling: a new target for cancer therapy. Cancer Res 71:293–297. https://doi.org/10.1158/0008-5472.CAN-10-2463
49. Henkels KM, Boivin GP, Dudley ES, Berberich SJ, Gomez-Cambronero J (2013) Phospholipase D (PLD) drives cell invasion, tumor growth and metastasis in a human breast cancer xenograph model. Oncogene 32:5551–5562. https://doi.org/10.1038/onc.2013.207
50. Sant S, Johnston PA (2017) The production of 3D tumor spheroids for cancer drug discovery. Drug Discov Today Technol 23:27–36. https://doi.org/10.1016/j.ddtec.2017.03.002
51. Lovitt CJ, Shelper TB, Avery VM (2014) Advanced cell culture techniques for cancer drug discovery. Biology (Basel) 3:345–367. https://doi.org/10.3390/biology3020345
52. Vinci M, Gowan S, Boxall F, Patterson L, Zimmermann M, Court W, Lomas C, Mendiola M, Hardisson D, Eccles SA (2012) Advances in establishment and analysis of three-dimensional tumor spheroid-based functional assays for target validation and drug evaluation. BMC Biol 10:29. https://doi.org/10.1186/1741-7007-10-29
53. Noble AR, Maitland NJ, Berney DM, Rumsby MG (2018) Phospholipase D inhibitors reduce human prostate cancer cell proliferation and colony formation. Br J Cancer 118:189–199. https://doi.org/10.1038/bjc.2017.391
54. Utter M, Chakraborty S, Goren L, Feuser L, Zhu YS, Foster DA (2018) Elevated phospholipase D activity in androgen-insensitive prostate cancer cells promotes both survival and metastatic phenotypes. Cancer Lett 423:28–35. https://doi.org/10.1016/j.canlet.2018.03.006
55. Yonezawa T, Katoh K, Obara Y (2004) Existence of GPR40 functioning in a human breast cancer cell line, MCF-7. Biochem Biophys Res Commun 314:805–809
56. Miyauchi S, Hirasawa A, Iga T, Liu N, Itsubo C, Sadakane K, Hara T, Tsujimoto G (2009) Distribution and regulation of protein expression of the free fatty acid receptor GPR120. Naunyn Schmiedebergs Arch Pharmacol 379:427–434. https://doi.org/10.1007/s00210-008-0390-8
57. Liebmann C (2011) EGF receptor activation by GPCRs: an universal pathway reveals different versions. Mol Cell Endocrinol 331:222–231. https://doi.org/10.1016/j.mce.2010.04.008

Publisher's Note Springer Nature remains neutral with regard to jurisdictional claims in published maps and institutional affiliations.

BBA - Molecular Basis of Disease 1865 (2019) 1540–1554

Contents lists available at ScienceDirect

BBA - Molecular Basis of Disease

journal homepage: www.elsevier.com/locate/bbadis

GDF11 exhibits tumor suppressive properties in hepatocellular carcinoma cells by restricting clonal expansion and invasion

Monserrat Gerardo-Ramírez[a,b], Roberto Lazzarini-Lechuga[c], Sharik Hernández-Rizo[a,b], Javier Esteban Jiménez-Salazar[c], Arturo Simoni-Nieves[a,b], Carmen García-Ruiz[d], José Carlos Fernández-Checa[d], Jens U. Marquardt[e], Cedric Coulouarn[f], María Concepción Gutiérrez-Ruiz[b,g], Benjamín Pérez-Aguilar[b,1], Luis E. Gomez-Quiroz[b,g,*,1]

[a] Posgrado en Biología Experimental, DCBS, Universidad Autónoma Metropolitana-Iztapalapa, Mexico City, Mexico
[b] Departamento de Ciencias de la Salud, Universidad Autónoma Metropolitana-Iztapalapa, Mexico City, Mexico
[c] Departamento de Biología de la Reproducción, Universidad Autónoma Metropolitana-Iztapalapa, Mexico City, Mexico
[d] Department of Cell Death and Proliferation, Instituto de Investigaciones Biomédicas de Barcelona, CSIC, Liver Unit, Hospital Clinic, IDIBPAS and CIBERehd, Barcelona, Spain
[e] 1st Department of Medicine, University Medical Center, Johannes Gutenberg University Mainz, Langenbeckstrasse 1, 55131 Mainz, Germany
[f] INSERM, Inra, University of Rennes, UMR 1241, Nutrition Metabolisms and Cancer, Rennes, France
[g] Laboratorio de Medicina Experimental, Unidad de Medicina Translacional, Instituto de Investigaciones Biomédicas, UNAM/Instituto Nacional de Cardiología Ignacio Chavez, Mexico City, Mexico

ARTICLE INFO

Keywords:
GDF11
Huh7 cells
HCC
Cell cycle
Liver cancer
Hep3B cells

ABSTRACT

Growth differentiation factor 11 (GDF11) has been characterized as a key regulator of differentiation in cells that retain stemness features, despite some controversies in age-related studies. GDF11 has been poorly investigated in cancer, particularly in those with stemness capacity, such as hepatocellular carcinoma (HCC), one of the most aggressive cancers worldwide. Here, we focused on investigating the effects of GDF11 in liver cancer cells. GDF11 treatment significantly reduced proliferation, colony and spheroid formation in HCC cell lines. Consistently, down-regulation of CDK6, cyclin D1, cyclin A, and concomitant upregulation of p27 was observed after 24 h of treatment. Interestingly, cell viability was unchanged, but cell functionality was compromised. These effects were potentially induced by the expression of E-cadherin and occludin, as well as Snail and N-cadherin repression, in a time-dependent manner. Furthermore, GDF11 treatment for 72 h induced that cells were incapable of sustaining colony and sphere capacity in the absent of GDF11, up to 5 days, indicating that the effect of GDF11 on self-renewal capacity is not transient. Finally, in vivo invasion studies revealed a significant decrease in cell migration of hepatocellular carcinoma cells treated with GDF11 associated to a decreased proliferation judged by Ki67 staining. Data show that exogenous GDF11 displays tumor suppressor properties in HCC cells.

1. Introduction

Liver diseases represent one of the main challenges in public health. Changes in human habits tend to increase the prevalence of severe liver diseases, such as steatohepatitis, cirrhosis, viral hepatitis and liver cancer [1]. Hepatocellular carcinoma (HCC) is one of the most prevalent and aggressive tumor worldwide with high rate of postsurgical recurrence [2–4], and despite the outstanding progress made in the last decade in identifying new therapeutic approaches to target canonical proliferation and survival pathways, the potential use of non-canonical molecules and the molecular basis of their anti-proliferating activity are currently being studied directed to provide new therapeutic targets [5].

Growth differentiation factor 11 (GDF11) is a member of the subfamily of the bone morphogenic proteins, and of the superfamily of the transforming growth factor beta (TGF-β). GDF11 is critical for organogenesis and development, particularly for skeletal system. Knock-out for mouse Gdf11, or for the furin-like convertase (Pcsk5), which activates GDF11 to a mature form, results in skeletal development defects

* Corresponding author at: Departamento de Ciencias de la Salud, Universidad Autónoma Metropolitana Iztapalapa, Av. San Rafael Atlixco 186, Col. Vicentina, Iztapalapa, 09340 Mexico City, Mexico.
E-mail address: legq@xanum.uam.mx (L.E. Gomez-Quiroz).
[1] Shared Senior authorship.

https://doi.org/10.1016/j.bbadis.2019.03.003
Received 20 August 2018; Received in revised form 26 February 2019; Accepted 14 March 2019
Available online 16 March 2019
0925-4439/ © 2019 Elsevier B.V. All rights reserved.

and lethality *in uterus* [6,7].

Recently, some controversies have emerged about the effects of GDF11 in rejuvenation process [8]. While some groups report that GDF11 expression reduces with age, and its restoration induces proliferation and differentiation of progenitor cells (satellite cells) in the skeletal [9] and cardiac muscle [10], reversing the age-related hypertrophy, others state that GDF11 significantly inhibits muscle regeneration and decreases satellite cell expansion in mice [11,12]. This debating question is also associated with the great similarity of GDF11 with myostatin (or GDF8) and the poor specificity of some commercial antibodies [13]. Aside of these controversial functions of GDF11 in age-related disorders, both outlooks have in common that cells, with some stemness properties, are targeted by the GDF11, notably in development process [14–16].

Given that cancer cells, with stemness features, are recognized as key therapeutic target, due to their capacity of sustained proliferation and migration, possibly driving tumor progression and resistance to treatment, we aimed at figure out the effects of GDF11 in HCC-derived cell lines. Although some studies revealed that GDF11 expression correlates with poor prognosis in colorectal [17] and breast cancer [18], it has been poorly studied in this kind of disease. Recently, Bajikar and collaborators [19] reported that GDF11 exerts tumor suppressive functions in triple-negative breast cancer cells. Loss of function of GDF11 in breast cancer has been notably related to deficient maturation due to the convertase PCSK5, which activates bioactive GDF11 from its immature form. The present study is the first one related to liver cancer and provides evidence that GDF11 could be a good candidate for new therapeutic options.

2. Materials and methods

2.1. Cell culture

Huh7, Hep3B, Hepa1–6, HepG2, SNU-182 and MDA-MB-231 cell lines were obtained from the American Type Culture Collection (ATCC, Manassas, VA, USA). Cells were cultured in William's medium supplemented with 10% fetal bovine serum (FBS, Hy-Clone, Logan, UT, USA), 100 U/ml ampicillin and 100 μg/ml streptomycin (Thermo Fisher Scientific, Waltham, MA, USA). Cells were maintained at 37 °C in a 5% CO_2 and 90% humidity atmosphere. Cells were plated in plastic culture bottles (Sigma-Aldrich, Saint Louis, MO, USA). All cell lines were mycoplasma free.

2.2. Main experimental design

Cells were exposed to 50 ng/ml GDF11 [20] for different times. GDF11 was added to culture media every 24 h and cells were recovered after 72 h for experiments, as depicted in Supplementary Fig. 1A.

In order to determine whether GDF11 effects are not transient, and remain after growth factor withdrawal, we performed additional experiments, in which cells were treated every 24 h up to 72 h, then harvested and re-plated without GDF11. Spheroid and colony formation were evaluated up to 5 days in the absent of GDF11 (Supplementary Fig. 1B).

2.3. Western blotting

Western blot was conducted as we previously reported [21]. PVDF membranes were probed with specific antibodies as described in the Supplementary Table 1. Horseradish peroxidase-conjugated antibodies were used according to the primary antibodies. Blots were exposed using Super Signal West Pico Chemiluminescent substrate (Pierce Biotechnology, USA). Signal was detected using Gel Logic 2500 (Kodak, Rochester, NY, USA).

2.4. Immunofluorescence assays

Immunofluorescence was conducted as previously reported [22], briefly, cells were treated for different times with GDF11, and then fixed with 4% paraformaldehyde in phosphate-buffered saline (PBS). Samples were permeabilized with 0.01% (v/v) Triton-X 100 for 30 min and blocked with 3% (w/v) bovine serum albumin (BSA) in PBS for 30 min and subsequently incubated with primary antibodies anti-occludin (Santa Cruz Biotechnology 81812, dilution 1:100), anti-snail (Santa Cruz Biotechnology 28199, dilution 1:100), anti-E-cadherin (Santa Cruz Biotechnology 21791, dilution 1:100) and anti-N-cadherin (Santa Cruz Biotechnology 59987, dilution 1:100). Nuclei were counterstained with 1 μg/ml 4′,6-diamidino-2-phenylindole (DAPI) (Sigma-Aldrich). Images were obtained using a multi-photon confocal microscope (Carl Zeiss LSM-780 NLO, Oberkochen, Germany).

2.5. Cell proliferation

Cell proliferation was addressed by CCK-8 kit (Dojindo Lab, Kumamoto, Japan), following manufacturer's instructions.

2.6. Spheroid formation

Cells were seeded in six-well low attachment plates (Millipore-Sigma, Saint Louis MO, USA). The cultures were supplemented every 24 h with 50 ng/ml of GDF11 for five days. The spheroids were counted and photographed using an inverted microscope Carl Zeiss VERT.A1.

2.7. Wound-healing assay

Cells were seeded in six-well plates to approximately 90% of confluency. In each well a couple of wounds were created with a 20 μl pipette tip. Plates were washed three times with PBS to remove detached cells. Subsequently, media were added supplemented or not with FBS in presence or absent of GDF11.

The healing response was monitored every 24 h up to 72 h when photography register was performed.

2.8. Cell functionality by MTT assay

Cell functionality was addressed by the 3-(4,5-dimethylthiazol-2-yl)-2,5-diphenyltetrazolium bromide (MTT) test, using the Vybrant MTT Cell Proliferation Assay Kit (Thermo Fisher Scientific), following manufacturer's instructions.

2.9. Clonogenic assay

After 72 h under GDF11 treatment, 1×10^3 cells were seeded into 6-well plates in triplicate and maintained in GDF11-free media, in presence or absent of FBS. After 10 days, colonies were stained with crystal violet, photographed and counted.

2.10. Invasion study using a chick embryo chorioallantoic membrane (CAM) assay

Chick embryo CAM model was used to study invasion properties, following previous method reported by our group and others [23–25]. Briefly, ten fertile chick (*Gallus domesticus*) eggs (ALPES SA Farms, Puebla, Mexico) were randomly separated in two groups. Eggs were incubated at 37.8 °C and 60% humidity up to 22 HH of embryo stage development. Then, shells were wiped with 70% ethanol, and 1 cm^2 window was done. The vitelline membrane was dissected and 1×10^6 cells, treated or not with GDF11 for 72 h and labeled with vibrant CFDA SE cell tracer kit (Thermo Fisher Scientific), were introduced onto the CAM, in the convergence of two blood vessels, using 30 μl of Matrigel (Sigma-Aldrich) as substrate. The window in the shells was covered

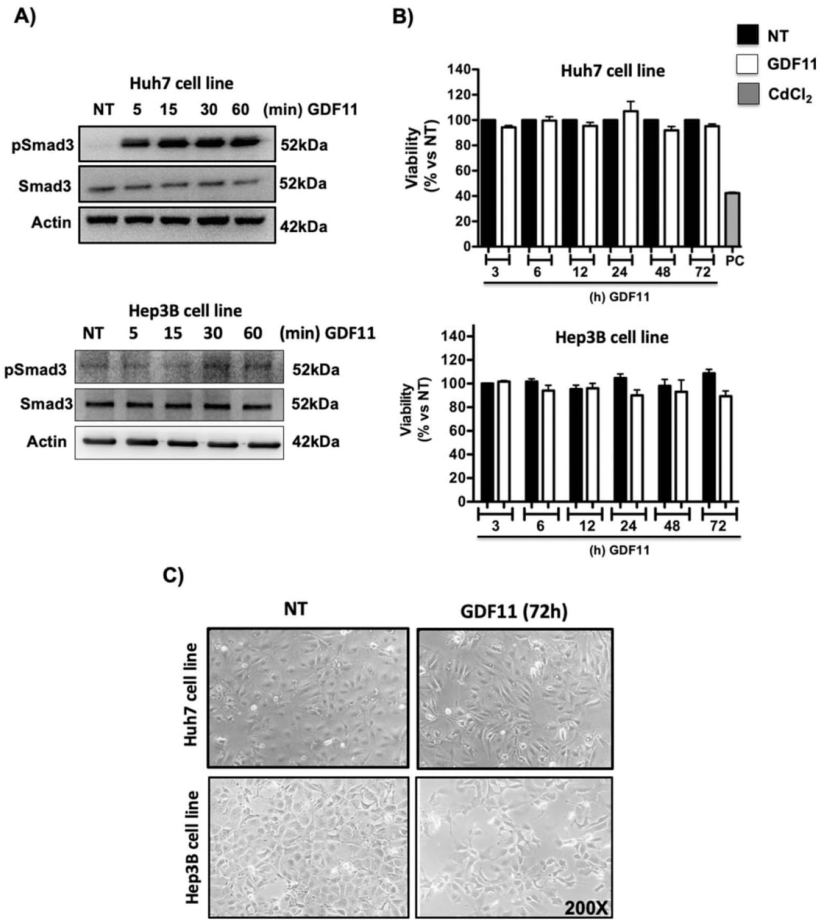


Fig. 1. HCC cells respond to GDF11 treatment activating Smad3 with no effects on cell viability. Huh7 and Hep3B cells were treated for different times with GDF11 (50 ng/ml). A) Western blot analysis of the Smad3 phosphorylation. Actin was used as loading control. B) Time-course analysis of cell viability determined by crystal violet staining, cadmium chloride ($CdCl_2$, 5 μM for 6 h) was used as positive control (PC). Each column represents the mean ± SEM of at least four independent experiments carried out by triplicate. C) Cell morphology under GDF11 treatment at 72 h, cells were treated every 24 h with GDF11 up to 72 h. Representative images of at least four independent experiments. Original magnification 200×.

with sterile adhesive tape and eggs were incubated as above for 2 and 4 days. CAM were recovered and immediately fixed with 4% paraformaldehyde in PBS. Paraffin sections (5 μm) were obtained for immunofluorescence using anti-beta-catenin antibody (Cell Signaling #9562). Proliferation was addressed by immunofluorescence using anti-Ki67 antibody (abcam 15580; dilution 1:100). Nuclei were counterstained with 1 μg/ml DAPI. Images were acquired using a multiphoton confocal microscope (Carl Zeiss LSM-780 NLO).

2.11. Real-time quantitative reverse transcriptase-polymerase chain reaction (qRT-PCR)

One μg total RNA was reverse transcribed in 20 μl reaction volume with a SuperScript (Invitrogen Corp.) first-strand synthesis kit according to the manufacturer's instructions. Oligonucleotide primers were designed using Primer3 v.0.4.0 (http://frodo.wi.mit.edu/primer3/) as describe [26]. The qRT-PCR analysis was performed with a CFX96 Touch (Bio-Rad) thermal cycler in a 96-well reaction plate. The 10 μl PCR reaction mix contained 5 μl 2× SYBR Green PCR Master Mix (Bio-Rad), 200 nM of each primer, and 1 μl cDNA template. Reactions were incubated for 10 min at 95 °C followed by 40 cycles of 30 s at 95 °C and 60 s at specific primer temperature. The expression level of ribosomal protein S18 (rs18) was used as reference. Relative gene expression levels were calculated using the formula $2^{(-\Delta\Delta Ct)}$. Primer sequences are listed in Supplementary Table 2.

2.12. Protein quantification

The protein content was determined by using the bicinchoninic acid method (BCA, Pierce, Thermo Fisher Scientific), following the manufacturer's instructions.

2.13. Statistical analysis

The results are presented as the average of at least three independent experiments. A One-way ANOVA followed by Tukey post-test was performed for the analysis of cell viability, mitochondrial functionality by MTT, number of spheroids and number of colonies in cell sensitization experiments whit GDF11. t-Student test was performed for the analysis of the numbers of spheroids.

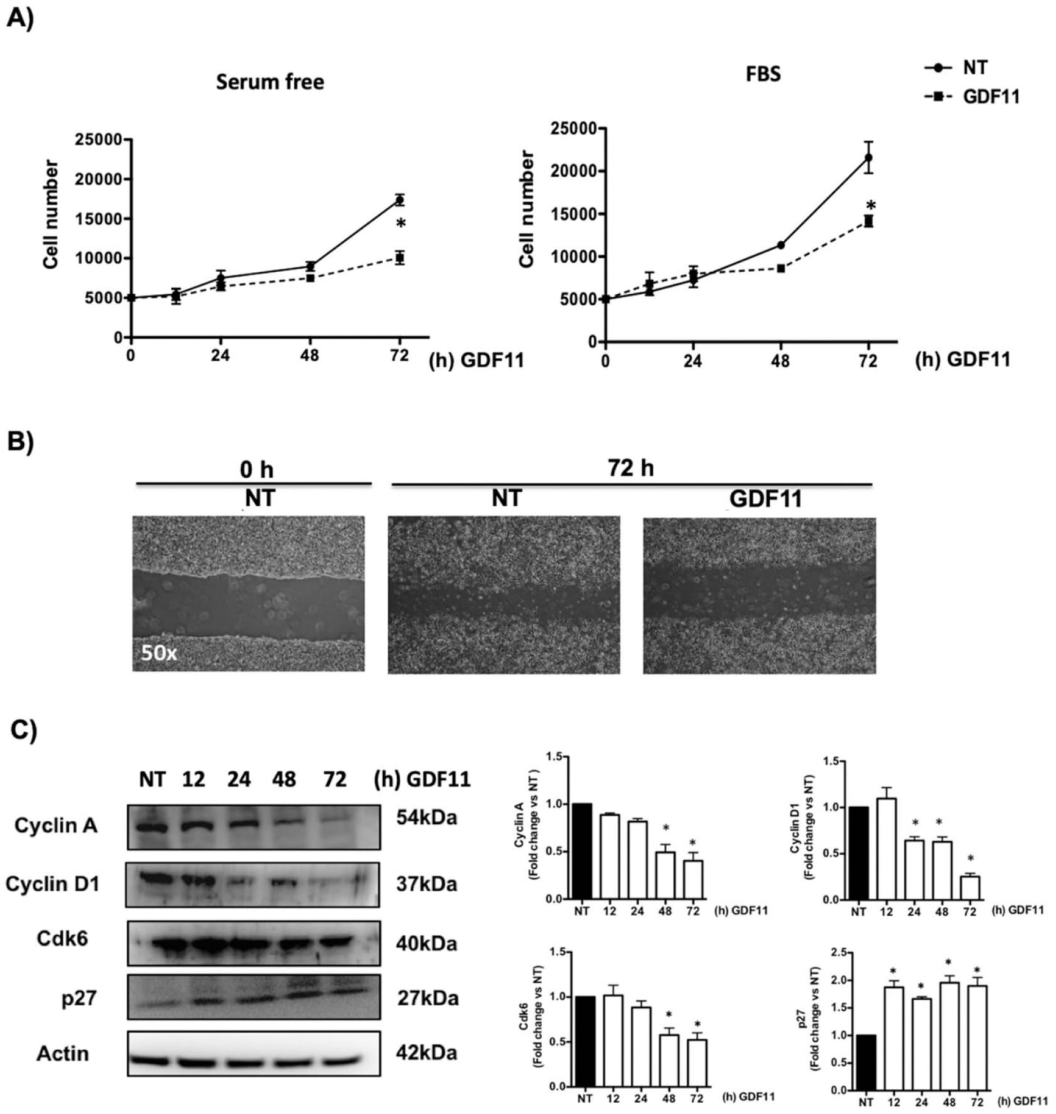


Fig. 2. GDF11 impairs proliferation, migration and cellular function. A) Huh7 cell proliferation addressed by CCK-8 in the absent or the presence of fetal bovine serum (FBS). B) Wound-healing assay, Huh7 cells were treated every 24 h with GDF11 up to 72 h. Representative images of at least four independent experiments. C) Western blot of the main cell cycle proteins and densitometric analysis. D) Hep3B cell proliferation addressed by CCK-8 in the absent or the presence of FBS. Each point represents the mean ± SEM of at least four independent experiments carried out by triplicate, F) wound-healing assay, Hep3B cells were treated every 24 h with GDF11 up to 72 h. Representative images of at least four independent experiments. G) Mitochondrial functionality by MTT assay in HCC cell lines, each column represents the mean ± SEM of at least three independent experiments carried out by triplicate. Images are representative of at least three independent experiments. *, $p \leq 0.05$ vs NT cells at 72 h.

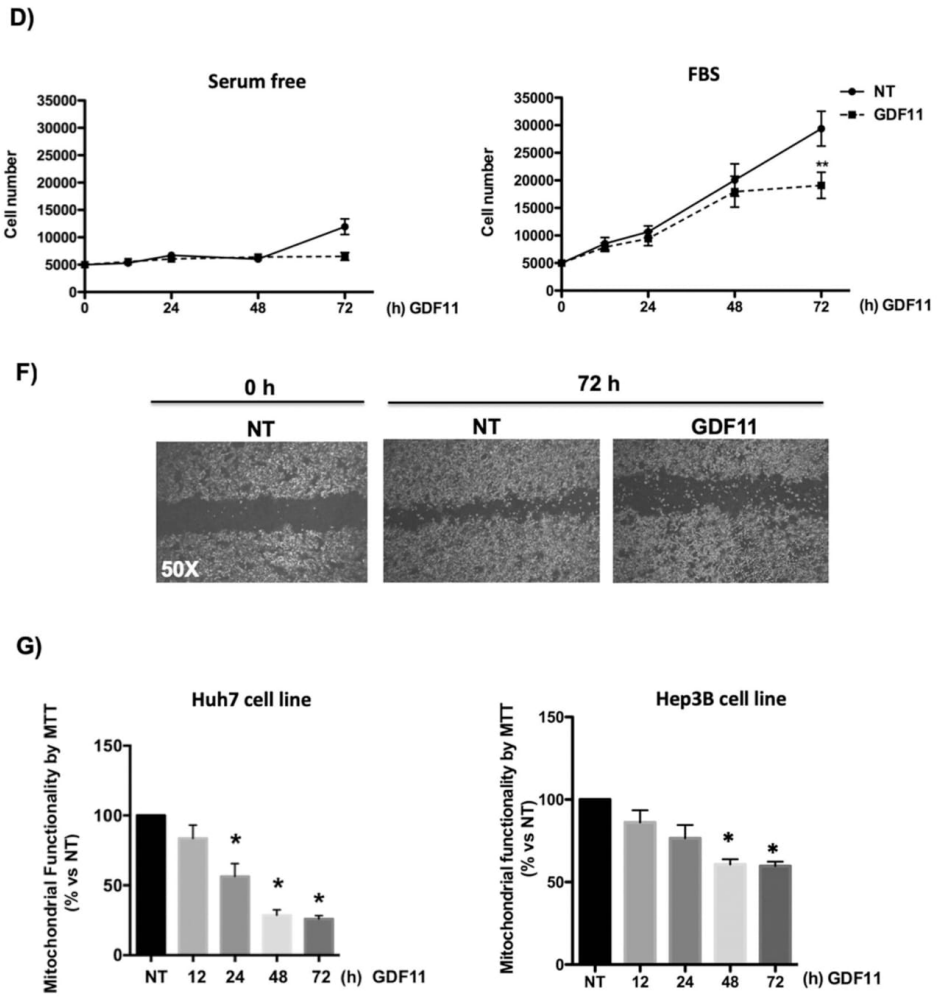


Fig. 2. (*continued*)

3. Results

3.1. HCC cells respond to GDF11 treatment by activating Smad3

To figure out whether HCC-derived cells respond to GDF11, Huh7 and Hep3B cells were treated with 50 ng/ml GDF11 up to 60 min. Activation of the canonical signaling pathway was addressed by immunoblot of Smad3. Fig. 1A shows that Smad3 is rapidly activated by phosphorylation 5 min, in Huh7 cell line, and 30 min in Hep3B cell line, after GDF11 treatment. Activation remains up to 60 min. To explore impact in cell viability, Huh7 and Hep3B cells were treated at different times with GDF11. Time-course analysis up to 72 h of treatment demonstrates that GDF11 has no significant impact on cell viability (Fig. 1B), while $CdCl_2$ (5 μM, 6 h), used as a positive control, reduces cell viability. In addition, morphology inspection of cell culture at 72 h revealed small changes in cells, including a flat-like phenotype and a decrease in cell density in both cell lines (Fig. 1C).

3.2. GDF11 impairs cell proliferation and cycle progression

Next, we decided to address cell proliferation; although no significant effect was observed on cell viability, GDF11 was shown to decrease Huh7 cell proliferation starting after 48 h GDF11 treatment and being statistically significantly at 72 h in the absence or presence of FBS (Fig. 2A), which was used as a competitor. In addition, a wound-healing assay revealed an impaired repair process at 72 h under GDF11 treatment compared with untreated cells (Fig. 2B). The analysis of the content of key cell cycle proteins shows that positive regulators such as Cyclin A, Cyclin D1 and CDK6 decreases in a time dependent manner, while CDK inhibitor p27 increases (Fig. 2C). Consistent with results observed in Huh7 cells, Hep3B cells under GDF11 treatment showed similar effects in cell proliferation (Fig. 2D) and wound-healing assay (Fig. 2F). Although viability was not affected in both HCC-derived cell lines, cell functionality, evaluated by MTT assay was significantly decreased starting after 24 h of treatment, in Huh7 cells, and 48 h in

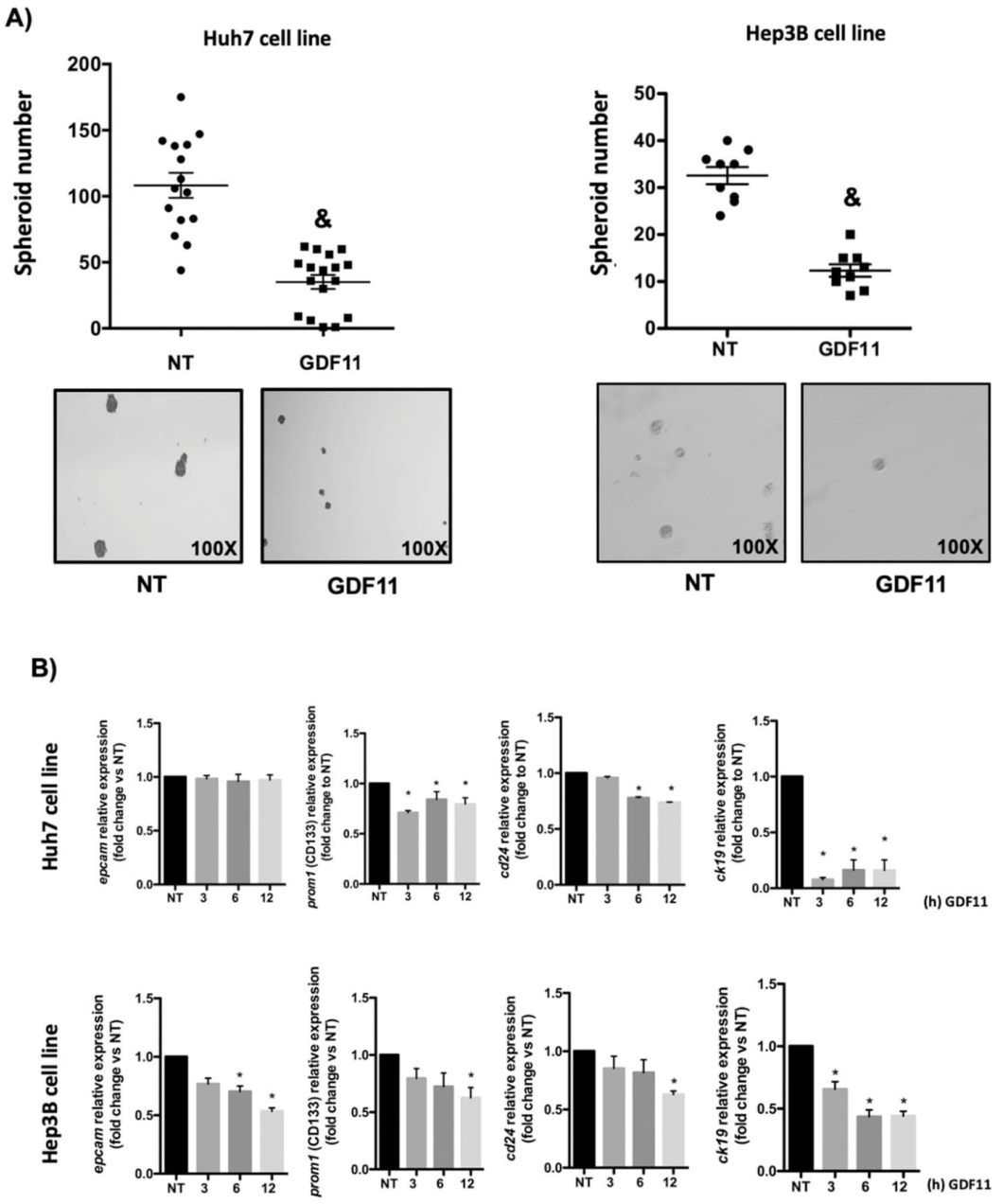


Fig. 3. GDF11 decreases spheroid formation capacity and the expression of genes related to aggressiveness. A) Spheroid counting at 72 h, Huh7 and Hep3B cells were treated every 24 h with GDF11 (50 ng/ml) up to 72 h, each point represents an independent experiment, we reported the median ± SEM of at least ten independent experiments. Images are representative of at least ten independent experiments, original magnification 100×. &, $p \leq 0.05$ vs NT cells at 72 h. B) Messenger RNA levels of key genes related to cancer aggressiveness, relative expression to not treated (NT) cells is demonstrated as means ± SEM. *, $p \leq 0.05$ vs NT cells.

Hep3B cells, explaining the effects observed in proliferation and wound-healing (Fig. 2G).

3.3. GDF11 decreases spheroid formation capacity and the expression of genes related to aggressiveness

Previous results strongly suggest that GDF11 exerts tumor suppressive effects. To gain more evidence, we performed studies of spheroid formation under GDF11 treatment every 24 h for 5 days. Cells treated with GDF11 exhibited fewer spheroids at day 5 (39%, in Huh7 cells; and 34% in Hep3B), as compared with untreated cells at the same time (Fig. 3A). Even more, spheroids observed under the GDF11 treatment were smaller (25% in Huh7 cells; and 40% in Hep3B) than those formed in the absent of treatment.

The analysis of the expression of some of the key well-characterized markers of cancer cell aggressiveness, revealed an increment of

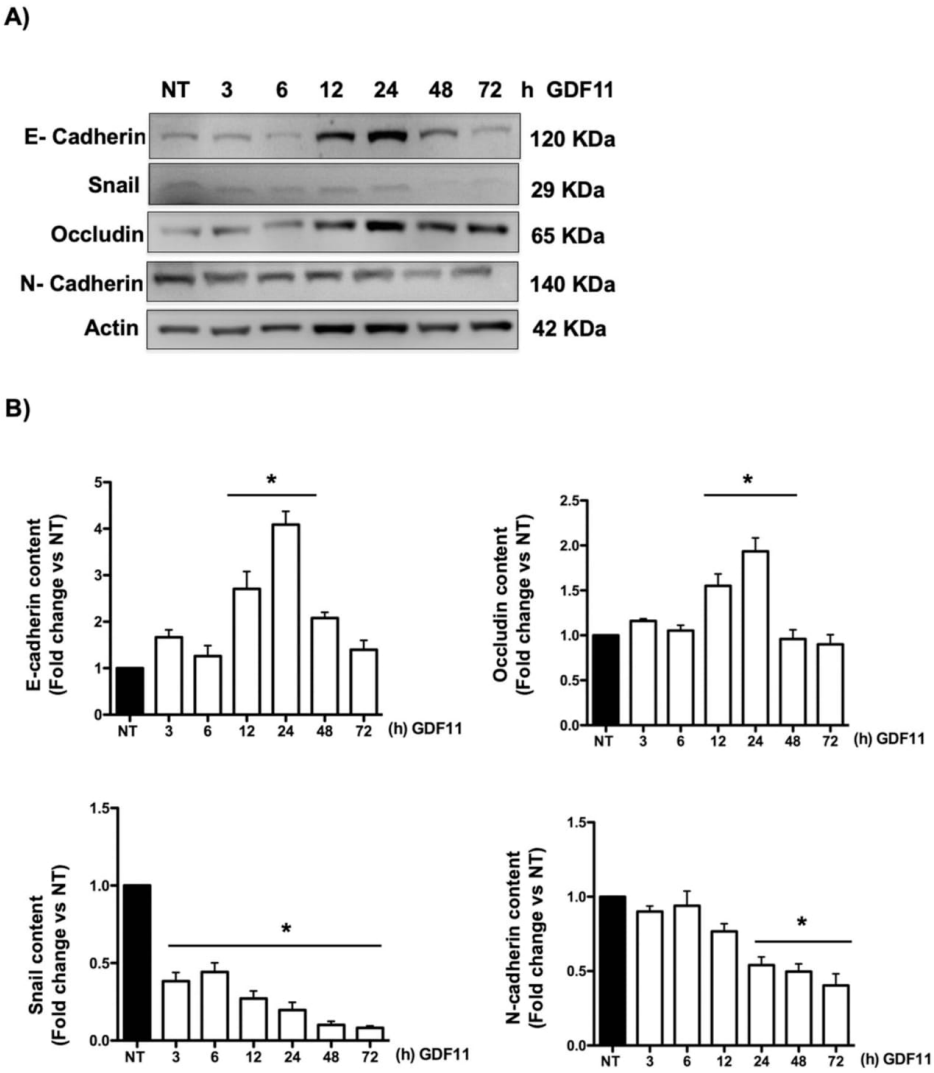


Fig. 4. GDF11 promotes mesenchymal to epithelial transition. A) Time-course analysis by Western blot of representative epithelial (E-cadherin and occludin) and mesenchymal (Snail and N-cadherin) markers in Huh7 cells treated with GDF11 (50 ng/ml) and, B) corresponding densitometric analysis. Each column represents the mean ± SEM of at least three independent experiments carried out by triplicate. Images are representative of at least three independent experiments. *, $p \leq 0.05$ vs NT cells. Immunofluorescence determined by confocal microscopy of C) Snail and E-cadherin content and, D) N-cadherin and occludin content. Images are representative of at least three independent experiments. Original magnification 360×.

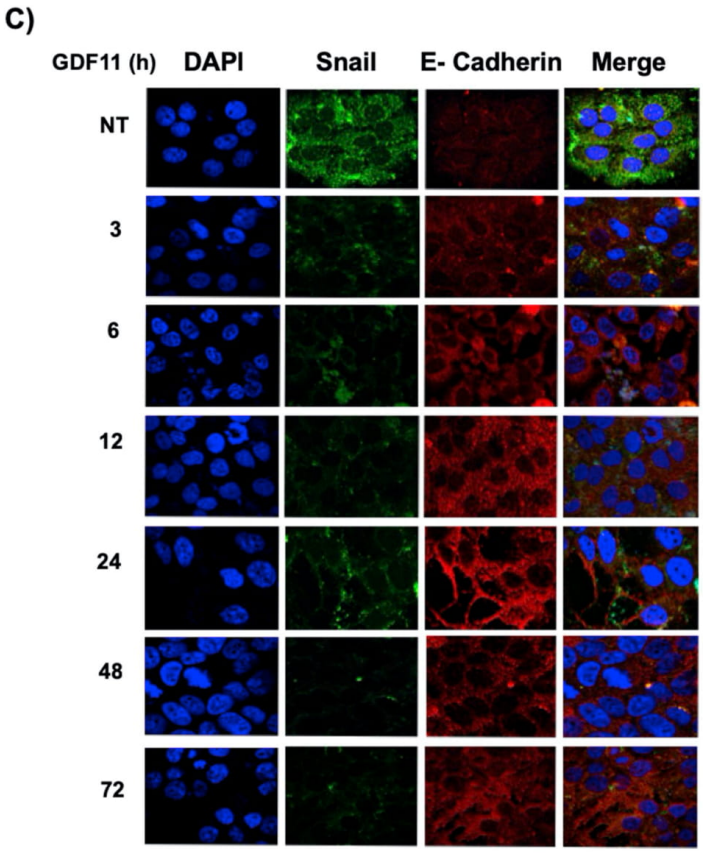


Fig. 4. (*continued*)

messenger RNA of CD133, CD24, CK19 and EpCAM particularly, the last one was significantly diminished only in Hep3B with no changes in Huh7 cells (Fig. 3B).

3.4. GDF11 promotes mesenchymal epithelial transition

Next, we decided to address the expression of some mesenchymal and epithelial key markers in cells under GDF11 treatment. The immunoblot revealed a decrement of mesenchymal markers, such as Snail and N-cadherin, and the increment of epithelial markers, such as occludin and E-cadherin, in a time-dependent manner (Fig. 4A and B), interestingly mesenchymal markers remain below levels of not treated cells, while epithelial markers decrement peaked at 24 h and then decreased to control values. To gain more confidence of these data, we analyzed the content of these proteins by immunofluorescence, Fig. 4C and D show the colocalization of Snail and E-cadherin; and N-cadherin and occludin, respectively, in both cases the expression of the mesenchymal proteins (Snail or N-cadherin) was considerably diminished, and the epithelial ones was increased, confirming the immunoblot experiments. Similar results were obtained in Hep3B exhibiting an increment in the expression of E-cadherin and occludin, and decrement in N-cadherin, in a time-dependent manner (Supplementary Fig. 2).

3.5. The effects elicited by GDF11 for 72 h of treatment remain in the absence of the factor

To figure out whether the effects displayed by GDF11 induce a long-lasting or a transient cellular reprograming, cells were treated with GDF11 every 24 h for three days then, cells were harvested and processed to explore the capacity of colony and spheroid formation for five days, in presence or absence of serum as competitor. Fig. 5A shown that Huh7 cells treated with GDF11 remarkably decreased the ability to form colonies, in the presence or absence of FBS. Similarly, spheroid formation was significantly diminished in both cell lines (Fig. 5B and C), interestingly a better effect was observed in Huh7 cell line practically abrogating the spheroid formation capacity. Serum supplementation in the media did not rescue cells from the static phenotype (Supplementary Fig. 3), but the number of spheroids were different in the presence or absent of FBS in NT cells. Reprogramming experiments showed that cells exposed to GDF11 were unable of sustaining their colony and sphere forming capacity, indicating that the effect of GDF11 on self-renewal capacity is not transient.

3.6. GDF11 impairs invasion capacity

To address one of the key hallmarks of malignancy, we assayed

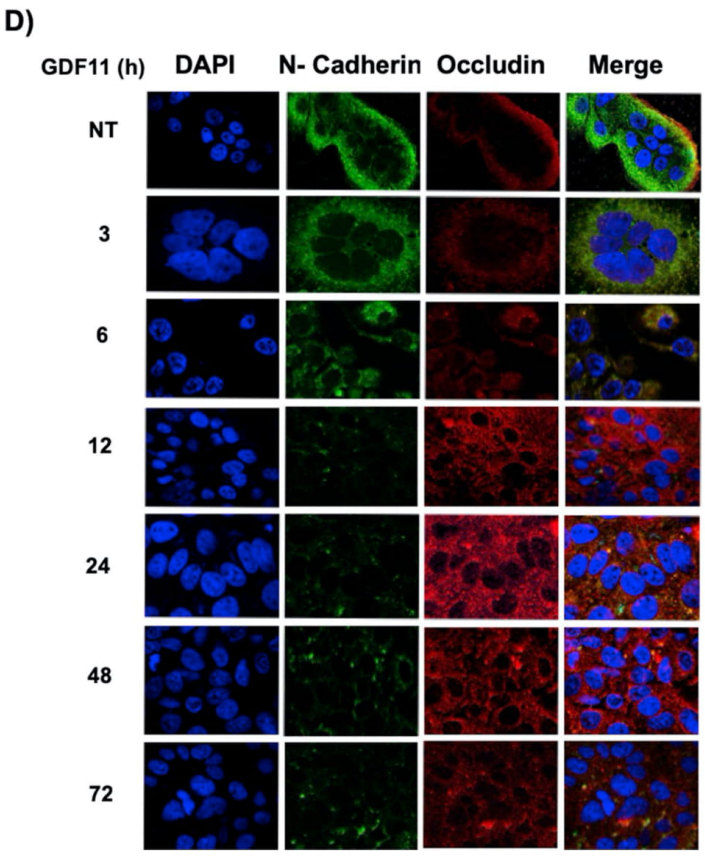


Fig. 4. (*continued*)

invasion property in cells treated or not with GDF11. 1×10^6 cells were grafted in the CAM of the chick embryo (Fig. 6A). Fig. 6C shows the complete control CAM with no cells, in order to observe normal morphology of the CAM. Cells were grafted in the area labeled with the yellow circle; the eggshell was covered with sterile tape. After two or four days of incubation at 37 °C, the CAM was recovered fixed and paraffin embedded for immunofluorescence and confocal microscopy. We started exploring the effect at day four; at this time we observed embryo lethality only with not treated cells (Fig. 6B). Microscopy inspection revealed few disaggregated not treated cells remaining in the grafted zone (Supplementary Fig. 4A, white arrows), and some cells were observed in the distal zone of the CAM (green cells), indicating an ongoing invasion process (Supplementary Fig. 4C). The same experimental setting with GDF11 treated cells revealed some significant compacted aggregates of cells (Supplementary Fig. 4B, yellow arrow heads), and some of them in transit (Supplementary Fig. 4B, white arrows). No cell was detected in the distal CAM (Supplementary Fig. 4D). Remarkably, chick embryos in the eggs inoculated with GDF11 treated cells were still alive (Fig. 6B).

In order to analyze the invasion process at an early time point, we decided to incubate the eggs only for two days. Microscopic analysis of the complete CAM revealed that most of the untreated cells were gone (Fig. 6D). In fact, some of chick embryo dies also at this time, however, cells treated for three days with GDF11 remained covered by the CAM and cell localization suggests an attempt of migration, but most of the cells still there (Fig. 6E). The CAM zones near to the cell cumulous strongly express beta catenin (yellow arrow, and figure inset), probably as a response to Huh7 cells reprograming induced by GDF11; in comparison, beta catenin expression in CAM with non-treated cells, was weak, suggesting degradation. In order to address the cell proliferation status in the invasion experiment, we proceeded to detect Ki67 protein content by immunofluorescence; Fig. 6F shows more proliferating cells in CAM grafted with not treated Huh7 cells comparing with those under GDF11 treatment; remarkably, Ki67 positive cells were more abundant in the lower zone of the CAM, indicating more proliferative capacity (yellow arrow; Fig. 6F).

To corroborate the GDF11-induced invasion restriction, we performed the CAM experiment using Hep3B cells. The results depicted in Supplementary Fig. 3E show disaggregated not treated cells in the engraftment zone, cells seems to be disabled to form cell to cell interactions, in comparison with GDF11 treated cells that exhibited a well compacted cell cumulous with well defined cell interactions, the vascular zone exhibited not treated cells in blood vessels, effect that was absent in GDF11-treated cells, interestingly, the tumor was well delimited (white arrows, Supplementary Fig. 4), suggesting that treated cells were able to degrade the basal membrane, as observed in an in situ

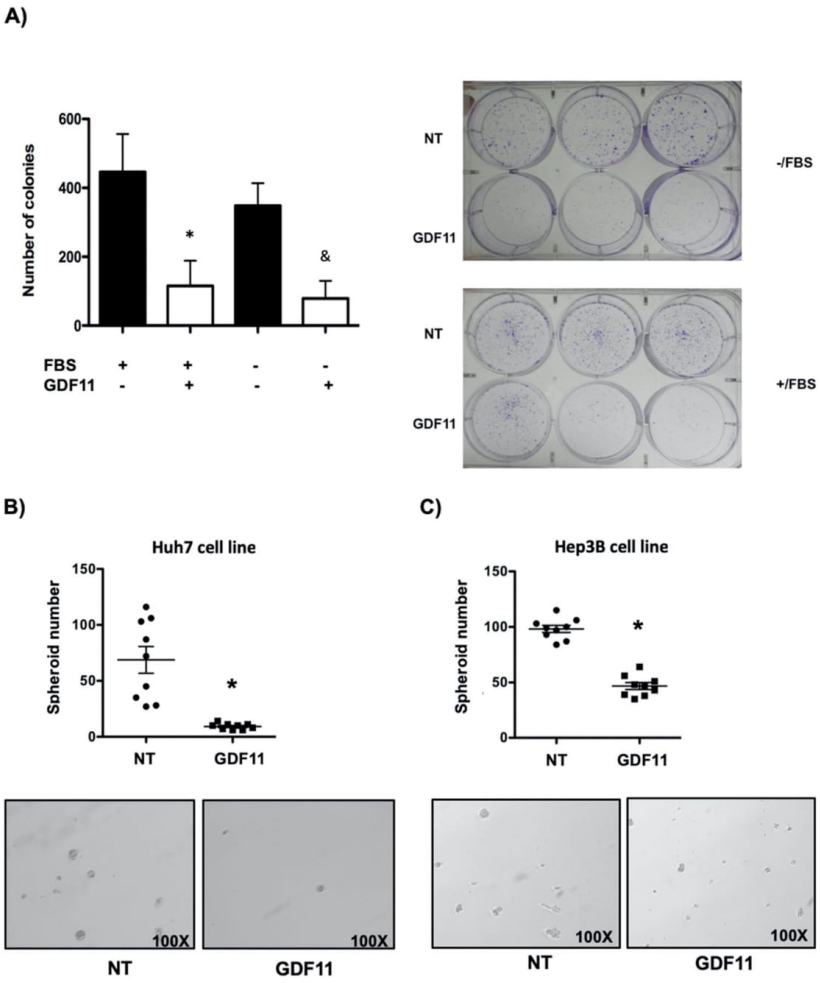


Fig. 5. The effects elicited by GDF11 remains in the absent of the growth factor. Cells were treated every 24 h with GDF11 (50 ng/ml) up to 72 h, after that, cells were harvested and we proceeded to analyze: A) colony formation and, B) spheroid formation with deprivation of GDF11. Experiments were conducted in the presence or absence of fetal bovine serum (FBS). For the number of colonies each column represents the mean ± SEM of at least three independent experiments carried out by triplicate. Representative images of the six-well plates. For spheroid formation, each point represents an independent experiment; we reported the median ± SEM of at least nine independent experiments. *, $p \leq 0.05$ vs NT cells in presence of FBS (+FBS); &, $p \leq 0.05$ vs NT cells in the absence of FBS (−FBS).

tumor. The distal zone in the experiment with not treated cells shows many disaggregated cells in the CAM, in comparison of the GDF11 experiment with few cells; remarkably, the size of this zone was thicker than that with not treated cells. Thus, these data strongly suggest that GDF11 significantly reduces invasive property.

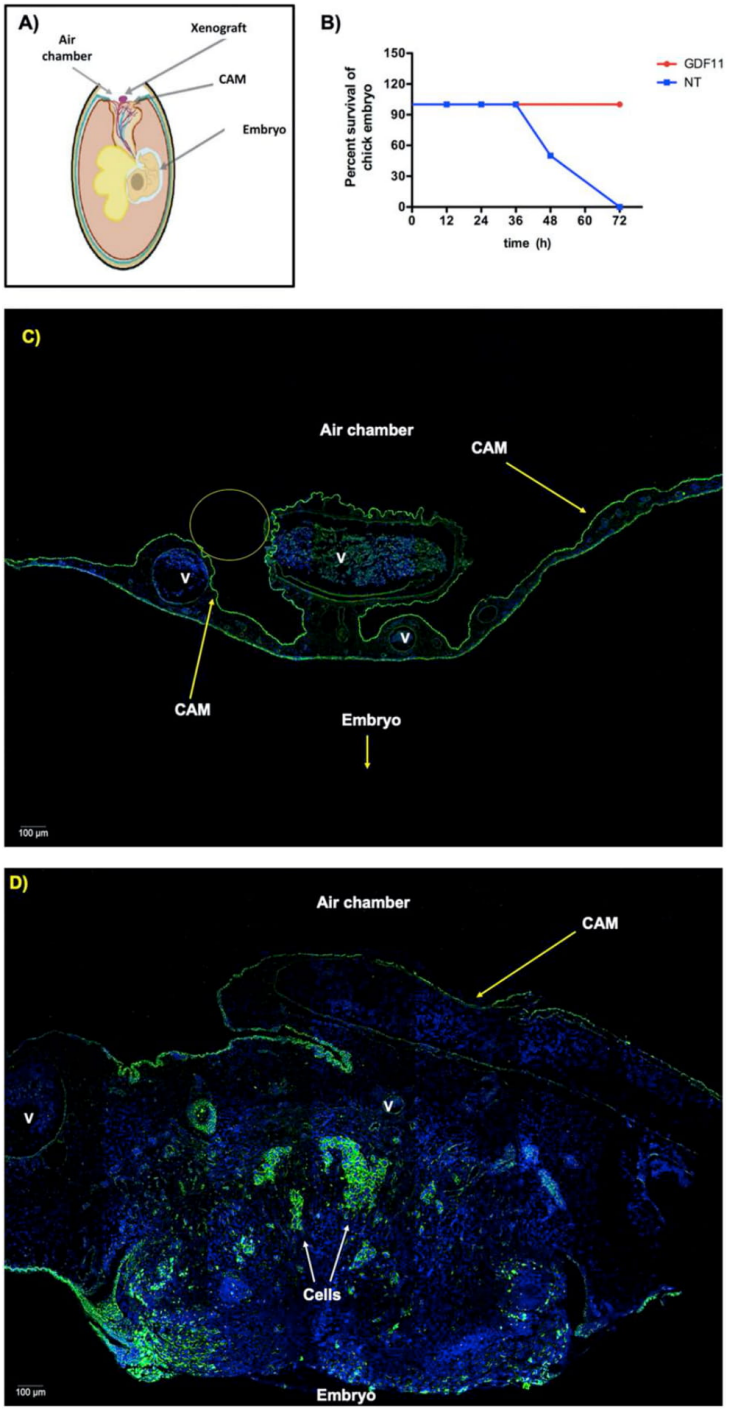
3.7. GDF11 decreases spheroid formation in other cancer cell lines

Finally, to corroborate that the tumor suppressive effects displayed by GDF11 are not restricted to Huh7 and Hep3B cell line, we treated for three days the human hepatoma cell line HepG2 (Fig. 7A), the mouse HCC cell line Hepa1–6 (Fig. 7B), the human breast cancer cell line MDA-231 (Fig. 7C), and the human HCC cell line SNU-182. In all cases, GDF11 significantly decreases spheroid-forming capacity, suggesting a conserved effect among cancer cells with some stemness phenotype.

4. Discussion

HCC accounts for 90% of primary liver cancer, with increasing new cases every year, raising a warning worldwide [4,27]. Although, some therapeutic options are currently well established, such as sorafenib administration for advanced tumors, local ablation or resection, these options only provide some limited benefits in terms of patient survival. Besides, liver transplantation remains a great challenge due to the limited number of donors.

Investigation of signaling pathways involved in the control of proliferation, survival or the metabolism of cancer cells is crucial to define novel alternative therapeutic approaches.



(caption on next page)

Fig. 6. GDF11 impairs invasive capacity. The chick embryo chorioallantoic membrane (CAM) model was used to address the invasion capacity as specified in Material and Methods. 1×10^6 cells treated or not with GDF11 for 72 h, were engrafted in the top of the CAM in 30 μl of Matrigel. A) Schematic representation of the model used in the study. B) Survival plot of the chicken embryo, n = 6 in each treatment. C) Representative confocal image composition of the control complete CAM, the yellow circle indicates the place were cells were placed. D) Confocal microscopic inspection of the entire CAM that received not treated Huh7 cells. E) Confocal microscopic inspection of the entire CAM that received GDF11 treated Huh7 cells for 72 h. CAM is identified by immunofluorescence of beta catenin (membrane in green, yellow arrows), DAPI was used for nuclei identification, Huh7 cells were traced with Vybrant CFDA SE cell tracer kit (white arrows). F) Ki67 immunofluorescence, positive cells in green (Alexa flour 488), nuclei in red (propidium iodide). V, blood vessel. Images are representative of at least 6 eggs per condition.

GDF11, a relatively new member of the TGF-β superfamily, has been showed to display biological effects in a wide range of cell types. It is particularly interesting that most of the cells that respond to GDF11 exhibit some degree of stemness phenotype [9,20]. Along this characteristic, we hypothesized that this growth factor could exert some effects in HCC-derived cell lines, particularly in those retaining stemness features. It was reported that Huh7 cell line expresses some of the key stemness markers, such as Nanog, Oct4 or Sox2. It has been also reported that increased expression of these genes in Huh7 cells is related to the increment of stemness [28,29], particularly when cells are forming spheroids [30]. The first evidence that Huh7 and Hep3B cells respond to GDF11 was the activation of one of the canonical signal transducers, specifically the phosphorylation of Smad3 [11,20], which was strongly detected after 5 min of GDF11 treatment in the case of Huh7 and, at 30 min in Hep3B cells, and remained activated along 60 min (Fig. 1A). It is well-characterized that some members of the TGF-β display effects in epithelial cells that modulate survival or proliferation [31]. Interestingly, we found that viability is unaffected up to 72 h under GDF11 treatment (Fig. 1B), with no outward changes in cell phenotype. However, cell proliferation is clearly diminished at 72 h, in presence or not, of the proliferative action of FBS (Fig. 2A and D), suggesting cytostatic effects similar to those observed with other members of the TGF-β family. Indeed, it is reported that TGF-β by itself, displays cytostatic and apoptotic functions that restrain cell growth, avoiding the hyperproliferative disorders, even in Huh7 and Hep3B cells [32,33]. This novel effect, elicited by GDF11 in liver cancer cells, confirms the well-conserved cytostatic effect in the TGF-β family, as exemplified by the analysis of the content of the main cell cycle regulating proteins; cyclins A and D1, and cdk6 were downregulated, and p27 was overexpressed, these effects being particularly evident at 72 h (Fig. 2C). Similarly, GDF11 significantly attenuated the proliferation of the neural stem cell line Cor-1, downregulating key positive cell cycle proteins [20]. In addition, this work by Williams and collaborators showed that cell migration is impaired by GDF11 as we also observed (Fig. 2B and F).

Based in the fact that stemness feature is increasing in spheroid or 3D culture, particularly in cells used in this study [29,30], we observed that the number and the size of spheroids decreased in the presence of GDF11 at 72 h of repeated treatment (50 ng/ml, every 24 h) in both HCC cell lines. We found similar effects in HepG2 (Fig. 7A), a human hepatoma cell line capable to form spheroids as well [30], and in SNU-182, another human HCC cell line from a high aggressive tumor. Interestingly, when comparing the human liver cancer cell lines, GDF11 displayed greater effects in Huh7 and Hep3B than in HepG2, although, in the last one, decrement in sphere formation was statistically significant, confirming the preference of GDF11 on cells with stemness feature. Similar results were reported by Bajikar and collaborators in triple negative breast cancer cell lines [19], even more, Hepa1–6, MDA-MB-231 and SNU-182 cell lines presented similar effects with some differences in the number of spheroids, but in all cases with significant changes (Fig. 7).

To gain more evidence, we performed the analysis of the messenger RNA levels of key molecular markers for aggressive cancers and stemness (Fig. 3B), cytokeratin 19 (ck19) has been closely related to poor prognosis and high recurrence in HCC [34], the effect on ck19 expression, induced by GDF11, was the most relevant, in terms of absolute values comparing with NT cells, prom1 (CD133) and epcam (EpCAM) also are well characterized stemness markers, being CD133 most significant in stages I, while the prognostic role of EpCAM is more effective in advanced stages [35], interestingly, the effect of GDF11 in epcam expression was different in the HCC cell lines studied here, Huh7 cells did not respond to the GDF11 treatment exhibiting no changes in the expression, however, Hep3B, which a more aggressive cell line, diminished the expression since 6 h of treatment, supporting the findings by Chang and coworkers [35]. These results strongly suggest that GDF11 antitumorigenic properties are more relevant in advanced tumors. Finally, cd24 is another well-known marker for stemness and aggressive HCC [36], our data clearly show a decrement since 6 h in Huh7 and at 12 h in Hep3B, once again the difference in stemness capacity is evident in both cell lines, but in both cases GDF11 displays antitumorigenic effects.

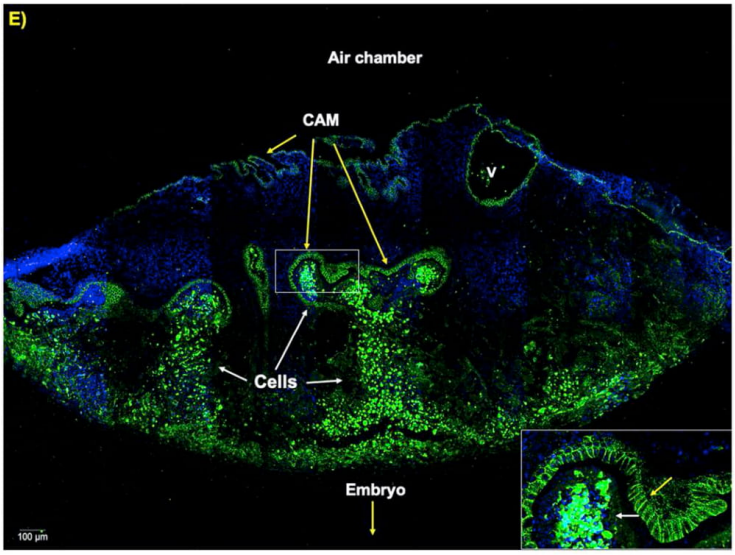
The analysis of mesenchymal and epithelial markers revealed a clear GDF11-induced mesenchymal to epithelial transition phenotype. A time-dependent decrement in the expression of mesenchymal-related proteins such as Snail and N-cadherin, and increased of epithelial markers, such as E-cadherin and occludin (Fig. 4) [37], was confirmed by Western blot and immunofluorescence. The gain of an epithelial phenotype was simultaneously associated to a significant decrease in colony and spheroid formation capacity (Fig. 5), and to a decreased capacity in invasion (Fig. 6), as addressed by the CAM assay. Interestingly, in the CAM assay we observed a degradation of the basal membrane, a key condition for invasion in the experiment using not treated cells, and in the case of the experiment with GDF11 treated cells the membrane was preserved suggesting a distinctive phenotype of an in situ tumor, in addition treated cells were presented forming cumulous, probably because the increment of E-cadherin expression (Fig. 4 and Supplementary Fig. 2).

All these data clearly show that GDF11 induces an anti-tumor response in HCC cells, directed to decreases aggressiveness by attempting reverse the mesenchymal to epithelial phenotype.

The decrement of the invasive phenotype was also found in triple negative breast cancer cell lines [19]. The effect was associated to an increase in the expression of E-cadherin, supporting our findings in HCC-derived cells. Importantly, we reported that GDF11 effects were not transient, and may evoke a cellular reprograming in HCC cells. Indeed, treatment for 72 h with GDF11 sustained the effects even five days in culture in the absent of GDF11.

Although, a low frequency of mutations in GDF11 and a significant enrichment in the convertase PCSK5 locus have been reported in breast cancer [19], we did not find significant presence of mutations in those genes in HCC according to The Cancer Genome Atlas (TCGA, data not shown). However, in human HCC the expression level of GDF11 observed no changes, but in cholangiocellular carcinoma (CCC), significant differences were found increasing 1.55-fold change in tumors versus normal tissue (Supplementary Fig. 5), (36 patients for CCC and 371 for HCC; https://portal.gdc.cancer.gov and http://firebrowse.org), in the case of PCSK5 gene expression the TCGA reports significant changes in both HCC and CCC (1.56-fold and 2.31-fold change versus normal tissue.

These data suggest that changes in basal expression in GDF11 and PCSK5 genes, are rare events in HCC and probably not responsible to the loss of function of GDF11, maybe some epigenetic silencing mechanism could be related to loss of function of GDF11. Nevertheless, we clearly demonstrated that recombinant human GDF11 induces an



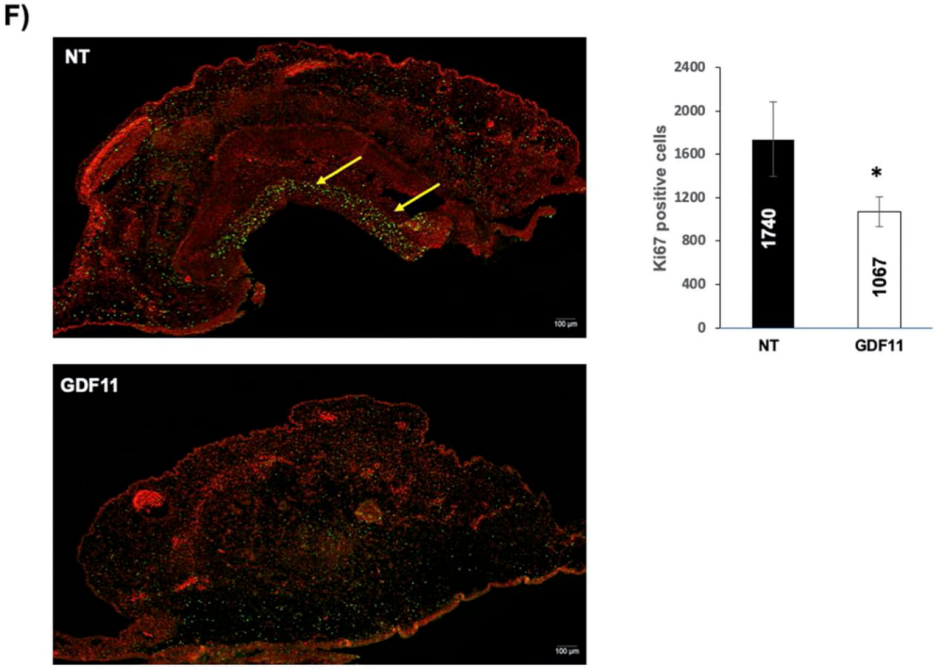


Fig. 6. (*continued*)

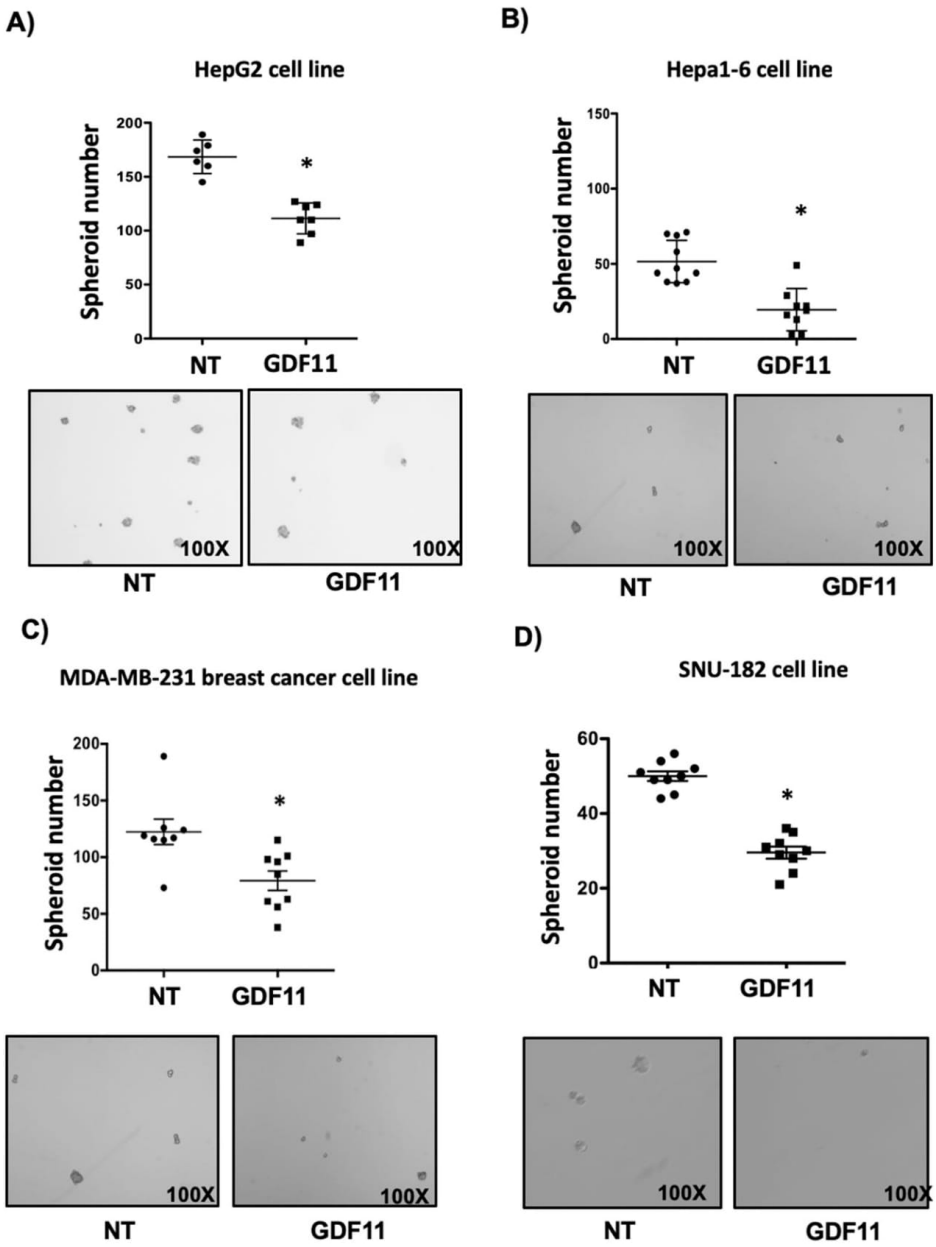


Fig. 7. GDF11 decreases spheroid formation property in other cancer cell lines. Cells were treated every 24 h with GDF11 (50 ng/ml) up to 72 h and we proceeded to spheroid counting in A) HepG2, hepatoblastoma cell line B) Hepa1–6, mouse hepatocellular carcinoma cell line, C) MDA-MB-231, triple negative breast cancer cell line, D) SNU-182, grade III/IV human hepatocellular carcinoma cell line. Each point represents an independent experiment; we reported the median ± SEM of at least six independent experiments. *, $p \leq 0.05$ vs NT cells at 72 h.

antitumorigenic effect with no relevance in cell death, but lessening aggressiveness by promoting a cytostatic phenotype and repressing invasion.

In conclusion, we are reporting tumor suppressive properties of GDF11 in HCC-derived cells restricting self-renewal capacity, setting GDF11 as a good candidate for therapy and biomarker in liver cancer.

Conflicts of interest

The authors declare no conflict of interest.

Transparency document

The Transparency document associated with this article can be found, in online version.

Acknowledgements

This work was partially funded by a grant from the Consejo Nacional de Ciencia y Tecnología (CONACYT; CB-252942 and Fronteras de la Ciencia-1320) and Universidad Autónoma Metropolitana. We thank the confocal core units of the Universidad Autonoma Metropolitana Iztapalapa, and Instituto Nacional de Cancerología de Mexico, for the assistance. MGR, SHR, ASN are scholarship holders from Conacyt.

Appendix A. Supplementary data

Supplementary data to this article can be found online at https://doi.org/10.1016/j.bbadis.2019.03.003.

References

[1] N. Mendez-Sanchez, E. Garcia-Villegas, B. Merino-Zeferino, S. Ochoa-Cruz, A.R. Villa, H. Madrigal, R.A. Kobashi-Margain, Y. Gutierrez-Grobe, N. Chavez-Tapia, G. Ponciano-Rodriguez, M. Uribe, Liver diseases in Mexico and their associated mortality trends from 2000 to 2007: a retrospective study of the nation and the federal states, Ann. Hepatol. 9 (2010) 428–438.

[2] A. Forner, J.M. Llovet, J. Bruix, Hepatocellular carcinoma, Lancet 379 (2012) 1245–1255.

[3] P. Kaposi-Novak, J.S. Lee, L. Gomez-Quiroz, C. Coulouarn, V.M. Factor, S.S. Thorgeirsson, Met-regulated expression signature defines a subset of human hepatocellular carcinomas with poor prognosis and aggressive phenotype, J. Clin. Invest. 116 (2006) 1582–1595.

[4] J. Ferlay, I. Soerjomataram, R. Dikshit, S. Eser, C. Mathers, M. Rebelo, D.M. Parkin, D. Forman, F. Bray, Cancer incidence and mortality worldwide: sources, methods and major patterns in GLOBOCAN 2012, Int. J. Cancer 136 (2015) E359–E386.

[5] J. Bruix, M. Colombo, Hepatocellular carcinoma: current state of the art in diagnosis and treatment, Best Pract. Res. Clin. Gastroenterol. 28 (2014) 751.

[6] A.C. McPherron, A.M. Lawler, S.J. Lee, Regulation of anterior/posterior patterning of the axial skeleton by growth/differentiation factor 11, Nat. Genet. 22 (1999) 260–264.

[7] R. Essalmani, A. Zaid, J. Marcinkiewicz, A. Chamberland, A. Pasquato, N.G. Seidah, A. Prat, In vivo functions of the proprotein convertase PC5/6 during mouse development: Gdf11 is a likely substrate, Proc. Natl. Acad. Sci. U. S. A. 105 (2008) 5750–5755.

[8] C.E. Brun, M.A. Rudnicki, GDF11 and the mythical fountain of youth, Cell Metab. 22 (2015) 54–56.

[9] M. Sinha, Y.C. Jang, J. Oh, D. Khong, E.Y. Wu, R. Manohar, C. Miller, S.G. Regalado, F.S. Loffredo, J.R. Pancoast, M.F. Hirshman, J. Lebowitz, J.L. Shadrach, M. Cerletti, M.J. Kim, T. Serwold, L.J. Goodyear, B. Rosner, R.T. Lee, A.J. Wagers, Restoring systemic GDF11 levels reverses age-related dysfunction in mouse skeletal muscle, Science 344 (2014) 649–652.

[10] F.S. Loffredo, M.L. Steinhauser, S.M. Jay, J. Gannon, J.R. Pancoast, P. Yalamanchi, M. Sinha, C. Dall'Osso, D. Khong, J.L. Shadrach, C.M. Miller, B.S. Singer, A. Stewart, N. Psychogios, R.E. Gerszten, A.J. Hartigan, M.J. Kim, T. Serwold, A.J. Wagers, R.T. Lee, Growth differentiation factor 11 is a circulating factor that reverses age-related cardiac hypertrophy, Cell 153 (2013) 828–839.

[11] M.A. Egerman, S.M. Cadena, J.A. Gilbert, A. Meyer, H.N. Nelson, S.E. Swalley, C. Mallozzi, C. Jacobi, L.L. Jennings, I. Clay, G. Laurent, S. Ma, S. Brachat, E. Lach-Trifilieff, T. Shavlakadze, A.U. Trendelenburg, A.S. Brack, D.J. Glass, GDF11 increases with age and inhibits skeletal muscle regeneration, Cell Metab. 22 (2015) 164–174.

[12] D.J. Glass, Elevated GDF11 is a risk factor for age-related frailty and disease in humans, Cell Metab. 24 (2016) 7–8.

[13] M.J. Schafer, E.J. Atkinson, P.M. Vanderboom, B. Kotajarvi, T.A. White, M.M. Moore, C.J. Bruce, K.L. Greason, R.M. Suri, S. Khosla, J.D. Miller, H.R. Bergen 3rd, N.K. LeBrasseur, Quantification of GDF11 and myostatin in human aging and cardiovascular disease, Cell Metab. 23 (2016) 1207–1215.

[14] G. Finkenzeller, G.B. Stark, S. Strassburg, Growth differentiation factor 11 supports migration and sprouting of endothelial progenitor cells, J. Surg. Res. 198 (2015) 50–56.

[15] F. Jeanplong, S.J. Falconer, J.M. Oldham, N.J. Maqbool, M. Thomas, A. Hennebry, C.D. McMahon, Identification and expression of a novel transcript of the growth and differentiation factor-11 gene, Mol. Cell. Biochem. 390 (2014) 9–18.

[16] K.K. Gokoffski, H.H. Wu, C.L. Beites, J. Kim, E.J. Kim, M.M. Matzuk, J.E. Johnson, A.D. Lander, A.L. Calof, Activin and GDF11 collaborate in feedback control of neuroepithelial stem cell proliferation and fate, Development 138 (2011) 4131–4142.

[17] T. Yokoe, T. Ohmachi, H. Inoue, K. Mimori, F. Tanaka, M. Kusunoki, M. Mori, Clinical significance of growth differentiation factor 11 in colorectal cancer, Int. J. Oncol. 31 (2007) 1097–1101.

[18] C. Wallner, M. Drysch, M. Becerikli, H. Jaurich, J.M. Wagner, S. Dittfeld, J. Nagler, K. Harati, M. Dadras, S. Philippou, M. Lehnhardt, B. Behr, Interaction with the GDF8/11 pathway reveals treatment options for adenocarcinoma of the breast, Breast 37 (2018) 134–141.

[19] S.S. Bajikar, C.C. Wang, M.A. Borten, E.J. Pereira, K.A. Atkins, K.A. Janes, Tumor-suppressor inactivation of GDF11 occurs by precursor sequestration in triple-negative breast cancer, Dev. Cell 43 (2017) 418–435 e413.

[20] G. Williams, M.P. Zentar, S. Gajendra, M. Sonego, P. Doherty, G. Lalli, Transcriptional basis for the inhibition of neural stem cell proliferation and migration by the TGFbeta-family member GDF11, PLoS One 8 (2013) e78478.

[21] C. Enriquez-Cortina, M. Almonte-Becerril, D. Clavijo-Cornejo, M. Palestino-Dominguez, O. Bello-Monroy, N. Nuno, A. Lopez, L. Bucio, V. Souza, R. Hernandez-Pando, L. Munoz, M.C. Gutierrez-Ruiz, L.E. Gomez-Quiroz, Hepatocyte growth factor protects against isoniazid/rifampicin-induced oxidative liver damage, Toxicological sciences: an official journal of the Society of Toxicology 135 (2013) 26–36.

[22] J.U. Marquardt, D. Seo, L.E. Gomez-Quiroz, K. Uchida, M.C. Gillen, M. Kitade, P. Kaposi-Novak, E.A. Conner, V.M. Factor, S.S. Thorgeirsson, Loss of c-Met accelerates development of liver fibrosis in response to CCl(4) exposure through deregulation of multiple molecular pathways, Biochim. Biophys. Acta 1822 (2012) 942–951.

[23] J.P. Quigley, P.B. Armstrong, Tumor cell intravasation alu-cidated: the chick embryo opens the window, Cell 94 (1998) 281–284.

[24] D. Ribatti, The chick embryo chorioallantoic membrane (CAM) assay, Reprod. Toxicol. 70 (2017) 97–101.

[25] R. Lazzarini-Lechuga, O. Alcantar-Ramirez, R. Jaime-Cruz, L. Gómez-Quiroz, Efecto teratogénico de nanopartículas de oro de 20 nm durante la septación cardiaca, Munod Nano 7 (2014) 69–77.

[26] C. Czauderna, M. Palestino-Dominguez, D. Castven, D. Becker, L. Zanon-Rodriguez, J. Hajduk, F.L. Mahn, M. Herr, D. Strand, S. Strand, S. Heilmann-Heimbach, L.E. Gomez-Quiroz, M.A. Worns, P.R. Galle, J.U. Marquardt, Ginkgo biloba induces different gene expression signatures and oncogenic pathways in malignant and non-malignant cells of the liver, PLoS One 13 (2018) e0209067.

[27] A. Jemal, E.M. Ward, C.J. Johnson, K.A. Cronin, J. Ma, B. Ryerson, A. Mariotto, A.J. Lake, R. Wilson, R.L. Sherman, R.N. Anderson, S.J. Henley, B.A. Kohler, L. Penberthy, E.J. Feuer, H.K. Weir, Annual report to the nation on the status of cancer, 1975–2014, featuring survival, J. Natl. Cancer Inst. 109 (2017).

[28] L. Ghisolfi, A.C. Keates, X. Hu, D.K. Lee, C.J. Li, Ionizing radiation induces stemness in cancer cells, PLoS One 7 (2012) e43628.

[29] H. Hirschfield, C.B. Bian, T. Higashi, S. Nakagawa, T.Z. Zeleke, V.D. Nair, B.C. Fuchs, Y. Hoshida, In vitro modeling of hepatocellular carcinoma molecular subtypes for anti-cancer drug assessment, Exp. Mol. Med. 50 (2018) e419.

[30] H.S. Seol, S.E. Lee, J.S. Song, J.K. Rhee, S.R. Singh, S. Chang, S.J. Jang, Complement proteins C7 and CFH control the stemness of liver cancer cells via LSF-1, Cancer Lett. 372 (2016) 24–35.

[31] Y. Zhang, P.B. Alexander, X.F. Wang, TGF-beta family signaling in the control of cell proliferation and survival, Cold Spring Harb. Perspect. Biol. 9 (2017).

[32] P.M. Siegel, J. Massague, Cytostatic and apoptotic actions of TGF-beta in homeostasis and cancer, Nat. Rev. Cancer 3 (2003) 807–821.

[33] J. Zhang, O. Yamada, S. Kida, Y. Matsushita, T. Hattori, Down-regulation of osteopontin mediates a novel mechanism underlying the cytostatic activity of TGF-beta, Cell Oncol (Dordr) 39 (2016) 119–128.

[34] C.W. Lee, S.E. Lin, H.I. Tsai, P.J. Su, C.H. Hsieh, Y.C. Kuo, C.M. Sung, C.Y. Lin, C.N. Tsai, M.C. Yu, Cadherin 17 is related to recurrence and poor prognosis of cytokeratin 19-positive hepatocellular carcinoma, Oncol. Lett. 15 (2018) 559–567.

[35] A.W. Chan, J.H. Tong, S.L. Chan, P.B. Lai, K.F. To, Expression of stemness markers (CD133 and EpCAM) in prognostication of hepatocellular carcinoma, Histopathology 64 (2014) 935–950.

[36] Y. Li, R. Wang, S. Xiong, X. Wang, Z. Zhao, S. Bai, Y. Wang, Y. Zhao, B. Cheng, Cancer-associated fibroblasts promote the stemness of CD24(+) liver cells via paracrine signaling, J Mol Med (Berl) 97 (2019) 243–255.

[37] W. Chengye, T. Yu, S. Ping, S. Deguang, W. Keyun, W. Yan, Z. Rixin, L. Rui, G. Zhenming, Y. Mingliang, W. Liming, Metformin reverses bFGF-induced epithelial-mesenchymal transition in HCC cells, Oncotarget 8 (2017) 104247–104257.

Received: 30 June 2018 | Accepted: 4 September 2018

DOI: 10.1002/jcp.27474

ORIGINAL RESEARCH ARTICLE

WILEY Journal of Cellular Physiology

Cholesterol burden in the liver induces mitochondrial dynamic changes and resistance to apoptosis

Mayra Domínguez-Pérez[1,2,3] | Arturo Simoni-Nieves[1,2] | Patricia Rosales[2] | Natalia Nuño-Lámbarri[4] | Mónica Rosas-Lemus[5] | Verónica Souza[1,6] | Roxana U. Miranda[1,6] | Leticia Bucio[1,6] | Salvador Uribe Carvajal[5] | Jens U. Marquardt[7] | Daekwan Seo[8] | Luis E. Gomez-Quiroz[1,6] | María Concepción Gutiérrez-Ruiz[1,6]

[1]Laboratorio de Fisiología Celular, Departamento de Ciencias de la Salud, CBS Universidad Autónoma Metropolitana Iztapalapa, Mexico City, México

[2]Posgrado en Biología Experimental, DCBS, Universidad Autónoma Metropolitana Iztapalapa, Mexico City, México

[3]Laboratorio de Genómica de Enfermedades Cardiovasculares, Instituto Nacional de Medicina Genómica, Mexico City, México

[4]Unidad de Investigación Traslacional, Fundación Clínica Médica Sur, Mexico City, Mexico

[5]Departamento de Genética Molecular, Instituto de Fisiología Celular, UNAM, México City, Mexico

[6]Laboratorio de Medicina Experimental, Unidad de Medicina Translacional, Instituto de Investigaciones Biomédicas, UNAM/ Instituto Nacional de Cardiología Ignacio Chavez, Mexico City, Mexico

[7]First Department of Medicine, University Medical Center, Johannes Gutenberg University Mainz, Mainz, Germany

[8]Bioinformatics Department, Macrogen Corp, Rockville, Maryland,

Correspondence
María Concepción Gutiérrez-Ruiz, Departamento de Ciencias de la Salud, DCBS, Universidad Autónoma Metropolitana-Iztapalapa, Av. San Rafael Atlixco 186, Colonia Vicentina, Iztapalapa, D.F. 09340, México.
Email: mcgr@xanum.uam.mx

Funding information
Consejo Nacional de Ciencia y Tecnología, Grant/Award Numbers: CB-166042, CB252942; Universidad Autónoma Metropolitana Iztapalapa; SEP-PRODEP, Grant/Award Number: 913026-14612111

Abstract

Non-alcoholic fatty liver disease (NAFLD) encompasses a broad spectrum of histopathological changes ranging from non-inflammatory intracellular fat deposition to non-alcoholic steatohepatitis (NASH), which may progress into hepatic fibrosis, cirrhosis, or hepatocellular carcinoma. Recent data suggest that impaired hepatic cholesterol homeostasis and its accumulation are relevant to the pathogenesis of NAFLD/NASH. Despite a vital physiological function of cholesterol, mitochondrial dysfunction is an important consequence of dietary-induced hypercholesterolemia and was, subsequently, linked to many pathophysiological conditions. The aim in the current study was to evaluate the morphological and molecular changes of cholesterol overload in mouse liver and particularly, in mitochondria, induced by a high-cholesterol (HC) diet for one month. Histopathological studies revealed microvesicular hepatic steatosis and significantly elevated levels of liver cholesterol and triglycerides leading to impaired liver synthesis. Further, high levels of oxidative stress could be determined in liver tissue as well as primary hepatocyte culture. Transcriptomic changes induced by the HC diet involved disruption in key pathways related to cell death and oxidative stress as well as upregulation of genes related to glutathione homeostasis. Impaired liver function could be associated with a decrease in mitochondrial membrane potential and ATP content and significant alterations in mitochondrial dynamics. We demonstrate that cholesterol overload in the liver leads to mitochondrial changes which may render damaged hepatocytes proliferative and resistant to cell death whereby perpetuating liver damage.

KEYWORDS
apoptosis, cholesterol, mitochondrial dynamics, oxidative stress

 © 2018 Wiley Periodicals, Inc.

1 | INTRODUCTION

Non-alcoholic fatty liver disease (NAFLD) is the most common form of chronic liver disease (Lonardo et al., 2017). Patients with NAFLD are at high risk of developing inflammatory steatohepatitis (NASH) which can progress into fibrosis, cirrhosis, and ultimately, hepatocellular carcinoma (HCC; Calvisi et al., 2011). Several lines of evidence indicate that structural and functional alterations of mitochondria significantly contribute to changes of the cellular lipid metabolism as well as oxidant stress response. Consistently, mitochondrial dysfunction is frequently associated with the development of NAFLD (Auger, Alhasawi, Contavadoo, & Appanna, 2015; Serviddio & Sastre, 2010). Oxidative stress is one of the key mediators of hepatic damage and a major contributor to the progression from steatosis to NASH, particularly when mitochondria are compromised (Bellanti et al., 2018). Oxidative stress can result in various deleterious processes that stem from an imbalance between the excessive formation of pro-oxidants and the counteracting antioxidant mechanisms (Gomez-Quiroz, Gutierrez Ruiz, Marquardt, Factor, & Thorgeirsson, 2017). It is well known that mitochondrial dysfunction can be induced by dietary-induced hypercholesterolemia, leading to organ insufficiency or failure, particularly in the liver (Marí et al., 2006). Although mitochondria, particularly the inner membrane, only have low levels of cholesterol in the cell, cholesterol content is essential for the proper functionality of mitochondria (Garcia-Ruiz et al., 2009). Alterations in mitochondrial cholesterol have been associated with a wide range of pathological conditions, including steatosis and cancer (Enríquez-Cortina et al., 2017). Recently, it has been published that a high cholesterol (HC) diet (1.25% cholesterol) in combination with a high fat diet (60% cocoa butter) synergistically enables development and progression of NAFLD to NASH by a mechanism driven by cholesterol derivatives (oxysterols) in presence of free fatty acids with impact in mitochondrial function and dynamics (Bellanti et al., 2018), but the effects displayed by dietary cholesterol alone remains partially characterized. In the present work, we were aimed to figure out the effects of cholesterol overload in the liver, particularly in hepatocytes, and the influence on the transcriptome and in the cholesterol-overloaded mitochondria dynamic.

2 | MATERIAL AND METHODS

All chemicals and reagents were of the highest analytical grade, and most of them were purchased from Sigma (St. Louis, MO). Reagents obtained from other suppliers are detailed in the text.

2.1 | Animal model

C57BL/6 male mice (8–10 weeks old) were purchased from Jackson Laboratory (Bar Harbor, ME) and were maintained in pathogen-free conditions with controlled temperature and humidity on a 12 hr light–dark cycle in the animal facility at the Universidad Autonoma Metropolitana. The experimental protocols used were approved and performed in accordance with the Animal Care Committee of the Universidad Autonoma Metropolitana and the NIH Guide for the Care and Use of Laboratory Animals.

2.2 | Experimental design

Twenty mice were randomly divided in two groups, 10 animals were fed with an HC diet (2% cholesterol and 0.5% sodium cholate; Gomez-Quiroz et al., 2016; Nuño-Lámbarri et al., 2016) for 30 days, the second group was fed with control standard Chow diet (LabDiet #5001) for the same period. After 30 days, animals were killed. Liver weight was monitored, and liver tissue, as well as serum, was collected for subsequent analyzes.

2.3 | Histological analysis

Liver sections from all groups were fixed in absolute ethanol and embedded in paraffin for routine hematoxylin and eosin (H&E) staining, and both, morphometric and NAFLD activity score (NAS; Kleiner et al., 2005) studies were performed. For morphometric study five H&E slides, five random- view fields were selected, and 100 cells were counted in each field. Data are reported as cell percentage considering normal, regenerative, and death phenotypes (Enriquez-Cortina et al., 2013). Tissue for Oil Red O staining were fixed in 4% paraformaldehyde/phosphate-buffered saline (PBS) for 30 min and was stained with freshly diluted 0.2% Oil red O solution for 4 hr after that we proceeded to microphotography.

2.4 | Primary mouse hepatocytes isolation and culture

Hepatocytes were isolated from HC and Chow mice by the two-step collagenase perfusion, as we previously reported (Gómez-Quiroz et al., 2008). The viability was assessed by trypan blue exclusion and generally exceeded >90%. Hepatocytes were seeded at 2.5×10^5 cells per cm^2 either in Lab-Tek chambered slides or in 10-cm dishes (Nalge, Nunc) in Ham's F-12/Dulbecco's modified Eagle's basal hepatocyte growth medium supplemented with 10% fetal bovine serum. After 24 hr, cells were used for reactive oxygen species (ROS) determination, Oil Red O staining, cholesterol, and mitochondrial potential determination.

2.5 | Biochemical determinations and analysis of liver function

Blood samples were obtained from the orbital venous plexus under Avertin (2-2-2 tribromoethanol) anesthesia before sacrifice. Serum activity of aspartate aminotransferase (AST), alanine transferase (ALT), and alkaline phosphatase (ALP) were determined by an automated method using Reflovet Plus (Roche, Mannheim, Germany).

2.6 | Cholesterol determination

For total cholesterol determination, 10 mg of liver or mitochondrial protein was saponified with alcoholic KOH in a 60°C heating block for 30 min. After the mixture had cooled, 3 ml of hexane and 600 µl of distilled water were added and shaken to ensure complete mixing. Appropriate aliquots of the hexane layer were evaporated under nitrogen with vacuum (Speed Vac, Savant, Cranbury, NJ) and used for cholesterol measurement with O-phthalaldehyde dissolved in acetic acid (0.5 mg/ml). After that sulfuric acid (1 ml) was added and then read at 550 in a spectrophotometer (Rudel & Morris, 1973).

2.7 | Triglycerides determination

Triglycerides (TG) content was determined using the triglyceride determination kit (Sigma-Aldrich, St Louis, MO) following manufacturer's instructions.

2.8 | Oil red O staining

To detect intracellular neutral lipids accumulation, the cells were seeded into 24-well chambers. After treatments, cells were washed with ice-cold PBS and then fixed with 2.5% paraformaldehyde for 1 hr. The cells were stained with freshly diluted 0.2% Oil red O solution for 4 hr; after that, we proceeded to microphotography.

2.9 | In situ ROS determination

Animals were euthanized in parallel exclusively for in situ ROS determination. Fresh tissue was rapidly sectioned, frozen in liquid nitrogen, and embedded in optimum cutting temperature reagent (Sakura Finetec, Torrance, CA). Subsequently, 8-µm frozen sections were obtained in a cryostat (Leica CM-3050S) at −20°C and the slides were immediately incubated for 15 min, in the dark, at room temperature with either 2′,7′–dichlorofluorescin diacetate (DCFDA, 5 µM), a cell-permeable non-fluorescent probe that is intracellularly de-esterified and converted to the highly fluorescent 2′,7′-dichlorofluorescein (DCFH) upon oxidation by ROS, particularly peroxides, or with dihydroethidium (DHE, 1 µM) for determination of superoxide anion radical detecting ethidium fluorescence. Samples were covered and observed using a confocal microscope at excitation and emission wavelengths of 480 and 520 nm, respectively, for DCFDA; and excitation and emission wavelengths of 485 and 570 nm, respectively, for DHE-derived ethidium fluorescence, as we previously reported (Nuño-Lámbarri et al., 2016).

2.10 | Western blot

The whole liver homogenate was prepared in ice-cold PBS using dounce homogenizer. The cellular pellet was suspended in 200 µl of M-PER (Pierce Chemical, Rockford, IL); lysis buffer was supplemented with proteases and phosphatases inhibitors (Roche). Lysis was performed on ice for 15 min, and cell debris was removed by centrifugation at 13,000*g* at 4°C for 10 min and the supernatant was recovered (Hernández et al., 2015). Total protein concentration was determined using a bicinchoninic acid kit (Pierce Thermo Scientific, Rockford, IL), according to the manufacturer's instructions. Proteins were separated by electrophoresis using 10% gradient Duramide precast gels (Cambrex, Rockland, ME) and transferred to a polyvinylidene difluoride membranes (Invitrogen, Carlsbad, CA; Clavijo-Cornejo et al., 2013). Immunodetection was performed using antibodies listed in Supporting Information Table 1.

2.11 | Mitochondria isolation

Mitochondria were obtained by homogenization and differential centrifugation. Briefly, cells were suspended 50% w/v in mitochondrial buffer 0.22 M mannitol, 0.7 M sucrose, 2 mM HEPES, pH 7.4) plus 0.1% BSA and were homogenized. The homogenate was centrifuged in an F21- 8 × 50 y Sorvall rotor at 1017*g* for 5 min. Then the supernatant was recovered and centrifuged at 10,700*g* for 10 min. The pellet was suspended in mitochondrial buffer containing BSA and centrifuged at 3,600*g* for 5 min. The supernatant was recovered and centrifuged at 17,000*g* for 10 min. The resulting pellet was suspended in a small volume of mitochondrial buffer (without BSA), and protein was determined by Biuret (Rosas-Lemus, Uribe-Alvarez, Chiquete-Félix, & Uribe-Carvajal, 2014).

2.12 | Mitochondrial transmembrane potential ($\Delta\Psi$)

The $\Delta\psi$ was determined using 10 µM safranine-O, following the absorbance changes at 511–533 nm in a DW2000 Aminco spectrophotometer in dual mode (Åkerman & Wikström, 1976). At the end of each trace, $\Delta\psi$ was collapsed by adding 5 µM of the protonophoro m-chlorophenylhydrazone (CCCP). Additionally, changes in mitochondria membrane potential were addressed by using the rhodamine-based dye Mito Red, which upon mitochondria localization emits fluorescence in a membrane potential-dependent manner.

2.13 | ATP determination

Hepatic ATP concentration was determined colorimetrically in liver homogenates of Chow and HC mice using the Abcam ATP-assay kit (Abcam, MA) according to the manufacturer's instructions. Briefly, 30 mg of liver was lysed in the ATP assay buffer and centrifuged at 13,000*g* for 2 min to pellet-insoluble materials. Samples were deproteinized and neutralized with PCA-KOH. The supernatant was added to a 96-well plate and followed by the addition of 50 µl of the Reaction Mix to each well and was incubated at the room temperature in the dark for 30 min. Absorbance was read at 570 nm using a multimode detector DTX 880 (Beckman Coulter). The ATP content was calculated based on a standard curve generated at the same time.

2.14 | Electron microscopy

Tissues were fixed with 2% glutaraldehyde in 0.1 M phosphate buffer (pH 7.4) followed by 1% OsO_4. After dehydration, thin sections were stained with uranyl acetate and lead citrate for observation under an EOL JEM 12000 EII transmission electron microscope (TEM).

2.15 | Global transcriptomic analysis by microarray

Microarray analysis was performed as we previously described (Gomez-Quiroz et al., 2016). As input, 200 ng total RNA from liver tissue were used for the in vitro transcription reactions, which were incubated for 16 hr at 37°C. Hybridization, washing, detection (Cy3-streptavidin, Amersham Biosciences, GE Healthcare), and scanning were performed on an Illumina iScan system (Illumina) using reagents and protocols supplied by the manufacturer. The biotinylated cRNA (750 ng per sample) was hybridized on Sentrix whole genome beadchips mouse Ref-8v2 for 18 hr at 58°C while rocking (5 rpm). The beadchip covers ~24,000 RefSeq transcripts. Image analysis and data extraction were performed automatically using Illumina GenomeScan Software. Gene expression values were adjusted by subtracting background noises in each spot by GenomeStudio (Illumina) and normalized by quantile normalization method across all samples. A signal intensity with a detection *p*-value greater than 0.05 was treated as a missing value, and only genes with sufficient representation across the samples were included in further data analysis (presence in ≥2 replicates/group). Differentially expressed genes were identified by Bootstrap *t*-test with 10,000 repetitions (Neuhauser & Jockel, 2006). Genes with a Bootstrap *p*-value ≤ 0.01 were considered significantly different. Only genes with more than two fold differences and *p*-value ≤ 0.01 were included in further analyzes. Ingenuity Pathway Analysis tool (IPA, Ingenuity Systems Inc.) was used to explore the functional relationships among the differentially expressed genes. The significance of each network, function, and pathway was determined by the scoring system provided by IPA tool. The microarray datasets have been deposited to the Gene Expression Omnibus database (http://www.ncbi.nlm.nih.gov/geo, accession number GSE30651).

2.16 | Caspase 3 activity

Tissue was lysed in reaction buffer and incubated for 30 min on ice. For each reaction, caspase 3 synthetic tetrapeptide fluorogenic substrate (Ac-DEVD-AMC) was added (BD Pharmigen) and then the tissue lysate; after that, the samples were incubated for 1 hr. The amount of AMC released was measured by fluorometry at an excitation wavelength of 380 nm and an emission wavelength of 420 nm.

2.17 | Statistical analysis

The data are presented as mean ± standard error (*SE*). for at least three independent experiments. Comparisons between groups were made using Student's *T*-test follow post ad hoc by U Mann–Whitney using GraphPad Prism 6 for Mac OSX, a $p \leq 0.05$ was considered significant.

3 | RESULTS

3.1 | An HC diet consumption resulted in hepatic steatosis and liver damage

Livers of C57BL/6 mice fed with HC diet for 30 days showed hepatomegaly, the characteristic pale color of the fatty liver and increased liver to body weight ratio (Figure 1b,c). An increase in lipid content in the tissue was confirmed by Oil Red staining (Figure 1e). Further, total liver cholesterol increased 6.5-fold and triglycerides 5.2-fold compared with Chow diet fed mice (Figure 1f,g). Consistently, a steatotic phenotype and alterations of the liver architecture was present (Figure 1i), dispersed inflammation (white arrow) and hepatocyte ballooning (yellow arrow) were consistent with NASH according to the NAS (or Kleiner Scoring System, Supporting Information Table 2; Kleiner et al., 2005).

In addition, cellular hypertrophy with numerous hyperchromatic hepatocytes unveiling nuclear condensation were observed (Figure 1i, asterisks). The morphometric analysis confirmed significantly higher percentages of both, dead and proliferating cells, as well as a decrease in normal cells in liver from HC fed animals (Figure 1j). Mice fed with HC showed increased signs of liver injury, judged by an increased activity in ALT, AST, and ALP (Figure 1k).

In confirmation of the steatotic phenotype observed and the increment of neutral lipids in the liver of HC mice, oil red O staining, and filipin fluorescence further demonstrated that cultured primary hepatocytes isolated from HC mice maintained high levels neutral lipids (Supporting Information Figure 1b), and free cholesterol content (Supporting Information Figure 1d).

3.2 | Global transcriptomic analysis

Next, transcriptomic profiling of HC diet livers was performed. In comparison to Chow, a total of 938 differentially expressed genes (439 upregulated and 499 downregulated (Supporting Information Table 3) could be detected. These genes were highly efficient in separating the two different diets using unsupervised clustering analysis (Figure 2a). We found that a significant number of differentially expressed genes related to hepatic cell death and oxidative stress (Ccnd1, Cers2, E2F1, Sod2, Scd, Pon3, Hmox 1, Sod1, Plin5, App, Usp10, Adar, Casp7, Nr1i3, Gstz1, Gnmt, Irf5; Figure 2b–d). Interestingly, most of the genes related to glutathione homeostasis were upregulated (Gsta1, Gsta2, Gstm4, Gpx4, Gss), and many nuclear genes encoding mitochondrial proteins were downregulated (Abcb8, Abcb6, Mtif3, Shmt2, Slc25a23, Slc25a10, Hmgcs2, Gls2, Hsd17b10Bcat2) clearly indicating a compromise of mitochondrial functions.

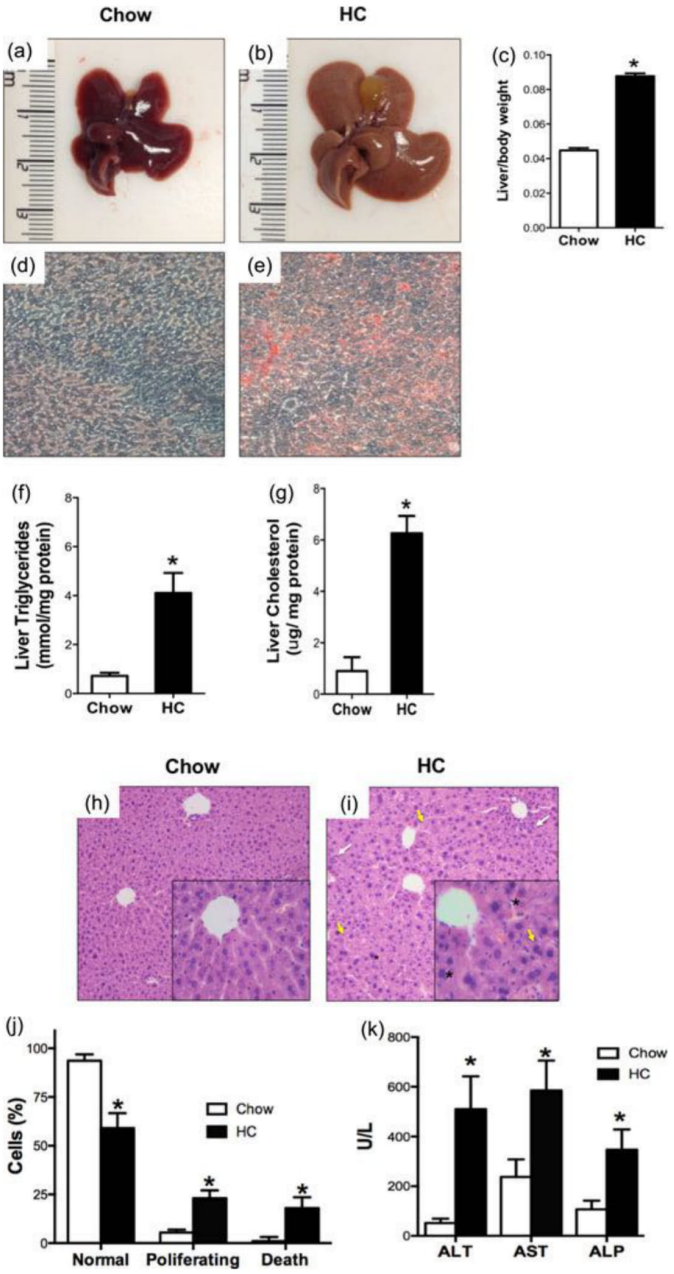
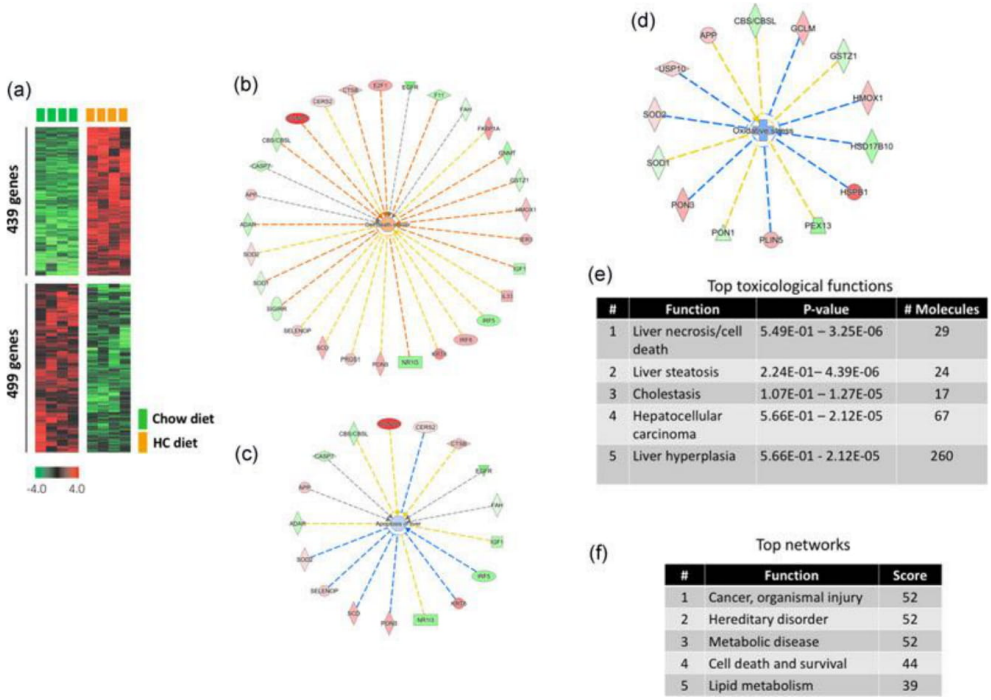


FIGURE 1 A high cholesterol diet consumption resulted in hepatic steatosis and liver damage. Gross inspection of the liver from mice fed with (a) chow control diet, (b) HC diet, (c) Liver to body weight ratio. Neutral lipid content determined by oil red O staining in liver tissue from animals fed with (d) chow control diet (e), HC diet. Biochemical determination of (f) triglycerides and, (g) cholesterol content in liver tissue. Histology analysis by H&E staining of liver tissue from mice fed with (i) HC diet or, (h) chow control diet. Original magnification 100 ×, (inset 200 ×), yellow arrow, hepatocyte ballooning; asterisk, nuclei condensation; white arrow inflammation. (h) Morphometric analysis of the H&E staining. (k) Liver function test. Each column represents the mean ± standard error of the mean (*SEM*) in at least four different mice. $^{*}p \leq 0.05$ versus Chow control mice. Images are representative of at least three independent experiments. ALT, alanine aminotransferase; AST, aspartate aminotransferase; ALP, alkaline phosphatase; HC: high cholesterol; H&E: hematoxylin and eosin

Consistently, affected toxicological functions were involved in liver cell death, steatosis, cholestasis, and HCC (Figure 2e), while top networks affected were cancer, organismal injury, metabolic diseases and lipid metabolism, among others (Figure 2f). Data clearly show an extensive impact in gene expression, indicating a profound adaptation of the cholesterol-overloaded liver.



#	Function	P-value	# Molecules
1	Liver necrosis/cell death	5.49E-01 – 3.25E-06	29
2	Liver steatosis	2.24E-01– 4.39E-06	24
3	Cholestasis	1.07E-01 – 1.27E-05	17
4	Hepatocellular carcinoma	5.66E-01 – 2.12E-05	67
5	Liver hyperplasia	5.66E-01 - 2.12E-05	260

#	Function	Score
1	Cancer, organismal injury	52
2	Hereditary disorder	52
3	Metabolic disease	52
4	Cell death and survival	44
5	Lipid metabolism	39

FIGURE 2 Global transcriptomic analyzes by microarray. (a) Unsupervised hierarchical cluster analyses of liver tissue from mice fed with an HC diet or normal Chow diet for 30 days. A total of 938 differentially expressed genes were identified using bootstrap *t*-test with 10,000 repetitions (*p*-value 0.01). Gene regulatory networks associated with (b) cell death, (c) apoptosis and (d) oxidative stress in the liver overloaded with cholesterol, determined by IPA analysis. (e) Top toxicological functions and (f) top networks involved in cholesterol overload in the liver, determined by IPA analysis. HC: high cholesterol; IPA: ingenuity pathway analysis

3.3 | An HC diet induces increment of reactive oxygen species and oxidative stress

To evaluate the effect of cholesterol overload in the production of ROS, peroxides and superoxide were determined using specific probes for the superoxide anion (DHE) and peroxides (DCFH). Data show that lipid overload remarkably increased DHE fluorescence, showing that superoxide increased in both, liver tissue (Figure 3b,e) cultured primary hepatocytes (Supporting Information Figure 2b). Also, peroxides were considerably elevated, as shown by increased DCFH fluorescence (Figure 3d,e Supporting Information Figure 2d).

Next, we determined the content of the main enzymes responsible for peroxide and superoxide detoxification, as well as the levels of Nrf2, a key transcription factor involved in antioxidant response (Figure 3f). As expected, Nrf2 expression decreased dramatically in livers of animals fed with HC diet, whereas catalase content did not change. Further, while SOD1, a cytoplasmic enzyme responsible for converting superoxide radical to molecular oxygen and hydrogen peroxide, decreased in HC livers, SOD2, a mitochondrial manganese-dependent SOD increased dramatically. GST, an enzyme that conjugates xenobiotics, among them hydroperoxides to glutathione (GSH) and thereby detoxify cellular environments, markedly raised in lipid-overloaded tissue.

We also assessed the content of two intracellular GSH-dependent selenoperoxidases known to catalyze organoperoxides detoxification, GPx-1 and GPx-4. Consistent with our results from the gene expression profiling GPx-1 levels were significantly lower in HC livers, while GPx-4 significantly increased (Figure 3f). All Western blot results corroborate the data obtained by microarrays. Densitometric analysis of Western blots could be found in Supporting Information Figure 3.

3.4 | The development of hepatic steatosis and altered mitochondrial homeostasis in HC livers

Consistent with the hypercholesterolemic phenotype, cholesterol content in isolated mitochondria of HC livers revealed a two-fold increment compared to Chow (Figure 4a). To further characterize the influence of cholesterol overload in mitochondria functionality, we determined mitochondrial membrane potential using Mito Red. A significantly reduced fluorescence was observed in HC hepatocytes

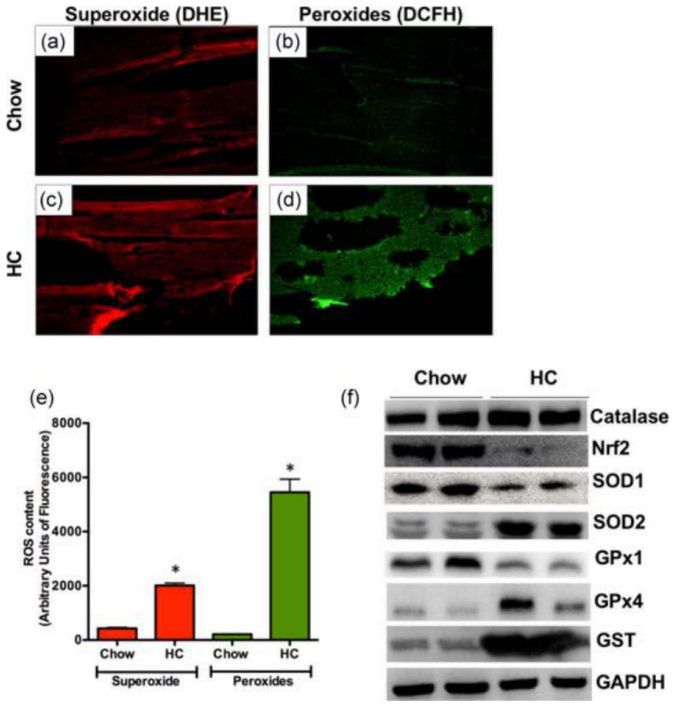


FIGURE 3 A high cholesterol diet induces increment of reactive oxygen species and oxidative stress. Reactive oxygen species content in liver tissue were determined by both, DHE (1 μM, in red) and DCFH (5 μM in green) fluorescence, in liver tissue from mice fed with Chow diet (a,c), and high cholesterol diet (b,d), representative images obtained by confocal microscopy. Original magnification ×100. (e) Fluorescence quantification. Each column represents the mean ± standard error of the mean (*SEM*) in at least four different mice. $^{*}p \leq 0.05$ versus Chow control mice. (f) Western blot analysis of the main antioxidant proteins using antibodies depicted in Supporting Information Figure 1. GAPDH was used as loading control. Images are representative of at least three independent experiments. DCFH: 2′,7′-dichlorofluorescein; DHE: dihydroethidium; GAPDH: glyceraldehyde-3-phosphate dehydrogenase

(Figure 4c), indicating that the membrane potential of mitochondria was decreased when compared cwith hepatocytes from Chow fed mice (Figure 4b). This result was corroborated in isolated mitochondria from mice under both diets. A significantly diminished membrane potential of liver mitochondria from HC fed mice determined by spectrophotometry using safranine was present (Figure 4d). HC mitochondria exhibited 50% of loss in membrane potential compared with those from Chow livers. In line with this, a 60% decrease in ATP content could be revealed for HC livers (Figure 4e), clearly suggesting impairment of mitochondrial functionality.

3.5 | HC diet causes imbalance of mitochondrial dynamics and fission

To estimate the structural impairment of mitochondria induced by HC diet, we performed TEM. HC diet led to abnormal mitochondria, with loss of cristae, rarefied matrix, and lipid droplet accumulation (Figure 5b). These signs of mitochondrial damage were not seen in cells from Chow fed mice (Figure 5a). Congruently, while the number of mitochondria was significantly increased the corresponding size in HC livers was reduced (Figure 5c). To evaluate the impact of HC diet on mitochondrial dysfunction, we studied the content of the main proteins involved in mitochondrial dynamic: PGC-1α, a central regulator of mitochondrial biogenesis through interactions with multiple transcription factors; Drp1, a main regulator in mitochondrial fission; OPA1, a mitochondrial dynamin like GTPase located at the inner membrane that regulates mitochondrial fusion and cristae remodeling alongside with mitofusin (Mfn) 1 and 2. Figure 5d, Supporting Information Figure 4, show an increase in the activation of Drp1 (Ser-616), and in the expression of PGC-1α, whereas OPA1, Mfn1, and Mtn2 all decreased significantly in the hepatocytes from HC mice. These results suggest that components regulating mitochondrial fission and biogenesis were increased by HC diet, contributing to the imbalance in mitochondrial dynamics.

3.6 | HC diet promotes cell survival

Compromised mitochondria homeostasis might affect cellular survival. Therefore, we evaluated the expression levels of the main mitochondrial survival-related proteins (Figure 6a, Supporting Information Figure 5). Interestingly, pro-apoptotic Bax protein was significantly increased and Bcl-2 was downregulated, but feasible compensatory antiapoptotic response was displayed by the increment of Bcl-X_L and, remarkably by Mcl-1.

The outstanding elevation in Mcl-1 was also associated with a strong activation of Stat3 in HC samples, its main transcription factor. As expected, apoptosis was unaffected, judged by caspase 3 activity, (Figure 6b), suggesting that cholesterol overload in mitochondrial

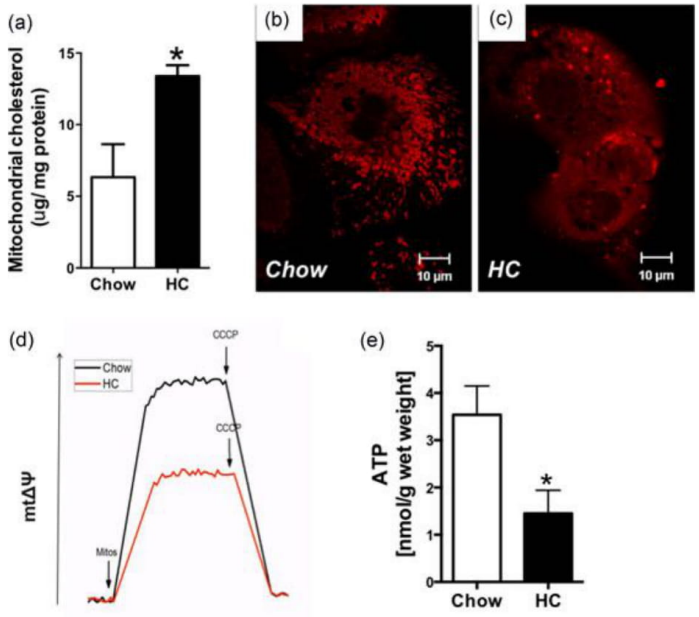


FIGURE 4 The high cholesterol diet induces mitochondria overload in mitochondria altering mitochondrial morphology and functionality. (a) Mitochondrial cholesterol content. Confocal Microscopy inspection of the mitochondrial transmembrane potential assayed by Mito Red fluorescence in cultured primary hepatocytes isolated from (b) HC diet fed mice and (c) Chow diet fed mice. (d) Mitochondrial transmembrane potential ($\Delta\Psi$) determined by using 10 µM safranine-O, following the absorbance changes at 511–533 nm. $\Delta\psi$ was collapsed by adding 5 µM of the protonophoro m-chlorophenylhydrazone (CCCP). Images are representative of at least three independent experiments. (e) ATP determination in liver homogenates from both HC and Chow diet fed mice. Each column represents the mean ± standard error of the mean (*SEM*), at least four independent experiments. $^*p \leq 0.05$ versus Chow

might yield to apoptosis resistance, despite ROS overproduction by a mechanism that could be mediated, particularly, by Mcl-1.

4 | DISCUSSION

We and others have reported that cholesterol overload in the liver promotes oxidative stress, liver damage and sensitizes to a more severe damage (Domínguez-Pérez et al., 2016; López-Islas et al., 2016; López-Reyes et al., 2015; Mari et al., 2006) in the context of relevant cytotoxic stimuli ultimately leading to advanced liver disease as well as cancer (Enríquez-Cortina et al., 2017). Moreover, mitochondrial dysfunction has been implicated in the progression of steatosis to NASH (Kim et al., 2017). Although mitochondria dysfunction has been frequently associated to chronic liver diseases and hepatocarcinogenesis, detailed molecular and functional characteristics remain partially characterized, in addition to the unknown effect in global gene expression signature.

In the current study, we aimed to dissect the effects of cholesterol overload in the mouse liver with emphasis on the mitochondria homeostasis and the relevance in the transcriptome.

An increased liver content of TG and cholesterol were observed, although HC mice maintained the same body weight as control, due to both experimental diets being isocaloric. Histopathological examination of the liver revealed microvesicular steatosis after 30 days of HC diet feeding (Figures 1i, and 5b), phenotype in agreement with that observed in rats under same diet (Marí et al., 2006). Liver function tests were elevated, and an increase in ROS content was found in tissue and in hepatocytes primary culture. Previous data from our group showed the ratio of reduced GSH to oxidized GSH (GSSG) was significantly decreased by the HC diet as compared to the corresponding Chow fed mice. HC mice also displayed a greater increase in lipid oxidation as measure by the rate of production of thiobarbituric acid-reactive substances (Gomez-Quiroz et al., 2016).

One of our main interest was to address the gene expression profile induced by cholesterol liver overload, HC diet induced dysregulation 938 genes, 493 were upregulated, and 499 downregulated, indicating a prominent impact in gene expression tending to an adaptive response, that could be related, among other physiological processes, to apoptosis resistance in a mechanism involving mitochondria homeostasis and function, narrowed linked to changes in mitochondria redox state, judged by the overexpression of SOD2 (Figures 2b and 3f) key regulator

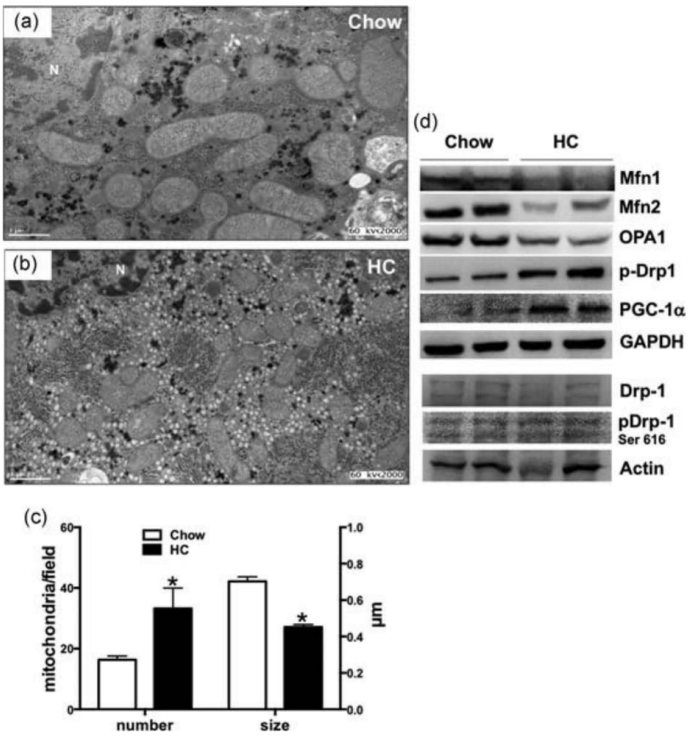


FIGURE 5 High cholesterol diet induces an imbalance in mitochondrial dynamics favoring the susceptibility to fission. TEM of primary hepatocytes isolated from mice fed with (a) Chow control diet, or (b) high cholesterol diet. (c) Morphometric analysis of TEM. Each column represents the mean ± standard error of the mean (*SEM*) in at least four independent experiments. *$p \leq 0.05$ versus Chow. (d) Western blot analysis of the main mitochondria dynamics-related proteins using antibodies depicted in Supporting Information Table 1. GAPDH and actin were used as loading control. GAPDH: Glyceraldehyde-3-phosphate dehydrogenase; TEM: transmission electron microscopy

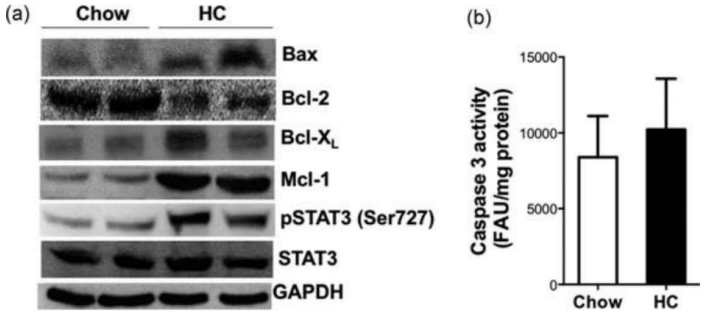


FIGURE 6 High cholesterol diet promotes cell survival. (a) Western blot analysis of the main apoptosis-related proteins using antibodies depicted in Supporting Information Figure 1. GAPDH was used as loading control. (b) Caspase 3 activity. Each column represents the mean ± standard error of the mean (*SEM*) in at least three independent experiments. GAPDH: glyceraldehyde-3-phosphate dehydrogenase

of the mitochondria redox status, and the selenoprotein (Selenop) another antioxidant protein particularly expressed in the liver. Figure 2e,f show that this gene expression signature favoring particularly hepathopaties such as cholestasis, HCC, and hyperplasia, consistent with our previous findings in a mice model of HCC (Enríquez-Cortina et al., 2017), previous work we have reported that under HC diet, and in the presence of a carcinogenic stimulus, mice develop an aggressive phenotype of HCC (Enríquez-Cortina et al., 2017), correlating with the present transcriptomic data; interestingly, we found the overexpression of Hspb1, a gene encoding the HSP 27, which has been reported to be associated with poor clinical outcome (Choi et al., 2017), in fact, we reported the finding of metastasis in lungs, and resistance to

cell death, but in the present work we are observing that this issue is related to cholesterol overload rather than N-diethylnitrosamine carcinogenic effect.

HC diet induced liver damage and dysfunction, associated with a decrease in mitochondrial membrane potential and ATP content. It has been reported that increased mitochondrial cholesterol content can lead to mitochondrial dysfunction (Balboa et al., 2017), including reduced fluidity of mitochondrial membranes (Garcia-Ruiz et al., 2009), reduced ATP generation (Yu et al., 2005), and decreased mitochondrial GSH import (Marí et al., 2006). Our data show decreased mitochondrial membrane potential, ATP production, and increased cholesterol levels in the organelle.

From the perspective of HC diet, we found that it induced several patterns of mitochondrial alteration: (a) increment in cholesterol content, which plays an important role in the change of membrane fluidity (Marí et al., 2006), (b) it induced sensitization to oxidative stress, leading to mitochondrial insufficiency and metabolic abnormality, (c) it impaired mitochondrial bioenergetics, and (d) it promoted steatohepatitis, leading to the retardation of mitochondrial function, as it has been recently reported (Bellanti et al., 2018). Mitochondria obtained from HC liver presented twice cholesterol content compared to control, and biogenesis and mitochondrial fission were observed. Mitochondrial cholesterol content is relevant for the transport of mitochondrial-reduced GSH. In fact, it has been found that cholesterol incorporation in isolated mitochondria decreases mGSH stores (Fernandez-Checa & Kaplowitz, 2005). Furthermore, we found alterations in mitochondrial dynamics in HC cells. Our study provides evidence of an increase in the activation of Drp1 related with increased fission (increased mitochondrial number), but not fusion, as suggested by the downregulation of Mfn1, Mfn2 and OPA-1 in addition, the increment of PGC-1α, strongly suggest mitochondrial biogenesis Both fission and fusion are critical mechanisms for the growth, redistribution, and maintenance of healthy mitochondria or disease-related processes, especially apoptosis and mitophagy. In the current study, HC diet induced the imbalance of fission and fusion proteins as shown by a high activation of Drp-1 and a low expression of OPA-1 and mitofusins.

An increased content of antiapoptotic proteins, particularly Mcl-1, in HC livers explains the result of caspase 3 activity which shows no changes despite Bax increment and Bcl-2 decrement.

Lucken-Ardjomande and coworkers (Lucken-Ardjomande, Montessuit, & Martinou, 2008) using the cationic sterol U18666A as a tool to increase mitochondrial cholesterol levels, reported that cholesterol prevents apoptosis impeding Bax activation after its insertion into the mitochondrial outer membrane. Mitochondria could sense stress to allow for cellular adaptation to the environment, with the flexibility to adapt. Our results show that mitochondria adapt to high levels of cholesterol content increasing fission. Also, a decrease in apoptosis was observed conferring cell survival in HC adverse condition. Thus, an increase in cholesterol could favor that damaged hepatocytes do not enter apoptosis and proliferate, perpetuating liver damage.

STAT3, a cell proliferation related transcription factor that modulates many genes related to apoptosis, cell cycle and epithelial to mesenchymal transition, was activated in HC hepatocytes.

All findings in this study, and the increase in p-STAT3 (Ser727) content and DNA oxidation (data not shown) in liver after one month HC diet could suggest that damaged hepatocytes could proliferate and perpetuate liver damage. NAFLD is an increasing cause HCC.

Recently, we have reported that an HC diet increases oxidative DNA damage and a rapid carcinogenic process, this was associated to an impairment in the activation of DNA repair enzymes, resulting in liver tumors with an aggressive phenotype in comparison with animals under Chow diet (Enríquez-Cortina et al., 2017), demonstrating that certainly, cholesterol could display tumor promoter properties. Even more, recently it was published that free fatty acids and cholesterol derivatives by autoxidation, synergically facilitates development and progression of NAFLD to NASH by impairing mitochondria function, supporting our findings particularly on cholesterol effects (Bellanti et al., 2018), although This study remarkably shows the relevance of cholesterol participation in NAFLD to NASH progression, our work focuses on the impact of cholesterol alone, providing evidence that mitochondria impairment is independent of free fatty acids overload.

In summary, cholesterol overload in the liver, and particularly in mitochondria, induces remarkably transcriptomic changes, mainly associated to mitochondria function and dynamic which favors oxidative stress, apoptosis resistance that could promote transformation, as we recently probed.

ACKNOWLEDGMENTS

This study was partially funded by a grant from CONACYT: Fronteras de la Ciencia #1320, CB-166042, CB252942, and SEP-PRODEP 913026-14612111, Universidad Autónoma Metropolitana Iztapalapa. We thank Roberto Lazzarini and the Confocal Core Unit of the DCBS-UAM-I for technical support and Jorge Sepúlveda for TEM.

CONFLICTS OF INTEREST

The authors declare that they have no conflicts of interest.

ORCID

María Concepción Gutiérrez-Ruiz http://orcid.org/0000-0003-0501-7226

REFERENCES

Auger, C., Alhasawi, A., Contavadoo, M., & Appanna, V. D. (2015). Dysfunctional mitochondrial bioenergetics and the pathogenesis of hepatic disorders. *Frontiers in Cell and Developmental Biology*, *3*, 40.

Balboa, E., Castro, J., Pinochet, M. J., Cancino, G. I., Matías, N., José sáez, P., … Zanlungo, S. (2017). MLN64 induces mitochondrial dysfunction

associated with increased mitochondrial cholesterol content. *Redox Biology*, *12*, 274–284.

Bellanti, F., Villani, R., Tamborra, R., Blonda, M., Iannelli, G., di Bello, G., … Serviddio, G. (2018). Synergistic interaction of fatty acids and oxysterols impairs mitochondrial function and limits liver adaptation during nafld progression. *Redox Biology*, *15*, 86–96.

Calvisi, D. F., Wang, C., Ho, C., Ladu, S., Lee, S. A., Mattu, S., … Evert, M. (2011). Increased lipogenesis, induced by AKT-mTORC1-RPS6 signaling, promotes development of human hepatocellular carcinoma. *Gastroenterology*, *140*(3), 1071–1083.

Choi, B., Choi, S. K., Park, Y. N., Kwak, S. Y., Lee, H. J., Kwon, Y., … Lee, Y. S. (2017). Sensitization of lung cancer cells by altered dimerization of HSP27. *Oncotarget*, *8*(62), 105372–105382.

Clavijo-Cornejo, D., Enriquez-Cortina, C., López-Reyes, A., Domínguez-Pérez, M., Nuño, N., Domínguez-Meraz, M., … Gómez-Quiroz, L. E. (2013). Biphasic regulation of the NADPH oxidase by HGF/c-Met signaling pathway in primary mouse hepatocytes. *Biochimie*, *95*(6), 1177–1184.

Domínguez-Pérez, M., Nuño-Lámbarri, N., Clavijo-Cornejo, D., Luna-López, A., Souza, V., Bucio, L., … Gutiérrez-Ruiz, M. C. (2016). Hepatocyte growth factor reduces free cholesterol-mediated lipotoxicity in primary hepatocytes by countering oxidative stress. *Oxidative Medicine and Cellular Longevity*, *2016*, 7960386–7960388.

Enriquez-Cortina, C., Almonte-Becerril, M., Clavijo-Cornejo, D., Palestino-Domínguez, M., Bello-Monroy, O., Nuño, N., … Gómez-Quiroz, L. E. (2013). Hepatocyte growth factor protects against isoniazid/rifampicin-induced oxidative liver damage. *Toxicological Sciences: An Official Journal of the Society of Toxicology*, *135*(1), 26–36.

Enríquez-Cortina, C., Bello-Monroy, O., Rosales-Cruz, P., Souza Arroyo, V., Miranda, R. U., Toledo-Pérez, R., … Gomez-Quiroz, L. (2017). Cholesterol overload in the liver aggravates oxidative stressmediated DNA damage and accelerates hepatocarcinogenesis. *Oncotarget*, *8*(61), 104136–104148.

Fernandez-Checa, J. C., & Kaplowitz, N. (2005). Hepatic mitochondrial glutathione: Transport and role in disease and toxicity. *Toxicology and Applied Pharmacology*, *204*(3), 263–273.

Garcia-Ruiz, C., Mari, M., Colell, A., Morales, A., Caballero, F., Montero, J., … Fernández-Checa, J. C. (2009). Mitochondrial cholesterol in health and disease. *Histology and Histopathology*, *24*(1), 117–132.

Gomez-Quiroz, L., Gutierrez Ruiz, M. C., Marquardt, J. U., Factor, V. M., & Thorgeirsson, S. S. (2017). Redox regulation by HGF/c-Met in liver disease. In Muriel, P. (Ed.), *Liver pathophysiology therapies and antioxidants*. USA: Academic Press

Gomez-Quiroz, L. E., Seo, D., Lee, Y. H., Kitade, M., Gaiser, T., Gillen, M., … Marquardt, J. U. (2016). Loss of c-Met signaling sensitizes hepatocytes to lipotoxicity and induces cholestatic liver damage by aggravating oxidative stress. *Toxicology*, *361-362*, 39–48.

Gómez-Quiroz, L. E., Factor, V. M., Kaposi-Novak, P., Coulouarn, C., Conner, E. A., & Thorgeirsson, S. S. (2008). Hepatocyte-specific c-Met deletion disrupts redox homeostasis and sensitizes to Fas-mediated apoptosis. *The Journal of Biological Chemistry*, *283*(21), 14581–14589.

Hernández, I., Domínguez-Pérez, M., Bucio, L., Souza, V., Miranda, R. U., Clemens, D. L., … Gutiérrez-Ruiz, M. C. (2015). Free fatty acids enhance the oxidative damage induced by ethanol metabolism in an in vitro model. *Food and Chemical Toxicology: An International Journal Published for the British Industrial Biological Research Association*, *76*, 109–115.

Kim, H. J., Han, Y. H., Na, H., Kim, J. Y., Kim, T., Kim, H. J., … Lee, M. O. (2017). Liver-specific deletion of RORalpha aggravates diet-induced nonalcoholic steatohepatitis by inducing mitochondrial dysfunction. *Scientific Reports*, *7*(1), 16041.

Kleiner, D. E., Brunt, E. M., Van Natta, M., Behling, C., Contos, M. J., Cummings, O. W., … Nonalcoholic Steatohepatitis Clinical Research, N. (2005). Design and validation of a histological scoring system for nonalcoholic fatty liver disease. *Hepatology*, *41*(6), 1313–1321.

Lonardo, A., Nascimbeni, F., Maurantonio, M., Marrazzo, A., Rinaldi, L., & Adinolfi, L. E. (2017). Nonalcoholic fatty liver disease: Evolving paradigms. *World Journal of Gastroenterology*, *23*(36), 6571–6592.

Lucken-Ardjomande, S., Montessuit, S., & Martinou, J. C. (2008). Bax activation and stress-induced apoptosis delayed by the accumulation of cholesterol in mitochondrial membranes. *Cell Death and Differentiation*, *15*(3), 484–493.

López-Islas, A., Chagoya-Hazas, V., Pérez-Aguilar, B., Palestino-Domínguez, M., Souza, V., Miranda, R. U., … Gutiérrez-Ruiz, M. C. (2016). Cholesterol enhances the toxic effect of ethanol and acetaldehyde in primary mouse hepatocytes. *Oxidative Medicine and Cellular Longevity*, *2016*, 9209825–9209829.

López-Reyes, A. G., Martínez-Flores, K., Clavijo-Cornejo, D., Nuño-Lámbarri, N., Palestino-Domínguez, M., Souza, V., … Gutiérrez-Ruiz, M. C. (2015). Cholesterol overload in hepatocytes affects nicotinamide adenine dinucleotide phosphate oxidase (NADPH) activity abrogating hepatocyte growth factor (HGF) induced cellular protection. *Gaceta Medica de Mexico*, *151*(4), 456–464.

Marí, M., Caballero, F., Colell, A., Morales, A., Caballeria, J., Fernandez, A., … García-Ruiz, C. (2006). Mitochondrial free cholesterol loading sensitizes to TNF- and Fas-mediated steatohepatitis. *Cell Metabolism*, *4*(3), 185–198.

Neuhauser, M., & Jockel, K. H. (2006). A bootstrap test for the analysis of microarray experiments with a very small number of replications. *Applied Bioinformatics*, *5*(3), 173–179.

Nuño-Lámbarri, N., Domínguez-Pérez, M., Baulies-Domenech, A., Monte, M. J., Marin, J. J., Rosales-Cruz, P., … Gomez-Quiroz, L. E. (2016). Liver Cholesterol overload aggravates obstructive cholestasis by inducing oxidative stress and premature death in mice. *Oxidative Medicine and Cellular Longevity*, *2016*, 9895176.

Rosas-Lemus, M., Uribe-Alvarez, C., Chiquete-Félix, N., & Uribe-Carvajal, S. (2014). In *Saccharomyces cerevisiae* fructose-1,6-bisphosphate contributes to the Crabtree effect through closure of the mitochondrial unspecific channel. *Archives of Biochemistry and Biophysics*, *555-556*, 66–70.

Rudel, L. L., & Morris, M. D. (1973). Determination of cholesterol using o-phthalaldehyde. *Journal of Lipid Research*, *14*(3), 364–366.

Serviddio, G., & Sastre, J. (2010). Measurement of mitochondrial membrane potential and proton leak. *Methods in Molecular Biology*, *594*, 107–121.

Yu, W., Gong, J. S., Ko, M., Garver, W. S., Yanagisawa, K., & Michikawa, M. (2005). Altered cholesterol metabolism in Niemann-Pick type C1 mouse brains affects mitochondrial function. *The Journal of Biological Chemistry*, *280*(12), 11731–11739.

Åkerman, K. E. O., & Wikström, M. K. F. (1976). Safranine as a probe of the mitochondrial membrane potential. *FEBS Letters*, *68*(2), 191–197.

SUPPORTING INFORMATION

Additional supporting information may be found online in the Supporting Information section at the end of the article.

How to cite this article: Domínguez-Pérez M, Simoni-Nieves A, Rosales P, et al. Cholesterol burden in the liver induces mitochondrial dynamic changes and resistance to apoptosis. *J Cell Physiol*. 2019;234:7213–7223. https://doi.org/10.1002/jcp.27474

www.impactjournals.com/oncotarget/ Oncotarget, 2017, Vol. 8, (No. 61), pp: 104136-104148

Research Paper

Cholesterol overload in the liver aggravates oxidative stress-mediated DNA damage and accelerates hepatocarcinogenesis

Cristina Enríquez-Cortina[1,2], Oscar Bello-Monroy[1,2], Patricia Rosales-Cruz[1,2], Verónica Souza[2], Roxana U. Miranda[2], Rafael Toledo-Pérez[1,2], Armando Luna-López[3], Arturo Simoni-Nieves[1,2], Rogelio Hernández-Pando[4], María Concepción Gutiérrez-Ruiz[2], Diego F. Calvisi[5], Jens U. Marquardt[6], Leticia Bucio[2,*] and Luis Enrique Gomez-Quiroz[2,*]

[1]Posgrado en Biología Experimental, DCBS, Universidad Autónoma Metropolitana Iztapalapa, México City, México

[2]Laboratorio de Fisiología Celular, Departamento de Ciencias de la Salud, Universidad Autónoma Metropolitana Iztapalapa, México City, México

[3]Instituto Nacional de Geriatría, S.S., México City, México

[4]Departamento de Patología Experimental, Instituto Nacional de Ciencias Médicas y Nutrición Salvador Zubirán, México City, México

[5]Institute of Pathology, University of Greifswald, Greifswald, Germany

[6]1st Department of Medicine, University Medical Center, Johannes Gutenberg University Mainz, Mainz, Germany

[*]Shared senior authorship

Correspondence to: *Luis Enrique Gomez-Quiroz,* ***email:*** *legq@xanum.uam.mx*

Keywords: *cholesterol; oxidative stress; ATM; DNA damage; carcinogenesis*

Received: *August 06, 2017* ***Accepted:*** *September 20, 2017* ***Published:*** *October 24, 2017*

Copyright: Enríquez-Cortina et al. This is an open-access article distributed under the terms of the Creative Commons Attribution License 3.0 (CC BY 3.0), which permits unrestricted use, distribution, and reproduction in any medium, provided the original author and source are credited.

ABSTRACT

Primary liver cancers represent the second leading cause of cancer-related deaths worldwide. Diverse etiological factors include chronic viral hepatitis, aflatoxin and alcohol exposure as well as aberrant liver lipid overload. Cholesterol has been identified as a key inducer of metabolic impairment, oxidative stress and promoter of cellular dysfunction. The aim of this work was to address the oxidative stress-mediated DNA damage induced by cholesterol overload, and its role in the development of hepatocellular carcinoma.

C57BL/6 male mice were fed with a high cholesterol diet, followed by a single dose of N-diethylnitrosamine (DEN, 10 μg/g, ip). Reactive oxygen species generation, DNA oxidation, antioxidant and DNA repair proteins were analyzed at different time points. Diet-induced cholesterol overload caused enhanced oxidative DNA damage in the liver and was associated with a decrease in key DNA repair genes as early as 7 days. Interestingly, we found a cell survival response, induced by cholesterol, judged by a decrement in Bax to Bcl2 ratio. Importantly, N-acetyl-cysteine supplementation significantly prevented DNA oxidation damage. Furthermore, at 8 months after DEN administration, tumor growth was significantly enhanced in mice under cholesterol diet in comparison to control animals. Together, these results suggest that cholesterol overload exerts an oxidative stress-mediated effects and promotes the development of liver cancer.

INTRODUCTION

Aberrant lipogenesis has a major effect on many diseases, in addition to well-known metabolic disorders such as obesity and/or metabolic syndrome, lipid disorders also have crucial impact on tumor development. Lipids are essential building blocks, for new cellular membranes [1], but also are required for post-translational modifications in cell cycle-related proteins, such as Ras or heterotrimeric G proteins [2, 3], and are a major source of energy supply for cells [1]. Hepatocellular carcinoma (HCC), one of most frequent cancers globally, shows a remarkable dependence on sustained lipid synthesis [4]. Moreover, HCC aggressiveness is directly associated to the levels of lipogenic enzymes, related to fatty acid and cholesterol synthesis. Several reports have shown that increased activation of fatty acid synthase (FASN), ATP citrate lyase (ACLY), Acetyl-CoA carboxylase (ACC), mevalonate kinase (MVK), squalene synthase (SQS), and the 3-Hydroxy-3-methylglutaryl-CoA reductase (HMGCR), among others significantly drive the tumorigenic process and increases the aggressiveness of the tumors [5-7]. Although recent evidence supports the notion that exogenous free fatty acids play a major role in liver cancer development [8], the relevance of excessive dietary cholesterol in this context is less well understood. A recent report demonstrated that expression of HMGCR and MVK is significantly enriched in HCC human tissue when compared with the surrounding and normal liver tissue [6]. Furthermore, free cholesterol is increased in liver tissue from patients with non-alcoholic steatohepatitis (NASH), and this is associated to an increment in the expression of the sterol regulatory element binding protein (SREBP) 2 and steroidogenic acute regulatory protein (StAR) [9], both critically linked to HCC development and progression [10].

We and others have shown that cholesterol overload in the liver induces profound cellular redox imbalances, leading to the aggravation of different chronic liver diseases [11-14], predominantly by affecting mechanisms related to loss of glutathione (GSH) homeostasis in hepatocyte growth factor (HGF) and its receptor c-Met dependent manner [15, 16]. Oxidative stress is a well-addressed mechanism for DNA damage and carcinogenesis [17]. Therefore, redox imbalance can also enhance the carcinogenic effects of canonical DNA damage inducers such as *N*-nitrosodiethylamine (DEN) [18].

Given the chemical and biological properties of cholesterol and its effect for redox, we hypothesized that cholesterol can participate in the carcinogenic process, particularly by aggravating DNA damage in early stages of hepatocarcinogenesis. In the present work, we investigated the contribution of dietary cholesterol overload in the liver on chemically-induced DNA damage, and its effects on the redox status, antioxidant and DNA repair enzymes, to characterize a possible role of cholesterol as a tumor promoter in the liver.

RESULTS

Cholesterol overload enhances DEN-induced oxidative liver damage

Given the well-known role of cholesterol as inducer of oxidative stress we, first addressed the extent of liver damage at 2, 7 and 14 days in all experimental groups.

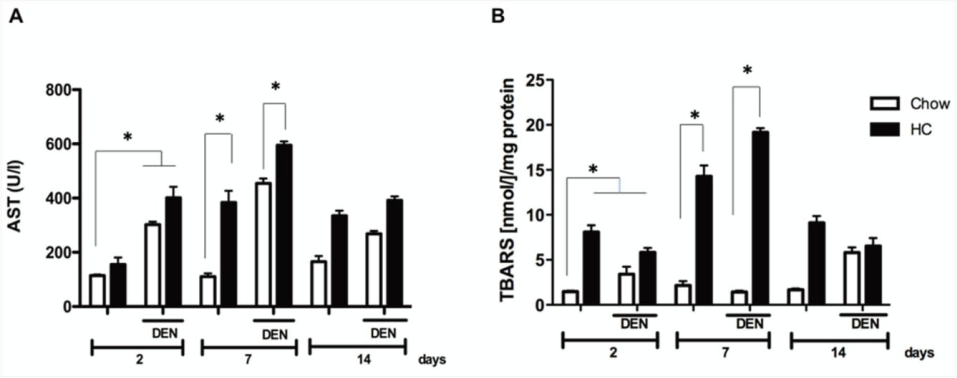


Figure 1: Cholesterol overload in the liver exacerbates the damage induced by *N*-nitrosodiethylamine. Mice were subjected to both high cholesterol (HC) or Chow diet and two days later received, or not, a single dose of *N*-nitrosodiethylamine (DEN, 10 μg/g body weight), serum and liver tissue were recovered at 2, 7 and 14 days after DEN treatment. **(A)** Serum aspartate aminotransferase (AST) activity, and **(B)** lipid peroxidation determination assayed by thiobarbituric acid reactive substances (TBARS). Each column represents the mean ± SEM in at least five different mice. *, $p \leq 0.05$.

HC fed mice displayed a transient increase in AST serum levels starting two days under the treatment, peaking at 7 days when compared with animals under the CW diet and treated with DEN (DCW, Figure 1A). Interestingly, AST activity decreased after 14 days of treatment, suggesting liver healing response after the acute damage.

To address the degree of oxidative damage, lipid peroxidation was determined in whole liver tissue. In accordance to the increased activity of AST, levels of TBARS were significantly increased at 7 days in animals under HC diet, (7-fold *vs* CW and DCW), returning to similar levels observed at day 2 at day 14 (Figure 2B). Data clearly show a maximal damage response at 7 days.

To figure out the ROS involvement in cholesterol-mediated liver damage, we addressed both, superoxide radical ($O_2^{\cdot-}$), by DHE; and peroxides, such as H_2O_2, by DCFDA fluorescence, in fresh liver sections at 7 and 14 days. Representative confocal images of ROS determination are shown in Figure 2. It is of notice that the HC diet alone increases both $O_2^{\cdot-}$ and peroxides cellular content at 7 days, approximately 8-fold versus CW, which is related to TBARS content and AST activity. ROS content was exacerbated in DEN-treated HC group, indicating a greater loss of redox homeostasis. ROS content was significantly diminished at 14 days, confirming that day 7 is the time for maximal oxidative stress generation (Figure 2B).

The assessment of some of the main protective and antioxidant proteins revealed an adaptive response in DHC mice (Figure 2C). Remarkably, the levels of GSH-related enzymes such as γ-GCS, GSTM and GPx4 increased in the DHC group (densitometric analysis in Supplementary Figure 2), suggesting that GSH system is required for this kind of damage as we and others previously reported [11, 14, 18]. Interestingly, the GSH to GSSG ratio determined at day 7 exhibited a significant decrease in livers from HC fed animals, but HC and DEN treated mice show similar values of GSH than control Chow (Figure 2D), this finding agrees with γ-GCS content observed in HC-DEN group, other antioxidant and protective enzymes such as SOD1, HO-1 and HSP70 were also increased in this group comparing with Chow and Chow-DEN animals.

Since effects were most striking at 7 days, we measured total cholesterol levels in liver tissue from animals of all groups. Figure 3A shows that mice fed with HC diet certainly exhibited significant cholesterol increment. Macroscopic inspection of livers shows the characteristic steatotic pale color in HC fed animals

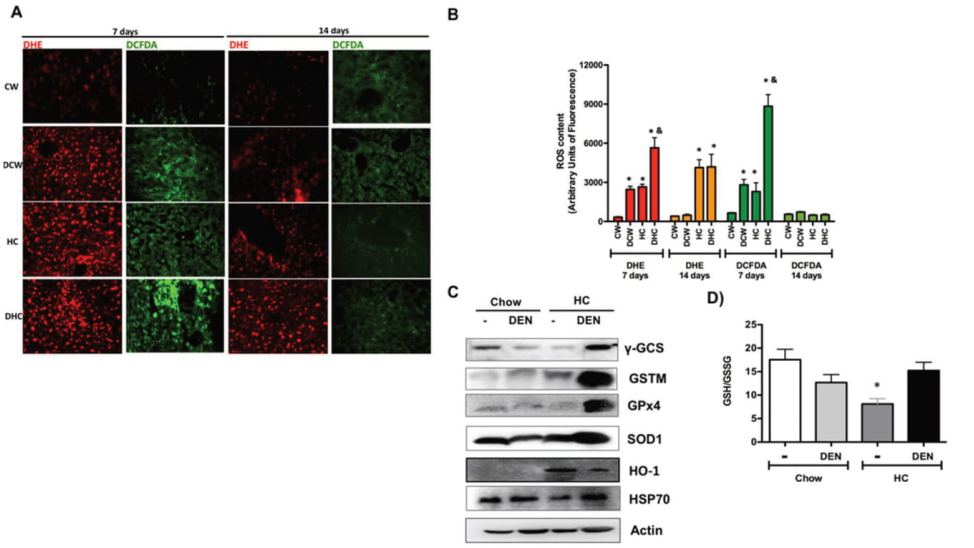


Figure 2: Cholesterol overload in the liver disrupt redox homeostasis. **(A)** Reactive oxygen species content in liver tissue were determined by dihydroethidium (DHE, 5 μM, in red) and 2',7' –dichlorofluorescin diacetate (DCFDA, 5 μM, in green). Representative images obtained by confocal microscopy. Original magnification X100. **(B)** Fluorescence quantification of ROS determination. **(C)** Western blot of the main antioxidant and protective proteins at day 7. Images are representative of at least three independent experiments. Actin was used as loading control. **(D)** Determination of reduced glutathione (GSH) and oxidized GSH (GSSG) in livers at day 7. Each column represents the mean ± SEM in at least four different mice. *, $p \leq 0.05$ vs respective Chow samples at the same time. &, $p \leq 0.05$ vs Chow-DEN at the same time.

(Figure 3B). Gallbladder hypertrophy was also observed in HC-fed animals, and these characteristics were related to a slight, but significant, increment in liver to body weight ratio in both groups under HC diet (Figure 3C).

Histology analysis revealed multivesicular steatosis in both groups under HC diet, with the DEN treated group exhibiting a mild inflammatory infiltration. Mitogenic activity was also corroborated by the observation of chromatin distended nuclei (arrow), nucleoli acidophilic staining, a key indication of cellular metabolism activation and constant rRNA synthesis (Figure 3D).

HC promotes an antiapoptotic response and DNA damage

Although there is an increment in antioxidants enzymes and GSH in animals under HC diet and DEN treatment, ROS content is significantly increased as well, suggesting an inefficient antioxidant response. This sustained pro-oxidant environment could promote apoptosis. To assess the apoptosis status in the respective groups, we assayed Bax to Bcl2 expression ratio in the livers. As expected, DEN treatment led to a significant increase in the ratio in animals treated with chow diet. However, HC fed animals treated with DEN showed a striking activation of Bcl-2 and concomitant downregulation of Bax (Figure 4A). Apoptosis was corroborated by caspase 3 activity in whole liver homogenate (Figure 4B) observing a decrease in caspase 3 activity in HC fed animals treated with DEN comparing with Chow-DEN. Thus, these data suggest that the HC diet induces apoptosis resistance that might facilitate a cell transformation due to an unresolved cell damage.

Cholesterol overload in the liver enhances the DNA damage induced by DEN and impairs DNA repair-related proteins activation

Next, we determined the activation of the histone 2AX (H2AX), a surrogate marker of DNA damage, in samples from 7 days of treatment. Consistent with the increased liver damage and ROS activation, Figure 5A shows an increment in the phosphorylation of the H2AX in HC groups, particularly in those treated with DEN, damage was corroborated by measuring the deoxyguanosine (dG) oxidation into 8-oxo-dG, another key marker of DNA oxidation. Of note, at 7 days HC fed animals showed a significant increase in 8-oxodG (Figure 5B), particularly in those treated with DEN.

To dissect the underlying molecular mechanism, we evaluated the levels of key proteins involved in DNA repair. Figure 5C shows representative immunoblot images of p-ATM, p-BRCA1, p-ATR, p-CHK1, p-CHK2 and p-p53; importantly, all proteins were

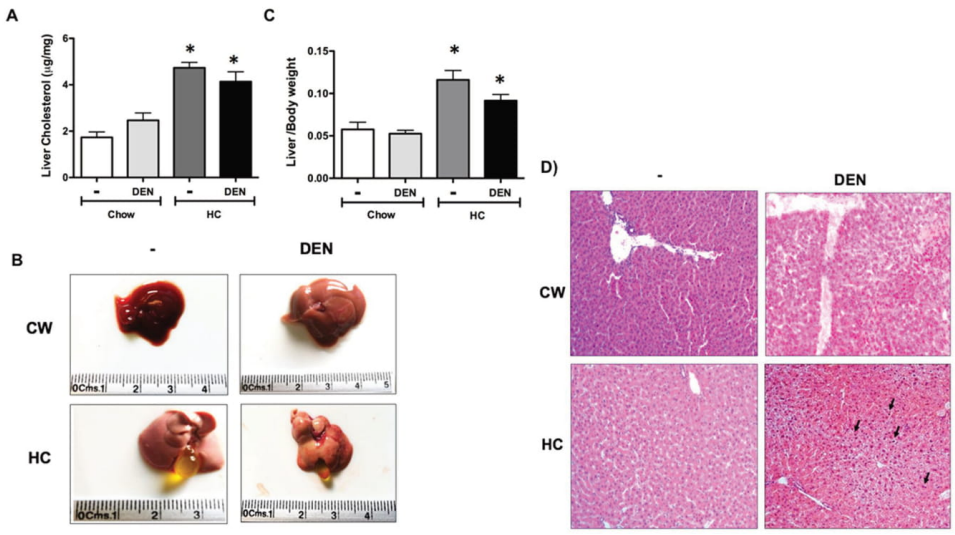


Figure 3: Macroscopic and microscopic inspection of the liver under HC diet and DEN treatment. **(A)** Cholesterol content in liver tissue. **(B)** Macroscopic aspect of the liver from different groups. **(C)** Liver to body weight ratio. Each column represents the mean ± SEM in at least four different mice. *, $p \leq 0.05$ vs Chow control animals. **(D)** Histology appearance by H&E staining, arrows show cells with mitogenic activity corroborated by chromatin distended nuclei. Images are representative of at least 4 different mice, original magnification X200.

significantly decreased in DHC mice, whereas p-ATM increased in Chow fed animals (densitometric analysis in Supplementary Figure 3).

NAC treatment counteracts ROS generation and the oxidative DNA damage

The disruption of cellular redox status aggravates the harmful effects mediated by DEN, and our data clearly show an impairment of the GSH system. To elucidate whether the redox homeostasis could be re-established we added NAC (80 mmol/L) in drinking water along HC diet for 7 days. As expected, NAC significantly decreases ROS content in all conditions, particularly in those under HC diet and DEN treatment (Figure 6A and Supplementary Figure 1), while concomitantly leading to an improvement in liver function (Figure 6B) and a decrease in DNA damage judged by dG oxidation (Figure 6C).

A HC diet promotes tumor progression

To address if the exacerbated DNA damage observed in DHC could be associated to progression of HCC and an aggressive phenotype, we explored the different investigated groups at 1, 3, 5 and 8 months as we previously reported [18]. The kinetics of tumor development was assessed by incidence and multiplicity. In agreement with our findings from the acute model, chronic cholesterol overload in the liver led to a more rapid development of tumors than in DCW mice (Figure 7A). Indeed, at 3 months 44 % (4 of 9, $p \leq 0.05$) of DHC mice developed tumors comparing with 0% in DCW mice, at 5 months all DHC animals developed tumors versus 40% of DCW. The tumor incidence in DHC mice was higher compared with DCW at 3, 5 and 8 months after DEN treatment (Figure 7B). At 8 months of treatment, the liver to body weight ratio (Figure 7C) was higher in DHC animals comparing with HC and CW animals, and the data agree with the incidence and multiplicity of the lesions. Gross liver inspection of DHC livers revealed multiple tumors (Black arrow), bigger and evidently, more vascularized than those seen in DCW. Small lesions were observed in HC livers (white arrow).

Additionally, histological analysis of HC tissue (Figure 7E), revealed steatohepatitis, picnotic nuclei and increased mitotic activity, perilobular, periportal inflammation (black arrow), and signs of cholestasis (yellow arrow). All the observed cells by the field were identified as neoplastic due the loss of nucleus/ cytoplasm ratio, granular cytoplasm that indicates massive mitochondrial presence and more than five nucleoli per nucleus. Along with these cellular alterations, the liver normal architecture was completely lost. DHC livers exhibited multi-vesicular steatosis, increased mitotic activity, that extensively describes a well-differentiated carcinoma. Hepatocytes displayed acidophilic nuclei,

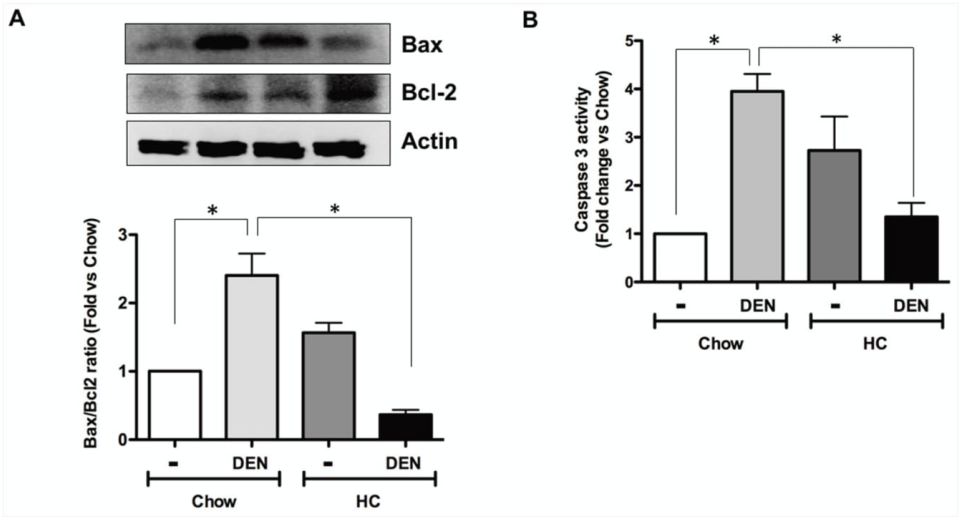


Figure 4: HC promotes an antiapoptotic response and DNA damage. (A) Bax to Bcl2 ratio of protein content determined by Western blot in samples from all animal groups, representative images of at least three different mice. Actin was used as loading control. **(B)** Caspase 3 activity in whole tissue homogenates. Each column represents the mean ± SEM in at least four different mice. *, $p \leq 0.05$.

loss of liver normal architecture and perilobular and periportal inflammation (·), it is clear the difference between the transformed cells that conform the tumor (T) when compared with those on the surrounding tissue (ST). The tumor cellular changes observed in this tissue were much more dramatic than those found in DCW treated liver sections. Interestingly, we found metastasis in lungs only in some animals (5 of 9) under HC diet and DEN treatment (Supplementary Figure 4).

DISCUSSION

Aberrant lipogenesis is a critical event in many pathologies, such as obesity, metabolic syndrome, some viral infections, among others [19]. Increasing evidence supports that, in cancer, lipogenesis is overacting to support the tumor growth [20], because lipids are required as fuel, building blocks for new cellular membranes, and some lipid intermediaries are essential for post-translational modifications in key proteins such as Ras or heterotrimeric G proteins [2, 3]. Particularly, in human HCC, Calvisi and coworkers, outstandingly proved that aberrant lipogenesis is directly associated to an aggressive phenotype and poor prognosis [6]. The expression of key proteins associated with lipogenesis was found to be increased in HCC, being higher as HCC malignancy progress. Among the proteins correlated with a poorer outcome are the fatty acid synthase (FASN), acetyl-coenzyme A carboxylase, and the overactivation of their main transcription factor, such as SREBP 1. Remarkably, those related to mevalonate pathway were also increased such as mevalonate kinase, HMGCR, and the master transcription factor SREBP 2, suggesting that cholesterol could be positioned as a key element in HCC progression.

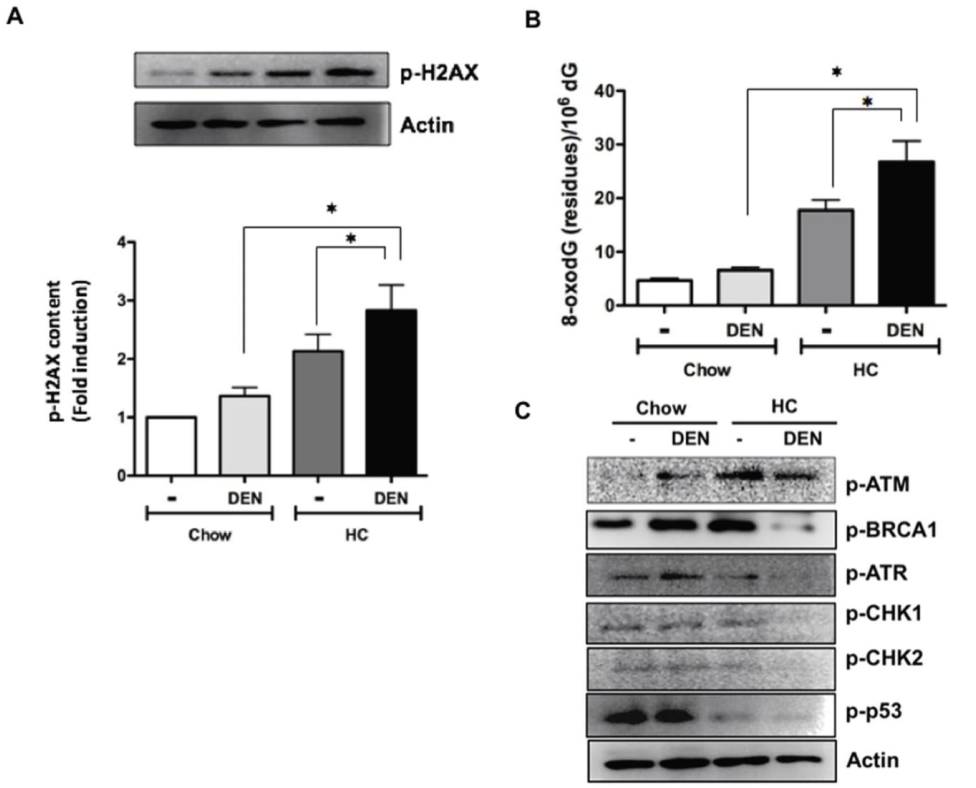


Figure 5: Cholesterol overload in the liver potentiates the DNA damage induced by DEN impairing DNA repair enzymes activation. **(A)** Phosphorylation of histone 2AX (p-H2AX) determined by Western blot. **(B)** Guanine oxidation judged by 8-oxodeoxiGuanine (8-oxodG) determined by HPLC. **(C)** Representative images of Western blot analysis of the main proteins related to DNA repair. Actin was used as loading control. Each column represents the mean ± SEM in at least four different mice. *, $p \leq 0.05$.

We were focused to figure out if cholesterol plays determinant role in DNA damage and HCC initiation.

We and others have been proved that the consumption of a high cholesterol diet induces a cholesterol overload in the liver rising a complex response in hepatocytes characterized by mitochondria dysfunction and oxidative stress [12-14], but, interestingly, hepatocytes with cholesterol overload seems to be resistant to cell death under unstimulated conditions. Nonetheless, they are sensitized to a second aggression, particularly those directed to mitochondria by a mechanism related to mitochondrial-glutathione depletion [14]. In DHC mice, we found that GSH-related enzymes were remarkably increased (Figure 2C) perhaps as a compensatory response, because GSH levels are considerably decreased in hepatocytes with cholesterol overload as we and others have demonstrated [11, 13, 14], interestingly DHC tissue exhibited GSH levels compared as Chow control animals (Figure 2D), suggesting that both harmful stimulus, cholesterol and DEN display different regulatory pathways directed to control redox homeostasis. GPx4 is a mitochondria-resident antioxidant enzyme directed to reduce hydrogen peroxides and lipid hydroperoxides, and the enzyme is fundamental for redox mitochondria homeostasis [21]. It is relevant that GPx4 is overexpressed in DHC tissue, recently, Guerriero and coworkers [22] showed that the overexpression of GPx4 is correlated to malignancy, exhibiting a higher expression in HCC grade III comparing with I and II.

Oxidative stress is the leading mechanism of damage in the liver with high cholesterol content as we have confirmed in the present work (Figure 1 and 2). However, exploration of some markers of cell death revealed that cells seem to be resistant to death as judged by the Bax to Bcl2 ratio and caspase 3 activity (Figure 4). It has been reported that mitochondria isolated from HCC exhibit high levels of cholesterol, resistance to mitochondrial membrane permeabilization, and release of proapoptotic

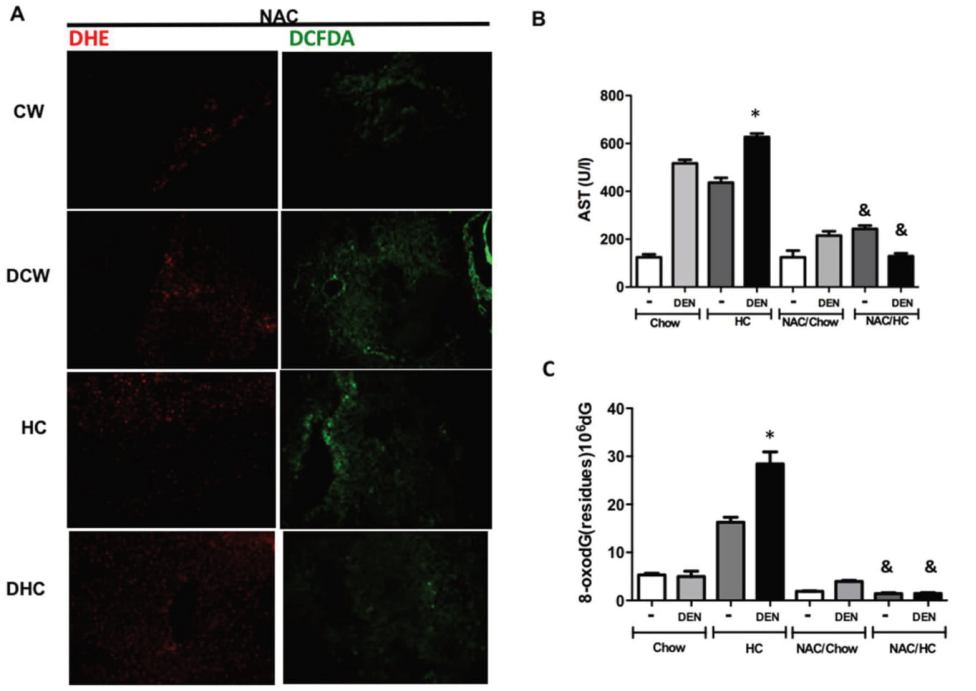


Figure 6: N-acetylcysteine prevents oxidative stress and DNA oxidative damage. A cohort of animals treated for 7 days received 80 mmol/L N–acetyl–L-cysteine (NAC) in drinking water *ad libitum*. **(A)** Reactive oxygen species content in liver tissue were determined by dihydroethidium (DHE, 5 μM, in red) and 2',7' –dichlorofluorescin diacetate (DCFDA, 5 μM, in green). Representative images obtained by confocal microscopy. Original magnification X100. **(B)** Serum aspartate aminotransferase (AST) activity, **(C)** 8-oxodeoxiGuanine (8-oxodG) content determined by HPLC. Each column represents the mean ± SEM in at least four different mice. *, $p \leq 0.05$ vs Chow control animals; &, $p \leq 0.05$ vs DEN treated Chow.

mediators such as cytochrome c and Smac/Diablo, being resistance to Bax activity [23], these characteristics confers an aggressive phenotype and contributes to chemotherapy resistance. Although, cholesterol overload has been associated to apoptosis resistance, we gain evidence that, part, such response could be mediated by Bcl2 expression when liver is in presence of DEN (Figure 4A), this was related to a decrease in Bax content indicating a clear antiapoptotic effect corroborated by caspase 3 activity. Under HC diet, mitochondrial cholesterol overload [14] disturbing metabolism and impairing mitochondrial membrane dynamic [24], this could explain the antiapoptotic effect, profounder attention requires the cholesterol-mediated Bcl2 expression to exploit the potential therapeutic intervention.

ROS are the main inducers of DNA damage and, consequently, of mutations. Indeed, particularly mitochondria-derived ROS have been implicated to initiation, progression and aggressiveness of cancer [25-27]. Figure 5 shows the increment of two well-documented markers of DNA damage. The level of 8-oxodG in plasma, urine, and cerebrospinal fluids has been used as marker of DNA damage [28]. In addition, the formation of 8-oxodG is linked to epigenetic instability in human HCC [29], and it has been identified as a risk factor for the development of HCC in patients with chronic hepatitis C virus infections. In addition, it has been suggested that these patients must be monitored carefully [30]. Taking into consideration the confidence on 8-oxodG determination as a good marker of DNA damage, our findings are remarkable indicating a broad damage induced by DEN in an hypercholesterolemic environment. Even more, activation of the H2AX, another excellent marker for DNA damage in humans [31], confirms the exacerbation of the genomic damage promoted by the high cholesterol liver content and DEN treatment.

The extensive DNA damage triggers a mechanism named DNA damage response (DDR), which detects and repairs DNA by inducing cell cycle arrest to guarantee that only cells in good conditions can progress and proliferate. Some reports indicate that activation of DDR proteins can be increased during early stages of tumorigenesis [32, 33]. It has been suggested that this response can work as a barrier for tumor development, but this is dependent of p53 activation [34]. In our system, as Figure 5D shows, p53 phosphorylation is practically abrogated in animals under HC diet, suggesting the progression of aberrant cells into the cell cycle conditioning to tumorigenesis. The results also indicate that, although ataxia-telangiectasia mutated (ATM) activation is increased in HC tissue, in DHC is downregulated but not abrogated as the other repair enzymes are. It seems that the ATM-initiated signal

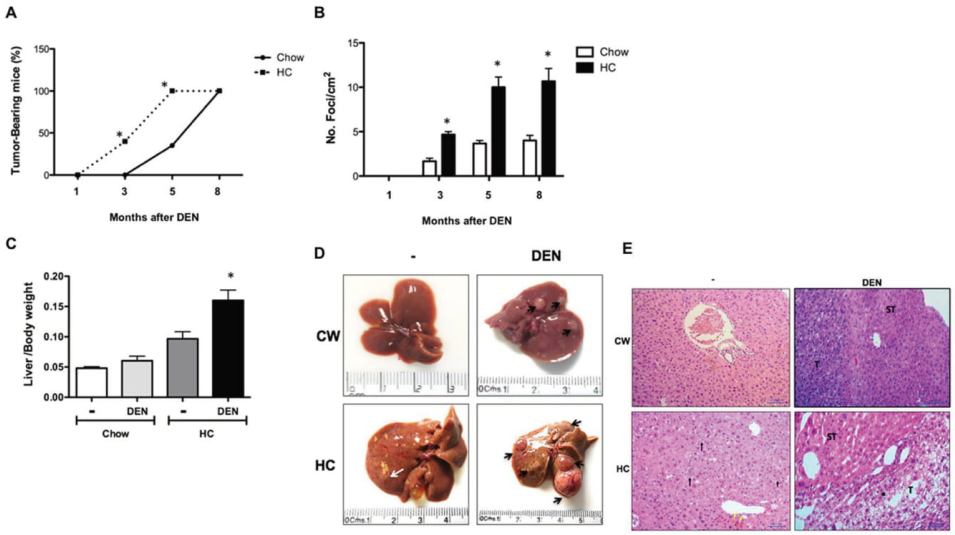


Figure 7: Mice subjected to HC diet are more susceptible than Chow mice to DEN-induced hepatocarcinogenesis. **(A)** Incidence and time course of hepatic lesions from 1 to 8 months after DEN treatment, **(B)** multiplicity of foci per square centimeter. **(C)** Liver to body weight ratio at month 8. Each column or point represent the mean ± SEM in at least four different mice. *, $p \leq 0.05$ vs Chow control animals; &, $p \leq 0.05$ vs DEN treated Chow, **(D)** Macroscopic inspection of the livers at month 8, **(E)** Histology appearance by H&E staining, perilobular, periportal inflammation (black arrow), cholestasis (yellow arrow), inflammation (·), tumor (T), surrounding tissue (ST). Images are representative of at least 4 different mice, original magnification X200.

transduction is partially impaired due to one of the main downstream effectors, CHK2, which is decreased only in DHC tissue.

ATM is primarily activated by double-stranded DNA breaks (DSB), but ATR also responds to a broad spectrum of damages [35]. We have the evidence that cholesterol overload in the liver induces DNA oxidation as judged by 8-oxodG, and this triggers ATM activation. This supports previous findings that ATM and oxidative stress are related each other and, particularly, ATM seems to display protective effects [36]. Accordingly, our data clearly indicate a relation of ATM levels with a protective effect (Figure 5D). HA2X is a downstream substrate of ATM leading to the enhancement of the DDR, confirming that in high cholesterol-induced DNA damage ATM is leading the protective response.

We have previously reported that NAC supplementation can prevent carcinogenic effects of oxidative stress [18], and in the present work we confirmed once again this relevant property of NAC (Figure 6). It has been reported that $ATM^{-/-}$ cells are under oxidative stress and an increment in 8-oxodG has been observed, this condition was reverted by NAC treatment counteracting genetic instability [36, 37].

Our work offers the mechanism driving the enhancement of a canonical carcinogenic effect by cholesterol overload in the liver, which can promote a faster development of tumors (Figure 7) with an aggressive phenotype, judged by lung metastasis (Supplementary Figure 4), in fact, lipid metabolism has extensively been related to cancer metastasis [38], and it has recently been reported that cholesterol metabolism plays key role in metastasis in an experimental model of pancreatic cancer, the abrogation acyl-CoA cholesterol acyl transferase-1 (ACAT-1), significantly suppresses tumor growth and metastasis [39], even more, the use of simvastatin, an inhibitor of cholesterol synthesis, blocks the transforming growth factor beta-induced epithelial-mesenchymal transition, a hallmark for cancer metastasis [40], our data, leave clear the relevance of cholesterol content in cancer metastasis.

The assessment of the activation of ATM and HA2X, and the content of GPx4 and GSTM in early liver lesions could represent good prognosis factors for aggressive presentations of HCC, although many reports indicate that cancer therapies with antioxidants do not provide benefits, but detriments in some cases, definitively in carcinogenesis processes antioxidants could be fundamental, particularly those serving as precursors for endogenous antioxidants synthesis such as NAC, that cells can manages properly as we previously demonstrated [18] and confirmed in the present work.

Data confirm that cholesterol can play a relevant role not only in HCC progression but in cell transformation, by a mechanism related to the increment of ROS levels and apoptosis decrement at early times that lead to DNA damage and initiation of carcinogenesis. Our findings are in agreement with data published by Dr. Calvisi and colleagues [6], indicating that cholesterol homeostasis-related proteins are overexpressed in HCC with poor prognosis, even more RNA-seq analysis of human HCC revealed disorders in lipid metabolism, metabolism of xenobiotics, and ATM signaling [41], some genomic reports also confirm that our mouse data are relevant in human, particularly those related with oxidative stress, DNA damage and lipid metabolism [42]. Our findings are positioning cholesterol cellular overload in the liver as a tumor promoter, inducing oxidative stress, impairing DNA damage repair system and promoting and accelerated tumor progression (Supplementary Figure 5). Hypercholesterolemia should be closely monitored in those patients with HCC risk factors.

MATERIALS AND METHODS

Animals

Sixty 14-days old male mice (C57/BL6) were randomly separated in four groups: i.) fed with a high cholesterol diet (HC, 2% cholesterol and 0.5% sodium cholate) as previously reported [11, 13, 14]; ii.) HC diet and a single intraperitoneal (ip) injection of 10 μg/g body weight of DEN (Sigma-Aldrich) as previously reported [18]; control animals received regular Chow diet (CW) with iii.) or without iv.) DEN. An extra cohort of mice fed HC or Chow diet for 7 days and treated or not with DEN, received 80 mmol/L N–acetyl–L-cysteine (NAC, Sigma-Aldrich) in drinking water *ad libitum*.

Mice were euthanized and serum and liver tissue were examined at 2, 7 or 14 days and 1, 3, 5 and 8 months. All animals were maintained in specific pathogen-free housing and cared in accordance with the NIH Guide for the Care and Use of Laboratory Animals.

Histology

Livers were fixed in 10% neutral formalin overnight at 4°C. Paraffin sections (5 μm) were stained with routine H&E for histology and quantification of liver lesions (foci). Analysis was conducted by an expert pathologist (R.H.P.).

Western blot

Western blot was performed as we previously reported [43], using specific antibodies listed in Supplementary Table 1.

Lipid peroxidation

Lipid peroxidation was assayed by the production of thiobarbituric acid reactive substances (TBARS) using spectrophotometry as described by Buege and Aust [44].

DNA extraction, enzymatic hydrolysis, and analysis of 8-oxo-7,8-dihydro-2'-deoxyguanosine (8-oxodG) by HPLC/electrochemical detection

DNA was extracted from fresh liver samples using the chaotropic-NaI method, as we previously reported [45]. After DNA quantification using Nanodrop 2000c (Thermo Scientific Inc), samples were digested with nuclease P1 and *E. coli* acid phosphatase. 8-oxodG detection was performed as we reported previously [45]. Briefly, 100 µg of digested DNA was loaded into a HPLC coupled with an electrochemical detector (EC, Waters Inc) and the system was connected to a Supelcosil LC-18 (Supelco, Bellefonte, PA, USA) reverse-phase column (250X4.6 mm, i.d. particle size 5 µm). The eluent was 50mM potassium phosphate buffer, pH 5.5, with 8% methanol at 1 ml/min flow rate. The molar ratio of 8-oxodG in each DNA sample was determined based on EC detection at 290 mV for 8-oxodG and absorbance at 254 nm for dG.

ROS in situ determination

Animals were euthanized in parallel exclusively for *in situ* ROS determination [12]. Fresh tissue was rapidly sectioned, frozen in liquid nitrogen, and embedded in optimum cutting temperature reagent (OCT, Sakura Finetec, Torrance, CA). Subsequently, 8-µm frozen sections were obtained in a cryostat (Leica CM-3050S) at −20°C and the slides were immediately incubated for 15 min, in the dark, at room temperature with either 2',7' –dichlorofluorescin diacetate (DCFDA, 5 µM), a cell-permeable non-fluorescent probe that is intracellularly de-esterified and converted to the highly fluorescent 2′,7′-dichlorofluorescein upon oxidation by ROS, particularly peroxides, or with dihydroethidium (DHE, 5 µM) for determination of superoxide anion radical detecting ethidium fluorescence. Samples were covered and observed using a confocal microscope at excitation and emission wavelengths of 480 and 520 nm, respectively, for DCFDA; and excitation and emission wavelengths of 485 and 570 nm, respectively, for DHE-derived ethidium fluorescence, as we previously reported [46].

Caspase 3 activity

Caspase 3 activity was quantified using the caspase 3 synthetic fluorogenic tetrapeptide substrate Ac-DEVD-AMC (BD Pharmingen) as previously we reported [12] using fresh liver tissue, values were normalized regarding Chow sample and reported as fold change.

Serum detection of alanine aminotransferase activity

Blood samples were obtained from each animal. Serum levels of alanine aminotransferase (ALT) were determined by the automated method using Reflovet Plus (Roche).

Glutathione determination

Both reduced and oxidized glutathione (GSH and GSSG, respectively) were determined using the Glutathione assay kit (Sigma-Aldrich # CS0260) following manufacturer´s instructions. Values are reported as GSH to GSSG ratio.

Protein content

Protein content was evaluated by the bicinchoninic acid protein assay (BCA) kit following the manufacturer´s instructions (Thermo Scientific).

Statistical analysis

Data are presented as mean ± SEM of at least three independent experiments carried out in triplicate. Comparisons between groups were made using Student's *t* test, Mann Whitney and Tukey-Kramer test. GraphPad Prism 6 software for OSX was used to run analysis. Differences were considered significant at $p \leq 0.05$.

Abbreviations

DEN, N-diethylnitrosamine; HC, high cholesterol; CW, Chow regular diet; ROS, reactive oxygen species; HCC, hepatocellular Carcinoma; FASN, fatty acid synthase; ACLY, ATP citrate lyase; ACC, Acetyl-CoA carboxylase; MVK, mevalonate kinase; SQS, squalene synthase; HMGCR; the 3-hydroxy-3-methylglutaryl-CoA reductase; SREBP, sterol regulatory element binding protein GSH, reduced glutathione; GSSG, oxidized glutathione; AST, aspartate aminotransferase; TBARS, thiobarbituric acid reactive substances; 8-oxodG, 8-oxo-7,8-dihydro-2′-deoxyguanosine; DCFDA, 2′,7′-dichlorofluorescein diacetate; DHE, dihydroethidium; NAC, N-acetyl-L-cysteine.

Author contributions

Cristina Enríquez-Cortina, performed Western blot experiments, cared animals, processed tissue, collaborated in manuscript draft.

Oscar Bello-Monroy, prepared tissue for histology analysis and performed histological experiments.

Patricia Rosales. Performed ROS detection in tissue

Verónica Souza. Performed ROS detection in tissue and prepared images.

Roxana U. Miranda, conducted microscopy analysis.

Rafael Toledo-Pérez, performed HPLC DNA damage experiments.

Armando Luna-López, performed HPLC DNA damage experiments and analyzed that data

Arturo Simoni-Nieves, conducted apoptosis experiments and GSH determination

Rogelio Hernández-Pando. Main pathologist, interpreted the histological analysis and emitted the result.

María Concepción Gutiérrez-Ruiz, Provided funding, revised manuscript.

Diego F. Calvisi, participated in experimental design, revised manuscript.

Jens U Marquardt, participated in experimental design, revised manuscript

Leticia Bucio, performed experiments related to DNA damage

Luis Enrique Gomez-Quiroz, leader of the study, participated in experimental design, wrote manuscript, provided funding.

ACKNOWLEDGMENTS AND FUNDING

We thank CONACYT for financial support for Cristina Enriquez-Cortina Ph.D. studies. We also thank Roberto Lazzarini for technical support and the Confocal Core Unit of the DCBS-UAM-I, and Hiram Castillo for assistance in the animal maintenance at the animal facility of the National Rehabilitation Institute. We also thank to Dr. Carlos Pineda and Dr. Alberto López-Reyes for assistance in the project. This work was partially funded by a grant from CONACYT: Fronteras de la Ciencia #1320, SEP-PRODEP 913026–14612111, Universidad Autónoma Metropolitana Iztapalapa.

CONFLICTS OF INTEREST

All authors declare that they have no conflicts of interest.

REFERENCES

1. Beloribi-Djefaflia S, Vasseur S, Guillaumond F. Lipid metabolic reprogramming in cancer cells. Oncogenesis. 2016; 5:e189.
2. Wedegaertner PB, Wilson PT, Bourne HR. Lipid modifications of trimeric G proteins. J Biol Chem. 1995; 270:503-506.
3. Vogel A, Reuther G, Weise K, Triola G, Nikolaus J, Tan KT, Nowak C, Herrmann A, Waldmann H, Winter R, Huster D. The lipid modifications of Ras that sense membrane environments and induce local enrichment. Angew Chem Int Ed Engl. 2009; 48:8784-8787.
4. Kaposi-Novak P, Lee JS, Gomez-Quiroz L, Coulouarn C, Factor VM, Thorgeirsson SS. Met-regulated expression signature defines a subset of human hepatocellular carcinomas with poor prognosis and aggressive phenotype. J Clin Invest. 2006; 116:1582-1595.
5. Che L, Pilo MG, Cigliano A, Latte G, Simile MM, Ribback S, Dombrowski F, Evert M, Chen X, Calvisi DF. Oncogene dependent requirement of fatty acid synthase in hepatocellular carcinoma. Cell Cycle. 2017; 19:499-507.
6. Calvisi DF, Wang C, Ho C, Ladu S, Lee SA, Mattu S, Destefanis G, Delogu S, Zimmermann A, Ericsson J, Brozzetti S, Staniscia T, Chen X, et al. Increased lipogenesis, induced by AKT-mTORC1-RPS6 signaling, promotes development of human hepatocellular carcinoma. Gastroenterology. 2011; 140:1071-1083.
7. Morales A, Mari M, Garcia-Ruiz C, Colell A, Fernandez-Checa JC. Hepatocarcinogenesis and ceramide/cholesterol metabolism. Anticancer Agents Med Chem. 2012; 12:364-375.
8. Cao D, Song X, Che L, Li X, Pilo MG, Vidili G, Porcu A, Solinas A, Cigliano A, Pes GM, Ribback S, Dombrowski F, Chen X, et al. Both de novo synthetized and exogenous fatty acids support the growth of hepatocellular carcinoma cells. Liver Int. 2017; 37:80-89.
9. Caballero F, Fernandez A, De Lacy AM, Fernandez-Checa JC, Caballeria J, Garcia-Ruiz C. Enhanced free cholesterol, SREBP-2 and StAR expression in human NASH. J Hepatol. 2009; 50:789-796.
10. Kolly P, Dufour JF. Surveillance for hepatocellular carcinoma in patients with NASH. Diagnostics (Basel). 2016.
11. Gomez-Quiroz LE, Seo D, Lee YH, Kitade M, Gaiser T, Gillen M, Lee SB, Gutierrez-Ruiz MC, Conner EA, Factor VM, Thorgeirsson SS, Marquardt JU. Loss of c-Met signaling sensitizes hepatocytes to lipotoxicity and induces cholestatic liver damage by aggravating oxidative stress. Toxicology. 2016; 361-362:39-48.
12. Nuno-Lambarri N, Dominguez-Perez M, Baulies-Domenech A, Monte MJ, Marin JJ, Rosales-Cruz P, Souza V, Miranda RU, Bucio L, Montalvo-Jave EE, Concepcion Gutierrez-Ruiz M, Garcia-Ruiz C, Fernandez-Checa JC, Gomez-Quiroz LE. Liver cholesterol overload aggravates obstructive cholestasis by inducing oxidative stress and premature death in mice. Oxid Med Cell Longev. 2016; 2016:9895176.
13. Dominguez-Perez M, Nuno-Lambarri N, Clavijo-Cornejo D, Luna-Lopez A, Souza V, Bucio L, Miranda RU, Munoz L, Gomez-Quiroz LE, Uribe-Carvajal S, Gutierrez-Ruiz MC. Hepatocyte growth factor reduces free cholesterol-mediated lipotoxicity in primary hepatocytes by countering oxidative stress. Oxid Med Cell Longev. 2016; 2016:7960386.
14. Mari M, Caballero F, Colell A, Morales A, Caballeria J, Fernandez A, Enrich C, Fernandez-Checa JC, Garcia-Ruiz C. Mitochondrial free cholesterol loading sensitizes to TNF- and Fas-mediated steatohepatitis. Cell Metab. 2006; 4:185-198.
15. Gomez-Quiroz LE, Factor VM, Kaposi-Novak P, Coulouarn C, Conner EA, Thorgeirsson SS. Hepatocyte-specific c-Met deletion disrupts redox homeostasis and

sensitizes to Fas-mediated apoptosis. J Biol Chem. 2008; 283:14581-14589.

16. Clavijo-Cornejo D, Enriquez-Cortina C, Lopez-Reyes A, Dominguez-Perez M, Nuno N, Dominguez-Meraz M, Bucio L, Souza V, Factor VM, Thorgeirsson SS, Gutierrez-Ruiz MC, Gomez-Quiroz LE. Biphasic regulation of the NADPH oxidase by HGF/c-Met signaling pathway in primary mouse hepatocytes. Biochimie. 2013; 95:1177-1184.
17. Linhart K, Bartsch H, Seitz HK. The role of reactive oxygen species (ROS) and cytochrome P-450 2E1 in the generation of carcinogenic etheno-DNA adducts. Redox Biol. 2014; 3C:56-62.
18. Takami T, Kaposi-Novak P, Uchida K, Gomez-Quiroz LE, Conner EA, Factor VM, Thorgeirsson SS. Loss of hepatocyte growth factor/c-Met signaling pathway accelerates early stages of N-nitrosodiethylamine induced hepatocarcinogenesis. Cancer Res. 2007; 67:9844-9851.
19. Ameer F, Scandiuzzi L, Hasnain S, Kalbacher H, Zaidi N. De novo lipogenesis in health and disease. Metabolism. 2014; 63:895-902.
20. Deep G, Schlaepfer IR. Aberrant lipid metabolism promotes prostate cancer: role in cell survival under hypoxia and extracellular vesicles biogenesis. Int J Mol Sci. 2016.
21. Liang H, Van Remmen H, Frohlich V, Lechleiter J, Richardson A, Ran Q. Gpx4 protects mitochondrial ATP generation against oxidative damage. Biochem Biophys Res Commun. 2007; 356:893-898.
22. Guerriero E, Capone F, Accardo M, Sorice A, Costantini M, Colonna G, Castello G, Costantini S. GPX4 and GPX7 over-expression in human hepatocellular carcinoma tissues. Eur J Histochem. 2015; 59:2540.
23. Montero J, Morales A, Llacuna L, Lluis JM, Terrones O, Basanez G, Antonsson B, Prieto J, Garcia-Ruiz C, Colell A, Fernandez-Checa JC. Mitochondrial cholesterol contributes to chemotherapy resistance in hepatocellular carcinoma. Cancer Res. 2008; 68:5246-5256.
24. Ribas V, Garcia-Ruiz C, Fernandez-Checa JC. Mitochondria, cholesterol and cancer cell metabolism. Clin Transl Med. 2016; 5:22.
25. Ishikawa K, Takenaga K, Akimoto M, Koshikawa N, Yamaguchi A, Imanishi H, Nakada K, Honma Y, Hayashi J. ROS-generating mitochondrial DNA mutations can regulate tumor cell metastasis. Science. 2008; 320:661-664.
26. Sabharwal SS, Schumacker PT. Mitochondrial ROS in cancer: initiators, amplifiers or an Achilles' heel? Nat Rev Cancer. 2014; 14:709-721.
27. Sullivan LB, Chandel NS. Mitochondrial reactive oxygen species and cancer. Cancer Metab. 2014; 2:17.
28. Poulsen HE, Nadal LL, Broedbaek K, Nielsen PE, Weimann A. Detection and interpretation of 8-oxodG and 8-oxoGua in urine, plasma and cerebrospinal fluid. Biochim Biophys Acta. 2014; 1840:801-808.
29. Nishida N, Arizumi T, Takita M, Kitai S, Yada N, Hagiwara S, Inoue T, Minami Y, Ueshima K, Sakurai T, Kudo M. Reactive oxygen species induce epigenetic instability through the formation of 8-hydroxydeoxyguanosine in human hepatocarcinogenesis. Dig Dis. 2013; 31:459-466.
30. Chuma M, Hige S, Nakanishi M, Ogawa K, Natsuizaka M, Yamamoto Y, Asaka M. 8-Hydroxy-2'-deoxy-guanosine is a risk factor for development of hepatocellular carcinoma in patients with chronic hepatitis C virus infection. J Gastroenterol Hepatol. 2008; 23:1431-1436.
31. Rey S, Quintavalle C, Burmeister K, Calabrese D, Schlageter M, Quagliata L, Cathomas G, Diebold J, Molinolo A, Heim MH, Terracciano LM, Matter MS. Liver damage and senescence increases in patients developing hepatocellular carcinoma. J Gastroenterol Hepatol. 2017; 32:1480-1486.
32. Bartkova J, Horejsi Z, Koed K, Kramer A, Tort F, Zieger K, Guldberg P, Sehested M, Nesland JM, Lukas C, Orntoft T, Lukas J, Bartek J. DNA damage response as a candidate anti-cancer barrier in early human tumorigenesis. Nature. 2005; 434:864-870.
33. Gorgoulis VG, Vassiliou LV, Karakaidos P, Zacharatos P, Kotsinas A, Liloglou T, Venere M, Ditullio RA Jr, Kastrinakis NG, Levy B, Kletsas D, Yoneta A, Herlyn M, et al. Activation of the DNA damage checkpoint and genomic instability in human precancerous lesions. Nature. 2005; 434:907-913.
34. Weber AM, Ryan AJ. ATM and ATR as therapeutic targets in cancer. Pharmacol Ther. 2015; 149:124-138.
35. Marechal A, Zou L. DNA damage sensing by the ATM and ATR kinases. Cold Spring Harb Perspect Biol. 2013.
36. Takao N, Li Y, Yamamoto K. Protective roles for ATM in cellular response to oxidative stress. FEBS Lett. 2000; 472:133-136.
37. Reliene R, Fischer E, Schiestl RH. Effect of N-acetyl cysteine on oxidative DNA damage and the frequency of DNA deletions in atm-deficient mice. Cancer Res. 2004; 64:5148-5153.
38. Luo X, Cheng C, Tan Z, Li N, Tang M, Yang L, Cao Y. Emerging roles of lipid metabolism in cancer metastasis. Mol Cancer. 2017; 16:76.
39. Li J, Gu D, Lee SS, Song B, Bandyopadhyay S, Chen S, Konieczny SF, Ratliff TL, Liu X, Xie J, Cheng JX. Abrogating cholesterol esterification suppresses growth and metastasis of pancreatic cancer. Oncogene. 2016; 35:6378-6388.
40. Xie F, Liu J, Li C, Zhao Y. Simvastatin blocks TGF-beta1-induced epithelial-mesenchymal transition in human prostate cancer cells. Oncol Lett. 2016; 11:3377-3383.
41. Huang Q, Lin B, Liu H, Ma X, Mo F, Yu W, Li L, Li H, Tian T, Wu D, Shen F, Xing J, Chen ZN. RNA-Seq analyses generate comprehensive transcriptomic landscape and reveal complex transcript patterns in hepatocellular carcinoma. PLoS One. 2011; 6:e26168.
42. Niu ZS, Niu XJ, Wang WH. Genetic alterations in hepatocellular carcinoma: an update. World J Gastroenterol. 2016; 22:9069-9095.

43. Clavijo-Cornejo D, Gutierrez-Carrera M, Palestino-Dominguez M, Dominguez-Perez M, Nuno N, Souza V, Miranda RU, Kershenobich D, Gutierrez-Ruiz MC, Bucio L, Gomez-Quiroz LE. Acetaldehyde targets superoxide dismutase 2 in liver cancer cells inducing transient enzyme impairment and a rapid transcriptional recovery. Food Chem Toxicol. 2014; 69:102-108.

44. Buege JA, Aust SD. Microsomal lipid peroxidation. Methods Enzymol. 1978; 52:302-310.

45. Luna-Lopez A, Triana-Martinez F, Lopez-Diazguerrero NE, Ventura-Gallegos JL, Gutierrez-Ruiz MC, Damian-Matsumura P, Zentella A, Gomez-Quiroz LE, Konigsberg M. Bcl-2 sustains hormetic response by inducing Nrf-2 nuclear translocation in L929 mouse fibroblasts. Free Radic Biol Med. 2010; 49:1192-1204.

46. Enriquez-Cortina C, Almonte-Becerril M, Clavijo-Cornejo D, Palestino-Dominguez M, Bello-Monroy O, Nuno N, Lopez A, Bucio L, Souza V, Hernandez-Pando R, Munoz L, Gutierrez-Ruiz MC, Gomez-Quiroz LE. Hepatocyte growth factor protects against isoniazid/rifampicin-induced oxidative liver damage. Toxicol Sci. 2013; 135:26-36.

Facultad de Medicina

Versión electrónica en http://tab.facmed.unam.mx

MENSAJE BIOQUÍMICO

Mens. Bioquim. 41 (2017) 108-115

TAB

Memoria del 44º Taller de Actualización Bioquímica, Facultad de Medicina; UNAM

Fundamentos de la señalización redox: Lecciones de los sistemas generadores de especies reactivas de oxígeno

Basics in redox signaling: Lessons from reactive oxygen species generating systems

Salas-Silva, Elsy Soraya [1,2]; Simoni-Nieves, Arturo [1,2]; Miranda-Labra, Roxana U. [1] y Gómez-Quiroz, Luis Enrique[1,*]

1. Laboratorio de Fisiología Celular, Departamento de Ciencias de la Salud, Universidad Autónoma Metropolitana Unidad Iztapalapa.
2. Doctorado en Biología Experimental, Departamento de Ciencias de la Salud, Universidad Autónoma Metropolitana Unidad Iztapalapa
*Correspondencia. Departamento Ciencias de la Salud, UAM-I, Av. San Rafael Atlixco 186, Col. Vicentina, Iztapalapa, Ciudad de México. CP, 09340. Tel. +52(55)58044730, legq@xanum.uam.mx

Resumen

En la actualidad, las especies reactivas de oxígeno están tomando cada vez relevancia por su implicación en la señalización celular, sobre todo en procesos claves como la proliferación, la diferenciación, la apoptosis, e incluso en la sobrevivencia, lo que deja claro que estas moléculas ya no sólo deben ser consideradas como entidades tóxicas. Se han identificado reguladores maestros de la señalización redox, entre ellos el factor de crecimiento de hepatocitos y su receptor c-Met, quienes juegan un rol importante en la señalización mediada por estas especies, modulando sistemas como el de las NADPH oxidasas o la mitocondria, y permitiendo la expresión diferencial de antioxidantes, lo cual permite a la célula responder de manera adecuada ante los estímulos del ambiente extracelular.

Palabras Clave: ROS, NADPH oxidasa, Nrf2, c-Met, HGF, Romo1

Abstract

Nowadays, reactive oxygen species-mediated cellular signaling is a growing field. The evidence of the requirement of these species in cellular processes such as proliferation, differentiation, apoptosis and even, survival, is leaving clear that reactive oxygen species are not just noxious entities, not anymore. As it happens in many biological systems, homeostasis is the key for a proper cellular and tissue physiology, including apoptosis or inflammation. New master regulators have been identified. The hepatocyte growth factor and its receptor c-Met, play pivotal roles in the redox signaling, modulating free radicals generator systems, such as NADPH oxidase or mitochondria; or the expression of antioxidants, leading to a specific cellular response against the stimulus from the extracellular environment.

Keywords: ROS, NADPH oxidase, Nrf2, HGF, Romo1

Introducción

Las especies reactivas de oxígeno (ROS, por sus siglas en inglés, *Reactive Oxygen Species*), siguen siendo poco comprendidas, tal vez, por la mala fama que les generó sus efectos tóxicos en sistemas biológicos, quizá, estudiados de manera muy general. Si bien es innegable el potencial de daño que pueden tener, las ROS son igualmente necesarias para mantener funciones fisiológicas relevantes como la diferenciación, la proliferación, la sobrevivencia, el metabolismo, etc.[1,2]; esto en

gran medida por la capacidad que tienen de modificar químicamente residuos de aminoácidos de proteínas claves en la señalización, induciendo cambios conformacionales que permiten exponer sitios catalíticos, secuencias de localización nuclear, dominios de unión al DNA, entre otros, pero como hemos dicho, se conoce más de los efectos tóxicos y muchas veces se exagera de ello en la literatura no especializada e incluso se han identificado errores relacionados con una mala interpretación en la literatura especializada. ¿Qué tan malos son las ROS? es una pregunta difícil de contestar, tan complicada de responder como ¿Qué tan buenos son los antioxidantes?, que es la otra cara de la moneda con una idea generalizada de que son especies moleculares buenas que uno debería consumir, incluso en exceso, por los aparentes beneficios que nos dan, particularmente en el contexto de varias enfermedades, sin embargo no olvidemos que ambas entidades están en cada uno de los platos de una balanza (Figura 1), por lo que basta con concebir esta imagen para darnos cuenta de que el desbalance, hacia cualquier lado, rompe con la homeostasis, conduciendo, cuando las ROS suben o las antioxidantes bajan, en lo que conocemos como estrés oxidante (Figura 2). De hecho, se ha reportado que los antioxidantes lejos de ayudar en el tratamiento del cáncer lo pueden empeorar [3,4].

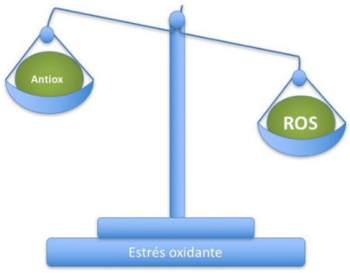


Figura 1. Balance óxido-reducción, entre especies prooxidantes y antioxidantes.

De este modo, se debe ver a las ROS, junto con otras especies prooxidantes (radicales libres, especies reactivas de nitrógeno, etc.), y a los antioxidantes, desde la óptica de la homeostasis, del equilibrio [5]. Las consecuencias son diversas cuando el equilibro se rompe.

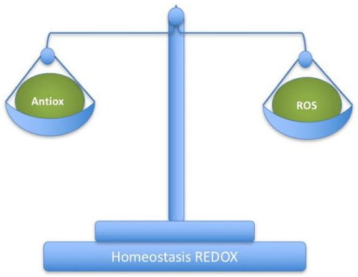


Figura 2. Desequilibrio óxido-reducción. Estrés oxidante.

La función primaria en la producción controlada de ROS dentro de la célula es la transducción de señales tendiente a la regulación de la expresión génica[6], pasando por la estimulación de fenómenos fisiológicos como la inflamación o la apoptosis, en niveles ligeramente incrementados, hasta llegar a procesos de daño como la necrosis, cuando los niveles exceden el umbral y rompen el equilibrio (Figura 3).

En el presente texto hacemos una revisión de conceptos básicos de la transducción de señales mediada por cambios en el estado redox celular, haciendo énfasis en el sistema del factor de crecimiento de hepatocitos (HGF) y su receptor c-Met como reguladores maestros del estado redox celular, particularmente en epitelios.

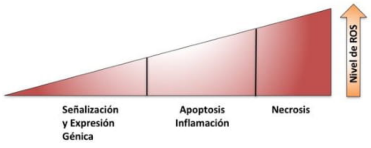


Figura 3. Relación entre los niveles de especies reactivas de oxígeno y fenómenos celulares.

© 2017 Mensaje Bioquímico. Todos los derechos reservados. ISSN-0188-137X
Comité Editorial: Cárdenas Monroy, C.A.; González Andrade, M.; Lara Lemus, R.; Martínez González, J.J.; Molina Jijón, E.; Torres Durán, P.V. *Publicado por el Departamento de Bioquímica de la Facultad de Medicina; UNAM.*

Homeostasis redox

Hablar de moléculas prooxidantes nos lleva casi de inmediato a pensar en las ROS, pero no son las únicas, también tienen relevancia las especies reactivas de nitrógeno entre otras; ahora bien, no todas las ROS son radicales libres, definidas como moléculas o átomos que presentan un electrón desapareado; a la par de ellas, están moléculas con una alta capacidad oxidante, tal vez la más destacada de ellas sea el peróxido de hidrógeno (H_2O_2), que si bien no es un radical libre puede producir a uno de los más reactivos que existen y sin función fisiológica conocida, el radical hidroxilo (HO•), capaz de oxidar prácticamente a cualquier molécula con la que interactúe, como a los ácidos nucleicos, a las proteínas, o a los lípidos, generando disfunción celular, mutaciones y eventualmente la muerte.

La célula está generando constantemente ROS como producto de procesos celulares normales, como la respiración, el metabolismo o la biotransformación de xenobióticos (como el citocromo P450 2E1) [7]. El radical anión superóxido ($O_2^{\cdot-}$) se genera fácilmente cuando el oxígeno molecular gana un electrón. Esta ROS interviene frecuentemente en procesos de señalización, pero también puede inducir daño cuando se incrementa su producción o cuando enzimas como las superóxido dismutasas (SOD) disminuyen su expresión o actividad [8].

La célula tiene un sistema muy eficiente para el mantenimiento del balance redox que se muestra en la figura 4. El $O_2^{\cdot-}$ producido por sistemas metabólicos como la respiración, la xantina oxidasa, la ciclo oxigenasa, entre otros, o por sistemas canónicos de producción de ROS como la NADPH oxidasa, de la cual hablaremos más adelante, es dismutado por las SOD, de la cual existen tres variantes [9]. La dismutación genera al H_2O_2 que, como se mencionó, puede producir al HO• en presencia de metales como el Fe^{2+} o el Cu^{+1}, en un proceso químico conocido como reacción de Fenton [10]. El H_2O_2 es reducido en H_2O por varias enzimas, siendo las más relevantes la catalasa y la glutatión peroxidasa (GSHPx), que usa dos moléculas de glutatión (GSH) como poder reductor.

En estados fisiológicos, esta serie de reacciones acopladas permiten el equilibrio redox y una correcta progresión en las funciones celulares normales, pero el desbalance conduce al mal funcionamiento, una vez más, el mecanismo central es la activación anómala de rutas de transducción y expresión génica tendiente a equilibrar o a solucionar dicho disturbio (Figura 4).

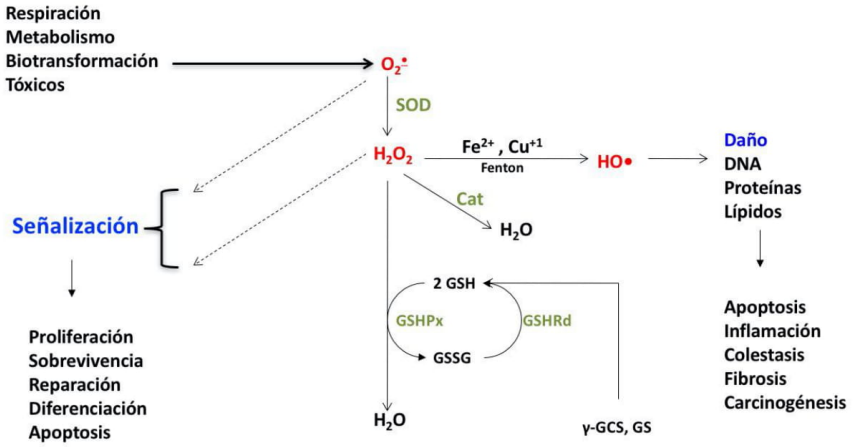


Figura 4. Control de la homeostasis redox.

© 2017 Mensaje Bioquímico. Todos los derechos reservados. ISSN-0188-137X
Comité Editorial: Cárdenas Monroy, C.A.; González Andrade, M.; Lara Lemus, R.; Martínez González, J.J.; Molina Jijón, E.; Torres Durán, P.V. *Publicado por el Departamento de Bioquímica de la Facultad de Medicina; UNAM.*

Modulación de sistemas prooxidantes y antioxidantes como estrategia para la señalización redox

El balance que hemos venido refiriendo está perfectamente controlado por la expresión de enzimas antioxidantes, y la regulación de los sistemas prooxidantes. Si bien, como hemos dicho, sistemas como la xantina oxidasa, o la ciclooxigenasa, generan ROS, como subproductos en sus reacciones, no se sabe con certeza si esto puede ser utilizado, más allá del accidente, por la célula con fines regulatorios o de señalización

La NADPH oxidasa y la mitocondria están bien caracterizadas que son capaces de producir ROS con el único objetivo de señalizar, con umbrales que permiten éste proceso y no el daño celular [11].

La NADPH oxidasa

En nuestro grupo de investigación identificamos recientemente una sobreactivación anómala de la NADPH oxidasa en ratones que carecen de la señalización del receptor del HGF, c-Met [2], los hepatocitos de estos ratones presentan un incremento significativo en la actividad del complejo y por lo tanto una generación excesiva de ROS [2,12], esto es un buen ejemplo de que si bien existe un incremento en ROS, no necesariamente la célula está en estrés oxidante, ya que esto va acompaño del incremento en enzimas antioxidantes y GSH, equilibrando la balanza. Investigaciones posteriores nos permitieron caracterizar y proponer que el HGF/c-Met es un regulador maestro del estado redox celular, que tiende a la activación de rutas de señalización para fines de protección y sobrevivencia[13] .

Podría parecer irónico, que, si bien las ROS pueden inducir muerte celular, también puedan promover sobrevivencia, la respuesta de esto ésta en la cantidad y en la temporalidad de la producción de ROS[13] .

Las NADPH oxidasas son sistemas exclusivos para señalizar en células no fagocíticas, como ejemplo las epiteliales, esto aunado a la muy bien caracterizada función en estallido respiratorio en células fagocíticas profesionales[14].

La familia está compuesta por varios complejos enzimáticos, conformada por 7 homólogos catalíticos unidos a la membrana, como Nox1, Nox2, Nox3, Nox4 y Nox5, además de DUOX1 y 2 [14]. A los componentes catalíticos se unen, en la mayoría de ellas, proteínas regulatorias, tanto citosólicas, como p47phox o p67phox, como de membrana, como el caso de p22phox, que es usada por las Nox1-4 [11].

Existen, además, diferencias en cuanto al tipo de ROS que producen. El $O_2^{\cdot-}$ es generado particularmente por las Nox1, 2, 3 y 5, mientras que la Nox 4 y las Duox generan H_2O_2, marcando en ello posibles diferencias en las rutas de señalización activadas, aspecto que no ha quedado del todo claro, más allá de la expresión diferencial tejido dependiente de las oxidasas [11,15,16]. Sin embargo, como se ha mencionado, el $O_2^{\cdot-}$ puede ser fácilmente dismutado a H_2O_2 teniendo un punto más de regulación en las rutas donde están involucradas.

Las rutas de señalización que han sido identificadas en relación a la NADPH oxidasa están en número creciente, entre otras se puede mencionar a PI3K/Akt/mTOR, TLR4, TNF-alfa, NF-kB, Angiotensina II, HIF-1 alfa, ADAM17, Nrf2, etc.; éste último ha sido caracterizada en hepatocitos por nuestro grupo, formando un eje entre el factor de crecimiento de hepatocitos, NADPH oxidasa y Nrf2, la activación de esta ruta está dirigida hacia respuestas de protección y sobrevivencia.

HGF y c-Met como modelo de regulación de las NADPH oxidasas en señalización.

La NADPH oxidasa puede ser activada tanto por receptores acoplados a proteínas G, como por receptores con actividad de cinasa de tirosinas (RTK) [13]. Se sabe que los RTK pueden inducir la actividad de la oxidasa a través de la ruta de Ras/Erk, o por la fosfolipasa C gama, que facilita la activación de la proteína cinasa C (PKC), dando lugar a la fosforilación de p47phox, regulador de la Nox2, aunque esta función también ha sido atribuida a la cinasa Akt, que es parte también de las rutas canónicas iniciadas por los RTK [11].

Recientemente hemos publicado una serie de trabajos en los que se deja patente la relación de la NADPH oxidasa y c-Met con fines de señalización y que tiende a inducir una señal de protección y sobrevivencia. HGF/c-Met ejercen una regulación bifásica en el hepatocito que tiende a la activación de respuestas de sobrevivencia y reparación[13].

En la primera etapa, la activación de c-Met por el HGF promueve la actividad de la NADPH oxidasa, induciendo la generación de ROS,

© 2017 Mensaje Bioquímico. Todos los derechos reservados. ISSN-0188-137X
Comité Editorial: Cárdenas Monroy, C.A.; González Andrade, M.; Lara Lemus, R.; Martínez González, J.J.; Molina Jijón, E.; Torres Durán, P.V. *Publicado por el Departamento de Bioquímica de la Facultad de Medicina; UNAM.*

particularmente $O_2^{\bullet-}$, en un mecanismo dependiente del tiempo, que llega a valores máximos a los 5 min posterior al estímulo, y que se mantiene hasta los 30 min, cayendo a valores basales 60 min después del tratamiento[13].

Esta fase de respuesta temprana va dirigida a la activación del factor de transcripción Nrf2 y a la producción de proteínas de protección, como antioxidantes o de fase II y III de destoxificación [17,18], destacando enzimas como NAD(P)H quinona oxidorreductasa 1 (NQO1), o la gama glutamilcisteina sintetasa (GCS), la enzima limitante en la síntesis de GSH (Figura 5).

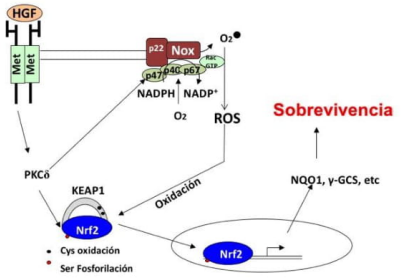


Figura 5. Mecanismo molecular del efecto temprano del HGF/c-Met. Activación de la ruta NADPH oxidasa/Nrf2.

La segunda etapa es de respuesta tardía y es opuesta a la primera en términos de actividad de la oxidasa, ya que disminuye significativamente lo cual se relaciona en la producción de ROS, cayendo a niveles por debajo de los basales a las 12 h y manteniéndose hasta las 24 h[13].

El estudio de los efectos (opuestos), inducidos por el HGF, reveló que ambos mecanismos van dirigidos a la activación de respuestas de protección y sobrevivencia en el hepatocito.

En la etapa temprana, c-Met induce la activación de PKC delta, en un proceso dependiente de la fosfolipasa C [2]. En este punto PKC delta toma un papel dual, siendo el primero la fosforilación de p47phox, lo que permite el ensamble y activación de la NADPH oxidasa[13]. Las ROS producidas permiten la oxidación de cisteínas (cys) específicas en la proteína Keap1, inhibidor del factor de transcripción Nrf2, estas cisteínas juegan un papel central en la activación del factor de transcripción, particularmente la cys 151 juega un papel de sensor de los cambios en el estado redox celular. La oxidación de las cys inducen un cambio conformacional en el complejo que estabiliza a Nrf2 en el citosol, conformado, entre otras proteínas, por la ligasa de ubiquitinas tipo 3 Cullin 3 (Cul3), quien usa a Keap1 para la ubiquitinación constitutiva de Nrf2 en un estado celular inclinado hacia el potencial reductor [19]. El cambio conformacional permite que el sitio catalítico de Cul3 se aleje de los sitios de ubiquitinización, por lo que la degradación por el proteosoma 26S se evita y permite su migración al núcleo. La activación de Nrf2 no está aún completa, se requiere de la fosforilación de serinas específicas, situación que representa la segunda función de PKC delta, que fue activada por c-Met [13].

Nrf2 una vez en el núcleo se une a su secuencia consenso, el elemento de respuesta antioxidante (ARE), en genes que codifican principalmente para proteínas de fase II y III de destoxificación, y para antioxidantes. Si la respuesta de la NADPH oxidasa, iniciada por la señalización de HGF/c-Met, se abroga con inhibidores específicos de la oxidasa como el DPI, Nrf2 no se activa y la célula queda sensibilizada a los efectos prooxidantes que puedan derivar de la mitocondria, por ejemplo, cuando se exponen las células a bloqueadores de la cadena respiratoria como la Antimicina A [13] (Figura 5).

La NADPH oxidasa, canónicamente es usada por algunas proteínas con la finalidad de inducir estrés oxidante y apoptosis, como el factor de crecimiento transformante (TGF) beta, que ejerce dicha acción en células epiteliales (Figura 6)[11].

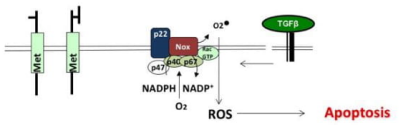


Figura 6. Efectos citotóxicos mediados por la NADPH oxidasa inducidos por el factor de crecimiento transformante beta

La segunda fase o respuesta tardía, muestra, como se mencionó, un decremento en la actividad de la NADPH oxidasa en tiempos largos del tratamiento con HGF, el efecto está asociado al decremento en la expresión de varias subunidades de la NADPH oxidasa como p22phox, p67phox, Nox2 y Nox4 (Figura 7). El mecanismo, tendiente a la abrogación en la expresión de los componentes de la oxidasa, aún no se han determinado por

© 2017 Mensaje Bioquímico. Todos los derechos reservados. ISSN-0188-137X
Comité Editorial: Cárdenas Monroy, C.A.; González Andrade, M.; Lara Lemus, R.; Martínez González, J.J.; Molina Jijón, E.; Torres Durán, P.V. *Publicado por el Departamento de Bioquímica de la Facultad de Medicina; UNAM.*

completo, pero sabemos que dicha respuesta esta mediada por un mecanismo complejo que involucra mecanismos transcripcionales y post-traduccionales, observándose la participación de Akt y la función del proteosoma 26 S, así como una interacción directa entre c-Met y la subunidad regulatoria p22phox (datos sin publicar).

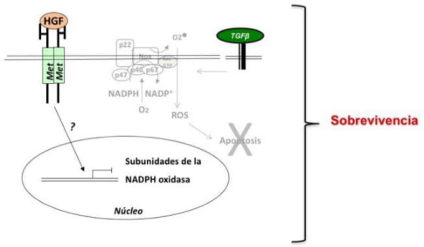


Figura 7. Mecanismo parcial del efecto tardío del HGF/c-Met. Represión transcripcional de los componentes de la NADPH oxidasa.

Una vez más las células que son retadas bajo las condiciones de represión de la NADPH oxidasa ejercidas por c-Met, presentan resistencia al efecto citotóxico, en este caso por el factor de crecimiento transformante beta, que usa a la oxidasa para iniciar apoptosis [13].

El disturbio que genera la ausencia en la señalización de c-Met en el hígado (como en el caso de los ratones deficiente del receptor), está siempre ligado al estrés oxidante y al inicio o progresión de enfermedades hepáticas como el cáncer hepatocelular [12,20], la fibrosis [21], la enfermedad hepática alcohólica [7], la esteatosis y la colestasis [22,23], entre otras, por lo que las implicaciones en la pérdida del control del estado redox que conduce el HGF y c-Met son notables y el conocimiento y la caracterización de ello puede permitir la implementación de nuevas estrategias terapéuticas.

Las mitocondrias

La mitocondria suele ser considerada como la generadora de ROS por excelencia. Existe la concepción, poco precisa, de que la producción de ROS por el organelo es consecuencia "accidental" de la fuga de electrones que son captados por el oxígeno molecular. Existe evidencia de que la mitocondria presenta algunos mecanismos bien regulados que permiten la producción de ROS con la finalidad de conducir procesos celulares bien definidos [24].

Nuestro grupo tiene experiencia con dos sistemas que regulan la generación de ROS con fines de señalización en la mitocondria, la proteína moduladora de ROS 1 (Romo1) y el ganglíosido GD3.

Romo1 es una proteína mitocondrial descubierta y caracterizada muy recientemente [25] que tiene la función particular de inducir y regular la producción de ROS, de hecho se ha sugerido que el incremento en la expresión observada de Romo1 en varias líneas celulares derivadas de tumores, tiene una relación directa con el estrés oxidante que presentan éstas células, lo que contribuye a la acumulación de más mutaciones y a la agresividad [25,26].

El mecanismo en la generación de ROS aún no está caracterizado, sin embargo, se cuenta con evidencia que la expresión de Romo1 está estrechamente vinculada a la activación de la ruta de señalización de Erk1/2, la cual es de la familia de las MAPK, y de NF-kB que a su vez conduce a la activación del ciclo celular y a la proliferación, esto tanto en condiciones normales como patológicas [27,28] (Figura 8).

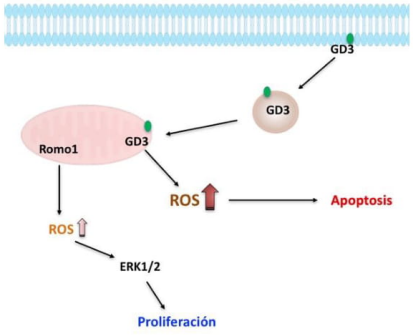


Figura 8. Los mecanismos mitocondriales de generación controlada de especies reactivas de oxígeno y sus efectos fisiológicos.

Aún queda mucho camino para determinar la magnitud de la relevancia de Romo 1, al parecer es una proteína muy conservada, se ha identificado recientemente incluso en lampreas [29], lo que nos habla de la necesidad evolutiva en el control de estado redox, y se ha empezado a relacionar en otras patologías, más allá del cáncer, como en la esteatosis no alcohólica [22], que se sobreexpresa en ausencia de la señalización de c-Met, o en ciertas

© 2017 Mensaje Bioquímico. Todos los derechos reservados. ISSN-0188-137X
Comité Editorial: Cárdenas Monroy, C.A.; González Andrade, M.; Lara Lemus, R.; Martínez González, J.J.; Molina Jijón, E.; Torres Durán, P.V. *Publicado por el Departamento de Bioquímica de la Facultad de Medicina; UNAM.*

enfermedades reumáticas, no necesariamente en artritis, en lo cual nos hemos enfocado recientemente [30]. ¿Cuáles son los mecanismos moleculares que permiten la modulación de ROS y sus implicaciones celulares? es una pregunta que se debe responder en busca de nuevas opciones terapéuticas, al menos, en la lucha contra el cáncer. El ganglióside GD3 es otro caso de la regulación de las ROS en la mitocondria[31]. El GD3 pertenece a la familia de los glucolípidos, lípidos especializados caracterizados por tener una región polar grande formada de oligosacáridos, así como dos colas hidrofóbicas, conformadas por un ácido grasos y la otra por la esfingosina. El GD3 forma parte estructural de las balsas lipídicas cuya función es básicamente en la señalización, muchos de los RTK están en estas balsas, pero también se ha reportado recientemente su participación en la formación de autofagosomas [32].

En realidad, el GD3 señaliza como parte de la ruta del TNF-alfa, el cual induce la activación de la esfingomielinasa ácida y la liberación del GD3 que se dirige a la mitocondria [33] promoviendo la generación de ROS y la apoptosis [31,34] (Figura 8).

El mecanismo detallado en la generación de ROS esta por ser completamente dilucidado, pero más allá de los cambios a nivel de membrana mitocondrial y su desestabilización, pareciera haber más puntos de regulación, tal vez una activación de Romo1. En sí la participación de GD3 en la generación controlada de ROS por la mitocondria está sumamente confirmado y representa un mecanismo central en la inducción de apoptosis como respuesta iniciada por el TNF-alfa[31,33].

Los efectos mostrados por el GD3 y Romo1 muestran una respuesta diferencial de la mitocondria que está, en gran medida, determinado por los niveles de ROS. En general podemos afirmar que niveles relativamente bajos de ROS promueven efectos como proliferación o sobrevivencia, mientras que el incremento puede promover apoptosis (Figura 8).

Una reflexión final

El uso de las ROS como entidades en la señalización, podría posicionarlas en el viejo concepto de "segundo mensajero", y representan un claro triunfo en términos de adaptación, de llevarlas de especies altamente tóxicas, a su control con fines positivos para la fisiología celular.

La generación y el uso de ROS representa ventajas para la célula, son entidades que se forman con relativa facilidad, en procesos regulados, dependientes del gasto de poder reductor; o de manera colateral en procesos metabólicos que, si bien éstos pueden salirse de control en un primer nivel, pueden contrarrestarse con la acción de las enzimas antioxidantes que, de hecho, su expresión suele estar controlada por señalización redox.

Es importante hacer hincapié en dejar a un lado el concepto de que las ROS son entidades negativas, si esto fuera así, lo serían igualmente los antioxidantes. Como en prácticamente todos los sistemas biológicos la homeostasis o equilibrio determina los paradigmas celulares y el estado redox es un caso que debe cada vez más tomarse en cuenta en el contexto de cualquier evento molecular de la célula.

Agradecimientos

El trabajo fue escrito con el apoyo, y como producto de los proyectos financiados por el CONACYT: CB-252942, CB–222578, Fronteras de la Ciencia 1320, así como por la Universidad Autónoma Metropolitana Iztapalapa.

1

Referencias

1. Miranda, R. U., Gomez-Quiroz, L. E., Mejia, A., and Barrios-Gonzalez, J. (2013). *Fungal biology* **117**, 85-93
2. Gomez-Quiroz, L. E., Factor, V. M., Kaposi-Novak, P., Coulouarn, C., Conner, E. A., and Thorgeirsson, S. S. (2008). *J Biol Chem* **283**, 14581-14589
3. Sayin, V. I., Ibrahim, M. X., Larsson, E., Nilsson, J. A., Lindahl, P., and Bergo, M. O. (2014). *Sci Transl Med* **6**, 221ra215
4. Le Gal, K., Ibrahim, M. X., Wiel, C., Sayin, V. I., Akula, M. K., Karlsson, C., Dalin, M. G., Akyurek, L. M., Lindahl, P., Nilsson, J., and Bergo, M. O. (2015). *Sci Transl Med* **7**, 308re308
5. D'Autreaux, B., and Toledano, M. B. (2007). *Nat Rev Mol Cell Biol* **8**, 813-824
6. Gomez-Quiroz, L., and Cuevas-Bahena, D. (2008) Especies reactivas de oxígeno y señalización. in *Radicales Libres y estrés oxidativo. Aplicaciones Médicas* (Konigsberg, M. ed.), El Manual Modenor, México. pp 487-500
7. Valdes-Arzate, A., Luna, A., Bucio, L., Licona, C., Clemens, D. L., Souza, V., Hernandez, E., Kershenobich, D., Gutierrez-Ruiz, M. C., and Gomez-Quiroz, L. E. (2009). *Free Radic Biol Med* **47**, 424-430

© 2017 Mensaje Bioquímico. Todos los derechos reservados. ISSN-0188-137X
Comité Editorial: Cárdenas Monroy, C.A.; González Andrade, M.; Lara Lemus, R.; Martínez González, J.J.; Molina Jijón, E.; Torres Durán, P.V. *Publicado por el Departamento de Bioquímica de la Facultad de Medicina; UNAM.*

8. Clavijo-Cornejo, D., Gutierrez-Carrera, M., Palestino-Dominguez, M., Dominguez-Perez, M., Nuno, N., Souza, V., Miranda, R. U., Kershenobich, D., Gutierrez-Ruiz, M. C., Bucio, L., and Gomez-Quiroz, L. E. (2014). *Food Chem Toxicol* **69**, 102-108
9. Gomez-Quiroz, L., and Cuevas-Bahena, D. (2008) Sueróxidos dismutasas. in *Radicales libres y estres oxidativo. Aplicaciones Médicas* (Konigsberg, M. ed.), El Manual Moderno. pp 169-182
10. Valko, M., Jomova, K., Rhodes, C. J., Kuca, K., and Musilek, K. (2016). *Arch Toxicol* **90**, 1-37
11. Brandes, R. P., Weissmann, N., and Schroder, K. (2014). *Free radical biology & medicine* **76**, 208-226
12. Kaposi-Novak, P., Lee, J. S., Gomez-Quiroz, L., Coulouarn, C., Factor, V. M., and Thorgeirsson, S. S. (2006). *J Clin Invest* **116**, 1582-1595
13. Clavijo-Cornejo, D., Enriquez-Cortina, C., Lopez-Reyes, A., Dominguez-Perez, M., Nuno, N., Dominguez-Meraz, M., Bucio, L., Souza, V., Factor, V. M., Thorgeirsson, S. S., Gutierrez-Ruiz, M. C., and Gomez-Quiroz, L. E. (2013). *Biochimie* **95**, 1177-1184
14. Lambeth, J. D., and Neish, A. S. (2014). *Annu Rev Pathol* **9**, 119-145
15. Bedard, K., Lardy, B., and Krause, K. H. (2007). *Biochimie* **89**, 1107-1112
16. Brown, D. I., and Griendling, K. K. (2009). *Free radical biology & medicine* **47**, 1239-1253
17. Aleksunes, L. M., Slitt, A. L., Maher, J. M., Augustine, L. M., Goedken, M. J., Chan, J. Y., Cherrington, N. J., Klaassen, C. D., and Manautou, J. E. (2008). *Toxicol Appl Pharmacol* **226**, 74-83
18. Klaassen, C. D., and Reisman, S. A. (2010). *Toxicol Appl Pharmacol* **244**, 57-65
19. Zhang, Q., Pi, J., Woods, C. G., and Andersen, M. E. (2010). *Toxicol Appl Pharmacol* **244**, 84-97
20. Takami, T., Kaposi-Novak, P., Uchida, K., Gomez-Quiroz, L. E., Conner, E. A., Factor, V. M., and Thorgeirsson, S. S. (2007). *Cancer Res* **67**, 9844-9851
21. Marquardt, J. U., Seo, D., Gomez-Quiroz, L. E., Uchida, K., Gillen, M. C., Kitade, M., Kaposi-Novak, P., Conner, E. A., Factor, V. M., and Thorgeirsson, S. S. (2012). *Biochim Biophys Acta* **1822**, 942-951
22. Gomez-Quiroz, L. E., Seo, D., Lee, Y. H., Kitade, M., Gaiser, T., Gillen, M., Lee, S. B., Gutierrez-Ruiz, M. C., Conner, E. A., Factor, V. M., Thorgeirsson, S. S., and Marquardt, J. U. (2016). *Toxicology* **361-362**, 39-48
23. Nuno-Lambarri, N., Dominguez-Perez, M., Baulies-Domenech, A., Monte, M. J., Marin, J. J., Rosales-Cruz, P., Souza, V., Miranda, R. U., Bucio, L., Montalvo-Jave, E. E., Concepcion Gutierrez-Ruiz, M., Garcia-Ruiz, C., Fernandez-Checa, J. C., and Gomez-Quiroz, L. E. (2016). *Oxid Med Cell Longev* **2016**, 9895176
24. Zorov, D. B., Juhaszova, M., and Sollott, S. J. (2014). *Physiol Rev* **94**, 909-950
25. Chung, Y. M., Kim, J. S., and Yoo, Y. D. (2006). *Biochem Biophys Res Commun* **347**, 649-655
26. Chung, J. S., Lee, S. B., Park, S. H., Kang, S. T., Na, A. R., Chang, T. S., Kim, H. J., and Yoo, Y. D. (2009). *Free Radic Res* **43**, 729-737
27. Na, A. R., Chung, Y. M., Lee, S. B., Park, S. H., Lee, M. S., and Yoo, Y. D. (2008). *Biochem Biophys Res Commun* **369**, 672-678
28. Shyamsunder, P., Verma, R. S., and Lyakhovich, A. (2015). *Cancer Lett* **361**, 33-38
29. Zhao, C., Feng, B., Cao, Y., Xie, P., Xu, J., Pang, Y., Liu, X., and Li, Q. (2013). *Fish Shellfish Immunol* **35**, 278-283
30. Blancas-Meza, C., Martínez-Nava, G., López-Reyes, A., Zamudio-Cuevas, Y., Martinez-Flores, K., Clavijo-Cornejo, D., Miranda, R. U., Gutierrez Ruiz, M. C., Gomez Quiroz, L., Pineda, C., and Fernández-Torres, J. (2016). *Investigación en Discapacidad* **5**, 139-145
31. Garcia-Ruiz, C., Colell, A., Paris, R., and Fernandez-Checa, J. C. (2000). *FASEB J* **14**, 847-858
32. Matarrese, P., Garofalo, T., Manganelli, V., Gambardella, L., Marconi, M., Grasso, M., Tinari, A., Misasi, R., Malorni, W., and Sorice, M. (2014). *Autophagy* **10**, 750-765
33. Garcia-Ruiz, C., Colell, A., Morales, A., Calvo, M., Enrich, C., and Fernandez-Checa, J. C. (2002). *J Biol Chem* **277**, 36443-36448
34. Garcia-Ruiz, C., Colell, A., Mari, M., Morales, A., Calvo, M., Enrich, C., and Fernandez-Checa, J. C. (2003). *J Clin Invest* **111**, 197-208



DR. LUIS ENRIQUE GÓMEZ QUIROZ

Profesor Investigador Titular C del Departamento de Ciencias de la Salud. Químico de formación, con maestría y doctorado en Biología Experimental (UAM-I) y postdoctorado en Biología Celular y Molecular del cáncer hepático en el National Cancer Institute del NIH, Bethesda, Maryland, USA. Actual coordinador del Posgrado en Biología Experimental.

Principales líneas de investigación: regulación de la expresión génica por cambios en el estado redox, hepatocarcinogenesis y progresión tumoral en hígado y páncreas, y transducción de señales. Es miembro del Sistema Nacional de Investigadores nivel III, de la Academia Mexicana de Ciencias, del International Liver Cancer Association, y de la Sociedad Mexicana de Bioquímica, entre otras.

© 2017 Mensaje Bioquímico. Todos los derechos reservados. ISSN-0188-137X
Comité Editorial: Cárdenas Monroy, C.A.; González Andrade, M.; Lara Lemus, R.; Martínez González, J.J.; Molina Jijón, E.; Torres Durán, P.V. *Publicado por el Departamento de Bioquímica de la Facultad de Medicina; UNAM.*

Annals of Hepatology 19 (2020) 489–496

Contents lists available at ScienceDirect

Annals of Hepatology

journal homepage: www.elsevier.es/annalsofhepatology

Original article

Mediterranean-like mix of fatty acids induces cellular protection on lipid-overloaded hepatocytes from western diet fed mice

Lyssia Castellanos-Tapia[a,b], María Elizabeth Tejero-Barrera[a], Soraya Salas-Silva[b,c], Arturo Simoni-Nieves[b,c], Alejandro Escobedo-Calvario[b,c], Luis E. Gomez-Quiroz[c,*]

[a] Nutrigenomics Laboratory, National Institute of Genomic Medicine, Mexico City, Mexico
[b] Posgrado en Biologia Experimental, DCBS, Universidad Autonoma Metropolitana Unidad Iztapalapa, Mexico City, Mexico
[c] Departamento de Ciencias de la Salud, Universidad Autónoma Metropolitana Iztapalapa, Mexico City, Mexico

ARTICLE INFO

Article history:
Received 16 April 2020
Accepted 19 June 2020
Available online 12 July 2020

Keywords:
PUFA
MUFA
Mediterranean diet
Western diet
NAFLD

ABSTRACT

Introduction and objective. Non-alcoholic fatty liver disease remains as one of the main liver disorders worldwide. It is widely accepted that is the kind of lipid, rather than the amount deposited in the cells that determines cell damage. Cholesterol and saturated free fatty acids are deleterious lipids when accumulated but, in contrast, there are some valuable lipids that could counteract those with harmful properties. Much of this knowledge arises from studies using a single fatty acid, but the effects of a combination of fatty acids, as obtained by diet has been poorly addressed. In the present work, we were focused to figure out the cellular effect of two different mixes of fatty acids, one with high proportion of saturated fatty acids, and another one with high proportion of unsaturated fatty acids (Mediterranean-like) in a cellular model of steatosis. Material and methods. Primary mouse hepatocytes from animals fed with a western diet (high fat and carbohydrates diet), were treated with both mixes of fatty acids for 24 h. Results. Our data clearly show that only the high unsaturated fatty acid mix induced a decrease in triglycerides (47.5%) and cholesterol (59%) content in steatotic hepatocytes mediating cellular protection associated to the decrement of ROS and oxidative damage. The mixture of high saturated fatty acids exhibited no effects, preserving high levels of cholesterol and triglycerides and oxidative damage. In conclusion, our results show that Mediterranean-like mix of fatty acids exerts cellular protection in steatosis by decreasing triglycerides, cholesterol, ROS content and oxidative damage.

© 2020 Fundación Clínica Médica Sur, A.C. Published by Elsevier España, S.L.U. This is an open access article under the CC BY-NC-ND license (http://creativecommons.org/licenses/by-nc-nd/4.0/).

1. Introduction

Non-alcoholic fatty liver disease (NAFLD) remains as one of the main liver disorders worldwide, with increasing prevalence every year [1]. It is associated with metabolic disorders, such as diabetes, dyslipidemia, metabolic syndrome, or obesity [2], but also to the consumption of fatty foods, particularly those rich in cholesterol, saturated free fatty acids (FFA) and carbohydrates such as western-style diet [3,4].

We and others have reported that is the type of lipid, rather than the amount that determines the severity of the disease [5–7]. In this context, high cholesterol overload in hepatocytes seems to be the main cellular noxious stimulus in NAFLD particularly because cholesterol targets mitochondria inducing oxidative stress, ATP decrement and susceptibility to cell death due to a second hit [5,7], such as alcohol toxicity [8], obstructive cholestasis [9], or deficiencies in signaling pathways, such as HGF/c-Met [10]; as a consequence oxidative stress is exacerbated increasing damage and, eventually, leading to carcinogenesis [6].

Diet could also be the counterbalance in NAFLD particularly due to the differential lipid content. It is recognized that Mediterranean diet is rich in monounsaturated and polyunsaturated fatty acids (MUFA and PUFA, respectively), which in addition present antioxidant properties, among others [11].

Diet is a determining factor that influences the concentration and composition of fatty acids in plasma and for instance, in the liver. Some studies have shown that certain fatty acids alone or in combination induce significant changes in liver physiology and

Abbreviations: NAFLD, Non-alcoholic fatty liver disease; NASH, Non-alcoholic steatohepatitis; TG, Triglyceride; HMPFA, High mono and polyunsaturated fatty acids; HSFA, High proportions of saturated fatty acids; MUFA, Monounsaturated fatty acids; PUFA, Polyunsaturated fatty acids; FFA, Free fatty acid; AST, Aspartate aminotransferase; ALT, Alanine transferase; ROS, Reactive Oxygen Species; TBARS, Thiobarbituric acid-reactive substances.

* Corresponding author.
E-mail address: legq@xanum.uam.mx (L.E. Gomez-Quiroz).

https://doi.org/10.1016/j.aohep.2020.06.005
1665-2681/© 2020 Fundación Clínica Médica Sur, A.C. Published by Elsevier España, S.L.U. This is an open access article under the CC BY-NC-ND license (http://creativecommons.org/licenses/by-nc-nd/4.0/).

pathophysiology. Hepatic cells treated with palmitic acid and n-3 PUFA increased the expression of genes related with beta oxidation, diminishing the toxic effects of the palmitic acid [12]. In primary rat hepatocytes stimulated with oleic acid in the presence of palmitic acid alleviated ER stress induced by palmitic acid [13].

There is evidence that high levels of palmitic, palmitoleic and myristic fatty acids in hepatic tissue from mice with steatosis is correlated with severity of NASH [14], similar findings have been reported in patients with NASH where high content of palmitic, myristic, palmitoleic, vaccenic and oleic acids were found in liver, this FFA mix was toxic in both human primary hepatocytes and in HepG2 cell line [15]. Furthermore, in terms of nutrition, dietary fatty acids come in complex combinations which can vary greatly in the content of SFA, MUFA or PUFA.

In the present work, we were focused to study the cellular effects of two different combinations of fatty acids, where the proportion of them was variable, to explore the differential response in lipid overloaded hepatocytes from mice fed with a western diet, as a mouse model of NAFLD.

2. Materials and methods

2.1. Experimental design

All animal procedures were carried out according to the guidelines of the NIH Guide for the Care and the Use of the Laboratory Animals and Univerisidad Autonoma Metropolitana Iztapalapa (UAM-I) animal facility guide. The research was approved by the ethical committee of the UAM-I. Twenty 8-10 weeks old BALB/c mice were randomly separated in two groups. The first one was fed with a western diet (ssniff EF R/M acc TD88137 mod, catalog # E15721-34, 10 mm pellets. ssniff Spezialdiaten GmbH, Soest, Germany) for 1 week. The second group was fed with control diet (ssniff EF R/M CD88137 Control, catalog #E15720-04, 10 mm pellets), the nutrient contents are the same that the western diet, except that the atherogenic components were removed. All animals received water and diet *ad libitum*.

2.2. Analysis of liver function

Serum activity of aspartate aminotransferase (AST), and alanine transferase (ALT) were determined by using automated analyzer for clinical chemistry (Spotchem EZ, Arkray USA Inc, Minneapolis, MN, USA) following manufacturerś instructions. Blood samples were obtained by coauthor S.S.S. in the perfusion procedure, as follows.

2.3. Primary mouse hepatocytes isolation, purification and culture

Hepatocytes were isolated from mice by the two-step collagenase perfusion technique, followed by isodensity purification in percoll gradient, as we previously described [16]. Briefly, mice were anesthetized with avertin, perfusion was performed in the mouse liver through the inferior vena cava via the right atrium, at this point blood was collected. The organ was perfused 5 min with Hank' balanced solution w/o calcium and magnesium containing 10 mM HEPES and 0.2 mM EGTA followed by 10–15 min perfusion with William's medium E containing 10 mM HEPES and 0.03% collagenase H (0.19 U/mg) (Boehringer Mannheim Biochemica).

Hepatocytes were seeded at 2.13×10^5 cells per cm^2 either in Lab-Tek chambered slides or 10-cm dishes (Nalge, Nunc) in the Ham's F-12/Dulbecco's modified Eagle's basal hepatocyte growth medium supplemented with ITS+ (Collaborative Research) (insulin 6.25 mg/ml, transferrin 6.25 mg/ml, selenious acid 6.25 ng/ml, bovine serum albumin 1.25 mg/ml, 2 mM glutamine, 30 mg/ml proline (Gibco Inc), 1 mg/ml galactose (Gibco), 18 mM HEPES, 1 mM sodium pyruvate (Gibco), 1.4×10^{-2} M sodium bicarbonate (Gibco) and 10% fetal bovine serum (Hyclone Laboratories, Inc., Logan, UT). After 4 h attachment, the medium was replaced by serum-free basal hepatocyte growth medium. The following day, cells were treated with different mix of FFA, according to Table 1. All reagents were purchased from Sigma-Aldrich (St. Louis, MO, USA), except when otherwise stated.

Table 1
Fatty acids composition of the two mixes.

FFA	HMPFA %	HSFA %	Sigma–Aldrich Catalog #
Palmitic	57	60	P0500
Myristic	0.5	1.5	M3128
Palmitoleic	1	3	P9417
Oleic	27	23	O1008
n-3 PUFA (EPA/DHA, 7/2)	14.5	6.5	E2011/D2534

Primary hepatocytes were treated with both FFA mixtures, the first one contained high proportions of saturated FFA (HSFA) and the second mixture contains high proportion of FFA monounsaturated (MUFA) and polyunsaturated (PUFA), and it is referred as (HMPFA) as Table 1 shows. All FFA were supplied by Merck and Co. (Kenllworth, NJ, USA). Treatments were carried out using 100 μM, final concentration, of each FFA mixture, for 24 h.

2.4. FFA mix formulation

Cell cultures (80% confluence) were under serum free media containing 1% antibiotics for 12 h at 37 °C, 5% CO_2. FFA mix formulation was based on previous report [17]. FFA (all >99% purity and purchased from Sigma-Aldrich, Saint Louis, MO, USA) mixes were prepared as follow: 100 mM stock of Palmitic acid and Myristic acid were dissolved in 100% ethanol at 70 °C, meanwhile oleic, palmitoleic acids and PUFA n-3: docosahexaenoic acid (DHA), and eicosapentaenoic acid (EPA); (7:2 EPA/DHA,) in 100% ethanol at 40 °C. Previously, albumin (fatty acids free, Sigma-Aldrich) was prepared in William medium (25 mg/mL), prewarmed at 40 °C until solve and filtered (0.45 μm). The conjugation of BSA-FFA was added to a prewarmed 25 mg/mL BSA solution and 2 mM of two mixes fatty acids overnight (40 °C). The conjugated mix was added to a pre-warmed media (40 °C) to achieve a final FFA mix concentration of 100 μM. Mix of FFA was based on the reported composition in human plasma of participants exposed to a diet with a high content of saturated fat [18] and persons living in the Mediterranean area [19]. The mixtures included same fatty acids with two different proportions of SFA, MUFA and PUFA n-3, as Table 1 depicts. The graphical experimental design is depicted in Supplementary Fig. S1.

2.5. Red oil staining

Neutral lipids cellular content was assayed by red oil O staining as previously published [20]. Briefly, cells were seed in chamber slides, after treatments, cells were washed with ice-cold PBS and then fixed with paraformaldehyde for one h. Then, cells were stained with 0.2% oil red O solution (Sigma-Aldrich, Inc) for 4 h. Cells were washed three times with isopropanol for 10 min. Nuclei were counterstained with hematoxylin. Microphotography was obtained in an Axioscope microscope (Carl Zeiss AG, Oberkochen, Germany)

2.6. Cell functionality by MTT

Cell functionality was addressed by the 3-(4,5-dimethylthiazol-2-yl)-2,5 diphenyltetrazolium bromide (MTT) test, using the

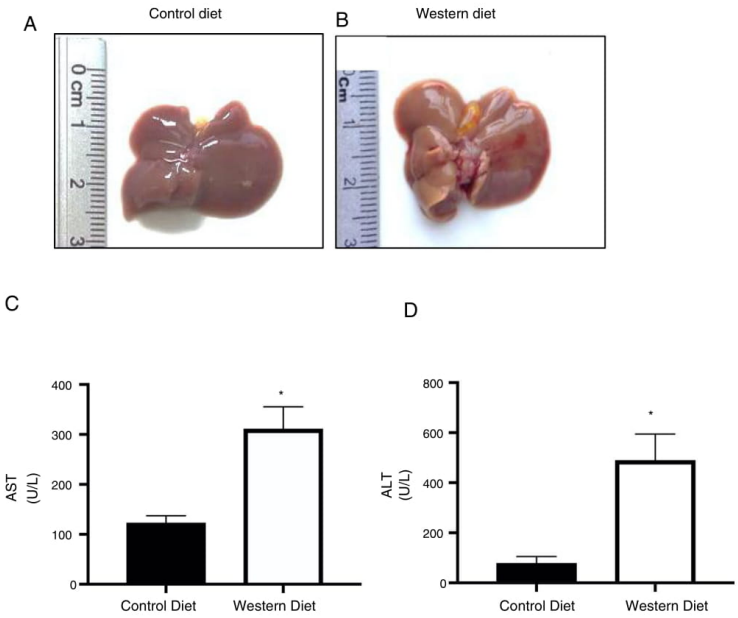


Fig. 1. Western diet induces liver dysfunction and steatosis. Macroscopic liver inspection A) Liver from mouse fed with control balanced diet; B) Liver from mouse fed with western diet for 7 days; C) Aspartate aminotransferase (AST) activity; D) Alanine aminotransferase (ALT) activity. The images are representative of at least four experimental animals. Each bar represents the mean ± SEM in at least four different mice, * $p < 0.01$ vs control diet.

Vybrant MTT Cell Proliferation Assay Kit (Thermo Fisher Scientific, Waltham, MA, USA), following manufacturer's instructions.

2.7. Reactive oxygen species determination

Reactive oxygen species (ROS) cellular content was determined by dihydroethidium (DHE, 50 μM) fluorescence, for 15 min, in the dark, at room temperature as we previously reported [21]. DHE-derived fluorescence was recorded in a Multimodal reader (DTX 880, Beckman Coulter, Inc. Brea, CA, USA) at wavelength 520 nm for excitation and 570 nm for emission. Data is reported in arbitrary fluorescence units (AFU).

2.8. Lipid peroxidation

Lipid peroxidation was assayed by the production of thiobarbituric acid-reactive substances (TBARS) using spectrophotometry as described previously [21]

2.9. Protein content determination

Protein content was determined using the bicinchoninic acid (BCA), kit (Thermo Fisher Scientific), according to manufacturer's instructions.

3. Statistical Analysis

Data are presented as mean ± SEM of at least three independent experiments carried out by triplicate. Comparisons between groups were made using Student's *t* test, Mann Whitney and Tukey–Kramer test. GraphPad Prism 8 software for OSX was used to run analysis. Differences were considered significant at $p \leq 0.05$.

4. Results

We fed BALB/c mice with either western or control diet for seven days. As Fig. 1B shows, livers from animals under western diet exhibit the characteristic pale color of steatosis, comparing with control diet (Fig. 1A) even more, these animals presented high serum activity of AST and ALT, two well-accepted markers of liver damage (Fig. 1C and D), confirming liver injury due to high lipid diet consumption.

Due to the main objective of the present work was to figure out the impact of different combination of FFA in the lipid-overloaded hepatocyte, we proceeded to liver perfusion and hepatocytes isolation and culture (Supplementary Fig. S1).

To confirm the lipid overload in hepatocytes, neutral lipids were assessed by the oil red O staining, hepatocytes from animals under western diet showed increased lipid content in comparison with hepatocytes from control mice (Fig. 2A and B). To gain more confidence, we confirmed cellular lipid accumulation biochemically by measuring both triglycerides (TG) and cholesterol content. TG increased 2.65-fold (Fig. 2C) and cholesterol 4.98-fold (Fig. 2D) in western diet hepatocytes regarding control.

Results clearly show that western diet induces liver impairment and lipid overloaded hepatocytes, confirming that these cells represent a good model to study the cellular effects of differential FFA mixture in steatotic hepatocytes.

Cells from both groups of animals, were treated with 100 μM of HMPFA or HSFA mixes of FFA (Table 1) for 24 h. Interestingly, the treatment with HMPFA for 24 h remarkably decreased the lipid content (Fig. 3D) induced by western diet consumption (Fig. 3B), but no differences were observed in HSFA-treated cells (Fig. 3F). Control cells showed a slight increment in lipid content under the treatment with HMPFA, judged by oil red O staining, comparing

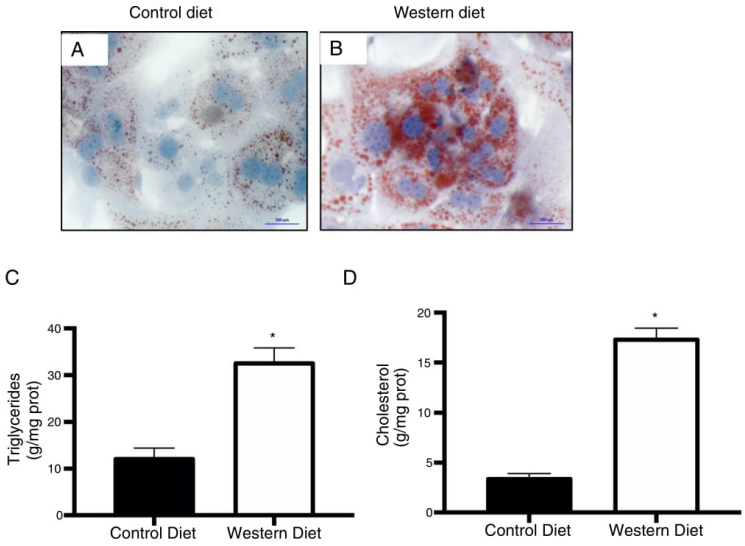


Fig. 2. Hepatocytes from mouse fed with western diet exhibits lipid overload. Neutral lipids content determined by oil red O staining. Primary hepatocytes from A) mouse fed with control balanced diet; B) mouse fed with western diet for 7 days; C) Liver triglyceride content; D) liver total cholesterol content. Data are normalized versus mg of cellular total protein. The images are representative of at least four animals. Reference bar 500 μm. Each bar represents the mean ± SEM in at least four different mice, *p < 0.01 vs control diet.

with not treated control cells (Fig. 3A), however these cells treated with HSFA observed a notable increment in lipid content (Fig. 3E). These results clearly show a favorable effect induced by the FFA Mediterranean-like mix treatment in steatotic hepatocytes.

To gain more confidence, we proceeded to biochemically measure both TG and cholesterol cellular content. Fig. 3G clearly shows that HMPFA treatment significantly reduces 2.1-fold the TG content in western hepatocytes, similar findings were found in cholesterol decreasing 1.7-fold regarding western hepatocytes (Fig. 3H), but HSFA mix did not observe any change, remaining TG and cholesterol values similar to those observed in western hepatocytes.

Cellular functionality, addressed by MTT assay, revealed a significant improvement in cell function in western hepatocytes treated with HMPFA mix comparing with not treated western cells (Fig. 4), while HSFA mix worsened cell function of western hepatocytes.

To gain mechanistic enlightenments, and due to oxidative stress is one of the main inducers of cell damage in steatosis as we previously published [6,7], we proceeded to measure the ROS content in cells under different treatments as previously reported [6]. Fig. 5A shows a remarkable increment in ROS in western cells compared with control hepatocytes, consistent with our previous findings. HMPFA mix remarkably reduced ROS production, while HSFA treatment did not induce significant changes in ROS content in western hepatocytes, even more, it increased the ROS in control hepatocytes comparing with not treated cells. These data were in agreement with lipid peroxidation, a well-accepted marker of oxidative damage, Fig. 5B shows that western hepatocytes increased 208.7% the TBARS regarding control cells, while HMPFA treatment decreased them 52% regarding western hepatocytes. Interestingly, HSFA increased TBARS in control cells, with no significant change in western hepatocytes, suggesting a kind of saturation in the oxidative damage.

5. Discussion

Recently, it has been published the last annual report to the nation on the status of cancer [22], this dossier leaves clear that liver malignancies are the most prevalent among all types of cancers. This is alarming. In part, the phenomenon could be related to the remarkable prevalence of NAFLD, not only in USA but worldwide [23], which seems to be increasing particularly by sedentary lifestyle and inadequate dietary behaviors. Although, it is well known that practically all liver diseases present a natural history starting with steatosis, this could also be as a consequence of the high consumption of fat and carbohydrates characterizing the typical western diet.

In the present work, we were aimed to address the cellular effects of different mixes of dietary FFA in lipid-overloaded primary mouse hepatocytes.

Although, many cancer-derived cell lines naturally present aberrant lipogenesis leading to lipid overload [24], the anomalous gene expression of these cells could mask potential interesting effects, particularly in metabolism, proliferation or survival. To address both, the effect of cellular lipid overload, and the impact of the treatment with specific lipids mixtures, we used a proper cellular model, with naturally occurring lipid overload. Standard commercial western diet (ssniff, E15721-34) provides high content of fat and carbohydrates (crude fat, 21.2%; cholesterol, 2.071%, and carbohydrates 33.2%) certainly resembling the western diet consumed in Mexico and developed countries such as USA [25].

Hepatocytes obtained from mice fed with western diet for one week, presented a clear lipid overload characterized by increased content of TG and free cholesterol (Fig. 2). Mice under western diet presented increased serum activity of AST and ALT and the characteristic pale color of the organ, indicating liver dysfunction due to the steatosis (Fig. 1).

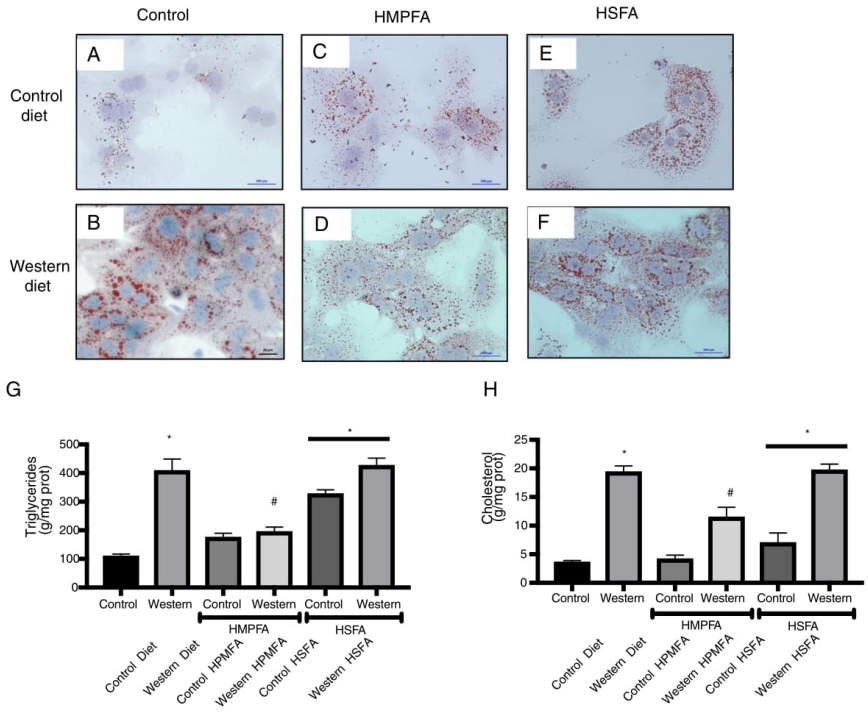


Fig. 3. Treatment with different lipid mixtures induces differential response in steatotic hepatocytes. Neutral lipids content determined by oil red O staining. Primary hepatocytes from mouse fed with control balanced control diet A), C) and E); or western diet B), D) and F) for 7 days. Cells were treated or not with high mono and polyunsaturated fatty acids (HMPFA) or high saturated fatty acids (HSFA) according Table 1, for 24 h. G) cellular triglycerides content and, H) total cellular cholesterol content. The images are representative of at least four animals. Reference bar 500 μm (200X original magnification). Each bar represents the mean ± SEM in at least four different mice. * $p < 0.05$ vs control cells, # $p < 0.05$ vs western cells.

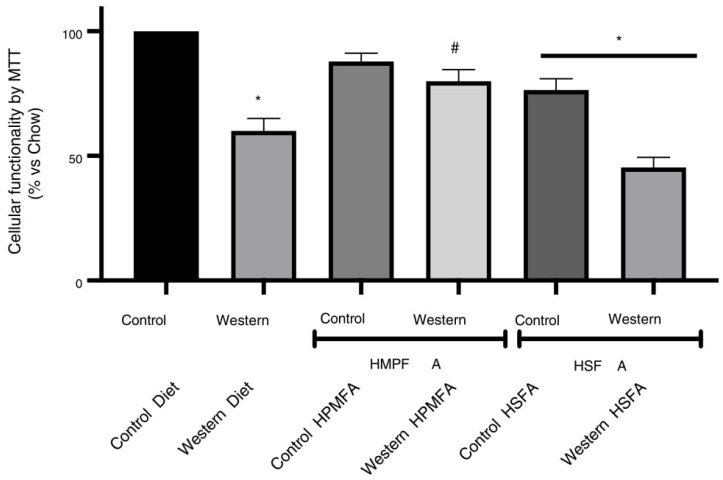


Fig. 4. Cellular functionality by MTT assay. Control and western cells were treated or not with high mono and polyunsaturated fatty acids (HMPFA) or high saturated fatty acids (HSFA) according Table 1, for 24 h. Each bar represents the mean ± SEM in at least four mice, *$p < 0.05$ vs control cells, # $p < 0.05$ vs western cells.

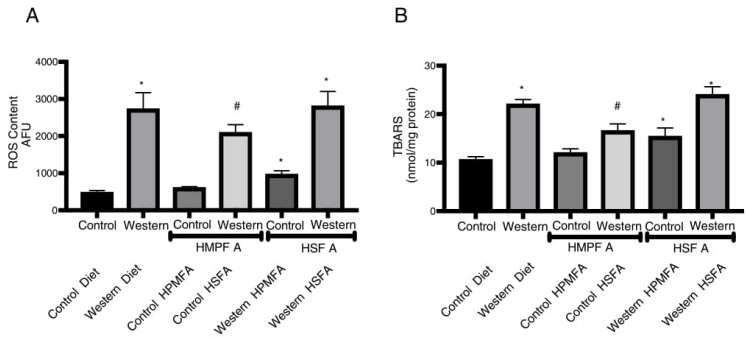


Fig. 5. Mediterranean-like mix of fatty acids protects lipid-overloaded hepatocytes from the oxidative damage. Control and western cells were treated or not with high mono and polyunsaturated fatty acids (HMPFA) or high saturated fatty acids (HSFA) according Table 1, for 24 h. (A) Reactive oxygen species (ROS) content determined by the superoxide radical probe dihydroethidium as reported in material and methods section; (B) Lipid peroxidation assayed by thiobarbituric acid reactive substances (TBARS). Each group represents mean ± SEM in at least three mice, *p < 0.05 vs control cells, # p < 0.05 vs western cells.

We and others have reported that is the kind of lipid rather than the amount of them that determines the grade of cellular damage [5,6,9], particularly the increment in hepatic cholesterol governs severity of liver diseases as we previously reported [8,9,26]. In our *in vitro* model, we show that cholesterol is significantly increased (5-fold) in hepatocytes. The excess of cholesterol in cells particularly targets mitochondria, inducing oxidative stress, mitochondria fission, decrement in ATP production and sensitization to damage [5,7]. Hepatocytes isolation by the two-step collagenase perfusion leads to the preservation of the steatotic phenotype, as we clearly show (Fig. 2). Cholesterol overload in addition, represents another challenge, persistent liver accumulation could induce apoptosis resistance [7] promoting tumorigenesis, as we recently reported [6].

There is no doubt regarding the problem of liver cholesterol accumulation. New alternatives directed to decrease noxious lipids are required, particularly nutritional ones.

It has been extensively published that the Mediterranean diet which is plant-centric, but moderate to low amounts of animal components, could play key role in chronic disease prevention [27–29]. Recently, it has been published that Mediterranean diet also provides beneficial effects in patients with NAFLD, diminishing parameters of severity such as lipid profile, glycemic index, serum liver enzymes activity, among others [30,31].

Focused exclusively in some the main types of FFA such as those find in plasma in persons who consume Mediterranean diet [19,32], we explored, at the cellular level, the effects induced by this FFA mix (HMPFA) on steatotic hepatocytes, comparing with a saturated FFA mix (HSFA). It is important to emphasize that both FFA mixtures are composed with the same lipids but with different content (Table 1).

It could be paradoxical, but our data clearly show that the presence of some lipids could influence the content of others. Fig. 3 depicts that HMPFA induces lipid content reduction in western hepatocytes, while HSFA seems to have no influence judged by oil red staining.

In addition to essential nutritional functions, FFA activate multiple signaling pathways, particularly those related to metabolism, by interacting with specific FFA receptors [33]. It is evident that HMPFA are activating changes in lipid metabolism or mobility, effect not observed with the saturated-rich mix. Although, both lipid combinations have the same fatty acids, the HMPFA has more n-3 PUFA. Some studies have shown that dietary supplementation with n-3 PUFA in obese mice under a high fat diet reduces hepatic lipid content, normalize TG with an improvement in the inflammatory response and decreasing oxidative stress, favoring insulin sensitivity, same effects have been observed in hepatic cells with lipid overload [34–36].

It is interesting that HMPFA exerted differential effect preferent controlling TG (Fig. 3G) rather than cholesterol (Fig. 3H), although cholesterol certainly decreased with the HMPFA treatment regarding untreated animal under western diet, cholesterol levels remain significantly increased when comparing with cells from control diet fed mice however, the decrement in cholesterol was related to an improvement in mitochondrial function judged by MTT test (Fig. 4).

It has been extensively published that cholesterol overload in hepatic cells is particularly relevant in mitochondrial functionality. Cholesterol accumulates in this organelle inducing oxidative stress and sensitization to a second insult [5,6,9].

Our data clearly show that, although the decrement of cholesterol induced by HMPFA treatment, it did not reach basal values, but it was good enough to decrease ROS content (Fig. 5A) and oxidative damage, judged by lipid peroxidation (Fig. 5B). Although, it has been observed that Mediterranean diet has the ability to decrease ROS by a polyphenol-dependent mechanism [37], the antioxidant properties elicited by mono or polyunsaturated FFA should be revisited, particularly in the context of NAFLD as recently published [11], and as our results clearly show.

Olive oil represents the main fat source in the Mediterranean diet, it is composed particularly of monounsaturated fatty acids (mainly oleic acid, 55-83%) and polyunsaturated fatty acids (4–20%) [11], in fact these FFA are excellent ROS scavengers due to the capacity of their double bonds to react with reactive substances, our data provide evidence that the HMPFA induced a decrement in ROS content and cellular lipid peroxidation (Fig. 5), mediated by the western diet.

PUFA, particularly n-3, have demonstrated to display protective effects in the liver, in fact, it is well known that enteral nutrition in hospitals is associated to deterioration of liver function, n-3 PUFA induced an improvement in the liver [38], the effect was associated to the downregulation of Cyp450 enzymes, this could represent an adaptive mechanism tending to improve oxidative stress phenomena.

Aside this remarkable protective effect induced by HMPFA, the HSFA mix did not exert any change in lipid-overloaded hepatocytes. As expected, treatment with HSFA in control hepatocytes increased cellular lipid overload by a significant increment of TG but not cholesterol. HSFA treatment resulted in a slight increment in ROS content and lipid peroxidation.

6. Conclusion

Our results show that combination of increased proportions of MUFA and PUFA exert cellular protective effects by controlling the levels of TG and cholesterol and decreasing the ROS production and the oxidative damage in hepatocytes with lipid overload induced by the feeding of a western diet. Consumption of increased combination of MUFA and PUFA and low content of saturated FFA, induces a protective effect in steatotic hepatocytes, leading to the improvement of cellular function by decreasing oxidative stress. The ingestion HMPFA (or Mediterranean-like diet) could potentially be a good adjuvant treatment in fatty liver diseases. Although, the *in vitro* study is confined to the effects in the hepatocytes, validation in *in vivo* models and, even more in humans, would be of great interest to stablish dietary supportive intervention in the treatment of NAFLD.

Conflict of interest

The authors have no conflicts of interest to declare.

Acknowledgments

This work was supported by National Institute of Genomic Medicine. Cátedra Nestlé-INMEGEN, CONACYT: Fronteras de la Ciencia 1320 and CB-252942. Universidad Autonoma Metropolitana Unidad Iztapalapa.

Appendix A. Supplementary data

Supplementary material related to this article can be found, in the online version, at doi:https://doi.org/10.1016/j.aohep.2020.06.005.

References

[1] Spengler EK, Loomba R. Recommendations for diagnosis, referral for liver biopsy, and treatment of nonalcoholic fatty liver disease and nonalcoholic steatohepatitis. Mayo Clin Proc 2015;90:1233–46, http://dx.doi.org/10.1016/j.mayocp.2015.06.013.

[2] Brunt EM, Wong VW, Nobili V, Day CP, Sookoian S, Maher JJ, et al. Nonalcoholic fatty liver disease. Nat Rev Dis Primers 2015;1:15080, http://dx.doi.org/10.1038/nrdp.2015.80.

[3] Mozaffarian D, Hao T, Rimm EB, Willett WC, Hu FB. Changes in diet and lifestyle and long-term weight gain in women and men. N Engl J Med 2011;364:2392–404, http://dx.doi.org/10.1056/NEJMoa1014296.

[4] Costa CS, Del-Ponte B, Assuncao MCF, Santos IS. Consumption of ultra-processed foods and body fat during childhood and adolescence: a systematic review. Public Health Nutr 2018;21:148–59, http://dx.doi.org/10.1017/S1368980017001331.

[5] Mari M, Caballero F, Colell A, Morales A, Caballeria J, Fernandez A, et al. Mitochondrial free cholesterol loading sensitizes to TNF- and Fas-mediated steatohepatitis. Cell Metab 2006;4:185–98, http://dx.doi.org/10.1016/j.cmet.2006.07.006.

[6] Enriquez-Cortina C, Bello-Monroy O, Rosales-Cruz P, Souza V, Miranda RU, Toledo-Perez R, et al. Cholesterol overload in the liver aggravates oxidative stress-mediated DNA damage and accelerates hepatocarcinogenesis. Oncotarget 2017;8:104136–48, http://dx.doi.org/10.18632/oncotarget.22024.

[7] Dominguez-Perez M, Simoni-Nieves A, Rosales P, Nuno-Lambarri N, Rosas-Lemus M, Souza V, et al. Cholesterol burden in the liver induces mitochondrial dynamic changes and resistance to apoptosis. J Cell Physiol 2019;234:7213–23, http://dx.doi.org/10.1002/jcp.27474.

[8] Lopez-Islas A, Chagoya-Hazas V, Perez-Aguilar B, Palestino-Dominguez M, Souza V, Miranda RU, et al. Cholesterol enhances the toxic effect of ethanol and acetaldehyde in primary mouse hepatocytes. Oxid Med Cell Longev 2016;2016:9209825, http://dx.doi.org/10.1155/2016/9209825.

[9] Nuno-Lambarri N, Dominguez-Perez M, Baulies-Domenech A, Monte MJ, Marin JJ, Rosales-Cruz P, et al. Liver cholesterol overload aggravates obstructive cholestasis by inducing oxidative stress and premature death in mice. Oxid Med Cell Longev 2016;2016:9895176, http://dx.doi.org/10.1155/2016/9895176.

[10] Gomez-Quiroz LE, Seo D, Lee YH, Kitade M, Gaiser T, Gillen M, et al. Loss of c-Met signaling sensitizes hepatocytes to lipotoxicity and induces cholestatic liver damage by aggravating oxidative stress. Toxicology 2016;361-362:39–48, http://dx.doi.org/10.1016/j.tox.2016.07.004.

[11] Abenavoli L, Milanovic M, Milic N, Luzza F, Giuffre AM. Olive oil antioxidants and non-alcoholic fatty liver disease. Expert Rev Gastroenterol Hepatol 2019;13:739–49, http://dx.doi.org/10.1080/17474124.2019.1634544.

[12] Albracht-Schulte K, Gonzalez S, Jackson A, Wilson S, Ramalingam L, Kalupahana NS, et al. Eicosapentaenoic acid improves hepatic metabolism and reduces inflammation independent of obesity in high-fat-fed mice and in HepG2 cells. Nutrients 2019;11, http://dx.doi.org/10.3390/nu11030599.

[13] Zeng X, Zhu M, Liu X, Chen X, Yuan Y, Li L, et al. Oleic acid ameliorates palmitic acid induced hepatocellular lipotoxicity by inhibition of ER stress and pyroptosis. Nutr Metab (Lond) 2020;17:11, http://dx.doi.org/10.1186/s12986-020-0434-8.

[14] Yamada K, Mizukoshi E, Sunagozaka H, Arai K, Yamashita T, Takeshita Y, et al. Characteristics of hepatic fatty acid compositions in patients with nonalcoholic steatohepatitis. Liver Int 2015;35:582–90, http://dx.doi.org/10.1111/liv.12685.

[15] Chiappini F, Coilly A, Kadar H, Gual P, Tran A, Desterke C, et al. Metabolism dysregulation induces a specific lipid signature of nonalcoholic steatohepatitis in patients. Sci Rep 2017;7:46658, http://dx.doi.org/10.1038/srep46658.

[16] Gomez-Quiroz LE, Factor VM, Kaposi-Novak P, Coulouarn C, Conner EA, Thorgeirsson SS. Hepatocyte-specific c-Met deletion disrupts redox homeostasis and sensitizes to Fas-mediated apoptosis. J Biol Chem 2008;283:14581–9, http://dx.doi.org/10.1074/jbc.M707733200.

[17] Najbjerg H, Young JF, Bertram HC, Afseth NK, Host V, Kohler A. High-throughput FTIR spectroscopy of intact HepG2 cells reveals additive and non-additive effects of individual fatty acids when given as mixtures. J Biophotonics 2013;6:446–56, http://dx.doi.org/10.1002/jbio.201200073.

[18] Hodson L, Eyles HC, McLachlan KJ, Bell ML, Green TJ, Skeaff CM. Plasma and erythrocyte fatty acids reflect intakes of saturated and n-6 PUFA within a similar time frame. J Nutr 2014;144:33–41, http://dx.doi.org/10.3945/jn.113.183749.

[19] Jenab M, Slimani N, Bictash M, Ferrari P, Bingham SA. Biomarkers in nutritional epidemiology: applications, needs and new horizons. Hum Genet 2009;125:507–25, http://dx.doi.org/10.1007/s00439-009-0662-5.

[20] Hernandez I, Dominguez-Perez M, Bucio L, Souza V, Miranda RU, Clemens DL, et al. Free fatty acids enhance the oxidative damage induced by ethanol metabolism in an in vitro model. Food Chem Toxicol 2015;76:109–15, http://dx.doi.org/10.1016/j.fct.2014.12.005.

[21] Salas-Silva S, Simoni-Nieves A, Razori MV, Lopez-Ramirez J, Barrera-Chimal J, Lazzarini R, et al. HGF induces protective effects in alpha-naphthylisothiocyanate-induced intrahepatic cholestasis by counteracting oxidative stress. Biochem Pharmacol 2020;174:113812, http://dx.doi.org/10.1016/j.bcp.2020.113812.

[22] Henley SJ, Ward EM, Scott S, Ma J, Anderson RN, Firth AU, et al. Annual report to the nation on the status of cancer, part I: national cancer statistics. Cancer 2020, http://dx.doi.org/10.1002/cncr.32802.

[23] Perumpail BJ, Khan MA, Yoo ER, Cholankeril G, Kim D, Ahmed A. Clinical epidemiology and disease burden of nonalcoholic fatty liver disease. World J Gastroenterol 2017;23:8263–76, http://dx.doi.org/10.3748/wjg.v23.i47.8263.

[24] Gerardo-Ramirez M, Lazzarini-Lechuga R, Hernandez-Rizo S, Jimenez-Salazar JE, Simoni-Nieves A, Garcia-Ruiz C, et al. GDF11 exhibits tumor suppressive properties in hepatocellular carcinoma cells by restricting clonal expansion and invasion. Biochim Biophys Acta Mol Basis Dis 2019;1865:1540–54, http://dx.doi.org/10.1016/j.bbadis.2019.03.003.

[25] Batis C, Hernandez-Barrera L, Barquera S, Rivera JA, Popkin BM. Food acculturation drives dietary differences among Mexicans, Mexican Americans, and Non-Hispanic Whites. J Nutr 2011;141:1898–906, http://dx.doi.org/10.3945/jn.111.141473.

[26] Lopez-Reyes A, Clavijo-Cornejo D, Fernandez-Torres J, Medina-Luna D, Estrada-Villasenor EG, Gomez-Quiroz LE, et al. Fast morphological gallbladder changes triggered by a hypercholesterolemic diet. Ann Hepatol 2018;17:857–63, http://dx.doi.org/10.5604/01.3001.0012.3160.

[27] Trichopoulou A, Martinez-Gonzalez MA, Tong TY, Forouhi NG, Khandelwal S, Prabhakaran D, et al. Definitions and potential health benefits of the Mediterranean diet: views from experts around the world. BMC Med 2014;12:112, http://dx.doi.org/10.1186/1741-7015-12-112.

[28] Sofi F, Abbate R, Gensini GF, Casini A. Accruing evidence on benefits of adherence to the Mediterranean diet on health: an updated systematic review and meta-analysis. Am J Clin Nutr 2010;92:1189–96, http://dx.doi.org/10.3945/ajcn.2010.29673.

[29] Sofi F, Macchi C, Abbate R, Gensini GF, Casini A. Effectiveness of the Mediterranean diet: can it help delay or prevent Alzheimer's disease? J Alzheimers Dis 2010;20:795–801, http://dx.doi.org/10.3233/JAD-2010-1418.

[30] Moosavian SP, Arab A, Paknahad Z. The effect of a Mediterranean diet on metabolic parameters in patients with non-alcoholic fatty liver disease: A systematic review of randomized controlled trials. Clin Nutr ESPEN 2020;35:40–6, http://dx.doi.org/10.1016/j.clnesp.2019.10.008.

[31] Bullon-Vela V, Abete I, Tur JA, Pinto X, Corbella E, Martinez-Gonzalez MA, et al. Influence of lifestyle factors and staple foods from the Mediterranean diet on non-alcoholic fatty liver disease among older individuals with metabolic syndrome features. Nutrition 2020;71:110620, http://dx.doi.org/10.1016/j.nut.2019.110620.

[32] Saadatian-Elahi M, Slimani N, Chajes V, Jenab M, Goudable J, Biessy C, et al. Plasma phospholipid fatty acid profiles and their association with food intakes: results from a cross-sectional study within the European Prospective Investigation into Cancer and Nutrition. Am J Clin Nutr 2009;89:331–46, http://dx.doi.org/10.3945/ajcn.2008.26834.

[33] Hara T, Kimura I, Inoue D, Ichimura A, Hirasawa A. Free fatty acid receptors and their role in regulation of energy metabolism. Rev Physiol Biochem Pharmacol 2013;164:77–116, http://dx.doi.org/10.1007/112_2013_13.
[34] Valenzuela R, Espinosa A, Gonzalez-Manan D, D'Espessailles A, Fernandez V, Videla LA, et al. N-3 long-chain polyunsaturated fatty acid supplementation significantly reduces liver oxidative stress in high fat induced steatosis. PLoS One 2012;7:e46400, http://dx.doi.org/10.1371/journal.pone.0046400.
[35] Jung UJ, Millman PN, Tall AR, Deckelbaum RJ. n-3 fatty acids ameliorate hepatic steatosis and dysfunction after LXR agonist ingestion in mice. Biochim Biophys Acta 2011;1811:491–7, http://dx.doi.org/10.1016/j.bbalip.2011.06.003.
[36] Kang S, Huang J, Lee BK, Jung YS, Im E, Koh JM, et al. Omega-3 polyunsaturated fatty acids protect human hepatoma cells from developing steatosis through FFA4 (GPR120). Biochim Biophys Acta Mol Cell Biol Lipids 2018;1863:105–16, http://dx.doi.org/10.1016/j.bbalip.2017.11.002.
[37] Abenavoli L, Boccuto L, Federico A, Dallio M, Loguercio C, Di Renzo L, et al. Diet and non-alcoholic fatty liver disease: the Mediterranean way. Int J Environ Res Public Health 2019;16, http://dx.doi.org/10.3390/ijerph16173011.
[38] Bechynska K, Daskova N, Vrzackova N, Harant K, Heczkova M, Podzimkova K, et al. The effect of omega-3 polyunsaturated fatty acids on the liver lipidome, proteome and bile acid profile: parenteral versus enteral administration. Sci Rep 2019;9:19097, http://dx.doi.org/10.1038/s41598-019-54225-8.

Epilogue.

Although intensive research work is done everyday for many scientist in the translational medicine field to unmask the pathological mechanisms of various diseases, sometimes we forget the ultimate link in this arduous task, the patients. Throughout my entire journey as a student, I always had my mentors not only as an invaluable guide on this cobbled path called science but also to remind me that our work should always be conducted thinking about the well-being of patients, either to improve treatments and to provide them with a better life quality.

So the only and most important thing that I can offer to those readers who come across this manuscript; it is that during their training and during their academic and research life they lead themselves on the path of excellence thinking about the end point of their research, "THE PATIENTS".

Take care and thank you for taking your time to read this manuscript.

Arturo Simoni Nieves

Casa abierta al tiempo
UNIVERSIDAD AUTÓNOMA METROPOLITANA

ACTA DE DISERTACIÓN PÚBLICA

No. 00125
Matricula: 2163802393

The consumption of a high cholesterol diet conditions the development of a subtype of HCC with high aggressiveness and poor prognosis.



ARTURO SIMONI NIEVES
ALUMNO

REVISO

MTRA. ROSALIA SERRANO DE LA PAZ
DIRECTORA DE SISTEMAS ESCOLARES

Con base en la Legislación de la Universidad Autónoma Metropolitana en la Ciudad de México se presentaron a las 12:00 horas del día 10 del mes de marzo del año 2021 POR VÍA REMOTA ELECTRÓNICA, los suscritos miembros del jurado designado por la Comisión del Posgrado:

DR. JU SEOG LEE
DRA. MARIA CONCEPCION GUTIERREZ RUIZ
DR. HECTOR FERNANDO SERRANO
DR. CEDRIC COULOUARN MICHEL

Bajo la Presidencia del primero y con carácter de Secretario el último, se reunieron a la presentación de la Disertación Pública cuya denominación aparece al margen, para la obtención del grado de:

DOCTOR EN BIOLOGIA EXPERIMENTAL

DE: ARTURO SIMONI NIEVES

y de acuerdo con el artículo 78 fracción IV del Reglamento de Estudios Superiores de la Universidad Autónoma Metropolitana, los miembros del jurado resolvieron:

Aprobar

Acto continuo, el presidente del jurado comunicó al interesado el resultado de la evaluación y, en caso aprobatorio, le fue tomada la protesta.

DIRECTORA DE LA DIVISIÓN DE CBS

DRA. SARA LUCIA CAMARGO RICALDE

PRESIDENTE

DR. JU SEOG LEE

VOCAL

DRA. MARIA CONCEPCION GUTIERREZ RUIZ

VOCAL

DR. HECTOR FERNANDO SERRANO

SECRETARIO

DR. CEDRIC COULOUARN MICHEL